



CONFERENCE PROCEEDINGS



UGC Sponsored
National Conference on

Recent Advancements in Science and Technology

VOLUME I : Chemistry



:: Organized by ::

Vidya Bharati Shaikshanik Mandal's

Vidya Bharati Mahavidyalaya, Amravati

Re-accredited with Grade 'A' by the NAAC (CGPA 3.23 - Third Cycle)
College with Potential for Excellence (CPE Status Thrice by the UGC)
Star College Status by DBT, New Delhi, Mentor College under Paramarsh by UGC
Identified as Lead College by S.G.B. Amravati University, Amravati

:: In Collaboration with ::

S.S.S.K.R. Innani Mahavidyalaya

Karanja (Lad), Dist. Washim 444105 (M.S.), India
NAAC Re-Accredited 'A+' Grade (CGPA 3.28)
C.P.E. Status Awarded by UGC, New Delhi
Affiliated to Sant Gadge Baba Amravati University, Amravati

ISBN : 978-81-19931-25-5



CONFERENCE PROCEEDINGS



UGC Sponsored
National Conference on

Recent Advancements in Science and Technology

VOLUME I : Chemistry



:: Organized by ::

Vidya Bharati Shaikshanik Mandal's

Vidya Bharati Mahavidyalaya, Amravati

Re-accredited with Grade 'A' by the NAAC (CGPA 3.23 - Third Cycle)
College with Potential for Excellence (CPE Status Thrice by the UGC)
Star College Status by DBT, New Delhi, Mentor College under Paramarsh by UGC
Identified as Lead College by S.G.B. Amravati University, Amravati

:: In Collaboration with ::

S.S.S.K.R. Innani Mahavidyalaya

Karanja (Lad), Dist. Washim 444105 (M.S.), India
NAAC Re-Accredited 'A+' Grade (CGPA 3.28)
C.P.E. Status Awarded by UGC, New Delhi
Affiliated to Sant Gadge Baba Amravati University, Amravati

SAI JYOTI PUBLICATION, NAGPUR

UGC Sponsored
National Conference on

Recent Advancements in Science and Technology

VOLUME I : Chemistry

Chief Editor

Dr. Pradnya S. Yenkar

Principal, Vidya Bharati Mahavidyalaya, Amravati

ISBN : 978-81-19931-25-5

Date : 10th Feb., 2024

Publisher :

Sai Jyoti Publication

Itwari, Nagpur

E-mail : sjp10ng@gmail.com

Type Setting & Printing

LASER POINT,

Gadge Nagar, Amravati

No part of this book shall be reproduced, stored in retrieval system, or translated in any form or by any means, electronic, mechanical, photocopying and/or otherwise without the prior written permission of the publishers.

• **Disclaimer :**

- The publishers, The Principal, Vidyabharti Mahavidyalaya, Amravati and the organizers are not responsible for the content of any of the research paper/article published in this conference proceedings.
- The authors/Co-authors are responsible for the plagiarism
- For any conflict of interests, the Author/Co-Authors are responsible.
- For any query/issue/ethical aspects contact the corresponding Author.

CONFERENCE PROCEEDINGS

UGC Sponsored National Conference on Recent Advancements in Science & Technology

Date : 10th Feb, 2024

:: Organized by ::

Vidya Bharati Shaikshanik Mandal's

Vidya Bharati Mahavidyalaya, Amravati

:: In Collaboration with ::

S.S.S.K.R. Innani Mahavidyalaya

Karanja (Lad), Dist. Washim 444105 (M.S.), India

Editorial Board

VOLUME I : Chemistry

Chief Editor
Dr. Pradnya S. Yenkar Principal, Vidya Bharati Mahavidyalaya, Amravati
Editors
Prof. Dr. M. M. Rathore , Associate Editor Dr. V. H. Masand , Member Dr. P. S. Bodkhe , Member Dr. C. N. Deshmukh , Member Mr. Varun Mahale , Member Dr. P. P. Nalawade , Member Dr. J. R. Bansod , Member Mr. C. N. Jadhav , Member

CONTENTS

Chemistry

S.No.	Title	Author/s	Page No.
1	QSAR evaluation of Glucagon Receptor (GCGR) antagonists for the anti-hyperglycaemic lead development	Ajaykumar Gandhi Pooja Gaikwad Jyoti Dahatonde Archana Chapolikar	1-7
2	Synthesis and Biological Evaluation of Pyrazole Derivative	A P Thakare S R Kolteke	8-12
3	Healthy hydroponic cattle feed (grass) development eco-friendly & economically	Dr. Ramesh Tukaram Parihar, Dr A.G.Gaddamwar	13-18
4	Design and Synthesis of Heterocyclic Active Moieties of Pyrazoles and Its Importance's	Somwanshi A.R.	19-22
5	QSAR analysis of sodium glucose co-transporter 1 (SGLT1) inhibitors for anti-hyperglycaemic lead development	Archana Chapolikar, Jyoti Dahatonde, Pooja Gaikwad, Ajaykumar Gandhi	23-34
6	Preparation and Acetone Gas Sensing Properties of Cd Substituted Magnesium Ferrites	A. V. Kadu	35-40
7	Studies of Acoustic Properties of Substituted Chalcone in Different Percentage of Dioxane-Water Mixture	A. D. Khambre	41-44
8	Synthesis, Physicochemical evaluation of heteryl amino derivatives of bis[5-cyano-1,6-dihydro-6-imino-2-isopropyl-4-(methylthio) pyrimidine] diazene	Girish Deshmukh Avinash Thakare, Chanda Gawande	45-49
9	Novel Synthesis and Characterization of Some Substituted Chlorosubstituted Aryl Substituted 1,3-Thiazole as Antibacterial Agents	Chhaya D. Badnakhe	50-58
10	Mini Review on biological aspects of 1,3,4-Thiadiazoles	Mr. N.D. Dahake, Dr. V.H. Masand	59-61
11	Simultaneous Non-aqueous Conductometric Investigation of Pharmaceutically Potent Ibuprofen-Paracetamol Combination Drugs	Pradip P. Deohate, Aakanksha S. Dongare Anushri R. Jalamkar	62-64
12	Cp*Co(III) Catalyzed Redox-Neutral Annulation: A Powerful Tool for Isoquinoline Synthesis from <i>N</i> -Cbz Hydrazones	Dewal S. Deshmukh Bhalchandra M. Bhanage	65-67

13	Design, synthesis, spectral characterization and anti-microbial screening of some novel 1, 2, 4-dithiazole with Coumarin moiety	K. U. Dongare S. A. Waghmare S. B. Sarkate R. N. Ingole	68-72
14	Effect Of metal-ligand complexon germination of some vegetable plants	Prof. M.M.Rathore C.N.Deshmukh	73-78
15	Preparation of Adsorbent from various natural materials for removal of heavy metal ions from waste water: Critical review	Sandhya B. Gaikwad	79-82
16	Evaluation of Antioxidant Activity by DPPH Method of Thiocarbamides	P.L. Harale M.E. Shelke D.T. Tayade	83-86
17	Investigations of Proximate Compositions of <i>Xanthium Strumarium L</i> Roots from Tisgaon (PIN Code 431002) of Taluka and District Aurangabad, India	Jawerea Nayab Mohammad Jamil Rahim Ullah Sharafat Ullah	87-89
18	Synthesis, Structural Study Of Substituted Heterocyclic Compounds	Kavita. M. Heda	90-93
19	Characterization of Diesel Mixtures by Ultrasonic Methods	K. P. Belsare N. B. Selukar	94-96
20	Phytochemical and Proximate Analysis of Leaves of <i>Heteropogon Contortous</i> (L.) Beauv	Miss Mosim Raza H. Shaikh	97-100
21	A Review of Computer-Aided Drug Discovery (CADD)	Manojkumar O. Malpani	101-105
22	Synthesis and Anti-microbial Activity of Novel 3-[(3-substitutedamino-1,2,4-thiadiaz-3-yl)]amino-5-N-TAG-amino-1,2,4-thiadiazole [11b]	M. R. Raghuvanshi	106-109
23	Sulfate promoted zirconia-based mixed oxide as solid acid catalysts for organic transformations	Sushil V. Shelke Sambhaji T. Dhumal Abhay L. Ghodke Meghshyam K. Patil	110-112
24	Structure, Physical and Chemical Properties of Thiourea with Their Derivatives	A.P. Mitake S.P. Rathod	113-119
25	Study of Proton and Metal-Ligand Stability Constants of hydroxy Substituted Chalcone Complexes pH-Metrically	Mohd. Wajid Shaikh Mohd Waris	120-123
26	Ecofriendly synthesis and characterization of Ethyl 2-imino-6-methyl-4-substituted phenyl-1, 2, 3, 4-tetrahydropyrimidine-5-carboxylate compounds	Nilesh B. Jadhav	124-126

27	Effect of Fe Dopant on Structural & Electrical Properties of Copper Oxide Nanoparticles	N. N. Gour A. P. Pinjarkar H. G. Wankhade P. R. Padole	127
28	Preliminary Phytochemical Studies of <i>Cesalpinia crista</i> L.	Nitin G. Asole Ramesh T. Parihar Anand S. Jadhao	128-131
29	Removal of Methylene Blue using <i>Cajanus Cajan</i> Activated Carbon	Vilayatkar N.D. Chaudhari D.L. Kadu N.S. Kurzekar R.R.	132-134
30	Conductometric Studies of [CPHDD] and [CTMBCD] at Different Molar Concentrations and Different Percentage Compositions in Water-Ethanol Mixture	K.P. Jumde Sanghapal S. Padhen Saleem R. Khan D.T. Tayade	135-140
31	Synthesis and Characterization of Some Substituted Chalcone by the Green Synthesis Way (Grinding Method)	Nilesh S. Padole Murlidhar P. Wadekar Shubhangi Y. Deshmukh Vinod M. Sherekar	141-144
32	In-Silico Prediction of Phytoconstituents From <i>Solanum Indicum</i> for Antiepileptic Activity	Pooja.P.Patle Parimal Katolkar Pradeep Raghatate Jagdish Baheti	145-156
33	Deep Discoveries in Chemistry: Unraveling the Mysteries at the Molecular Level	Dr. Prashant R. Mahalle	157-159
34	Synthesis, Characterization of (3-Chloro-benzylidene) – (4-Phenyl-thiazol-2-yl) amine and Studied their antioxidant Activity	Ghodile R.D Chaudhari P.S. Dharamkar R. R	160-164
35	Synthesis and Characterization of Schiff Bases Using Different Amines and their Biological Activities	Priyadarshani N Deshmukh	165-167
36	Physico-Chemical Assessment of Soil Sample in Jarud Region in Amravati District of Maharashtra (India)	Dr. Priyanka U. Belsare Ku Tejashri M. Ghotkar	168-171
37	Synthesis ,Characterization And Antimicrobial Study Of Co(II),Cu(II) and Fe(III) Complexes Of Substituted 4,4'-Dimethoxybenzoinhydrazones	P. M. Dahikar	172-175
38	Study of Extraction and Chemical Screening of <i>T. cordifolia</i> (Guduchi) Stem & Leaves	Ramesh Tukaram Parihar S A Quazi Shaikh Farah T	176-178

39	In-silico QSAR-based virtual screening recognition of novel anaphylactic lymphoma kinase inhibitor	Rahul D. Jawarkar Praveen Sharma Sachin Kumar Jain	179-196
40	Synthesis, characterization and biocidal study of some novel 2-hydroxy 4,6-disubstituted phenyl pyrimidines bearing 4-bromo phenol moiety	Rajendra M. Pathade Pravin. S. Bodkhe	197-203
41	Investigation of antimicrobial Activities of Dihydropyrazines	Manish Fukate Sheryil Malvilayils Roshan Jaiswal Swati Bawiskar	204-208
42	Synthesis and Spectral Characterization of Novel 1,2,4-Dithiazole Derivatives	Mr Ramdas N Ingole Dr Siddharth S Waghmare Dr Pravin S Bodkhe	209-211
43	Synthesis of Substituted Flavanones and their Impact on Seed Germinations	S. P. Rathod R.T.Parihar A.P.Mitake T.M.Bhagat S. B. Waghmare	212-215
44	Antimicrobial Resistance : A Global Challenge	Reshal Deshmukh	216-217
45	Wings across Reservoirs: Understanding and Safeguarding the Migration Patterns of Insectivorous Birds in Anthropogenic Landscapes	Dr. Chandrashekhar R. Kasar Ku. Revati Kishor Lonkar	218-222
46	Synthesis and Characterization of Pyrazolone and its derivatives	Mr. R. N. Gaikwad	223-225
47	Preliminary Phytochemical analysis of Leaves extract of the plant <i>Justicia Adhatoda</i>	Swapnil D. Bhagat Sopan D. Ingole Varun A. Mahale Nandkishor S. Thakare Chandrakant U. Dhanwad	226-229
48	<i>In-Silico</i> Prediction of Phytoconstituents From <i>Solanum Indicum</i> for Antistress Activity Targeting Ask 1 Inhibitor	Sakshi Mude Parimala Katolkar Pradeep Raghatate Jagdish Baheti	230-241
49	Design, Synthesis, Spectral Characterisation and Antibacterial Screening of Some Novel 4-Substitutedimino-1,3,5-Dithiazine Along With Pyrimidine Nucleus	S. B. Sarkate ^a S. A. Waghmare K. U. Dongare R. N. Ingole	242-245
50	Comparative Account of Partial Molar Volumes and Compressibilities of Aqueous-(L-Arginine + Glucose/Lactose) Solutions at 310.15 K	R. V. Dudhate H. N. Pawar B. R. Bhosle S. D. Deosarkar S. D. Deshmukh P. S. Bodkhe	246-249

51	Studies in the Synthesis of 5-(3-Substitutedthiocarbamido) Aminoindole by Microwave Technique	M. B. Shahakar R.D. Isankar P.V. Raut	250-254
52	Understanding the Role of Lipophilicity and Pharmacophore Elements in Pyrimidinedione based BCAT1 Inhibitory Activity	S. R. Deshmukh P.P. Nalawade V. H. Masand S. D. Thakur P. S. Navale	255-258
53	Use of Formic Acid as Co Surrogates in Palladium Catalyzed Carbonylation Reaction	Shoeb R. Khan Pratik E. P. Michael Mayur V. Khedkar	259-264
54	<i>In-Silico</i> Prediction of Phytoconstituents From <i>Solanum Indicum</i> for Antianxiety Activity	Shweta Dhole Parimal Katolkar Pradeep Raghatate Jagdish Baheti	265-275
55	Computational Insight on the Argentophilic Interactions of Axially Chiral Ag-NHC Complex of R-BINOL Scaffold via TD-DFT	Sonali Ramgopal Mahule	276-279
56	Agricultural Influence and application of Mn(III), Fe(III) and VO(IV) Schiff base metal Complexes	S. R. Kelode	280-283
57	Recent Applications of Deep Eutectic Solvent (DES), a Greener Media in Organic Synthesis	Suchita B. Wankhede	284-290
58	Synthesis, Characterization and Pharmacological Evaluation of Some New Functionalized Flavone Derivatives From B-Diketones	Sushil K. Pagariya Pravin S. Bodkhe	291-297
59	Design, Synthesis, Spectral Characterisation and Antibacterial Screening of Some Novel 4-Substitutedimino-1,3,5-Dithiazine Along With Pyrimidine Nucleus	S. B. Sarkate S. A. Waghmare K. U. Dongare R. N. Ingole	298-302
60	Colorimetric Phytochemical Analysis of <i>Tinospora Cordifolia</i> and FTIR Study of Its Medicinal Sample Giloy Ghanvati	Dr Swaroopa Rani N. Gupta	303-317
61	Determination of Hydrochloric Acid Neutralizing Capacity of Different Antacid Tablet by Back Titration Method and Its FTIR Analysis	Dr Swaroopa Rani N. Gupta	318-328
62	Investigation of Physico-chemical parameters of groundwater from Barshitakli tehsil region, Akola district, Maharashtra, India	Dr. S. S Deshmukh Dr. Tejas R. Patil	329-332

63	Identification of confluence of multiple scaffolds required for Aurora Kinase A inhibition	Vijay H. Masand S.D. Thakur M.M. Rathore	333-335
64	Synthesis, Characterization and Biological Evaluation of 4-(4-Bromo-1-Hydroxy Naphthalen-2-Yl)-6-(4-Hydroxy Phenyl)-5,6-Dihydropyrimidine-2(1h)-One	Dr. V. M. Sherekar Mr. Nilesh S. Padole	336-339
65	Efficient Synthesis of Salicylaldehyde-Based Schiff Bases Using Hydrothermal Sonication: A Green Approach	Vivek Ramkrushna Mate Datta Anandrao Patil Kalpana B. Gawande Sanjay R. Thakare Rajkumar Uddhavrao Pokalwal	340-345
66	Viscometric Technique for Evaluation of 1-Phenyl-3-[4-(2-Ethylimino-4-T-Butylimino-1,3,5-Dithiazino)Amino- Phenyl]Prop-2-Ene-1-One in Ethanol-Water Mixture	S.S. Padhen A.B. Wadekar	346-348
67	An Overview on Green Chemistry	Dr. Rupali.S. Talegaonkar	349-353
68	3D Printing Technology for development of Transdermal Drug Delivery Systems	Dr. Amar Deshpande Dr. Jagdish Baheti	354-358
69	<i>In-silico</i> Prediction of Phytoconstituents from <i>Hymenodictyon excelsum</i> for Antimalarial Activity Targeting Hypoxanthine-guanine phosphoribosyltransferase (HPRT1)	Parimal Katolkar Jagdish Baheti	359-372
70	Spectrophotometric Complexation Study of Cu(II) with 8-Hydroxyquinoline based Azo dye	Santosh M. Chavan Nilesh V. Rathod Manoj S. More Chandrakant D. Ghugare Ravi E. Khadse Jayshri S. Jadhao Akash V. Kubade Parikshit S. Thakare	373-377
71	A Comprehensive Review on Various Method of Synthesis and Biological Activities of Schiff Bases with Heterocyclic Moiety	Rahul P. Rahate	378-383
72	Revolutionizing Applications: A Comprehensive Review of Schiff Base Nanoparticles at the Nanoscopic Scale	S. R. Khandekar	384-389
73	Screening Of Antioxidant Property Present In Psidium Guajava Linn	V D Mane P P Mhasal	390-394

74	In-Silico Prediction of Phytoconstituents From Solanum Indicum for Antiepileptic Activity	Pooja P. Patle Parimal Katolkar Pradeep Raghatate Jagdish Baheti	395-405
75	Development and Characterization of Piroxicam Matrix Based Transdermal Patch	Pragati Hasbe Zohra Firdous M.S.A Pankaj Dhapke Jagdish Baheti	406-410
76	Analytical Method Development and Validation of Antidiabetic Drugs	Prajakta Sontakke Disha Dhabarde Jagdish Baheti	411-414
77	Synthesis of colloidal metal oxide using reverse micelle technique and its application in coupling reactions for Benzoxazole formation	Ramesh N. Zade Pravin S. Bodakhe Kishor B. Raulkar Bhupesh M. Mude	415-418
78	Synthesis, Characterization and Biological Evaluation of Coumarin – Chalcone Derivatives	Disha M. Dhabarde Punam B. Rathi Ashish Telrandhe	419-420
79	Synthesis and Characterization of (3-(3,5-dichloro-2-hydroxyphenyl)-5-(pyridin-2-yl) isoxazol -4-yl)(phenyl) methanone with microwave irradiation	P. S. Nandurkar M. M Rathore	451-424
80	Microbial Examination of Nanoparticle of Tetra-O-acetyl-B-D-Glucosyl-5aryl-4-Dithiobiurets	Ashish G. Sarap P.T. Agrawal	425-428
81	Synthesized PANI/Cu-NPs / Aloe-Vera thin films Biocomposites for ammine gas sensor stimulator	Dr. D. B. Dupare	429-435
82	Structural and Ion-Exchange Properties of Copolymer Derived from 4, 4'-Biphenol - Benzidine – Formaldehyde	P. P. Kalbende M. S. Dhore S. S. Butoliya	436-445
83	Navigating the Therapeutic Landscape: Discovery and Pharmacophore Modeling of BRD4 Inhibitors for Prostate Cancer Precision Treatment	Mr. P S. Nawale Ms. A D. Mehakare Dr. J R. Bansod Prof. Capt. M M. Rathore	446-451

.

Chemistry

1

QSAR evaluation of Glucagon Receptor (GCGR) antagonists for the anti-hyperglycaemic lead development

Ajaykumar Gandhi¹, Pooja Gaikwad¹, Jyoti Dahatonde¹, Archana Chapolikar^{1*}.

¹Department of Chemistry, Government College of Arts and Science, Aurangabad, Maharashtra, India, 431004
(achapolikar49@gmail.com , ppbhagile19@gmail.com, jyotidorge29@gmail.com, gascajay18@gmail.com)

*Correspondence: achapolikar49@gmail.com, Mobile Number- (+91)9657538276.

ABSTRACT: GA-MLR based QSAR evaluation has been effectuated on a small dataset of GCGR antagonists abide by OECD principles. Present study revealed some of the structural features such as minimum possible occurrence of -H₂CCH-, PhCH₂- moieties and more number of carbon atoms at topological distance of 10 from halogen(s) as crucial for better GCGR antagonistic activity. Developed QSAR model performed very well for all the approved statistical parameters such as, $R^2 = 0.90$, $Q^2_{\text{LOO}} = 0.87$, $Q^2_{\text{LMO}} = 0.82$, $Q^2_{\text{F}^n} = 0.86\text{--}0.92$, $\text{CCC}_{\text{ext}} = 0.93$. Applicability domain analysis and Y-randomization test also enhanced the credibility of this study.

KEYWORDS: QSAR, GCGR, hyperglycaemia

ABBREVIATIONS:

CADD- Computer Aided Drug Designing, **GCGR-** Glucagon Receptor, **GCGRA-** Glucagon Receptor Antagonist, **SMILES-** Simplified Molecular-Input Line-Entry System, **GA-** Genetic Algorithm, **MLR-** Multiple Linear Regression, **QSAR-** Quantitative Structure-Activity Relationship, **QSARINS-** QSAR Insurbria, **OECD-** Organization for Economic Co-operation and Development, **OFS-** Objective Feature Selection, **SFS-** Subjective Feature Selection

1. INTRODUCTION

A lifestyle induced metabolic disorder, Type 2 Diabetes Mellitus (T2DM) is the prevalent and ever escalating type of the diabetes, worldwide. To date, 463 million people have diabetes and an estimated global projection for diabetes is 578 million adults by 2030[1]. Cardiovascular discomfort, retinopathy, nephropathy are some of the health complications that are consequences of hyperglycaemia. Glucagon – a peptide hormone, known to elevate hepatic glucose production by stimulating gluconeogenesis and glycogenolysis and regulates blood glucose homeostasis collaboratively with insulin. In both, type 1 and type 2 diabetes, increase in glucagon level and/or insufficient glucagon suppression contribute to the hyperglycaemia. Glucagon Receptor (GCGR) antagonism emerged as a promising therapy to control hyperglycaemia. BAY 27-9955 was the first clinically approved GCGR antagonist. MK-357732, MK-0893, PF-06291874, LY- 2409021, and LGD-6972 under trial GCGR antagonist[2]–[5]. GCGR is a well-established target for glucagon suppression and hence further optimization of reported compounds may possibly suffice a better lead of desired anti-hyperglycemic potency with minimum and less serious side effects

Computer Aided Drug Designing (CADD)[6]–[8] being result oriented, time- and cost-efficient, and eco-friendly approach, is now an established drug discovery approach. QSAR—is a multidisciplinary approach wherein experimentally determined bio-activity of molecule is statistically correlated to its molecular features (expository QSAR) which further assist in an *in silico* bio-activity prediction (statistical QSAR)[9]–[11]. Expository QSAR intelligibly aligned with statistical QSAR provides better insights for the pharmacokinetics[12]–[19].

In the recent work, a QSAR model using dataset of 44 GCGRAs with experimentally determined GCGR binding activity is developed. Decidedly this model will assist synthetic organic chemists in the development of better GCGRA as anti-hyperglycemic lead.

2. MATERIALS AND METHODS

A. Selection of data-set:

A dataset of 44 Glucagon Receptor Antagonists (GCGRAs) with *in vitro* GCGR binding activity in terms of half-maximal inhibitory concentration (IC_{50}) ranging from 0.02 to 131.1 μM (converted to pIC_{50}) is used [20], [21]. The variation in GCGR binding activity with chemical features, illustrated using five least and five most active compounds (**Figure. 1**). The SMILES strings with reported IC_{50} and pIC_{50} values for all the GCGRAs are present in the Table S1 in the supplementary material. (A google drive for supplementary information provided at the end)

B. Molecular Structure Drawing and Optimization:

Free and open source software, ChemSketch 12 Freeware (www.acdlabs.com) is used to draw 2D structures and further conversion to 3D structures is achieved using OpenBabel 2.4.0. A geometry optimized molecule is characterized by its lowest energy i.e. most stable conformation. Geometry optimization ensures the normalization of all such a physico-chemical properties for all the molecules from dataset and makes it a necessarily important step prior to molecular descriptor calculation. As a step forward, force field MMFF94 available in TINKER is used for optimization of the molecules.

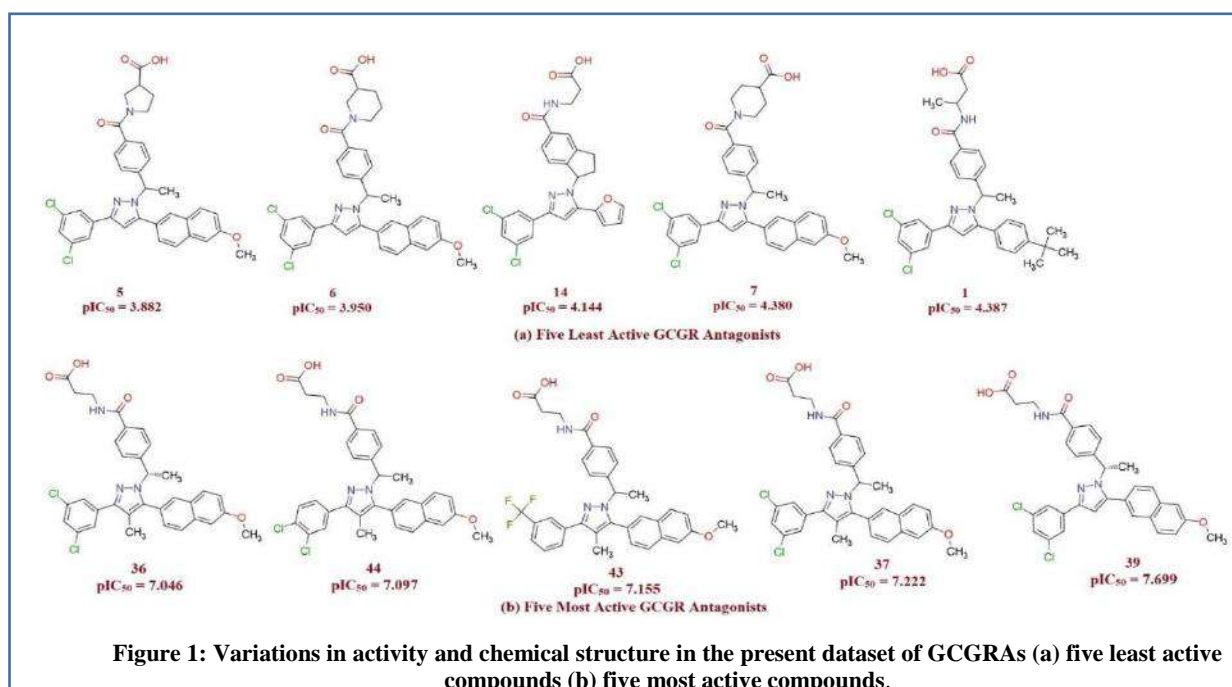


Figure 1: Variations in activity and chemical structure in the present dataset of GCGRAs (a) five least active compounds (b) five most active compounds.

C. Molecular Descriptor Calculation and Objective Feature Selection (OFS):

A molecular descriptor is a structural and physico-chemical property of a molecule or specific part of the molecule. More than 18,000 molecular descriptors were calculated for each molecule using PyDescriptor [22] and PaDEL [23]. In the data pruning step, Objective Feature Selection (OFS) in QSARINS v2.2.4 [24], [25] screened out multi-collinear and spurious molecular descriptors (i.e. with nearly constant values >95%, co-linearity $|R| > 0.95$) and contracted molecular descriptor pool with 1145 variables is generated. Contracted though, molecular descriptor pool has covered adequately comprehensive chemical space being comprised of 0D- to 3D- descriptors, structural, constitutional properties and charge descriptors etc.

D. Subjective Feature Selection, QSAR Model – Development and Validation:

In accordance with the OECD principles, firstly, apt variable selection method GA-MLR [26] in Subjective Feature Selection (SFS) operation in QSARINS v2.2.4 is used to perform simple and easy to interpret QSAR models. Then, all the derived models were subjected to the thorough

statistical validation, Y-scrambling and Applicability Domain analysis. The steps in QSAR building process:

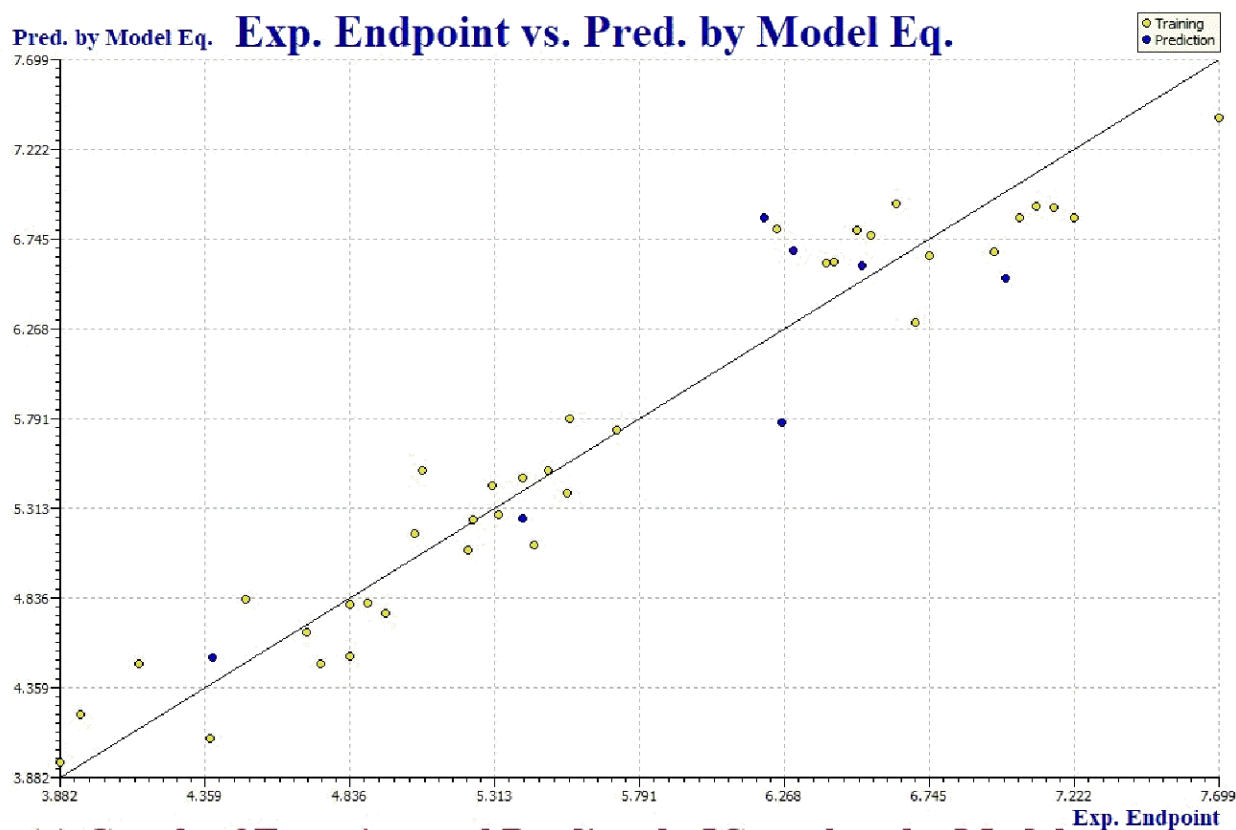
- I. Random split operation in QSARINS v2.2.4 split given dataset into a training set with 35 molecules (80%) and a prediction set with 9 molecules (20%) prediction. Molecules in training set were utilized for QSAR model development and external validation was performed on 9 molecules in prediction set.
- II. QSAR models were built using Subjective Feature Selection (SFS) operation in QSARINS v2.2.4 (at default settings) by setting Q^2_{LOO} as fitness function. Insignificant increase in Q^2_{LOO} value was observed after 5 variables and hence to avoid overfitting SFS operation is confined to 5 variables which additionally helped in deriving easy and informative QSAR models. (See supplementary information Table S2)
- III. (a) Leave-One-Out (LOO) and Leave-Many-Out (LMO) parameter based internal validation; (b) External validation; (c) Y-scrambling and model Applicability Domain (AD) analysis, performed for legitimate validation.
- IV. Performance of each model, measured by close inspection of the various statistical parameters meter the robustness of the GA-MLR based QSAR model. The QSAR model with best values of these parameters and with best predicative ability is selected.

3. RESULTS

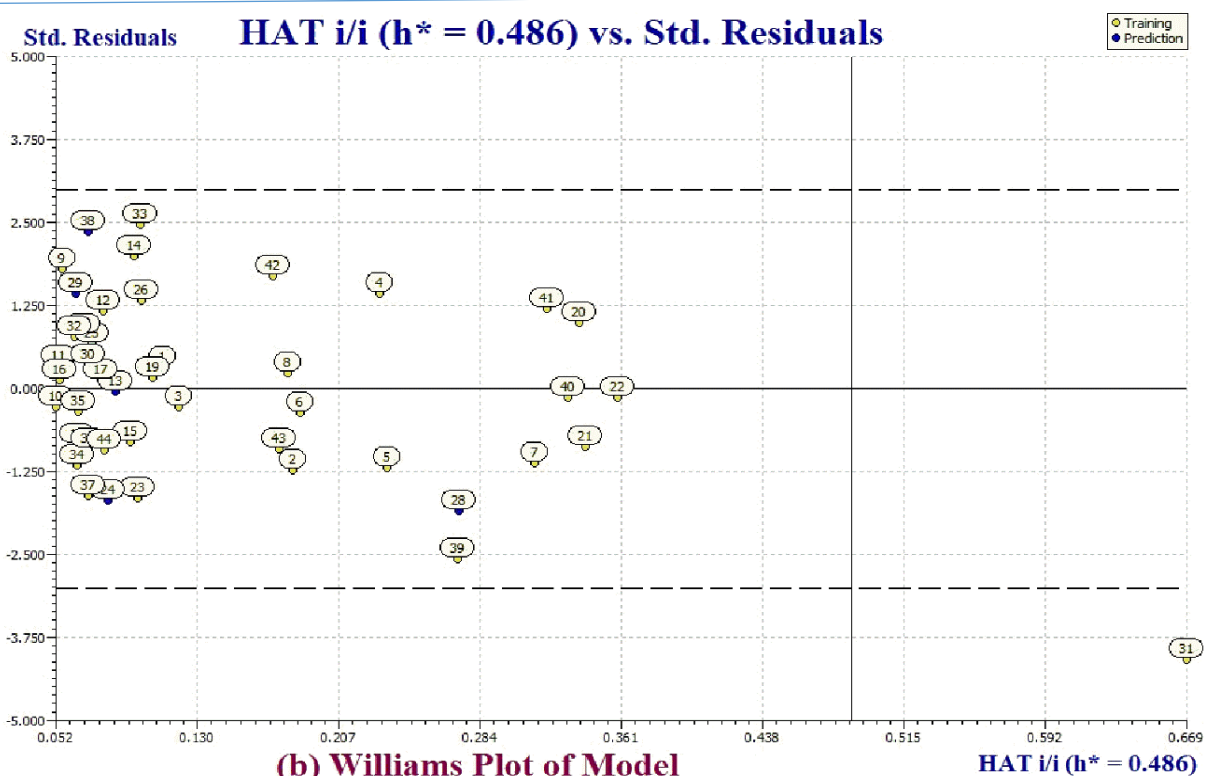
- Values of Fitting, Internal Validation, and External Validation are very well above the approved threshold values.
- The predictiveness of the generated QSAR model can be corroborated from **Figure 2a**.
- Moreover, Model applicability domain (AD) of the model is corroborated from Williams plot (Figure.2b).
- **QSAR Model** (Divided Set: Training Set-80% and Prediction Set-20%):

$$pIC_{50} = 7.941(\pm 1.078) - 0.148(\pm 0.068)H_{don_8B} - 1.594(\pm 0.204)KRFPC298 - 1.700(\pm 0.490)KRFPC582 + 0.106(\pm 0.047)APC2D10_C_X$$

$$[R^2 = 0.90, R^2_{adj} = 0.88, Q^2_{LOO} = 0.87, Q^2_{LMO} = 0.82, RMSE_{tr} = 0.25, MAE_{tr} = 0.25, RSS_{tr} = 3.86, CCC_{tr} = 0.95, s = 0.35, F = 70.22, RMSE_{cv} = 0.36, MAE_{cv} = 0.29, PRESS_{cv} = 4.80, CCC_{cv} = 0.93, R2_{ext} = 0.90, Q2-F1 = 0.88, Q2-F2 = 0.86, Q2-F3 = 0.92, CCC_{ext} = 0.93]$$
- Compounds 13, 40, 22, 17 and 16 with Predicted Models Equation Residual values in the range -0.012 to +0.032 are best predicted for their GCGR activity (pIC_{50}) in the present QSAR evaluation (Figure. 3).
- All these five compounds fall within Applicability Domain, as evident from William Plots (Figure. 2b). On the other hand, GCGR binding activity of Compound 31 is worst predicted for by the QSAR models and turned out as an outlier.



(a) Graph of Experimental Predicted pIC_{50} values by Model



(b) Williams Plot of Model

Figure 2: For QSAR Model (a) Graph of Experimental vs. Predicted pIC_{50} values (b) Williams plot.

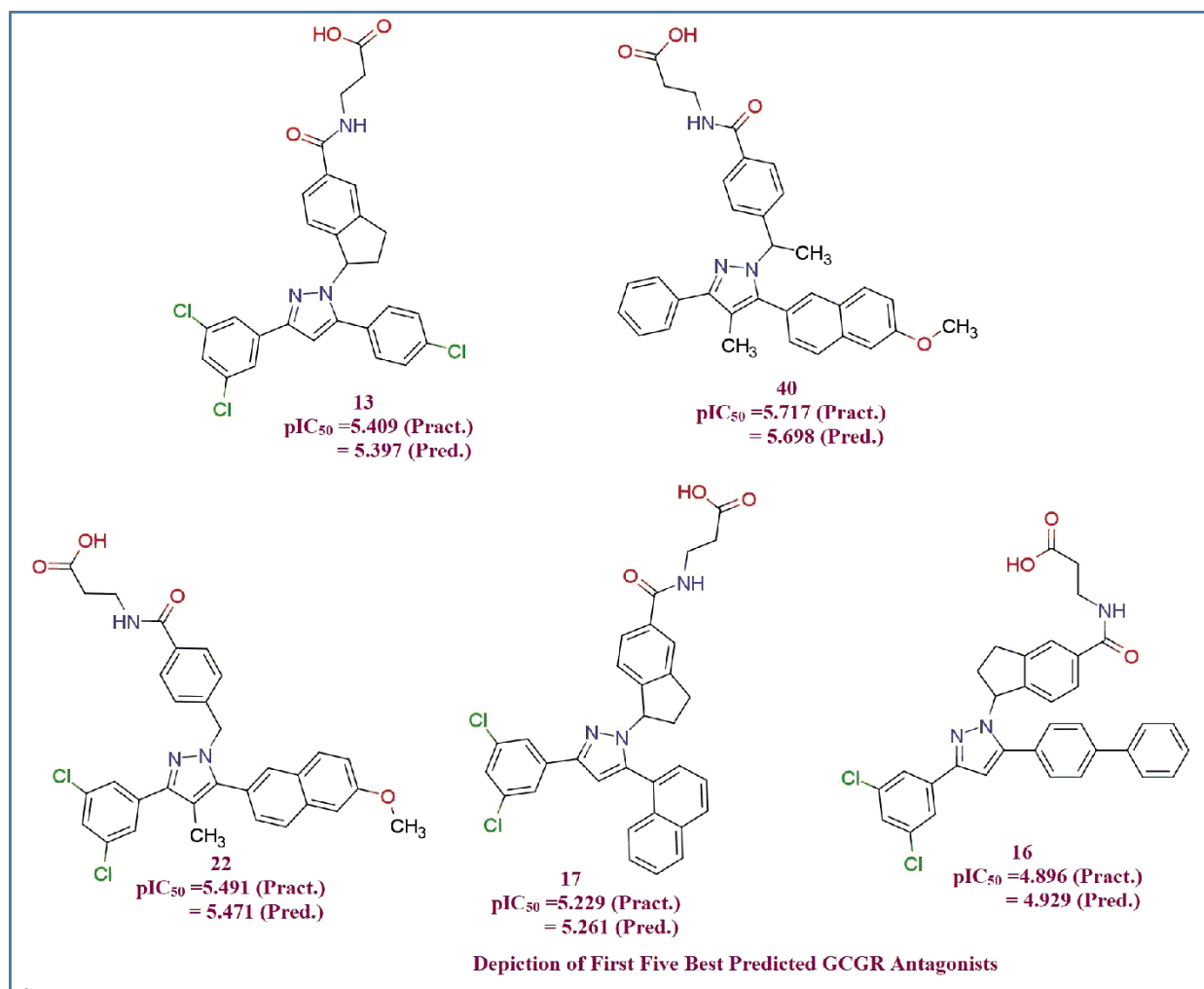


Figure 3: Depiction of first 5 Best Predicted Molecules

4. DISCUSSION

- H_don_8B (-VE correlation with GCGR binding potency) small possible number of Hydrogen atoms within 8 bonds from HBD atom is advisable for more potent GCGR antagonist
- KRFPC298 and of KRFPC582 8B (-VE correlation with GCGR binding potency) less frequent occurrence of H_2C-CH and of $PhCH_2-$ structural fragments, respectively are recommended for better GCGR binding potency.
- APC2D10_C_X (+VE correlation with GCGR binding potency) more frequent occurrence of Carbon at topological distance of 10 from any halogen is advocated by QSAR evaluation

5. CONCLUSIONS

Decidedly, a QSAR evaluation of a given series of compounds revealed some prominent structural/chemical traits that are responsible for the enhanced activity of the compound, such as minimum occurrence of $-H_2CCH-$ and $PhCH_2-$ structural fragments, and less possible number of hydrogen atoms within eight bonds from hydrogen bond donor atoms, and more number of Carbons at topological distance of ten from halogen(s) which revealed the scope for optimization of the lead for better GCGR binding potency. The QSAR model will assist in optimizing leads to better GCGR binding potency to curb hyperglycaemia and diabetes.

ACKNOWLEDGMENTS: The authors are thankful to Dr. Paola Gramatica and her team for providing QSARINS-v2.2.4 and developers of TINKER, ChemSketch 12 Freeware (ACD labs), and PyDescriptor for providing the free versions of their software.

REFERENCES:

- [1] IDF Diabetes Atlas 9th edition, "IDF Diabetes Atlas 9th edition 2019," 2019. Accessed: August 4, 2021. [Online]. Available: <https://diabetesatlas.org/en/>.
- [2] E. G. Vajda *et al.*, "Pharmacokinetics and pharmacodynamics of single and multiple doses of the glucagon receptor antagonist LGD-6972 in healthy subjects and subjects with type 2 diabetes mellitus," *Diabetes, Obes. Metab.*, vol. 19, no. 1, pp. 24–32, 2017, doi: 10.1111/dom.12752.
- [3] M. F. Sammons and E. C. Y. Lee, "Recent progress in the development of small-molecule glucagon receptor antagonists," *Bioorganic Med. Chem. Lett.*, vol. 25, no. 19, pp. 4057–4064, 2015, doi: 10.1016/j.bmcl.2015.07.092.
- [4] J. Z. Peng *et al.*, "A semi-mechanistic model for the effects of a novel glucagon receptor antagonist on glucagon and the interaction between glucose, glucagon, and insulin applied to adaptive phase ii design," *AAPS J.*, vol. 16, no. 6, pp. 1259–1270, 2014, doi: 10.1208/s12248-014-9648-x.
- [5] Y. Xiong *et al.*, "Discovery of a novel glucagon receptor antagonist N-[(4-[(1 S)-1-[3-(3, 5-dichlorophenyl)-5-(6-methoxynaphthalen-2-yl)-1 H -pyrazol-1-yl]ethyl}phenyl) carbonyl]-β-alanine (MK-0893) for the treatment of type II diabetes," *J. Med. Chem.*, vol. 55, no. 13, pp. 6137–6148, 2012, doi: 10.1021/jm300579z.
- [6] A. Baldi, "Computational approaches for drug design and discovery: An overview," *Syst. Rev. Pharm.*, vol. 1, no. 1, pp. 99–105, 2010, doi: 10.4103/0975-8453.59519.
- [7] A. Jain, "Computer aided drug design," *J. Phys. Conf. Ser.*, vol. 884, no. 1, 2017, doi: 10.1088/1742-6596/884/1/012072.
- [8] J. S. Smith, A. E. Roitberg, and O. Isayev, "Transforming Computational Drug Discovery with Machine Learning and AI," *ACS Med. Chem. Lett.*, vol. 9, no. 11, pp. 1065–1069, 2018, doi: 10.1021/acsmmedchemlett.8b00437.
- [9] "M.H. Baig, K. Ahmad, S. Roy, J.M. Ashraf, M. Adil, M.H. Siddiqui, S. Khan, M.A. Kamal, I. Provaznik, I. Choi, Computer aided drug design: success and limitations, *Curr. Pharmaceut. Des.* 22 (2016) 572–581."
- [10] S. Joy, Y. M. Vijayakumar, and G. Sunhye, "Role of computer-aided drug design in modern drug discovery," *Arch. Pharm. Res.*, 2015, doi: 10.1007/s12272-015-0640-5.
- [11] E. N. Muratov *et al.*, "QSAR without borders," *Chem. Soc. Rev.*, vol. 49, no. 11, pp. 3525–3564, 2020, doi: 10.1039/d0cs00098a.
- [12] A. Cherkasov *et al.*, "QSAR modeling: Where have you been? Where are you going to?," *J. Med. Chem.*, vol. 57, no. 12, pp. 4977–5010, 2014, doi: 10.1021/jm4004285.
- [13] T. Fujita and D. A. Winkler, "Understanding the Roles of the 'two QSARs,'" *J. Chem. Inf. Model.*, vol. 56, no. 2, pp. 269–274, 2016, doi: 10.1021/acs.jcim.5b00229.
- [14] J. Huang and X. Fan, "Why QSAR fails: An empirical evaluation using conventional computational approach," *Mol. Pharm.*, vol. 8, no. 2, pp. 600–608, 2011, doi: 10.1021/mp100423u.
- [15] N. Chirico and P. Gramatica, "Real external predictivity of QSAR models. Part 2. New intercomparable thresholds for different validation criteria and the need for scatter plot inspection," *J. Chem. Inf. Model.*, vol. 52, no. 8, pp. 2044–2058, 2012, doi: 10.1021/ci300084j.
- [16] P. Gramatica, S. Cassani, P. P. Roy, S. Kovarich, C. W. Yap, and E. Papa, "QSAR modeling is not 'Push a button and find a correlation': A case study of toxicity of (Benzo-)triazoles on Algae," *Mol. Inform.*, vol. 31, no. 11–12, pp. 817–835, 2012, doi: 10.1002/minf.201200075.
- [17] T. M. Martin *et al.*, "Does rational selection of training and test sets improve the outcome of QSAR modeling?," *J. Chem. Inf. Model.*, vol. 52, no. 10, pp. 2570–2578, 2012, doi: 10.1021/ci300338w.
- [18] V. H. Masand, D. T. Mahajan, G. M. Nazeruddin, T. Ben Hadda, V. Rastija, and A. M. Alfeefy, "Effect of information leakage and method of splitting (rational and random) on external predictive ability and behavior of different statistical parameters of QSAR model," *Med. Chem. Res.*, vol. 24, no. 3, pp. 1241–1264, Aug. 2015, doi: 10.1007/s00044-014-1193-8.

-
- [19] P. Gramatica, "On the development and validation of QSAR models," *Methods Mol. Biol.*, vol. 930, pp. 499–526, 2013, doi: 10.1007/978-1-62703-059-5_21.
- [20] S. Shu *et al.*, "A novel series of 4-methyl substituted pyrazole derivatives as potent glucagon receptor antagonists: Design, synthesis and evaluation of biological activities," *Bioorganic Med. Chem.*, vol. 26, no. 8, pp. 1896–1908, 2018, doi: 10.1016/j.bmc.2018.02.036.
- [21] S. Shu *et al.*, "Design, synthesis, structure-activity relationships, and docking studies of pyrazole-containing derivatives as a novel series of potent glucagon receptor antagonists," *Bioorganic Med. Chem.*, vol. 24, no. 12, pp. 2852–2863, 2016, doi: 10.1016/j.bmc.2016.04.053.
- [22] V. H. Masand and V. Rastija, "PyDescriptor: A new PyMOL plugin for calculating thousands of easily understandable molecular descriptors," *Chemom. Intell. Lab. Syst.*, vol. 169, pp. 12–18, Oct. 2017, doi: 10.1016/j.chemolab.2017.08.003.
- [23] A. Allouche, "Software News and Updates Gabedit — A Graphical User Interface for Computational Chemistry Softwares," *J. Comput. Chem.*, vol. 32, pp. 174–182, 2012, doi: 10.1002/jcc.
- [24] P. Gramatica, S. Cassani, and N. Chirico, "QSARINS-chem: Insubria datasets and new QSAR/QSPR models for environmental pollutants in QSARINS," *J. Comput. Chem.*, vol. 35, no. 13, pp. 1036–1044, May 2014, doi: 10.1002/jcc.23576.
- [25] P. Gramatica, N. Chirico, E. Papa, S. Cassani, and S. Kovarich, "QSARINS: A new software for the development, analysis, and validation of QSAR MLR models," *J. Comput. Chem.*, vol. 34, no. 24, pp. 2121–2132, Sep. 2013, doi: 10.1002/jcc.23361.
- [26] A. K. Saxena and P. Prathipati, "Comparison of MLR, PLS and GA-MLR in QSAR analysis," *SAR QSAR Environ. Res.*, vol. 14, no. 5–6, pp. 433–445, 2003, doi: 10.1080/10629360310001624015.
- [27] K. Roy, S. Kar, and P. Ambure, "On a simple approach for determining applicability domain of QSAR models," *Chemom. Intell. Lab. Syst.*, vol. 145, pp. 22–29, 2015, doi: 10.1016/j.chemolab.2015.04.013.
- [28] T. M. De Assis *et al.*, "QSAR Models Guided by Molecular Dynamics Applied to Human Glucokinase Activators," *Chem. Biol. Drug Des.*, vol. 87, no. 3, pp. 455–466, 2016, doi: 10.1111/cbdd.12683.
- [29] P. Gramatica, "Principles of QSAR models validation: Internal and external," *QSAR Comb. Sci.*, vol. 26, no. 5, pp. 694–701, 2007, doi: 10.1002/qsar.200610151.
- [30] A. Arwansyah, A. R. Arif, G. Syahputra, S. Sukarti, and I. Kurniawan, "Theoretical studies of Thiazolyl-Pyrazoline derivatives as promising drugs against malaria by QSAR modelling combined with molecular docking and molecular dynamics simulation," <https://doi.org/10.1080/08927022.2021.1935926>, 2021, doi: 10.1080/08927022.2021.1935926.

2

Synthesis and Biological Evaluation of Pyrazole Derivative**¹A P Thakare & ²S R Kolteke**¹Department of Chemistry, Rajarshree Shahu Science College, Chandur Rly²Mahatma Fule Arts, Commerce & Sitaramji Chaudhari Science College, Warud

Email- anmol21086@gmail.com

Abstract:

Pyrazole, a five-membered heterocycle containing two nitrogen atoms, is extensively found as a core framework in a huge library of heterocyclic compounds that envelops promising agro-chemical, fluorescent and biological potencies. Attributed to its several potential applications, there is a rise in the significance of designing new pyrazoles. The current study presents the synthesis of pyrazole derivatives by the reaction of chalcones with aryl hydrazine hydrochlorides in acetic acid (30%) under reflux conditions in good yields. Structures of synthesized new pyrazoles were confirmed by spectral studies.

Biological activity of all the synthesized compounds was checked against gram positive and gram negative bacteria. It has been found that all compounds shows good antimicrobial activity.

Introduction:

Heterocyclic compounds are a highly valuable and unique class of compounds. These compounds demonstrate a broad spectrum of physical, chemical and biological characteristics. Amongst heterocyclic compounds, nitrogen-containing heterocycles are extensively found as a core framework in a huge library of heterocycles and show several employments in natural science and other areas of science. Additionally, nitrogen-containing heterocycles have striking structural features and they are widely observed in natural products, for instance, vitamins, hormones and alkaloids.

Chalcones are the principal precursors for the synthesis of bioactive small molecules such as benzothiazepines, pyrazolines, isoxazolines, cyclopropanes, oxadiazoles, etc., The chalcones are most commonly synthesized via Claisen-Schmidt reaction of an aromatic aldehyde with acetophenones. Chalcones has gained importance due to their simple structures and diverse pharmacological applications. Design and synthesis of simple heterocycles with various bioactivities is a worthwhile contribution in organic synthesis. The compounds with thiophene are the most important class in active pharmaceutical drugs and remain the choice for anti-inflammatory agents in spite of multiple attempts at exploring alternative scaffolds. [1-5]

II. EXPERIMENTAL

All melting points were determined in open glass capillaries and are uncorrected. The IR spectra were recorded on KBr disc using Perkin Elmer-1800 intrachord. ¹HNMR and ¹³C NMR spectra were recorded in CDCl₃ on Bruker Avance 400MHz spectrophotometer with TMS as internal standard (chemical shifts are expressed in δ ppm). The mass spectra were recorded on a Joel SX-102 (EI/CI/FAB) mass spectrometer at 70 eV. The reactions were monitored by the TLC on silica gel G plates in the solvent system benzene-methanol mixture (9:1). All reagents were purchased from commercial suppliers and used without further purification. The compound includes 2-hydroxy-4-methylacetophenone, benzaldehyde, p-chloro benzaldehyde, anisaldehyde, 4-methyl benzaldehyde.

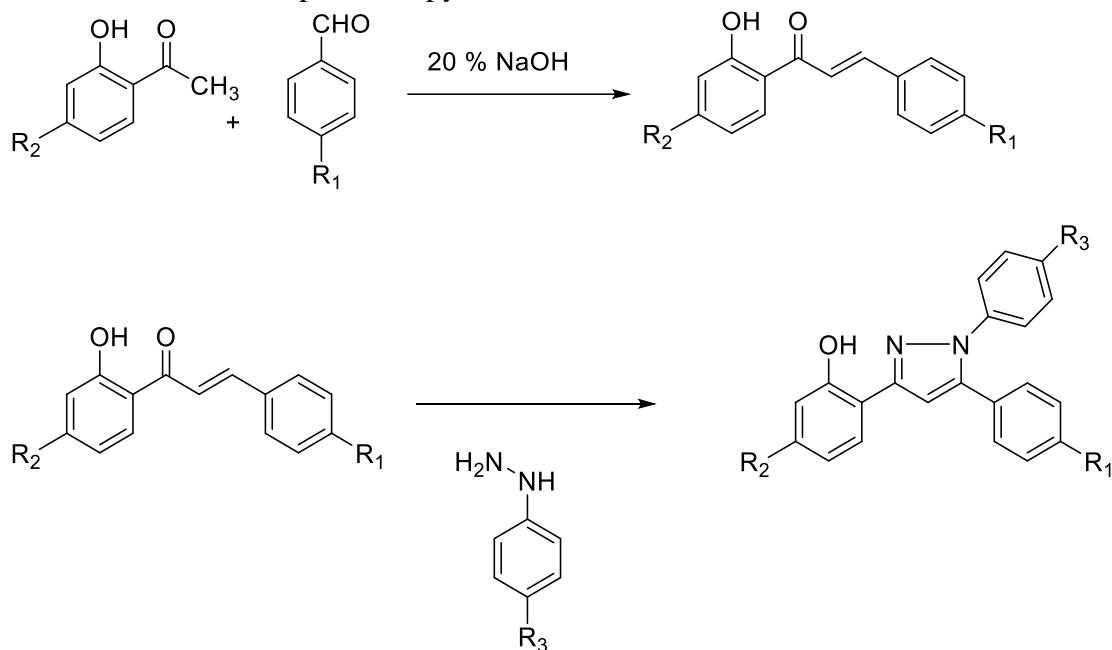
Synthesis of chalcone:

A mixture of 0.01 mol 2-hydroxy-4- methylacetophenone and 0.01 mol various aldehyde added into ethanol solvent. To this reaction mixture 20 % NaOH added and heated for several minutes

upto formation of solid residue. By keeping overnight residue neutralized by ice cold HCl solution, filtered and dried in oven.

Synthesis of Pyrazole:

A mixture of synthesized chalcone and aryl hydrazine hydrochloride in aqueous acetic acid under reflux condition produced pyrazole derivative.



Result & Discussion:

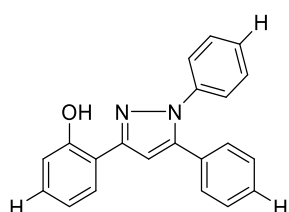
Sr No	Compounds	R ₁	R ₂	R ₃
1	2-(1,5-diphenyl-1H-pyrazol-3-yl)phenol	H	H	H
2	2-(1-phenyl-5-(p-tolyl)-1H-pyrazol-3-yl)phenol	CH ₃	H	H
3	2-(5-(4-chlorophenyl)-1-phenyl-1H-pyrazol-3-yl)phenol	Cl	H	H
4	2-(5-(4-methoxyphenyl)-1-phenyl-1H-pyrazol-3-yl)phenol	OMe	H	H
5	2-(5-(4-methoxyphenyl)-1-phenyl-1H-pyrazol-3-yl)-5-methylphenol	OMe	CH ₃	H
6	2-(5-(4-chlorophenyl)-1-phenyl-1H-pyrazol-3-yl)-5-methylphenol	Cl	CH ₃	H
7	5-methyl-2-(1-phenyl-5-(p-tolyl)-1H-pyrazol-3-yl)phenol	CH ₃	CH ₃	H

Table: Analytical Data of Synthesized Compounds

Sr No	Molecular formula	M.P. (°C)	Yield (%)	C %	H %	N %
1	C ₂₁ H ₁₆ N ₂ O	112	84	80.75	5.16	8.97

2	$C_{22}H_{18}N_2O$	119	78	80.96	5.56	8.58
3	$C_{21}H_{15}ClN_2O$	110	76	72.73	4.36	8.08
4	$C_{22}H_{18}N_2O_2$	123	81	77.17	5.30	8.18
5	$C_{23}H_{20}N_2O_2$	121	84	77.51	5.66	7.86
6	$C_{22}H_{17}ClN_2O$	120	80	73.23	4.75	7.76
7	$C_{23}H_{20}N_2O$	105	88	81.15	5.92	8.23

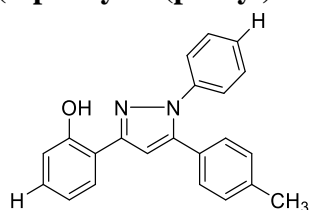
1) 2-(1,5-diphenyl-1H-pyrazol-3-yl)phenol



IR (KBr) ν : 3059(Ar C-H), 3345 (O-H), 1330 (C-N), 1226 (C-O).

1H -NMR (400 MHz, $CDCl_3$) δ (ppm) 7.05 (s, 1H, OH), 7- 8.26 (m, 14H, Ar)

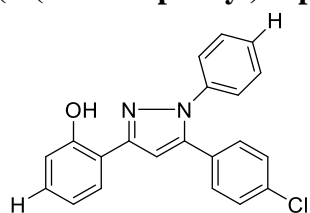
2) 2-(1-phenyl-5-(p-tolyl)-1H-pyrazol-3-yl)phenol



IR (KBr) ν : 3059(Ar C-H), 3345 (O-H), 2990 (aliphatic C-H), 1328 (C-N), 1226 (C-O).

1H -NMR (400 MHz, $CDCl_3$) δ (ppm) 7.05 (s, 1H, OH), 7- 8.26 (m, 13H, Ar), 2.34 (s, 3H, CH_3)

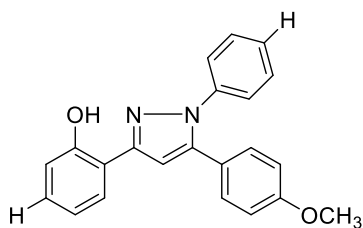
3) 2-(5-(4-chlorophenyl)-1-phenyl-1H-pyrazol-3-yl)phenol



IR (KBr) ν : 3059(Ar C-H), 3345 (O-H), 2990 (aliphatic C-H), 1328 (C-N), 1226 (C-O).

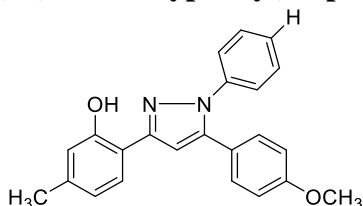
1H -NMR (400 MHz, $CDCl_3$) δ (ppm) 7.02 (s, 1H, OH), 7- 8.26 (m, 13H, Ar)

4) 2-(5-(4-methoxyphenyl)-1-phenyl-1H-pyrazol-3-yl)phenol



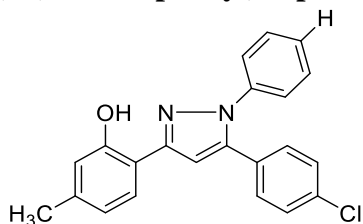
IR (KBr) ν : 3059(Ar C-H), 3345 (O-H), 2990 (aliphatic C-H), 1328 (C-N), 1226 (C-O).
 $^1\text{H-NMR}$ (400 MHz, CDCl_3) δ (ppm) 7.02 (s, 1H, OH), 7- 8.26 (m, 13H, Ar), 3.81 (s, 3H, OCH_3)

5) 2-(5-(4-methoxyphenyl)-1-phenyl-1H-pyrazol-3-yl)-5-methylphenol



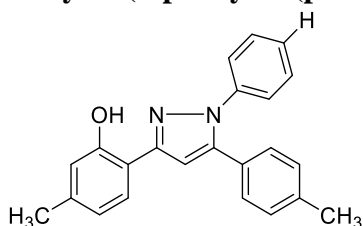
IR (KBr) ν : 3059(Ar C-H), 3345 (O-H), 2990 (aliphatic C-H), 1328 (C-N), 1226 (C-O).
 $^1\text{H-NMR}$ (400 MHz, CDCl_3) δ (ppm) 7.02 (s, 1H, OH), 7- 8.26 (m, 12H, Ar), 3.81 (s, 3H, OCH_3), 2.28 (s, 3H, CH_3)

6) 2-(5-(4-chlorophenyl)-1-phenyl-1H-pyrazol-3-yl)-5-methylphenol



IR (KBr) ν : 3059(Ar C-H), 3345 (O-H), 2990 (aliphatic C-H), 1328 (C-N), 1226 (C-O).
 $^1\text{H-NMR}$ (400 MHz, CDCl_3) δ (ppm) 7.02 (s, 1H, OH), 7- 8.26 (m, 12H, Ar), 2.28 (s, 3H, CH_3)

7) 5-methyl-2-(1-phenyl-5-(p-tolyl)-1H-pyrazol-3-yl)phenol



IR (KBr) ν : 3059(Ar C-H), 3345 (O-H), 2990 (aliphatic C-H), 1328 (C-N), 1226 (C-O).
 $^1\text{H-NMR}$ (400 MHz, CDCl_3) δ (ppm) 7.02 (s, 1H, OH), 6.89- 7.55 (m, 12H, Ar), 2.28 (s, 3H, CH_3)

Biological Activity

Compounds were screened for their antibacterial and antifungal activity using cup-plate agar diffusion method at a concentration of 40 mg, using Gram positive bacterial strains such as *B. cocous* and *B.subtillus* and Gram negative bacterium strain such as *Proteus vulgaris* and *Escherichia coli*. The antifungal testing was carried out against *Aspergillus niger*. Known antibiotics like Amoxycillin, Benzoylpenicillin, Ciprofloxacin, Erythromycin, and antifungal activity was compared with Greseofulvin. The zone of inhibition measured in mm. By

visualizing the antimicrobial data, it could be observed that most of the compounds exhibited significant activity.

References:

1. Manjunath B.C., Manjula M., Raghavendra K.R., Ajay Kumar K., Lokanath N.K. (2014) 4-(Thiophen2-yl)-2-[4-(trifluoromethyl)-phenyl]-2,3-dihydro-1,5-benzothiazepine. *Acta Cryst. Sect. E*, 70 (Part 3).
2. Kumar G.V., Govindaraju M., Renuka N., Khatoon B.B.A., Mylarappa B.N., Kumar K.A. (2012) Synthesis of 1,3,5-triaryl-4,6-dioxo-pyrrolo[3,4-d]-7,8-dihydropyrzoles and their antimicrobial and antioxidant activity. *Rasayan J. Chem.* 5 (3) 338–342.
3. Ajay Kumar K., Govindaraju M., Vasantha Kumar G. (2010) Synthesis of isoxazoles via 1,3-dipolar cycloaddition reactions and their antimicrobial activity. *Ind. J. Heterocycl. Chem.* 20 (4) 183-184.
4. Ajay Kumar K., Lokanatha Rai K.M., Vasanth Kumar G., Mylarappa B.N. (2012) A facile route for the synthesis of ethyl N-aryl-2,6-dioxo-piperid-3-ene-4-carboxylates and their biological activity. *Int. J. Pharm. Pharm. Sci.* 4 (Suppl 4) 564-568.
5. Ajay Kumar K., Lokanatha Rai K.M. (2004) Synthesis and evaluation of antimicrobial activity of 4,5-dihydro-12,4-oxadiazoles, *Bulg. Chem. Commun.* 36 (4) 249-252.
6. Chikulla, K V. Raja, S. Isoxazole-A Potent Pharmacophore, *I. J. of Pharmacy and Pharmaceutical Sci.*, 9(7): 13-24.
7. Jyothi, A N. Poojitha, J. Raju, G N. Nadendla, R R. Potential activities of isoxazole derivatives, *World J. of Pharmaceutical Research.* 4(12): 667-679.
8. Dou, G. Xu, P. Li, Q. Xi, Y. Huang, Z. Shi, D. 2013. Clean and Efficient Synthesis of Isoxazole Derivatives in Aqueous Media, *Molecules*, 18: 13645–13653.

3

Healthy hydroponic cattle feed (grass) development eco-friendly & economically**Dr. Ramesh Tukaram Parihar, Dr A.G.Gaddamwar***

Department of chemistry, Vidnyan Mahavidyalaya Malkapur, Dist-Buldhana, Affiliated to Sant Gadge Baba Amravati University Amravati, Maharashtra, India

Department of chemistry, Amolakchand Mahavidyalaya Yavatmal, Dist-Yavatmal, Affiliated to Sant Gadge Baba Amravati University Amravati, Maharashtra, India

Abstract

Dairy cattle require green fodder for high milk yield. However, it cannot available throughout the year and in some area, it is difficult to have access for green fodder. Thus, hydroponic fodder production has become an alternative way to fulfil this green fodder requirement of the dairy cow in low cost. According to WHO the production of milk in the India is 14 crore litres, but the consumption is 64 crore litres. It is being claimed that 68.7 percent of the milk and its products sold in the country are adulterated. In the US, the average dairy cow produces more than 7.5 gallons of milk per day and India's milk processing capacity is 126 million litres per day, the highest in the world, and lauded the dairy sector for increasing production from 22 MMT, or around 6 crore litres per day in 1977, to 58 crore litres per day in 2022. The adoption of this technique has enabled the production of fresh forage from grains without soil. Hydroponic fodder has high nutritive value due to the conversion of complex compounds into simpler and essential form, and activation of enzymes during germination. Thus, it contains high protein, vitamins and minerals which are essential for dairy cows. There were improvements in digestibility and intake of nutrients results in increased milk yields and quality like milk fat of dairy cow on the feeding of hydroponic fodder. Traditional fodder production has a number of limitations regarding soil & climatic conditions. In successful mulch animal rearing green fodder has its special significance.

Keywords: Hydroponics, Eco-friendly, Economics, nutritional value, Amino Acid.**Introduction**

The word hydroponics has been derived from the Greek word "water working". Hydro means "water" and phonic means "working" and it is a technology of sprouting grains or growing plants without soil, but only with water or nutrient rich solution. However, hydroponics fodder can be well produced with the use of fresh water only It is one of the most important agricultural techniques currently in use for green forage production in many countries especially in arid and semi-arid regions environmentally control houses. The population of Dairy livestock has increased immensely in our country, but still it is unable to fulfil the required milk Demand that we need to import it. Dairy cattle require green fodder for being healthy and higher Milk yield. The facts that deficiency of feed and fodder alone Account nearly 50 percent losses in livestock. To overcome these hydroponic cattle feed cultivation is introduced. Hydroponics fodder production has two aspects i.e. Physiology and nutrition of plant-animal system and Engineering of hydroponic technology. Hydrophobic is the science of soilless growing of plants in Nutrient rich solutions at regulated temperature and humidity. The main problems of feed scarcity emanate from land scarcity; actually, rapid urbanization is the major cause behind the decrease in land meant for grazing and fodder cultivation. With Water, labour shortage and elevated cost of fertilizers the farmer leans to cultivate commercial food crops over green fodder. Nevertheless, producing green fodder to meet the current demand has become a greatest

challenge among livestock farmers. In fact, green fodder is very important for productive and reproductive performance of animals.

Feeding green fodder can improve livestock products. Livestock production in most regions is limited due to poor production and pricy imported green fodder. Today, land scarcity presents an important limit towards forage production for animal especially sheep, goats and cattle. Unlike monogastric mammals, ruminant cannot solely dependent on cereal grains. That's why, alternative technologies, such hydroponics, are regarded as vital to face these issues. The use of this technology can help improve the long-term economic development of the livestock industry. Hydroponic fodder can also improve the performance of the animals by providing their nutrient needs. Hydroponic growing green fodder has high feed quality, rich with proteins, fibres, vitamins, and minerals effects on animals. The growth of the fodder crop mainly depends on moisture, temperature, RH and irrigation. Hydroponic Green fodder is the natural diet for livestock. Hydroponic green fodder consists of grass with grains, roots, stems and leaves which are highly nutritious and provide sustainable fodder production and conserve water take 8 days to develop seed to green fodder. It's production to meet current demand has become a greatest challenge among livestock farmers, due to temperature, humidity and contamination on the seed and fodder are restrict the optimum growth of fodder. Amount of yield and quality of fodder is influenced by grain quality, grain variety and treatments and growing environmental. Green fodder production crisis serious problems which are contamination of seeds that effect germination, and plant growth. This contamination further takes to fungus and mould infection which are not healthy for livestock animals. Temperature, relative humidity is also parameter to increase and decrease the fungus and mould infection. Hydroponic farming means growing of plants without soil by using nutrients water at desired temperature and humidity. Through hydroponics it is easy and quick to produce nutritive green fodder. Green fodder is the natural diet for livestock. Its production to meet the current demand has become a greatest challenge among livestock farmers. Due to many reasons, green fodder production has been facing a serious crisis and so the livestock productivity. Due to increasing intensive system of rearing livestock, the need for green fodder is enormous .As the gap between the demand and supply of the green fodder for livestock becoming unconquerable, researchers and farmers are in search for an alternative fodder or fodder production method, that would restore fodder and livestock production.

Hydroponics is the state of the art technology that has revolutionised the green fodder production in the 21st century. Hydroponics is a method of growing green fodder without soil in an environmentally controlled houses or machines. Many of the livestock farmers are switching to hydroponic fodder production from conventional production methods, as the fodder produced by this method are highly nutritious, provide sustainable fodder production round the year and conserve water. Though this method has made a greatest impact in the fodder production system, most of the farmers are facing some practical difficulties in profitably running the hydroponic machine for sustainable fodder production. This manual has been compiled with the essential manage mental practices that have to be carried out for an economically sustainable fodder production. Green fodder plays major role in feed of all livestock. Also, into the milch animals, Green fodder providing required nutrients for milk production and health of the dairy animals. Green fodder feeding to livestock is important for optimization of productivity. Animals Feeding and fodder production are the two important aspects for the sustainability of products and productivity in animal rearing. Although, India is the top producer of milk in the world But there are many challenges insufficient livestock feed, fodder is one of the constraints Affecting growth, health, production and reproduction potential of livestock. Green fodder is the natural diet for livestock. Its production to meet the current demand has become a greatest Challenge among livestock farmers. Due to many reasons, green

fodder production has been Facing a serious crisis and so the livestock productivity. Due to increased population day by Day hence agriculture land is converted into urbanization. Now days small land holdings Amongst farmers, non-availability of irrigated lands for fodder production is reduced, Unavailability of fertile land for fodder production, increasing mining and coastal line has Limited area for fodder production, deforestation, lack of scientific knowledge of feed and Fodder production among unemployed youths for fodder farming, higher labour cost and Small land holdings has left livestock as well as dairy farmer with many challenges for Animal rearing and milk production in all over the world. Also, due to increasing intensive System of rearing livestock, the need for green fodder is huge. To overcome all these shortage Issue of green fodder the new hydroponics technology came into exist. Hydroponics is the state-of-the-art technology that has revolutionised the green fodder production in the 21st century. In India only 4.9% of cropped land area is utilized for cultivating fodder. Indian livestock industry faces a deficit of 35.6% green fodder, 26% of dry fodder and 41% of concentrate feed ingredients.

Problem statement

A suitable combination of green & dry fodder is Very important for maintaining animal health& milk production. But in Scarcity condition traditional green fodder production become impossible Because of lack of irrigation water. In such condition the technique of Green fodder production by Hydroponic method is very useful tool. This technique does not require soil. Hence limitations like Saline soil, inferior soil, water logged soil etc can be easily overcome. This Technique requires very less quantity of water. Hence it can be easily undertaken in scarcity affected areas. Green fodder is the natural diet of cattle. Green fodder is the most Viable method to not only enhance milk production, but to also bring about A qualitative change in the milk produced by enhancing the content of Unsaturated fat,, Omega 3 fatty acids , vitamins, minerals and carotenoids. Hydroponics fodder growing is the state-of-the-art technological Intervention to supplement the available normal green fodder resources required by the dairy cattle. The contamination was starts from the seeds. When seeds were soaking for 24 hours in water there was problem of fermentation and because of that the fermented odour take place to the seeds which are resulted the fungus infection. After soaking the seeds, the seeds were placed into gunny bags at dark rooms for sprouting this resulted increase in fermentation odour. Sprouted seeds when placed into the hydroponic or office tray water sprayed to the seeds were for 2 minutes which are 1liter/min and because of that the maize seeds had higher amount of water which are not suitable for fodder and the water are not well drained from the trays this causes increase in fungus infection. Uncontrolled environment was also helping to increasing the fungus infection if there is temperature is greater than 35 °c and humidity higher than 70 to 80 % the fungus and mould infection were increases.

Materials and Method/procedures

Hydroponics fodder unit is nothing but a chamber with arrangement of temperature, humidity and light intensity for maximum sprouting & growth of fodder crop seeds (mainly maize, oat, barley, wheat etc). With 30 to 35 °C temperature, 60 to 75 % R humidity and 50 % shed 1 Kg of maize should yield 6 to 8 Kg green fodder in 7 to 9 days. It found that for 6-8 times mass increase around 2 litre water is sufficient per kg of seeds during summer season. So by this one can grow very good, healthy & economical viable fodder for dairy / goat farming. (We suggest to calculate economic output of system at your end based on input seed cost) There are plenty of manufacturer suppliers of hydroponics systems in market but farmers can build their own system as it's very easy to fabricate & all components available in market.

Following are required components with their specifications -

System components – Growing cabinet, Racks for trays, trays, seeds, watering system (fogger / mister / drip pipes) , timer, motor. (Photo look like are given below)

Growing cabinet – Square shape cabinet is most suitable & easy to fabricate , cabinet size can vary based on number of trays , cabinet can be fabricated with mild steel pipes (MS) , UPVC or bamboo. Just make square box and trays arrangement. Slotted angle racks can also be serve purpose. Cabinet need to be covered with 50 % green shed net and/or poly house covering film for reducing light intensity & conserves humidity.

Racks for trays – Can be of MS, UPVC or bamboo. Height of the tray racks need to be arranged as per day cycle of fodder i.e lower level 2 racks with 6 inch , above 2-3 racks on 8 to 12 inch and upper level racks 12 to 15 inch height. A gentle slope is beneficial for avoiding water lodging and fungal growth.

Trays – Various kind of trays are available in market based on quality of plastic & durability, specialized hydroponics trays are costly (2 feet * 2 feet tray cost approx. Rs.350) . We can use simple office tray (1.5 feet *1 feet) with perforations at bottom (simply drill holes on equal distance). Make sure there are sufficient holes made to avoid any kind of water lodging and avoid fungal infection. After every use, tray need to be disinfected by diluted hydrogen peroxide and sun drying.

Seeds – Maize, wheat, oat, barely suits best for hydroponics. You can choose based on availability and rate per unit. Seed should be free from any fungal infection. To remove broken seed, give brine water treatment and remove floating seeds. Soak seed further hours in potassium permanent. Once seeds sprouted 2 treatments of powder trichoderma Species will also help in lowering fungal Infection. Seed rate of 0.5 Kg / Ft² is sufficient for hydroponics fodder cultivation.

Watering system – Motor pump of 0.25 or 0.5 Hp is sufficient for 100 tray system. For lesser Capacity, minimum 0.25 Horse power motor will be required for operating fogger / misters. We prefer Jain Irrigation misters than foggers as they required less pressure & easy for maintains. Drip line – regular 16 mm HDEP drip line is best suited.

Timer – Various timers available in market. Timer best suited are generally 1 to 2 min operation Every / hour. We prefer Frontier TM-619-H-2 with 17 time intervals. If motor pump is above 3 Amp Additional really is preferable.

Engineering Aspects of Hydroponic Technology – Research in the following areas of engineering and machinery development will help in making the system more acceptable to the farmers.

Reservoir Engineering and Nutrient Solutions- The reservoir is the part of the hydroponic System that holds the nutrient solution. Depending on the type of hydroponic system, the Nutrient solution can be pumped from the reservoir up to the growing chamber (root zone) in cycles using a timer, as well as continually without a timer. Reservoir can be made out Of materials including the plastic that can hold water. Nutrient solutions can be developed separately for hydroponic fodder crop and sprouted grain crop.

Delivery System-The delivery of the hydroponic system's nutrient solution/water can be customized as per local needs.

Submersible Pump- Most hydroponic systems use a submersible pump to pump water/ Nutrient solution from the reservoir up to the growing chamber/root zone of the plants.

Air Pump- Other than in water culture systems, air pumps are optional in hydroponic Systems. However, using them has benefits. It helps to increase dissolved oxygen levels in the water up and keep the water oxygenated. This helps in keeping the nutrients evenly mixed all the time.

Grow Lights- Grow lights are optional part of hydroponic systems. One can choose to either Use natural sunlight or artificial light to grow the plants depending on the place of operation of the hydroponic system. These are generally used in commercial hydroponic systems for Growing fruits, vegetables and flowers.

Conclusion:

High initial investment on fully automated commercial hydroponic systems and high labour and energy costs in maintaining the desired environment in the system adds substantially to the net cost of hydroponic fodder production. Such systems are not successful in developing countries. Conversely, low cost hydroponic systems have been developed by utilizing locally available infrastructure where there is an acute shortage of fodder and water; local irrigation systems are not well established; transportation and fuel costs are high; and seasonal variations of fodder prices are extreme. Typical lean periods of fodder production are the norm, investment in controlling temperature and humidity are low, and so is the cost of labour. Under such situations the cost structure is often shifted in favour of hydroponic fodder production, and it may find a niche in increasing livestock production. Hydroponics fodder is nutritious, palatable and digestible and can be grown in low cost techniques with locally home grown grains. Against impending climate change and less availability land hydroponics fodder production is an effective alternative technology for sustainable livestock production in different agro climatic regions of India. The use of hydroponic culture modified the chemical composition of milk with respect to fat content, which is a desirable parameter. Moreover, principal component analysis revealed that with respect to proximate analysis, the quality of milk from cows from the GZ farm was superior to that of cows from the MT farm. The difference between minerals in the two farms may not be easily interpreted as the environment plays an important role, particularly with contaminants in the air, water, and soil. Further studies are needed to establish the effects of long-term feeding with different types of hydroponic fodder and to investigate the effects of these hydroponic fodders on the productive and reproductive performance of dairy cows. Further studies may be directed towards the development of feeding strategies with respect to the inclusion of hydroponic fodder under different agro climatic conditions. The challenges of Hydroponic fodder-cum-sprouted grain technology are enormous in producing quality green feed and fodder, and using it for value addition of products, such as milk rich in CLA, Omega-3, vitamins and micro minerals; cage-free poultry products, grass-fed meat and meat products. Better outcome will be possible with the strong policy support and technology back up. When used as supplement in the feeding of dairy animals, it will improve health and reproduction; boost productivity as well as nutritional quality of milk and other foods of animal origin, thus improving the income and profits of the farmers. However, before adoption of hydroponic feed/fodder on wider scale, several issues pertaining to HPFP technology, namely, economics, viability, sustainability and superiority of hydroponic Fodder require further research on priority.

Result and Discussion

For sustainable dairy farming, quality green fodder should be fed regularly to dairy animals. Hydroponic fodder is a good option in front of the farmer because it grows fast, it contains a high nutrient value, and the most important thing is animals like to eat. Green fodder is an important constituent in the feed of livestock. Due to many drastic Changes in agriculture

system, animal rearing and increased population there is shortage of Green fodder to the livestock. Green fodder production through hydroponics technology can be a real beneficial alternative source to overcome the fodder deficiency in livestock sector with many advantage. In developed countries where there is no dearth of quality feed and fodder, the hydroponic production of fodder is less competitive than traditional fodder production when compared on per kg dry matter basis.

References

1. Authored by Nisha Sharma, Somen Acharya, Kaushal Kumar, Narendra Singhand O.P. Chaurasia, in the Journal of Soil and Water Conservation 17(4): 364-371, October-December 2018
2. Authored by Bikram Pradhan and Bandita Deo, published in Current Science, Vol.116, No. 5.
3. Authored by Shailesh Solanki, Nitish Gaurav, Geetha Bhawani and Abhinav Kumar, published in International Journal of Advanced Research (IJAR), this paper focus on the challenges and possibilities to bring soil less farming in India.
4. Authored by Awadhesh Kumar, published in Acta Scientific Agriculture (ISSN:2581-365X) Volume 3, Issue 2, 2019.
5. Butler, J.D., 2006. Hydroponics as hobby growing plants without soil. Information Ofce of University of Illinois 18(2), 11-32.
6. Choi, B., Lee, S.S., 2012. Effects of waste nutrient solution on growth of Chinese cabbage (*Brassica campestris* L.) in Korea. Korean Journal of Environmental Agriculture 30(2), 125-131.
7. Folds, E., 2018. Where did hydroponics come from? Accessed on 16-08-2021. Liao, P., Liu, J., Sun, L., Chang, H., 2020. Can the Adoption of Protected Cultivation Facilities Affect Farm Sustainability? Sustainability 12(23), 70-99.
8. Miller, A., 2011. A Critical Appraisal of Current Development in Vertical Farming. Carleton University publisher 8(15), 23-45.
9. Resh, H.M., 2013. Hydroponic Food Production: A Definitive Guidebook for the Advanced Home Gardener and the Commercial Hydroponic Grower. CRC Publisher 11(23), 45-68. Resh, H.M., 1998.
10. Hydroponics: Questions and answers for successful growing. Woodbridge Publisher 5(4), 12-23. Yadav, D., 2020.

4

Design and Synthesis of Heterocyclic Active Moieties of Pyrazoles and Its Importance's

Somwanshi A.R.

Department of chemistry, J.D. Patil Sangludkar Mahavidyalaya, Daryapur, Amravati (Maharashtra)India
(Corresponding author: Somwanshi A.R., Email: anilsomwanshi40@gmail.com, Mob. No. 9822468944)

Abstract

Pyrazoles have totally concerned and great attention in organic and pharmaceutical fields, due to their promising value as synthetic intermediates for the generation of various bioactive compounds. Subsequently, the synthesis of pyrazoles is a significant focus on research for synthetic organic chemists. Similarly, fused pyrazoles such as pyrazolo based pyridines and pyrazolo pyrimidines have been broadly studied due to their various physiochemical and biological utilities based on the important structural electronic properties of these N-heterocyclic compounds. So, the synthesis of these fused heterocycles and of their derivatives is of distinguished interest to both reveal novel derivatives and exposed the new application. Several procedures have been explained in the literature for the preparation of pyrazoles and of their fused systems in recent years, which mostly involve condensation reactions. And the synthesized pyrazole-based derivatives were confirmed by ^1H NMR and GCMS analysis.

Keywords: *Pyrazole, N-Heterocyclic, bioactive, fused heterocycles*

Introduction

Heteroaromatic compound pyrazole compound of 5-membered ring having two adjacent nitrogen atoms [1]. NH-Pyrazoles are weak bases and also weak acids because they have tendency to accept the protons ($\text{C}=\text{N}$) and also nitrogen atom ($\text{N}-\text{H}$) in pyrrole have tendency to donate protons. [2] Similarly, the interaction between the heteroatoms and hydrogen i.e., hydrogen bonding is depending on structural units of pyrazoles [3].

A German chemist Ludwig Knorr in 1883, who tried to prepare the quinoline compound with antipyretic activity [4]. But unfortunately synthesized the pyrazole instead to quinoline [5]. Knorr has first familiarized the of pyrazole to this heterocycles core to represent that it was derived from pyrrole by the replacement of carbon atom by nitrogen [6]. the first to notice antipyretic action of pyrazole-based compounds in man, which has encouraged the interest in pyrazoles moiety [7]. Then in 1846, the Kosuge and Okeda extracted (a plant which is having antimicrobial activity), 3-n-nonylpyrazole from *Houttuynia cordata* and also levo- β -(1-pyrazolyl) alanine from watermelon seeds (*Citrullus vulgaris*) [8]. Until these findings it was thought that pyrazoles could not be found naturally [9]. The adaptability of pyrazole moiety-based compounds in biological utilities as well as synthetic also. It has been well recognized, being even one of the furthestmost studied compounds among the azole family, even though there are so many natural products containing the pyrazoles moiety [10].

A N-heterocyclic compounds as like composed pyrazoles, substitutes pyrazoles are important due to their wide applications [11]. Most of natural products shows the presence of fused pyrazole structure. A compound pyrazolo[4,3-d] pyrimidine is naturally present in Formicin A. Which is having different biological activity. Such as antiviral and antitumor.

In over-all, biological and pharmacological activities of these compounds containing pyrazole core moiety fused with five- and six-membered heterocyclic compounds. In particular, pyrazole-based pyridine and pyrimidines have taken part in drug discovery [12].

EXPERIMENTAL SECTION

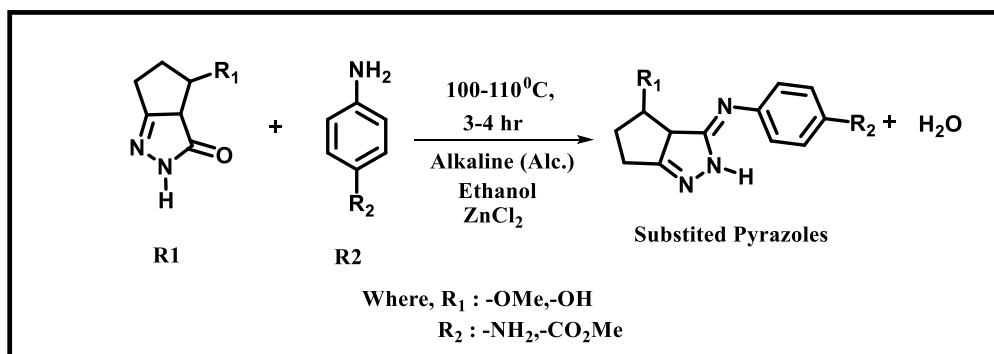
MATERIALS

Methanol (98%), Ethanol (98%) Acetonitrile (99%) and ethyl acetate (98%) were procured from Avra chemical Pvt. Ltd. Sodium hydroxide (98%) zinc chloride Were acquired from Sisco Research Laboratories Pvt. Ltd.

CHARACTERIZATION TECHNIQUE

The Chemical structure of synthesized compounds was confirmed by spectral data. $^1\text{H-NMR}$ spectra were recorded on BRUKER AVANCE NEO 500 MHz spectrometer using DMSO and CDCl_3 solvent and TMS as internal standards at SAIF, Punjab University, Chandigarh (India). Chemical shifts are expressed in ppm. Mass spectrums were recorded on Thermo Scientific TSQ 8000 Gas Chromatograph

General Reaction



Scheme 1. General Reaction for Synthesis of N-Heterocyclic Substituted Pyrazoles

Reactant (R1) (0.1 mmol) was heated with reactant (R2) (0.15 mmol) in oil bath at 100 °C to 110 °C, till complete removal of dehydrated water is ensured. The solid cream color precipitate was obtained and it filtered, washed with methanol and recrystallized by ethanol with preferable yield, m.p.-178°C as cream- white colored crystalline solid. (Scheme 1.)

Table 1. Synthesis of N-heterocyclic Pyrazoles Derivatives

Sr. No	R1	R2	Product	Time in Hrs.	Yield
1				4	86
2				4	81

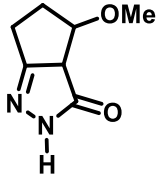
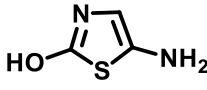
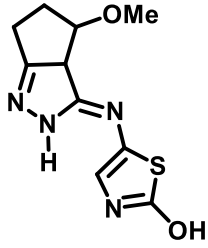
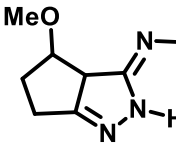
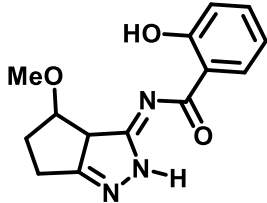
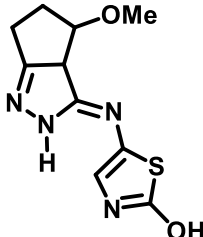
3				4	87
---	---	---	---	---	----

Table 2. Structural analysis of derivatives

Sr. No	Structure of Products	Structural analysis by ¹ HNMR and GCMS
1		¹ HNMR(500MHz,CDCl ₃):δ9.40(s,1H),6.747.20(m,4H),3.41(s,3H),3.2(q,1H),2.0-2.16(t,2H),1.56-1.81(t,2H),1.6(t,1H) GCMS: Cal m/z: 245.28, Found m/z: 244.16
2		¹ HNMR(500MHz,CDCl ₃):δ16.4(s,1H),6.747.68(m,5H),3.41(s,3H),3.2(d,1H),2.0-2.16(t,2H),1.56-1.81(t,2H),1.6(t,1H) GCMS: Cal m/z: 273.11, Found m/z: 273.06
3		¹ HNMR(500MHz,CDCl ₃):δ9.69(s,1H),7.68(s,1H),6.68(s,1H),3.41(s,3H),3.2(q,1H),2.06-2.16(q,2H),1.56-1.81(m,2H),1.6(t,1H) GCMS: Cal m/z: 252.29, Found m/z: 251.40

Conclusion

Synthesis of pyrazole derivatives and even their various functional group substituents are well established. Mostly, the bioactivity of the pyrazole derivatives was studied in detail. There are recent attempts in understanding different properties of the pyrazole derivatives. In addition, there are some challenges to overcome. These challenges include efficiency for high yields in synthesis, generating novel pyrazole derivatives with bioactivity in the sub micromolar range, and characterizing the properties of the derivatives accurately. For this reason, we believe there is a need for investigating new synthetic routes, studying different properties and seeking new applications of novel derivatives especially in blends with polymers. Therefore, the new trend in pyrazole derivatives will be towards new applications in various areas.

Acknowledgement

The author is thankful to Department of chemistry, J.D. Patil Sangludkar Mahavidyalaya for providing research facilities Authors are very much thankful to the Director, SAIF, Punjab University Chandigarh for providing spectral data.

Conflict of Interest: None

References

- 1) Bekhit, Adnan A., et al. "New heterocyclic hybrids of pyrazole and its bioisosteres: Design, synthesis and biological evaluation as dual acting antimalarial-antileishmanial agents." *European Journal of Medicinal Chemistry* 94 (2015): 30-44.
- 2) Farag, A. M., Ali, K. A., El-Debss, T. M., Mayhoub, A. S., Amr, A. G. E., Abdel-Hafez, N. A., & Abdulla, M. M. (2010). Design, synthesis and structure–activity relationship study of novel pyrazole-based heterocycles as potential antitumor agents. *European journal of medicinal chemistry*, 45(12), 5887-5898.
- 3) Abdelgawad, N., Ismail, M. F., Hekal, M. H., & Marzouk, M. I. (2019). Design, synthesis, and evaluation of some novel heterocycles bearing pyrazole moiety as potential anticancer agents. *Journal of Heterocyclic Chemistry*, 56(6), 1771-1779.
- Fayed, E. A., Eissa, S. I., Bayoumi, A. H., Gohar, N. A., Mehany, A. B., & Ammar, Y. A. (2019). Design, synthesis, cytotoxicity and molecular modeling studies of some novel fluorinated pyrazole-based heterocycles as anticancer and apoptosis-inducing agents. *Molecular diversity*, 23, 165-181.
- 4) Nossier, E. S., Fahmy, H. H., Khalifa, N. M., El-Eraky, W. I., & Baset, M. A. (2017). Design and synthesis of novel pyrazole-substituted different nitrogenous heterocyclic ring systems as potential anti-inflammatory agents. *Molecules*, 22(4), 512.
- Faisal, M., Saeed, A., Hussain, S., Dar, P., & Larik, F. A. (2019). Recent developments in synthetic chemistry and biological activities of pyrazole derivatives. *Journal of Chemical Sciences*, 131, 1-30.
- 5) M Abdelrazek, F., M Gomha, S., H Abdelrahman, A., Metz, P., & A Sayed, M. (2017). A facile synthesis and drug design of some new heterocyclic compounds incorporating pyridine moiety and their antimicrobial evaluation. *Letters in Drug Design & Discovery*, 14(7), 752-762.
- 6) Gangurde, K. B., More, R. A., Adole, V. A., & Ghotekar, D. S. (2024). Design, synthesis and biological evaluation of new series of benzotriazole-pyrazole clubbed thiazole hybrids as bioactive heterocycles: Antibacterial, antifungal, antioxidant, cytotoxicity study. *Journal of Molecular Structure*, 1299, 136760.
- 7) Reddy, G. M., Garcia, J. R., Yuvaraja, G., Venkata Subbaiah, M., & Wen, J. C. (2020). Design, synthesis of tri-substituted pyrazole derivatives as promising antimicrobial agents and investigation of structure activity relationships. *Journal of Heterocyclic Chemistry*, 57(5), 2288-2296.
- 8) Castillo, J. C., & Portilla, J. (2018). Recent advances in the synthesis of new pyrazole derivatives. *Targets Heterocycl. Syst*, 22, 194-223.
- Karati, D., Mahadik, K. R., & Kumar, D. (2022). Pyrazole Scaffolds: Centrality in Anti-Inflammatory and Antiviral Drug Design. *Medicinal Chemistry*, 18(10), 1060-1072.
- 9) Liu, X. R., Wu, H., He, Z. Y., Ma, Z. Q., Feng, J. T., & Zhang, X. (2014). Design, synthesis and fungicidal activities of some novel pyrazole derivatives. *Molecules*, 19(9), 14036-14051.
- 10) Ansari, A., Ali, A., & Asif, M. (2017). Biologically active pyrazole derivatives. *New Journal of Chemistry*, 41(1), 16-41.
- 11) Abd-El Gawad, N. M., Hassan, G. S., & Georgey, H. H. (2012). Design and synthesis of some pyrazole derivatives of expected anti-inflammatory and analgesic activities. *Medicinal chemistry research*, 21, 983-994.
- 12) Bakthavatchala Reddy, N., Zyryanov, G. V., Mallikarjuna Reddy, G., Balakrishna, A., Padmaja, A., Padmavathi, V., ... & Sravya, G. (2019). Design and synthesis of some new benzimidazole containing pyrazoles and pyrazolyl thiazoles as potential antimicrobial agents. *Journal of Heterocyclic Chemistry*, 56(2), 589-596.

5

QSAR analysis of sodium glucose co-transporter 1 (SGLT1) inhibitors for anti-hyperglycaemic lead development

Archana Chapolikar^{1,*}, Jyoti Dahatonde¹, Pooja Gaikwad¹, Ajaykumar Gandhi¹

¹Department of Chemistry, Government College of Arts and Science, Chhatrapati Sambhajnagar, Maharashtra, India, 431004 (achapolikar49@gmail.com)

*Correspondence: achapolikar49@gmail.com, Mobile Number- (+91)9657538276.

Abstract: GA-MLR based QSAR evaluation has been effectuated on a small dataset of **SGLT1 inhibitors** abide by OECD principles. Recent study revealed that the presence of *o*-xylene moiety, hydrogen atoms exactly five bonds from hydrogen bond donor atoms and ring carbon atoms within 2Å from hydrogen bond donor/acceptor atoms facilitate the SGLT1 inhibitory action of the compound. Developed QSAR models shown excellent performance on all the statistical parameters with values well above the approved thresholds, such as, $R^2 = 0.79-0.80$, $Q^2_{LOO} = 0.77$, $Q^2_{LMO} = 0.76$, $Q^2_{F^n} = 0.87-0.90$, $CCC_{ext} = 0.93-0.95$. Applicability domain analysis and Y-randomization test also enhanced the credibility of this study.

Keywords: QSAR, SGLT1, anti-hyperglycaemics.

ABBREVIATIONS:

CADD- Computer Aided Drug Designing, **SGLT1/2 -** sodium glucose co-transporter 1/2, **SMILES-** Simplified Molecular-Input Line-Entry System, **GA-** Genetic Algorithm, **MLR-** Multiple Linear Regression, **QSAR-** Quantitative Structure-Activity Relationship, **QSARINS-** QSAR Insubria, **OECD-** Organization for Economic Co-operation and Development, **OFS-** Objective Feature Selection, **SFS-** Subjective Feature Selection

1. INTRODUCTION

SGLT1 and SGLT2 play crucial role in renal glucose re-absorption. SGLT1 is present in both the renal tubules and small intestine and are responsible for active glucose absorption. SGLT1 is a low-capacity glucose transporter (relative to SGLT2), its higher glucose affinity than SGLT2 and additional galactose transportation capability has own an identity of anti-

hyperglycaemic target to SGLT1. Dual SGLT inhibitors i.e. inhibitors of both SGLT1 and SGLT2 are under clinical trial and unfortunately no SGLT1 inhibitor based drugs in the market are present.

C-phenyl 1-thio-D-glucitol scaffold based derivatives [10,11], Deuterated C-Aryl Glycoside[12], Indole-N-glucoside (TA-1887)[13], 1-methoxy-6,8-dioxabicyclo[3.2.1]octane[14], benzocyclobutane-C-glycosides[15], 6-hydroxyl C-aryl glucoside derivatives[16], benzocyclobutane-C-glycosides[17], 6-deoxy O-spiroketal C-arylglucosides [18] are some classes of compounds tested for SGLT1 inhibitory potency. But the search of sufficiently potent SGLT1 inhibitor with no or minimum side effect is still on. To contribute to the development of better SGLT1 inhibitor L. Burggraaff did attempt to identify SGLT1 inhibitors in silico (Burggraaff et al., 2019) with the application of proteochemometrics through machine learning. There is still huge scope for the development

of SGLT1 inhibitors as possibly effective anti-hyperglycaemic agent.

2. MATERIALS AND METHODS

A. Selection of data-set:

For the present work, 107 C-aryl glucoside derivatives with in vitro SGLT1 inhibitory activity in terms of half-maximal inhibitory concentration i.e. $IC_{50} = 0.4$ to 100000 nM were used [19- 22]. The dataset consists of benzocyclobutane-C- (Placeholder1), deuterated C-Aryl Glycoside, series of C-phenyl D-glucitol derivatives, 6-deoxy O-spiroketal-C-arylglucosides, C-phenyl 1-thio-D-glucitol, and C5-fluoro-hexose derivatives. A dataset truly comprised of diverse set of molecules with plenty of pharmacophoric features embedded along with the different scaffolds and hence has covered large chemical space. A QSAR model developed using such a dataset will certainly have large applicability domain that cover the class of the compounds presently under the process of optimization towards more potent SGLT1 inhibitors to treat hyperglycaemia.

The IC_{50} values in nanomolar (nM) unit were converted into molar (M) unit by multiplying factor 10^{-9} . The five least and the five most active C-aryl glucoside derivatives from the present dataset are depicted in **Figure 1** to demonstrate the variation in bio-activity with chemical features. The SMILES strings with the reported IC_{50} (in nM and M unit) and pIC_{50} values for all the molecules are given in Supplementary information. Before OSAR analysis

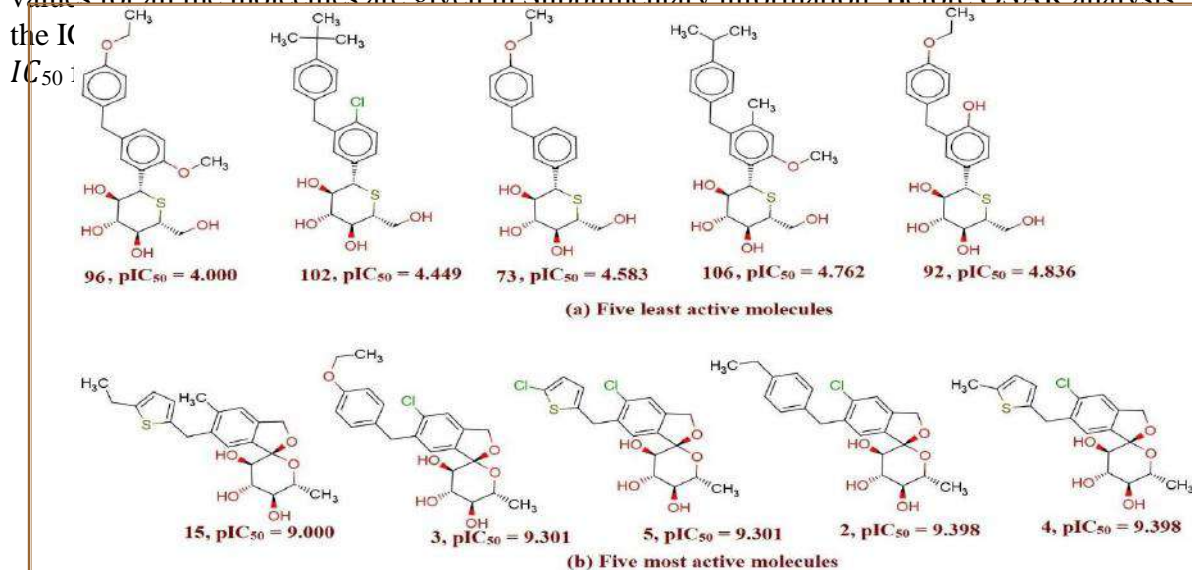


Figure 1: Variations in activity and chemical structure in the dataset used for development of QSAR Models

B. Molecular Structure Drawing and Optimization:

Free and open source software, ChemSketch 12 Freeware (www.acdlabs.com) is used to draw 2D structures and further conversion to 3D structures is achieved using OpenBabel

2.4.0. A geometry optimized molecule is characterized by its lowest energy i.e. most stable conformation. Geometry optimization ensures the normalization of all such a physico-chemical properties for all the molecules from dataset and makes it a necessarily important step prior to molecular descriptor calculation. As a step forward, force field MMFF94 available in TINKER is used for optimization of the molecules.

C. Molecular Descriptor Calculation and Objective Feature Selection (OFS):

A molecular descriptor is a structural and physico-chemical property of a molecule

or specific part of the molecule. More than 18,000 molecular descriptors were calculated for each molecule using PyDescriptor and PaDEL. In the data pruning step, Objective Feature Selection (OFS) in QSARINS v2.2.4 screened out multi-collinear and spurious molecular descriptors (i.e. with nearly constant values >95%, co-linearity $|R| > 0.95$) and contracted molecular descriptor pool with 1145 variables is generated. Contracted though, molecular descriptor pool has covered adequately comprehensive chemical space being comprised of 0D– to 3D– descriptors, structural, constitutional properties and charge descriptors etc.

D. Subjective Feature Selection, QSAR Model – Development and Validation:

In accordance with the OECD principles, firstly, apt variable selection method GA– MLR in Subjective Feature Selection (SFS) operation in QSARINS v2.2.4 is used to perform simple and easy to interpret QSAR models. Then, all the derived models were subjected to the thorough statistical validation, Y-scrambling and Applicability Domain analysis. The steps in QSAR building process:

I. Random split operation in QSARINS v2.2.4 split given dataset into a training set with 35 molecules (80%) and a prediction set with 9 molecules (20%) prediction. Molecules in training set were utilized for QSAR model development and external validation was performed on 9 molecules in prediction set.

II. QSAR models were built using Subjective Feature Selection (SFS) operation in QSARINS v2.2.4 (at default settings) by setting Q^2_{LOO} as fitness function. Insignificant increase in Q^2_{LOO} value was observed after 5 variables and hence to avoid overfitting SFS operation is confined to 5 variables which additionally helped in deriving easy and informative QSAR models. (See supplementary information Table S2)

III. (a) Leave-One-Out (LOO) and Leave-Many-Out (LMO) parameter based internal validation; (b) External validation; (c) Y-scrambling and model Applicability Domain (AD) analysis, performed for legitimate validation.

IV. Performance of each model, measured by close inspection of the various statistical parameters meter the robustness of the GA-MLR based QSAR model. The QSAR model with best values of these parameters and with best predicative ability is selected.

3. RESULTS

Statistical QSAR

After removing all the insignificants terms, the following GAMLR QSAR model-1 and model- 2 were obtained from GA-MLR analysis.

GAMLR QSAR Model-1 (Training Set: 80% and Prediction Set: 20%)

$$pIC_{50} = 22.737(\pm 0.2.253) + 0.608(\pm 0.275)_{ringC_2A} \\ + 0.289(\pm 0.121)_{onH5B} - 0.466(\pm 0.173)_{ringS_C_8Ac} \\ - 634.57(\pm 82.98)P.7$$

GAMLR QSAR Model-2 (Training Set: 80% and Prediction Set: 20%)

$$pIC_{50} = 18.274(\pm 0.2.440) + 0.657(\pm 0.308)_{KRFP3596} \\ + 0.258(\pm 0.116)_{fdonH5B} \\ - 0.206(\pm 0.073)_{fringSH6B} \\ - 424.535(\pm 82.051)P.7 \quad (1)$$

Statistical Parameters	Values	
	Model 5.1	Model 5.2
FITTING		
R^2	0.79	0.80
$R^2_{adj.}$	0.78	0.79
$R^2 - R^2_{adj.}$	0.01	0.01
LOF	0.32	0.32
K_{xx}	0.22	0.23
ΔK	0.14	0.15
$RMSE_{TR}$	0.52	0.51
MAE_{TR}	0.40	0.39
RSS_{TR}	22.85	22.48
CCC_{TR}	0.88	0.89
s	0.53	0.53
F	77.42	79.01
INTERNAL VALIDATION		
Q^2_{LOO}	0.77	0.77
$R^2 - Q^2_{LOO}$	0.02	0.03
$RMSE_{CV}$	0.55	0.54
MAE_{CV}	0.42	0.41
$PRESS_{CV}$	25.60	25.53
CCC_{CV}	0.87	0.87
Q^2_{LMO}	0.76	0.76
$R^2_{Y_{SCR}}$	0.05	0.05
$RMSE_{AV_{Y_{SCR}}}$	1.10	1.10
$Q^2_{Y_{SCR}}$	-0.07	-0.07
EXTERNAL VALIDATION		
$RMSE_{EXT}$	0.36	0.40
MAE_{EXT}	0.32	0.35
$PRESS_{EXT}$	2.78	3.43
R^2_{EXT}	0.90	0.88
Q^2_{F1}	0.90	0.87
Q^2_{F2}	0.90	0.87
Q^2_{F3}	0.90	0.87
CCC_{EXT}	0.95	0.93
$r^2_m avg.$	0.85	0.76
$r^2_m delta$	0.03	0.13
k'	1.00	0.99
k	1.00	1.00

The statistical parameters for developed GAMLQ QSAR models 1 and 2 have been presented in **Table 1**. A good number of statistical parameters for model 1 and 2, which are related to fitting, internal and external validation and Y-scrambling, have been calculated. From **Table 1**, it is clear that R^2_{TR} , CCC_{TR} , CCC_{cv} , $R^2_{adj.}$, and F satisfy the recommended threshold value, which shows that the QSAR models are statistically robust with adequate number of molecular descriptors in the models. Although the data are obtained from different publications, they pass the statistical compatibility as the values of statistical parameters for fitting criteria such as $R^2_{adj.} = 0.78$, $R^2 - R^2_{adj.} = 0.01$, $LOF = 0.32$, $CCC_{TR} = 0.88$, etc. are well above the approved threshold values for both models. From Fitting parameters such as, R^2_{TR} , CCC_{TR} , CCC_{cv} , $R^2_{adj.}$, and F satisfy the recommended threshold value which shows that the QSAR models are statistically robust with adequate number of molecular descriptors in them. The values for different cross-validation parameters such as Q^2_{LOO} , $RMSE_{cv}$, MAE_{cv} , CCC_{cv} , and Q^2_{LMO} support the statistical robustness of the QSAR models. The graphs; Experimental endpoint against Predicted endpoint for both the models [Figure 4a & 5a] and experimental endpoint against residuals [Figure 4b & 5b] represent the performance of the QSAR model 1 and 2, respectively, on both Training and Prediction set molecules.

The external predictive ability of the models is established by the high values of R^2_{EXT} , Q^2_{F1} , Q^2_{F2} , Q^2_{F3} , and CCC_{EXT} . In short, the developed QSAR models fulfill the recommended threshold values for many internal and external validation parameters. In addition, for a better validation of derived models, the model applicability domain (AD) was assured by plotting Williams plots for models 1 [Figure 4b & 5b]. Therefore, these models are statistically robust and possess good external predictive ability. Moreover, fulfilment of recommended threshold values for many parameters as well as low R^2 value after Y-randomization indicate that the model is not developed by chance.

The performance of the QSAR Model 1 and 2 for

each molecule from used dataset is given in Supplementary Information respectively. Compound 29 (Exp. pIC_{50} = 7.036 Pred. pIC_{50} = 7.042, PMER value = 0.006, HAT i/i = 0.037) and 85 (Exp. pIC_{50} = 7.456, Pred. pIC_{50} = 7.457, PMER value = 0.001, HAT i/i = 0.1 10) are the best predicted for their pIC_{50} values by model 1 and 2, respectively. Both compound 29 and 85 fall well within the AD of respective models as reflected from HAT i/I values. Possible reason for the best bioactivity P for the compound 29 [Figure 2] might be the presence of simple structural features, molecular planarity in a side chain of the glucoside scaffold maintained by simple methyl substituent and a fused ring substitution (benzocyclobutane) that minimized the errors in the bioactivity Prediction due to conformational changes in the molecules. Compound 85 (Figure 3) is with more number of pharmacophoric feature with large number of hydrogen bond donor and acceptor atoms (O, N, etc.). This might have helped molecule to attain optimum value for the molecular descriptors wherefrom QSAR equation is developed in subjective feature selection.

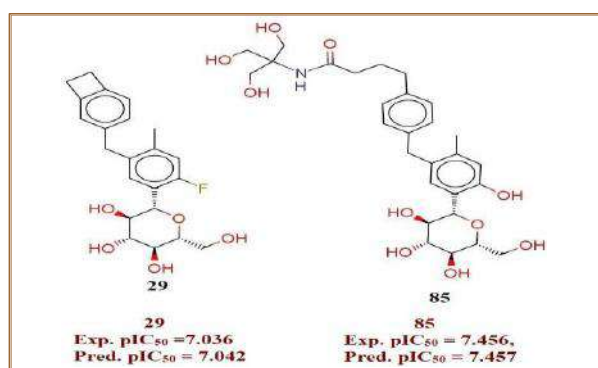


Figure 2: Representation of the best predicted compound by QSAR Model 1 and 2

Collective result of all these causes could be the reason for best SGLT1 inhibitory activity prediction for these compounds. Models developed in present study failed to predict precise bioactivity for some of the compound (see Figure 3). Compound 102 is the worst predicted compound (Exp. pIC_{50} = 4.449 Pred. pIC_{50} = 5.784, PMER value = 1.335, HAT i/i = 0.038) for its SGLT1 inhibitory activity by model 1 whereas compound 45 is the worst predicted compound (Exp. pIC_{50} = 5.933, Pred. pIC_{50} = 7.348, PMER value = 1.415, HAT i/i = 0.024) for SGLT1 inhibitory activity by model 5.2. In both the models, compound 14 is the third worst predicted compound (Exp. pIC_{50} = 7.578, by model 5.1; Pred. pIC_{50} = 8.893, PMER value = 1.306, HAT i/i = 0.079 and by model 5.2; Pred. pIC_{50} = 8.858, PMER value = 1.271, HAT i/i = 0.079).

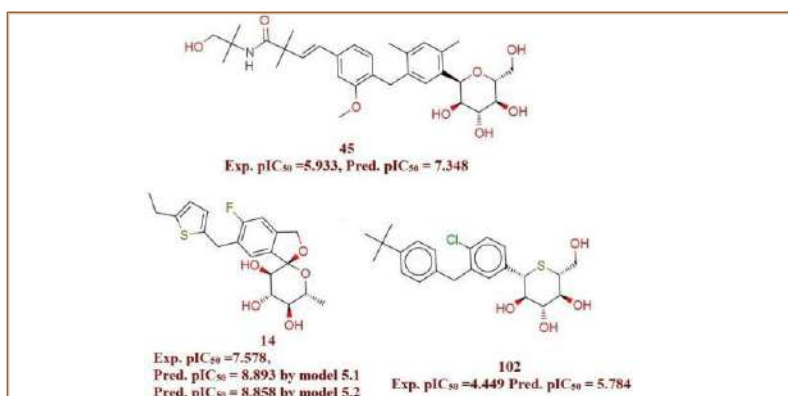


Figure 3: Representation of worst predicted and outlier compounds

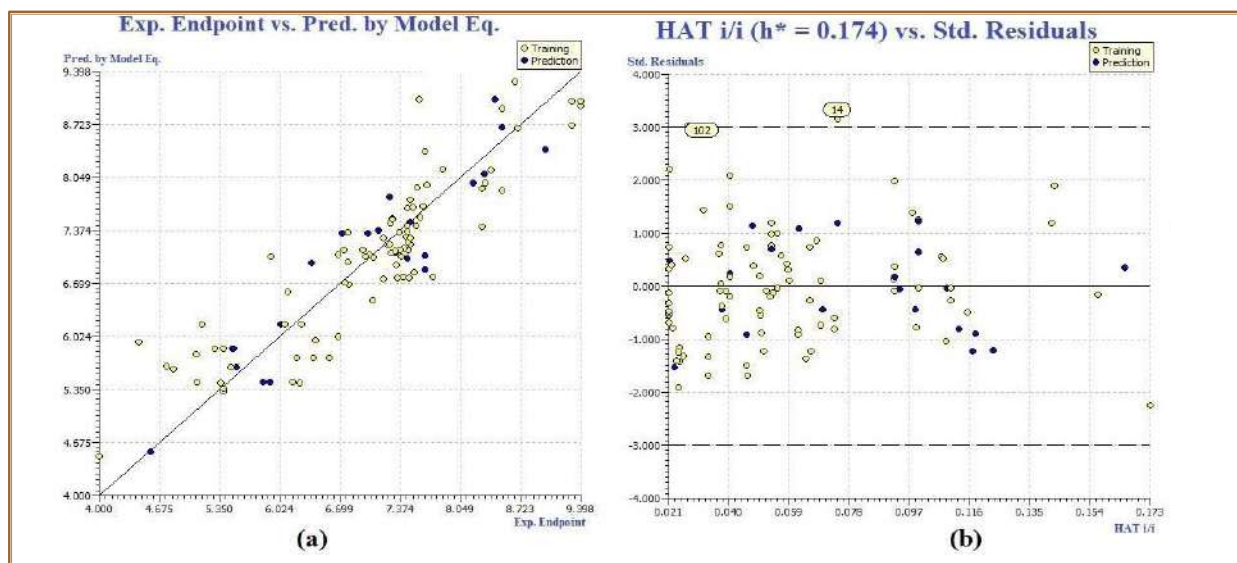


Figure 4: (a) Graph of Experimental vs. Predicted Endpoint values (b) Williams plot for QSAR Model-1

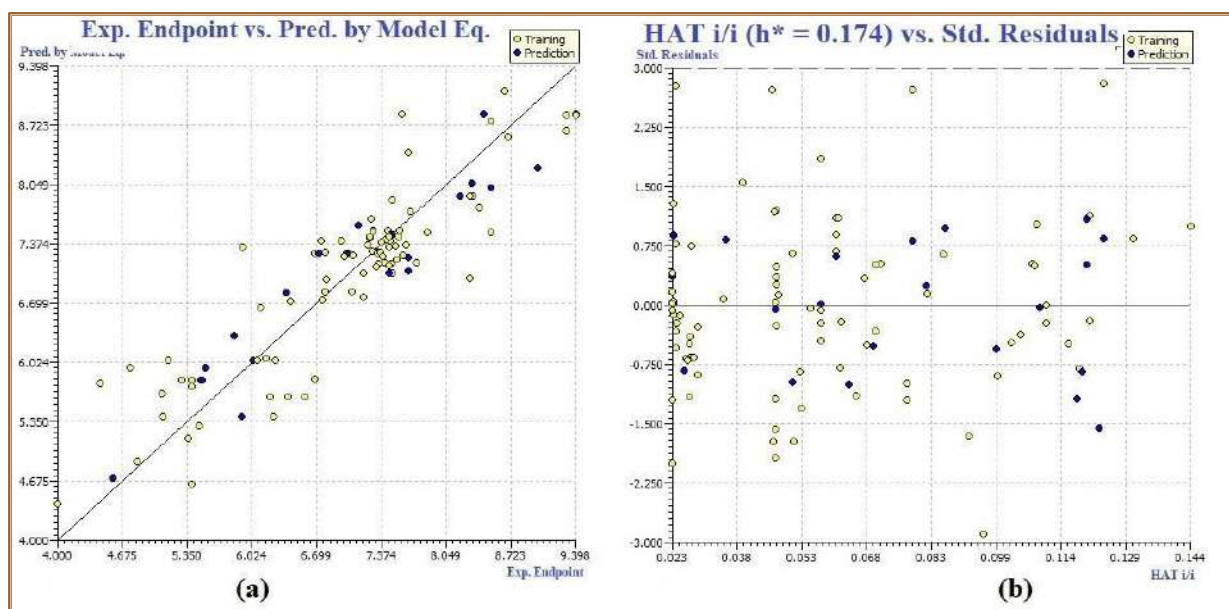
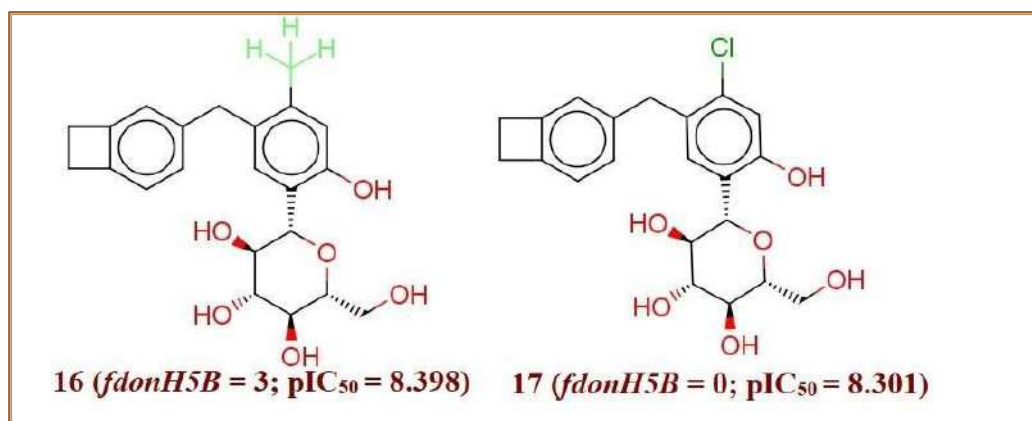


Figure 5: (a) Graph of Experimental vs. Predicted Endpoint values (b) Williams plot for QSAR Model-2

Descriptive QSAR *fdonH5B*

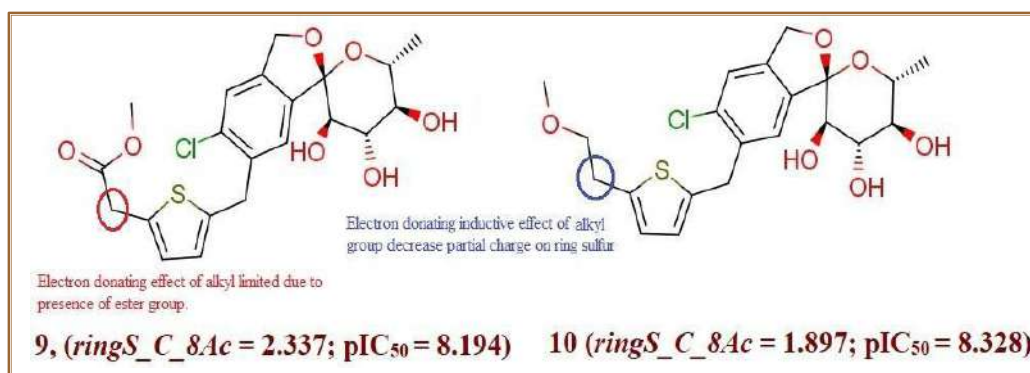
The molecular descriptor *fdonH5B* encode the information on frequency or number of Hydrogen atoms exactly five bonds from HBD atom. It has positive coefficient, thus increase in the value of *fdonH5B* increase the pIC_{50} value i.e. SGLT1 inhibitory potency of the compound. To support this observation, a pair of compound 44 (*fdonH5B* = 2; pIC_{50} = 6.754) and 30 (*fdonH5B* = 1; pIC_{50} = 6.686) is appropriate. Compound 17 (*fdonH5B* = 0; pIC_{50} = 8.301) and 16 (*fdonH5B* = 3; pIC_{50} = 8.398) is yet another pair of compound that appropriately support the same observation (Figure 6). The substituent $-Cl$ in compound 17 on replacement by $-CH_3$ added three Hydrogens which got placed exactly five bond from HBD i.e. $-OH$ group ortho glycoside residue.



ringS_C_8Ac

Figure 6: Illustration of the molecular descriptor *fdonH5B*

The molecular descriptor *ringS_C_8Ac* encode the information on the sum of partial charges of ring Sulfur atoms within 8Å from C atom. As it has negative coefficient, decrease in the value of *ringS_C_8Ac* enhance the SGLT1 inhibitory potency of the compound. The significance of this molecular descriptor is highlighted by comparing compound 9 (*ringS_C_8Ac* = 2.337; *pIC*₅₀ = 8.194) with 10 (*ringS_C_8Ac* = 1.897; *pIC*₅₀ = 8.328) wherein decrease in the value of *ringS_C_8Ac* furnished more potent SGLT1 inhibitor (see **Figure 7**). The close observation of the structures of compound 9 and 10 reveal that this molecular descriptor indirectly provide information on substituent on ring containing Sulfur atom. In compound 9, the electron donating inductive effect of $-CH_2-$ group is limited by an electron withdrawing inductive effect of ester $-C(O)O$ group whereas in compound there is ether functionality that too separated by one more CH_2 group and hence an electron donating effect of CH_2 group is retained. This feature in compound 10 diminish the partial positive charge on ring Sulfur.



da_ringC_2A

Figure 7: Illustration of the molecular descriptor ringS_C_8Ac

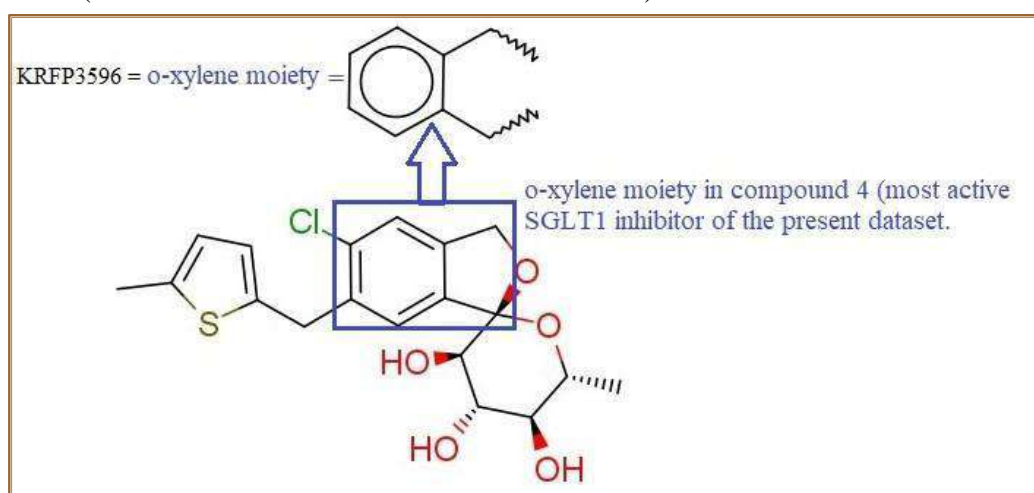
The molecular descriptor, *da_ringC_2A* encode the information on number of ring Carbon atoms within 2Å from HBD and HBA. It has positive coefficient and hence increase in the value of this descriptor cause increase in the SGLT1 inhibition activity of the compound. Comparison of compound 44 (*da_ringC_2A* =2; pIC₅₀ = 6.754) with 30 (*da_ringC_2A* =1;

pIC₅₀ = 6.686) rationalize the observation. Compound 48 (*da_ringC_2A* =3; pIC₅₀ = 7.444) with 47 (*da_ringC_2A* =4; pIC₅₀ = 7.638) is yet another pair of the compound to support this fact.

KRFP3596

It is a Klekota-Roth fingerprint abbreviated as KRFP. It encode the information on the presence of various chemical substructures. KRFP3596 molecular descriptor encode specifically the presence of substructure represented by *o*-xylene moiety (see **Figure 8**). This molecular descriptor has positive coefficient and hence the presence of *o*-xylene substructure own better SGLT1 inhibitory potency to the compound. This observation can be supported by the observation of whole dataset. All the most active compounds with pIC₅₀ ≥ 7.036. *o*-xylene substructure is present (KRFP3596 = 1) whereas in the least active compounds with pIC₅₀ ≤

5.514 (with few exceptions) there is no *o*-xylene substructure present (i.e. KRFP3596 = 0). In **Figure 8** *o*-xylene moiety quantitatively encoded as KRFP3596 is depicted using compound 4 (a most active SGLT1 inhibitor of the series).



ASP.7

Figure 8: Illustration of the molecular descriptor KRFP3596

ASP.7 i.e. average simple path, order 7 abbreviated as ASP.7 is one of the χ Chi Path descriptor. It has negative coefficient in both the models. Therefore, decrease in the value of ASP.7 increase the value of pIC₅₀ i.e. SGLT1 inhibitory potency of the compound. Significance of the smaller value of ASP.7 molecular descriptor for better SGLT1 inhibitory potency is supported

by comparing compound 1 (ASP.7 = 0.027, pIC₅₀ = 7.652) with compound 2 (ASP.7 = 0.026, pIC₅₀ = 9.398). Decrease in the value of ASP.7 by just 0.001 unit elevated the potency of compound 3 by about 1.7 unit.

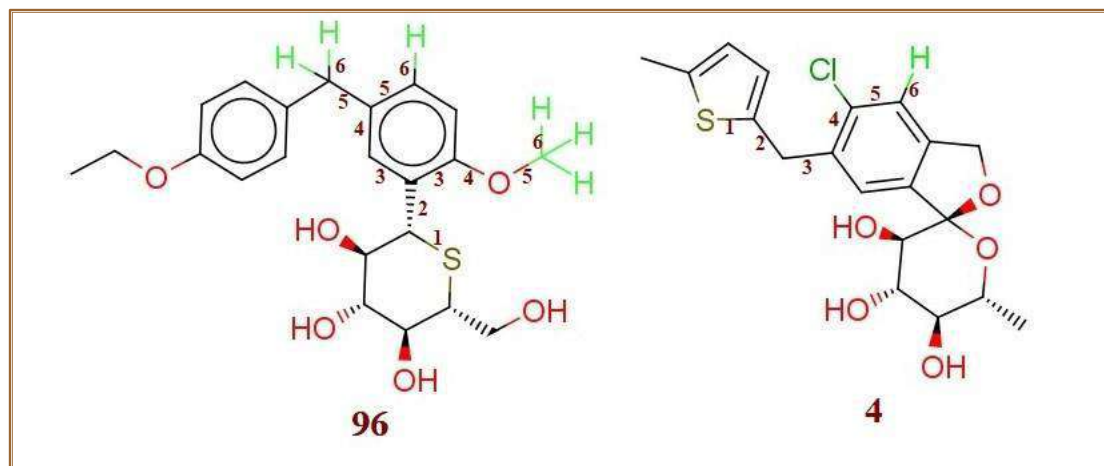
fringSH6B

The molecular descriptor, *fringSH6B* encode the information on the number of Hydrogen within 6 bonds from ring Sulfur. It has negative coefficient and hence decrease in the value of *fringSH6B* could increase the SGLT1 inhibitory potency of the compound. The least active SGLT1 inhibitor of the series i.e. compound 96 there are 6 such a hydrogens are present (**Figure 9**) and last 7 least active compounds have at least 2 such hydrogens (i.e. *fringSH6B* = 2 in their structure. On the contrary, the 4 most active compounds of the series have only 1 or even no (0) such a hydrogens (**Figure 9**). This molecular descriptor provide an easy ground for optimization of present SGLT1 inhibitors toward more potent leads. For example, in compound 4 (the most potent SGLT1 of the series) just repositioning of –Cl that replace hydrogen at 6 bond from sulfur could furnish more potent SGLT1 inhibitor. In case of presence of –OCH₃ group as a bearer of such hydrogens can be replaced by –OCF₃ or –OH group and more SGLT1 inhibitor can be expected.

Figure 9: Illustration of the molecular descriptor fringSH6B

4. CONCLUSIONS

Statistical accomplishment of both the models is quite satisfactory as reflected from values of the various statistical parameters that are well above the approve threshold values. High value of Q₂LOO = 0.77, Q₂LMO = 0.76, R₂EXT = 0.88-0.90, and Q₂F_n = 0.87-0.90 and



CCCEXT

= 0.93-0.95 mark the acceptable predictive ability of the Model 1 and 2. Applicability domain analysis based on leverage approach provided an information on the most appropriate classes of the compounds with distinguished scaffold and pharmacophoric features for reliable prediction of SGLT1 inhibition potential prior to their wet-lab synthesis and/or in-vitro/in-vivo

studies. Information on PMER values for all the compounds and best predicted compound(s) help to have precise guess on the predicted activity. The knowledge of worst predicted compound(s) and/or outlier(s) help the user to identify compound(s) unsuitable for the application of the models for reliable SGLT1 inhibitory potential.

Presence of o-xylene moiety, Hydrogen atoms exactly five bonds from HBD atom and ring Carbon atoms within 2Å from HBA and HBD atoms, facilitate the SGLT1 inhibitory action of the compound, as suggested by QSAR evaluations. In the course of optimization of the existing SGLT1 inhibitors within applicability domain of the models developed, it is advisable to ensure the more number of Hydrogens exactly five bond and ring Carbons within 2Å from HBA and/or HBD atoms. Introduction of ring substituent within 2Å from HBA and HBD atoms or substituting existing ring system with optimum number of functionalities with HBA and HBD atoms could suffice to have required structural modification and hence highly recommended during structural derivatization. QSAR evaluation also suggest that the ring

Sulfur atoms within 8Å from Carbon atom, Hydrogen atoms within 6 bonds from ring Sulfur are detrimental to the activity of the SGLT1 inhibitors. In the compounds from dataset, sulfur present in two different scaffold systems viz. S-glycoside ring and thiophene ring. It is observed that, occurrence of S-glycoside moiety set to zero towards the end of most potent SGLT1 inhibitors. However, thiophene has not proved that detrimental to SGLT1 inhibitory potency of the compound as it is present in some of the relatively more potent SGLT1 inhibitors. Removal of thiophene is not advisable but, it is suggestive to not to substitute thiophene ring with substituent that could intensify the positive charge on Sulfur of the thiophene through electron withdrawing inductive/resonance effect such as -Cl, -COR, -C(O)OR etc.

In conclusion, the present QSAR analysis was effective in identifying interdependent, interconnected astounding structural features which are otherwise hard to recognize by mere observation. Strategic optimization of the present SGLT1 inhibitors within applicability domain of the model with recommended Structural modifications could lead to the discovery of more active SGLT1 inhibitor(s) as an effective anti-hyperglycaemic agent with acceptable ADMET profile.

ACKNOWLEDGMENTS: The authors are thankful to Dr. Paola Gramatica and her team for providing QSARINS-v2.2.4 and developers of TINKER, ChemSketch 12 Freeware (ACD labs), and PyDescriptor for providing the free versions of their software.

REFERENCES:

- [1] IDF Diabetes Atlas 9th edition, *IDF Diabetes Atlas 9th edition 2019*, International Diabetes Federation Diabetes Atlas, Ninth Edition/2019.
- [2] Y. Huang, X. Cai, W. Mai, M. Li and Y. Hu, *Association between prediabetes and risk of cardiovascular disease and all cause mortality: Systematic review and meta-analysis*, BMJ 355 (2016), .
- [3] A.G. Tabák, C. Herder C, W. Rathmann, E.J. Brunner, M. Kivimäki. *Prediabetes: a high-risk state for diabetes development*. Lancet. 2012 Jun 16;379(9833):2279-90, doi: 10.1016/S0140- 6736(12)60283-9.
- [4] Y. Heianza, S. Hara, Y. Arase, K. Saito, K. Fujiwara, H. Tsuji et al., *HbA1c 5.7-6.4 and impaired fasting plasma glucose for diagnosis of prediabetes and risk of progression to diabetes in Japan (TOPICS 3): A longitudinal cohort study*, Lancet 378 (2011), pp. 147–155.
- [5] J. Yeboah, A.G. Bertoni, D.M. Herrington, W.S. Post and G.L. Burke, *Impaired fasting glucose and the risk of incident diabetes mellitus and cardiovascular events in an adult population: MESA (Multi-Ethnic Study of Atherosclerosis)*, J. Am. Coll. Cardiol. 58 (2011), pp. 140–146.
- [6] M.J. Davies, D.A. D'Alessio, J. Fradkin, W.N. Kernan, C. Mathieu, G. Mingrone et al., *Management of hyperglycaemia in type 2 diabetes, 2018. A consensus report by the American Diabetes Association (ADA) and the European Association for the Study of Diabetes (EASD)*, Diabetologia 61 (2018), pp. 2461–2498.
- [7] G. Ferrannini and L. Rydén, *Sodium-glucose transporter 2 inhibition and cardiovascular events in patients with diabetes: Information from clinical trials and observational real-world data*, Clin. Sci. 132 (2018), pp. 2003–2012.
- [8] H.J.L. Heerspink, B.A. Perkins, D.H. Fitchett, M. Husain and D.Z.I. Cherney, *Sodium Glucose Cotransporter 2 Inhibitors in the Treatment of Diabetes Mellitus: Cardiovascular and Kidney Effects, Potential Mechanisms, and Clinical Applications*, Circulation 134 (2016), pp. 752–772.
- [9] *Phlorizin: A review*. Diabetes Metab Res Rev, 2005.
- [10] A. Oku, K. Ueta, K. Arakawa, T. Ishihara, M. Nawano, Y. Kuroshima et al., *T-1095, an inhibitor of renal Na⁺-glucose cotransporters, may provide a novel approach to treating diabetes*, Diabetes 48 (1999), pp. 1794–1800.
- [11] K. Katsuno, Y. Fujimori, Y. Takemura, M. Hiratochi, F. Itoh, Y. Komatsu et al., *Sergliflozin, a novel selective inhibitor of low-affinity sodium glucose cotransporter (SGLT2), validates the critical role of SGLT2 in renal glucose reabsorption and modulates plasma glucose level*, J. Pharmacol. Exp. Ther. 320 (2007), pp. 323–330.
- [12] Y. Fujimori, K. Katsuno, I. Nakashima, Y. Ishikawa-Takemura, H. Fujikura and M. Isaji, *Remogliflozin etabonate, in a novel category of selective low-affinity sodium glucose cotransporter (SGLT2)*

- inhibitors, exhibits antidiabetic efficacy in rodent models*, J. Pharmacol. Exp. Ther. 327 (2008), pp. 268–276.
- [13] W. Meng, B.A. Ellsworth, A.A. Nirschl, P.J. McCann, M. Patel, R.N. Girotra et al., *Discovery of dapagliflozin: A potent, selective renal sodium-dependent glucose cotransporter 2 (SGLT2) inhibitor for the treatment of type 2 diabetes*, J. Med. Chem. 51 (2008), pp. 1145–1149.
- [14] S. Nomura, S. Sakamaki, M. Hongu, E. Kawanishi, Y. Koga, T. Sakamoto et al., *Discovery of canagliflozin, a novel C-glucoside with thiophene ring, as sodium-dependent glucose cotransporter 2 inhibitor for the treatment of type 2 diabetes mellitus (1)*, J. Med. Chem. 53 (2010), pp. 6355–6360.
- [15] M. Imamura, K. Nakanishi, T. Suzuki, K. Ikegai, R. Shiraki, T. Ogiyama et al., *Discovery of Ipragliflozin (ASP1941): A novel C-glucoside with benzothiophene structure as a potent and selective sodium glucose co-transporter 2 (SGLT2) inhibitor for the treatment of type 2 diabetes mellitus*, Bioorganic Med. Chem. 20 (2012), pp. 3263–3279.
- [16] N.C. Goodwin, R. Mabon, B.A. Harrison, M.K. Shadoan, Z.Y. Almstead, Y. Xie et al., *Novel L-xylose derivatives as selective sodium-dependent glucose cotransporter 2 (SGLT2) inhibitors for the treatment of type 2 diabetes*, J. Med. Chem. 52 (2009), pp. 6201–6204.
- [17] V. Mascitti, B.A. Thuma, A.C. Smith, R.P. Robinson, T. Brandt, A.S. Kalgutkar et al., *On the importance of synthetic organic chemistry in drug discovery: Reflections on the discovery of antidiabetic agent ertugliflozin*, Medchemcomm 4 (2013), pp. 101–111.
- [18] W. Zhang, A. Welihinda, J. Mechanic, H. Ding, L. Zhu, Y. Lu et al., *EGT1442, a potent and selective SGLT2 inhibitor, attenuates blood glucose and HbA1c levels in db/db mice and prolongs the survival of stroke-prone rats*, Pharmacol. Res. 63 (2011), pp. 284–293.
- [19] Y. Wang, Y. Lou, J. Wang, D. Li, H. Chen, T. Zheng et al., *Design, synthesis and biological evaluation of 6-deoxy O-spiroketal C-arylglucosides as novel renal sodium-dependent glucose cotransporter 2 (SGLT2) inhibitors for the treatment of type 2 diabetes*, Eur. J. Med. Chem. 180 (2019), pp. 398–416.
- [20] H. Kakinuma, T. Oi, Y. Hashimoto-Tsuchiya, M. Arai, Y. Kawakita, Y. Fukasawa et al., *(1 S)- 1,5-anhydro-1-[5-(4-ethoxybenzyl)-2-methoxy-4-methylphenyl]-1-thio- d -glucitol (TS-071) is a potent, selective sodium-dependent glucose cotransporter 2 (SGLT2) inhibitor for type 2 diabetes treatment*, J. Med. Chem. 53 (2010), pp. 3247–3261.
- [21] S. Kuroda, Y. Kobashi, T. Oi, K. Kawabe, F. Shiozawa, L. Okumura-Kitajima et al., *Discovery of potent, low-absorbable sodium-dependent glucose cotransporter 1 (SGLT1) inhibitor SGL5213 for type 2 diabetes treatment*, Bioorganic Med. Chem. 27 (2019), pp. 394–409.
- [22] S. Kuroda, Y. Kobashi, T. Oi, H. Amada, L. Okumura-Kitajima, F. Io et al., *Discovery of a potent, low-absorbable sodium-dependent glucose cotransporter 1 (SGLT1) inhibitor (TP0438836) for the treatment of type 2 diabetes*, Bioorganic Med. Chem. Lett. 28 (2018), pp. 3534–3539.
- [23] G.H. Kuo, M.D. Gaul, Y. Liang, J.Z. Xu, F. Du, P. Hornby et al., *Synthesis and biological evaluation of benzocyclobutane-C-glycosides as potent and orally active SGLT1/SGLT2 dual inhibitors*, Bioorganic Med. Chem. Lett. 28 (2018), pp. 1182–1187.
- [24] G. Xu, M.D. Gaul, G.H. Kuo, F. Du, J.Z. Xu, N. Wallace et al., *Design, synthesis and biological evaluation of (2S,3R,4R,5S,6R)-5-fluoro-6-(hydroxymethyl)-2-aryltetrahydro-2H-pyran-3,4-diols as potent and orally active SGLT dual inhibitors*, Bioorganic Med. Chem. Lett. 28 (2018), pp. 3446–3453.
- [25] A. Baldi, *Computational approaches for drug design and discovery: An overview*, Syst. Rev. Pharm. 1 (2010), pp. 99–105.
- [26] A. Jain, *Computer aided drug design*, J. Phys. Conf. Ser. 884 (2017), .
- [27] J.S. Smith, A.E. Roitberg and O. Isayev, *Transforming Computational Drug Discovery with Machine Learning and AI*, ACS Med. Chem. Lett. 9 (2018), pp. 1065–1069.
- [28] M.H. Baig, K. Ahmad, S. Roy, J.M. Ashraf, M. Adil, M.H. Siddiqui, S. Khan, M.A. Kamal, I. Provaznik, I. Choi, *Computer aided drug design: success and limitations*, Curr. Pharmaceut. Des. 22 (2016) 572–581, .
- [29] S. Joy, Y.M. Vijayakumar and G. Sunhye, *Role of computer-aided drug design in modern drug discovery*, Arch. Pharm. Res. (2015), .
- [30] E.N. Muratov, J. Bajorath, R.P. Sheridan, I. V. Tetko, D. Filimonov, V. Poroikov et al., *QSAR without borders*, Chem. Soc. Rev. 49 (2020), pp. 3525–3564.
- [31] A. Cherkasov, E.N. Muratov, D. Fourches, A. Varnek, I.I. Baskin, M. Cronin et al., *QSAR modeling: Where have you been? Where are you going to?*, J. Med. Chem. 57 (2014), pp. 4977–5010.
- [32] T. Fujita and D.A. Winkler, *Understanding the Roles of the “two QSARs,”* J. Chem. Inf. Model. 56 (2016), pp. 269–274.

-
- [33] J. Huang and X. Fan, *Why QSAR fails: An empirical evaluation using conventional computational approach*, Mol. Pharm. 8 (2011), pp. 600–608.
- [34] N. Chirico and P. Gramatica, *Real external predictivity of QSAR models. Part 2. New intercomparable thresholds for different validation criteria and the need for scatter plot inspection*, J. Chem. Inf. Model. 52 (2012), pp. 2044–2058.
- [35] P. Gramatica, S. Cassani, P.P. Roy, S. Kovarich, C.W. Yap and E. Papa, *QSAR modeling is not “Push a button and find a correlation”*: A case study of toxicity of (Benzo-)triazoles on Algae, Mol. Inform. 31 (2012), pp. 817–835.
- [36] T.M. Martin, P. Harten, D.M. Young, E.N. Muratov, A. Golbraikh, H. Zhu et al., *Does rational selection of training and test sets improve the outcome of QSAR modeling?*, J. Chem. Inf. Model. 52 (2012), pp. 2570–2578.
- [37] V.H. Masand, D.T. Mahajan, G.M. Nazeruddin, T. Ben Hadda, V. Rastija and A.M. Alfeefy, *Effect of information leakage and method of splitting (rational and random) on external predictive ability and behavior of different statistical parameters of QSAR model*, Med. Chem. Res. 24 (2015), pp. 1241–1264.
- [38] P. Gramatica, *On the development and validation of QSAR models*, Methods Mol. Biol. 930 (2013), pp. 499–526.
- [39] M.C. Sharma and S. Sharma, *Molecular modeling studies of thiophenyl C-aryl glucoside sglt2 inhibitors as potential antidiabetic agents*, Int. J. Med. Chem. 2014 (2014), .
- [40] X. Zhao, B. Sun, H. Zheng, J. Liu, L. Qian, X. Wang et al., *Synthesis and biological evaluation of 6-hydroxyl C-aryl glucoside derivatives as novel sodium glucose co-transporter 2 (SGLT2) inhibitors*, Bioorganic Med. Chem. Lett. 28 (2018), pp. 2201–2205.
- [41] G. Xu, B. Lv, J.Y. Roberge, B. Xu, J. Du, J. Dong et al., *Design, synthesis, and biological evaluation of deuterated C-aryl glycoside as a potent and long-acting renal sodium-dependent glucose cotransporter 2 inhibitor for the treatment of type 2 diabetes*, J. Med. Chem. 57 (2014), pp. 1236–1251.
- [42] S. Nomura, Y. Yamamoto, Y. Matsumura, K. Ohba, S. Sakamaki, H. Kimata et al., *Novel indole- N-glucoside, TA-1887 As a sodium glucose cotransporter 2 inhibitor for treatment of type 2 diabetes*, ACS Med. Chem. Lett. 5 (2014), pp. 51–55.
- [43] V.H. Masand and V. Rastija, *PyDescriptor: A new PyMOL plugin for calculating thousands of easily understandable molecular descriptors*, Chemom. Intell. Lab. Syst. 169 (2017), pp. 12– 18.
- [44] P. Gramatica, S. Cassani and N. Chirico, *QSARINS-chem: Insubria datasets and new QSAR/QSPR models for environmental pollutants in QSARINS*, J. Comput. Chem. 35 (2014), pp. 1036–1044.
- [45] P. Gramatica, N. Chirico, E. Papa, S. Cassani and S. Kovarich, *QSARINS: A new software for the development, analysis, and validation of QSAR MLR models*, J. Comput. Chem. 34 (2013), pp. 2121–2132.
- [46] A.K. Saxena and P. Prathipati, *Comparison of MLR, PLS and GA-MLR in QSAR analysis*, SAR QSAR Environ. Res. 14 (2003), pp. 433–445.
- [47] K. Roy, S. Kar and P. Ambure, *On a simple approach for determining applicability domain of QSAR models*, Chemom. Intell. Lab. Syst. 145 (2015), pp. 22–29.
- [48] T.M. De Assis, G.C. Gajo, L.C. De Assis, L. Santos Garcia, D.R. Silva, T.C. Ramalho et al., *QSAR Models Guided by Molecular Dynamics Applied to Human Glucokinase Activators*, Chem. Biol. Drug Des. 87 (2016), pp. 455–466.
- [49] P. Gramatica, *Principles of QSAR models validation: Internal and external*, QSAR Comb. Sci. 26 (2007), pp. 694–701.
- [50] A. Arwansyah, A.R. Arif, G. Syahputra, S. Sukarti and I. Kurniawan, *Theoretical studies of Thiazolyl-Pyrazoline derivatives as promising drugs against malaria by QSAR modelling combined with molecular docking and molecular dynamics simulation*, <https://doi.org/10.1080/08927022.2021.1935926> (2021), .
-

6

Preparation and Acetone Gas Sensing Properties of Cd Substituted Magnesium Ferrites

A. V. Kadu

Prof Ram Meghe College of Engineering and Management, Badnera, Amravati, M.S. India.

Mail id: kadu.aashish@gmail.com

Abstract :

In this work, we report the preparation and gas sensing performance of pure and doped MgFe_2O_4 were prepared by sol gel method. The structural characteristics of the material were studied by using X-ray diffraction and Scanning Electron Microscopy. The XRD pattern shows a nanocrystalline solid solution of MgFe_2O_4 with an orthorhombic phase and the crystallite sizes is found to be in the range of 30-40 nm. The gas sensing performance of the unmodified and surface modified films was tested for various gases such as H_2S , NH_3 , LPG and acetone. $\text{Mg}_{0.4}\text{Cd}_{0.6}\text{Fe}_2\text{O}_4$ powder showed large response to 200 ppm acetone gas at an operating temperature 180°C . The sensitivity, selectivity of $\text{Mg}_{0.4}\text{Cd}_{0.6}\text{Fe}_2\text{O}_4$ thick films was measured.

Keywords: Acetone sensor, $\text{Mg}_{0.4}\text{Cd}_{0.6}\text{Fe}_2\text{O}_4$, Gas sensing properties, Response time.

1. Introduction:

Magnesium ferrites (MgFe_2O_4) have emerged as promising candidates for gas sensing applications owing to their inherent chemical stability, high surface area, and tunable electrical properties. The ability to detect volatile organic compounds (VOCs) such as acetone is of particular interest due to its relevance in various industrial, environmental, and healthcare sectors. However, enhancing the sensitivity, selectivity, and response time of gas sensors based on magnesium ferrites remains a key challenge.

Dopant-mediated modifications offer a promising strategy for tailoring the gas sensing properties of magnesium ferrites. Among the dopants explored for this purpose, cadmium (Cd) substitution has garnered significant attention due to its potential to influence the structural and electronic properties of the host material. By introducing Cd ions into the magnesium ferrite lattice, it is possible to induce changes in the surface morphology, defect structure, and gas interaction mechanisms, thereby enhancing the sensing performance towards acetone and other VOCs.

The detection of acetone gas holds immense importance in various applications, including industrial process monitoring, environmental pollution control, and medical diagnostics. Reliable and efficient gas sensors capable of detecting acetone at low concentrations are essential for ensuring workplace safety, environmental compliance, and early disease diagnosis.

Chemical methods [1-3], microwave sintering method [4,5], Citrate precursor method [6], wet chemical method [7] and Sol-gel method [8] etc. The sol-gel method has been identified as the most straightforward approach for preparing ferrites in bulk form. In this paper the results are presented of the ferrites prepared by using sol gel method.

The development of Cd-substituted magnesium ferrite-based gas sensors presents an exciting opportunity to address these challenges and advance the state-of-the-art in gas sensing technology. Structural properties of Mg^{2+} and Al^{3+} co-substituted lithium ferrites were studied by Modi et al [9]. X-ray and infrared studies of chromium substituted magnesium ferrite was reported by Kawade et al [10] and found that, the lattice parameters decrease with Cd^{3+} substitution and the X-ray density decreases as Cd^{3+} content increases. The distance between magnetic ions in both octahedral and tetrahedral sites decreases with increase in Cd^{3+} .

In this research paper, we present a systematic investigation of the preparation and acetone gas sensing properties of Cd-substituted magnesium ferrites. Through a combination of synthesis techniques, structural characterization, and gas sensing measurements, we aim to elucidate the influence of Cd doping on the microstructure, surface chemistry, and sensing performance of the synthesized materials.

2. Experimental Details

2.1. Material Synthesis

Analytical grade reagents were utilized throughout the experiment. Nanostructured MgFe_2O_4 and $\text{Mg}_{0.4}\text{Cd}_{0.6}\text{Fe}_2\text{O}_4$ were synthesized by the sol-gel method. Initially, a precursor was prepared using the sol-gel citrate method, employing the stoichiometric ratio of ferrous nitrate, magnesium nitrate, cadmium nitrate, and citric acid. This precursor was then dissolved in ion-free water at 80°C for 2 hours. Subsequently, ethylene glycol was introduced with continuous stirring to achieve a homogeneous and stable sol. The solution underwent further heating in a pressure vessel at approximately 130°C for 12 hours. Throughout this process, the transparent solution underwent a transformation into a gel state with notably high viscosity. The material was subsequently subjected to heating in a furnace at 350°C for 3 hours, resulting in a vigorous combustion that spontaneously propagated until all the gel was consumed, leaving behind a loose powder. This powder is calcination at 650°C for 6 hours to enhance the crystallinity of the materials.

2.2. Characterization techniques

The synthesized samples were characterized for their structure and morphology by X-ray powder diffraction (XRD; Siemens D5000) and Scanning electron microscopy (SEM; Hitachi-800). The X-ray diffraction data were recorded by using $\text{CuK}\alpha$ radiation (1.5406 \AA).

2.3. Measurement of sensing properties

The gas-sensing properties of prepared $\text{Mg}_{0.4}\text{Cd}_{0.6}\text{Fe}_2\text{O}_4$ powders were studied for reducing gases such as H_2S , NH_3 , LPG and acetone whose concentration were fixed at 1000 ppm in air. The gas sensitivity (S) was defined as: $S = (R_a - R_g)/R_a = \Delta R/R_a$; where, R_a and R_g are the resistance of sensor in air and the test gas, respectively. The gas-sensing properties were measured in a temperature range of $50 - 350^\circ\text{C}$.

3. Results and Discussion

3.1. X-ray Diffraction Study

The XRD pattern of the $\text{Mg}_{0.4}\text{Cd}_{0.6}\text{Fe}_2\text{O}_4$ prepared by sol-gel method calcined at 650°C is presented in Figure 1. Study of X-ray diffraction reveals that all the compositions under investigations were found to be face centered cubic spinel structure. The XRD pattern indicates that the product has high degree of crystallinity judged from the high and sharp diffraction peaks. The average particle size of the nanocrystalline $\text{Mg}_{0.4}\text{Cd}_{0.6}\text{Fe}_2\text{O}_4$ according to the scherrer formula were in the range of 30–40 nm.

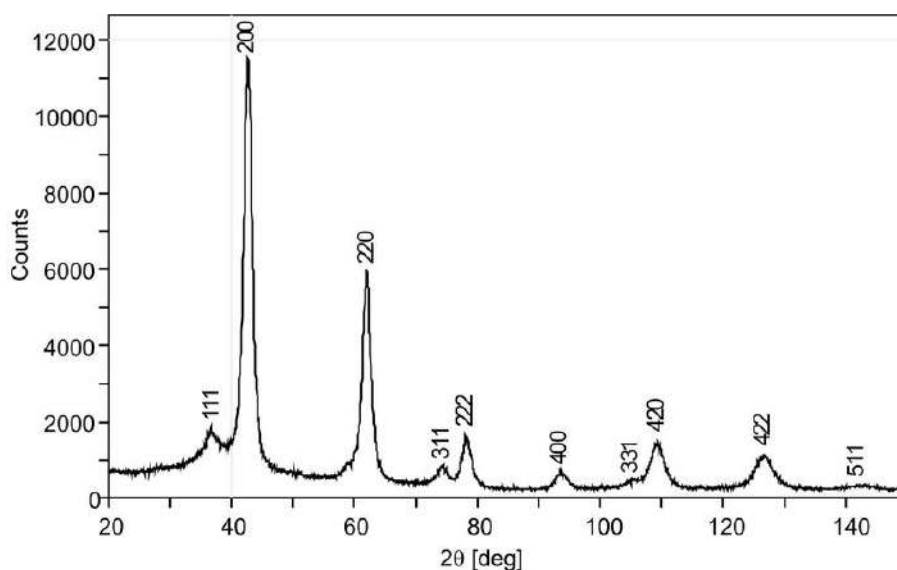


Fig 1 XRD pattern of $\text{Mg}_{0.4}\text{Cd}_{0.6}\text{Fe}_2\text{O}_4$ calcined at 650°C

3.2 Scanning Electron Microscopy

The powder sample's morphology was examined using scanning electron microscopy (SEM). Figure 2 displays the SEM image of the $\text{Mg}_{0.4}\text{Cd}_{0.6}\text{Fe}_2\text{O}_4$ powder, revealing a uniform distribution of grain sizes with a slight tendency for agglomerate formation. The formation of polycrystalline material led to particle sizes ranging between 30 to 40 nm.

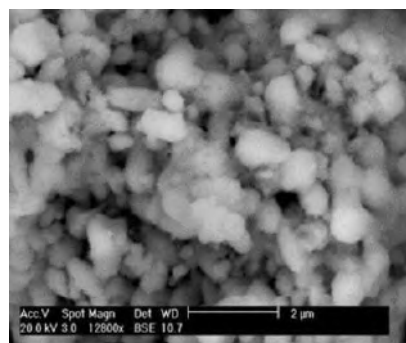


Fig 2 SEM image of $\text{Mg}_{0.4}\text{Cd}_{0.6}\text{Fe}_2\text{O}_4$ calcined at 650°C

3.3. Gas Sensing Properties

Figure 3 illustrates the sensor response (S) plotted against the operating temperature for undoped MgFe_2O_4 nanopowder, which was calcined at 650°C for 6 hours, when exposed to different reducing gases such as H_2S , NH_3 , LPG, and acetone. The sensor exhibits a notably higher response to acetone gas compared to LPG, NH_3 , and H_2S at an operating temperature of 250°C.

To enhance the gas response properties, various atoms or additives are introduced into the base sensing semiconductor. Figure 4 illustrates the gas response concerning different amounts of Cd-doped MgFe_2O_4 ($x = 0.2, 0.4, 0.6$, and 0.8). The response to acetone gas exhibits a consistent increase with the rise in Cd concentration. The highest response is observed for $\text{Mg}_{0.4}\text{Cd}_{0.6}\text{Fe}_2\text{O}_4$ ($x = 0.6$) due to the increased availability of sites for oxygen adsorption, facilitating the oxidation of the test gas. Conversely, a decrease in response may stem from an inadequate number of available sites on the surface. The partial replacement of Mg by Cd ions leads to a reduction in grain size, resulting in a higher density of grain boundaries and consequently, an increased effective exposure area of the film to ammonia gas. Additionally, the chemical composition of the semiconductor is a critical parameter influencing its sensing performance. Indeed, the composition alone can impact the microstructure and thereby dictate the sensing properties.

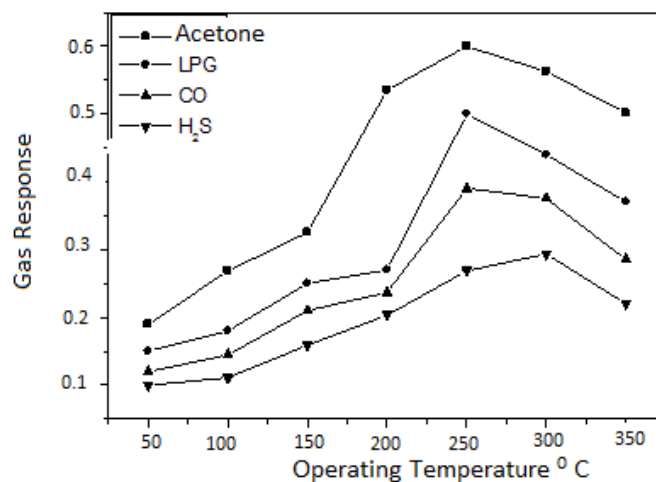


Fig 3 Gas sensing characteristics of undoped MgFe_2O_4 for various reducing gases as a function of operating temperature.

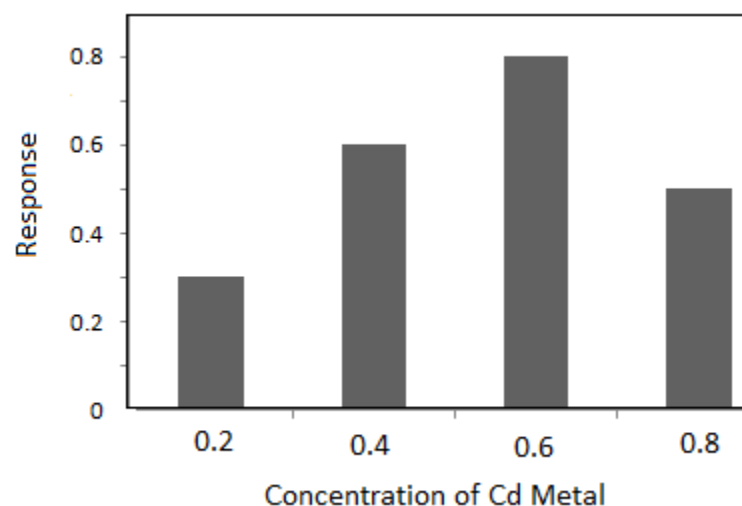


Fig 4 Sensor Response of MgFe_2O_4 doped with different amount of Cd calcined at 650°C . (a) $x=0.2$, (b) $x=0.4$, (c) $x=0.6$ and (d) 0.8

Figure 5 depicts the gas response of $\text{Mg}_{0.4}\text{Cd}_{0.6}\text{Fe}_2\text{O}_4$ across various operating temperatures. It is evident that the sensor exhibits a notably higher response to acetone gas compared to H_2S , NH_3 , and LPG at 180°C . This heightened sensitivity to acetone gas can be attributed to the surface modification achieved by Cd over the $\text{Mg}_{0.4}\text{Cd}_{0.6}\text{Fe}_2\text{O}_4$ film. The enhanced selectivity can be elucidated as follows: Upon adsorption of O_2^- on the surface of $\text{Mg}_{0.4}\text{Cd}_{0.6}\text{Fe}_2\text{O}_4$, it captures electron(s) from the n-type semiconductive $\text{Mg}_{0.4}\text{Cd}_{0.6}\text{Fe}_2\text{O}_4$ body due to the strong electronegativity of the oxygen atom, resulting in the formation of negatively charged chemisorbed oxygen species such as O_2^- , O^- , and O^{2-} . Consequently, the electron concentration within the n-type $\text{Mg}_{0.4}\text{Cd}_{0.6}\text{Fe}_2\text{O}_4$ diminishes, thereby leading to an increase in the material's resistance.

Figure 6 shows the dependence of gas response of the $\text{Mg}_{0.4}\text{Cd}_{0.6}\text{Fe}_2\text{O}_4$ sensor on the concentration level of acetone gas at 180°C . It is clear from the graph that with the increase in the concentration, the response increases linearly up to 200 ppm of acetone gas, after that it saturates. The graph also indicates that at low concentration response has a linear relationship with concentration because there may be sufficient number of available surface states to act on acetone gas. After 200 ppm level of acetone gas, the curve flattens because there would not be enough ionosorbed oxygen species to contribute to detecting mechanisms.

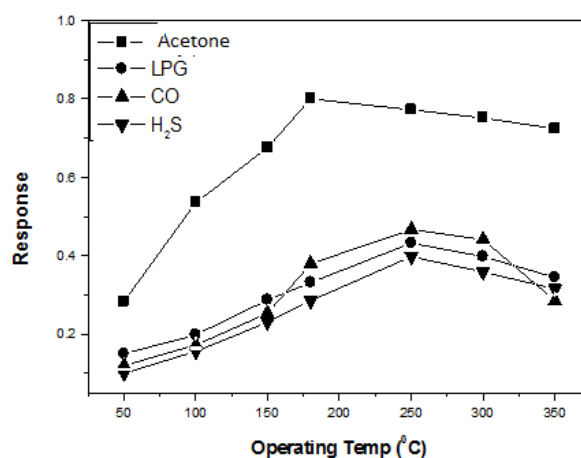


Fig 5 Response to different reducing gases of $\text{Mg}_{0.4}\text{Cd}_{0.6}\text{Fe}_2\text{O}_4$ as a function of operating temperature.

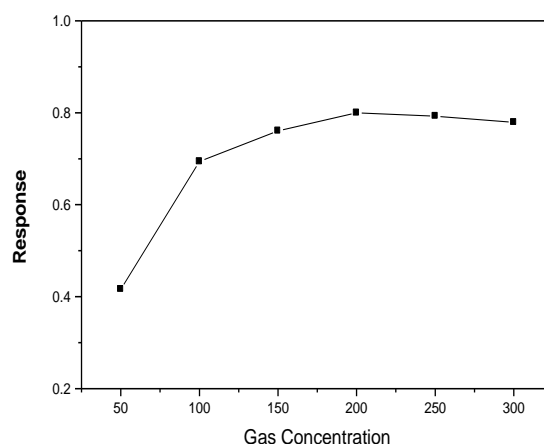


Fig 6 Response of $\text{Mg}_{0.4}\text{Cd}_{0.6}\text{Fe}_2\text{O}_4$ to acetone gas of different concentration at an operating temperature 180°C .

Figure 7 shows the response time of the sensor at 180°C . The response time in this case is ~ 40 sec. It was observed that the response time comes to saturated at 55 sec. It suggests that after this time there is no more O^- species left to react with the acetone gas vapour. It also indicates that by increasing the surface area i.e. increasing the grain size of the film, one can increase the response time.

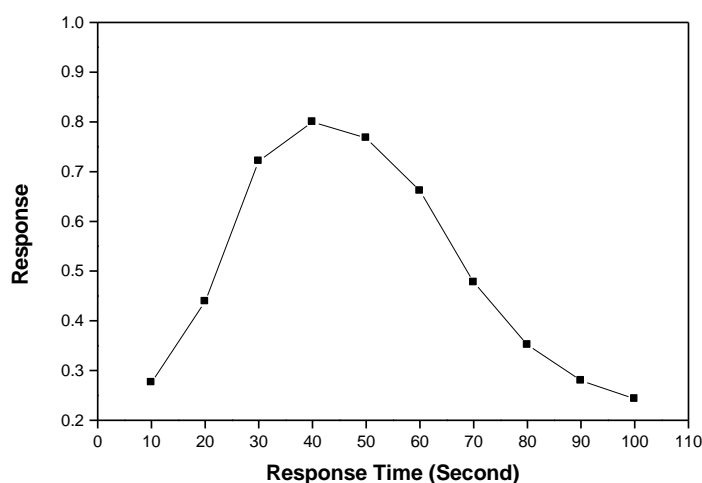


Fig 7 Response characteristics of $\text{Mg}_{0.4}\text{Cd}_{0.6}\text{Fe}_2\text{O}_4$ at 180°C .

4. Conclusion

In this study the preparation and gas sensing properties of both pure and doped MgFe_2O_4 materials synthesized through a chemical method. Structural analysis via X-ray diffraction and scanning electron microscopy revealed a nanocrystalline solid solution of MgFe_2O_4 exhibiting an orthorhombic phase, with crystallite sizes ranging between 30-40 nm. Gas sensing experiments were conducted on unmodified and surface-modified films, assessing their responses to various gases including H_2S , NH_3 , LPG, and acetone. Specifically, $\text{Mg}_{0.4}\text{Cd}_{0.6}\text{Fe}_2\text{O}_4$ powder demonstrated a significant response to 200 ppm acetone gas at an operational temperature of 180°C . The sensitivity and selectivity of $\text{Mg}_{0.4}\text{Cd}_{0.6}\text{Fe}_2\text{O}_4$ thick films were also evaluated. These findings underscore the potential of MgFe_2O_4 -

based materials for gas sensing applications, particularly in detecting acetone gas, with implications for diverse industrial and environmental monitoring scenarios.

References :

- [1] I.Z. Rahman and T.F. Ahmed., *J. Mag. and Mag. Mater.*, **2005**, 290,1576.
- [2] E.E. Sileo and S.E. Jacobo., *Phys.B: Condens. Matter.*, **2004**, 354,241.
- [3] M.V. Islam, T. Abbas, S.B. Niaz. Z. Ahed, S. Sabeen and M.A. Choudary., *Solid State Comm.*, **2004**, 130, 353.
- [4] A. Bhaskar, B. Rajinikanth and S.R. Murthy., *J. Mag. and Mag. Mater.* , **2004**, 283,109.
- [5] Y.J.Yang, C.I Sheu, S.Y. Cheng and H. Chang., *J. Mag. and Mag. Mater.*, **2004**, 284, 220.
- [6] A.Thakur and M. Singh., *Ceramics Inter.*, **2003**, 29, 505.
- [7] K.M. Jadhav, V.B. Kawade, K.B. Modi, G.K. Bichile, R.G. Kulkarni., *Phys.B: Conds. Matter.* **2000**, 291, 379.
- [8] S. Yan, J. Geng, L. Yin and E. Zheu., *J. Mag. and Mag. Mater.*, 2004, 277, 84.
- [9] K. B. Modi J. D. Gajera, M. C. Chhantbar, K. G. Saija, G. J. Baldha and H. Joshi., *Mater. Lettrs.*, **2003**, 57,4049.
- [10] V. B. Kawade, G. K. Bichile and K. M. Jadhav., *Mater. Lettrs.*,**2000**, 42, 33.

Studies of Acoustic Properties of Substituted Chalcone in Different Percentage of Dioxane-Water Mixture

A. D. Khambre*

*Departments of Chemistry, Sant Gadge Baba Amravati University, Amravati (MS), India
Sant Gadge Baba Amravati University, Amravati
Email id _asmitakhambre@rediffmail.com

ABSTRACT--Ultrasonic velocity and density measurement of synthesized Dibromo chalcone ligand were carried out in different percentage of Dioxane-water mixture at $30 \pm 0.1^\circ\text{C}$. The obtained experimental data have been used to evaluate acoustical parameters such as intermolecular free length, specific acoustic impedance, relative association, adiabatic compressibility, apparent molal compressibility, and apparent molal volume. These parameters are used to interpret solute-solvent, solute-solute interaction in the system.

Keywords --- 1,4-Dioxane, ligand, Ultrasonic velocity, intermolecular free length, metal ions etc.

INTRODUCTION

The ultrasonic velocity technique is one of the most powerful techniques for studying the nature of intermolecular interaction in liquid. The ultrasonic velocity and other acoustic parameters can be measured with great accuracy and provides a powerful way to determine intermolecular interactions. The ultrasonic studies are useful in extensive research in different field of science [1-4]. This is because of its ability of characterizing physicochemical behaviour of liquid medium [5-6]. The measurements of ultrasonic velocity are helpful to interpreted solute- solvent, ion-solvent interaction in aqueous and non-aqueous medium [7-8]. Numerous workers have done the acoustical study by the measurement of density and ultrasonic velocity of different aqueous and non-aqueous system at different temperature, different concentration of solute and in different percentage of organic solvent [9-11]. The ultrasonic and viscometric studies of α amino acids in different percentage of aqueous dioxane systems have been carried out by Raut et al [12]. The ultrasonic interferometric investigations of 3-(chloroaryl)-5-aryl-1-substituted pyrazolines in different percentage of dioxane medium at different temperature have studied by Deshmukh and Raghuvanshi [13]. They are reported that the ultrasonic velocity decreases with increase in percentage of organic solvent. Thorat S. A. and Thakur S. D. have studied the ultrasonic behaviour and molecular interaction of substituted 3,5-diaryl isoxazoline in different percentage DMF-water mixture at 305 K. They reported that there is weak solute-solvent interaction in all systems [14]. Deosarkar et al investigated the acoustical studies of some pyrazoles in different percentage of dioxane-water mixture at 303.15 K at 2 MHz frequency. They observed that the interactions are exist between pyrazoles and dioxane water mixture and solute-solvent interactions are more favorable than other interactions [15]. The ultrasonic behaviour and study of molecular interactions of chalcone in dioxane at different concentrations and in different percentages of dioxane- water mixture at 305 K at 1 MHz frequency have been investigated by Pathare [16]. The present work deals with the effect of different percentage of Dioxane-water mixture on acoustical parameters of synthesized Schiff base ligand at $30 \pm 0.1^\circ\text{C}$.

EXPERIMENTAL

The Dibromo Chalcone ligand were synthesized in the laboratory by literature method [17]. All the chemicals used are of good analytical grade (AR). The solution of solute was

prepared by dissolving required amount of ligand in different percentage of purified Dioxane-water solvent. The acoustical parameters are determined at fixed concentration of solute 1×10^{-3} M. The density of solvent and solutions were measured by specific gravity bottle having 10 ml capacity. The ultrasonic velocities were measured by using ultrasonic interferometer having frequency 2MHz (Mittal Enterprises Model No. F-80). The constant temperature was maintained by circulating water through the double wall measuring cell, made up of glass.

THEORY AND CALCULATION

The sound velocity of ligand was measured in different percentage of dioxane-water mixture. The wavelength of ultrasonic wave is calculated using relation,

$$2D = \lambda \quad \text{----- (1)}$$

Where, λ is wave length and D is distance in mm. The ultrasonic velocity is calculated by using relation,

$$\text{Ultrasonic velocity (U)} = \lambda \times \text{Frequency} \times 10^3 \quad \text{----- (2)}$$

Some acoustical parameters have been calculated using the standard relations. The adiabatic compressibility (β_s) of solvent and solution are calculated by using equations

$$\text{Adiabatic compressibility solution } (\beta_s) = 100 / U_s^2 \times d_s \quad \text{----- (3)}$$

$$\text{Adiabatic compressibility solvent } (\beta_0) = 100 / U_0^2 \times d_0 \quad \text{----- (4)}$$

$$\text{Acoustic impedance (Z)} = U_s \times d_s \quad \text{----- (5)}$$

Where, U_0 , d_0 , β_0 and U_s , d_s , β_s are ultrasonic velocity, density and adiabatic compressibility of solvent and solution respectively.

$$\text{Intermolecular free length (Lf)} = K \times \sqrt{\beta_s} \quad \text{----- (6)}$$

$$\text{Relative association (R}_A\text{)} = (d_s / d_0) \times (U_0 / U_s)^{1/3} \quad \text{----- (7)}$$

Where, K is Jacobson's constant[19] is calculated by using relation,

$$K = (93.875 + 0.375 \times T) \times 10^{-8} \quad \text{----- (8)}$$

Where, T is temperature at which experiment is carried out.

Apparent molal compressibility (ϕ_k) has been calculated by using the relation,

$$\beta_s d_0 - \beta_0 d_s = \beta_s \times M$$

$$(\phi_k) = 1000 \times \beta_s d_0 - \beta_0 d_s / m \times d_s \times d_0 + \beta_s \times M / d_s \quad \text{----- (9)}$$

Apparent molal Volume (ϕ_v) has been calculated by using the relation,

$$M (d_0 - d_s) \times 1000 (\phi_v) = M / d_s \times (d_0 - d_s) \times 1000 / m \times d_s \times d_0 \quad \text{----- (10)}$$

$$\phi_k(s) = \phi_k^0(s) + S_{k(s)} \sqrt{m} \quad \text{----- (11)}$$

$$\phi_v = \phi_v^0 + S_v \sqrt{m} \quad \text{----- (12)}$$

RESULT AND DISCUSSION

In the present investigation, different acoustical properties such as ultrasonic velocity (U_s), density (d_s), adiabatic compressibility (β_s), intermolecular free length (Lf), specific acoustic impedance (Z), apparent molal volume (ϕ_v), apparent molal compressibility ($\phi_k(s)$),

relative association (R_A) are listed in table. It is found that ultrasonic velocity decreases with decrease in percentage of dioxane. The ultrasonic velocity is related to intermolecular free length. The variation of ultrasonic velocity in solution depends upon the increase or decrease of intermolecular free length after mixing the solute is based on a model for sound propagation proposed by Eyring and Kincaid[20]. The intermolecular free length (L_f) increases with increasing the percentage of dioxane, hence decrease in ultrasonic velocity with increasing the percentage of dioxane. This indicates that there is a weak interaction between ion and solvent molecules which suggesting a structure non-promoting behavior of the added solute. This also implies increase in number of free ions showing the occurrence of ionic dissociation due to weak ion-ion interactions.

The value of specific acoustic impedance (Z) decreases with decrease in the percentage of dioxane for given system. This is due to decrease in the strength of intermolecular attraction. The specific acoustic impedance (Z) is directly proportional to ultrasonic velocity and inversely proportional to adiabatic compressibility and shows similar behaviour to that of ultrasonic velocity and opposite to that of adiabatic compressibility. It was found that the value of adiabatic compressibility increases with decrease in percentage of dioxane indicates that there is weak solute-solvent interaction may be due to departure of solvent molecules around ions. The relative association is the property used to understand the interaction in solution. The relative association is measure of extent of association of the component in the mixture. The value of relative association decreases with decrease in percentage of Dioxane-water solvent.. This is due to the breaking up of the associated solvent molecules on addition of dioxane in it. It was observed that apparent molal volume decreases with decrease in percentage of Dioxane-water solvent the system. It indicates the existence of weak ion-solvent interaction. The apparent molal volume increases due to decreasing dielectric constant of medium with increase in percentage of Dioxane-water solvent.

The value of apparent molal compressibility decreases with decreases in percentage of Dioxane-water solvent for the system. The positive value of apparent molal compressibility shows the strong electrostatic attractive force in the vicinity of ions causing electrostatic solvation of ions

Table

Acoustic Properties of ligand (L) at different percentages in Dioxane-water Mixture

% of Dioxane	U_s (m.sec ⁻¹)	ρ_s (g.cm ⁻³)	B_s (bar ⁻¹)	L_f (Å)	ϕ_v (cm ³ mole ⁻¹)	$\phi_{k(s)}$ (cm ³ mole ⁻¹ bar ⁻¹)	R_A	Z (cm.sec ⁻¹ .cm ⁻³)
100	1630.22	0.9039	5.04×10^{-4}	13.51×10^2	1006.11	25.36	0.9176	14773.55
95	1584.30	0.9125	4.77×10^{-4}	13.14×10^2	900.18	15.92	0.9194	1467.57
90	1560.45	0.9275	4.52×10^{-4}	12.80×10^2	723.23	10.42	0.9285	1456.59
85	1544.15	0.9385	4.35×10^{-4}	12.56×10^2	595.86	6.92	0.9354	1449.18
80	1514.65	0.9481	4.20×10^{-4}	12.33×10^2	487.63	3.42	0.9410	1436.04
75	1480.85	0.9510	4.03×10^{-4}	12.08×10^2	455.46	1.09	0.9479	1408.28

CONCLUSION

The present study shows the experimental data for ultrasonic velocity, density at $30 \pm 0.1^\circ\text{C}$ for synthesized Dibromo Chalcone in 70% Dioxane-water mixture. From experimental

data, the acoustical properties were calculated. The solute-solvent interaction and ion-ion / solute-solute interaction existing between Dibromo Chalcone ligand and different percentage of dioxane were also studied with the help of experimental data. Lastly it has been concluded from the experimental data, that the solute-solvent interaction in Dibromo Chalcone and dioxane systems are weak.

ACKNOWLEDGEMENT

The Author are thankful to Principal, vidarbha mahavidyalay, amravati for providing necessary facilities and for kindly cooperation.

REFERENCES

- [1] K. Balaramamoorthy, V. A. Chandramouli and N. Kondal Rao, J. Sci. Ind, Res., 32(12), 1973, 747.
- [2] Y. Tanaka, M. Ido, Y. Umeki and S. Honda, Bull. Jp. Soc. Prec. Eng., 1975, 9(4), 99.
- [3] D. A. Bell, Br. Brit. Cer. Trans., 1989, 88.
- [4], 133. [4] O. Doutres, Y. Salissou, N. Atalla and R. Panneton, Appl. Acous., 2010, 71, 506..
- [5] M. Gupta and J. P. Shukla, Indian J Pure Appl Phys., 1996, 34, 772.
- [6] Pankaj and C. Sharma, Ultrasonics, 1991, 29, 344.
- [7] S. Balaja and S. Oza, Fluid Phase Equilibria, 2002, 200, 11-18.
- [8] S. S. Aswale, D. T. Tayade, S. R. Aswale and P. B. Raghuvanshi, Proceedings of 1st International Society Bio-Technology Conference, Gangtok, 2008, 325.
- [9] S. D. Thakur, D. T. Mahajan and M. L. Narwade, J. Ind. Chem. Soc., 2007, 84(5), 480..
- [10] S. A. Ikhe, P. R. Rajput and M. L. Narwade, Ind. J. Chem. A, 2005, 44(12), 2495.
- [11] G. V. Ramana, E. Rajagopal and N. M. Murthy, J. Pure Appl. Ultrason., 2005, 27, 98..
- [12] Raut A. R., Mhaske S. T. and Murhekar G. H. (2015), Int. J. Curr. Res. Chem., Pharma. Sci., 2(10), 79-83..
- [13] Deshmukh A. O. and Raghuvanshi P. B. (2015), Int. J. Chem. Tech. Res., 8(10), 375-382. [14] Thorat S. A. and Thakur S. D. (2015), Sci. Revs. Chem. Commun., 5(2), 57-61..
- [15] Deosarkar S. D., Jahagirdar H. G. and Talwatkar V. B. (2010), Rasayan J. Chem., 3(4), 757-760..
- [16] Pathare Unnati A. (2016), J. Appli. Chem., 9(2), 68-70.
- [17] S. S. Lamani Kumar, Oblennavar Kotresh, M. A. Phaniband and J. C. Kadakol, E. Journal of Chemistry, 2009, 6 (S1), S239-S246..
- [18] Vogel's "A Text Book of Practical Organic Chemistry" (1989), Vth edition, Longman Scientific and Technical, John Wiley and Sons, New York, 401.
- [19] K. Sreekanth, D. Sravanakumar, J. Chem. Pharma Res., 2011, 3(4), 29-41.
- [20] Eyring H. and Kincaid J. F. (1938), J. Chem. Phys., 6, 620.

8

Synthesis, Physicochemical evaluation of heteryl amino derivatives of bis[5-cyano-1,6-dihydro-6-imino-2-isopropyl-4-(methylthio) pyrimidine] diazene**Girish Deshmukh*¹ Avinash Thakare², Chanda Gawande³**

1, 2. Shankarlal Agrawal Science College, Salekasa

3. S.Chandra Mahila Mahavidyalaya, Amgaon, Maharashtra (INDIA)

Email: girish.deshmukh2@gmail.com**Abstract:**

Study of the synthesis and pharmacological evaluation of heteryl amino derivatives of bis[5-cyano-1,6-dihydro-6-imino-2-isopropyl-4-(methylthio)pyrimidine]diazene, we obtained good result Antimycobacterium activity and Antityphoid activity.

Introduction:

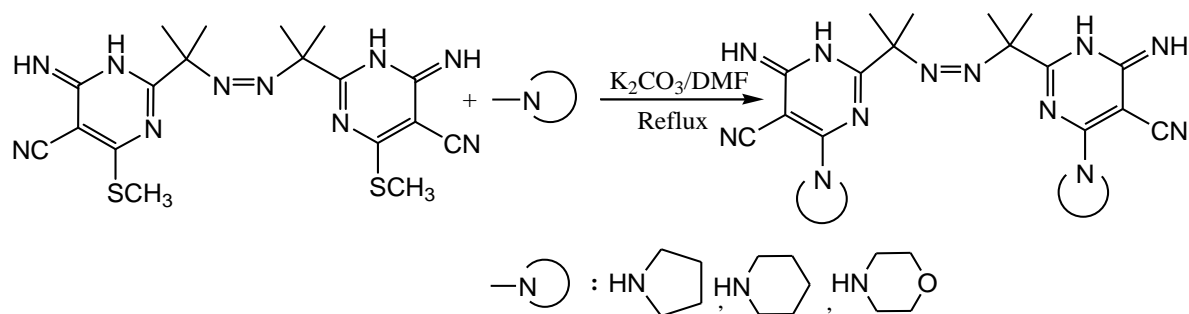
The understanding of principles of drug design and development of the drug molecules is important study the physicochemical properties of chemical compounds used to develop novel pharmacologically active compounds. The biological activities, mechanism of actions, possible biological activities of the metabolites and significance of stereochemistry for molecules are important factors for new drug design [1]. All these principles are based on the basic organic chemistry, physical chemistry and biochemistry. Heterocyclic compounds contain, one or more atoms of other elements apart from carbon, common hetero atoms are sulphur, nitrogen and oxygen [2]. The heterocyclic compounds having less common atoms such silicon, bromine, phosphorus, tin, boron are much investigated in recent years. The heterocycles with five or six atoms in the ring are the most important [3]. The practice of medicinal chemistry is devoted to the research in development of new disease treating agent. The process of finding a new drug is complex and involves talent of people from variety of disciplines [4]. The important aspect of medicinal chemistry is to establish a relationship between pharmacological activity and chemical structure [5].

Pyrimidine is a six membered cyclic compound containing 2 nitrogen and 4 carbon atoms which is pharmacologically inactive however its substituted derivatives shows an important place in modern medicine [6]. Pyridazine 1, oxygenated derivative-pyridazinone 2 and benz fused pyridazine or phthalazine 3 are heterocyclic compounds that contain two adjacent nitrogen atoms (1,2-diazine) in the ring structure [7]. They show a high range of pharmacological activities and are found in different natural compounds with different biological activities [8]. Many heterocyclic compounds obtained from synthetic as well as natural sources, generally in practice have one or more nitrogen in the heterocyclic ring system. Diazines (1,2/1,3/1,4) are important heterocyclic rings. Recently, much attention has been focused on diazine derivatives for their broad-spectrum pharmacological activities [9].

Present Work:

The newly synthesised molecule possesses two methylthio groups which can be easily substituted with heteryl amines that can be marked.

Heteryl amino derivatives of can be prepared by reacting it with substituted heteryl amines in 1:2 proportion using DMF solvent and anhydrous K₂CO₃ catalyst to yield compounds



Scheme: Synthesis of heteraryl amino derivatives of bis[5-cyano-1,6-dihydro-6-imino-2-isopropyl-4-(methylthio) pyrimidine] diazene

Results and Discussion:

In the study of optimization of reaction condition and solvent for the synthesis of heteraryl amino derivatives of bis[5-cyano-1,6-dihydro-6-imino-2-isopropyl-4-(methylthio) pyrimidine] diazene we have obtained low yield at room temperature than the reaction carried out at the reflux condition.

Experimental Section:

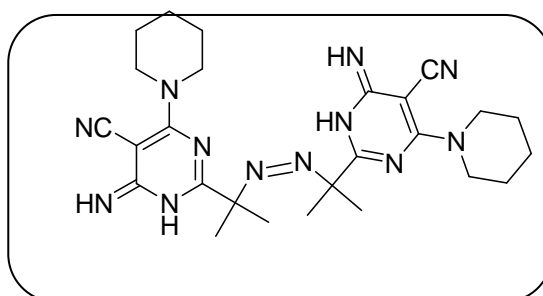
All chemicals procured from spectrochem, Alfa Aesar, SDfine, Sigma Aldrich were used without further purification. The IR spectra were recorded with Shimadzu FTIR. The melting points were recorded using Veego digital melting point apparatus. The NMR spectra were recorded with Bruker 400MHz using DMSO-d₆ solvent.

General Procedure:

Compound (0.442 g, 1 mmol) and different heteraryl amines, (1 mmol) in 1:2 proportion using 15 ml of DMF as solvent and catalyst anhydrous K₂CO₃ as catalyst (10 mg) reflux for 5-7 hours, the progress of reaction was monitored by TLC. The reaction mixture was cooled to room temperature and poured into ice cold water. The separated solid product was filtered off, washed many times with water and recrystallized from ethanol.

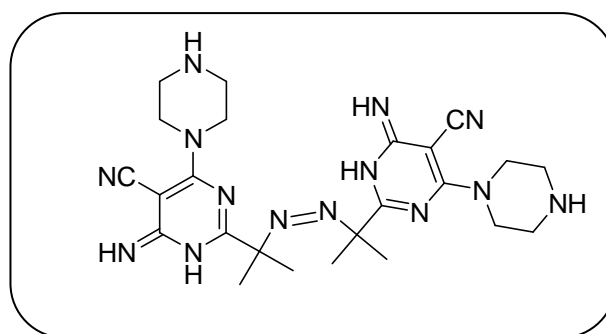
Spectral Data:

1) bis[5-cyano-1,6-dihydro-6-imino-2-isopropyl-4-(piperidinyl) pyrimidine] diazene



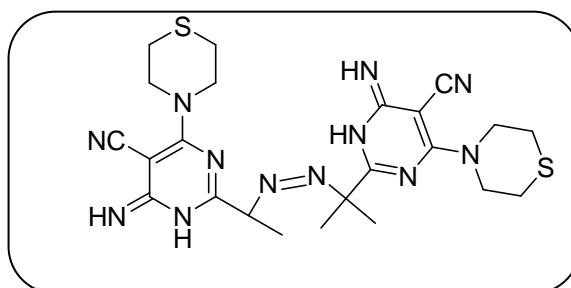
- **Molecular Formula** : C₂₆H₃₆N₁₂
- **Mol. Weight (g/mol)** : 516.6
- **IR(KBr) (cm⁻¹)** : 3300(=NH), 2198 (CN), 1616 (C=N)
- **¹H NMR (δ, ppm) (DMSO-d₆)** : 1.24 (q, 8H), 1.36 (s, 12H), 2.82 (t, 8H), 3.86 (s, 2H), 9.21(s, 2H)
- **Mass (m/z)** : 372.2, 516.4 (M⁺)

2) bis[5-cyano-1,6-dihydro-6-imino-2-isopropyl-4-(p-piperazinyl) pyrimidine]

diazene

- **Molecular Formula** : $C_{24}H_{34}N_{14}$
- **Mol. Weight (g/mol)** : 518.6
- **IR(KBr) (cm^{-1})** : 3309 (=NH), 2204 (CN), 1610 (C=N)
- **1H NMR (δ , ppm) (DMSO- d_6)** : 1.35 (s, 12H), 3.08 (t, 8H), 3.10 (t, 8H), 3.82 (s, 2H), 8.00 (s, 2H)
- **Mass (m/z)** : 332.6, 518.9(M^{+})

3) bis[5-cyano-1,6-dihydro-6-imino-2-isopropyl-4-(4-thiomorpholino)pyrimidine] diazene



- **Molecular Formula** : $C_{24}H_{32}N_{12}S_2$
- **Mol. Weight (g/mol)**: 552.7
- **IR(KBr) (cm^{-1})** : 3301 (=NH), 2198 (CN), 1606 (C=N)
- **Mass (m/z)** : 477.1, 552.6 (M^{+})

Table: Synthesis of heteryl amino derivatives of bis[5-cyano-1,6-dihydro-6-imino-2-isopropyl-4-(methylthio) pyrimidine] diazene

Entry	Substrate	Product	Reaction Time (h)	Yield (%)	M.P. ($^{\circ}C$)
a			5.0	74	194

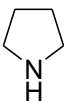
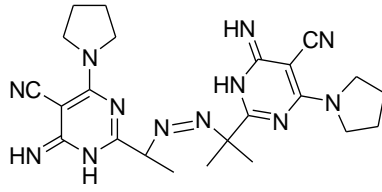
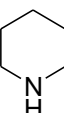
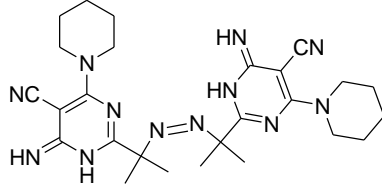
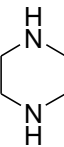
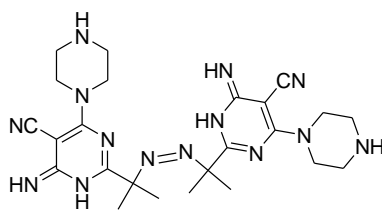
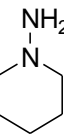
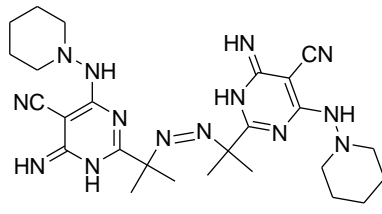
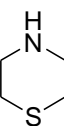
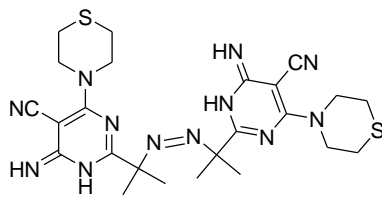
b			5.5	70	186
c			6.5	67	180
d			4.5	78	203
e			5.0	79	178
f			6.5	83	182

Table : Physicochemical evaluation of heteryl amino derivatives bis[5-cyano-1,6-dihydro-6-imino-2-isopropyl-4-(methylthio) pyrimidine] diazene
Solvent: DMSO

Sr. No.	Compound (0.1M)	Density (ρ) (g/cm³)	Viscosity (μ*10³) poise	Refractive Index (n)
1	3.19a	0.9520	6.3465	1.5423
2	3.19b	0.9689	6.8745	1.5279
3	3.19c	0.9588	7.9472	1.5364
4	3.19d	0.9637	6.3120	1.5457
5	3.19e	0.9697	7.1857	1.5663
6	3.19f	0.9884	6.4412	1.4666

References:

1. Zanatta, N.; Flores, D. C.; Madruga, C. C.; Flores, A. F. C.; Bonacorso, H. ; *Tetrahedron Lett.***2006**, 47, 573.
2. Amir M., Javed SA, Kumar H ;*Indian J. Pharm. Sciences*, **2007**, 69(3): 337.
3. Jain M. K., Sharnevas SC,*Organic Chem.* **2008**, 3: 997.
4. Sasada T, Kobayashi F, Sakai N, Konakahara T; *Org. Lett.***2009**, 11, 2161.
5. Zhichkin P, Fairfax D J, Eisenbein S A; *Synthesis*, **2002**, 720.
6. Ahmad O. K., Hill M D, Movassaghi M; *J. Org. Chem.*, **2009**,74: 8460.
7. Barthakur M. G., Borthakur M, Devi P, Saikia C J, Saikia A, Bora U; *Synlett*, **2007**, 223.
8. Karpov S. and Mulle T J J; *Synthesis*, **2003**, 2815.
9. Movassaghi M., Hill M. D.; *J. Am. Chem. Soc.*, **2006**, 128: 14254.
10. Ghorab M. M., Heiba MI, Hassan AA; *JACS*.**2011**,7(1),1063.
11. Kappe C. O.; *Eur J Med Chem*.**2000**, 35(12), 1043.
12. Brown D. J. *New York: Pergamon press*, **1984**. 57.
13. Callery P., Gannett P.; *Philadelphia Lippincott Williams and Wilkins*, **2002**. 934.
14. Polak A., Scholer HJ. ;*Chemotherapy*. **1975**, 21, 113.
15. Cheng C., Roth B. In: Ellis GP; *8th ed. London: Butterworths*, **1982**. 267.
16. Ghomi A. S., Ali M.; Dig J Nanomater Biostruct **2010**,5(2):303.
17. Lagoja I. M.; *Chem Biodivers***2005**, 2(1):1.
18. Brown D. J., Evans R. F., Cowden UK; *Pergamon Press Oxford*; **1984**.15.
19. Elderfield R. C. *John Wiley & Sons New York*; **1957**. 6.
20. Agarwal O. P. *Krishna Prakashan Media (P) Ltd.*; **2006**. 735.
21. Porter A. E. *Pregamon Press, Elsevier Science BV Amsterdam*; **1979**. 14.
22. Gavilan M. D., Gomez-Vidal J. A., Serrano F. R.;*Chem Lett***2008**; 18, 1457.
23. Ali M., Azad M., Siddiquia H. L., Nasim F. H.; *J Chinese Chem Soc*, **2008**; 55, 394.
24. Siddiqui A. B., Trivedi A. R., Kataria V. B., Shah ;*Bioorg Med Chem Lett*,**2014** 15, 24, 1493.
25. S. Cao, X. Qian, G. Song, B. Chai, and Z. Jiang; *Journal of Agricultural and Food Chemistry*,**2003**, 51, 152.
26. K. Abouzid, M. Abdel Hakeem, O. Khalil, and Y. Maklad; *Bioorganic & Medicinal Chemistry*, 2008,16, 1, 382.
27. W. Malinka, A. Redzicka, O. Lozach, ;*Il Farmaco*, **2004**,59, 6, 457.
28. Jain, K. S.; Chitre, T. S.; Miniyar, P. B.; Kathiravan, M. K.; Bendre, V. S.; Veer, V.S. *J. Curr. Sci.* **2006**, 90, 793.
29. Botta, M.; Corelli, F.; Maga, G.; Manetti, F.; Renzulli, M.; Spadari, S.; *Tetrahedron***2001**, 57, 8357.

Novel Synthesis and Characterization of Some Substituted Chlorosubstituted Aryl Substituted 1,3-Thiazole as Antibacterial Agents

Chhaya D. Badnakhe¹

¹ Department of Chemistry, Dr.Manorama and Prof.H.S.Pundkar, Arts, Commerce and Science College, Balapur, Dist. Akola.

E-mail : chhayadeotalu@rediffmail.com

Abstract :- The synthesis, spectral analysis and biological activities of 5-(2'-hydroxy-3',5'-dichlorophenyl)-4-heptan-1-one-2-[4-(2-hydroxy-3,5-dichlorophenyl)-2-mercapto-imidazolo]-1,3-thiazole (8d₂) (J'') have been carried out. In this case 5-(2'-hydroxy-3',5'-dichlorophenyl)-4-(heptan-1-one)-2- amino-1,3-thiazole (8d) (J), 5-(2'-hydroxy-3',5'-dichlorophenyl)-4-heptan-1-one-2-[(2-hydroxy-3,5-dichlorophenyl) ethanonylamino]-1,3-thiazole (8d₁) (J') & 5-(2'-hydroxy-3',5'-dichlorophenyl)-4-heptan-1-one- 2-[4-(2-hydroxy-3,5-dichlorophenyl)-2-mercapto-imidazolo]-1,3-thiazole (8d₂) (J'') have been screened. The compound (J) was synthesized from 1-(2'-Hydroxy-3',5'-dichlorophenyl)-2-bromo-1,3-nonanedione (a₄) by the action of thiourea, while (J'') was synthesized from (J) by reaction with α -bromo, 2-hydroxy-3,5 dichloroacetophenone to get 5-(2'-hydroxy-3',5'-dichlorophenyl)-4-heptan-1-one-2-[(2-hydroxy-3,5-dichlorophenyl)ethanonylamino]-1,3-thiazole (8d₁) (J'). Further (J') on treatment with KSCN was dissolved in acetic acid gave (J''). The nanoparticles of the compounds J, J' and J'' have been prepared by using ultrasonic technique. The newly synthesized titled compound and it's nanoparticles were screened for their antibacterial activity against some pathogens ; Gram+ve bacteria viz. Staphylococcus pneumoniae, Staphylococcus aureus and Gram-ve bacteria viz. Escherichia coli and Pseudomonas fluorescens by using agar disc diffusion method. All the newly synthesized compounds were found to be active against test pathogens.

Keywords : Chalcone, thiazine, thiourea, α -bromo,2-hydroxy-3,5 dichloroacetophenone, KSCN was dissolved in acetic acid, antibacterial assay.

INTRODUCTION : Heterocyclic nucleus plays an important role in medicinal chemistry and it is a key template for the growth of various therapeutic agents. Thiazole is a heterocyclic compound featuring both a nitrogen atom and sulfur atom as part of the aromatic five-membered ring. Thiazoles and related compounds are called 1,3-azoles (nitrogen and one other hetero atom in a five-membered ring). They are isomeric with the 1,2-azoles, the nitrogen and sulphur containing compound being called isothiazoles. Thiazoles are found naturally in the essential vitamins. Molecules that possess sulfur atoms are important in living organisms. Chalcones and their analogues having α , β -unsaturated carbonyl system are very versatile substrates for the evolution of various reactions and physiologically active compounds. Plant Pathology or Phytopathology deals with the cause, etiology, resulting losses and control or management of the plant diseases.

. It is the scientific study of diseases in plants caused by pathogens (infectious organisms) and environmental conditions (physiological factors). Organisms that cause infectious disease include fungi, oomycetes, bacteria, viruses, phytoplasmas, protozoa, nematodes and parasitic plants.

The researchers⁽¹⁻⁶⁾ have reported the synthesis of several thiazoles and also their potent biological activities such as antimicrobial⁷, antibacterial⁸, antifungal⁹, fungicidal¹⁰ and

insecticidal agent¹¹.

Now a days nanotechnology is a promising field of interdisciplinary research. It opens up a wide array of opportunities in various fields like medicine, pharmaceuticals, electronics and agriculture. Since the physiochemical properties of nanoforms vary greatly, it becomes important to examine the effect of nanoparticles on microorganisms to harness the benefit of this technology in the plant protection especially against phytopathogens. Previous studies confirmed that metal nanoparticles are effective against pathogens, insects and pests. Hence nanoparticles can be used in the preparation of new formulations like nanomedicines for the diseases like diagnosing & treating cancer¹², enhancing outer membrane of living cells¹³, inhibiting tumour growth in human being¹⁴, brain cancer¹⁵. Nanotechnology has the potential to revolutionize the different sectors of agriculture and food industry with modern tools for the treatment of diseases by providing the medicines for rapid diseases like malaria¹⁶, cancer & HIV¹⁷, breast cancer¹⁸, localized diseases¹⁹.

In the present study, the chlorosubstituted 1,3-thiazole & their imidazole derivatives (J'') have been prepared along with their nanoparticles and screened them for their antibacterial activities against some Gram+ve bacteria viz. *Staphylococcus pneumoniae*, *Staphylococcus aureus* and Gram-ve bacteria viz. *Escherichia coli* and *Pseudomonas*. All the newly synthesized compounds were found to be active against test pathogens.

EXPERIMENTAL :-

All the glasswares used in the present work were of pyrex quality. Melting points were determined in hot paraffin bath and are uncorrected. The purity of compounds was monitored on silica gel coated TLC plate. IR spectra were recorded on Perkin-Elmer spectrophotometer in KBr pellets, ¹H NMR spectra on spectrophotometer in CDCl₃ with TMS as internal standard. UV spectra were recorded in nujol medium. The analytical data of the titled compounds was highly satisfactory. All the chemicals used were of analytical grade. All the solvents used were purified by standard methods. Physical characterisation data of all the compounds is given in Table 1.

2'-Hydroxy 3,5'-Dichloroacetophenone:

2-Hydroxy-5-chloroacetophenone was dissolved in acetic acid (5 ml), Sodium acetate (3g) was added to the reaction mixture and then chlorine in acetic acid reagent (40 ml; 7.5 w/v) was added dropwise with stirring. The temperature of the reaction mixture was maintained below 20°C. The mixture was allowed to stand for 30 minutes. It was poured into cold water with stirring. A pale yellow solid then obtained was filtered, dried and crystallized from ethanol to get the compound 2'-hydroxy 3,5'-dichloroacetophenone.

Preparation of 1-(2'-hydroxy-3',5'-dichloro-4-hexylchalcone :

2-Hydroxy-3,5-dichloroacetophenone (0.01 mol) dissolved in ethanol (50 ml) treated with heptanaldehyde (0.1 M) at its boiling temperature. Aqueous sodium hydroxide solution [40%, 40 ml] was added dropwise and the mixture was stirred mechanically at room temperature for about 1 hour. It is then kept for 6 to 8 hours followed by decomposition with ice cold HCl [1:1]. The yellow granules thus obtained were filtered, washed with 10% NaHCO₃ solution and finally crystallized from ethanol-acetic acid solvent mixture to get the compound.

Preparation of 1-(2'-hydroxy-3'-5'-dichlorophenyl)-2,3-dibromononan-1-one (a₁) :

2'-Hydroxy-3',5'-dichloro-4-hexylchalcone (0.01 M) was suspended in bromine—

glacial acid reagent [25% w/v] [6.4 ml]. The reagent was added dropwise with constant stirring. After complete addition of reagent the reaction mixture was kept at room temperature for about 30 minutes. The solid product, thus separated, was filtered and washed with a little petroleum ether to get the compound (a_1).

Preparation of 2-(4''-hexyl)-6,8-dichloroflavone (a_2):

1-(2'-Hydroxy-3',5'-dichlorophenyl)-2,3-dibromo-nonan-1-one (0.01 mol) was dissolved in ethanol (25 ml). To this, aqueous solution of KOH (25 ml) was added. The reaction mixture was refluxed for 1 hour, cooled and diluted with water. The product, thus separated, was filtered and crystallized from ethanol to get the compound (a_2).

Preparation of 1-(2'-hydroxy-3',5'-dichlorophenyl)-1,3-nonanedione (a_3) :

2-(4''-Hexyl)-6,8-dichloroflavone (0.01 mol) was dissolved in ethanol (25 ml). To this, aqueous solution of HCl (25 ml) was added. The reaction mixture was then refluxed for one hour, cooled and diluted with water. The solid product, thus obtained, filtered and crystallized from ethanol to get the compound (a_3).

Preparation of 1-(2'-hydroxy-3',5'-dichlorophenyl)-2-bromo-1,3-nonanedione (a_4) :

1-(2'-Hydroxy-3',5'-dichlorophenyl)-1,3-nonanedione (0.01 mol) was dissolved in a mixture of ethanol (10 ml) and dioxane (10 ml). To this, calculated amount of liquid bromine (0.5 ml) was added. The product was not separated even after standing for one hour. It was then diluted with water and washed with water several times and extracted with ether. The solvent was removed under reduced pressure to get the white solid of the compound (a_4).

Preparation of 5-(2'-hydroxy-3',5'-dichlorophenyl)-4-(heptan-1-one)-2-amino-1,3-thiazole (J) :

1-(2'-Hydroxy-3',5'-dichlorophenyl)-2-bromo-1,3-nonanedione (a_4) (0.01 mol) and thiourea (0.01 mol) were dissolved in ethanol (25 ml). To this, aqueous KOH solution (0.01 mol) was added. The reaction mixture was then refluxed for three hours, cooled, diluted with water and acidified with conc HCl. The product, thus separated, was filtered and crystallized from ethanol to get the compound (J).

Preparation of 5-(2'-hydroxy-3',5'-dichlorophenyl)-4-heptan-1-one-2-[(2-hydroxy-3,5-dichlorophenyl)ethanonylamino]-1,3-thiazole (J'):

A stoichiometric mixture of 5-(2'-hydroxy-3',5'-dichlorophenyl)-4-(heptan-1-one)-2-amino-1,3-thiazole (J) and α -bromo-2-hydroxy-3,5-dichloro acetophenone was dissolved in ethanol and refluxed for one hour. It was then cooled, diluted with water and crystallized from ethanol to get the compound (J').

Preparation of 5-(2'-hydroxy-3',5'-dichlorophenyl)-4-heptan-1-one-2-[4-(2-hydroxy-3,5-dichlorophenyl)-2-mercapto-imidazolo]-1,3-thiazole (J''):

A stoichiometric mixture of 5-(2'-hydroxy-3',5'-dichlorophenyl)-4-heptan-1-one-2-[(2-hydroxy-3,5-dichlorophenyl)ethanonylamino]-1,3-thiazole(J') and KSCN was dissolved in acetic acid, refluxed for 4.5 hours, cooled, diluted with water, and solid product, thus obtained crystallized from ethanol to get the compound (J'').

The UV, IR, and NMR spectral data :-

Compound (J) :

UV : Spectrum No. 1

The UV-Vis spectrum of the compound (J) reported in dioxane showed λ_{\max} value 410 nm corresponding to $n \rightarrow \pi^*$ transition.

IR (KBr) :- Spectrum No. 2

3036.60 cm⁻¹ (-OH phenolic), 2955.55 cm⁻¹ (aliphatic -C-H stretching), 3036.60 cm⁻¹ (aromatic -C-H stretching), 3797.72 cm⁻¹ (-NH₂ stretching), 1538.48 cm⁻¹ (-C=N stretching), 1228.56 cm⁻¹ [(C-N=) stretching], 756.57 cm⁻¹ (C-Cl stretching in aliphatic), 1073.66 cm⁻¹ (C-Cl stretching in aromatic).

PMR :- Spectrum No. 3

δ 5.2 (hump, 2H, -N-**H**₂) ; δ 6.7 (d, 1H, -CH=C-**H**) ; δ 6.8 (d, 1H, -CH=C-H) ; δ 7 to 7.8 (m, 6H, Ar-**H**) ; offset (region not observed, observed, O-**H**)

Compound (J'') :**UV :** Spectrum No. 4

The UV-Vis spectrum of the compound J'' reported in dioxane showed λ_{max} value 399 nm corresponding to n→π* transition.

IR (KBr) :- Spectrum No. 5

1649 cm⁻¹ (=C=O stretching), 3391 cm⁻¹ (-OH phenolic), 2925 cm⁻¹ (aliphatic -C-H stretching), 3068 cm⁻¹ (aromatic -C-H stretching), 1435.8 cm⁻¹ (-C=N stretching), 1305 cm⁻¹ [(C-N) (C-NO₂) stretching], 738 cm⁻¹ (C-Cl stretching in aliphatic), 2547 cm⁻¹ (-S-H stretching).

PMR :- Spectrum No. 6

δ 7.4 to 8.25 (m, 4H, Ar-**H**) ; δ 0.80 (t, 3H, -CH₂-CH₃, δ 1.064 (envelope of CH₂, **10H**, -(CH₂)-CH₃).

Preparation of Nanoparticles of the Titled Compound:

Ultrasonic Processor Sonapros PR-250MP was used to produce nanoparticles of the test compound. The test compound was dissolved in dioxane to prepare 0.1 M solutions. This solution was taken in a beaker and the probe of the sonapras 250 MP was dipped in solution. These solution was exposed to sonopros MP 250 for 10 minutes separately. The test compound was converted to nanoparticles. The solvent dioxane was evaporated by conventional heating method. The size of nanoparticles of the test compound was confirmed by X-ray diffraction studies using Benchtop x-ray diffraction (XRD) instrument (Miniflex).

The thin film of the nanoparticles of the test compound was prepared on glass slide. This slide was introduced to the X-ray diffraction instrument to get graphical information which was used for the calculation of the crystal size of test compounds.

Characterisation of Size of Nanoparticles of the Test Compound:

The crystal size of nanoparticles of the test compound is calculated by using Debye - Scherrer equation.

$$D = \frac{0.94 \lambda}{\beta \cdot \cos \theta}$$

Where,

D = The average crystalline size.

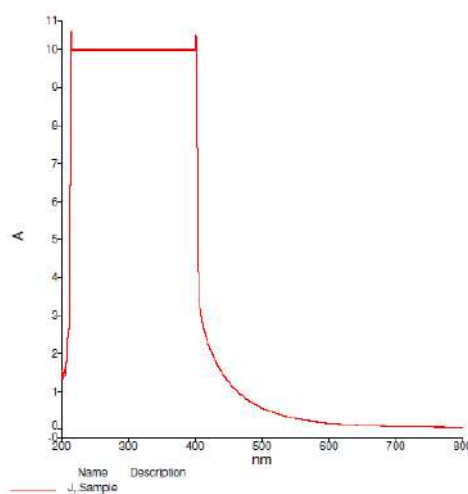
0.94 = The particle shape factor which depends on the shape and size of the particle.

λ = is the wavelength.

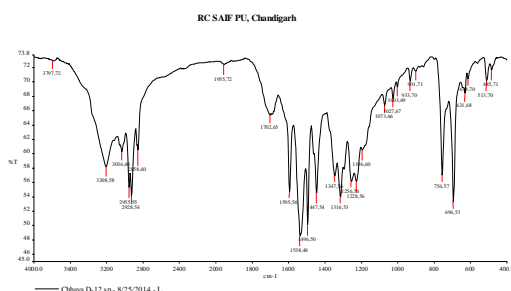
Δ = is the full width at half maximum [FWHM] of the selected diffraction peaks ($\beta = 0.545$)

2θ = is the Bragg's angle obtained from 2θ values which was corresponding to the maximum intensity peak

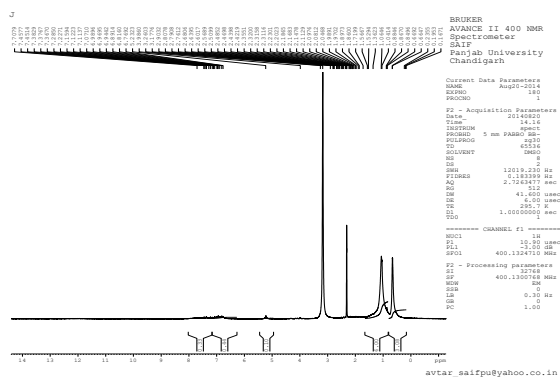
in XRD pattern ($\Delta = 0.7501$ rad).



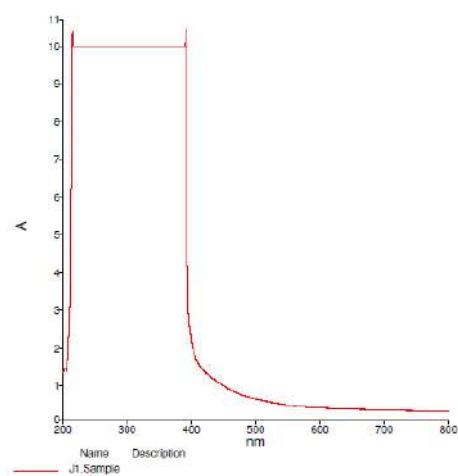
Spectrum No. 01



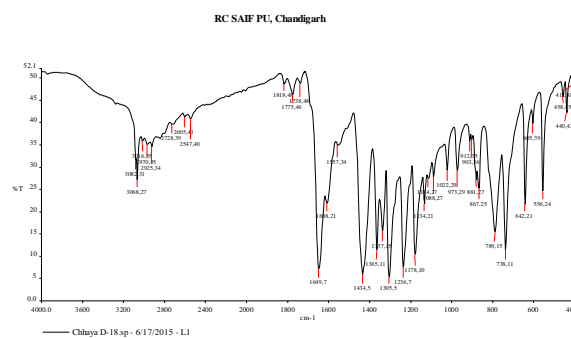
Spectrum No. 02



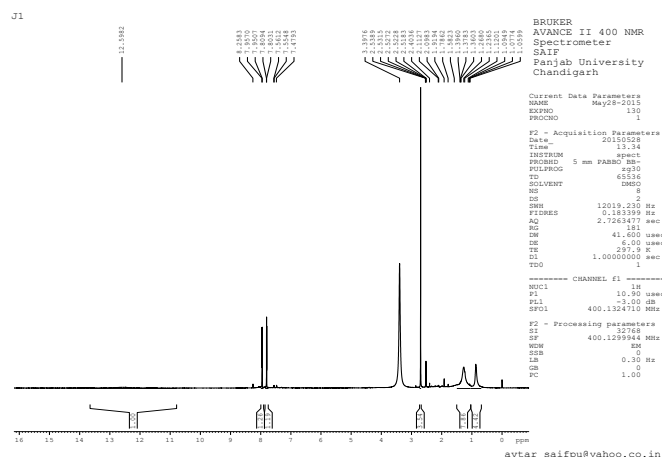
Spectrum No. 03



Spectrum No. 04



Spectrum No. 05

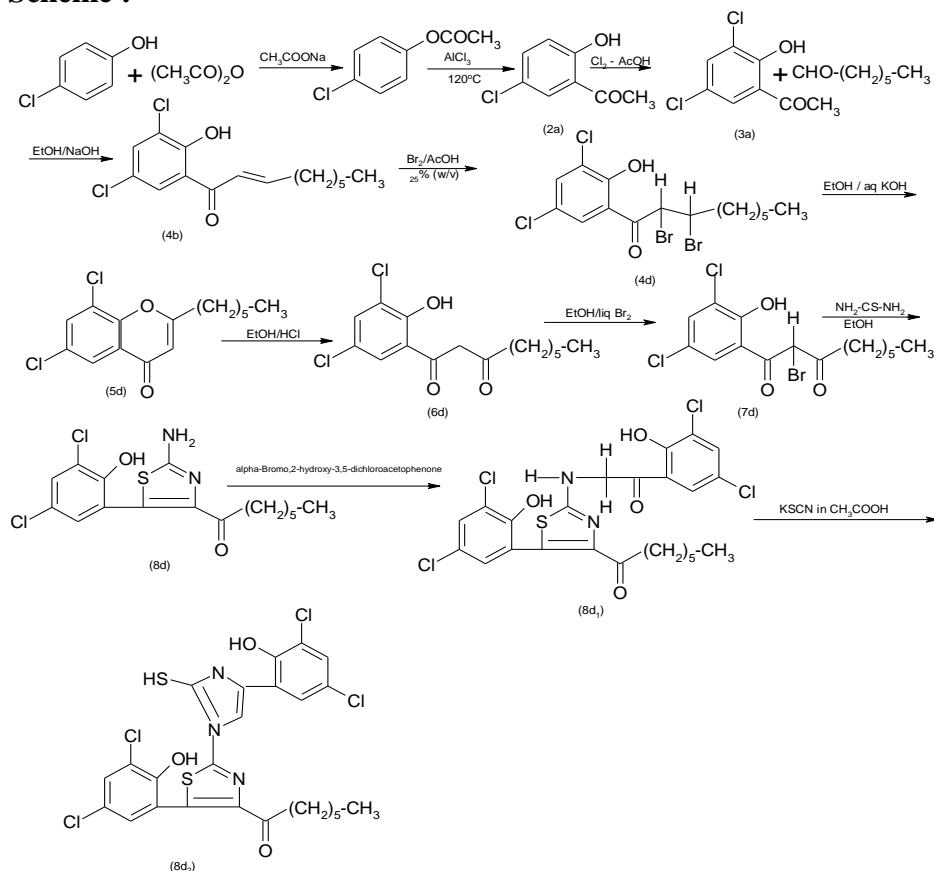


Spectrum No. 06

Table 1 : Characterisation data of newly synthesized compounds :

Compounds	Molecular formula	M.P. in °C	% of yield	% of element					
				C	H	N	S	Cl	Br
	C ₈ H ₆ O ₂ Cl ₂	54	80	47.90/48	2.95/3			34.15/34.58	
a	C ₁₅ H ₉ O ₄ NCl ₂	250	70	53.10/53.25	2.40/2.66	3.98/4.18		21/21.77	
a ₁	C ₁₅ H ₉ O ₄ NCl ₂ Br ₂	72	70	36.01/36.14	1.78/1.80	2.78/2.81		14.20/14.25	32.08/32.12
a ₂	C ₁₅ H ₇ O ₄ NCl ₂	132	60	53.14/53.57	2.07/2.08	4.13/4.16		21.03/21.13	
a ₃	C ₁₅ H ₉ O ₅ NCl ₂	117	50	50.74/50.84	2.45/2.54	3.90/3.95		20.03/20.05	
a ₄	C ₁₅ H ₈ O ₅ NCl ₂ Br	78	60	41.12/41.57	1.78/1.84	3.20/3.23		16.08/16.39	18.34/18.47
J	C ₁₆ H ₂₀ O ₂ N ₂ Cl ₂ S	96	60	51.10/51.20	5.30/5.33	7.40/7.46	7.67/7.76	17.20/17.23	
J'	C ₂₄ H ₂₂ O ₄ N ₂ Cl ₄ S	94	70	49.85/50.00	3.78/3.81	4.78/4.86	5.50/5.55	24.50/24.65	
J''	C ₂₅ H ₂₁ O ₃ N ₃ Cl ₄ S ₂	108	70	48.60/48.62	3.38/3.40	6.75/6.80	10.35/10.37	23.00/23.01	

Scheme :



Where :

1) $R_1 = -H, -C_6H_5$

2) $R_2 = -H, -C_6H_5$

EXPERIMENTAL DETAILS AND DISCUSSION OF RESULTS :

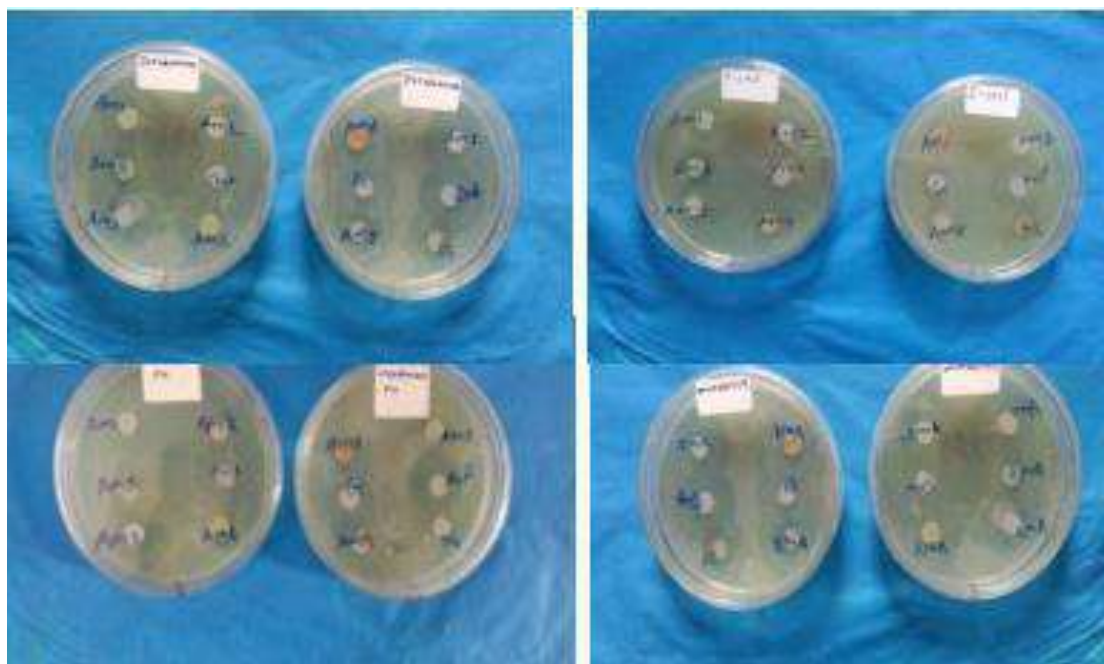
Antibacterial Assay :

The compounds (a – J'') were screened for their antibacterial activity against Gram +ve bacteria viz. *Staphylococcus pneumoniae*, *Staphylococcus aureus* and Gram -ve bacteria viz. *Escherichia coli* and *Pseudomonas fluorescens* at conc. of 1000 ppm by using Agar disc diffusion method. Ofloxacin used as a standard and chloroform as solvent control. The zones of inhibition formed were measured in mm and are shown in Table No.2.

Table No.2- Impact of test compounds against plant pathogens :

Sample Code	(Gram positive)		(Gram Negative)	
	<i>Staphylococcus pneumoniae</i>	<i>Staphylococcus aureus</i>	<i>Escherichia coli</i>	<i>Pseudomonas fluorescens</i>
a	-	15	12	12
a₁	-	13	-	12
a₂	17	14	12	15
a₃	15	-	12	25
a₄	14	12	15	12
J	14	15	15	-
J'	12	13	12	18
J''	12	-	14	25
Reference Antibiotic	(Ofloxacin)	(Ofloxacin)	(Ofloxacin)	(Ofloxacin)

Diameter of inhibition zone (mm)



RESULT AND DISCUSSION :

Most of the test compounds have shown remarkable and very encouraging antibacterial activities. A further detailed study in the light of plant pathology is advised.

ACKNOWLEDGEMENTS :

The authors are thankful to Dr.D.H.Pundkar, Principal, Dr.Manorama & Prof.H. S.Pundkar, Arts, Commerce & Science College, Balapur, Dr.B.B.Wankhade, Principal, Malkapur Vidnyan Mahavidyalaya, Malkapur, and Shri Shankarlal Khandelwal College, Akola for providing help in carrying out the antibacterial activities & for providing necessary facilities to carry out the research work.

REFERENCES :-

- (1) K. Anilkumar, P.K., K. Shrivastava Rao, Reddana P., *Ind. J. of chem. sec., B*, pp. 1033-1037, June **2007**.
- (2) Kakade B.S., "*Synthesis in heterocyclic compounds Ph.D. Thesis*", Nagpur University, **1983**.
- (3) Seiji Miwatashi, Yasayoshi Arikawa, Shigonori Ohkawa, Keiko Ugo-*Chem., Pharm, Bull.* 56 (8), Vol. 56, No. 8, pp.no. 1126-1137, **2008**.
- (4) Airody Vasudeva Adhikari, Karabasanagouda T., Ramgopal Dhanwad and G. Parameshwarappa, *Indian J. of Chem.*, vol. 47 B, pg.no. 144-152, Jan. **2008**.
- (5) Yasuda, Nobuyuki, Karikome, Michinori, Toda, Takashi, *Chem., Lett.* (12), 1141-2-1995.
- (6) Bhavin Sutariya, Raziya S.K., S. Mohan and S.V. Sombassiva Rao, *Indian J. of Chem.* Vol. 46 B, pp.no. 884-887, May **2007**.
- (7) Airody Vasudeva Adhikari, Karabasanagouda T., Ramgopal Dhanwad and G. Parameshwarappa, *Indian J. of Chem.*, vol. 47 B, pg.no. 144-152, Jan. **2008**.
- (8) Mr. Prakash Anil Castelina, Dr. Jagdish Prasad, Dr. Prasanntha Naik, Vol 4/ISSUE : 3/Mar. (**2014**)/ISSN-2249-555 x.
- (9) Khare, P.K., H. Singh, Shrivastava, *Indian J. Chem., Sec., B*, 875-879, May **2007**.
- (10) Pathan S.R., Dighe N. and S. Shinde, H.V. *Asian J. of Research chem.*, 2 (2), April-June **2009**.
- (11) Suman Adhikari, S.B. Bari, A. Samanta, *Journal of Applied Research*, 8, 1, 31-40 [**2014**].
- (12) Piotr Grodzinski, *American cancer society*, 3 Aug. (**2012**) ; DOI : 10.1002/CnCr. 27766.
- (13) Yue Yaun, Xijun Wang Bin Mei, *Dongxin Zhan Scientific Reports* 3, Article number : 3523, doi : 10.1038/srep 035 23 ; 29 November (**2013**).
- (14) Andrei L. Gartel, *Scientifica*, volume (**2014**) (2014), Article ID 59 658, <http://dx.doi.org/10.1155/2014/596528>.
- (15) Dr. Ho, Nanotech advancements, *Scientific hardness nanotechnology to better diagnose and tract cancer*, 120 : 2781-2783 ; doi 10.1002/Cner.28982.
- (16) Patricia Urban and Xavier Fernandez Busquets, *Bentham science, Current Medicinal chemistry*, ISSN 1875-533 x. Volume 22, 38 Issues (**2015**).
- (17) Chun-Mao Lin and Tan-Yi Lu, *Bentham Science*, ISSN : 2212-4020.
- (18) Ming Wang, Mariana Holasia, Kasim Kabirov, Aryamitra Banerjee, *Cell Cycle*, vol. 11, issue 18, (**2012**).
- (19) Oriol Planas, Thibault Gallavardin and Santi Nonell, Institut Quimic de Sarria, Universitat Ramon Lull Via Augusta, 390, 08017, DOI : 10.1039/C4CC 09070 E ICommun, **2015**, 51, 5586-5589.

* * * * *

Mini Review on biological aspects of 1,3,4-Thiadiazoles

Mr. N.D. Dahake*, Dr. V.H. Masand

Abstract: Thiadiazols are a significant class of heterocyclic compounds with a wide range of uses in biological, pharmacological, and chemical synthesis. They are also well-known for their benefits as metal chelating agents, cyanine dyes, oxidation inhibitors, and anti-corrosion agents. Researchers from all around the world are working on this moiety because of its wide range of uses, which has helped to enhance the chemistry of thiadiazols. The most recent information on advancements, novel approaches, synthetic strategies, methods used for thiadiazole synthesis, and their various medicinal uses, as well as the structure-activity relationship of the most effective compounds and their physical characteristics, is provided in this review article. For medicinal and organic chemists working on developing newer compounds with thiadiazole moiety that may be safer and more effective agents, this article can be a valuable resource.

Key words: Semi carbazide, thiadiazole, antitumour, antioxidant, anti-inflammatory.

Antibiotic Activity: It has been found that 1,3,4-thiadiazoles have a wide range of antibacterial activity. Through its several reactivity sites, which have been outlined above, the thiadiazole ring frequently served as a framework to which various pharmacophore compounds with comparable antibacterial properties were connected. Quinoline, pyrazole, triazole, piperine, imidazoline, and other well-known pharmacophore agents were known to exhibit a range of bioactivities (Schem – 1). In order to test the in vitro antibacterial activity of 2,8-substituted quinolin-1,3,4-thiadiazoleyl acetamide derivatives against *Staphylococcus aureus*, *Streptococcus pyogenes*, *Salmonella typhimurium*, and *Escherichia coli*, Bhat et al. Compounds 183 and 184 demonstrated superior inhibitory effects against *S. aureus* at MIC = 16 µg/mL (controlled to amoxicillin MIC = 32 µg/mL), while compounds 185 and 186 demonstrated superior outcomes against *pyogenes* at MIC = 16 µg/mL (controlled to amoxicillin MIC = 32 µg/mL).

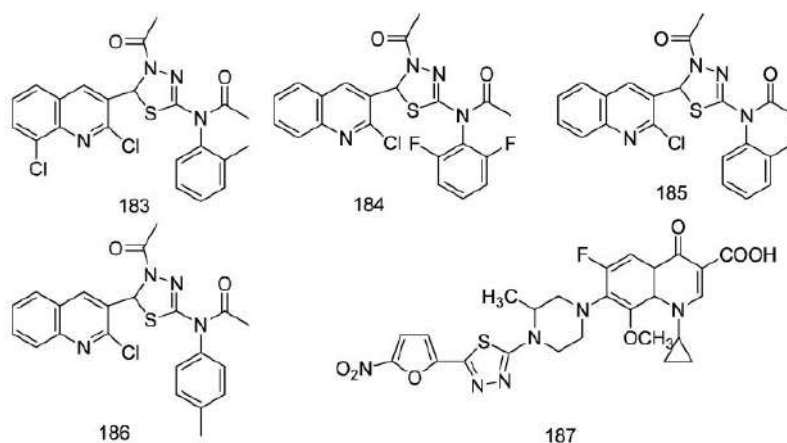


Figure 4- Scheme -1

Antiviral Activity: Research on 1,3,4-thiadiazoles' antiviral efficacy was unsatisfactory. Despite their best efforts, the majority of the time the researchers only saw moderate or even lower activity. Triazolo 1,2,4-[3,4-b]In vitro anti-HIV-1 (IIIB) and HIV-2 (ROD) activity in MT-4 cells was significantly lower with -1,3,4-thiadiazoles with 3,6-substituted by substituted phenyl, heterocyclic groups such as furan, thiophene, pyroazine, pyridine, pyrrole, coumarin, etc., adamantyl and acyclic C-nucleosides (compound

214) than the reference drug (Scheme 2). Moreover, 2-arylthioacetamino-1,3,4-thiadiazoles were produced and assessed for their ability to block HIV-1 reverse transcriptase as non-nucleoside inhibitors (NNRTIs) through an allosteric interaction with the non-nucleoside inhibitor binding site, or NNBS, which is a location next to the NRTI binding site. The new 1,3,4-thiadiazole compounds did not perform as well as their benzoimidazole analogues and the reference drug zidovudine, despite the fact that the nitrogen atom and the amino group of thiadiazole can form H bonds with the RT NNBS residues and the 5-position substituent can also contribute to the interaction with NNBS observed through docking simulation. Comparing thiadiazole compounds to their benzoimidazole equivalents and the reference medication zidovudine, they did not perform as well.

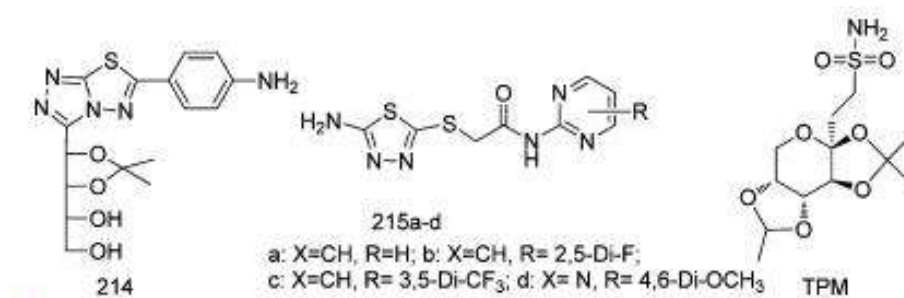


Figure 5 - Antiviral Analogues of 1,3,4-Thiadiazole

Antioxidant Activity: Antioxidants can stop chain reactions that could harm or kill a cell by removing free radical intermediates from oxidation events. Usually, they are reducing agents like polyphenols, ascorbic acid, or thiols. Similar to chemical antioxidants, a network of interacting antioxidant enzymes, including catalase, peroxiredoxins, thioredoxin and glutathione systems, superoxide dismutase (SODs), and catalase, protects cells from oxidative stress. There is a lot of literature on the antioxidant properties of 1,3,4-thiadiazoles. Compared to the reference antioxidant propyl gallate, N-(2,4-Dimethylphenyl)-5-(4-nitrophenyl)-1,3,4-thiadiazol-2-amine exhibited more superoxide anion scavenging action. The presence of a potent electron-withdrawing group (NO₂) may be responsible for stabilising the negatively charged adduct that superoxide forms. This outcome supported the report by Chidananda. Notwithstanding the unsurprising results, some (benzo)-imidazothiadiazoles and triazolothiadiazoles demonstrated potential antioxidant activities against a variety of in vitro systems, including superoxide radical, 2,2-diphenyl-1-picrylhydrazyl DPPH radical, microsomal NADPH-dependent inhibition of lipid peroxidation LP levels, nitric oxide scavenging activity, and microsomal ethoxy resorufin O-deethylase (EROD). When used to scavenge free radicals (DPPH•, ABTS•+, and •OH) in vitro, thiol and aminothiols compounds formed from 1,3,4-thiadiazoles have been shown to have much greater antioxidant properties than their comparable analogues derived from benzothiazoles, with thiols being superior to aminothiols. In comparison to the radioprotectors WR-2721 and WR-1065, analogue provided 83% protection against 2-deoxyribose degradation by •OH at 60 μM, scavenging DPPH• and ABTS•+ free radicals with IC₅₀ values of 0.053 and 0.023 mM, respectively. However, in vivo tests revealed that benzothiazoles had a more effective radioprotective effect. It was proposed that there is a direct connection between the aromatic ring's ability to trap radicals and the thiol function's ability to capture them. Furthermore, studies in the literature have shown that 1,3,4-thiadiazoles had less antioxidant activity than oxadiazole units in both nitric oxide and DPPH techniques.^{61a,b} The mutagenicity effect of cyclophosphamide was able to be mitigated by melatonin, the pineal gland indole, and its thiadiazol indole derivatives. This reduction in mutagenicity effect may have been caused by the antioxidant activity of these compounds in male mice. Additionally, the thiadiazole ring's existence was unable to interfere with its action.

Melatonin activity, however, was not affected by the mere existence of a thiadiazole ring fused to a melatonin moiety with an acetonitrile side chain.

References

1. Bhat, A. R.; Tazeem; Azam, A.; Choi, I.; Athar, F. *Eur. J. Med. Chem.* 2011, 46, 3158.
2. xiaohe, Z.; Yu, Q.; Hong, Y.; Xiuqing, S.; Rugang, Z. *Chem. Biol. Drug Des.* 2010, 76, 330.
3. (a) Limon-Pacheco, J.; Gonsebatt, M. E. *Mutat. Res., Genet. Toxicol. Environ. Mutagen.* 2009, 674, 137. (b) Pastore, A.; Federici, G.; Bertini, E.; Piemonte, F. *Clin. Chim. Acta* 2003, 333, 19. (c) Rahman, I.; Biswas, S. K. *Encyclopedia of Respiratory Medicine*; Academic Press: Oxford, 2006
4. Pandey, A., Rajavel, R., Chandraker, S., Dash, D., *Eur. J. Chem.* 2012, 9(4), 2524-2531.
5. Kai, Z., Wang, P., Li-Na, X., Xiao-Yun, F., Fen, J., Sha, L., Yuming, L., Bao-Quan, C., *Bioorg. Med. Chem. Lett.* 2014, 24, 5154-5156.
6. Raj, M. M., Patel, H. V., Raj, L. M., Patel, N. K., *Int. J. Pharma. Chem. Bio. Sci.* 2013, 3(3), 814-819.
7. Husam, A. A., Ahlam, J. Q., Iraqi. *J. Pharm. Sci.* 2012, 21(1), 98-104.
8. Ahmad, T., Singh, A. K., Jaiswal, N., Singh, D., *Int. Res. J. Pharm.* 2012, 3, 70-82.
9. Plonka, W., Paneth, A., Paneth, P., *Mol.* 2020, 25(20), 4645.
10. Ming, C., Wen, G. D., Gui, S. L., Zhong, T. F., Xiu, W., *Mol.* 2021, 26(6), 1708.
11. Georgeta, S., *Mol.* 2020, 25(4), 942.
12. Wadher, S. J., Puranik, M. P., Karande, N. A., Yeole, P. G., *Int. J. Pharm. Tech. Res.* 2009, 1(1), 22-33.
13. Akocak, S., Lolak, N., Nocentini, A., Karakoc, G., Tufan, A., & Supuran, C. T., *Bioorg. Med. Chem.* 2017, 25(12), 3093-3097.
14. Hamadneh, L. A., Sabbah, D. A., Hikmat, S. J., Al-Samad, L. A., Hasan, M., Al-Qirim, T. M., & Al-Dujaili, A. H., *Mol. Cell. Biochem.* 2019, 458(1), 39-47.
15. Akram, E., Daham, S. N., Rashad, A. A., & Mahmood, A. E., *Al-Nahrain J. Sci.* 2019, 22(1), 25-32.
16. Gaber, M., El-Wakiel, N., El-Baradie, K., & Hafez, S., *J. Iran. Chem. Soc.* 2019, 16(1), 169-182.
17. Godhani, D. R., Mulani, V. B., Mehta, J. P., & Kukadiya, N. B., *World. Scient. News.* 2018, 100, 51-60.
18. Rajavel, P., Senthil, M. S., Anitha, C., *E-J. Chem.* 2008, 5(3), 620-626.
19. Pandey, A. K., *Bangladesh. J. Pharmacol.* 2019, 14(3), 127-128.
20. Ibrahim, D. H., Saleem, A. J., Awad, A. A., Ahmed, H. S., & Shneshil, M. K., *Insti. Phys. Publis.* 2019, 1294(5), 052029.

Simultaneous Non-aqueous Conductometric Investigation of Pharmaceutically Potent Ibuprofen-Paracetamol Combination Drugs

Pradip P. Deohate, Aakanksha S. Dongare and Anushri R. Jalamkar

Department of Chemistry, Shri Radhakisan Laxminarayan Toshniwal College of Science, Akola-444001, India

E-mail : pradip222091@yahoo.co.in

Abstract

Simultaneous non-aqueous conductometric investigation of pharmaceutically potent ibuprofen-paracetamol combination drugs has been accomplished using the solvent isopropanol and the titrant KOH in isopropanol. Drugs ibuprofen and paracetamol are distinctly acidic in nature. These drug combinations are extensively used in medicines and pharmaceuticals. In present work, ibuprofen-paracetamol combination drugs are simultaneously investigated by non-aqueous conductometric titration method using the dip type of glass conductivity cell. This method has been found to be precise for assay of combination drugs and can be used even in common laboratories. The results are compared to those obtained by Indian Pharmacopoeia (IP) method.

Keywords : Non-aqueous, conductometric investigation, ibuprofen-paracetamol

Introduction

The literature survey showed that, different pharmaceutical drugs and organic compounds have been analyzed by the conductometric method¹⁻³. Good amount of literature is available on determination of pharmaceutical compounds by acid-base titration method in non-aqueous solvents as well as other methods. Procedures for non-aqueous titrations are described in the main pharmacopoeias⁴⁻⁶. Conductometric titration method using conductivity cell is also recommended by the pharmacopoeias. Determination of pharmaceutical compounds by non-aqueous titration method is discussed and reviewed by many authors⁷⁻⁹. In the literature, different methods are given for the determination of ibuprofen^{10,11}. Non-aqueous conductometric estimation of ibuprofen in perchloric acid has been reported earlier¹². For the determination of combination drugs, different methods have been suggested and these are mostly concerns with the separation of components followed by individual component estimation using suitable technique. Investigation of pharmaceutically potent ibuprofen-paracetamol combination drugs by conductometric titration method using solvent isopropanol was not yet reported in literature. As the drugs ibuprofen and paracetamol are distinctly acidic in nature, could not be titrated directly with aqueous alkali because of their hydrolysis. The basic titrants are superior to the alkoxide solvents. These are more susceptible to the atmospheric moisture and carbondioxide.

Herein, the easy method to investigate the pharmaceutically potent drugs is reported. It will help in the investigation of raw materials and products for quick check of spurious drugs that are feared to penetrate the markets. In the reported work, conductometric titrations in non-aqueous medium using the solvent isopropanol and titrant KOH in isopropanol were carried out to analyze the ibuprofen and paracetamol in two component combination drugs without any separation.

Material and Methods

All the titrations were performed by a digital conductometer (Systronics-304) with dip type of glass conductivity cell having outer diameter of 15 mm and cell constant 1. Conductivity cell was conditioned in the desired solvent for 24 hours before the use. Conductometric titrations were carried out at constant temperature using thermostatic bath and the volume of titration solution was always kept constant (20 ml). Suitable volume corrections

were applied whenever necessary. Weightings of required drugs and chemicals were made on Contech, CAH-123 (± 0.001 g) balance. Chemicals and solvents used were AR grade. Solvents were purified and made anhydrous by standard methods¹³ and titrants were protected from atmospheric moisture and CO₂. Drugs used in present work were obtained from pharmaceutical laboratories. These are pharmaceutical in nature and included in pharmacopoeias⁴⁻⁶.

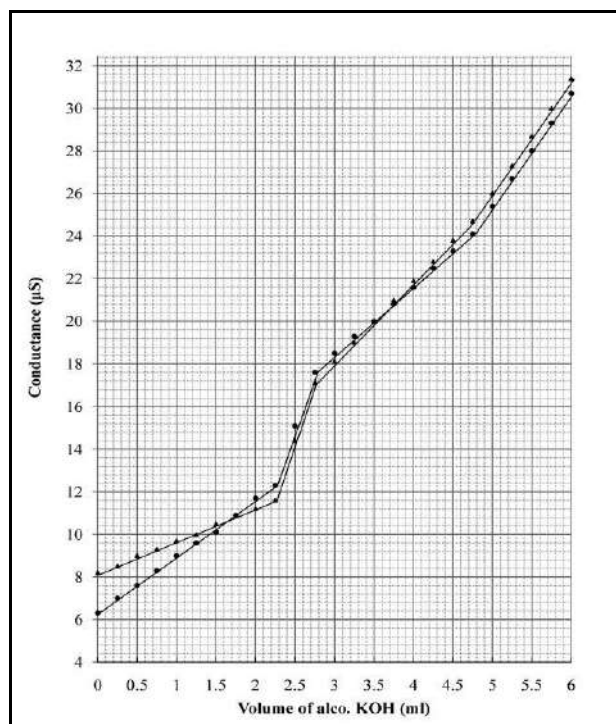
Ten tablets of the same batch of ibuprofen-paracetamol drugs were accurately weighed and powdered for the present investigation. As per the requirement, quantity of powder equivalent to about 400 mg of ibuprofen and 325 mg of paracetamol was weighed accurately, treated with 50 ml of isopropanol and stirred vigorously for dissolving the active component of the tablets. Binding agents and fillers remained insoluble. Common additives present in the tablets i.e. calcium carbonate, glucose, lactose, starch, gum etc. were mostly insoluble in isopropanol. Solutions were filtered, residues were washed with small portions of isopropanol for three to four times and volumes of solutions were made to 100 ml with isopropanol. Aliquots of 10 ml of these solutions were diluted to 20 ml with isopropanol and titrated with 0.1 M solution of KOH in isopropanol by conductometric method using a conductivity cell. Conductometrically, titrant was standardized with 0.1 M benzoic acid in isopropanol. End points were found out by plotting the graphs and later on amount of drugs present in titrated weights of tablet powder were calculated. Amount of active components (drugs) present in one tablet was calculated from the average weight of the tablet. Same tablets were also analyzed by the method given in pharmacopoeias so as to compare the results.

Results and Discussion

Ten tablets of the same batch of drugs ibuprofen and paracetamol were weighed and powdered. Powder equivalent to 400 mg of ibuprofen and 325 mg of paracetamol was exactly weighed, extracted with isopropanol and volume was made to 100 ml. The 10 ml of this solution was diluted to 20 ml with isopropanol and titrated conductometrically with KOH in isopropanol. Standardization of titrant was done using standard benzoic acid in isopropanol by conductometric titration. Weight of drugs ibuprofen and paracetamol in titrated amount of tablets was calculated. Investigation of same tablets was done by IP method and result for two tablets of different brands was tabulated. It was observed that, the reported method of non-aqueous conductometric titration gives quite accurate and comparable results to those obtained by IP method (**Table-1**). It is simple, precise and free from indicator error or interferences. Acidic drugs get hydrolyzed in presence of aqueous alkali, but in non-aqueous medium it can be avoided. As per the US Pharmacopoeia, alcoholic solution of the acidic drugs is to be titrated with aqueous alkali and such titration must be performed very fastly for minimizing the hydrolysis. Present method has not this limitation. The most common additives present in the tablets i.e. calcium carbonate, sugars, gum etc. are insoluble in isopropanol and do not affect the results. Conductometric breaks obtained using isopropanol as solvent are quite pronounced and prominent with minimum error (**Graph-1**). At the end point, solvent isopropanol permitted a large change in the concentration of solvated proton. Solvent isopropanol can be purified and made anhydrous very easily. Its dielectric constant is smaller. Present method is simple than other one, where the components are separated and investigated by spectrophotometric, chromatographic or other techniques.

Table-1 : Conductometric investigation of ibuprofen-paracetamol combination drugs

Sample	Label Claim (mg)		Weight Found by IP method (mg)		Weight Found by present method (mg)	
	Ibuprofen	Paracetamol	Ibuprofen	Paracetamol	Ibuprofen	Paracetamol
DT-01	400	325	398.80	326.80	399.10	327.50
DT-02	400	325	401.90	317.10	402.60	319.70

Graph-1 : Conductometric investigation of ibuprofen-paracetamol combination drugs**Conclusion**

Simultaneous non-aqueous conductometric investigation of pharmaceutically potent ibuprofen-paracetamol combination drugs is fast, simple, precise method. It can be worked out in all common laboratories without the use of any kind of sophisticated equipments. For titration of drugs in non-aqueous medium, solvent isopropanol was found to be good one with accurate results. KOH in isopropanol was found to be better basic titrant to the alkoxide solvents that are susceptible to atmospheric moisture and carbondioxide.

Acknowledgement

Authors are thankful to Principal, Shri Radhakisan Laxminarayan Toshniwal College of Science, Akola for providing sophisticated equipments and necessary laboratory facilities.

References

1. S. Ashour and H. Aboudan, *Int. J. Pharm. Chem.*, **4(1)**, 8 (2018).
2. F. M. Salama, K. A. M. Altia, R. A. M. Said, A. El-Olemy and A. M. Abdel-Raoof, *J. Adv. Pharm. Res.*, **2(2)**, 113 (2018).
3. M. Ayad, M. El-Balkiny, M. Hosny and Y. Metias, *Ind. J. Adv. Chem. Sci.*, **4(2)**, 149 (2016).
4. "Pharmacopoeia of India", Directorate of Publications, New Delhi (2007).
5. "British Pharmacopoeia", Her Majesty's Stationary Office, London (2004).
6. "United States Pharmacopoeia XX and National Formulary XV", U.S. Pharmacopeia Convention, Rockville (1980).
7. L. Safarik and M. Kasova, *Pharmazie*, **36**, 843 (1984).
8. M. Beslova, Z. Bezakova, M. Bachrata and J. Subter, *J. Farmaceuticky Obzor.*, **56**, 97 (1987).
9. P. N. Vyas and R. B. Kharat, *J. Ind. Chem. Soc.*, **65**, 885 (1988).
10. E. M. Costi, I. Goryacheva, M. D. Sicilia, S. Rubio and D. Perez-Bendito, *J. Chromatogr.*, **1210(1)**, 1 (2008).
11. R. Hamoudova and M. Pospisilova, *J. Pharm. Biomed. Anal.*, **41(4)**, 1463 (2006).
12. S. Ghora, O. Halder, A. Bagchi, P. Mukherjee, A. Raha and M. Pal, *Int. J. Pharm. Res. Health*, **6(3)**, 2643 (2018).
13. J. Kucharsky and L. Safarik, "Titrations in non-aqueous solvents", Elsevier, New York (1965).

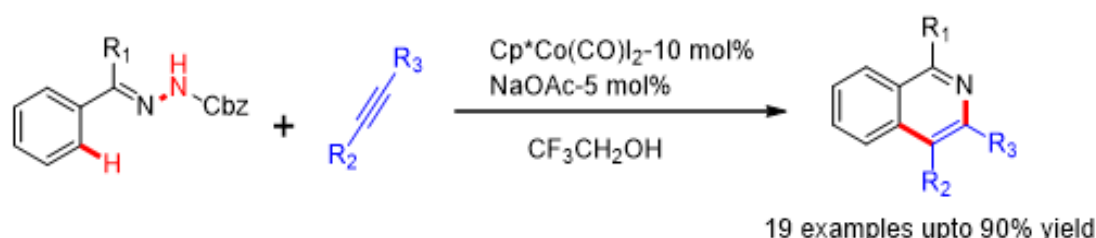
12

Cp*Co(III) Catalyzed Redox-Neutral Annulation: A Powerful Tool for Isoquinoline Synthesis from *N*-Cbz Hydrazones**Dewal S. Deshmukh^{1*} and Bhalchandra M. Bhanage²**¹*Department of Chemistry, J. D. Patil Sangludkar Mahavidyalaya, Daryapur- 444803 (MH)*²*Department of Chemistry, Institute of Chemical Technology, Matunga, Mumbai-400019**e-mail id: dewalsdeshmukh@rediffmail.com***Abstract**

A new cascade oxidative cyclization reaction of *N*-Cbz hydrazones with internal alkynes has been explored for the preparation of isoquinoline derivatives using Cp*CoIII-catalyst via C-H and N-N bond functionalization. *N*-Cbz hydrazones are rarely explored as directing group for redox-neutral [4+2] cyclization reaction through the cyclometallation and this catalyst system does not require any external oxidizing agent as well as silver or antimony salt. The demonstrated efficient approach has been utilized for the synthesis of different isoquinoline derivatives with good regioselectivity and yields.

Introduction

Transition metal-catalyzed C-H bond functionalization is vital for modifying organic molecules, particularly in drug synthesis and green chemistry. Current efforts are directed at enhancing Cp*Co(CO)I₂-catalyzed C-H bond activation with first-row transition metals [1-5]. Isoquinoline derivatives, essential for diverse pharmacological applications and as catalyst ligands, are employed in materials, dye, and paint industries using various name reactions. In recent decades, C-H bond activation has become a pivotal pathway for achieving high yields in isoquinoline derivative synthesis [6-12].



Scheme 1. Transition metal catalyzed annulation reaction for the synthesis of isoquinoline.

Exploring transition metal-catalyzed isoquinoline synthesis has faced challenges like external oxidant requirements, expensive catalysts, and limited starting materials. Addressing these issues, the Zhu group showcased the use of the affordable cobalt catalyst for C-H/N-N bond activations. [13–17]. Challenges in existing protocols, such as the use of air and silver salt, highlight the need for a cost-effective Co-catalyzed synthetic protocol without external oxidants [18].

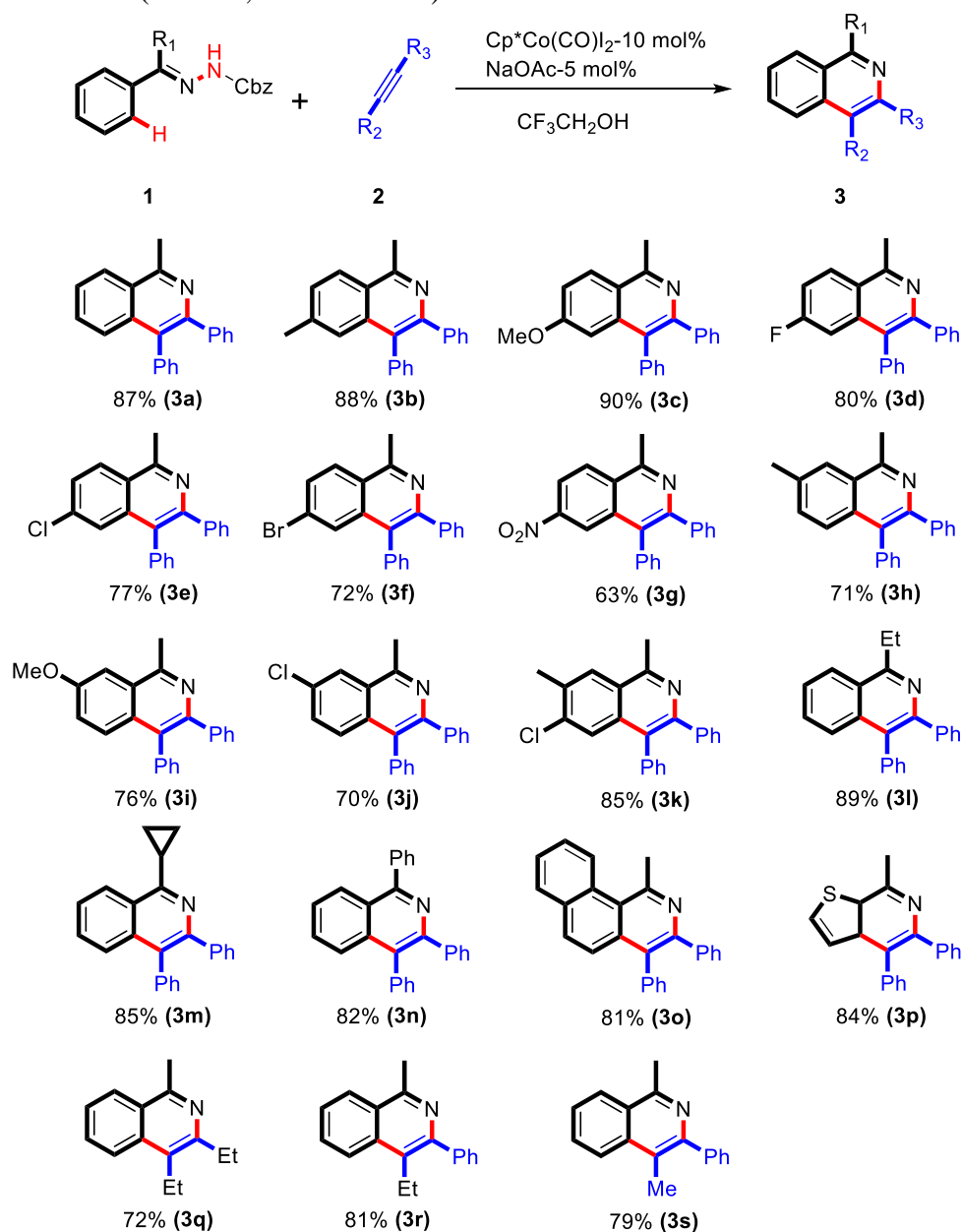
Our research expedites ortho C-H bond activation, utilizing Cp*Co(III) in a redox-neutral cyclization with the seldom-studied *N*-Cbz hydrazone, providing an elegant, cost-effective, and user-friendly method for isoquinoline synthesis without the need for silver salt and with an external oxidant.

Results and discussion

Optimizing reaction conditions using 0.5 mmol *N*-Cbz hydrazone and diphenylacetylene in 2 mL trifluoroethanol with Cp*Co(CO)I₂, NaOAc, and AgSbF₆ resulted

in a satisfactory 71% yield for isoquinoline 3a at 100 °C for 16 hours; further screening revealed varying impacts of acetate sources and solvents on product yield, with the absence of silver hexafluoroantimonate salt surprisingly having no effect on the final yield.

Raising the reaction temperature to 110°C significantly impacted product yield, while no change was observed at 120°C. Extending reaction time to 18 hours had no effect, but reducing it to 14 hours resulted in a lower yield. The optimal catalyst loading for the model reaction was found to be 10 mol% (Table 1, entries 12–17).



Scheme 2. The scope of substituted *N*-Cbz hydrazones and Alkynes.^a

Under optimized conditions, our versatile protocol produced promising isoquinoline products (87–78% yield) from various substituted *N*-Cbz hydrazones, showcasing adaptability with electron-donating and -withdrawing groups. Notably, substituting *N*-Cbz hydrazone without a substitute yielded product 3a significantly, and introducing methyl and methoxy groups increased yields (88% and 90% for 3b & 3c). Electron-deficient groups (fluoro, chloro, bromo, nitro) yielded products with 80%, 77%, 72%, and 63% yields (3d-3g), and varied

positions of functional groups minimally impacted yields. The reaction with diphenyl acetylene and meta-methyl N-Cbz hydrazone resulted in a 71% yield (3h). Annulating disubstituted N-Cbz hydrazones yielded product 3k with an 85% yield. Isoquinoline products from various ketones (3l, 3m, 3n, 3o) showed yields of 89%, 85%, 82%, and 81%, respectively.

Diphenyl acetylene and N-Cbz hydrazone, derived from a heterocyclic ketone, effectively yield the desired product (3p) in satisfactory yield. Exploring various N-Cbz hydrazones, we further investigated different alkynes for isoquinoline derivative preparation, where 3-hexyne and unsymmetrical alkynes (but-1-yn-1-ylbenzene and prop-1-yn-1-ylbenzene) produced the corresponding products (3q, 3r, 3s) with good yields.

Conclusion

Developed a redox-neutral Cp*CoIII-catalyzed dehydrative cyclization of N-Cbz hydrazones with alkynes, eliminating the need for silver salt or an external oxidant, yielding multi-substituted isoquinoline derivatives efficiently.

References

- [1] Jordan, F.; Szostak, M.; Nareddy, P. *ACS Catal.* **2017**, *7*, 5721-5745. DOI: [10.1021/acscatal.7b01645](https://doi.org/10.1021/acscatal.7b01645).
- [2] Abrams, D. J.; Provencher, P. A; Sorensen E. J. *Chem. Soc. Rev.* **2018**, *47*, 8925-8967. DOI: [10.1039/C8CS00716K](https://doi.org/10.1039/C8CS00716K).
- [3] Ping, Y.; Ding, Q.; Peng, Y., *ACS Catal.* **2016**, *6*, 5989-6005. DOI: [10.1021/acscatal.6b01632](https://doi.org/10.1021/acscatal.6b01632).
- [4] Liu, W.; Ackermann, L. *ACS Catal.* **2016**, *6*, 3743-3752. [10.1021/acscatal.6b00993](https://doi.org/10.1021/acscatal.6b00993).
- [5] Wang, S.; Chen, S. Y.; Yu, X. Q. *Chem. Commun.* **2017**, *53*, 3165-3180. DOI: [10.1039/C6CC09651D](https://doi.org/10.1039/C6CC09651D).
- [6] Bentley, K. W. *Nat. Prod. Rep.* **2006**, *23*, 444-463. DOI: [10.1039/B509523A](https://doi.org/10.1039/B509523A).
- [7] Tsuboyama, A.; Iwawaki, H.; Furugori, M.; Mukaide, T.; Kamatani, J.; Igawa, S.; Moriyama, T.; Miura, S.; Takiguchi, T.; Okada, S.; Hoshino, M.; Ueno, K. *J. Am. Chem. Soc.* **2003**, *125*, 12971-12979. DOI: [10.1021/ja034732d](https://doi.org/10.1021/ja034732d).
- [8] Fisher, N. I.; Hamer, F. M. *J. Chem. Soc.* **1934**, 1905-1910. DOI: [10.1039/JR9340001905](https://doi.org/10.1039/JR9340001905).
- [9] Whaley, W.; Govindachari, T. In *Organic Reactions*, ed. R. Adams, Wiley, New York, **1951**, *6*, 151.
- [10] Gensler, W. In *Organic Reactions*, ed. R. Adams, Wiley, New York, **1951**, *6*, 191.
- [11] Whaley, W.; Govindachari, T. In *Organic Reactions*, ed. R. Adams, Wiley, New York, **1951**, *6*, 74.
- [12] He, R.; Huang, Z. T.; Zheng, Q. Y.; Wang, C. *Tet. Lett.* **2014**, *55*, 5705. DOI: [10.1016/j.tetlet.2014.08.077](https://doi.org/10.1016/j.tetlet.2014.08.077).
- [13] Sen, M.; Kalsi, D.; Sundararaju, B. *Chem. Eur. J.* **2015**, *21*, 15529-15533. DOI: [10.1002/chem.201503643](https://doi.org/10.1002/chem.201503643).
- [14] Zhang, S.; Huang, D.; Xu, G.; Wang, S.C.R.; Peng, S.; Sun, J. *Org. Biomol. Chem.* **2015**, *13*, 7920-7923. DOI: [10.1039/C5OB01171J](https://doi.org/10.1039/C5OB01171J).
- [15] Wang, Y. F.; Toh, K. K.; Lee, J. Y.; Chiba, S. *Angew. Chem. Int. Ed.* **2011**, *50*, 5927-5931. DOI: [10.1002/anie.201101009](https://doi.org/10.1002/anie.201101009).
- [16] Zhang, S. S.; Liu, X. G.; Chen, S. Y.; Tan, D. H.; Jiang, C. Y.; Wu, J. Q.; Li, Q.; Wang, H. *Adv. Synth. Catal.* **2016**, *358*, 1705-1710. DOI: [10.1002/adsc.201600025](https://doi.org/10.1002/adsc.201600025).
- [17] Zhou, S.; Wang, M.; Wang, L.; Chen, K.; Wang, J.; Song, C.; Zhu, J. *Org. Lett.* **2016**, *18*, 5632-5635. DOI: [10.1021/acs.orglett.6b02870](https://doi.org/10.1021/acs.orglett.6b02870).
- [18] Pawar, A. B.; Agarwal, D.; Lade, D. M. *J. Org. Chem.* **2016**, *81*, 11409-11415. DOI: [10.1021/acs.joc.6b02001](https://doi.org/10.1021/acs.joc.6b02001).

Design, synthesis, spectral characterization and anti-microbial screening of some novel 1, 2, 4- dithiazole with Coumarin moiety.

K. U. Dongare^{a*} S. A. Waghmare^b, S. B. Sarkate^c, R. N. Ingole^d

^{a,b,c}Department of Chemistry, Ghulam Nabi Azad Arts, Commerce and Science College Barshitakli Dist. Akola 444401 (M.S.), India

^dDepartment of Chemistry, Shri Vitthal Rukhmini College, Sawana, Mahagaon, Dist. Yavatmal, (M.S.), India

*Corresponding author-kuldipdongare1994@gmail.com

ABSTRACT

One step synthesis of 7-(3-substitutedimino-1,2,4-dithiazolo)-4-methyl-2H-chromen-2-one (IIa-e) was carried out by oxidative cyclisation of 7-(5-substituted-2,4-dithiobiureto)-4-methyl-2H-chromen-2-one (Ia-e) by using liquid bromine in chloroform medium as an oxidizing agent. The synthesized compounds from these reaction conditions were characterized on the basis of elemental analysis, chemical characteristic and IR, PMR MASS, spectral data and antimicrobial activity against gram positive and gram-negative bacteria such as *S. typhi*, *E. coli*, *S. aureus*, *A. aerogenes*, *B. subtilis* and *B. megatherium*. etc.

Keywords: 7-(5-substituted-2,4-dithiobiureto)-4-methyl-2H-chromen-2-one, liquid bromine, chloroform, ammonium hydroxide ethanol, gram positive and gram-negative bacteria etc.

INTRODUCTION

Organic compounds containing thiadiazol¹ as the heterocycles in their structure are identified for their biological activities, pharmaceutical activities, industrial applications, agricultural purposes and in medicinal sciences²⁻³. Basically, structure of thiadiazol is five member nitrogen and sulphur containing heterocyclic compound. Presence of sulphur and nitrogen in its structure enhances the biological potential of the thiadiazol. Kalogirou⁴ had reported 1,2,3-dithiazole for the antimicrobial activities, Laitinen *et al.*⁵ reported the 1,2,3-dithiazole for the antibacterial activities, Matysiak⁶ had reported thiadiazol and some different substituents attached thiadiazol directly or indirectly shows effect directly in their biological, medicinal property.

Similarly, Sayed⁷ has prepared the thiadiazol based coumarin the best antimicrobial activities. The biological as well as industrial applications of coumarin⁸ get enhanced due the presence of the thiadiazol nucleus in their structure. This 1,2,4-dithiazole synthesis technique is quicker, less complicated, less expensive and requires less time.

MATERIAL AND METHOD

Material

All the chemical used were of loba chemie (AR grade).

Method:

In the present experiment for the synthesis of different substituted 7-(3-substitutedimino-1,2,4-dithiazolo)-4-methyl-2H-chromen-2-one by using liquid bromine in chloroform medium. Reaction mixture was kept at room conditions for 4 hours.

EXPERIMENTAL

All the chemicals used for the synthesis must be purified. After refluxing the purity of the compounds were checked by TLC (aluminium TLC) with thin layer thickness of 200 um. The melting points of all synthesise compounds will be recorded using hot paraffin bath. The carbon and hydrogen analysis were carried out on Carlo-Ebra-1106 analyser Nitrogen estimation were carried out with colmon-N-analyzer-29. IR spectra were recorded with Bruker

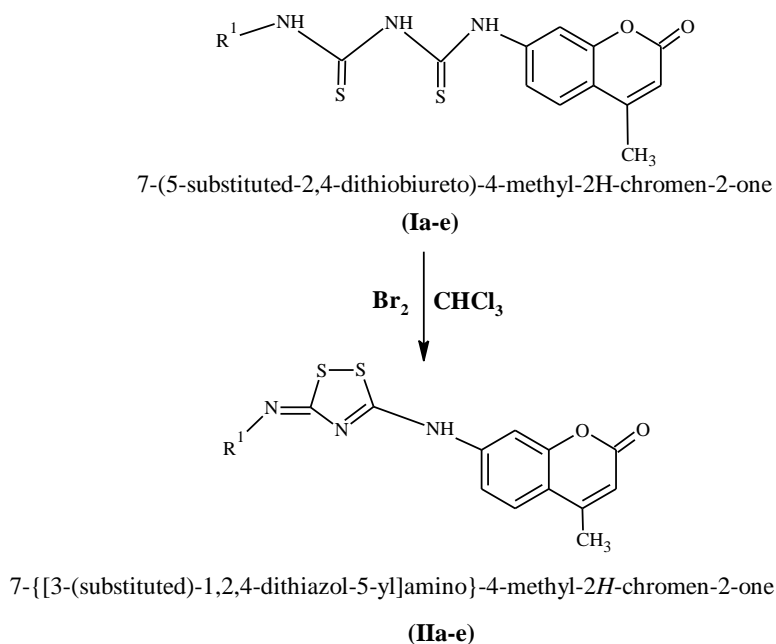
spectrometer in the range 4000-400 cm^{-1} . PMR spectra were recorded on VARIAN 400 MHz spectrometer with TMS as internal standard using CDCl_3 and DMSO Solvent.

GENERAL PROCEDURE

In a clean China dish paste of 7-(5-substituted-2,4-dithiobiureto)-4-methyl-2H-chromen-2-one (**Ia-e**) was prepared in chloroform and 5% liquid bromine in chloroform (2 ml) was added with constant stirring at room conditions. During the addition of bromine solution to firstly the colour of bromine disappear, addition of bromine was continued till colour of bromine appears and persists to the paste. Reaction mixture was kept for 4 hours at room conditions. On basification of the reaction mixture with dilute ammonium hydroxide solution, pale yellow solid of (**IIa-e**) obtained.

Similar procedure was adopted for the synthesis of all the derivatives in the series. The tentative reaction for the formation of product is depicted below,

Reaction



Similarly, 4-methyl-7-([3-(phenylimino)-1,2,4-dithiazol-5-yl]amino)-2H-chromen-2-one (**IIb**), 7-([3-(*tert*-butylimino)-1,2,4-dithiazol-5-yl]amino)-4-methyl-2H-chromen-2-one (**IIc**), 4-methyl-7-([3-[(4-methylphenyl)imino]-1,2,4-dithiazol-5-yl]amino)-2H-chromen-2-one (**IId**) and 7-([3-[(4-chlorophenyl)imino]-1,2,4-dithiazol-5-yl]amino)-4-methyl-2H-chromen-2-one (**IIe**) were synthesized from the oxidative cyclisation 7-(5-phenyl-2,4-dithiobiureto)-4-methyl-2H-chromen-2-one (**Ib**), 7-(5-*tert*-butyl-2,4-dithiobiureto)-4-methyl-2H-chromen-2-one (**Ic**), 7-[5-(4-methylphenyl)-2,4-dithiobiureto]-4-methyl-2H-chromen-2-one (**Id**) and 7-[5-(4-chlorophenyl)-2,4-dithiobiureto]-4-methyl-2H-chromen-2-one (**Ie**) with liquid bromine in chloroform medium respectively by the above mentioned procedure.

RESULT AND DISCUSSION

Spectral characterization results for all the synthesized compounds are given below

Spectral Characterization

1) 7-([3-(Ethylimino)-1,2,4-dithiazol-5-yl]amino)-4-methyl-2H-chromen-2-one (**IIa**)

Yellow solid, $\text{C}_{14}\text{H}_{13}\text{N}_3\text{O}_2\text{S}_2$, Yield-87%, M.P.-142 $^\circ\text{C}$. %Composition found (**calculated**): C-52.59(52.64), H-4.07(4.10), N-13.14(13.15), O-10.01(10.01) and S-20.03(20.07). **IR spectrum** (cm^{-1}): 3130.50 (Ar C-H stretching), 1140.12 (C=S stretching), 3340.43 (NH stretching) and 1740.41 (C=O stretch lactone). **PMR spectrum**: The spectrum of a compound was carried out in CDCl_3 . This spectrum distinctly displayed the signals due to singlet 3 protons of $-\text{CH}_3$ gives singlet at δ 2.4 ppm

due to attachment with aromatic ring, 3 protons of $-\text{CH}=\text{}$ of aromatic ring gives doublet at δ 7.7, 7.74 and 7.3 ppm, 1 proton of $-\text{CH}=\text{}$ of conjugated lactone gives singlet at δ 5.84 ppm, 2 protons of $-\text{CH}_2$ gives quartet at δ 3.5 ppm, 3 protons of $-\text{CH}_3$ gives triplet at δ 1.38 ppm, 1 proton $-\text{NH}$ attached between thionyl group and phenyl ring also deshielded due to thioamide position and gives signal at δ 3.9 ppm. **Mol. Wt.:** 319.40.

2) **4-Methyl-7-[[3-(phenylimino)-1,2,4-dithiazol-5-yl]amino]-2H-chromen-2-one (IIb)**

Yellow solid, $\text{C}_{18}\text{H}_{13}\text{N}_3\text{O}_2\text{S}_2$, Yield-85%, M.P.-134 $^\circ\text{C}$. **%Composition found (calculated):** C-58.78(58.83), H-3.53(3.56), N-11.43(11.43), O-8.70(8.70) and S-17.41(17.45). **IR spectrum (cm^{-1}):** 3050.12 (Ar C-H stretching), 1090.06 (C=S stretching), 3400.12 (NH stretching), 1753.94 (C=O stretch lactone) and 1580.29 (NH bending). **PMR spectrum:** The spectrum of a compound was carried out in CDCl_3 . This spectrum distinctly displayed the signals due to singlet 3 protons of $-\text{CH}_3$ gives singlet at δ 2.4 ppm due to attachment with aromatic ring, 4 protons of $-\text{CH}=\text{}$ of aromatic ring gives doublet at δ 7.7, 7.3, 7.4 and 7.6 ppm, 1 proton of $-\text{CH}=\text{}$ of conjugated lactone gives singlet at δ 5.85 ppm, 1 proton $-\text{NH}$ attached between thionyl group and phenyl ring also deshielded due to thioamide position and gives signal at δ 3.8 ppm. **Mol. Wt.:** 367.44.

3) **Synthesis of 7-[[3-(tert-butylimino)-1,2,4-dithiazol-5-yl]amino]-4-methyl-2H-chromen-2-one(IIc)**

Yellow amorphous solid, $\text{C}_{16}\text{H}_{17}\text{N}_3\text{S}_2\text{O}_2$, yield 85%, M.P. 110 $^\circ\text{C}$, **% Composition found (calculated),** C-55.33(55.33), H-4.94(4.93), N-12.09(12.09), O-9.20(9.20), S-18.45(18.45). **IR spectrum (cm^{-1}):** 3450.12 (N-H stretching), 3034.72 (C-H Ar Stretching), 1560.56 (N-H Bending), 1120.12 (C=S stretching) and 1740.40 C=O stretching(lactone). **PMR spectrum:** The spectrum of a compound was carried out in CDCl_3 . This spectrum distinctly displayed the signals due to singlet of 3H of $-(\text{CH}_3)$ at δ 2.42 ppm, singlet of 9H of $-(\text{CH}_3)_3$ at δ 1.35 ppm, singlet of 1H of $-\text{CH}=\text{}$ of conjugated lactone gives singlet at δ 5.8 ppm, 3 protons of $-\text{CH}=\text{}$ of aromatic benzene ring gives doublet at δ 7.7, 7.4 and 7.7 ppm and singlet of $-\text{NH}$ at δ 3.4 ppm. **Mol. Wt.:** 347.45.

4) **4-Methyl-7-[[3-[(4-methylphenyl)imino]-1,2,4-dithiazol-5-yl]amino]-2H-chromen-2-one (IId)**

Yellow solid, $\text{C}_{19}\text{H}_{15}\text{N}_3\text{O}_2\text{S}_2$, Yield-88%, M.P.-118 $^\circ\text{C}$. **%Composition found (calculated):** C-59.76(59.82), H-3.93(3.96), N-11.01(11.01), O-8.38(8.38) and S-19.77(16.81). **IR spectrum (cm^{-1}):** 3052.15 (Ar C-H stretching), 1050.20 (C=S stretching), 3470.12 (NH stretching), 1735.12 (C=O stretch lactone), 1570.12 (NH bending) and 2930.52 C-H (CH_3 stretching). **PMR spectrum:** The spectrum of a compound was carried out in CDCl_3 . This spectrum distinctly displayed the signals due to singlet 3 protons of $-\text{CH}_3$ gives singlet at δ 2.4 and 2.02 ppm due to attachment with aromatic ring, 5 protons of $-\text{CH}=\text{}$ of aromatic ring gives doublet at δ 7.2, 7.7, 7.03, 7.3 and 7.6 ppm, 1 proton of $-\text{CH}=\text{}$ of conjugated lactone gives singlet at δ 5.8 ppm, 1 proton $-\text{NH}$ attached between thionyl group and phenyl ring also deshielded due to thioamide position and gives signal at δ 3.5 ppm. **Mol. Wt.:** 381.47.

5) **7-[[3-[(4-Chlorophenyl)imino]-1,2,4-dithiazol-5-yl]amino]-4-methyl-2H-chromen-2-one (IIe)**

Yellow solid, $\text{C}_{18}\text{H}_{12}\text{N}_3\text{O}_2\text{S}_2\text{Cl}$, Yield-84%, M.P.-130 $^\circ\text{C}$. **%Composition found (calculated):** C-53.74(53.79), H-2.98(3.009), N-10.45 (10.45), O-7.96(7.95) and S-15.92(15.95). **IR spectrum (cm^{-1}):** 3080.45 (Ar C-H stretching), 1160.50 (C=S stretching), 3470.15 (NH stretching), 1745.12 (C=O stretch lactone), 1570.01 (NH bending) and 2950.63 C-H (CH_3 stretching). **PMR spectrum:** The spectrum of a compound was carried out in CDCl_3 . This spectrum distinctly displayed the signals due to singlet 3 protons of $-\text{CH}_3$ gives singlet at δ 2.3 ppm due to attachment with aromatic ring, 4 protons of $-\text{CH}=\text{}$ of aromatic ring gives doublet at δ 7.29, 7.78, 7.54, 7.35 and 7.60 ppm, 1 proton of $-\text{CH}=\text{}$ of conjugated lactone gives singlet at δ 5.86 ppm, 1 proton $-\text{NH}$ attached between thionyl group and phenyl ring also deshielded due to thioamide position and gives signal at δ 3.5 ppm. **Mol. Wt.:** 401.88.

CONCLUSION

In the present research work is cheaper and less time consuming method for synthesis of organic compound (IIa-e). In all the synthesized compounds give the maximum yield of product (II a-e). A variety of coumarin based 1,2,4-dithiazole derivative can be synthesised for their antimicrobial activities adopting the method.

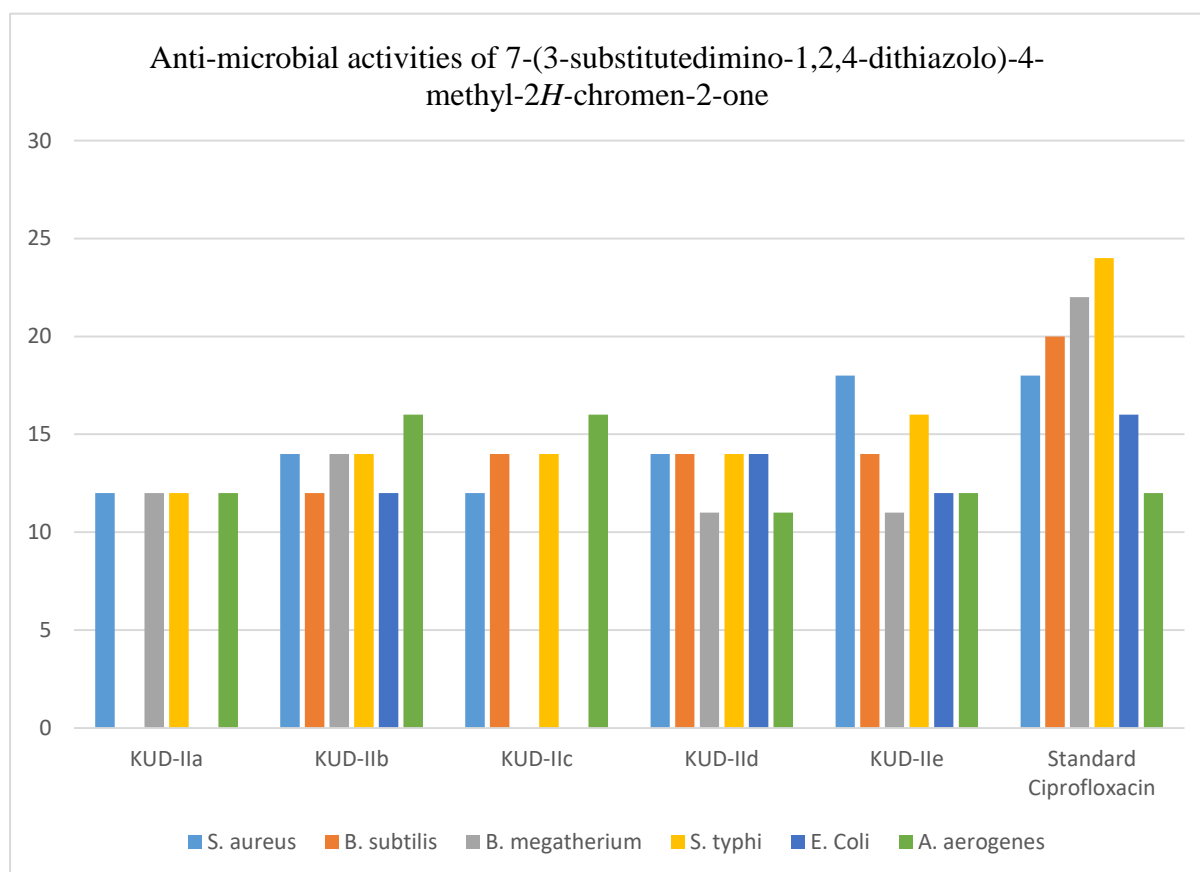
PHARMACOLOGICAL STUDIES

Antimicrobial Activity

All the synthesized compounds (**II-a**) to (**II-e**) were screened for antibacterial activity against *S. typhi*, *E. coli*, *S. aureus*, *A. aerogenes*, *B. subtilis* and *B. megatherium*. by disc diffusion method was performed using Mueller Hinton agar as well as nutrient agar medium. Each and every compound was tested at conc. 50 µg/ml in ethanol. The zone of inhibition of all the synthesized compounds were measured after 24-hour incubation at 37 °C. Standard drug used for comparison the activity was Ciprofloxacin.

Table 1: Synthesized compound **IIa-e** activity against Gram +ve and Gram -ve bacteria.

Table No. 1.1– Antimicrobial sensitivity test against bacteria (after 24 hours at 37 °C temp.) (zone of inhibition in mm)							
SR No .	Compd.	Gram positive			Gram negative		
		<i>S. aureus</i>	<i>B. subtilis</i>	<i>B. megatherium</i>	<i>S. typhi</i>	<i>E. Coli</i>	<i>A. aerogenes</i>
11	KUD-IIa	12	00	12	12	00	12
12	KUD-IIb	14	12	14	14	12	16
13	KUD-IIc	12	14	00	14	00	16
14	KUD-IId	14	14	11	14	14	11
15	KUD-IIe	18	14	11	16	12	12
27	Standard Ciprofloxacin	18	20	22	24	16	12



REFERENCES

1. Ibrahim, S. A., Salem, M. M., Abd Elsalam, H. A., & Noser, A. A. (2022). Design, synthesis, in-silico and biological evaluation of novel 2-Amino-1, 3, 4-thiadiazole based hydrides as B-cell lymphoma-2 inhibitors with potential anticancer effects. *Journal of Molecular Structure*, 1268, 133673, 1-14.
2. Kollu, U., Avula, V. K. R., Vallela, S., Pasupuleti, V. R., Zyryanov, G. V., Neelam, Y. S., & Chamarthi, N. R. (2021). Synthesis, antioxidant activity and bioinformatics studies of L-3-hydroxytyrosine templated N-alkyl/aryl substituted urea/thioureas. *Bioorganic chemistry*, 111, 104837, 1-13.
3. Tayade, D., T., Kale, P., R., Waghmare, S., A. & Nagrale, A., P. (2016). Studies in the antimicrobial activities of some newly synthesized [1,4]substitutedbenzodiazepines by Disc diffusion method and MIC Method, *Haya: The Saudi Journal of Life Sciences*, 1(2), 72-75.
4. Kalogirou, A. S., Oh, H. J., & Asquith, C. R. (2023). The Synthesis and Biological Applications of the 1, 2, 3-Dithiazole Scaffold. *Molecules*, 28(7), 3193, 1-33.
5. Laitinen, T., Baranovsky, I. V., Konstantinova, L. S., Poso, A., Rakitin, O. A., & Asquith, C. R. (2020). Antimicrobial and Antifungal Activity of Rare Substituted 1, 2, 3-Thiaselenazoles and Corresponding Matched Pair 1, 2, 3-Dithiazoles. *Antibiotics*, 9(7), 369, 1-15.
6. Matysiak, J. (2015). Biological and pharmacological activities of 1, 3, 4-thiadiazole based compounds. *Mini reviews in medicinal chemistry*, 15(9), 762-775.
7. Sayed, M. T., Elsharabasy, S. A., & Abdel-Aziem, A. (2023). Synthesis and antimicrobial activity of new series of thiazoles, pyridines and pyrazoles based on coumarin moiety. *Scientific Reports*, 13(1), 9912, 1-9.
8. Chandrakanth, M., Thomas, N. M., Arya, C. G., Fabitha, K., & Banothu, J. (2023). Coumarin-1, 2, 4-Triazole Hybrids: Recent Advances in Synthesis and Medicinal Applications. *Journal of Molecular Structure*, 137197, 1-36.
9. Al-Warhi, T., Sabt, A., Elkaeed, E. B., & Eldehna, W. M. (2020). Recent advancements of coumarin-based anticancer agents: An up-to-date review. *Bioorganic Chemistry*, 103, 104163, 1-15.
10. Fordyce, E. A., Morrison, A. J., Sharp, R. D., & Paton, R. M. (2010). Microwave-induced generation and reactions of nitrile sulfides: an improved method for the synthesis of isothiazoles and 1, 2, 4-thiadiazoles. *Tetrahedron*, 66(35), 7192-7197.
11. Nandgude, T. D., Bhise, K. S., & Gupta, V. B. (2008). Characterization of hydrochloride and tannate salts of diphenhydramine. *Indian journal of pharmaceutical sciences*, 70(4), 482.
12. Maffuid, K. A., Koyioni, M., Torrice, C. D., Murphy, W. A., Mewada, H. K., Koutentis, P. A., ... & Asquith, C. R. (2021). Design and evaluation of 1, 2, 3-dithiazoles and fused 1, 2, 4-dithiazines as anti-cancer agents. *Bioorganic & Medicinal Chemistry Letters*, 43, 128078, 1-5.
13. Gupta, A., Mishra, P., Kashaw, S. K., & Jatav, V. (2008). Synthesis, anticonvulsant, antimicrobial and analgesic activity of novel 1, 2, 4-dithiazoles. *Indian journal of pharmaceutical sciences*, 70(4), 535-538.

14

Effect Of metal-ligand complexon germination of some vegetable plants**Prof. M.M.Rathore and C.N.Deshmukh**

Department of Chemistry, VidyaBharti Mahavidyalaya, Amravati

Plant physiology will probably also assume an increasingly important role in agricultural research problems. As world population increases, mankind faces enormously complex problems. One of the primary tasks of the future will be to increase food, forage, fiber and wood production substantially throughout the world. Today the application of various chemical salts to soils is a basic feature of agricultural practice.

In the present work, Chalcone(an α,β -dihydroxy Ketone)treatment on Vegetable plant' is selected for study as they have both nutritional as well as medicinal value. Since organic drugs have intense biological activity and since no work is reported on the biological applications of binary complexes of Fe (III) with ligand(chalcone) and comparing with pure ligand, metal and control solution doubly distilled water to study the effect of complex, metal, ligand and control solution on germination survival, seedling height, etc. on fenugreek and Spanish plants in order to make suggestion whether complex, metal and ligands can be used as plant growth regulators.

The following aspects were studied in laboratory.

- 1) Estimation of Root / Shoot Ratio in soil & soilless media.
- 2) Estimation of chlorophyll contents in soil & soilless media.

EXPERIMENTAL:-

The information about the role of metal complexes in biological systems, their concentration and presence in different equilibria is of immense importance. Greshon et. al.¹,² reported that the activity of metal chelates is considerably increased as compared to that of the free metal and ligand alone on their complexation. The Shel et. al.³ and Shashindharam et. al.⁴ observed the antifungal and antibacterial activities of complexes shows that they are more active as compared to free ligand and metal involved.

Rare earth ions are used as probe in bio-chemistry of calcium. Zielinski et. al.⁵ showed that, Lanthanide ion could substitute the calcium ion to produce active enzyme system. Some bivalent metal ions have been reported to be useful in agriculture as plant growth regulators. Such a vast uses of lanthanide necessitate concentrating on the study of lanthanides and ligands for studying the germination pattern.

The complexes of transition metal with bis-alkyl thiourea are prepared and their herbicidal and plant growth regulating activity are tested with wheat and cucumbers by Darnall et. al.⁶.

Sayed amir et.al.⁷ studied effect of some heavy metals on seed germination of canola, wheat, safflower evaluate phytoremedial potential.

K. Abraham et. al.⁸ also studied effect of heavy metals on seed germination of archis hypogaeae. L

Shivakumar C. K. et. al.⁹ also observed the presence of beneficial fungus and effect of copper and zinc metal absorption on growth and metal uptake of legumeneous plants as although these metals are required in traces but are important for growth.

A. Ramteke et. al.¹⁰ studied the effect of chlorosubstituted pyrrazole and their complexes

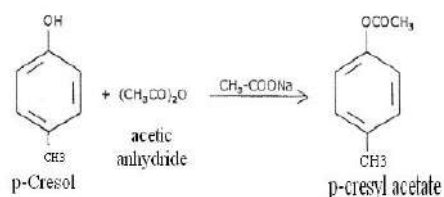
on spinach at different pH.

Recently J.G.Wu et. al¹¹ 18, 23 studied effect of complex on plants.

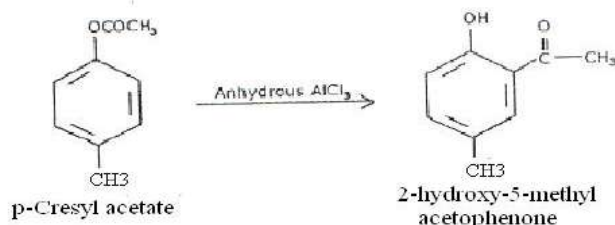
SYNTHESIS OF CHALCONE BY KNOWN METHOD

THE CHALCONE WAS PREPARED BY KNOWN LITERATURE METHOD AND WAS CONFIRMED BY MELTING POINT AND ALSO THE STRUCTURE WAS CONFIRMED BY IR SPECTROSCOPY AS SHOWN IN SPECTRA.

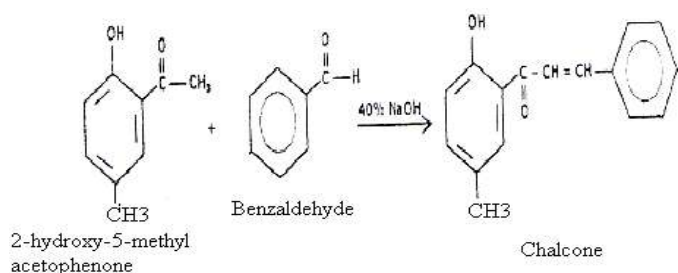
Step I: Preparation of p-cresyl acetate from p-cresol



Step II: Preparation of 2-hydroxy-5-methylacetophenone from p-cresyl acetate



Step III: Preparation of chalcone from 2-hydroxy-5-methylacetophenone



MATERIAL AND EXPERIMENTAL METHODS

• Metal ions:-

The solutions of metal ion in the form of FeCl_3 and MgCl_2 of 0.1 M concentration were prepared using distilled water and the seeds of fenugreek and Spinach were soaked in both metal solvents.

• Ligand:-

The organic compound was prepared were dissolved in proper solvent and above seeds are soaked for 2-3 hours.

Metal ion + Ligand:- The mixture of FeCl_3 and organic compound (chalcone) and MgCl_2 and organic compound (chalcone) were dissolved in the distilled water and seeds are soaked.

Media:-For the germination of the above vegetables seeds, two types of the medias are used.

- 1) Soil media (media A)
- 2) Soilless media (media B)

EXPERIMENTS PERFORMED :-

In general practice, various chemicals are used in agricultural as an important ingredient of various pesticides, insecticides, fertilizers, etc. to improve the crop yield. Amongst several economical important plants Fenugreek and Spinach are selected as a plants system. These plants are in ideal systems to study the germination and growth pattern. Further, their economical importance is reflected by its wide use for food. The important uses these plants in daily life are persuasive to study its response against metal ion, ligand and its complex regarding to physiological processes; particularly germination is a vital process for the growth of plants. Therefore, these plants are selected as a plant system.

1]Healthy seeds were taken and thoroughly washed using doubly distilled water. Seeds from these healthy seeds of equal size were chosen, immersed in tested solution. These seeds soaked were taken out of each solution the seeds are sown in germination trays of all medias.

2]Effect of ligand, metal Fe (III), complex and metal Mg (II), complex on chlorophyll in the leaves of vegetables plants were studied.

After sufficient growth, green fresh leaves were collected, as they contain chlorophyll pigments and chlorophyll content was determined spectrophotometrically given by Jahagirdar D. V.¹²

ESTIMATION OF CHLOROPHYLL IN LEAF PIGMENT:-

Procedure:- Collect the fresh leaves weigh around 1 gm of leaves and cut them into small pieces. Add 5 ml of water and transfer the mixture to a blender. Homogenize the mixture by blending it intermittently for 3-4 minutes. Take 0.5 ml of homogenous mixture and add 4.5 ml of 80% acetone to it. Thoroughly shake the content, centrifuge it. Collect the supernatant liquid and measure its optical density at 645 and 663 nm.

- **Parameters:-**Plants growth is decided on the basis of parameters such as percentage of germination survival, seedling height, shoot length, root length (root length / shoot length) and thickness of young leaf having high values compared to control system. The germination was noted after 7 days, 14 days and 22 days for all Plants. After noting the survival of the plants, they were taken out of the medias. The seedling height (root length / shoot length) was measured. The average values of these parameters are presented in Table 1

RESULT AND DISCUSSION

Some attempts have been made by Bera et. al.¹³ to study the effect of tannery effluent on seed germination, seedling growth and chloroplast pigment content in mungbean. Adhikari et. al.¹⁴ have observed the effect of raw sewage water on mustard. Recently Farzin

M. Parabia et. al.¹⁵ in their present investigation, effect of ligand, complex and metal ion on percentage seed germination, root length, shoot length (root / shoot ratio) has been studied.

ROOT LENGTH, SHOOT LENGTH AND ROOT / SHOOT RATIO

Germination starts when the seed shows emergence phase of growth, which begins, with penetration of embryo from the seed coat and end with development of root and shoot system. The elongation of shoot axis follows emergence of radical.

The rate and extent of elongation is subjected to a variety of controls, including nutrition, hormones and environmental factors. Though the root and shoot development start within a fraction of time but the further developments may vary according to the nutrients required for the development of root and shoot independently. Therefore, root and shoot length differs from each other.

Table 1:-Effect of Different Treatment on Vegetable Plant in Respect of Parameters in Soil and

Soilless Media.

Sr.N o.	Parameters	Fenugreek		Spinach	
		Soil	Soilless	Soil	Soilless
1	% Germination	73.6%	86%	88%	90.4%
2	Seedling Height(cm)	11.96	12.26	9.77	10.6
3	Shoot Length(cm)	6.44	6.46	6.04	6.29
4	Root length(cm)	5.52	5.76	3.74	4.28
5	Shoot/Root Ratio	1.17	1.15	1.68	1.50

Table 1 clearly indicates that percent germination in soilless medium is higher followed soil media. Similarly the root length and shoot length which is called as seedling height shows a significant development of root / shoot length i.e. height of seedling highest in chalcone + Mg as compared to over all the treatments and subsequently followed by chalcone + Fe, metal ion Mg, chalcone and control (d/w) respectively in all cases. When we compare the performance of all the treatments for different parameters in soil and soilless media. The germination & growth parameters are studied in soil and soilless media. Soilless media shows better performance as against soil media in all the treatments.

Mg is a major constituent for the formation of chlorophyll molecule which helps in the process of photosynthesis for the production of food materials in the plant i.e. sugar synthesis. With combination of chalcone + Mg plays a pinnacle role in keeping all the system working properly. This may be the reason for the better performance.

Fe plays major role in energy transfer within the plants and also brings about chlorophyll development and formation. It is also a constituent of certain enzyme and protein. With the combination of chalcone plays a major role in keeping all the plant system working properly may be the reason for a good performance.

The germination of seed and development of the seedling is better in soilless media than the soil media. Because there is less resistance for the root development and shoot

development in soilless media than the soil media may be the reason for better, overall development of the plant.

• **CHLOROPHYLL CONTENT**

Photosynthesis is the process in which the light energy will be converted into chemical energy. There are some basic requirements for the process of photosynthesis as CO₂, H₂O and light energy besides of course, the structural framework of green plant in the form of chloroplast, which is a unique cell having most important role in all the physiological reactions, starting from the absorption of light energy. Basically, among the smallest group of coordinating pigment molecules necessary to effect a photochemical

act, the most important pigments involved in photosynthesis are chlorophyll and carotenoid.

Table 2-3 clearly shows that absorption of plant leaves is higher at 663 nm in all the treatments. These tables also clearly indicates that the amount of chlorophyll is more in chalcone + Mg. Followed by chalcone + Fe, metal ion Mg, chalcone and control (d/w) in both soil and soilless media.

Obviously the chlorophyll content is highest in chalcone + Mg in both soil and soilless medias. Because of Mg is major constituent for the formation of chlorophyll.

Table 1:-Effect of different treatment on chlorophyll content in respect to soil media

Sr.No.	Name of vegetable plants	Treatment with Ligand	Treatment with Ligand+Mg	Treatment with Ligand+Fe	Treatment with Metal ion Mg	Treatment with distilled water
1	Fenugreek	8.22x10 ⁻³	10.162x10 ⁻³	8.363x10 ⁻³	11x10 ⁻³	5.64x10 ⁻³
3	Spinach	4.71x10 ⁻³	7.65x10 ⁻³	5.61x10 ⁻³	8.09x10 ⁻³	4.50x10 ⁻³

Table 2:-Effect of different treatment on chlorophyll content in respect to soilless media

Sr.No.	Name of vegetable plants	Treatment with Ligand	Treatment with Ligand+Mg	Treatment with Ligand+Fe	Treatment with Metal ion Mg	Treatment with distilled water
1	Fenugreek	11.9x10 ⁻³	14.8x10 ⁻³	12.5x10 ⁻³	19.3x10 ⁻³	10.3x10 ⁻³
3	Spinach	7.41x10 ⁻³	8.45x10 ⁻³	8.31x10 ⁻³	9.93x10 ⁻³	5.41x10 ⁻³

When we compare the performance of all treatments for different parameters, in soil and soilless medias. It is clearly observed that soil less media shows better result in respect of germination percentage, development of seedling during the experimental period.

Result of effect of metal ion Mg, Chalcone, Chalcone+ Mg and control (d/W) and chalcone+ fe, on germination, seedling development clearly reveals that, Chalcone +Mg shows significant better performance overall the treatments. All the parameters are considered, while finding out the results. In general order in all the parameters performance wise Chalcone+Mg stood first followed by metal ion Mg, Chalcone Chalcone+fe and control (D/W).

The germination and growth parameter are studied in soil and soilless media. The soilless media shows better performance as against the soil media in all the treatments.

Mg is major constituents for the formation of chlorophyll molecule which helps in the process of photosynthesis for the production of food materials in the plants ,i.e sugar synthesis with the combination of Mg chalcone plays a pinnacle role in keeping all the plant system working properly may be the reason for a better performance.

Mg is a secondary importance element essential for the plant growth. Which is also a constituents of many enzyme the detail information about Mg is already mention in the above para. So, keeping in view of all the characteristics of Mg plays a pivotal role for a good performance against the other treatments.

Germination of seed and development of seedling is better in the soilless media than the soil media, because there is less resistance for the root development and shoot development on the soilless media than the soil media, may be the reason for better overall development of the plant.

The analysis perform for finding out the total chlorophyll in green leaves of the plant. The results of analysis clearly indicates that metal ion Mg is having highest chlorophyll content in both soil and soilless media than the remaining treatment like Chalcone+Mg, Chalcone+fe , Chalcone and control (D/W).

REFERENCES

- 1] Greshon, H; Parmegiani, R., and Nicerson, W. J. : *Appl. Microbiol.*, **10**, 556 (1962).
- 2] Greshon, H., Parmegiani, R. : *Appl. Microbiol.*, **11**, 62 (1963).
- 3] Shel, A. M., Shariel, E. A., Gharib, A. and Ammar, Y. A. : *J Ind.Chem. Soc.*, **60**, 1067 (1968).
- 4] Shashindharam, P. and Ramchandra, L. K. : *J. Ind. Chem. Soc.*, **62**, 920 (1985).
- 5] Zielinski, S. Lomosik, L. and Wojciechowska, A. : *Mh. chem.*, **245**, 6484 (1970).
- 6] Darnell, D. W. and Brinhawn, E. R. : *J. Bio. Chem.*, **245**, 6484 (1970).
- 7] Sayed Amir et. al. : *J.of Agri. Science*, vol (4) No.9, (2012)
- 8] K. Abrahm et. al.: peparment of environment of science S. U. University Tirupati.
- 9] Shivakumar C. K.: *International multidisciplinary research journal* vol(2), 06-12,(2012).
- 10] A. A. Ramteke et. al.: *J. of chem.. and phrm. Research* vol(4) 1889-1894, (2012).
- 11] Jahagirdar, D.V. : Experiments in Chemistry, 1st Edition, Himalaya Publishing House (1994).
- 12] Bera, A. K. and Bokaria, K. : *Envir. Ecol.*, **17**(4), 958 (1999).
- 13] Adhikari, S., Mitra, A. and Gupta, S. K. : *J. Instr. Publ. Hlth. Engrs.*, India, **2**, 5 (1998).
- 14] J.G.Wu, R.N.Den, Z.N.Chen: *Trans. Met.Chem.*18, 23 ,2020

15

Preparation of Adsorbent from various natural materials for removal of heavy metal ions from waste water: Critical review.**Sandhya B. Gaikwad**

(shreyaantre@gmail.com),

MVP SAMAJ'S K.T.H.M. COLLEGE, Nashik

(K.R.T. Arts, B.H. Commerce and A.M. Science College.)

Abstract

Anthropogenic and industrial activities release heavy metal ions into the water. They may be poisonous or carcinogenic in nature and has serious risks to both aquatic environments and people. Heavy metal removal from wastewater is a severe issue as a result. The adsorption method is advantageous for removing heavy metals from wastewater due to its accessibility, affordability and eco-friendliness. High removal capacity of commercial adsorbents and bio adsorbents are both utilized to remove heavy metals from wastewater. This review article intends to gather erratically collect data on the many adsorbents used for heavy metal removal and to provide details on the commercially available and natural bio adsorbents utilized in particular for the removal of copper, lead, Nickel and cadmium.

KEYWORDS: Biosorption, Bio adsorbent, Heavy Metals ions.

1. Introduction

Environmental contamination is one of the major issues of this century as a result of industrial development and the manufacturing of diverse industrial products around the world. ^[1] Heavy metal mercury can accumulate more quickly in cropland and bodies of water as a result of mining, smelting and sewage irrigation. Through sewage irrigation, mercury can go to crops, which could be harmful to human health. ^[2] A significant amount of chromium is found in the waste water from chromium mining, smelting, manufacturing, planting, metal processing, tanning, paints and pigments, printing and dyeing. Recently there has been a lot of interest in studying how to use agricultural waste products as adsorbents to remove heavy metals from industrial effluents. A component of biotechnology is the use of agricultural by-products in the process known as bio-sorption to remove heavy metal ions from the environment. This is acknowledged as a new method for treating heavy metal-polluted streams. The metals of immediate concern, according to the World Health Organization are Cr (III), Cr (VI), Zn, Cd, Cu, Ni, Hg, Pb, Al and Mn. ^[4] Environmental pollution brought on by human activity has grown dramatically over the past few decades and has reached alarming levels in terms of its negative effects on living things. ^[5] The higher concentration of heavy metals causes adverse changes in color, test, odor of water and it also stains clothes and utensils. The Overload of heavy metals may cause severe health problems such as liver cancer, diabetes, cirrhosis of liver, disease related to heart and central nervous systems, infertility, etc. ^[10]

2.Material and Methods: -

Sr no .	Name of adsorbent used	Heavy metal ion removal	Initial conc. ppm or mg/l-	pH	Contact time in minuts/hr.	Adsorbent amount	Maximum adsorption capacity	Langmuir isotherm fit	Referen ce
1	Soybean oil residue	Cd, Zn, Pb	100-300	1-5	1-60 Cd=40min Zn=20min Pb=10min.	0.02-2gm			T.Mahamudiono(2022)
2	1.Biochar(B) 2.Modified biochar (MB) 3.Bentonite (BE) 4.Biochar – bentonite composite	Hg ²⁺	0.5-20		2hr		11.722 ,9.152		Y.Bai and J. Hong (2021)
3	Wheat straw, Corn straw	Cr(VI) Cr(III)	200	3 5			125.6 68.9 87.4 62.3	Langmuir	Y.Chen (2020)
4	1.Carbonized corn husk 2.Uncarbonized corn husk 3.carbonised Millet husk 4. uncarbonized Millet husk 5.carbonized husk 6.Uncarbonized husk	Cr Ni Mn	1.5	2-10	20min-40min	0.2-0.6 Agitation rate(100-300 rpm			S.M. Batagrawa (2019)
5	Wheat Bajra Sugarcane corn	Cu	5.55	5 5.6 5.8 5.6			98%		N.N. Bandela (2016)

6	Carbonized millet husk, Acid treated carbonised millet husk	Pb(II) Cd(II)Ni (II)			40min 100rpm	50mg 100rpm	98% 94% 94% 97% 92% 94%	FTIR SEM	S.M .Batagarawa (2017)
7.	Modified Nanokaoline (NK), Modified Nanobentonite (NB)	Zn ²⁺	4	6	70	400	167mgg-1 143mgg-1	Langmuir Freundlich, Temkin Dubnin Raushkevich SEM	B.U. Maheswari (2019)

3.Discussion

The synthetic and industrial waste water samples were treated by using different natural materials to remove different types of heavy metal ions. These natural materials are adsorbents are simple to produce and their raw materials are widely accessible. Hence, it is a green technology that significantly improves the wastewater treatment process. In general, the most practicable approaches are chemical, adsorption, and membrane techniques. There should be more study done on the introduction of low-cost materials and techniques for heavy metal removal from wastewater. Future study should consider the best methods for achieving effective metal recovery with minimal negative effects on the environment and low costs.

4.Conclusion

One such method that not only addresses the removal of heavy metals from wastewater but is also eco-friendly and has a small environmental impact is adsorption. Adsorbents like activated carbon are commonly employed, although their use is limited by their expensive price. As a result, it's important to consider sustainable solutions that also address the problem's wider implications. Agricultural wastes, industrial wastes, and biochar are inexpensive, easily accessible, renewable, and have a strong affinity for heavy metals, the use of these low-cost bio sorbents is used. As a result, the availability of agro-wastes as a cheap method for removing harmful heavy metals from waste water⁽⁵⁾. The adsorbents are simple to produce and their raw materials are widely accessible. Hence, it is a green technology that significantly improves the wastewater treatment process.

5. Acknowledgement

Further work on creating more affordable adsorbents may aid in the remediation of heavy metals.

6. References

- T.Mahamudiono,D.Bokov,G.Widjaja,I.S.Konstantinov,K.Setiyawan,W.K.Abdelbasset, H.S.Majdi, M.M.Kadhim, H.A.Kareem, K.Bansal- Removal of heavy metals using food industry waste as a cheap adsorbent DOI:<https://doi.org/10.1590/fst.111721>, (2022).
- Y. Bai and J. Hong- Preparation of a Novel Millet Straw Biochar –Bentonite Composite and its Adsorption Property of Hg²⁺ in aqueous solution. Materials,14,1117.<https://doi.org/10.3390/ma14051117>,(2021).

- Y.Chen,Q.Chen,H.Zhao, J.Dang,R.Jin, W.Zhao,Y.Li.-Wheat Straws and Corn Straws as adsorbents for the removal of Cr(VI) and Cr (III) from aqueous solution :kinetics, isotherm, and mechanism. ACS Omega 5, 6003-6009, (2020).
- S.M.Batagarawa,A.K.Ajibola.-Comparative evolution for the adsorption of toxic heavy metals on to millet corn and rice husks as adsorbents.Journal of analytical and pharmaceutical research.8,3 (2019).
- N.N.Bandela, M.G.Babrekar,O.K.Jogdand,G.Kaushik.-Removal of copper from aqueous solution using local agricultural wastes as low cost adsorbent. J.Mater.Envirn.Sci.7 (6)1972-1978,(2016).
- S.M.Batagarawa,L.Y.Dayo -Millet husk as efficient adsorbent for removal of Lead, Cadmium and Nickel ions from aqueous Solution. Dutse Journal of Pure and Applied Science(DUJOPAS).3,1. (2017).
- B.U.Maheswari,V.M.Siyakumar,M.Thirumarimurugan.- Synthesis, characterization of modified nano adsorbent and its application in removal of Zn^{2+} ions from battery effluent.Environmental Chemistry and Ecotoxicology,1,2-11, (2019).
- A.Farhad, M.S.Hossain,T.S.Moin,S.Ahmed,A.M.Chowdhury- Utilization of waste chicken feather for the preparation of eco-friendly and sustainable composite.<https://doi.org/10.1016/j.clet.2021.100190>,(2021).
- H.G.Roh,S.G.Kim,J.Jung- Adsorption of heavymetal ions(Pb^{2+} , Cu^{2+}) on Perm-lotion –to treated human hair. Korean J.Chem Eng.31(2),310-314, (2014).
- V.Kumar,P.K.Bharati,M.Talwar,A.K.Tyagi,P.Kumar- Studies on high iron content in water resources of Moradabad district (UP), India. Water Science 31, 44-51, (2017).
- W.C.Moon,P.Alaniandy- A review on interesting properties of chicken feather as low –cost adsorbent. International journal of integrated engineering Vol.11 No.2,136-146, (2019).

Evaluation of Antioxidant Activity by DPPH Method of Thiocarbamides

P.L. Harale¹, M.E. Shelke², D.T. Tayade²

1. Research Centre and Department of Chemistry, Padmashri Vikhe Patil College, Pravaranagar.

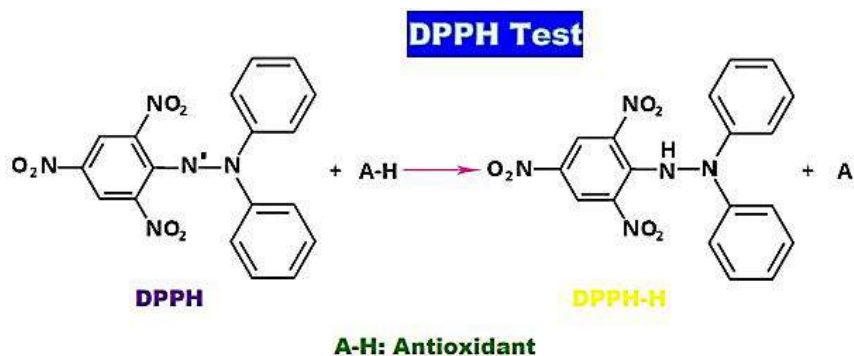
2. Department of Chemistry, Govt. Vidarbha Institute of Science and Humanity, Amaravati.

ABSTRACT

The DPPH free radical scavenging method is recognized and reliable for the evaluation of the antioxidant activity of chemical compounds. The antioxidant capability of thiocarbamate compounds was characterized by its color change with DPPH (2,2-Diphenyl-2-Picrylhydrazyl) and further analyzed its percentage scavenging activity with strong absorption at 517 nm. Utmost thiocarbamate compounds had incomparable percentage scavenging activity and displayed lower IC₅₀ values (effective concentration for scavenging 50% of the initial DPPH value (for μM) resolved excellent antioxidant activity as compared to ascorbic acid.

Keywords: Thiocarbamides, Antioxidant activity, DPPH method, IC₅₀ value

Graphical Abstract:



1. Introduction:

Thiocarbamide compounds have wide spectrum applications in various fields such as pharmaceutical, agriculture, medicinal, and synthetic chemistry¹⁻⁵. An antioxidant prevents the oxidation of molecules inside a cell. Free radicals produced during the biological oxidation chain reaction can lead to damage to a cell. Antioxidants act as reducing agents by terminating a biological chain reaction and eliminating free radical mediates, also preventing oxidative damage and protecting cells from severe body complaints⁶⁻⁹. Researchers are constantly working on synthesizing compounds with highly potent antioxidant activity¹⁰⁻¹⁵. The DPPH test is one of the very stable and reliable free radical scavenging methods to measure the antioxidant activity of organic compounds¹⁶⁻²¹. DPPH is reduced by accepting hydrogen from hydrogen donor compounds and free radical scavenging compounds reduction shows a colour change from violet to yellow. A study of antioxidant activity synthesized compounds was done by calculating its % scavenging activity values and half-maximal inhibitory concentration

values or effective concentration for scavenging 50% of the initial DPPH value (IC_{50} value) ²²⁻²⁴.

In the present study, the antioxidant activity of novel substituted thiocarbamide compounds was investigated by using the DPPH free radical scavenging method and comparing its activity with ascorbic acid.

2. Experimental Section:

2.1. General

All synthesized substituted thiocarbamide compounds were purified by recrystallization with ethanol. DPPH (2,2-Diphenyl-2-Picrylhydrazyl) and ascorbic acid of AR grade were used. Micropipettes are used for the preparation of the microliter solution. Absorption at 517nm was measured using a Systronic (2202 model) make Double-beam UV Spectrophotometer.

2.2. Antioxidant activity / DPPH free radical scavenging activity

Novel thiocarbamide compounds displayed antioxidant activity and were determined by using free radical scavenging against 2,2-Diphenyl-2-Picrylhydrazyl (DPPH). 0.2 μ M DPPH solution was prepared in 95 % ethanol and used as the negative control. Then, different substituted novel thiocarbamide compounds 200 μ g/ mL were mixed with DPPH solution which was then incubated in the dark for 30 min. at room temperature. Vitamin C is used as a standard for comparison because of its high inhibition ability with the presence of OH group stabilized free radical. The absorbance of the reaction mixtures was then measured at 517 nm. By using a spectrophotometer. Plotting the % scavenging against concentration gave the standard curve and the percentage scavenging was calculated from the following equation:

$$\% \text{ scavenging activity} = [(Abs. Blank - Abs. Sample) / Abs. Blank] \times 100.$$

Thiocarbamides have significant antioxidant activity show low IC_{50} value (half-maximal inhibitory concentration) by the DPPH method.

Table 1: Antioxidant activity expressed as IC_{50} values of TD5 thiocarbamides

Concentration (μ g/ml) of TD5	% Scavenging Activity	IC_{50} value
50	45.03	1.44
100	56.12	6.57
150	65.48	11.70
200	74.44	16.84
250	85.58	21.97
300	93.73	27.11

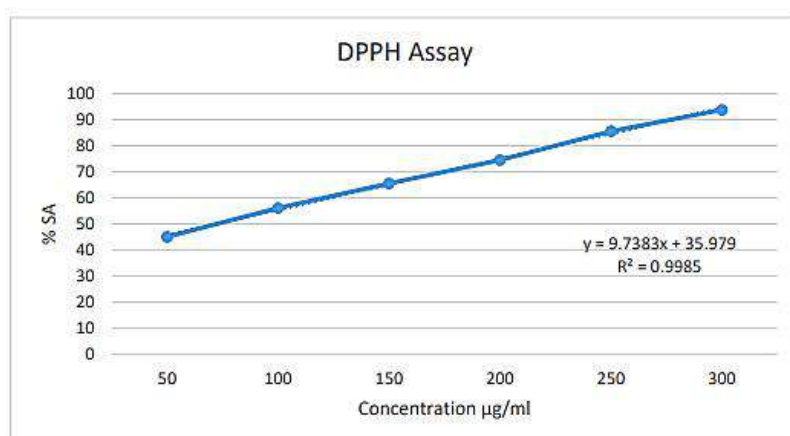
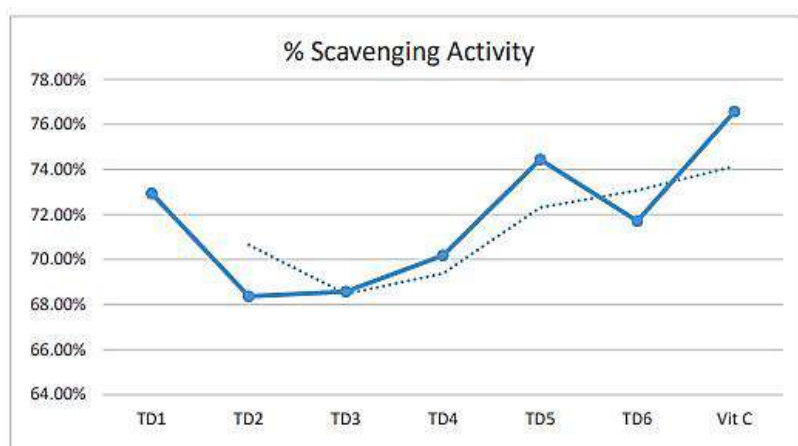


Table 2: Antioxidant activity of different thiocarbamides TD1-TD6

Thiocarbamide Derivatives 200 (μ M) solution	Ph-R	Abs.	% Scavenging Activity at 200 (μ M)
TD1	-H	0.254	72.94
TD2	-Me	0.297	68.37
TD3	-Allyl	0.295	68.58
TD4	-Ph	0.289	70.18
TD5	-PClPh	0.235	74.44
TD6	-mClPh	0.265	71.71
Vit.C		0.220	76.57



3. Result and Discussion:

Novel thiocarbamide compounds were investigated for their free radical scavenging ability in ethanol by using DPPH assay as DPPH radical changes from Purple to yellow color when quenched by antioxidants. DPPH radical scavenging was monitored by a Spectrophotometer at wavelength 517 nm. Most of the derivatives showed notable antioxidant properties as compared to Vitamin C. The Order of the activity depends on the free radical stability form in the derivatives.

In the present research work, all the thiocarbamide compounds showed excellent antioxidant activity with minimum IC₅₀ values and at the lower concentration due to the presence of the N-H group in its structure.

Acknowledgment:

We are thankful to the Research Center of the Department of Chemistry, Govt. Vitharbha Institute of Science and Humanity, Amaravati and Research Center of the Department of Chemistry, Loknete Dr.Balasaheb Vikhe Patil (Padmabhushan Awardee), Pravara Rural Education Society's, Padmashri Vikhe Patil College, Pravaranagar.

Declaration:

Conflict of interest: The authors declare that they have no conflict of interest.

Ethical approval: This has not been published elsewhere and is not currently under consideration for publication elsewhere

5. References:

1. Shah, Habib Ur Rehman, et al., Journal of Molecular Structure 1272, 134162, 2023.
2. Umapriya, Kollu, et al., AIP Conference Proceedings, 2390.1, 2022.
3. Al-Mulla, Abbas, Der Pharma Chemica 9.13,141-147, 2017.
4. Yanagimoto, Kenichi, et al., Journal of agricultural and food chemistry 50.19, 5480-5484, 2002.
5. Nishiyama, Tomihiro, et al., Polymer degradation and stability, 79.2, 225-230, 2003.
6. Fujisawa, Seiichiro, et al. Toxicology 177.1, 39-54,2002.
7. Beal, M. Flint., Annals of neurology 38.3, 357-366, 1995
8. Cheng, Zhihong, Jeffrey Moore, and Liangli Yu., Journal of agricultural and food chemistry 54.20, 7429-7436, 2006.
9. Manojkumar, Parameswaran, Thengungal Kochupappy Ravi, Acta Pharmaceutica 59.2,159-168, 2009.
10. Tsolaki, E., et al., Current Topics in Medicinal Chemistry 14.22, 2462-2477, 2014.
11. Santosh, Rangappa, et al., Chemistry Select 3.23, 6338-6343, 2018.
12. Mi, Yingqi, et al., International Journal of Biological Macromolecules 181, 572-581, 2021.
13. Radwan, Tasneem Mokhtar, et al., Journal of Heterocyclic Chemistry 57.3,1111-1122, 2020.
14. Kaddouri, Yassine, et al., Current Drug Delivery 18.3, 334-349, 2021.
15. Mahdi, Saba H., Dhuha Khudhair Rashid Al-Musawi, and Lekaa K. Abdul Kareem., Journal of Population Therapeutics and Clinical Pharmacology 30.14, 327-335, 2023.
16. Tsolaki, E., et al., Current Topics in Medicinal Chemistry 14.22, 2462-2477.17, 2014.
17. Jarallah, Shahad A., Olfat A. Nief, and Abdul Jabar Kh Atia., Journal of Pharmaceutical Sciences and Research 11.3, 1010-1015, 2019.
18. Kizilkaya, Hakan, et al., Journal of the Chinese Chemical Society 67.9, 1696-1701,2020.
19. Shanty, Angamaly Antony, and Puzhavorparambil Velayudhan Mohanan., Spectrochimica Acta Part A: Molecular and Biomolecular Spectroscopy 192, 181-187, 2018.
20. Payet, Bertrand, Alain Shum Cheong Sing, and Jacqueline Smadja., Journal of agricultural and food chemistry 53.26 (2005): 10074-10079.
21. Pontiki, Eleni, et al., Bioorganic & medicinal chemistry letters 16.8, 2234-2237, 2006.
22. Ludwig, Iziar A., et al., Food research international 61, 67-74, 2014.
23. Ouaket, Amine, et al., Mediterranean Journal of Chemistry 8.2, 103-107, 2019.
24. Lehuédé, Jacques, et al., European journal of medicinal chemistry 34.11, 991-996, 1999.

Investigations of Proximate Compositions of *Xanthium Strumarium L* Roots from Tisgaon (PIN Code 431002) of Taluka and District Aurangabad, India

Jawerea Nayab Mohammad Jamil^{1*}, Rahim Ullah Sharafat Ullah¹

1: Department of Chemistry, Government Vidarbha Institute of Science and Humanities
Amravati 444 604

*: Corresponding Author

Email ID: mirzanayabphd@gmail.com

Abstract

Xanthium Strumarium L showed anti-oxidant, anti-inflammatory, anti-cancer activities as well as various medicinal significances hence it created sufficient interest to carry out proximate investigations of roots of *Xanthium Strumarium L* of Tisgaon (PIN Code 431002) of Taluka and District Sambhaji Nagar (Aurangabad), India which is hitherto unknown from this region. Recently proximate investigations of roots of *Xanthium Strumarium L* of Tisgaon were successfully carried out and the present work deals with the quantitative analysis and identification of ash content moisture content as well water solubility, acid and base solubilities of *Xanthium Strumarium L*. which is important and essential part of herbal drugs in pharmacokinetics and pharmacodynamics of that particular drug. These factors directly hamper pharmacokinetics and pharmacodynamics of particular drugs and ultimately drug activity and drug effect of any synthetic, semi-synthetic and herbal drugs, hence it become essential to carry out proximate analysis of roots of *Xanthium Strumarium L* as they possess medicinal applications and significances. During this study it is investigated that, the roots of *Xanthium Strumarium L*. contain moisture and ash contents as well as acid-insoluble ash value, is determination of solubilities in cold water, hot water, and 1 percent NaOH, HCl, CH₃COOH are also investigated.

Keywords: *Xanthium Strumarium L*, roots, proximate investigations, quantitative analysis.

Introduction

In the tropical regions of India, *Xanthium Strumarium L.*, a member of the Composite family, is frequently seen growing along roadsides, in fields, and in hedges. The word "xanthium" refers to the seedpods, which change from green to yellow as they ripen (later they become deep yellow to brown), and is derived from the ancient Greek words "xanthos," which means "yellow," and "Strumarium," which means "cushion-like swelling." It is frequently referred to as "chota-gokhru" because of the fruit's resemblance to a cow's toe. It is used to treat the common condition hemicrania and is known as adhasisi in various parts of India. There are 25 species in the genus *Xanthium*, all of which are native to America. The medicinal plants *Xanthium Spinosum Linn.* and *X. Strumarium Linn.* are used in Europe and North America.

Sambhaji Nagar previously known as Aurangabad is one of the oldest and historical city in Maharashtra state of India encompass numbers of medicinal plants. Warmer climate is good for *X. Strumarium L*. It is an annual herb and grows up to 1 m tall and has a short, sturdy, hairy stem. The roots of *X. Strumarium L* contain tap root and secondary roots which are irregularly lobed. *Xanthium Strumarium L* is traditional herbal medicine which is used to treat bacterial, antifungal, urticaria and rheumatism infections as well as for the treatment of arthritis, rhinitis, nasal sinusitis, headache problems by vaidu and *X. Strumarium L*. showed reportable gastric ulcer, malaria, cancer, leprosy and leucoderma activities¹⁻⁸. As a wider

program of this laboratory on natural products; various proximate investigations of different plants of various regions have been investigated in sufficient details⁹⁻¹³, considering all these facts it was thought interesting to investigate proximate constituents present in roots of *Xanthium Strumarium L.* of Tisgaon (PIN Code 431002) of Taluka and District Aurangabad, India.

Materials and Methodology

All chemicals used during the research work were of A.R. grade. Freshly prepared solutions were used throughout the research work. The solvents were purified by known literature methods¹⁴.

Sample Preparation: The plants were collected from farms of Tisgaon of Taluka and District Aurangabad, India in May 2023. The plants were cut along with the stem and shade dried. Dried roots were taken in mortar pestle and crushed to prepare fine powder. This fine powder is used for proximate investigations by known literature methods¹⁵.

Proximate Analysis

The determination of physicochemical parameters such as moisture content, total ash value, acid-insoluble ash value, and solubility of the sample was carried out by the known literature methods¹⁵. Solubility of the sample was checked in cold water, hot water and 1 percent NaOH, HCl, CH₃COOH solution. Percentage of moisture and ash contents and acid insoluble ash are determined by using following formula,

$$\% \text{ of moisture} = \frac{\text{Loss of weight of sample}}{\text{Weight of sample taken}} \times 100$$

while,

Percentage of solubility is determined by using following formula,

$$\% \text{ of Solubility} = (\text{loss of weight of sample}) / (\text{weight of sample taken}) \times 100$$

The results obtained are given in **Table-1**

Table-1

Sr. No	Proximate Parameters	Loss of weight of sample	Amount of sample taken (in grams)	%
1	Moisture content	0.220	1	22.00
2	Total ash content	0.165	1	16.50
3	Acid insoluble ash value	0.42	1	42.00
4	Coldwater solubility	0.67	1	67.00
5	Hot water solubility	0.48	1	48.00
6	NaOH solubility	0.46	1	46.00
7	HCl solubility	0.54	1	54.00
8	CH ₃ COOH solubility	0.137	1	13.70

Result and Discussion

Moisture content in any part of plant provides information for an activity of water-soluble enzymes and coenzymes needed for the metabolic activities of that plant and it is observed from Table No.-1 that, total moisture content in roots of was found to be 22.00% which is good for metabolic activities in the plant growth and development of the plant. It was found that the total ash content obtained from dry roots is 16.50% and acid insoluble ash value is 42.00% which are good and these proximate parameters of plant organs are useful for the determination of the mineral contents. Coldwater solubility and hot water solubility were found to be 67.00% and 48.00% respectively; these proximate parameters will give information regarding water soluble neutral, acidic, basic and hydrocarbons present in the samples in herbal chemistry. HCl solubility and CH₃COOH solubility were found to be 54.00% and 13.70% respectively, these proximate parameters gave information regarding basic organic components present in the sample and NaOH solubility was found to be 46.00% which gave information regarding acidic organic components present in the sample.

Conclusion

The Results obtained during proximate analysis were good and it can be conclude that, in roots of *Xanthium Strumarium L.* of Tisgaon (PIN Code 431002) of Taluka and District Aurangabad, India contain good proximate parameters and the physicochemicals well as physiological and anatomical activities of *Xanthium Strumarium L.* herbs at Tisgaon (PIN Code 431002) of Taluka and District Aurangabad, India are in natural form and can be used for medicinal purpose.

References:

1. Masvingwe . C., Mavengwa . M. Toxicological evaluation of the plant *Xanthium strumarium* in Pigs in Zimbabwe. J Venom AnimToxins 1998, 4, 2.
2. Chopra. R.N, Nayar .S.L, Chopra I.C. Glossary of Indian Medicinal Plants. New Delhi: Council of Scientific and Industrial Research; 1986, 259.
3. Moerman. D. Native American Ethnobotany. Oregon: Timber Press; 1998, 9.
4. Foster. S., Duke .J.A. A field Guide to Medicinal Plants. Eastern and Central N. America: Houghton Mifflin Co., 1990, 12
5. Singh. G., Kachroo. P. Forest Flora of Srinagar, A good flora of the western Himalayas but poorly illustrated, Some information on plant uses, 1976.
6. Kirtikar .K.R, Basu .B.D. Indian Medicinal Plants. Basu LM press,Allahabad, India. 1981:Edition 2nd, Vol.2, 1355.
7. Chopra .R.N, Nayar .S.L, Chopra .I.C. Glossary of Indian Medicinal Plants. New Delhi: Council of Scientific and Industrial Research; 1958, 438.
8. Shivpuri . D.N, Dua . K.L. Investigations in pollen allergy in Delhi area IV clinical investigation, Indian J Med Res, 1963, 51, 68.
9. Tayade. D .T, Shaikh R. S, Patil S. U. J. of Indian Chem Soc., 83, 1-3 (2006).
10. Shaikh. R .S, Ph. D. Thesis, Amravati University, Amravati. (2006).
11. Tayade .D .T, Shaikh.R. S, Asian J. of Chemistry”, 15, (3, 4), 1851-52 (2003).
12. Tayade .D. T, Shaikh. R.S , Indian J. applied and pure biology, 18 (2),115-157 (2003).
13. Naskari. P. N., M. Phil Dissertation, Alagappa University, Karaikudi, (2007)
14. M. Hiruy M., Bisrat. D., Asres.K., Natural Product Resources, 10, 1052-1056 (2021).
15. Sree.L.T., Vijayalakshmi K. Proximate Composition, Nutritional Evaluation and Mineral Analysis in the Roots of an Indigenous Medicinal Plant, *Alternanthera Sessilis*. Int J Heal Sci Res [Internet]. 2018;8(7):55. Available from: www.ijhsr.org

Synthesis, Structural Study of Substituted Heterocyclic Compounds

Kavita. M. Heda^a

^aDepartment of Chemistry, Shri R. L. T. College of Science, Akola – 444001 (M.S.) India

E-mail: kavita_heda25@gmail.com

Abstract: Dithiazolidine constitutes a major role in the synthesis of various heterocyclic moieties. They act as active precursors in synthetic heterocyclic chemistry. Synthesis of a series of novel five member ring containing nitrogen and sulphur are well known¹. A series of novel 3-thio-4-substituted-5-tolyl-[1, 2, 4]-dithiazolidine [hydrochloride] have been synthesized by the interaction of several Ammonium aryl dithiocarbamate with *N-p*-tolyl-*S*-chloro isothiocarbamoyl chloride in refluxing chloroform medium. The newly synthesized compounds have been characterized by analytical and IR, ¹H NMR and Mass spectral studies.

A small heterocyclic ring containing nitrogen and sulphur have been under investigation for a long time because of their important properties. Synthesis, structural properties and antimicrobial activities of various [1, 2, 4]-dithiazolidine have been reported earlier². The literature survey revealed that the [1,2,4]- dithiazolidine have been found to possess potent anti-tumors, anti-tuberculosis³, anti-diabetic and anti-cancer⁴ and anti inflammatory⁵ properties.

Thiocarbamides and their heterocyclic derivatives have gained recently much interest as inhibitors of Human Immunodeficiency Virus (HIV)⁶ and Therapeutic agents⁷. Some of the heterocyclic derivatives of thiocarbamides are found to possess diverse pharmacological activities like antifungal and anti-tubercular agents. In view of utility of thiocarbamides, *N*-aryl-*S*-chloro isothiocarbamoyl chloride have been used in synthesis of substituted [1, 2, 4] dithiazolidine by interacting with Ammonium aryl dithiocabamates. The drug containing 1, 2, 4-dithiazolidines show a diverse range of physiological activities, antimicrobial⁸⁻⁹, anti-inflammatory¹⁰⁻¹², anti-ulcer¹³⁻¹⁴, and anti-cancer¹⁵. Here is reported the synthesis of several 3-thio-4- substituted -5-tolyl-[1, 2, 4]-dithiazolidine [hydrochloride] (3a-g) have been synthesized by the interaction of several Ammonium aryl dithiocarbamate (1a-g) with *N-p*-tolyl-*S*-chloro isothiocarbamoyl chloride (2). The required Ammonium aryl dithiocarbamate (1a-g) were obtained by the interaction of interaction of different amines with carbon disulphide and Ammonia.

Results and discussion

Several 3-thio-4- substituted -5-tolyl-[1, 2, 4]-dithiazolidine [hydrochloride] (3a-g) have been synthesized by the interaction of several Ammonium aryl dithiocarbamate (1a-g) with *N-p*-tolyl-*S*-chloro isothiocarbamoyl chloride (2). in CHCl₃. After condensation, the solvent was distilled off to obtain a sticky residue. This residue was triturated several times with petroleum ether (60-80⁰C) to afford a pale yellow solid (3a-g). The product was found to be non-desulphurizable when boiled with alkaline lead acetate solution. The IR spectra of products shows bands due to Ar-H, C-H, C=N, C-C, C-N, C=S, C-S, S-S stretching and ¹HNMR spectra of products distinctly displayed signals due to aromatic protons and Acetyl protons. The Mass spectrum of product was also observed. The identities of these new 3-thio-

4-aryl-5-tolyl-[1, 2, 4]-dithiazolidine [hydrochloride] have been established on the basis of usual chemical transformations and also IR, ^1H NMR and Mass spectral studies¹⁶⁻¹⁸.

Experimental

General Methods

All chemicals were research grade. Melting points determined are uncorrected. IR spectra were recorded in KBr on a FT-IR Perkin-Elmer RXI(4000-450 cm^{-1}) spectrophotometer. ^1H NMR measurements were performed on a Bruker DRX-300 (300 MHz FT NMR) NMR spectrometer in CDCl_3 solution with TMS as internal reference. The Mass spectra were recorded on a THERMO Finnigan LCQ Advantage max ion trap Mass spectrometer. Thin layer chromatography (TLC) was performed on silica Gel G and spots were visualized by iodine vapour. The compounds describe in this paper were first time synthesized by the multistep reaction protocol.

Synthesis of Ammonium aryl dithiocarbamate¹⁹ (1a-g)

The compound Ammonium aryl dithiocarbamate was prepared by drop wise addition of Amine [9ml] in ice cold mixture of ammonium [15ml, density 0.88] and carbon disulphide [7.5ml] followed by the vigorous shaking. The reaction mixture was allowed to stand for 30min heavy precipitate of Ammonium aryl dithiocarbamate separates out. Filter it and dry it.

Synthesis of *N-p*-tolyl-*S*-chloro isothiocarbamoyl chloride (2)

The *N-p*-tolyl-*S*-chloro isothiocarbamoyl chloride was prepared by the interaction of *p*-tolyl isothiocyanate and by passing calculated quantity of Cl_2 gas. Details of typical experiment are as follows:

Through the chloroformic solution of *p*-tolyl isothiocyanate (0.002 M, 0.298 g in 15 mL) pure and dry chlorine gas (0.71g) was passed maintaining the temperature below 10°C . Chlorine gas was generated by the addition of 35% HCl to KMnO_4 . After the complete addition of chlorine gas, the resultant yellow solution was filtered to remove suspended impurities and the clear solution was mixed with petroleum ether ($60-80^\circ\text{C}$). The solvent was then removed by distillation under vacuum. The resultant oil was again diluted with petroleum ether and distilled under vacuum. *N-p*-tolyl-*S*-chloro isothiocarbamoyl chloride was obtained as pale yellow oil (1.00 g).

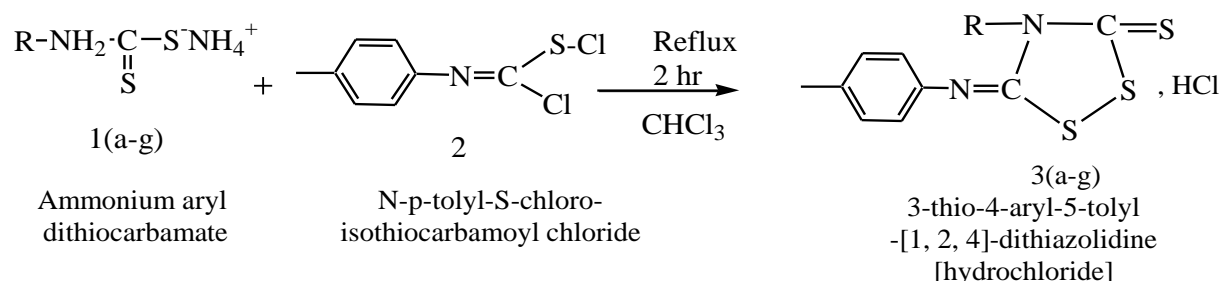
3a:- Synthesis of 3-thio-4-substituted-5-tolyl-[1, 2, 4]-dithiazolidine [hydrochloride]

A mixture of Ammonium phenyl dithiocarbamate (1a-g) and *N*-tolyl-*S*-chloro isothiocyanocarbamoyl chloride was gently refluxed for 2 hr during which evolution of HCl was noticed. The progress of reaction was monitored by TLC. After completion of the reaction, the reaction mixture was brought to room temperature and the solvent removed under reduced pressure to obtain residue. This residue was triturated several times with petroleum ether ($60-80^\circ\text{C}$) to afford a pale yellow solid (3a).

3a: IR (KBr) : ν 3155.5 (Ar-H), 2951.0 (C-H aliphatic), 1593.2 (C=N), 1508.3 (C-C), 1131.0 (C-N), 1143.7 (C=S), 752.2 (C-S), 503.4 (S-S), cm^{-1} ; ^1H NMR (δ in ppm, CDCl_3): δ 7.94-7.22 (9H, m),; δ 2.358-2.353 (3H, s, CH_3) Mass (m/z): 316 (M^+), 300, 225, 211, Anal. Calcd for $\text{C}_{15}\text{H}_{12}\text{N}_2\text{S}_3$, HCl: C, 56.96; H, 3.79; N, 8.86; S, 30.37; Found: C, 56.92; H, 3.75; N, 8.90; S, 30.34.

On the basis of all above facts the product with m. p. 122°C was assigned the structure 3-thio-4-phenyl-5-tolyl-[1, 2, 4]-dithiazolidine [hydrochloride]

When the reaction of *N-p*-tolyl-*S*-chloro-isothiocarbamoyl chloride was extended to several other Ammonium phenyl dithiocarbamate corresponding 3-thio-4-aryl-5-tolyl-[1, 2, 4]-dithiazolidine [hydrochloride] (3b-g) have been isolated.



Where, R= (a) Phenyl, (b) *o*-Cl-phenyl, (c) *m*-Cl-phenyl, (d) *p*-Cl-phenyl, (e) *o*-tolyl, (f) *m*-tolyl (g) *p*-tolyl.

3c: IR (KBr) : ν 3032.1 (Ar-H), 2769.7 (C-H aliphatic), 1593.2 (C=N), 1541.1 (C-C), 1131.0 (C-N), 1207.4 (C=S), 715.5 (C-S), 532.3 (S-S), cm^{-1} ; ^1H NMR (δ in ppm, CDCl_3): δ 7.94-7.22 (8H, m); δ 2.358-2.353 (3H, s, CH_3) Mass (m/z): 350 (M^+), 335, 315, 259, Anal. Calcd for $\text{C}_{15}\text{H}_{11}\text{N}_2\text{S}_3\text{Cl}$, HCl: C, 51.42; H, 3.14; N, 8.00; S, 27.42; Found: C, 51.46; H, 3.10; N, 8.04; S, 27.43.

Table -1: Physical data for characterization of compounds (3a-g)

Compd	Yield %	R_f	M.P. $^{\circ}\text{C}$	Analysis (%): Found	
				(calcd)	
				N	S
3a	78.00	0.65	122	8.90(8.86)	30.34(30.37)
3b	72.00	0.70	110	8.02(8.00)	27.38(27.42)
3c	68.00	0.50	101	8.04(8.00)	27.43(27.42)
3d	55.00	0.52	123	7.50(8.00)	27.38(27.42)

C and H analysis was found satisfactory in all cases.

Acknowledgement

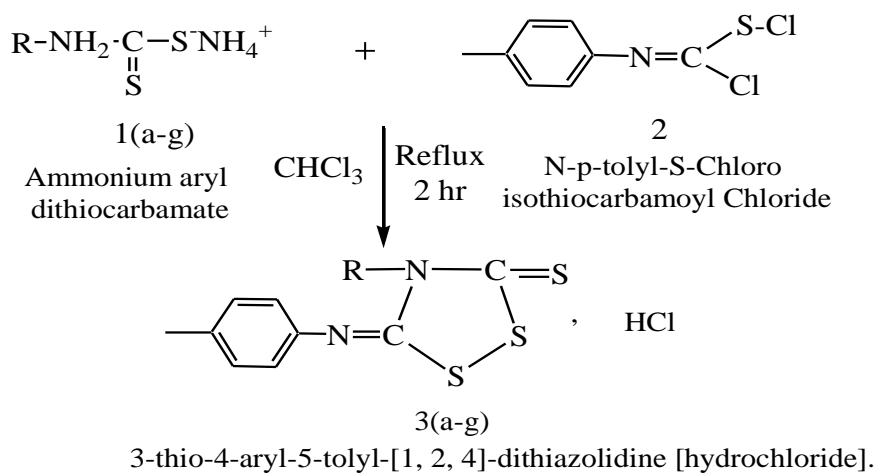
Authors are thankful to SAIF, CDRI, Chandigarh for providing the spectral data and also Dr. V. D. Nanoty for encouragement and necessary facilities.

References:

1. A. Dandia, R. Singh, S. Khaturia, C. Merienne, G. Morgant, and Loupy A, *Bioorg Med Chem.*, 1; **14**(7), (2006), 2409-17.
2. P. R. Kawle, P. Deohate, and B. N. Berad, *Int. J. of Chem. Sci.*, **10** (2012), 895-900.
3. R.M. Kharate, P.P. Deohate, and B.N. Berad, *Int. J. Chem. Sci.*, 7(4), (2009), 2843.

4. P. T. Agrawal, S. P. Deshmukh, *J. Indian Chem. Soc.*, **86**, (2009), 645-648.
5. P. Manna, R. Singh, K.K. Narang, and S.K. Manna, *Indian J. Chem.*, **44B**, (2005)1880.
6. Wilkerson W. W., Dax S., Cheatham W. W.; *J. Med. Chem.*; **40**, (1997), 4079-4088.
7. Nefzi A., Ostresh J. M., Houghten R. A.; *Chem. Rev.*; **97**, (1997), 449-472.
8. Z. A. Kaplancikli, G. Turan-Zitouni, A. Ozdemir, G. Revial, *Eur. J. Med. Chem.*, **43**, (2008), 155-159.
9. N. A. Al-Masoudi, Y. A. Al-Soud, M. Irene. Lagoja, *Carbohydr. Res.*, **318**, (1999), 67-74.
10. A. M. Abdel-Megeed, H. M. Abdel-Rahman, Gamal-Eldien S., *Eur. J. Med. Chem.*, **44**, (2009), 117-123.
11. P. X. Franklin, A. D. Pillia, P. D. Rathod, S. Yerande, M. Nivsarkar, H. Padh, K. K. Vasu, V. Sudarsanam, *Eur. J. Med. Chem.*, **43**, (2008), 129-134.
12. V. B. Jadhav, M. V. Kulkarni, V. P. Rasal, S. S. Biradar, M. D. Vinay, *Eur. J. Med. Chem.*, **43**, (2008), 1721-1729.
13. R. K. Rawal, R. Tripathi, S. B. Katti, C. Pannecouque, Erik De Clercq, *Eur. J. Med. Chem.*, **43**, (2008), 2800-2806.
14. K Ishihara, T Ichikawa, Y Komuro, S Ohara and K Hotta, *Arzneim Forsch, Drug Res*, **44** (1994), 827.
15. D. Havrytyuk, L. Mosula, B. Zimenkovsky, O. Vasylenko, A Gzella and R. Lesyk, *Eur. J. Med. Chem.*, **45(11)** (2010), 5012.
16. R. M. Silverstein, G. C. Bassler and T. C. Morrill, *Spectrometric Identification of Organic Compounds*, 5th ed., John Wiley and Sons, Inc, New York, (1991).
17. N.B. Colthup, L.H. Daly and S.E. Wibereley, *Introduction to Infrared and Raman spectroscopy* "Academic Press, New York, (1964).
18. D.H.Williams and L.Fleming, *Spectroscopic Methods in Organic Chemistry*, 4th ed., Tata-McGraw- Hill, (1988).
19. B.S. Furniss, A.J. Hannaford, W.G. Smith, A.R. Tatchell, "Vogel text book of practical organic, chemistry", FLBS, 4th ed.; p (a) 456 (b), 649 (1980).

Gaphical Abstract



R= (a) Phenyl, (b) *o*-Cl-phenyl, (c) *m*-Cl-phenyl, (d) *p*-Cl-phenyl,
 (e) *o*-tolyl, (f) *m*-tolyl, (g) *p*-tolyl

Kavita M. Heda*

Characterization of Diesel Mixtures by Ultrasonic Methods

K. P. Belsare¹ N. B. Selukar²

Department Of Chemical Technology,
Sant Gadge Baba Amravati University, Amravati, Maharashtra, India
Email: kmendhe29@gmail.com

Abstract: Petroleum fuel has a higher demand in the automobile sector. To meet this demand petroleum fuels are adulterated by some unwanted impurities. These impurities cause bad effects on fuel engines as well as the environment. To protect the environment and automobile engines; the detection of adulteration is important. The ultrasonic method is a recent technique for adulteration detection so the ultrasonic velocity method is used with physiochemical parameters for the characterization of Diesel.

Keywords: Diesel Mixture, Physiochemical characterization, ultrasonic method, Evaluation techniques

1. Introduction

Petroleum products have a lot of demand in the current market because of increasing automobile sectors to meet increasing demand for goods and public transport [1]. To meet this increasing demand there are some malpractices of adding adulterant in petroleum fuel and their presence can not be identified by simple visual inspection. But because of this adulteration, it is dangerous to the environment, human health as well as functioning of the engine. Therefore characterizing and determining its quality and being able to distinguish between these types is of utmost importance to protect the consumer as well as the environment. Adulteration of fuel becomes an acute problem today [2][3].

The ultrasonic method has recently used the Nondestructive method for the characterization of liquid fuel. Evaluation of petroleum fuel by ultrasonic method can be a better option. Density, viscosity, API gravity these physiochemical properties are of importance to characterize the different types of fuels but these are not sufficient to detect adulteration in fuel [3].

The objective of this study is to demonstrate the ability of ultrasonic methods to characterize petroleum products with physiochemical methods for detecting adulteration easily[4].

2. Materials and Methods

Diesel purchased from HP petrol pump. I have to study the adulteration of kerosene in diesel I purchased kerosene from the local market. The Kerosene purchased was blue. Both samples were kept in an airtight plastic tank. These diesel and kerosene were evaluated as per IP/ASTM norms. Then these results were compared with IS/ BIS norms for kerosene and diesel. Following Physiochemical characterization has been done on Diesel and kerosene samples.

- Density
- Specific Gravity
- API gravity
- Viscosity
- Ultrasonic velocity

2.1. Preparation of custom proportions of blends of fuel and adulterants

As an adulterated sample unwanted material is present in various amounts commonly in the range 20-80%. Hence the blends are prepared in such a way that it will cover the adulteration range. The blends are prepared as follows:

Sr. No.	% of kerosene	% of Diesel
1.	20	80
2.	40	60
3.	60	40
4.	80	20

Table 1. Percentages of Blends
These blends were kept in airtight bottles.

2.2. Evaluation of blends as per IP or ASTM norms:

The blended samples were subjected to various tests as per IP/ASTM norms such as Density, Specific Gravity, Viscosity, and ultrasonic velocity. Their tests have shown the variation in properties will indirectly indicate the quantity of adulterant in the sample.

3. Experimental Procedure:

The experimental procedure adopted for this experiment is given below

- 1) Specific gravity and API Gravity is calculated by the following formula

$$\text{Specific Gravity at } 25^{\circ}\text{C} = \frac{\text{Weight of sample}}{\text{Weight of distilled water}} \text{ (for equal volume)}$$

API Gravity is calculated by the formula

$$\text{API} = \frac{141.5}{\text{Sp. Gravity at } 15.6} - 131.5 \text{ (Sp. Gravity is calculated at } 15.6^{\circ}\text{C)}$$

- 2) Viscosity: The viscosity of the sample has been calculated by U – U-tube Viscometer.
- 3) Ultrasonic velocity measurement: Ultrasonic velocity has been measured by using Ultrasonic Interferometer. The formula used for measuring ultrasonic velocity is given below

$$\text{Velocity} = \text{Wavelength} \times \text{Frequency}$$

Where velocity is measured for different blends. And Observations are given in Table 2.

3.1. Experimental Observations

Diesel with kerosene is evaluated as follows: All tests were done at 25⁰ c.

Sample parameter	100% D + 0% K	80 % D + 20 % K	60 % D + 40 % K	40% D + 60 % K	20% D + 80 % K	0 % D +100 % K
Density	0.8322	0.8223	0.8222	0.8208	0.8181	0.7800
Specific Gravity	0.8336	0.8288	0.8187	0.8173	0.8146	0.7811
API Gravity	40.06	41.3140	41.3172	41.6289	42.1882	43.1992
Viscosity	4.35	2.93	2.73	2.59	2.47	2.38
Ultrasonic velocity	1325	1315.2	1281.6	1278.08	1277.4	1267.5

Table 2. Experimental Observation of Blends of Kerosene with Diesel

4. Results and Discussion

From the above experimental procedure, it is observed that, For the Kerosene diesel adulterated sample, as

- A. As the percentage of adulterants increases density of diesel decreases.
- B. As the percentage of kerosene increases in diesel, specific gravity also decreases.
- C. As the percentages of kerosene increase API gravity increases.
- D. viscosity decreases as the adulterant increases.
- E. Ultrasonic velocity decreases as percentages of kerosene in diesel increases.

References

1. Sh. R. Yadav, K. Murthy V, D. Mishra, and B. Baral, "Estimation of petrol and diesel adulteration with kerosene and assessment of the usefulness of selected automobile fuel quality test parameters", International Journal of Environmental Science and Technology, Vol.1, No. 4, pp. 253-255, (2005)
2. A. Jimenez, M.Rufdo, J.Panigua, A, Gonzalez-Mohino, L-S.Olegario, "New findings of edible oil characterization by ultrasonic parameters", Food Chemistry, vol. 374, pp 1-6, (2022)
3. G. M. Ramteke , L.B.Revatkar , R. V. Phadke , N.L.Chutke, " Analysis of Petrol : A Clarification for Purity of Petrol" , ESR Journal , pp. 1-8.(2016)
4. B. Alouache , F. K. Khechena, F. Lecheb , T. Boutkedjirt, " Characterization of Olive oil by Ultrasonic and Physiochemical Methods" , Elsevier, 70, 1875-3892 (2015).

Phytochemical and Proximate Analysis of Leaves of *Heteropogon Contortous* (L.) Beauv

Miss Mosim Raza H. Shaikh

Jagadamba Mahavidyalaya, Achalpur

mhshaikh214@gmail.com

ABSTRACT :

Recently Proximate analysis and phytochemical analysis of *Heteropogon Contortous* (L.) Beauv from Wazzar Village, located in Achalpur tehsil of Amravati, Maharashtra. The leaves sample contained tannin, saponin, protein, steriods, terpenoids, carbohydrate, alkaloids, flavonoids. Proximate analysis of moisture, ash, crude fiber, crude Protein, solubility were check. The values of it is moisture (27.78%), cold water (64.4%), hot water (50.4%), 1% NaOH (51.76%), 1% HCl (54.57%), ash content (13.48%). These results indicate that the *Heteropogon Contortous* (L.) Beauv. contains nutrients elements that will be useful in nutrition. Also the existence of some phytochemicals like tannin, saponin and steroids illustrated medicinal action of the plant in its therapeutic uses. The result of their phytochemcial screening could justify the observed activities and validate their use in herbal medicine.

Keywords: Proximate composition, Phytochemical analysis, *Heteropogon Contortous* (L.) Beauv

INTRODUCTION :

The term “medicinal plants” includes various type of plants used in herbalism and some of these plants have medicinal activities. Medicinal plants are the “backbone” of traditional medicine, which means more than 3.3 billion people in the less developed countries utilize medicinal plants on a regular basis [1].

Medicinal plants are an integral component of research developments in the Pharmaceutical industry. Such research focuses on the isolation and direct use of active medicinal constituents, or in the development of semi-synthetic drugs, or still again on the active screening of natural products to yield synthetic pharmacologically-active compounds. Natural products play an important role in drug discovery process including the provision of basic compounds affording less toxic and more effective drug molecules, serve as extremely useful natural drugs, exploration of biologically active prototypes towards newer and better synthetic drugs and modification of inactive natural products by suitable biological or chemical means into potent drugs [2].

Spear grass (*Heteropogon contortus* (L.) Beauv. ex Roem. & Schult.) Is a tropical perennial grass. It grows to a height of 50 to 150 cm, is tufted and highly variable. Its stems are geniculated at the base, erect at their upper levels, often branched, particularly at flowering [3]. The leaves are green or bluish green, usually glabrous or with few long hairs at the base. The leaf-blade is folded when young, and then flat at maturity, 3-30 cm long, 2-8 mm broad, and somewhat canoe-shaped at the apex [3, 4]. The inflorescence is a 3 to 8 cm long raceme borne single or in pairs at the axil of the upper leaves. The spikelets are paired and very dissimilar according to their position on the raceme. Male or sterile spikelets are awnless, sessile and borne at the base of the raceme, or pedicellate and borne at the apex. Bisexual spikelets are only borne at the apex and they are all awned. The long awns (5-10 cm long) and the way they become twisted as the seeds mature are a characteristic trait of spear grass. The seed is a

caryopsis, 3.5-4.5 mm long, grooved and whitish in colour [3, 4, 5]. There were considerable numbers of local species and varieties in the early botanical literature. Only a few commercial varieties are available, for example "Rocker" from Arizona and "Kahoolawe" from Hawaii [4]. Aside from phytoconstituent identification, it is also critical to analyze plants for their proximate and mineral compositions to expand knowledge of their nutritional health benefits. The review of the literature revealed that no previous work on the proximate analysis of *Heteropogon Contortous* (L.) Beauv. had been conducted.

MATERIALS AND METHODS

Collection of Samples

The leaves of the plant *Heteropogon contortus* (L) Beauv was collected from Wazzar Village, located in Achalpur tehsil of Amravati, Maharashtra. The whole plant was gently uprooted from the ground and then the leaves separated from the root after which they were dried at ambient temperature. The dried leaves were milled to fine powder, thereafter it was stored in an airtight container in the prior to its use.

Proximate analysis:

As per Aurveda, herbal drugs in the form of oral dosage are given to the patient as powdered materials mixed with water. For that, we performed proximate analysis to determine the physicochemical properties as well as solubility and nutrient content of herbal drug materials. Using a standard procedure and formula from the reported literature, the moisture content, ash content, crude protein, crude fiber, crude fat were determined.[6-8]

Moisture, ash and solubility were determined using the Association of official analytical chemists methods [5]. Crude fiber was estimated from the loss in weight on ignition of dried residue following digestion of fat-free samples.

Ash content:

An ignited and weighed silica crucible which contains 1gm of the powdered sample was incinerated slowly by raising the temperature in a muffle furnace at 450°C for 4 – 5 hours. It was cooled in desiccators and weighed. The procedure was repeated until a constant weight was obtained. The percentage of total ash was calculated.

Moisture Content:

The oven-drying method was used to determine moisture. The weight of the empty crucible was recorded and kept in the oven for 1 hour at 1100C, then 1 gm of dried sample was placed in a crucible (W1) and kept in the oven for 1 hour at 1100C. It was then cooled and weighed until the weight remained constant (W2). The moisture content (%) was calculated.

Crude fiber content:

After extraction with petroleum ether, 5 g of the dry material was boiled with 2% H₂SO₄ and NaOH solution for 30 minutes, respectively. It was filtered and washed the residue with boiling water and dried for 2 hrs at 130° C, cooled in a desiccator and weighed. Then the residue was ignited at 550 °C for 25 min. and cooled in a desiccator before reweighing.

Table -1

Sr.No.	Solubility in	Actual weight of sample taken in gm	Loss of wt. of sample in gm	%
1	Cold water	1.000	0.644	64.4
2	Hot water	1.000	0.504	50.4
3	Dil.NaOH	1.000	0.5176	51.76
4	Dil.HCl	1.000	0.5457	54.57
5	Ash Content	1.000	0.1348	13.48
6	Moisture Content	1.000	0.2778	27.78
7	Crude Fiber	---	---	33.7
8	Crude Protein	---	---	2.7

Phytochemical analysis :

Phytochemical analysis of the *Heteropogon contortus* (L) Beauv leaves.

S.No.	Content	Methanol	Aqueous
1	Amino Acids	-	-
2	Proteins	-	-
3	Carbohydrates	+	+
4	Saponins	-	+
5	Alkaloids	+	+
6	Phenols	+	+
7	Steroids	+	+
8	Terpenoids	+	+
9	Cardiac Glycosides	+	+
10	Flavonoids	+	+
11	Tannins	+	+
12	Anthroquinones	+	+

“+” = present, “-” = absent

RESULT AND DISCUSSIONS

The results of the proximate analysis support the use of the leaves as a food supplement. From the result, it was found that the total ash content obtained from dry leaves is 13%. Ash content is generally taken to be a measure of the mineral content of original food. The moderate moisture content provides for an activity of water-soluble enzymes and coenzymes needed for the metabolic activities of the plant. The total moisture content is 27.78 %. The proximate composition of the plant is depicted in table no.1.

The presence of flavonoids inferred that the leaves has the biological functions like antioxidant, allergies protection, free radical, inflammation, ulcers, hepatotoxins, tumor and viruses[8]. Flavonoids are water soluble free radical and antioxidants which prevent oxidative cell damage, and have strong anti-ulcer and anticancer activity[10]. Saponin content suggest that usefulness of the leaves as a productivity agent. The saponin level is low, either compared with the results from another works. Alkaloids are the most efficient medicinally significant bioactive substances in plants. Alkaloids and the synthetic derivatives are used as medicinal agents because of their bactericidal and analgesic properties. Tannins healing of wounds and inflamed mucous membranes. This are water soluble phenolic compounds which precipitate proteins. They exist in all plants. Tannins add to proteins making them bio-unavailable [11]

CONCLUSION

This type of study will be applicable for the pharmaceutical, medicinal, agricultural, industrial and biochemical sciences. This study also shown that proximate, phytochemical analysi of *Heteropogon contortus* (L) Beauv leaves is a balanced and rich source of macro- and micronutrients. So the further study will be carry out on this plant.

REFERENCES

1. Singh, R. (2015). Medicinal plants: A review. Journal of Plant Sciences, 3(1-1), 50-55.
2. Saad, R., Pohyeen, T., Khan, J., Wenji, L., Sultan, S., & Abdul Hameed, J. (2014). Phytochemical screening and antioxidant activity of different parts from five Malaysian herbs. International journal of science and technology, 19(2), 1336-1347.
3. Cook, B. G., Pengelly, B. C., Brown, S. D., Donnelly, J. L., Eagles, D. A., Franco, M. A., ... & Schultze-Kraft, R. (2005). Tropical Forages: an interactive selection tool. Tropical Forages: an interactive selection tool.
4. Soromessa, T. (2011). *Heteropogon contortus* (L.) P.Beauv. ex Roem. & Schult.. Record from Protabase. Brink, M. & Achigan-Dako, E.G. (Editors). PROTA (Plant Resources of Tropical Africa / Ressources végétales de l'Afrique tropicale), Wageningen, Netherlands
5. Food and Agricultural Organization (FOA), (2012). Grassland Index. A searchable catalogue of grass and forage legumes. FAO, Rome, Italy
6. Dhivya, R., & Manimegalai, K. (2013). Preliminary phytochemical screening and GC-MS profiling of ethanolic flower extract of *Calotropis gigantea* Linn.(Apocynaceae). Journal of Pharmacognosy and Phytochemistry, 2(3), 28-32.
7. P. K. Mukherjee, Elsevier, First Edition, 2019, 237-328, Quality Control Evaluation Herbal Drugs, doi: 10.1016/B978-012-813374-3.00007-7.
8. P. K. Mukherjee, Business Horizon Pharmaceutical Publications, New Delhi, 2008, 187-191.
9. AOAC, 20th edition. Rockville, Maryland, USA, 2016.
10. Akindahunsi A.A. & Salawu S.O., *African J. Biotech.*, 4, 2005, 497-501.
11. Sofora L.A., *Medicinal plants and traditional medicine in Africa*. (Spectrum books Ltd.)1993, p.55-71.

A Review of Computer-Aided Drug Discovery (CADD)

Manojkumar O. Malpani

Associate Professor

Department of Chemistry

Shankarlal Khandelwal Arts, Science and Commerce College, Akola, India

Email Id: manojkumarmalpani78@gmail.com

ABSTRACT

Computer-aided drug discovery (CADD) is an innovative approach that leverages computational tools to accelerate and improve the drug development process. With the advancement of technology, CADD has become an increasingly prevalent tool in the pharmaceutical industry. By simulating and analyzing molecular interactions, predicting drug-target binding affinities, and screening vast libraries of compounds, CADD has proven to be instrumental in identifying potential lead compounds with therapeutic potential. Through its ability to efficiently sift through enormous amounts of data and generate accurate predictions, CADD enables researchers to prioritize the most promising candidates for further investigation, ultimately streamlining the drug discovery timeline and increasing the chances of successfully developing effective treatments for various diseases.

Keywords: CADD, QSAR, Molecular docking.

1. INTRODUCTION

Drug discovery is a complex and time-consuming process that involves the identification and development of new therapeutic molecules to treat various diseases. Traditionally, this process heavily relied on experimental methods, which can be expensive, time-consuming, and limited in their ability to explore vast chemical space. However, with the advent of computational chemistry, a powerful field at the intersection of chemistry, biology, and computer science, drug discovery has witnessed significant advancements. Computational chemistry employs computer simulations, algorithms, and mathematical models to accelerate the drug discovery process, offering valuable insights into the behaviour of molecules and their interactions with biological targets. This review provides an overview of the role of computational chemistry in drug discovery, explores the techniques and tools employed, discusses the challenges and limitations, and highlights the future perspectives and advancements in this exciting field.

Overview of the drug discovery process

We are probably wondering how new drugs are discovered. It's not as simple as mixing random chemicals in a lab and hoping for the best. No, it's a carefully orchestrated process that involves a lot of trial and error, and a pinch of luck. The drug discovery process typically starts with identifying a target, which could be a receptor or an enzyme involved in a disease pathway. Once the target is identified, scientists embark on a mission to find a molecule that can interact with this target and either enhance or inhibit its function.

Now, you're probably thinking, "Well, that sounds like a lot of work!" And you're right! But fear not, because this is where computational chemistry swoops in to save the day.

Computational chemistry is like the superhero of drug discovery, using powerful computer modelling techniques to predict the behaviour of molecules and their interactions with targets.

2. ROLE OF COMPUTATIONAL CHEMISTRY IN DRUG DISCOVERY

Computational chemistry brings a whole host of advantages to the drug discovery table. For one, it saves time and money. Instead of blindly testing thousands of molecules in the lab, scientists can use computational methods to screen and prioritize the most promising candidates. It's like having a crystal ball that tells you which molecules are worth pursuing. Another advantage is that computational chemistry allows scientists to explore a vast chemical space. They can virtually generate and test millions of compounds without ever stepping foot in a lab. It's like having a magical laboratory that's not constrained by physical limitations.

Integration of Experimental and Computational Approaches

Now, you might be thinking, "Well, if computational chemistry is so amazing, can we just replace all the lab work with computers?" Not quite. While computational methods are incredibly powerful, they're not infallible. They still need to be validated with experimental data to ensure accuracy. That's why scientists often employ an integrated approach, combining both computational and experimental techniques. By synergizing the powers of computational chemistry and good old-fashioned test tubes, they can accelerate the drug discovery process and increase the chances of success.

3. TECHNIQUES AND TOOLS IN COMPUTATIONAL CHEMISTRY FOR DRUG DISCOVERY

Structure-Based Drug Design

Structure-based drug design is like playing molecular Tetris. Scientists use the three-dimensional structure of the target protein to design molecules that fit into specific pockets or binding sites. It's all about finding the perfect shape and electrostatic properties that will allow the molecule to interact with the target desirably.

Ligand-Based Drug Design

Ligand-based drug design takes a different approach. Instead of focusing on the target protein, scientists analyse molecules that have already shown activity against the target. They then extract common features and create new molecules based on those patterns. It's like reverse engineering a recipe to create a delicious new dish.

Quantitative Structure-Activity Relationship (QSAR)

Ever wondered if there's a mathematical equation for drug discovery? Well, QSAR comes pretty close. It's a technique that uses statistical models to establish correlations between the structure of a molecule and its biological activity. By understanding these relationships, scientists can predict the activity of new molecules and prioritize those with the highest chances of success.

4. VIRTUAL SCREENING AND MOLECULAR DOCKING IN DRUG DISCOVERY

Virtual screening is like speed dating for molecules. It involves screening large libraries of compounds against a target protein to identify potential hits. Instead of physically testing each molecule, scientists use computer algorithms to predict how well they will interact with

the target. It's a quick and efficient way to narrow down the options and focus on the most promising candidates.

Molecular Docking Methods

Molecular docking is like playing a game of molecular lock and key. Scientists use computational algorithms to predict how a small molecule (the ligand) will bind to a target protein (the receptor). By exploring different orientations and conformations, they can determine the most favourable binding pose. It's like solving a puzzle where the reward is a potential new drug.

Validation and Analysis of Docking Results

Of course, docking results are not to be taken at face value. They need to be validated and analysed to ensure their reliability and relevance. Scientists use various techniques, such as scoring functions and experimental validation, to assess the quality of the docking results. It's like a reality check for those molecules that thought they were the perfect match. And there you have it; a whirlwind tour of how computational chemistry shakes things up in the world of drug discovery. It's a fascinating field that combines science, technology, and a dash of creativity to create new medicines that can change lives. So next time you hear about a groundbreaking drug, you can appreciate the superheroes behind the scenes, harnessing the power of computers to make it happen.

5. MOLECULAR DYNAMICS SIMULATIONS AND QUANTUM MECHANICS IN DRUG DISCOVERY

Role of Molecular Dynamics Simulations

In the world of drug discovery, scientists are turning to computational chemistry techniques such as molecular dynamics simulations to understand the behavior of molecules at the atomic level. By simulating the movements and interactions of molecules over time, researchers can gain valuable insights into how drugs interact with their target proteins. This knowledge is crucial for designing and optimizing drug candidates with higher efficacy and fewer side effects.

Quantum Mechanics Applications in Drug Discovery

Quantum mechanics, on the other hand, provides a more detailed and accurate description of molecular properties and interactions. It allows scientists to calculate properties such as molecular energies, electronic structures, and reaction mechanisms. This information is vital in understanding the fundamental aspects of drug action and can guide the development of more potent and selective drugs.

Combining Molecular Dynamics and Quantum Mechanics

To achieve even greater accuracy, researchers often combine molecular dynamics simulations with quantum mechanics calculations. This hybrid approach, known as QM/MM (quantum mechanics/molecular mechanics), takes advantage of the strengths of both methods. It allows for a more realistic and comprehensive representation of the drug-target interactions, taking into account the dynamic nature of the system and the quantum effects that are critical for understanding complex biological processes.

6. CHALLENGES AND LIMITATIONS OF COMPUTATIONAL CHEMISTRY IN DRUG DISCOVERY

Accuracy and Reliability of Computational Models

Despite the significant advancements in computational chemistry, there are still challenges when it comes to the accuracy and reliability of the models used in drug discovery. The accuracy of predictions heavily relies on the quality of the force fields, parameterization methods, and approximations employed. It is essential for scientists to constantly refine and validate these models against experimental data to ensure their reliability.

Handling Large Data Sets and Computational Complexity

Another challenge is the exponential growth of data in drug discovery. With the increasing availability of genomic, proteomic, and chemical data, computational chemists must develop efficient algorithms and techniques to handle and analyze these large data sets. Additionally, the computational complexity of modeling drug-target interactions requires substantial computational resources, which can be a limiting factor for many research groups.

Limitations in Predicting Drug Efficacy and Safety

Computational chemistry methods have their limitations in accurately predicting drug efficacy and safety. While they can provide valuable insights into drug-target interactions, they cannot capture the complexities of the human body fully. Factors such as metabolism, pharmacokinetics, and off-target effects still require experimental validation. Therefore, computational chemistry should be considered as a complementary tool rather than a standalone solution in drug discovery.

7. FUTURE PERSPECTIVES AND ADVANCEMENTS IN COMPUTATIONAL CHEMISTRY FOR DRUG DISCOVERY

Emerging Technologies in Computational Chemistry

Exciting advancements in computational chemistry are on the horizon. Techniques such as accelerated molecular dynamics, enhanced sampling methods, and machine learning-based approaches are actively being developed to overcome the limitations of current methodologies. These emerging technologies hold promise for more accurate predictions and deeper insights into drug-target interactions.

Integration of Artificial Intelligence and Machine Learning

Artificial intelligence (AI) and machine learning (ML) are revolutionizing the field of drug discovery. By leveraging vast amounts of data, AI and ML algorithms can identify patterns, predict drug-target interactions, and even suggest novel drug candidates. The integration of these technologies with computational chemistry has the potential to significantly accelerate the drug discovery process and increase the success rate of developing new medications.

Potential Impact on Drug Discovery Process

The advancements in computational chemistry are poised to reshape the drug discovery landscape. By enabling faster and more accurate predictions, computational chemistry can help researchers prioritize potential drug candidates, optimize their properties, and reduce the need for extensive experimental screening. Ultimately, this can lead to a more efficient and cost-effective drug discovery process, benefiting patients worldwide by providing faster access to safer and more effective medications. In conclusion, computational chemistry has revolutionized the field of drug discovery, enabling scientists to expedite the identification and development of potential therapeutics with greater precision and efficiency. The integration of

computational methods with experimental approaches has proven to be a powerful combination, offering valuable insights into molecular interactions, structure-activity relationships, and drug efficacy. However, challenges such as accuracy, computational complexity, and the limitations of predictive capabilities still exist. Nonetheless, with the continuous advancements in technology, the future of computational chemistry in drug discovery holds immense promise. As researchers explore emerging technologies, incorporate artificial intelligence, and refine computational models, we can expect even greater strides in the discovery and development of novel drugs that improve the health and well-being of individuals worldwide.

CONCLUSION

The future of computational chemistry in drug discovery is promising. Emerging technologies such as artificial intelligence and machine learning are being integrated into computational chemistry workflows, allowing for more efficient and accurate predictions. Continued advancements in computational power and algorithms will further enhance the capabilities of computational chemistry. These advancements have the potential to revolutionize the drug discovery process, leading to the development of more effective and personalized therapeutics to address the unmet medical needs of patients.

REFERENCES:

1. Surabhi and B. K. Singh, COMPUTER AIDED DRUG DESIGN: AN OVERVIEW. Journal of Drug Delivery & Therapeutics. 2018; 8(5):504-509. <http://dx.doi.org/10.22270/jddt.v8i5.1894>.
2. J. J. Naikwadi, N. Desai, S. V. Patil, Computer aided drug design- an overview. IJCRT, Volume 9, Issue 10, October 2021, ISSN: 2320-2882.
3. K. S. Dhamal, S. A. Waghmare, H. Kamble, et.al., Role Of Computer Aided Drug Design In Drug Discovery & Development. International Journal of Research in Engineering and Science (IJRES). Volume 10, Issue 3, 2022, PP. 01-05.
4. I. Hoque, A. Chatterjee, S. Bhattacharya and R. Biswas, An Approach of Computer-Aided Drug Design (CADD) Tools for In Silico Pharmaceutical Drug Design and Development. Int. J. Adv. Res. Biol. Sci. (2017). 4(2): 60-71. <http://dx.doi.org/10.22192/ijarbs.2017.04.02.009>.
5. R. S. Waghmode, A. B. Lasure, S. B. Bavage, N. B. Bavage, Computer Aided Drug Design (CADD). IJIRT, Volume 8, Issue 3, ISSN: 2349-6002.

Synthesis and Anti-microbial Activity of Novel 3-[(3-substitutedamino-1,2,4-thiadiaz-3-yl)]amino-5-N-TAG-amino-1,2,4-thiadiazole [11b]

M. R. Raghuvanshi

Department of Chemistry, Arvindbabu Deshmukh Mahavidyalaya, Bharsingi, Dist-Nagpur, Maharashtra, India-441305 Corresponding author-meg.rag20@gmail.com

Abstract

In this study new 3-[(3-substituted amino -1,2,4-thiadiaz-3-yl)] amino-5-TAG-amino-1,2,4-thiadiazole [11] were synthesized by the oxidative cyclization of 1-[S-TAG-N-substitutedthioamido] dicyanadiamide [8] and 1-[(N-TAG) thioamido]-5-substitutedformamidino-2-imino-4-thiobiuret [9] respectively in chloroform medium using liquid bromine as oxidizing agent. The newly synthesized compounds isolated in these reaction were characterized and justified on the basis of conventional elemental analysis, chemical characteristics, IR, NMR and Mass spectral analysis. The synthesized compounds were screened for antimicrobial activities by disc diffusion method.

Keywords – Synthesis, Dicyandiamide, Thiadiazol, Antimicrobial activity

Introduction

During last few decades, heterocyclic molecules containing nitrogen, sulfur and oxygen (five and six membered rings) have become the area of interest for medicinal chemists and researchers owing to their wide spectrum of biological/pharmacological activities.¹ Thiadiazol, a five membered heterocyclic moiety containing one sulfur and two nitrogen atoms existing in four different isomeric forms, 1,2,3-thiadiazole; 1,2,4-thiadiazole and 1,2,5-thiadiazole and 1,3,4-thiadiazole has established its significant importance due to comprehensive pharmacological activities²⁻⁴. 1,2,4-Thiadiazoles are heteroatom rich heterocycles with a vital role in medicinal chemistry programmes; many clinically approved pharmaceuticals contain this heterocycle.⁵

1,2,4-thiadiazoles are considered as most significant subclass of bioactive five-membered organic compounds for medicinal chemistry⁶ and showed a remarkable biological activities such as cyclooxygenase inhibitors⁷, human leukemia⁸, antibacterial⁹, antiulcerative¹⁰, antihypertensive¹¹, cathepsin B inhibitors¹², anticonvulsant¹³, antidiabetic¹⁴, anti-inflammatory⁷, and allosteric modulators¹⁵.

The wide range of application of 1,2,4- thiadiazols as pharmacophores in medicinal chemistry has attracted great interest in their synthesis.¹⁶

As a part of research work presently been undertaken in this laboratory for the synthesis of heteroacycles and heterocycles, it was thought interesting to investigate the oxidative cyclization of 1-[(N-TAG) thioamido]-5-substitutedformamidino-2-imino-4-thiabiuret [9] with liquid bromine in chloroform medium to obtain a novel series of 3-[(3-substitutedamino-1,2,4thiadiaz-3-yl)] amino-5-N-TAG-amino-1,2,4-thiadiazole [11] In this study, a new series of 1,2,4-thiadiazole derivatives (11a-e) were synthesized in good yields, and the structures of the compounds were confirmed by IR, ¹H-NMR, and elemental analysis. For that The newly synthesized substituted derivatives of thiocarbamide were screened for its antibacterial activities against some gram positive & gram negative pathogens. The compounds showed good & moderate activity against the pathogens.

Experimental

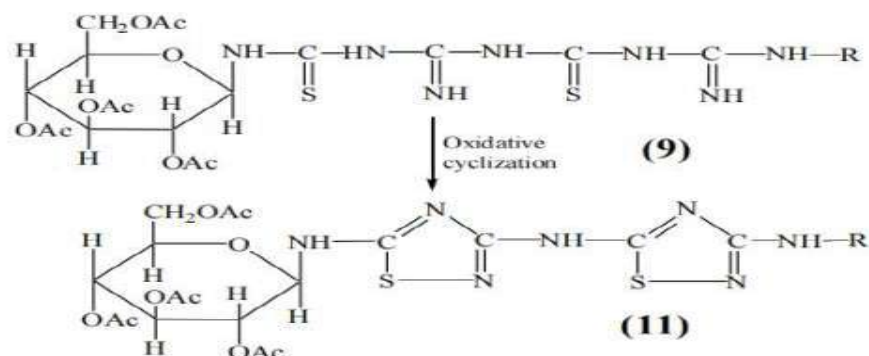
The melting points of all the synthesized compounds were recorded using hot paraffin bath and are uncorrected, The carbon and hydrogen analysis was carried out on Carlo-Ebra-1106 analyzer, nitrogen estimation was carried out on ColmanN-analyser-29. IR spectra were recorded on Perkin-Elmer spectrometer in the range 4000-400 cm^{-1} in KBr pellets. PMR spectra were recorded on Bruker AC-300F spectrometer with TMS as internal standard using CDCl_3 and $\text{DMSO}-d_6$ as solvent. The FAB mass spectra were recorded on a Joel SX 102/Da-600 mass spectrometer/ Data System using Argon. The accelerating voltage was 10kV and spectra were recorded at room temperature by using m-nitro benzyl alcohol as a matrix. The purity of the compounds was checked on Silica Gel-G plates by TLC with layer thickness of 0.3 mm. All chemicals used were of AR grade.

Synthesis of 3-[(3-phenylamino-1,2,4-thiadiaz-3-yl)]amino-5-N-TAG-amino-1,2,4-thiadiazole [11b]

In china dish a paste of 1-[N-TAG thioamido]-5-phenylthio formamidino-2-imino-4-thiobiuret [9b] was prepared in chloroform. To this liquid bromine in chloroform was added with constant stirring. Initially the colour of bromine disappeared, the addition of bromine was continued till the colour of bromine persisted to the reaction mixture. The reaction mixture was allowed to stand for 8 Hrs. at room conditions. It is dark brown in colour. After the basification of the reaction mixture afforded brown coloured product, which on crystallization gave brown crystals of [11b] yield 61%, m. p. 147°C .

The probable reaction mechanism of the formation of [11b] may be stated as follows.

Scheme



Where R = -H, -phenyl, -methyl, -ethyl and allyl.

Similarly 3-[(3-Amino-1,2,4-thiadiaz-3-yl)]-amino-5-N-TAG amino-1,2,4-thiadiazole [11a], 3-[(3-methylamino-1,2,4-thiadiaz-3-yl)]-amino-5-N-TAG amino-1,2,4-thiadiazole [11c], 3-[(3-ethylamino-1,2,4-thiadiaz-3-yl)]-amino-5-N-TAG amino-1,2,4-thiadiazole [11d], 3-[(3-allylamino-1,2,4-thiadiaz-3-yl)]-amino-5-N-TAG amino-1,2,4-thiadiazole [11e] were synthesized from 1-[(N-TAG)thioamidino]-5-formamidino-2-imino-4-thiobiuret [9a], 1-[(N-TAG)thioamidino]-5-methylformamidino-2-imino-4-thiobiuret [9c], 1-[(N-TAG)thioamidino]-5-ethylformamidino-2-imino-4-thiobiuret [9d], 1-[(N-TAG)thioamidino]-5-allylformamidino-2-imino-4-thiobiuret [9e] in bromine in chloroform medium respectively.

Result ad Discussion-

Spectral Evaluation-

The IR spectrum of compound 3-[(3-phenylamino-1,2,4-thiadiaz-3-yl)]amino-5-N-TAG-amino-1,2,4-thiadiazole was carried out in KBr pellets and is reproduce on plate No. IR-1. The IR spectrum clearly indicated the bands due to $\nu\text{-NH}$, $\nu\text{-C-H(Ar)}$, $\nu\text{-C=O}$, $\nu\text{-C=N}$, $\nu\text{-RC-N}$, $\nu\text{-RC-S}$ and an important absorption can be correlated in **Table No. 1**.

Table No.-1

Absorption	Assignment Observed	Absorption expected (Cm ⁻¹)
3374.5	-NH- stretching	3500-3100
1695.8	-C=O stretching	1900-1600
1585.0	-C=N stretching	1789-1471
1213.0	-C-N Stretching	1200-1000
757.4	-C-S Stretching	800-600

The PMR spectrum of compound 3-[(3-phenylamino-1,2,4-thiadiaz-3-yl)]amino-5-N-TAG-amino-1,2,4-thiadiazole was carried out in DMSO-d₆ and CDCl₃ and shown in figure 2. This spectrum distinctly displayed the signals due to -NH protons at δ 9.5-8.6 ppm, Ar. Protons at δ 7.77 - 7.01 ppm.

The FAB mass spectrum of 3-[(3-phenylamino-1,2,4-thiadiaz-3-yl)]amino-5-N-TAG-amino-1,2,4-thiadiazole [11b] was recorded at room temperature by using meta nitrobenzyl alcohol as the matrix m⁺ peak as well as other fragment peaks and the probable fragmentation pattern of the molecular ion.

Antimicrobial Activity

All the synthesized compounds were screened for antimicrobial activity using disc diffusion method¹⁷ and all the pathogen tested during analysis are human pathogens. For this Whatman filter paper No. 1 disks of 5mm diameter were sterilized in autoclave and soaked in sample solution, blotted on sterile filter paper. 0.1ml of the inoculums of test organism was spread using sterile glass spreader on the surface of nutrient agar. The filter paper disks soaked in Gentamycin (20 μ g/ml) (Glaxo India Ltd.) and Ciprofloxacin (20 μ g/ml) (Glaxo smith kline) were used as positive controls and the filter paper disc soaked in dimethyl sulphoxide (DMSO) were used as a solvent. The compounds were taken at a concentration or 1mg/ml using dimethyl sulphoxide as a solvent. Fluconazole (20 μ g/ml) as a standard for antifungal activity. The inhibition zones were measured in millimeter by the end of the incubation period (24 hrs. at 37°C for bacteria).

Table No-2

Compounds	Inhibition zone in mm					
	<i>S.Typhi</i>	<i>E.coli</i>	<i>P. aerogenosa</i>	<i>S.aures</i>	<i>A.nigar</i>	<i>c.albicanes</i>
9a	8	8	-ve	-ve	9	-ve
9b	10	9	-ve	8	12	10
9c	9	9	7	7	10	10
9d	9	8	9	9	9	9
9e	10	9	10	9	12	12
DMSO	-	-	-	-	-	-
Fluconazole	-	-	-	-	12	12
Ciprofloxacin	10	9	10	9	-	-

From the results it is clear that compounds showed remarkable and considerable antimicrobial activity against organism. The activity of compounds were tested against all the pathogen by disc diffusion method. The antimicrobial activity of different compound against micro-organisms were examined in the presence study and their potency, were assessed by the presence or absence inhibition zone and zone diameter. The result are given in Table No. 2. From this table clearly indicates that, all the compounds are active against *S. typhi*, *E.coli* & *A. nigar* but some compounds 9a and 9b are inactive against *P.aerogenosa*, *S.aurues* & *c.albicans*.

Conclusion-

This paper reports the synthesis of 3-[(3-phenylamino-1,2,4-thiadiaz-3-yl)]amino-5-N-TAG-amino-1,2,4-thiadiazole [11b] & 3-[(3-Substitutedamino-1,2,4-thiadiaz-3-yl)]amino-5-N-TAG-amino-1,2,4-thiadiazole (11a-e) derivatives and characterization by FT-IR, PMR and mass spectrograph indicating formation of the desired product. The compounds were studied to evaluate in vitro antibacterial and antifungal properties by disc diffusion method. The antimicrobial activity of different compound against micro-organisms were examined in the presence study and their potency, were assessed by the presence or absence inhibition zone and zone diameter. From results, most of these compounds found to be potent antibacterial and antifungal agent exhibited comparable antibacterial and antifungal activity than the standard. It means that the compounds showed remarkable and considerable antimicrobial activity.

Acknowledgement: The author acknowledges the help of SAIF, CDRI, Lucknow for providing the spectral data. Authors are thankful to the Department of Chemistry, Mahata Fule College of Science Warud for providing the necessary facilities to carry out the research work & Dr.Rahul Bhagat (Biotechnolgy) for his help in doing antimicrobial activity.

References

1. Yang Hu, Cui-Yun Li, Xiao-Ming Wang, Yong-Hua Yang, Hai-Liang Zhu., *Chem. Rev.* 2014, 114(10),pp5572–5610, <https://doi.org/10.1021/cr400131u>
2. V. Raj, A. Rai, S. Saha., *Anti-Cancer Agents Med Chem*, 2017,17(4),pp.500-523, [10.2174/1871520616666161013150151](https://doi.org/10.2174/1871520616666161013150151),PubMed: 27745547,View article View in Scopus Google Scholar
3. Serban.,*Molecules*,2020, 25 (4),pp.942, PubMed: 32093125. Pub Med Central: PMC7070519, View article View in Scopus Google Scholar
4. Y. Hu, C.Y. Li, X.M. Wang, Y.H. Yang, H.L. Zhu., *Chem Rev*, 2014,114 (10) , pp. 5572-5610, [10.1021/cr400131u](https://doi.org/10.1021/cr400131u), View article,View in Scopus Google Scholar
5. Daniel G. Anstis^a, Emma K. Davison, Jonathan Sperry ., *Tetrahedron*, **Volume 150**, 15 January 2024, 133767, <https://doi.org/10.1016/j.tet.2023.133767>
6. Kumar, D.; Kumar, N.-M.; Chang, K.-H.; Shah, K.: Synthesis and anticancer activity of 5-(3-indolyl)-1,3,4-thiadiazoles. *Eur. J. Med. Chem.* ,2010,**45**, pp 4664–4668
7. Unangst, P.C.; Shrum, G.P.; Connor, D.T.; Dyer, R.D.; Schrier, D.J.: Novel 1,2,4-oxadiazoles and 1,2,4-thiadiazoles as dual 5-lipoxygenase and cyclooxygenase inhibitors. *J. Med. Chem.* 1992,**35**, pp. 3691–3698
8. Romagnoli, R.; Baraldi, P.G.; Carrion, M.D.; Cruz-Lopez, O.; Preti, D.; Tabrizi, M.A.; Fruttarolo, F.; Heilmann, F.; Bermejo, J.; Estevez, F.,*Bioorg. Med. Chem. Lett.* ,2007,**17**, pp 2844–2848
9. Harai, R.; Sakamoto, K.; Hisamichi, H.; Nagano, N.: Structure–activity relationships of cephalosporins having a (dimethyl isoxazolidinone) vinyl moiety at their 3-position. *J. Antibiot.* ,1996,**49**, pp. 1162–1171
10. Kharimian, K.; Tam, T.F.; Leung-Toung, R.C.; Li, W.: Thiadiazole compounds useful as inhibitors of hb/kb atpase. *PCT Int. Appl.* WO9951584A1 ,1999
11. Kohara, Y.; Kubo, K.; Imamiya, E.; Wada, T.; Inada, Y.; Naka, T.,*J. Med. Chem.* ,1996,**39**, pp. 5228–5235
12. Leung-Toung, R.; Wodzinska, J.; Li, W.; Lowrie, J.; Kukreja, R.; Desilets, D.; KarimianK.; Tam. ,*Bioorg. Med. Chem.* ,2003,**11**, 5529–5537 (2003)
13. Castro, A.; Castano, T.; Encinas, A.; Porcal, W.; Gil, C., *Bioorg. Med. Chem.* **14**, 1644–1652 (2006)
14. Johnstone, C.; Mckercher, D.; Pike, K.G.; Waring, M.J., *PCT Int. Appl.*WO2005121110A1 ,2005.
15. van den Nieuwendijk, A.M.C.H.; Pietra, D.; Heitman, L.; Goblyos, A.; Ijzerman, A.P., *J. Med. Chem.* ,2004,**47**, 663–672
- 16.Armando Pombeiro Maximilian N Kopylovich, *European Journal of Organic Chemistry* 2017,(19), DOI:[10.1002/ejoc.201601642](https://doi.org/10.1002/ejoc.201601642)

Sulfate promoted zirconia-based mixed oxide as solid acid catalysts for organic transformations

Sushil V. Shelke^a, Sambhaji T. Dhumal^b, Abhay L. Ghodke^a, Meghshyam K. Patil^{a,*}

^aDepartment of Chemistry, Dr. Babasaheb Ambedkar Marathwada University, Sub-Campus, Dharashiv- 413501

^bDepartment of Chemistry, Ramkrishna Paramhansa Mahavidyalaya, Dharashiv-413501

E-mail: meghshyam_patil@yahoo.com

Abstract:

After gaining attention by sulfated zirconia as solid acid catalyst, various modified versions of zirconia based catalysts have attracted attention due some extra properties associated with stability of the catalyst. Among these modified versions, various sulfate promoted zirconia-based mixed oxides have been reported in the literature, which includes $\text{SO}_4^{2-}/\text{ZrO}_2\text{-CeO}_2$, $\text{SO}_4^{2-}/\text{SnO}_2\text{-ZrO}_2$, $\text{SO}_4^{2-}/\text{TiO}_2\text{-ZrO}_2$, sulfated zirconia catalyst supported on mesostructured $\gamma\text{-Al}_2\text{O}_3$, sulphated mesoporous $\text{La}_2\text{O}_3\text{-ZrO}_2$ composite oxides, and many more. In this article, we have summarized some of the organic transformations catalyzed by sulfate promoted zirconia-based mixed oxides. These organic transformations includes Friedel-Crafts benzylation of anisole with benzoyl chloride; dealkylation of 1,3,5-tri-*tert*butyl-benzene; synthesis of coumarins *via* Pechmann reaction; Mannich reaction between aldehyde, ketone and amines; synthesis of quinoxalines and synthesis of 2-aryl benzimidazoles and so on.

Keywords: Sulfate impregnation, sulfated zirconia, mixed oxide, organic transformations.

Introduction

Generally, liquid acid catalysts or homogeneous acid catalysts have been used to perform acid catalyzed reactions. Acid catalyzed reactions are efficiently carried out by these catalysts as these are soluble in the reaction medium and the reactant can easily reach to the active site of the catalyst and vice-versa. Whereas, some of these catalysts are very reactive and will not produce the product selectively. Further, the loopholes associated with the use of these systems are non-recoverable catalysts, tedious work-up procedures, and consequently responsible for pollution [1-5]. The scientific community was searching for a heterogeneous counterpart of these catalysts, that can work efficiently as a catalyst, gives high yield, recyclable, with easy and eco-friendly work-up procedure. In this regard, several heterogeneous catalysts such as zeolite, amberlite, nafion-H, molecular sieves, sulfated zirconia, and so on have been used as catalysts. Among these catalysts, sulfated zirconia is one of the important catalysts. It has been used extensively as a catalyst for processes/reactions such as alkylation, isomerization, cracking reactions, and several organic transformations [1-6]. In addition to this, many modified versions of sulfated zirconia can be used as catalysts. These modifications include different preparation procedures for sulfated zirconia catalysts, which can alter the properties of the catalyst. By using templated mesoporous, sulfated zirconia catalysts have been prepared. Other modification includes the use of MoO_x or WO_x as a promoter instead of SO_4^{2-} [7, 8]. Another important modification includes, sulfate impregnation of a mixed oxide of ZrO_2 with other metal oxide. In this article, we have discussed some of the organic transformation reactions, which are catalyzed by these sulfated zirconia-based mixed oxides.

Preparation of sulfated zirconia-based mixed oxides:

Several methods have been adopted in the literature for the preparation of sulfate impregnated zirconia based mixed oxides. These methods includes co-precipitation, sol-gel,

hydrothermal and so on. Reddy *et al.* prepared sulfated ceria-zirconia catalyst by co-precipitation followed by sulfated impregnation [9]. Ben Hamouda and Ghorbel used sol-gel method for preparation of sulfated zirconia supported by alumina [10]. Chakraborty *et al.* employed hydrothermal method for the preparation of silica sulphated zirconia [11]. These are some notable examples of use of different methods for synthesis of zirconia-based catalysts.

Organic Transformations by Sulfate promoted zirconia-based mixed oxide:

In this section, we have discussed some of the reactions reported by using sulfate promoted zirconia-based mixed oxide as a catalyst.

1. Friedel-Crafts benzoylation of anisole with benzoyl chloride and dealkylation of 1,3,5-tri-*tert*butyl-benzene:

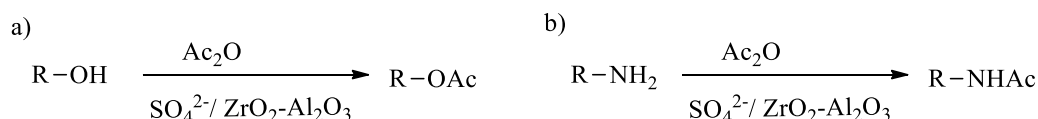
Zhao *et al.* have been prepared sulfated zirconia supported on mesostructured γ - Al_2O_3 as a catalyst used for Friedel-Crafts benzoylation of anisole with benzoyl chloride and dealkylation of 1,3,5-tri-*tert*butyl-benzene [12].

2. Pechmann reaction and Mannich reaction:

Reddy *et al.* synthesized sulfate promoted CeO_2 - ZrO_2 catalyst and utilized it for the synthesis of coumarins *via* Pechmann reaction as well as Mannich reaction between aldehyde, ketone and amines [9, 13].

3. Acetylation of alcohols and amines:

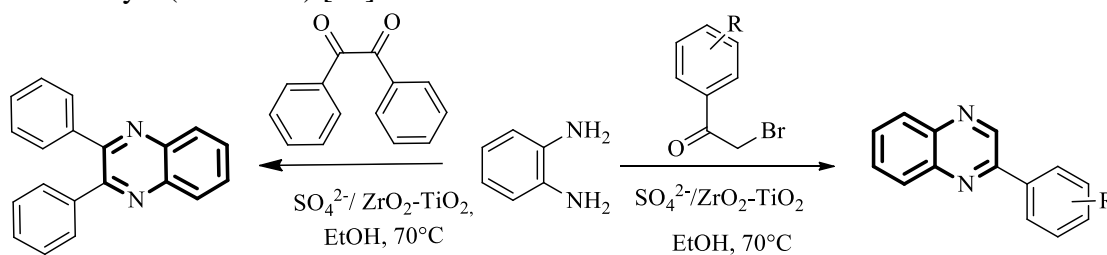
Sulfate promoted Al_2O_3 - ZrO_2 catalysts have been reported for acetylation of alcohol and amines with acetic anhydride (Scheme 1) [14].



Scheme 1. Sulfate ZrO_2 - Al_2O_3 catalyzed acylation of alcohols and amines.

4. Synthesis of quinoxalines

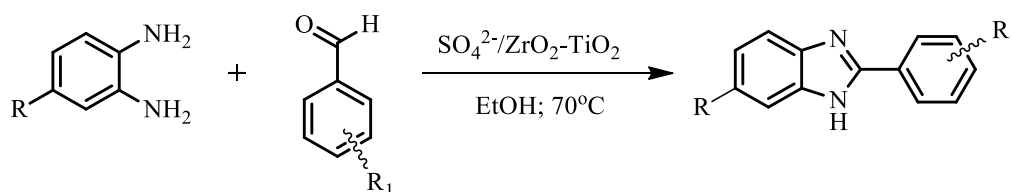
Recently, Shelke *et al.* reported the synthesis of quinoxalines by reaction between phenacyl bromides/benzil and *o*-phenylenediamine using sulfate promoted ZrO_2 - TiO_2 as a catalyst (Scheme 2) [15].



Scheme 2. $\text{SO}_4^{2-}/\text{ZrO}_2$ - TiO_2 catalyzed synthesis of quinoxalines.

5. Synthesis of 2-aryl benzimidazoles

Furthermore, Shelke *et al.* have also been reported the synthesis of 2-aryl benzimidazoles by reaction of *o*-phenylenediamines and different aromatic aldehydes (Scheme 3). This reaction is catalyzed by sulfate promoted ZrO_2 - TiO_2 [16].



Scheme 3. $\text{SO}_4^{2-}/\text{ZrO}_2$ - TiO_2 catalyzed synthesis of 2-aryl benzimidazoles.

Conclusion:

Sulfate promoted zirconia-based mixed oxides is a one of the promising group of catalysts in a family of solid acid catalysts. These catalysts have been used for variety of organic transformations. These catalysts are recyclable, easy work up procedures, promotes high yield, therefore it is an eco-friendly way to carried out many organic transformations such as Friedel-Crafts benzylation of anisole with benzoyl chloride; dealkylation of 1,3,5-*tert*-butyl-benzene; synthesis of coumarins *via* Pechmann reaction; Mannich reaction between aldehyde, ketone and amines; synthesis of quinoxalines and synthesis of 2-aryl benzimidazoles. Furthermore, these catalysts can be explored for various other organic transformations.

References:

- [1] M. K. Patil, A. N. Prasad, B. M. Reddy, *Curr. Org. Chem.*, **2011**, 15, 3961.
- [2] G. D. Yadav, J. J. Nair, *Microporous and Mesoporous Materials*, **1999**, 33, 1.
- [3] A. Feller, J. A. Lercher *Adv. Catal.*, **2004**, 48, 229.
- [4] A. Corma, *Catal. Rev.-Sci. Eng.*, **2004**, 46, 369.
- [5] K. Arata, *Green Chem.*, **2009**, 11, 1719.
- [6] G. X. Yan, A. Wang, I. E. Wachs, J. Baltrusaitis, *Appl. Catal. A: Gen.*, **2019**, 572, 210.
- [7] B. M. Reddy, M. K. Patil, B. T. Reddy, *Catal. Lett.*, **2008**, 125, 97.
- [8] B. M. Reddy, M. K. Patil, G. K. Reddy, B. T. Reddy, K. N. Rao, *Appl. Catal. A: Gen.*, **2007**, 332, 183.
- [9] B. M. Reddy, M. K. Patil, P. Lakshmanan, *J. Mol. Catal. A: Chem.* **2006**, 256, 290.
- [10] L. Ben Hamouda, A. Ghorbel, *J. Sol-Gel Sci. Tech.* **2003**, 26, 831.
- [11] B. Chakraborty, P. Dutta, S. K. Nandi, *Mater. Sci. Indian J.* **2013**, 9, 144.
- [12] J. Zhao, Y. Yue, W. Hua, H. He, Z. Gao, *Appl. Catal. A*, **2008**, 336, 133.
- [13] B. M. Reddy, P. M. Sreekanth, P. Lakshmanan, A. Khan, *J. Mol. Catal. A: Chem.*, **2006**, 244, 1.
- [14] B. M. Reddy, P. M. Sreekanth, Y. Yamada, T. Kobayashi, *J. Mol. Catal. A: Chem.*, **2005**, 227, 81.
- [15] S. V. Shelke, S. T. Dhumal, A. Y. Karale, T. R. Deshmukh, M. K. Patil, *Syn. Commun.* **2022**, 52, 597.
- [16] S. V. Shelke, S. T. Dhumal, T. R. Deshmukh, M. K. Patil, *Lett. Org. Chem.* **2023**, 206, 541.

Structure, Physical and Chemical Properties of Thiourea with Their Derivatives

A.P. Mitake, S.P. Rathod,

Department Of Chemistry G. S. Gawande Mahavidyalay Umarkhed Dist. Yavatmal

E-mail : mitake@gsgcollege.edu.in

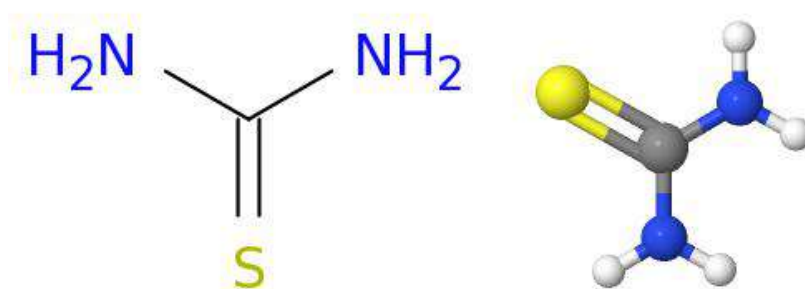
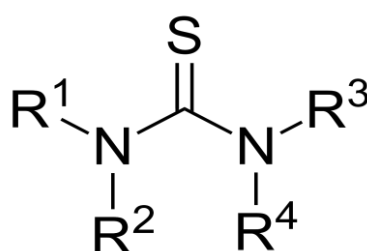
Abstract:

In this study six unsymmetrical thiourea derivatives, 1-isobutyl-3-cyclohexylthiourea (**1**), 1-*tert*-butyl-3-cyclohexylthiourea (**2**), 1-(3-chlorophenyl)-3-cyclohexylthiourea (**3**), 1-(1,1-dibutyl)-3-phenylthiourea (**4**), 1-(2-chlorophenyl)-3-phenylthiourea (**5**) and 1-(4-chlorophenyl)-3-phenylthiourea (**6**) were obtained in the laboratory under aerobic conditions. Compounds **3** and **4** are crystalline and their structure was determined for their single crystal. Compound **3** is monoclinic system with space group $P2_1/n$ while compound **4** is trigonal, space group $R^3:H$. Compounds (**1–6**) were tested for their anti-cholinesterase activity against acetylcholinesterase and butyrylcholinesterase (hereafter abbreviated as, AChE and BChE, respectively). Potentials (all compounds) as sensing probes for determination of deadly toxic metal (mercury) using spectrofluorimetric technique were also investigated.

Keywords: thiourea derivatives, enzyme inhibition,

Introduction:

It plays an important role in the construction of hetero-cycles, the compounds formed by the insertion of one or more, similar or different hetero-atoms (other than carbon or hydrogen atoms) in different cyclic systems. It appears as white crystals which are combustible and in contact with fire give off irritating or toxic fumes. It acts as a precursor to sulphide to produce metal sulphides like mercury sulphide. Thiourea is a reagent in organic synthesis, a special branch of chemical synthesis, and is concerned with the construction of organic compounds via organic reactions. "Thioureas" can refer to a broad class of compounds with the general structure $(R_1R_2N)(R_3R_4N)C=S$. Thiourea is also called by names such as "Thiocarbamide, and Pseudo thiourea" Thioureas belong to thioamides, a functional group with the general structure $R-CS-NR'R''$, where R, R', and R'' are organic groups. Examples include $RC(S)NR_2$, where R is methyl, ethyl, etc.

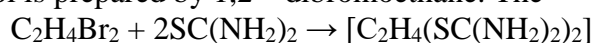
Structure of Thiourea molecule**Thiourea (CH₄N₂S)****Structure of Thiourea****Properties of Thiourea**

- It is an organic compound containing sulphur atoms.
- Its molar mass is 76.12 g.mol⁻¹.
- It is a white-coloured compound.
- It exists in a solid state at room temperature.
- The melting point of thiourea is 176 – 178°C.
- Its boiling point is 150 – 160°C
- Its density is 1.405 g.ml⁻¹.
- It is highly soluble in water. For instance, 142 g of thiourea can be dissolved in one litre of water at 25°.
- It is slightly acidic in nature
- Its crystals are highly combustible in contact with fire.
- It has pH value of more than 3.
- It is an odourless (with no smell) compound.
- Its surface tension is 1.04 10⁻² N/m.
- Thiourea on heating above 130°, forms ammonium thiocyanate. Upon cooling it again converts into thiourea.
- Reduction – Peroxides get reduced into their corresponding Diols (chemical compounds with two hydroxyl groups) by thiourea. During this reduction reaction, a by-product formed which is called endo-peroxide. Endo-peroxide is a highly unstable compound.
- Due to its non-volatile nature, it is also used in the ozonolysis of cyclic alkenes to give carbonyl compounds.
- It reacts with alkyl halides and forms thiols.

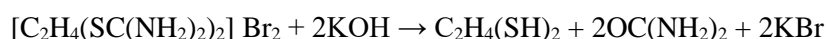
Uses of Thiourea

Total global production of thiourea approximately 40% is produced in Germany and another 40% in China. About 10,000 tonnes of thiourea is being manufactured globally in a year. Its bulk production clearly proves its significance in the market. Few of its applications are listed below:

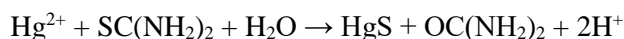
- Thiourea Dioxide (prepared by oxidation of Thiourea with Hydrogen peroxide) is used as a reducing agent in many chemical reactions used in textile processing.
- It is used in the production of flame-retardant resins, which prevents or slows down the spread of fires.
- It is used as a source of sulphide, a compound of sulphur with another element. It reacts with alkyl halides and changes them into thiols, a sulphur analogue of alcohols that is simple it is an organic compound consisting of compounds with a sulphur atom. For example, ethane – 1,2 – dithiol is prepared by 1,2 – dibromoethane. The reaction is given below:



Br_2



- Thiourea can be used as a source of sulphide in reactions with metal ions as well. For example, mercury sulphide is formed when mercury ion reacts with thiourea in presence of water and heat. The reaction is given below:



- Thiourea condenses with - dicarbonyl and forms pyrimidine derivatives. It is used in vulcanization accelerators.
- It is used as an auxiliary agent.
- It is used in silver – gelatine photographic prints, diazo paper, light-sensitive photocopy paper, etc.
- It is used in many electroplating processes such as Clifton – Philips and Beaver bright electroplating, etc.
- For copper printed circuits, tin (II) chloride solution is used. Thiourea is also used in the solution.
- It is used in silver cleaning products such as Tarn x which contains thiourea, sulfamic acid and detergent.
- It is used in gold and silver leaching. Lixiviants are used for this purpose and thiourea is an important ingredient of these. Lixiviant is a liquid medium used in hydrometallurgy to selectively extract the desired metal from the ore or mineral.
- Even short exposure to the Thiourea causes severe irritation and temporary skin infection.
- 125mg/kg of thiourea can be deadly for rats on oral ingestion.
- On chronic exposure, thiourea can cause a goitrogenic effect on humans. Goitrogens can reduce the thyroid's ability to produce the hormones your body needs to function normally.
- Enlargement of the thyroid gland is known as goiter disease. In this disease, goitrogens disrupt the production of thyroid hormones. This stimulates the pituitary gland to release TSH and TSH promotes the growth of thyroid tissues.

Six Different Derivatives of Thiourea

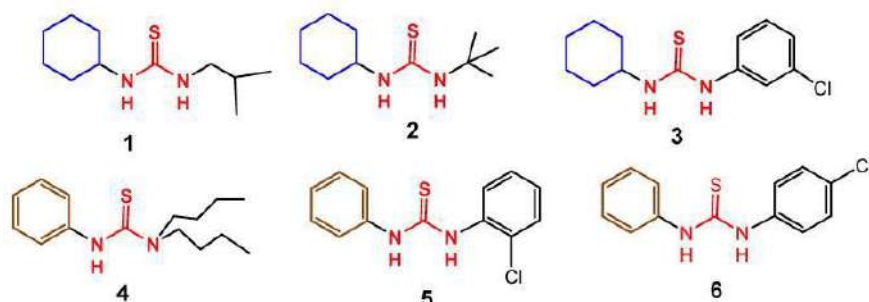


Figure 1: Structure of unsymmetrical thiourea derivatives, 1-cyclohexyl-3-(*iso*-butyl)thiourea (1), 1-cyclohexyl-3-(*tert*-butyl)thiourea (2), 1-cyclohexyl-3-(3-chlorophenyl)thiourea (3), 1-phenyl-3-(1,1-dibutyl)thiourea (4), 1-phenyl-3-(2-chlorophenyl)thiourea (5) and 1-phenyl-3-(4-chlorophenyl)thiourea (6) used in this study.

Material and Method:

All reactions were carried out under aerobic atmosphere and no special precautions were taken to exclude air or moisture during experiments. All chemicals were purchased from Vinit Chemicals, Nanded and were used without further purification. Thiourea derivatives described in this study are also commercially available in the market, we reproduced them in the laboratory, they were obtained as crystalline material. The formation of compounds was confirmed with the help of available spectroscopic techniques, such as ATR-FTIR spectrometer and ^1H - and ^{13}C NMR spectra (in order to assist readers these data is provided below). Thiourea derivatives were prepared by reactions as previously reported [1,2].

Experimental Work

1.1. 1-cyclohexyl-3-isobutylthiourea, 1

Compound 1 was synthesized by dropwise addition of cyclohexyl isothiocyanate (1 mL, 7.05 mmol) to isobutyl amine (0.7 mL, 7.05 mmol) in analytical grade acetone. The reaction mixture was allowed to stir over night at room temperature. The reaction led to the formation of precipitates and the progress was monitored by TLC. Solid material was separated from the mother liquor, washed with petroleum ether for removal of unreacted compounds and possible impurities. The solid was re-dissolved in ethanol and kept for slow evaporation. Spectroscopic data were collected and structure of the desired compound was deduced.

Yield = 70 %; Molecular formula = $\text{C}_{11}\text{H}_{22}\text{N}_2\text{S}$; m.p. = 102-105°C; FT-IR(ATR): $\nu(\text{cm}^{-1})$ = 3431br (NH), 3214br (N-H), 2930s, 2850w (CH), 1617 (C=S), 1379 (NCN), 1448 (CSasy);

1

^1H -NMR (300 MHz, DMSO-d_6) $\delta(\text{ppm})$ = 0.85 (d, $J(1\text{H},1\text{H}) = 6.7$ Hz, 6H, Me), 1.16, 1.25, 1.53, 1.63, 1.82 (overlapping multiplets of aliphatic protons), 3.18 (br, 1H, NH), 3.94(br, 1H, NH). ^{13}C -NMR (75 MHz, DMSO-d_6) $\delta(\text{ppm})$ = 20.1 (2C), 24.5 (2C), 25.1 (1C), 27.7 (1C), 32.3 (2C), 50.9 (1C), 51.6 (1C), 181.3 (C=S).

1.2. 1-cyclohexyl-3-(*tert*-butyl) thiourea, 2

In the similar manner as described above compound 2 was prepared by mixing *tert*butylamine (1 mL, 9.5 mmol) with a solution of cyclohexyl isothiocyanate (1.35 mL, 9.5

mmol) in dry acetone. Compound 2 was obtained as a colorless solid in ethanol.

Yield = 68 %; Molecular formula = C₁₁H₂₂N₂S; m.p.= 138-140°C; FT-IR (ATR): $\nu(\text{cm}^{-1})$ = 3421br, 3367br (N-H), 3050w, 2927w (C-H), 1636s (C=S), 1385 (NCN), 1544 (CSasy); ¹H-NMR (300 MHz DMSOd₆) $\delta(\text{ppm})$ = 1.03 (m, 2H, CH₂), 1.20 (m, 4H, CH₂), 1.61 (m, 4H, CH₂), 1.41 (s, 9H, Me), 1.83 (m, 1H, CH), 2.50 (p, 1H, CH), 3.16 (d, 1H, NH), 4.08 (br, 1H, NH); ¹³C-NMR (75 MHz, DMSO-d₆) $\delta(\text{ppm})$ = 24.4, 25.2, 29.0, 32.3, 50.6, 52.0, 180.2 (C=S).

1.3. 1-cyclohexyl-3-(3-chlorophenyl) thiourea, 3

A known amount of 3-chloroaniline (0.5 mL, 4.7 mmol) in 15 mL analytical grade acetone and equimolar amount of cyclohexyl isothiocyanate (0.6 mL, 4.7 mmol) was reacted together following the same method. Colourless crystals of 3 were obtained in EtOH in few days, were separated from the mother liquor, FT-IR and NMR data were collected and suitable crystal of the compound was mounted for X-ray data collection and structure confirmation.

Yield = 66 %; Molecular formula = C₁₃H₁₇ClN₂S, m.p. = 115-120°C, FT-IR(ATR): $\nu(\text{cm}^{-1})$ 3295br, 3206br (N-H), 3060w (Ar, C-H), 2993w, 2849w (C-H), 1700s (C=S), 1534s (NCN), 1435s (CSasy); ¹H-NMR (300 MHz, DMSO-d₆) $\delta(\text{ppm})$ = 1.26 (m, 4H, CH₂), 1.67 (m, 4H, CH₂), 1.92 (m, 2H, CH₂), 1.99 (m, 1H, CH), 4.17 (br, 1H, NH), 7.10, 7.26, 7.31, 7.82 (m, m, m, m, 4H, CH, Ph), 9.45 (br, 1H, NH); ¹³C-NMR (DMSO-d₆) $\delta(\text{ppm})$ = 25.0, 31.9, 39.8, 52.5, 121.0, 122.1, 123.5, 130.0, 132.9, 141.8, 179.5 (C=S).

1.4. 1-phenyl-3-(1,1-dibutyl) thiourea, 4

Phenyl isothiocyanate (1 mL, 8.3 mmol) and dibutyl amine (0.88 mL, 8.3 mmol) in 20 mL acetone was treated as discussed above. Colourless crystals of the desired compound 4 were obtained in the same solvent at ambient temperature.

Yield = 95%; Molecular formula = C₁₅H₂₄N₂S, m.p. = 85-87°C; FT-IR (ATR 400-4000 cm^{-1}) $\nu(\text{cm}^{-1})$ = 3700br (N-H), 2335w (C-H), 1529s (C=C), 1452s (NCN), 1205s (CSasy); ¹H-NMR (300 MHz, CDCl₃) $\delta(\text{ppm})$ = 0.96 (t, 6H, Me), 1.37 (m, 4H, CH₂), 1.69 (pent, 4H, CH₂), 3.65 (t, 4H, CH₂N), 7.05 (br, 1H, NH), 7.18, 7.31 (m, m, 5H, Ph); ¹³C-NMR (75 MHz, CDCl₃) $\delta(\text{ppm})$ = 13.7, 20.1, 29.4, 51.4, 125.5, 125.6, 128.5, 139.8, 181.0 (C=S).

1.5. 1-Phenyl-3-(2-chlorophenyl) thiourea, 5

In the similar manner as described above by reacting 2-chloroaniline (0.87 mL, 8.3 mmol) with phenyl isothiocyanate (1 mL, 8.3 mmol), the product 5 was obtained as colourless crystalline solid by recrystallization from ethanol. In the whole reaction process, the

reaction was monitored by TLC until single spot product was formed.

Yield = 69 %; Molecular formula = C₁₃H₁₁ClN₂S; m.p. = 90-92°C; FT-IR (ATR) : $\nu(\text{cm}^{-1})$ = 3700br (NH), 2335w (C-H), 1528s (C=S), 1452s (NCN), 1442s (CSasy); ¹H-NMR (DMSOd₆) $\delta(\text{ppm})$ = 7.16, 7.23-7.29, 7.32-7.39, 7.53, 7.63 (m, m, m, m, m, 9H, Aromatic protons), 9.43 (br, 1H, NH), 10.02 (br, 1H, NH); ¹³C-NMR (DMSO-d₆) $\delta(\text{ppm})$ = 123.8, 124.7, 127.2, 127.5, 128.6, 129.4, 129.8, 130.0, 136.4, 139.2, 180.3 (C=S).

1.6. 1-phenyl-3-(4-chlorophenyl) thiourea, 6

The derivative 6, was obtained as colourless solid by treating 4-chloroaniline (0.8 mL, 8.3 mmol) and phenyl isothiocyanate (1.0 mL, 8.3 mmol) in the same manner as reported

in literature [3]. Crystals were obtained in ethanol at room temperature by slow evaporation method.

Yield = 70 %; Molecular formula = C₁₃H₁₁ClN₂S; m. p. = 95-99°C; FT-IR (ATR): $\nu(\text{cm}^{-1})$ = 3436-3100br (N-H), 3000w (C-H), 1637s (C=S), 1549s (NCN), 1490s (CSasy); ¹H-NMR (DMSO-d₆) $\delta(\text{ppm})$ = 7.14, 7.37, 7.52 (m, m, m, 10H, Aromatic protons, NH), 9.88 (br, 1H, NH); ¹³C-NMR (DMSO-d₆) $\delta(\text{ppm})$ = 123.8, 124.6, 125.3, 128.3, 128.5, 138.5, 139.3, 179.3 (C=S).

3. NMR spectra of compounds 1–6

The ¹H- and ¹³C-NMR of all compounds were recorded on Bruker AM 300 MHz spectrometer. In the ¹H-NMR spectra, all the aliphatic and aromatic protons appeared in their characteristic and expected region, 0.8-3.4 ppm and 7.0-7.9 ppm, respectively [4]. The NMR data analysis of all compounds reveal that the reaction is straightforward and no side reactions were observed. As each compound contains two types of N-H protons with different environment (except 4), and accordingly two signals were observed for each of them. The N-H proton close to aromatic ring was observed in up-field region while the other appeared in down-field region. From 13

C-NMR spectra of compounds 1-6, it is evidenced that all the aliphatic and aromatic carbons appeared below 50 ppm and 120-140 ppm, respectively. The chemical shift corresponding to C=S bond was noticed in the region of ≈ 180 ppm, the presence of this carbon in the spectra of compounds 1-6 provides enough justification regarding the formation and presence of thiourea derivatives. Other carbon atoms belong to molecules of respective compounds appeared in their characteristic regions.

Table S1. UV-Visible spectroscopic data of compounds 1–3, 5 and 6.

Sr.No	Compound	Concentration ($\mu\text{g mL}^{-1}$)	Scan range (nm)	$\lambda_{\text{max}}(\text{nm})$
1	Comp -1	2	200-400	296
2	Comp - 2		200-400	294
3	Comp – 3		200-400	298
4	Comp -5		200-400	294
5	Comp - 6		200-400	295

Result and Conclusion:

Compounds 1–6 are structurally very simple; they are accessible in the market and can also be obtained in laboratory under ambient conditions [5]. Compounds structurally analogous to 1–6 are good corrosion inhibitors in acidic medium [6] and show excited results in affording metal sulfides for useful applications [7]. Compound 5 has been used as starting precursors for the preparation of benzothiazole derivatives under catalyst free conditions [8]. There are several other reports wherein simple thiourea molecules after certain modifications have shown efficiency as bioactive compounds [9]. Compound 6 has already been used for its inhibitory activity against melanin B16 cells and mushroom tyrosinase and its synthesis has been reviewed [10,11]. The IC₅₀ value as melanin B16 inhibitor was promising, 3.4 μM , while it exhibited moderate potency as mushroom tyrosinase inhibitor. The enzyme inhibition (AChE

and BChE) and metal sensing capability of compounds **1–6** (Figure 1) have not been reported so far. Since they are already in the field of bioorganic chemistry therefore these studies will help exploring their multidimensionality applications within a single system or organism whatever the case may be.

References:

1. Haribabu J., Subhashree G.R., Saranya S., Gomathi K., Karvembu R., Gayathri D. Synthesis, crystal structure, and in vitro and in silico molecular docking of novel acyl thiourea derivatives. *J. Mol. Struct.* 2015;1094:281–291. doi: 10.1016/j.molstruc.2015.03.035. [[CrossRef](#)] [[Google Scholar](#)] [[Ref list](#)]
2. Khan U.A., Badshah A., Tahir M.N., Khan E. Gold (I), silver (I) and copper (I) complexes of 2, 4, 6-trimethylphenyl-3-benzoylthiourea; synthesis and biological applications. *Polyhedron*. 2020;181:114485. doi: 10.1016/j.poly.2020.114485. [[CrossRef](#)] [[Google Scholar](#)] [[Ref list](#)]
3. P. Thanigaimalai: K.-C. Lee, V.K. Sharma, C. Joo, W.-J. Cho, E. Roh, Y. Kim, S.-H. Jung, *Bioorganic & Medicinal Chemistry Letters* 21 (2011) 6824–6828.
4. F.U. Rahman, M. Bibi, A.A. Altaf, M.N. Tahir, F. Ullah, E. Khan, *Journal of Molecular Structure* 1211 (2020) 128096.
4. Shetty P. Corrosion inhibition behaviour of thiourea derivatives in acid media against mild steel deterioration: An overview. *Surf. Eng. Appl. Electrochem.* 2017;53:587–591. doi: 10.3103/S1068375517060126. [[CrossRef](#)] [[Google Scholar](#)]
5. 37. Gan S.-F., Wan J.-P., Pan Y.-J., Sun C.-R. Highly efficient and catalyst-free synthesis of substituted thioureas in water. *Mol. Divers.* 2011;15:809–815. doi: 10.1007/s11030-010-9298-6. [[PubMed](#)] [[CrossRef](#)] [[Google Scholar](#)] [[Ref list](#)]
6. 38. Shetty P. Corrosion inhibition behaviour of thiourea derivatives in acid media against mild steel deterioration: An overview. *Surf. Eng. Appl. Electrochem.* 2017;53:587–591. doi: 10.3103/S1068375517060126. [[CrossRef](#)] [[Google Scholar](#)] [[Ref list](#)]
7. Owen J.S., Hendricks M.P., Campos M.P., Cleveland G.T., Jen-La PLANTE I., Hamachi L.S. Methods of Producing Metal Sulfides, Metal Selenides, and Metal Sulfides/Selenides Having Controlled Architectures Using Kinetic Control. 10,767,112. *U.S. Patent*. 2020 Sep 8; [[Ref list](#)]
8. 40. Wang R., Yang W.-j., Yue L., Pan W., Zeng H.-y. DDQ-Promoted C–S Bond Formation: Synthesis of 2-Aminobenzothiazole Derivatives under Transition-Metal-, Ligand-, and Base-Free Conditions. *Synlett*. 2012;23:1643–1648. doi: 10.1055/s-0031-1291159. [[CrossRef](#)] [[Google Scholar](#)] [[Ref list](#)]
- [9] 41. Mital A., Murugesan D., Kaiser M., Yeates C., Gilbert I.H. Discovery and optimisation studies of antimalarial phenotypic hits. *Eur. J. Med. Chem.* 2015;103:530–538. doi: 10.1016/j.ejmech.2015.08.044. [[PMC free article](#)] [[PubMed](#)] [[CrossRef](#)] [[Google Scholar](#)] [[Ref list](#)]
10. Thanigaimalai P., Lee K.-C., Sharma V.K., Joo C., Cho W.-J., Roh E., Kim Y., Jung S.-H. Structural requirement of phenylthiourea analogs for their inhibitory activity of melanogenesis and tyrosinase. *Bioorganic Med. Chem. Lett.* 2011;21:6824–6828. doi: 10.1016/j.bmcl.2011.09.024. [[PubMed](#)] [[CrossRef](#)] [[Google Scholar](#)] [[Ref list](#)]
11. 42. Štrukil V. Mechanochemical synthesis of thioureas, urea's and guanidine's. *Beilstein J. Org. Chem.* 2017;13:1828–1849. doi: 10.3762/bjoc.13.178. [[PMC free article](#)] [[PubMed](#)] [[CrossRef](#)] [[Google Scholar](#)] [[Ref list](#)]

Study of Proton and Metal-Ligand Stability Constants of hydroxy Substituted Chalcone Complexes pH-Metrically

Mohd. Wajid Shaikh Mohd Waris

Department of Chemistry, Yashwantrao Chavan Arts and Science Mahavidyalaya
Mangrulpir, Dist. Washim 444403, Maharashtra, India.
Wajid_shaikh369@rediffmail.com

ABSTRACT

In the present work, we have investigated the proton-ligand stability constants and metal-ligand stability constants of ligand 1-(5-bromo-2-hydroxyphenyl)-5-phenylpenta-2,4-dien-1-one (L_3) with transition metal ions like Cr (III) and Nd (III), which were determined pH-metrically at 0.1 M ionic strength. ($30 \pm 1^\circ\text{C}$) in a 70% dioxane-water mixture by the Bjerrum method as adopted by Calvin Wilson. 1:1 and 1:2 complexes were formed between 1-(5-bromo-2-hydroxyphenyl)-5-phenylpenta-2, 4-dien-1-one (L_3), Cr (III), and Nd (III). The values of pK and log k were evaluated and compared with the resultant data.

Keywords: Substituted chalcone, Dioxane – water mixture, stability constant.

1. Introduction

The stability constant, also known as the formation constant or association constant, is a measure of the strength of the bond formed between a ligand and a metal ion in a complex. It quantifies the stability or tendency of the complex to form and remain intact in a solution. Stability constants are determined through various experimental techniques, such as spectrophotometry or potentiometry. These constants are expressed as equilibrium constants and are typically denoted by the symbol K. The higher the stability constant, the more stable the complex is. Stability constants are important in various fields of chemistry, including coordination chemistry, biochemistry, environmental chemistry, and analytical chemistry. They play a crucial role in understanding the behavior of metal-ligand complexes in solution, their formation, and their potential applications.

The value of a stability constant depends on several factors, including the nature of the metal ion and ligand, the pH of the solution, temperature, and ionic strength. These constants provide valuable insights into the thermodynamics of complex formation and can be used to predict the stability of a complex under different conditions. Overall, stability constants are a fundamental concept in chemistry that helps to understand the formation and stability of metal-ligand complexes, and their importance extends to various areas of scientific research and applications.

A significant contribution was made to the field of stability constants of organic ligands and their metal complexes by Bjerrum¹ and Calvin². The Schiff base N-[2-hydroxy-1-naphthylidene]-2-methoxyaniline (3) was formed through condensation of 2-hydroxy-1-naphthylidene with 2-methoxyaniline. It was studied for its formation of transition elements and its stability constants, with the order of stability constant being $\text{Cu} > \text{Ni} > \text{Zn} > \text{Mn} > \text{Co}$ ³. Jagtap's study examined the stability constant of Ni (II) with substituted pyrazole carboxylic acid derivatives at 298K in a 70% DMF-water mixture.⁴ The stability constants of transition metals, including Cu (II) and Co (III) complexes with Schiff bases, were evaluated for anti-diabetic drugs. They were determined using the Calvin Bjerrum titration technique and

discussed in terms of order, ligand basis, and correlations.⁵ Thakur et al.⁶ studied the stability constant of Schiff bases with lanthanum using pH metric titration and the Calvin-Bjerrum method. They calculated thermodynamic parameters like Gibb's free energy change, entropy change, and enthalpy change. Thorat et al.⁷ studied the complex formation between Pr (III) and Sm (III) metal ions and 3-(2-hydroxy-3-nitro-5-methylphenyl)-5-(3-nitrophenyl) isoxazoline, 4-chlorophenyl isoxazoline, and 2-furyl isoxazoline. The study investigated the interaction of metal ions with the organic ligand N-[(E)-(4-Hydroxy-3-methoxyphenyl)methylene] isonicotinohydrazide. The ligand was synthesized using an anti-mycobacterial agent and aromatic aldehydes. The formation of these ligands was confirmed through various tests, with the stability constants arranged in a specific order.⁸ The stability constants and thermodynamic parameters of transition metal complexes of substituted aminothiazole Schiff bases have been studied by R.P. Giram et al.⁹

2. Experimental methodology

2.1 Material and Methods

All chemicals used are AR-grade. The ligand (L_3) was synthesized in the laboratory by the reported protocol¹⁰. The stock solution of the ligand was prepared by dissolving the required amount of ligand in a 70% (dioxane and water) mixture.

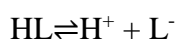
2.2 General procedure

Types of Titrations

i) Free acid HNO_3 (0.01 M)

ii) Free acid HNO_3 (0.01 M) and ligand ($20 \times 10^{-4}M$)

iii) Free acid HNO_3 (0.01 M) and ligand (20×10^{-4}) and metal ions ($4 \times 10^{-4}M$) against a standard 0.1N NaOH solution. The ionic strength of all the solutions was maintained at 1M by adding the appropriate amount of KNO_3 solution. All the titrations were carried out in a 70% (dioxane and water) mixture, and the readings were recorded for each 0.1 ml addition. The graph of the volume of alkali added (NaOH) against pH was plotted. The ligand involved in the present work may be considered a monobasic acid having only one dissociable H^+ ion from the phenolic OH group, and it can therefore be represented as HL. The dissociating equilibrium can be shown as.



By the law of mass action, we have,

$$K = [HL] / ([H^+] [L^-]) \quad (1)$$

Where, the quantities in bracket denote the activities of the Species at equilibrium.

3. Result and Discussion

3.1 Calculation of Proton-Ligand Stability Constant (n_A)

The plots between the volume of NaOH and the pH of the solution were used to determine the proton ligand stability constant (representing the replacement of H^+ ions from the functional group of the ligand with respect to the pH value). The horizontal difference ($V_2 - V_1$) was measured accurately between the titration curves of free acid and acid + ligand. It was

used to calculate the formation number n at various pH values and a fixed ionic strength $\mu = 0.1$ M using Irving and Rossotti's equation [1, 2].

$$n_A = \gamma \frac{(E_0 + N) (V_2 - V_1)}{(V_0 + V_1) T_L^0} \quad (2)$$

Where V^0 is the initial volume of the solution. E^0 and T_L^0 are the initial concentrations of the mineral acid and ligand, respectively. V_1 and V_2 are the volumes of alkali of normality N during the acid and ligand titration at a given pH. γ is the replaceable proton in the ligand. The data on n_A obtained at various pHs, along with the horizontal difference for some representative systems, are represented in Table 1. The metal ligand ligand formation number (n) is estimated by Irving-Rossotti's equation.

$$n = \frac{(E_0 + N) (V_3 - V_2)}{(V_0 + V_2) T_m^0} \quad (3)$$

Where the notations have the same meaning as given in the earlier equation. The horizontal difference ($V_3 - V_2$) between the metal complex ($A + M + L$) and reagent ($A + L$) curve is used to evaluate the value of n using Irving Rossotti's equation.

Table 1 Proton ligand stability constant (pK)

Ligand	System	pK	
		Half integral method	Point wise method
L3	1-(5-bromo-2-hydroxyphenyl)-5-phenylpenta-2,4-dien -1- One	7.7871	6.4506

Table 2: Metal-ligand stability constant (log K)

System	LogK ₁	LogK ₂	Δ LogK
Cr (III)+L ₃	5.7419	3.3126	2.4293
Nd (III)+L ₃	5.5310	3.5278	2.0032

Conclusion

From the titration curves, it is observed that the departure between the acid-ligand ($A + L$) curve and the acid-ligand-metal ($A + L + M$) curve for all systems started at pH 3.6. This indicated the commencement of complex formation. Also, the change in color from yellow to

orange in the pH range from 3.9 to 8.6 during titration showed the complex formation between metal and ligand.

The difference between $\text{Log}K_1$ and $\text{Log}K_2$ is less than 2.5, indicating the simultaneous formation of 1:1 and 1:2 complexes. When the difference is greater than 2.5, a stepwise complex formation takes place.¹¹ From Table 2, it is observed that in the all systems Cr (III)-L3 and Nd (III) + L3, the difference between $\log K_1$ and $\log K_2$ is sufficiently small, which indicates the simultaneous formation of complexes between metal ions and ligands takes place.

Acknowledgement

The author is also thankful to the Dr. R.D. Deshmukh, Principal, R.D.I.K. & N.K.D. College, Badnera, for providing useful guidance and facilities throughout the research work.

Reference

- 1 Bejerrum J. (1941). Metal Ammine formation in aqueous solution, haase, copenggan. 296p, 8(9), 20 (1982).
- 2 Calvin M, Wilson KW. (2003). stability of chelate compounds, J Am. Chem. Soc, 1945, 67.
- 3 Jadhav S, Rai M, Pardeshi R.K, Farooqui M. (2015). Determination of stability constant of metal ligand equilibria with special reference to Schiff base and transition elements. Der Pharmacia Lettre, 7 (12): 316-320. (<http://scholarsresearchlibrary.com/archive.html>)
- 4 Jagtap V. S (2019). Determination of Stability Constant of Some Coordination Compound by pH Metric Technique. Pramana Research Journal, 9 (8): 22-29. <https://pramanaresearch.org/>
- 5 Parihar R. T, Quazi S. A. (2019). Study of proton & Metal ligand stability constant of Schiff base complexes in 70% DMF solvent media pH metrically. Journal of Emerging Technologies and Innovative Research, 6 (1): 136-144.
- 6 Thakur S.V, Farooqui M.N, Jadhav R. L, Joshi S. U. (2021). Complexation of La (III) metal ion with novel Schiff bases. Thermodynamic study. Journal of Advanced Scientific Research, 12(2): 133-136. <http://www.sciensage.info>
- 7 Thorat, S.A, Thakur. S.D. (2015). Metal ligand stability constant of substituted 3,5-Diaryl isoxazolines complexes in 70% dioxane solvent media. J. Curr. Chem. Pharm. Science, 5(2): 67-74.
- 8 Omar Z. T, Jadhav S. L, Kayande D. D, Rai M. J. (2019). pH-metric Study of Metal-ligand Stability Constant of Transition Metal Complexes with Pharmacologically Active Ligand N-[(E)-(4-Hydroxy-3-methoxyphenyl) methylene] isonicotinohydrazide. Curr. Pharm. Res, 407, 58-65. <https://www.researchgate.net/publication/333365049>
- 9 Giram, R.P, Muthal, B.N, More, P.G. (2019). The study of stability constants and Thermodynamic parameters of transition metal complexes of substituted aminothiazole Schiff Bases. The Pharma Innvation Journal, 8(1): 249-252. <https://dx.doi.org/10.22271/tpi>
- 10 Swapnil, K.W, Kakade, K.P. (2013). Synthesis and characterization of substituted 5-bromo-2-benzylidene-1-benzofuran-3-one and its structural determination. International Journal of chemical and pharmaceutical science, 4(3): 119-122.
- 11 Deolankar, D. S, Deshpande, Y.H. (1987). La(III), Pr(III), Gd(III), Tb(III) and Dy(III) Complexes of aryl furyl and aryl thienyl β -diketones. Indian Journal of Chemistry, 26(A): 68-69. <http://nopr.niscpr.res.in/handle/123456789/47785>

Ecofriendly synthesis and characterization of Ethyl 2-imino-6-methyl-4-substituted phenyl-1, 2, 3, 4-tetrahydropyrimidine-5-carboxylate compounds

Nilesh B. Jadhav*

Department of Chemistry, Jagadamba Mahavidyalaya, Achalpur city
Email Id: jadhavnilesh29@gmail.com

Abstract: Ethyl acetoacetate, substituted aromatic aldehyde, and guanidine were the three components of a one-pot, three-component reaction that produced ethyl 2-imino-6-methyl-4-substituted phenyl-1, 2, 3, 4-tetrahydropyrimidine-5-carboxylate compounds [4a-c]. The reaction is effectively supported to provide the intended products, typically in high yields and within a brief timeframe. The newly synthesized chemicals structures were clarified by elemental and spectrum investigations. Using TLC, the purity of each compound was ascertained.

Keywords: Pyrimidine, Guanidine.

1. Introduction:

Heterocycles that include nitrogen are of synthetic importance since they belong to a significant class of both natural and artificial compounds, many of which have shown beneficial biological activity. the fascination with six-membered structures with two nitrogen atoms at positions one and three. In heterocyclic synthetic chemistry, the One Pot Multicomponent Reactions (MCRs), in which several reactions occur often in a single synthetic operation, have been heavily employed to generate carbon-carbon bonds. Similar reactions provide a multitude of options for efficiently building relatively complex molecules in a single phase of the process, so avoiding the laborious purification processes and allocating savings of both reagents and solvents. For this reason, understanding their biological conditioning and therapeutic applications is crucial for scientists working on drug discovery processes³. We have conducted the reactions in water, which is notable for its use as a non-flammable, non-hazardous, and green medium, based on the principles of green chemistry.

Pyrimidines have biological significance that motivates researchers to work on them. These activities include analgesic^{1,2,9}, antimicrobial activity^{3,4,7}, anticonvulsant⁵, antioxidant activity⁵, antimycobacterial⁶, antitumor⁷, antiviral⁸, anticancer^{9,10} and antifolate¹⁰.

2. Material and methods:

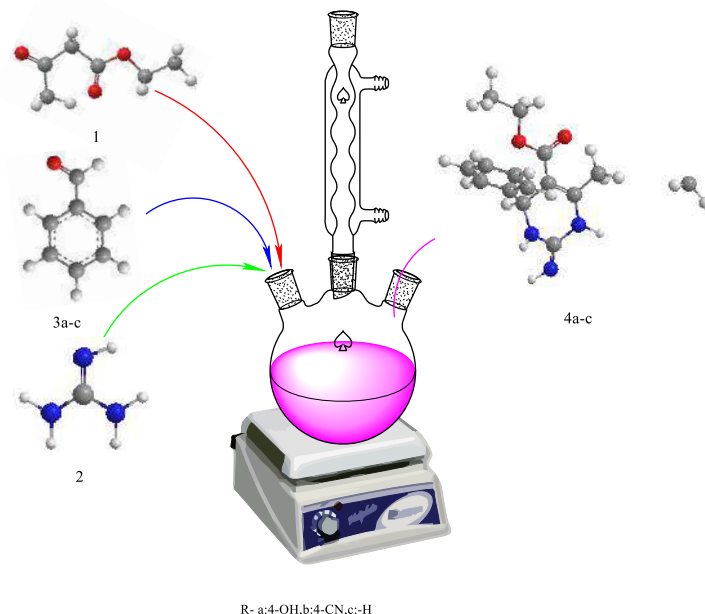
An uncorrected melting point was determined using open capillary tubes. Using an FTIR Agilent Technologies spectrometer at 4000-650, the FTIR spectra were recorded. Using tetramethyl silane (TMS) as an internal reference and d6-DMSO/CDCI₃ as the solvent, the ¹H NMR spectra were recorded on a Bruker spectrophotometer operating at 500 MHz. The units of chemical changes were ppm. We bought all of the solvents and reagents from Sigma Aldrich Chemicals Pvt Ltd. To maximize the reaction's purity and completeness, TLC was employed.

2.1 Synthesis Process in General:

2.1.1 Synthesis of phenyl-1,2,3,4-tetrahydropyrimidine-5-carboxylate by ethyl 2-imino-6-methyl-4 substitution[4a-c]:

Substituted aromatic aldehyde (0.01mol), ethyl acetoacetate (0.01mol), and guanidine (0.01mol) were added to 15 ml of distilled water in a dry 50 mL round-bottom flask, and the mixture was manually agitated for two minutes. The reaction mixture was then heated for an

hour at 90 degrees Celsius in a water bath. A solid began to deposit as the reaction went on, and an hour later the flask was full with solid. Using a spatula, the solid was carefully removed from the conical flask. One milliliter of cold water was used to wash the yellow solid. From ethanol, the crude product was recrystallized to remove impurities.



Scheme-1

3. Physiochemical and analytical data for compounds:

3.1 Ethyl 4-(4-hydroxy phenyl)-2-imino-6-methyl-1, 2, 3, 4-tetra hydro pyrimidine-5-carboxylate(4a):

M.F: $C_{14}H_{17}N_3O_3$. M.W:278. M.P: 124–126 °C. Yield: 77.35%. FT-IR: 1510(Ar-C=C), 1631(C=N), 1715(C=O), 2887(C-H), 3199(N-H), 3402(Ar-OH). 1H -NMR (500 MHz, DMSO d_6 , δ ppm): 7.81(s, 1H, =N-H), 6.91-6.71 (Ar-H), 4.50(s, 1H, R_2 -NH), 4.03(q, 2H, -CH₂), 1.25(t, 3H, -CH₃), 2.27 (s, 3H, Ar-CH₃), 9.1 (s, 1H, Ar-OH). Anal. Calcd. (in %): C, 61.07; H, 6.20; N, 15.21. Found: C, 61.11; H, 6.281; N, 15.35.

3.2 Ethyl 4-(4-cyano phenyl) -2-imino -6-methyl-1, 2, 3, 4-tetra hydro pyrimidine -5-carboxylate(4b):

M.F: $C_{15}H_{16}N_4O_2$. M.W:285. M.P: 112–114 °C. Yield: 76.81%. FT-IR: 1502(Ar-C=C), 1628(C=N), 1714(C=O), 2265(Ar-CN), 2888(C-H), 3195(N-H). 1H -NMR (500 MHz, DMSO d_6 , δ ppm): 7.81(s, 1H, =N-H), 7.76-7.28 (Ar-H), 4.48(s, 1H, R_2 -NH), 4.02(q, 2H, -CH₂), 1.20(t, 3H, -CH₃), 2.19(s, 3H, Ar-CH₃). Anal. Calcd. (in %): C, 63.39; H, 5.45; N, 19.83. Found: C, 63.35; H, 5.63; N, 19.69.

3.3 Ethyl 2-imino-6-methyl -4-phenyl-1, 2, 3, 4-tetra hydro pyrimidine- 5-carboxylate(4c):

M.F: $C_{14}H_{17}N_3O_2$. M.W: 260. M.P: 112–114 °C. Yield: 73.80%. FT-IR: 1509 (Ar-C=C), 1628(C=N), 1717 (C=O), 2882(C-H), 3199(N-H). 1H -NMR (500 MHz, DMSO d_6 , δ ppm): 7.81(s, 1H, =N-H), 7.28-7.17 (Ar-H), 4.59 (s, 1H, R_2 -NH), 4.12 (q, 2H, -CH₂), 1.20 (t, 3H, -CH₃), 2.31 (s, 3H, Ar-CH₃). Anal. Calcd. (in %): C, 64.79; H, 6.59; N, 16.25. Found: C, 64.15; H, 6.29; N, 16.89.

4. Conclusion:

The main focus of this research work was pyrimidine derivatives have been synthesized based on green chemistry principles (multicomponent synthesis) using water as a solvent. The structures of synthesized compounds were confirmed by FTIR, 1H NMR and elemental

analysis. The reaction is effectively supported to provide the intended products, typically in high yields and within a brief timeframe

5. References:

- 1) Huang, Zhibin, et.al. "Efficient one-pot three-component synthesis of fused pyridine derivatives in ionic liquid." *ACS Combinatorial Science* 13, no. 1 (2011): 45-49.
- 2) Arora, Neha, et.al. "Synthesis and analgesic activity of novel pyrimidine derivatives." *Synthesis* 11, no. 1 (2011): 010.
- 3) Saczewski, et.al. "Biological activities of guanidine compounds." *Expert opinion on therapeutic patents* 19, no. 10 (2009): 1417-1448.
- 4) Rawat, et.al. "synthesis and antimicrobial activity of some new heterocyclic guanidine derivatives." *world journal of pharmacy and pharmaceutical sciences* 5, no. 9 (2016): 1325-1337.
- 5) Mohana, et.al. "Synthesis and biological activity of some pyrimidine derivatives." *Drug invention today* 5, no. 3 (2013): 216-222.
- 6) Kumar, et.al. "Syntheses of novel antimycobacterial combinatorial libraries of structurally diverse substituted pyrimidines by three-component solid-phase reactions." *Bioorganic & medicinal chemistry letters* 12, no. 4 (2002): 667-669.
- 7) Baraldi, et.al. "Antimicrobial and antitumor activity of N-heteroimmine-1, 2, 3-dithiazoles and their transformation in triazolo-, imidazo-, and pyrazolopyrimidines." *Bioorganic & medicinal chemistry* 10, no. 2 (2002): 449-456.
- 8) Nasr, et.al. "Pyrido [2, 3-d] pyrimidines and Pyrimido [5', 4': 5, 6] pyrido [2, 3-d] pyrimidines as New Antiviral Agents: Synthesis and Biological Activity." *Archiv der Pharmazie: An International Journal Pharmaceutical and Medicinal Chemistry* 335, no. 6 (2002): 289-295.
- 9) Sondhi, et.al. "Anticancer, anti-inflammatory and analgesic activity evaluation of heterocyclic compounds synthesized by the reaction of 4-isothiocyanato-4-methylpentan-2-one with substituted o-phenylenediamines, o-diaminopyridine and (un) substituted o." *Australian Journal of Chemistry* 54, no. 1 (2001): 69-74.
- 10) Gangjee, et.al. "Synthesis, antifolate, and antitumor activities of classical and nonclassical 2-amino-4-oxo-5-substituted-pyrrolo [2, 3-d] pyrimidines." *Journal of medicinal chemistry* 44, no. 12 (2001): 1993-2003.

Effect of Fe Dopant on Structural & Electrical Properties of Copper Oxide Nanoparticles

N.N.Gour , A.P.Pinjarkar , H.G.Wankhade , P.R.Padole

Shri Shivaji Science College Amravati Corresponding Author: pramodpadole@gmail.com & wankhadehg@gmail.com

Abstract: Nanocrystalline Copper oxide (CuO_2) was synthesized by sol-gel citrate method. Further it was modified by doping Fe in it. Structural and Electrical study was carried out for modified and unmodified CuO_2 . From X-ray diffraction (XRD) studies it was observed that when CuO_2 doped with 2% Fe its Average Crystallite Size Increases from 41.32 nm to 54.51 nm on further doping with 0.1% & 0.3% Fe Its Average Crystallite Size decreases to 34.15 nm & 31.35 nm respectively. The electrical study of the nanocrystalline Copper Oxide is checked for different doping amount and also at different temperature for every sample. From the study it is observed that, conductivity changes with the concentration of dopant and also varies with temperature.

Keywords: Copper oxide, X-ray diffraction, crystallite size, Electrical Properties & Conductivity.

Preliminary Phytochemical Studies of *Cesalpinia crista* L.

Nitin G. Asole, Ramesh T. Parihar* and Anand S. Jadhao

Bapumiya Sirajoddin Patel Arts, Commerce and Science College, Pimpalgaon Kale, Tq. Jalgaon
(Jamod), Dist. Buldhana – Maharashtra

*Vidnyan Mahavidyalaya Malkapur, Tq. Malkapur, Dist. Buldhana – Maharashtra
Email Id: nitinasole2@gmail.com

Abstract:

Caesalpinia crista L. belongs to Fabaceae and commonly known as ‘sagargoti’ in Marathi. It is widely employed across the Asian and African continent for treatment of various kinds of diseases and disorders like abdominal pain, amenorrhea, cystic fibrosis, diabetes, leucorrhea, malaria fever, rheumatoid arthritis. The aim of present study was to investigate the presence of phytochemicals of root, stem, leaf and fruit of *Cesalpinia crista* L. Ethanol, acetone, hexane and petroleum ether extract of selected material were screen for the presence of different secondary metabolites, it revealed the existence of alkaloid, steroids, phytosterol, tannin, flavonoids, and glycosides. The findings of the present study provided evidence that crude organic solvent extracts of *Caesalpinia crista* L. contain medicinally important bioactive compound, it justifies their use in traditional medicines for the treatment of various kinds of diseases.

Key words: *Caesalpinia crista* L., organic solvents, phytochemicals

Introduction:

Caesalpinia crista L. an important medicinal plant belongs to Fabaceae (Caesalpinaceae), different parts of *C. crista* has several traditional medicinal applications and health benefit effects. *C. crista* generally presents in tropical areas and found almost in every part of India and Pakistan (**Bhanderi, et al., 2022**). Root, leaves, seed and bark is used in the treatment of different kinds of diseases such as pulmonary tuberculosis, malaria, pneumonia, colic fever, intermittent fever, swelling, menstrual complaints, skin diseases, tonic and as a uterine stimulant, to cleanse uterus and also alleviates edema and abdominal pain during this period. Various plant parts of *C. crista* traditionally used as antipyretic, periodic, tonic and vesicant for the treatment of backache, constipation, skin diseases, gynecological disorders, piles, ulcers and rheumatism (**Suryawanshi and Patel, 2011; Patil, K. S. 2005**).

The extracts different parts of *C. crista* have been reported to have anthelmintic activity antimalarial activity, antioxidant activity, anti-amyloidogenic, nootropic activity and cytotoxic activity (**Sadiya Afreen et al., 2016**). Literature on *C. crista* revealed presence of different compounds and most of them belong to diterpenes group. Several traditional medicinal plants have been reported to have strong antimicrobial properties and some of them have already been used in the treatment of animals and people suffering from viral infection (**Mandal, et al., 2011**).

Many plant and herbs that have potential as novel antiviral agents have been reported and wide spectrum of active secondary metabolites including alkaloids, coumarins, flavonoids, furyl compounds, lignans, polyphenolics, sulphides, saponins, terpenoids, thiophenes, proteins and peptides have been identified (**Srinivasa et al., 2003**). The decoction of *Caesalpinia crista* root has been used for its significant health benefits to treat rheumatism, backache and as a tonic. In Ayurveda Indian Medicine System heartwood is bitter, astringent, constipating,

hemostatic and sedative and it is useful in the treatment of burning sensation, convulsions, diabetes wounds, diarrhoea, dysentery, epilepsy, leucorrhoea, leprosy, menorrhagia, haemorrhages, ulcers, skin diseases, (**Kirtikar and Basu, 1989**).

Caesalpinia crista is a large woody climber height up to 15 m grows mainly on the river bank in tidal forests near eastern seacoast from Orissa and western sea coast from Konkan southwards and grown throughout India up to 800 meters elevation. Branches are finely grey-downy, armed hooked and straight hard yellow prickles on them. Bark is black, branchlets are glossy with recurved prickles. leaflets; 2-3 pair coriaceous, acute or obtuse, ovate or elliptic, upper surface shining, lower dull large, leaves bipinnate with recurved prickles at the base of pinnae, 2-5 pairs, often armed. Seeds of the plant are round, dry and hot, up to 1.2 cm in length, protected in a glossy yet very hard coat that may be green or ash gray in color, surface of the kernel is ridged and is furrowed and is about 1.23-1.75 cm in diameter (**Preedy et al., 2011; Pooja Upadhyay et al., 2019**).

Materials and Methods

Collection and Identification of materials:

The plant material i.e. roots, stem, leaves and fruits of *Caesalpinia crista* L., were collected from the botanical garden of Bapumiya Sirajoddin Patel Arts, Commerce and Science College, Pimpalgaon Kale, Tq. Jalgaon (Jamod), Dist. Buldhana – Maharashtra. The samples were collected during the year 2022-23. The Herbarium of *Caesalpinia crista* L., was prepared and authenticated from Department of Botany, Vidnyan Mahavidyalaya Malkapur. The root, stem and leaves were washed and kept for shade drying for 7-8 days or till it get the constant weight, whereas mature fruit was shade dried till get the constant weight. The fine powder of selected material were prepared with the help of mortle and pistle and finely powdered with the help of electric mixture grinder, prepared powder were stored in air tight container bottles at room temperature until used. 5 gram of the plant material powdered was wrapped in whatmann filter paper and placed in 100 ml beaker and selected solvent such as Ethanol, acetone, hexane and petroleum ether were added in each beaker and kept for overnight. Then extract was filtered through whatman filter paper and used for the detection of various phytochemical analyses.

Test for Phytochemicals

- **Alkaloids:** 2 ml of extract, few drops of Mayers reagents was added, white precipitate indicates existence of alkaloids.
- **Flavonoids:** To 2 ml of extract was taken, 10% of lead acetate was added, yellow precipitate indicate the presence of flavonoids.
- **Steroid:** 2 ml plant extract was taken in a test tube; 2 ml of CCl_3 and few drops of conc. H_2SO_4 were added in it and stir well. Chloroform layer appearance red and acid layer showed the greenish yellow florescence which indicated positive test for of steroid.
- **Glycosides:** 3 ml of extract, 4 ml of CCl_3 was added and stir well. The chloroform layer was separated then added 10% ammonium solution. The formation of pink colour indicate the presence of glycosides.
- **Carbohydrates:** About 0.5 ml of the extract was taken in which 0.5 ml of Benedict's reagent was added. The mixture was heated for 3 minutes in a boiling water bath. Appearance of red precipitate indicates the presence of carbohydrates.
- **Proteins:** 2 ml of extract, 2 ml of Millons reagent was added. White precipitates indicate the presence of proteins.

- **Amino acid:** 2 ml of extract, few drops of nitric acid was added. The existence of yellow colour it indicates the presence of protein and free amino acids.
- **Oil:** Small quantity of the extract was taken and pressed between two filter papers. Formation of spot indicates presence of oil.
- **Phenol:** About 4 ml of extract and 3 ml of 10% lead acetate solution was added. The formation of bulky white precipitate shows presence of phenol.
- **Tannins:** 5 ml of extract was taken and few drops of 5% FeCl₃ solution was added. The formation of dark green colour shows presence of tannins.
- **Saponins:** 0.5ml extract was vigorously shaken with few ml of distilled water. The formation of frothing is shows presence of saponins.
- **Terpenoids:** Salkowski's test- To 4 ml of plant extract, 2 ml of CCl₄ and 3ml Conc. H₂SO₄ were added carefully to form a layer, reddish brown colour of the inner face indicate the presence of terpenoids (Thimmaiah, S. R. 1999; Yadav and Agrwal, 2011; Shailaja J. R. 2015; Sridhar et al., 2016).

Observations and Results:

The phytoconstituents were extracted by using different solvents of increasing polarity like hexane, acetone, petroleum ether and ethanol. The Table 1 is representing the presence and absence of different phyto-constituents. Root, stem, leaf and seed extract of selected solvent revealed the presence of alkaloids, carbohydrate, protein and amino acids. Fruit extract shows the existence of oil. Glycosides were detected in root, stem, leaf and fruit. Stem extract showed the presence of phenol where as other parts showed negative test for phenol. Tannin, flavonoids, saponins, steroids, terpenoids were detected in all selected parts of *C. crista* in different solvents.

Table no: 1. Preliminary phytochemical screening of *Caesalpinia crista* L.

Sr. no.	Primary metabolites	Root				Stem				Leaf				Fruit			
		E	A	H	P	E	A	H	P	E	A	H	P	E	A	H	P
1.	Carbohydrates	+	+	+	+	+	+	+	+	+	+	+	+	+	+	+	+
2.	Proteins	+	+	+	+	+	+	+	+	+	+	+	+	+	+	+	+
3.	Amino acid	+	+	+	+	+	+	+	+	+	+	+	+	+	+	+	+
4.	Oils	-	-	-	-	-	-	-	-	-	-	-	-	+	+	+	+
5.	Glycosides	+	-	-	+	-	+	+	-	-	-	+	+	+	+	+	-
6.	Alkaloids	+	+	+	+	+	+	+	+	+	+	+	+	+	+	+	+
7.	Phenol	+	-	+	-	-	-	-	-	-	+	+	-	-	+	+	-
8.	Tannins	+	-	-	+	-	-	+	-	+	-	-	+	+	-	-	+
9.	Flavonoids	-	+	+	-	+	+	+	+	+	+	+	+	+	+	+	+
10.	Saponins	+	-	+	+	+	+	+	+	+	+	+	+	+	+	+	+
11.	Steroids	+	-	+	-	-	+	-	-	+	-	+	-	+	-	+	-
12.	Terpenoids	+	-	-	-	+	+	-	-	-	+	-	+	+	-	-	+

(A-Acetone, E-Ethanol, H-Hexane, P- Petroleum ether)

Conclusion:

It is concluded from the present results that, root, stem, leaf and fruit of *C. crista* in different solvent extract revealed the existence of various secondary metabolites. The medicinal properties such as activity antimalarial activity, antioxidant activity, anti-amyloidogenic, of burning sensation, convulsions, diabetes wounds, diarrhea, dysentery, epilepsy, leucorrhea, leprosy, menorrhagia, hemorrhages, ulcers, skin diseases and cytotoxic activity etc. are due the presence of various secondary metabolites. Hence isolation of individual compound from the *C. crista* may found a novel drug.

Acknowledgement:

Authors are grateful to principal of Vidnyan Mahavidyalaya Malkapur, Tq. Malkapur, Dist. Buldhana – Maharashtra and Bapumiya Sirajoddin Patel Arts, Commerce and Science College, Pimpalgaon Kale, Tq. Jalgaon (Jamod), Dist. Buldhana – Maharashtra for providing all the necessary facilities for the present research work.

REFERENCES:

- Bhanderi Chandani B., Kalpna D. Rakholiya and Mital J. Kaneria** (2022) Pharmacognostic and phytochemical evaluation of *Caesalpinia crista* L. leaf. *Journal of Medicinal Plants Studies*; 10(6): 37-39.
- Suryawanshi H. P. and Patel M. R.** (2011) Traditional Uses, Medicinal And Phytopharmacological Properties of *Caesalpinia Crista* Linn - An Overview, *International Journal Of Research In Pharmacy and Chemistry*.
- Sadiya Afrin, Raihana Pervin, Farah Sabrin , Md. Hossain Sohrab , Satyajit Roy Rony , Md. Emdadul Islam, Kazi Didarul Islam And Md. Morsaline Billah** (2016) Assessment of Antioxidant, Antibacterial and Preliminary Cytotoxic Activity of Chloroform Ond Methanol Extracts of *Caesalpinia Crista* L. Leaf Biotechnology And Genetic Engineering Discipline, Khulna University, Khulna-9208, Bangladesh. *Bangladesh J. Bot.* 45(5): 1061-1068.
- Mandal S., Hazra B., Sarkar R., Biswas S. and Mandal N.** (2011). Assessment of the antioxidant and reactive oxygen species scavenging activity of methanolic extract of *Caesalpinia crista* leaf. *Evid. Based Complement. Alternat.* 173768
- Srinivas K. V. N. S. Rao Y. K., Mahender I., Das B., Krishna K. V. S. R., Kishore K. H. and Murthy U. S.** (2003) Two new antibacterial flavonoids from the aerial part of *Caesalpinia pulcherrima* , *Phytochemistry*, 63:789-793.
- Kirtikar K. R. and Basu B. D.** (1989) Indian Medicinal Plants, Vol. II, Dehradun: International publishers.
- Pooja Upadhyay , Bhuwan Chandra Joshi, Ankush Sundriyal and Sushmita Uniyal** (2019) *Caesalpinia crista* L.: A review on traditional uses, phytochemistry and pharmacological properties, School of Pharmaceutical Sciences, Sardar Bhagwan Singh University, Balawala, Dehradun, Uttarakhand-248001, India yani Inder Singh Institute of Professional Studies, Dehradun, Uttarakhand-248003, India. *Curr Med Drug Res*, 3 (1): Article ID 191.
- Preedy, V. R., Watson R. R. and Patel V. B. (Eds.).** (2011). Nuts and seeds in health and disease prevention. *Academic press*.
- Thimmaiah, S. R.** (1999). Standard methods of biochemical analysis, *Kalyani Publishers*: 1-435.
- Yadav R. N. S., and Agarwala Munin** (2011) Phytochemical analysis of some medicinal plants, *Journal of Phytology*, 3(12): 10-14.
- Shailaja J. R.** (2015), Pharmacognostic & Phytochemical Analysis of *Gokshura* w.s.r. to Cardioprotective Activity, *Anveshana Ayurveda Medical Journal*, 1 (5): pp. 391-397.
- Sridhar, K., Rajesh, B., Sangeetha, K.** (2016), Phytochemical Screening and GC-MS Analysis of Ethanolic Extract of *Tribulus terrestris*, *International Journal of Pharmacology Research*, 6(1): pp. 44-50.
- Patil, K. S.** (2005) Wound healing activity of the seed kernels of *Caesalpinia crista* Linn *Journal of Natural Remedies*, 5(1): 26 – 30.

Removal of Methylene Blue using *Cajanus Cajan* Activated Carbon

^{1*}Vilayatkar N.D., ¹Chaudhari D.L., ²Kadu N.S., ³Kurzekar R.R.

¹S.S.Jaiswal college Arjuni/Morgoan-441701, India

²Bharatiya college, Amravati - 444605, India

³ C.J.Patel College, Tirora-442201, India

*Corresponding Author; Email: vilayatkar.niin@gmail.com Contact No. +91 9028631242

Abstract

Research is required to explore and test new and new low cost materials for removal of Methylene Blue. In the present research article, generation of activated carbon derived from *Cajanus cajan* pericarp, an agricultural waste product, followed by its characterization using modern techniques like FTIR and SEM studies have been reported. This newly obtained activated carbon has been tested to estimate its practical applicability for removal of methylene blue from aqueous solution. Batch adsorption experiments were performed for this purpose. The influence of pH, contact time, adsorbent doses and initial methylene blue concentration have also been studied and reported. The results revealed that the activated carbon adsorbent reported in this article is effective for removal of methylene blue from wastewater, and thus can be successfully used for control of methylene blue pollution.

Keywords: methylene blue, activated carbon, *Cajanus cajan*, adsorption isotherm.

Introduction-In water sources occurrence of synthetic dyes gives hazardous effects to aquatic organism and human health when discharge directly to environment. More than 10,000 dyes have been widely used in textile, paper, rubber, plastics, leather and cosmetic, pharmaceutical, and food industries[1]. The dyes consist of poisonous and complex components with slow degradation rate. Furthermore, the presence of dyes components affects the undesirable color change in water system. The unfavorable impact is not only from esthetics point of view but also from the decline of sun light penetration, thus reducing photosynthetic activity [2, 3]. As dyes are designed to resist breakdown with time, exposure to sunlight, soap and oxidizing agent cannot be easily removed by conventional wastewater treatment processes due to their complex structure and synthetic origins [4]. MB will cause increased heart rate, vomiting, shock, Heinz body formation, cyanosis, jaundice, quadriplegia and tissue necrosis in humans [5]. The commonly used methods for removing metal ions from waste water include precipitation, lime-coagulation, reduction, electrolytic removal, ion-exchange, reverse osmosis, membrane filtration, and solvent extraction[6-12]. A number of biosorbent have been used such as tree barks, saw dusts, activated rice husk, coconut shell, almond shell etc. for the adsorption of heavy metals. The objective of the present study is to investigate the possible use of activated carbon derived from *Cajanus Cajan pericarp* activated Carbon(CCPAC) as an alternative adsorbent material for removal of MB employing batch experiments.

Materials and Methods-All the chemicals used were of analytical or chemically pure grade. Distilled water was used throughout the investigation.

Preparation of activated carbon-*Cajanus cajan pericarp* was collected as an agricultural waste and washed several times with tap water followed by distilled water. The clean biomass so obtained was oven dried at 120°C for 24hrs. The dry biomass was milled and sieved to get fine particles. The biomass was subjected to pyrolysis process using Muffle Furness. During slow carbonization of raw material in the absence of air at temperature range 700-800°C, volatile product was removed and residue was converted into char. The char was then subjected

to chemical activation process using 25% zinc chloride solution. The adsorbent material obtained has been abbreviated as CCPAC.

Preparation of Methylene Blue solution -A stock solution of methylene blue of concentration 500 ppm (500 mg/L) was prepared by dissolving (0.5000)g of methylene blue in a 1000 mL volumetric flask, agitated by using a magnetic stirrer for a period of time and completed with distilled water up to the mark.

Characterization of CCPAC

FTIR analysis: FTIR of CCPAC is presented in Fig.1. The broad band at 3457.44 cm^{-1} indicates the presence of dissociated or associated -OH groups on the adsorbent surface. The band at 1637.05 cm^{-1} represents N-H bending. The band at 1119.11 cm^{-1} is indicative of CO stretching. The peak at 618.76 cm^{-1} appears to be due to stretching vibration of carbon hydrogen bonding of alkyne linkages.

Scanning Electron Microscopy (SEM) Analysis: The surface morphology of activated carbon under investigation was examined using scanning electron microscopy. At $\times 1000$ magnification, SEM micrograph clearly revealed that wide varieties of pores are present in activated carbon along with fibrous structure. It is found that there are holes and caves type openings on the surface of the adsorbent which would have created more surface area available for adsorption.

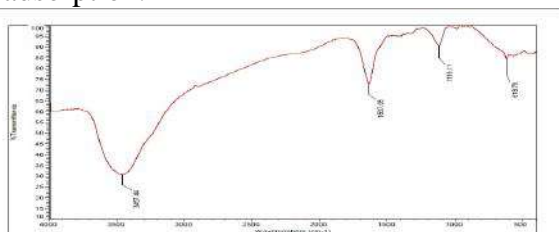


Fig1: FTIR of CCPAC

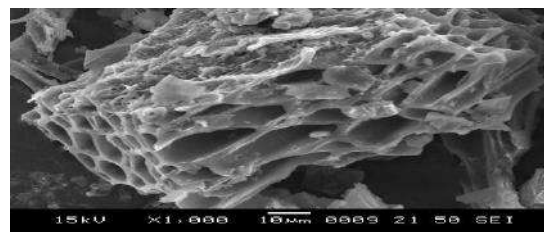


Fig 2: SEM of CCPAC

Results and discussion

Effect of pH-Effect of pH on the adsorption of MB using CCPAC as an adsorbent has been studied in the pH range 1 to 10. The relation between the pH of solution and percentage removal of MB has been shown in fig. 3. The most favorable adsorption was seen at basic pH 5–9 with 70 % removal of MG dye. So for further study pH 7–8 was maintained.

Effect of Contact time-Fig.4 represents the effect of contact time on removal of MB. The initial MB concentration taken was 30ppm. The percentage removal has found to increase with time from 35 to 76. After 100 minute negligible effect has been noticed on adsorption of MB. Thus 100 minute is the optimum time for these batch experiments.

Effect of adsorbent doses-The influence of CCPAC adsorbent doses was studied by varying it from 1 to 10 gm/lit for MB adsorption and the results are represented in Fig.5. The initial MB concentration taken was 30ppm. The percentage of MB removal was found to increase from 50 to 73. However after certain dose it becomes constant and it is treated as an optimum adsorbent dose, which is found to be 5gm/lit. for the CCPAC adsorbent.

Effect of Initial MB concentration-In the present study adsorption experiments were performed to study the effect of initial MB concentration by varying it from 10-100ppm solution is presented in Fig. 6. The results demonstrate that at a fixed adsorbent dose the percentage of MB removal decreases with increasing concentration of adsorbate.

Adsorption Isotherm-The isotherm data have been linearized using the Langmuir equation and is plotted between C_e/Q_e versus C_e . The Langmuir constant q_m , which is measure of the monolayer adsorption capacity of CCPAC is obtained as 2.85. The Langmuir constant b which denotes adsorption energy, is found to be 0.315. The high value (0.9122) of regression correlation coefficient (R^2) indicates good agreement between the experimental values and isotherm parameters and also confirms the monolayer adsorption of MB onto the CCPAC. The dimensional parameter, R_L , which is a measure of

adsorption favorability is found to be 0.0194 ($0 < R_L < 1$) which confirms the favorable adsorption process for MB on CCPAC adsorbent.

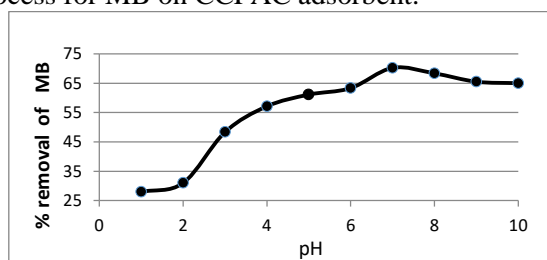


Fig.3: Effect of pH on adsorption of MB

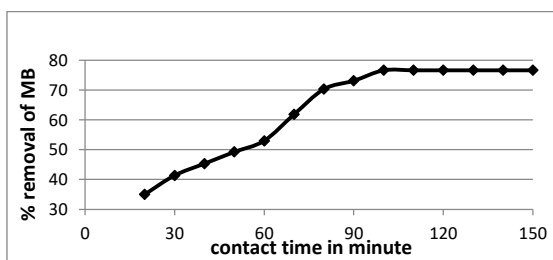


Fig.4: Effect of contact time on MB removal

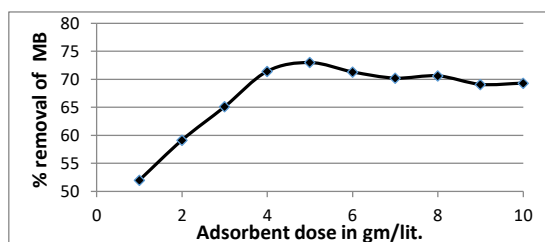


Fig. 5: Effect of adsorbent dose on MB adsorption

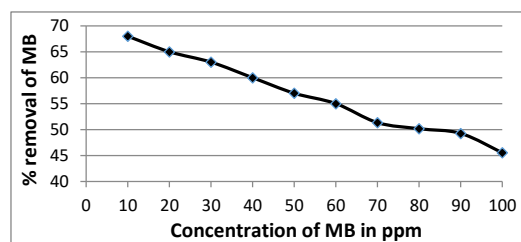


Fig 6: Effect of initial conc. of MB on adsorption

Conclusion-Utilization of waste material such as *Cajanus Cajan* pericarp for the removal of MB from the industrial waste-water is investigated. CCPAC is found to be better adsorbent for removal of MB. The maximum percentage for removal of MB is noticed at pH 7-8 with contact time 100 min. The percentage removal decrease with increase in initial MB concentration. At 5 gm/lit of optimum adsorption dose maximum removal efficacy has been noticed. The adsorption data are best fitted with Langmuir isotherm model which confirms the monolayer adsorption of MB onto CCPAC.

Acknowledgment- Authors are highly thankful to the Principal, S.S.Jaiswal college, Arjuni/Moregaon for providing necessary laboratory facilities. Authors are also thankful to Director SAIF Punjab University, Chandigarh and SAIF Cochin University, Kerala for characterization of Carbon.

Reference

- [1] S. Mondal, "Methods of dye removal from dye house effluent— an overview," *Environmental Engineering Science*, vol. 25, no. 3, 2008, pp. 383–396.
- [2] Spagnoli A A, Giannakoudakis D A and Bashkova S, Adsorption of methylene blue on cashew nut shell based carbons activated with zinc chloride: The role of surface and structural parameters, *Journal of Molecular Liquids* 229, 2017, 465–71
- [3] Tharaneedhar V, Kumar P S, Saravanan A, Ravikumar C and Jaikumar V. Prediction and interpretation of adsorption parameters for the sequestration of methylene blue dye from aqueous solution using microwave assisted corncob activated carbon *Sustainable Materials and Technologies* 11, 2017, 1–11.
- [4] L. Wang, J. Zhang, and A. Wang, "Removal of methylene blue from aqueous solution using chitosan-g-poly(acrylic acid)/montmorillonite superadsorbent nanocomposite," *Colloids and Surfaces A*, vol. 322, no. 1–3, 2008, pp. 47–53.
- [5] R. Ahmad and R. Kumar, "Adsorption studies of hazardous malachite green onto treated ginger waste," *Journal of Environmental Management*, vol. 91, no. 4, 2010, pp. 1032–1038.
- [6] Chakravarti A K , Choudhary S, Chakrabarty S and Mukharjee D C, liquid membrane Multiple emulsion process of chromium Cr(VI) separation from waste-water colloids, *surf A: Physio Chem. Engg. Aspects*, 1995, 103, 59-71.
- [7] Cimino G, Passerini A and Toscano G, Removal of toxic cations and Cr(VI) from aqueous solution by hazelnut shell water *Res*, 2000, 34(11) 2955-2962.
- [8] Gode F and pehlivan E, removal of Cr(VI) from aqueous solution by two lewattit-anion exchange resin, *J Hazard Mater*, 2005, 119 175-182.
- [9] Juang RS and Shiau RC , Metal removal from aqueous solution using Chitosan enhanced membrane filtration, *J Membr Sci*. 2000, 21(10), 1091-1097.
- [10] Lalvani SB, Hubner A and Wiltowski TC, Chromium adsorption in lignin, *Energy Sources* 2000, 22, 45-46.
- [11] Lu A, Zhong S, Chen J, Shi J, Tang J and lu X. Removal of Cr(VI) and Cr(III) from aqueous solution waste water by natural lino-pyrrhotite *Environ Sci. Technol*, 2006, 40(9), 3064-3069.
- [12] Rengaraj S: Yeon KH and Moon SH, Removal of Chromium from water and waste water by ion exchange resin *J. Hazard Mat*. 2001, 87,(1-3) 273-287.

Conductometric Studies of [CPHDD] and [CTMBCD] at Different Molar Concentrations and Different Percentage Compositions in Water-Ethanol Mixture

K.P. Jumde¹, Sanghapal S. Padhen², Saleem R. Khan³, D.T.Tayade³

¹ Department of Chemistry, Nilkanthrao Shinde Science and Arts College, Bhadrawati 442902 (M.S.) India.

² Department of Chemistry, Rajarshree Shahu Science College, Chandur Railway, Dist. Amravati 444904 (M.S.)

³ Department of Chemistry, Government Vidarbha Institute of Science and Humanities, Amravati, 444604, ³ Department of Chemistry, Government Vidarbha Institute of Science and Humanities, Amravati, 444604

Abstract

Conductivity play vital role in drug; diffusion, transmission, metabolism (drug activity and drug effect) and excretion in pharmacokinetics and pharmacodynamics of drugs. Thermodynamic parameters affected by substituent's of drug. Considering these facts recently in this laboratory, conductometrically thermodynamic parameters of 4-[4-(4-chlorophenyl)-4-hydroxypiperidin-1-yl]-N,N-dimethyl-2,2-diphenylbutanamide [CPHDD] and (2S,6R)-7-chloro-2,4,6-trimethoxy-6'-methyl-3H,4'H-spiro[1-benzofuran-2,1'-]cyclohex-2-ene]-3,4'-dione [CTMBCD] were investigated at different molar concentrations and different percentage compositions. This work mainly highlights on investigation of G , K and μ values. The thermodynamic parameters viz. ΔH , ΔS and ΔG for ion pair formation were determined from the value of ion association constant at 298K This technique is suitable and accurate to study pharmacokinetics and pharmacodynamics parameters.

Keywords: Conductometric measurements, thermodynamic parameters, [CPHDD], [CTMBCD] pharmacokinetics and pharmacodynamics.

Introduction:

Conductivity of drugs/ medicines play key role in medicinal chemistry. Conductometric measurements along with G , K and μ values, ΔH , ΔS and ΔG and biopharmaceutical parameters are responsible for the effective bioavailability of drug in vitro and in vivo correlations [1], which gives useful information regarding the permeability of drug in drug absorption and transmission of drug in pharmacokinetics and pharmacodynamics of drug in drug chemistry. Improvement of solubility and dissolution rate and oral bioavailability of poorly water soluble drugs are still the challenging aspects for the pharmaceutical technologists [2]. One of the safest methods of solubilisation is hydrotropic solubilisation [3] and by the addition of hydrotropic agents the aqueous solubilisation of insoluble drugs can be achieved. Many researchers highlighted the effect of the solubility enhancers (hydrotropic agents) [4, 5] and hence improved stability of the drug but no detailed explanation is available relating to the improvement phenomena.

Split of electrolyte conductivities into the ionic components ideally requires transference numbers, an accuracy to obtain exact readings for ground level laboratory for various parameters to chemist become difficult and important task and also serious experimental problems in many non-aqueous solvents for well equipped laboratories for pharmacokinetics and pharmacodynamics of drugs in drug chemistry. To overcome this problem conductance measurements provide very important and valuable information regarding ion-ion and ion-solvent interactions [6-7]. The conductometric studies of ionic association of divalent asymmetric electrolyte $\text{Cu}(\text{NO}_3)_2$ with Kryptofix-22 in mixed (MeOH-DMF) solvents at different temperatures were carried out by Gomaa and Al-Jahdalli [8].

Izonfuo and Obunwo [9] and Roy *et al* [10] studied the conductance of alkali metal in different mixtures mixed solvents. The thermodynamic parameters and Walden products of different complexes were studied by few researched and they also determined the comparison of transition metal complexes among the halide groups by [11]. Dubey [12] studied the interaction between sodium sulphate and 1-propanol, 1-butanol, 1-pentanol and 1-hexanol at different temperatures by conductometric technique [13]. The present investigation deals with the study of conductometric properties, thermodynamic behaviour and Walden product of 4-[4-(4-chlorophenyl)-4-hydroxypiperidin-1-yl]-N, N-dimethyl-2,2-diphenylbutanamide [CPHDD] and (2S, 6R)-7-chloro -2, 4, 6-trimethoxy-6'-methyl-3H, 4'H-spiro[1-benzofuran 2, 1']-cyclohex-2-ene]-3,4'-dione[CTMBCD] in ethanol-water mixture at different concentrations and different percentage compositions at constant temperature i.e. 27°C.

Experimental:

All the chemicals and solvents used for the synthesis were of A.R. grade. All the freshly prepared solutions were used for investigations. The solvents were purified by standard method [14]. Different concentration solutions of 0.1M 4-[4-(4-chlorophenyl)-4-hydroxypiperidin-1-yl]-N,N-dimethyl-2,2-diphenyl- butanamide [CPHDD] and (2S,6R)-7-chloro-2,4,6-trimethoxy-6'-methyl-3H,4'H-spiro[1-benzofuran-2,1']-cyclohex-2-ene]-3,4'-dione[CTMBCD] were prepared. 0.1M solution of each drug was prepared and then by serial dilution method 0.075M, 0.050M and 0.025M were prepared in 100% water and ethanol-water mixture respectively. Similar solutions were prepared for 80% and 70% water-ethanol mixture. All the solutions of drug were always used a fresh in the present investigation.

In 50 ml glass beaker drug solution was taken and it was kept inside the thermostat for 15-20 minutes to attain the thermal equilibrium (27°C). After achieving the thermal equilibrium, the conductivity was measured.

Results and Discussion:

During this investigation conductometric measurements of 100%, 80%, and 70% mixtures of water-ethanol were prepared. In first set 0.1M solution of [CPHDD] and in second set 0.1M solution of [CTMBCD] was prepared in conductivity water and by serial dilution method 0.075M, 0.050M and 0.025M solutions were prepared. At 27°C the conductance of each solution was measured by conductivity bridge and result are cited in Table 1 and Table 2. From the data observed conductance (G), specific conductance (k) and molar conductance (μ) were determined by known literature method.

Table 1: Conductometric Measurements of [CPHDD] at different concentration				
Determination of G, k and μ on different Concentrations at 27°C				
% of solution (Water- ethanol)	Concentration (M)	Observed conductance (G)	Specific conductance (k)	Molar conductance (μ)
100%	0.1 M	0.60×10^{-3}	0.5709606×10^{-3}	5.709606
	0.075 M	0.51×10^{-3}	0.4853165×10^{-3}	6.4708868
	0.050 M	0.37×10^{-3}	0.3520923×10^{-3}	7.0418474
	0.025 M	0.21×10^{-3}	0.1998362×10^{-3}	7.993448
80%	0.1 M	0.73×10^{-3}	0.6946687×10^{-3}	6.9466873
	0.075 M	0.70×10^{-3}	0.6661207×10^{-3}	8.8816093
	0.050 M	0.61×10^{-3}	0.5804766×10^{-3}	11.609532
	0.025 M	0.41×10^{-3}	0.3901564×10^{-3}	15.606256
70%	0.1 M	0.25×10^{-3}	0.2379002×10^{-3}	2.3790025
	0.075 M	0.22×10^{-3}	0.2093522×10^{-3}	2.7913629
	0.050 M	0.20×10^{-3}	0.1903202×10^{-3}	3.806404
	0.025 M	0.14×10^{-3}	0.1332241×10^{-3}	5.3289656

Table 2: Conductometric Measurements of [CTMBCD] at different concentration				
Determination of G, k and μ on different Concentrations at 27°C				
% of solution (Water- ethanol)	Concentration (M)	Observed conductance (G)	Specific conductance (k)	Molar conductance (μ)
100%	0.1 M	0.22X10-3	0.209352 X10-3	2.09352
	0.075 M	0.17 X10-3	0.161772 X10-3	2.15696
	0.050 M	0.12 X10-3	0.114192X10-3	2.28384
	0.025 M	0.08 X10-3	0.076128X10-3	3.04512
80%	0.1 M	0.16X10-3	0.152256X10-3	1.52256
	0.075 M	0.15 X10-3	0.14274X10-3	1.9032
	0.050 M	0.12 X10-3	0.114192X10-3	2.28384
	0.025 M	0.08 X10-3	0.076128X10-3	3.04512
70%	0.1 M	0.15 X10-3	0.14274X10-3	1.4274
	0.075 M	0.13 X10-3	0.123708X10-3	1.64944
	0.050 M	0.11 X10-3	0.104676X10-3	2.09352
	0.025 M	0.07 X10-3	0.066612X10-3	2.66448

From **Table-1 to Table-2**, it was observed that the observed conductance (G) and specific conductance (k) were decreases from [CPHDD] to [CTMBCD] continuously while molar conductance (μ) increases. Decrease in some conductance is due to number of phenolic-OH group present in the respective molecule. In [CPHDD] observed conductance continuously decreases from 0.1M concentration to 0.025M concentration continuously. This is due to the numbers of [CTMBCD] present in these solutions were continuously decreases. Same pattern was observed in percentage compositions of the mixture. Specific conductance of [CPHDD] decreases when the molar concentration and percentage composition of water decreases but the specific conductance increases at the same temperature. In [CPHDD] it was also observed that molar conductance increases from 0.1M concentration to 0.025M concentration as well as it increases in all percentage compositions. In 100% water molar conductance is highest while it will decreases from 100% to 70% water-ethanol percentage compositions. Molar conductance in 100% water is highest in all molar concentrations. Above results showed that [CPHDD] and [CTMBCD] are good drugs and will gave good pharmacokinetics and pharmacodynamics results of the standard drug. Same patterns of observed conductance, molar conductance and specific conductance were observed for [CTMBCD]. These results throw light on pharmacokinetics of these two drugs. During this investigation it was observed that the molar conductance of [CPHDD] is more than [CTMBCD] which clearly indicates the drug effect of [CPHDD] is comparatively good than [CTMBCD]. It means that the absorption, transformation and metabolism of [CPHDD] is better than [CTMBCD], so [CPHDD] possesses best drug activity and drug effect than [CTMBCD].

The specific constant (Ksp), log (Ksp) and thermodynamics parameter viz. change in free energy (ΔG), change in entropy (ΔS) and change in enthalpy (ΔH) of [CPHDD] and [CTMBCD] were determined by known literature method at various molar concentration, percentage compositions and temperatures and result are cited in **Table 1 to Table 8**.

Table 3 : Conductometric Measurements of [CPHDD] at different concentration						
Determination of Ksp, log Ksp, ΔG, ΔH and ΔS at different Concentrations at 27°C						
SYSTEM:DRUG CPHDD MEDIUM - 100% WATER						
Temp (°C)	Conc. (M)	Ksp	Log Ksp	ΔG	ΔH	ΔS
27	0.100	0.099790372	-1.000911358	5749.37757	-580158.4026	-1953.025934
	0.075	0.074842777	-1.125850107	6467.043561	-580158.4026	-1955.418154
	0.050	0.049895185	-1.301941363	7478.536846	-580158.4026	-1958.789798
	0.025	0.024947592	-1.602971367	9207.696116	-580158.4026	-1964.553662

Table 4 : Conductometric Measurements of [CPHDD] at different concentration						
Determination of Ksp, log Ksp, ΔG, ΔH and ΔS at different Concentrations at 27°C						
SYSTEM:DRUG [CPHDD] MEDIUM - 80% WATER						
Temp (°C)	Conc. (M)	Ksp	Log Ksp	ΔG	ΔH	ΔS
27	0.100	0.079832297	-1.097821375	6306.042527	-580158.4026	-1954.881484
	0.075	0.059874221	-1.222760124	7023.708518	-580158.4026	-1957.233704
	0.050	0.039916148	-1.398851376	8035.20178	-580158.4026	-1960.645348
	0.025	0.019958073	-1.699881393	9764.361124	-580158.4026	-1966.409212

Table 5 : Conductometric Measurements of [CPHDD] at different concentration						
Determination of Ksp, log Ksp, ΔG, ΔH and ΔS at different Concentrations at 27°C						
SYSTEM:DRUG [CPHDD] MEDIUM - 70% WATER						
Temp (°C)	Conc. (M)	Ksp	Log Ksp	ΔG	ΔH	ΔS
27	0.100	0.06985326	-1.155813321	6639.156535	-580158.4026	-1955.991864
	0.075	0.052389943	-1.280752074	7356.822548	-580158.4026	-1958.384084
	0.050	0.034926629	-1.456843323	8368.315793	-580158.4026	-1961.755728
	0.025	0.017463314	-1.757873327	10097.47506	-580158.4026	-1967.519592

Table 6: Conductometric Measurements of [CTMBCD] at different concentration						
Determination of Ksp, log Ksp, ΔG, ΔH and ΔS at different Concentrations at 27°C						
SYSTEM:DRUG [CTMBCD] MEDIUM - 100% WATER						
Temp (°C)	Conc. (M)	Ksp	Log Ksp	ΔG	ΔH	ΔS
27	0.100	3.925965087	0.593946433	-3411.713008	-580158.4026	-1922.488965
	0.075	2.944471816	0.469007696	-2694.047086	-580158.4026	-1924.881185
	0.050	1.962982544	0.292916437	-1682.553784	-580158.4026	-1928.252829
	0.025	0.981491271	-0.008113558	46.60543415	-580158.4026	-1934.016693

Table 7: Conductometric Measurements of [CTMBCD] at different concentration						
Determination of Ksp, log Ksp, ΔG, ΔH and ΔS at different Concentrations at 27°C						
SYSTEM:LIGAND [CTMBCD] MEDIUM - 80% WATER						
Temp (°C)	Conc. (M)	Ksp	Log Ksp	ΔG	ΔH	ΔS
27	0.100	3.14077207	0.49703642	-2855.048074	-580158.4026	-1924.344515
	0.075	2.355579053	0.372097683	-2137.382152	-580158.4026	-1926.736735
	0.050	1.570386035	0.196006424	-1125.88885	-580158.4026	-1930.108379
	0.025	0.785193016	-0.105023571	603.2703682	-580158.4026	-1935.872243

Table 8 : Conductometric Measurements of [CTMBCD] at different concentration						
Determination of Ksp, log Ksp, ΔG, ΔH and ΔS at different Concentrations at 27°C						
SYSTEM:DRUG [CTMBCD] MEDIUM - 70% WATER						
Temp (°C)	Conc. (M)	Ksp	Log Ksp	ΔG	ΔH	ΔS
27	0.100	2.748175561	0.439044473	-2521.934061	-580158.4026	-1925.454895
	0.075	2.061131671	0.314105736	-1804.268139	-580158.4026	-1927.847115
	0.050	1.374087781	0.138014477	-792.7748368	-580158.4026	-1931.218759
	0.025	0.687043889	-0.687043889	936.3843814	-580158.4026	-1936.982623

From **Table-3** to **Table-8** it was observed for these drugs Ksp, log Ksp, ΔH and ΔS decreases continuously while ΔG increases when we go from 0.1M concentration solution to 0.025M concentration. Same pattern was observed in percentage composition of the mixture i.e. these thermodynamic parameters are highest in 100% water while least in 70% water-ethanol solvent. In [CTMBCD] the values of all thermodynamic parameter as well as Ksp and log Ksp are the greatest than [CPHDD].

Conclusion:

From this investigation it is clear that various functional groups such as electron donating, electron withdrawing, acidic, basic and various functional groups present in the molecule directly affect conductance, specific conductance, molar conductance, Ksp, ΔH , ΔS and ΔG values of that drug. The structure of the drug as well as nature of that drug directly affects these parameters. The temperature molar concentrations and percentage compositions are also responsible for changing the values of these parameters. The solute (drug)-solvent interactions, solvent-solvent interactions, solvent-solvent-solute interactions and solute-solute-solvent interactions are another factor which directly hamper these parameters. The internal geometry as well as internal and intra hydrogen bonding affect these parameters.

During this investigation it was also observed that the molar conductance of [CPHDD] is highest than [CTMBCD] which clearly indicates the drug effect of [CPHDD] is comparatively more than [CTMBCD].

Disclosure of conflict of interest:

Authors wish to state that there is no conflict of interest on this work.

References:

- 1 S.Chakraborty, D.Shukla, A.Jain,B.Mishra and S.Singh, J.Coll.Int.Sci.,355,242-249,(2009).
- 2 S.Agrawal,S.S.Pancholi, N.K.Jainand G.P.Agrawal, Int.J.PHam.,274,149-155,(2004).
- 3 G.D.Pancholi and J.C.Gradock, J.PHarm.Sci.,68,728-732,(1974).
- 4 U.N.Dash and S.Supkar, Proc.Ind.Acad.Sci.Chem.Soc.,107, 541,(1995).
- 5 Agnieszka Boruń, Conductance and ionic association of selected imidazolium ionic liquids in various solvents: A review, Journal of Molecular Liquids, 276,2019, 214-224, <https://doi.org/10.1016/j.molliq.2018.11.140>.
- 6 E. A. Gomaa, B. M. Al-Jahdalli, *Conductometric Studies of Ionic Association of Divalent Asymmetric Electrolyte Cu(NO₃)₂ with Kryptofix -22 in Mixed (MeOH-DMF) Solvents at Different Temperatures*, American Journal of Condensed Matter Physics, Vol. 2 No. 1, 2012, pp. 16-21. doi: 10.5923/j.ajcmp.20120201.03.
- 7 W.A.L.Izonfuo, C.C.Obunwa, Ind.J.Chem.,38A,939,(1999).
- 8 M.N.Roy, D.Nandi, and D.K.Hazra, J.Ind.Chem.Soc.,70,121,(1993).
- 9 G.C.Bag, N.M.Singh, N.R.Singh, J.Ind.Chem.Soc.,77,146,(2000).
- 10 N.Dubey, J. Surface Sci. Technol., 24, 139-148, (2008).
- 11 A.B. Wadekar , D. T. Tayade, [2016], Conductometric Study of Substitutedthiocarbamidonaphthols in 70% Ethanol– Water Mixture at Different Molar Concentrations at Constant Temperature, International Journal of Science and Research 5(1),678-680
- 12 Agnieszka Boruń, Conductance and ionic association of selected imidazolium ionic liquids in various solvents: A review, Journal of Molecular Liquids, 276,2019,214-224, <https://doi.org/10.1016/j.molliq.2018.11.140>.
- 13 Bahram Ghalami-Choobar, Tayyebe Nosrati Fallahkar, [2019], Thermophysical properties of 1-ethyl-3-methylimidazolium bromide ionic liquid in water + ethylene carbonate mixtures at T = (298.2, 308.2 and 318.2) K Fluid Phase Equilibria, Volume 496, 42-60
- 14 A. B. Wadekar , D. T. Tayade, [2016], Thermodynamic study of substituted thiocarbamido-Napthnols at different concentrations and different Temperatures in mixed solvent media” European Journal of Pharmaceutical and Medicinal Research, 3(9), 635-637

Synthesis and Characterization of Some Substituted Chalcone by the Green Synthesis Way (Grinding Method)

Nilesh S. Padole¹, Murlidhar P. Wadekar², Shubhangi Y. Deshmukh³,
Vinod M. Sherekar⁴

¹Head and Assistant Professor, Vinayak Vidnyan Mahavidyalaya Nandgaon Khandeshwar 444708.

²Associate Professor, GVISH, Amravati, 444602.

³Research student, VBMV Camp, Amravati 444602.

⁴Assistant Professor, Vinayak Vidnyan Mahavidyalaya Nandgaon Khandeshwar 444708.

*Corresponding Author: Name: Mr. Nilesh S. Padole, E-mail: nileshongc021211@gmail.com Phone: +91-9096312784, Address: Vinayak Vidnyan Mahavidyalaya, Nandgaon Khandeshwar, 444708.

ABSTRACT

The presented chalcone were synthesized by Claisen- Schmidt condensation of 2-hydroxy-3-nitro-5-methyl acetophenone (3) and o-chloro benzaldehyde. m-chloro and indol-3-carboxy aldehydes. All the synthesized compounds were characterized through NMR, IR, and elemental analysis. The synthetic methods used proved successful synthesis of the desired compound. Grinding technique is used to follow the green synthesis way for the synthesis of chalcone.

KEYWORDS: Chalcones, Green Synthesis (Grinding Technique), Claisen- Schmidt condensation.

INTRODUCTION

Alpha-beta unsaturated ketones or commonly referred as chalcones are one of the important classes of organic compounds frequently encountered in synthetic chemistry. They are important intermediates not only as key building blocks for the synthesis of core heterocycles such as pyrazole, isoxazole, triazole, flavone, benzodiazepine and pyrimidine in medicinal chemistry, but also as an invaluable chelating ligand for various lanthanide and transition metals in material chemistry. Chalcones, α , β -unsaturated carbonyls, play a crucial role in many biological processes as well as are well-known intermediates for synthesizing various heterocycles¹ and bear a very good synthon so that variety of novel heterocycles with good pharmaceutical profile can be designed². Presence of enone functionality in chalcone shows the antibiotic activity.

Recent trends in organic synthesis utilize a non-conventional green technique such as ultrasound (sonochemistry), microwave irradiation, grinding and by using ionic liquids which have also been proved to have many advantages^{3,4,5}. Numerous solvents assisted and solvent-free methods have been reported for the preparation of pyrazoline derivatives. The present article elaborates on various green techniques reported previously for synthesis of chalcone derivatives, which will be useful for researchers for synthesizing chalcone derivatives in less time, yield effective and safely.

Green Synthesis of chalcone Derivatives "The design of chemical products and processes that are more environmentally benign and reduce negative impacts to human health and the environment"⁶. There are various green techniques available in the literature for synthesis of chalcone derivatives. Some green methods for organic synthesis of pyrazolines^{7,8} Microwave Irradiation Ultrasonic Irradiation Grinding Technique Ionic Liquids Microwave Irradiation Microwave, which consists of electric and magnetic field, acts as a non-ionising reaction that causes ionic motions and rotations, but there is no change in molecular structure. At least one liquid polar is required in microwave synthesis⁹. Polar mechanism shows the

microwave effect that when polarity is increased from ground state towards the transition state during the reaction¹⁰.

EXPERIMENTAL SECTION

The chalcones were synthesized by using 2-hydroxy-3-nitro-5-methyl acetophenone with some aldehydes (2-chloro Benzaldehyde, 3-chloro Benzaldehyde and Indol -3-carboxaldehyde) under alkaline condition. The chalcones were obtained yellow to brown and peach in colour and their synthesis were confirmed by melting point method and from spectral interpretation. This is the general Claisen-Schmidt reaction¹¹ but I used the reaction by grinding was carried out in a mortar and pestle at room temperature. During the grinding, sudden change in colour took place, indicating the progress of reaction. The full conversion of the reaction mixture to a solid mass indicates the completion of reaction¹²

The chemicals and solvents used were of highest purity purchased commercially from Merck, S.D. Fine and Alfa Aesar Company Ltd. The melting points of all the synthesized compounds were recorded by Thiele's melting point apparatus as uncorrected values. The elemental analysis was carried out on Thermo Scientific CHNS elemental analyser. IR spectra were recorded on a Shimadzu instrument using KBr pallet. ¹H NMR spectra were scanned by Bruker at 400 MHz using DMSO-d₆ as solvent and TMS as an internal reference. ¹³C NMR spectrum of one sample (4a) was recorded on same instrument at 100 MHz. Experimental procedure for synthesis of 3-(substituted)-1-(2-hydroxy-5-methyl-3-Nitro phenyl) prop-2-en-1-ones 5(a-c).

SYNTHESIS OF CHALCONES

Preparation of p-methylphenyl acetate (1)

The p-cresol was refluxed along with acetic anhydride and anhydrous sodium acetate for an hour. The reaction mixture was cooled and poured into the ice-cold water containing crushed ice. Acetate layer was separated by means of separating funnel and several times washed with water. It was finally purified by distillation and the distillate fraction was collected at about 236°C, to get the compound (1) b.p. 236°C yield: 84.74%.

Preparation of 2-hydroxy-5-methyl acetophenone (2)

p-methyl phenyl acetate (1) was mixed with anhydrous AlCl₃ (1) and heated at 120°C for 45 minutes on an oil bath. The reaction mixture was decomposed in ice cold water containing 10% hydrochloric acid and allowing the solution to fall drop by drop into ice cold water with constant stirring. Green solid compound i. e. crude ketone (2) was obtained, m.p. 47°C, yield: 89%.

Preparation of 2-hydroxy-3-nitro-5-methyl acetophenone (3):

2-hydroxy-5-methyl acetophenone (2) was dissolved in acetic anhydride in a beaker and reaction mixture was kept in ice bath by maintain temperature below 5°C. To this reaction mixture conc. HNO₃ was added dropwise with constant stirring till the solution becomes orange coloured and kept for 4-5 hrs. it was then decomposed with ice cold water. Yellow granules obtained were filtered and washed with water and then crystallized from ethanol, m.p. yield: 72%.

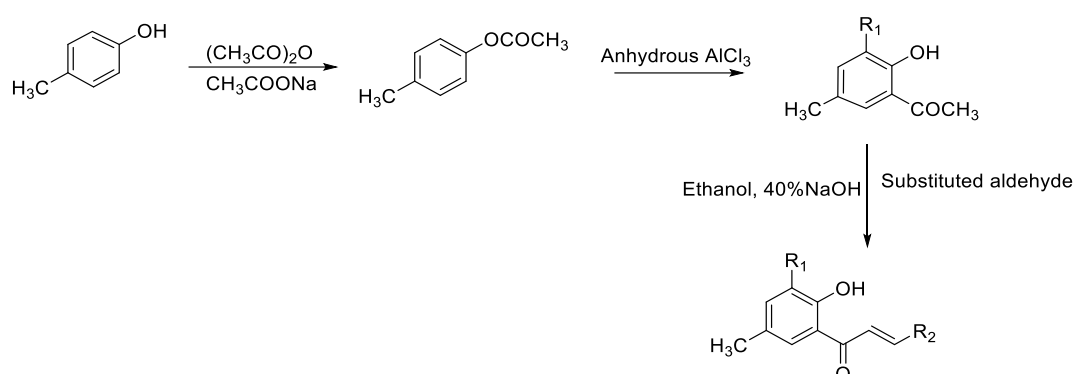
Preparation of β-unsaturated chalcones (4a–4c)

A mixture of 2-hydroxy-3-nitro-5-methyl acetophenone (3) (0.01mol) and chloro substituted aldehyde and indole 3-carboxyaldehyde, (0.01mol), aryl and ammonium bromide and

ammonium persulphate moist with few drops of water is ground at room temperature for 25 minutes in a mortar and pestle. The reaction mixture is allowed to stand for 25 min. Then Ice-cold water (30 ml) was added to the reaction mixture and acidified with conc. HCl. The product was collected by vacuum filtration and then recrystallized from ethanol. The same procedure of grinding was applied by using anhydrous Barium hydroxide and then result of two procedure was compared. Name of the chalcone prepared are entitled below.

- 3-(2-chlorophenyl)-1-(2-hydroxy-5-methyl-3-nitrophenyl)prop-2-en-1-one (4a) M.P. 112⁰C, yield: 74%.
- 3-(3-chlorophenyl)-1-(2-hydroxy-5-methyl-3-nitrophenyl)prop-2-en-1-one (4b) M.P 118⁰C, yield: 84%.
- 1-(2-hydroxy-5-methyl-3-nitrophenyl)-3-(1H-indol-3-yl)prop-2-en-1-one (4c) M.P 154⁰C, yield: 76%.

The complete experimental scheme for synthesis of above titled compounds is given below.



Scheme of 3-(substituted)-1-(2-hydroxy-5-methyl-3-Nitro phenyl) prop-2-en-1-ones 4(a-c). R₁ = NO₂; R₂ = 2-Chloro benzaldehyde, 3- Chloro benzaldehyde, Indol-3-carboxyaldehyde,

RESULTS AND DISCUSSION

Spectroscopic Data: The IR, ¹H NMR and ¹³C NMR spectral data showed expected signals or peaks which correspond to various groups present in each compound. Also, elemental analysis was found in full agreement with the proposed structures. The elemental analysis, IR, ¹H NMR and ¹³C NMR spectral data of compounds 4(a-c) are shown below

3-(2-chlorophenyl)-1-(2-hydroxy-5-methyl-3-nitrophenyl)prop-2-en-1-one (4a)

Brown solid; M.P. 112⁰C, yield: 74%; Elemental Anal. Calcd. for C₁₆H₁₂ClNO₄: C: 60.49, H: 3.81, O: 4.41, Cl: 11.16 Found: C: 53.10, H: 2.40, O: 3.98, Cl: 21.00. IR (KBr) cm⁻¹: 3120 (Phenolic OH stretch), 2980 (Aromatic C-H stretch), 2850 (Aliphatic C-H stretch), 1695 (C=O stretch), 1520 (Aromatic C=C stretch). ¹H NMR (400 MHz, DMSO-d₆) δ (ppm): 1.51 (s, 3H, -CH₃), 3.43 (s, 2H, -CH₂), 3.80 (s, 1H, -OH), 8.15-8.32 (m, 6H, Ar-H). ¹³C NMR (100MHz, DMSO-d₆) δ (ppm): 40 (-CH₂), 195 (C=O), 123-136 (Ar-C), 149-165 (C=C).

3-(3-chlorophenyl)-1-(2-hydroxy-5-methyl-3-nitrophenyl)prop-2-en-1-one (4b)

Dark brown solid; M.P 118⁰C, yield: 84%; Elemental Anal. Calcd. for C₁₆H₁₂ClNO₄; C: 53.10; H: 2.40; N: 3.98, Cl: 21.00. Found: C: 60.49; H: 3.81; N: 4.41, Cl: 20.91. IR (KBr) cm⁻¹: 3340 (Phenolic OH stretch), 2980 (Aromatic C-H stretch), 2910 (Aliphatic C-H stretch), 1615 (C=O stretch), 1515 (Aromatic C=C stretch), 1260 (C-O stretch). ¹H NMR (400MHz, DMSO-d₆) δ (ppm): 1.51 (s, 3H, -CH₃), 3.81 (s, 2H, -CH₂), 5.13 (s, 1H, -OH), 6.99-7.90 (m, 6H, Ar-H).

1-(2-hydroxy-5-methyl-3-nitrophenyl)-3-(1H-indol-3-yl)prop-2-en-1-one (4c)

Peach color solid; M.P 154⁰C, yield: 76%; Elemental Anal. Calcd. for C₁₈H₁₄N₂O₄: C, 67.08; H: 4.38; N: 3.98, found C: 53.10; H: 3.40; N: 7.90. ¹H NMR (400MHz, DMSO-d₆) δ (ppm): 1.50 (s, 3H, -CH₃), 3.38 (s, 2H, -CH), 4.10 (s, 1H, -OH), 6.77-7.65 (m, 6H, Ar-H).

CONCLUSION

In conclusion, a new series of 3-(substituted)-1-(2-hydroxy-5-methyl-3-Nitro phenyl) prop-2-en-1-ones i.e chalcones 4(a-c) bearing 4-methyl phenol i.e. p-cresol moiety were successfully synthesized in satisfactory yield by employing Claisen-Schmidt condensation of corresponding substituted 2-hydroxy-3-nitro-5-methyl acetophenone (3) and their structures were elucidated by chemical characteristics, elemental analysis and IR, ¹H NMR and ¹³C NMR spectroscopic techniques.

ACKNOWLEDGEMENT

Authors are thankful to Research centre of department of Chemistry, Government Vidharbha Institute of Science and Humanities, Amravati for providing research facilities.

REFERENCES

1. Khan SA, Asiri AM, Kumar S, Sharma K. European Journal of Chemistry. 2014 Mar 31;5(1):85-90. 7
2. Al-Bogami AS, Alkhatlan HZ, Saleh TS. 2013 Jul 21;25(11):6427
3. Deshmukh S.Y. Padole N.S. , Wadekar M.P. , Chaudhari M.A.; *Journal of Chemical and Pharmaceutical Research*, 2021, 13(7):01-06
4. . ElShora AI. Egypt J Sol. 2000;23:251-4.
5. Shubhangi Y. Deshmukh¹*, Nilesh S. Padole²; *JETIR*,2022,9(2): 794-801
6. Anastas PT, Warner JC. Principles of green chemistry. Green chemistry: Theory and practice. 1998:29-56.
7. Thirunarayanan G, Mayavel P, Thirumurthy K, Kumar SD, Sasikala R, Nisha P, Nithyaranjani A.. European Chemical Bulletin. 2013 Apr 18;2(9):598-605.
8. Chemat F, Esveld E. Chemical engineering & technology. 2001 Jul 1;24(7):735-44
9. Bougrin K, Loupy A, Soufiaoui M. Journal of Photochemistry and Photobiology C: Photochemistry Reviews. 2005 Oct 31;6(2):139-
10. Perreux L, Loupy A. Tetrahedron. 2001 Nov 5;57(45):9199-223.
11. Shubhangi Y Deshmukh, IJFMR,23-212,1-6, (2023).
12. K.P. Kakade, S. P. Kakade and S Y. Deshmukh, world journal of pharmacy and pharmaceutical science,4,1,1591-1597 (2014).

In-Silico Prediction of Phytoconstituents From *Solanum Indicum* for Antiepileptic Activity

Pooja.P.Patle*, Parimal Katolkar, Pradeep Raghatate, Jagdish Baheti

Kamla Nehru College of Pharmacy, Butibori, Nagpur 441108 (MS), INDIA

*Email: poojapatle000@gmail.com

ABSTRACT

Objective

A persistent, non-communicable brain disorder is epilepsy. Its distinctive characteristic is recurrent seizures. One or more parts of the body may experience partial or generalised seizures, which are short bursts of uncontrollable movement that can occasionally be followed by loss of consciousness and control over bowel or bladder function. Compounds found in medicinal plants have been the source of many conventional medications. *In-silico* testing of *Solanum indicum* phytoconstituents for antiepileptic efficacy was a part of our investigation.

Methods

Utilizing Discovery studio, molecular docking is done to assess the pattern of interaction between the phytoconstituents from the *Solanum indicum* plant and the crystal structure of the epilepsy proteins (PDB ID: 6O4L). Later, SwissADME and pkCSM were used to screen for toxicity as well as the pharmacokinetic profile. **Results**

The docked results suggest that Solafuranone (-7.8 kcal/mol), Isofraxidin (-6.1 kcal/mol) for 6O4L macromolecule has best binding towards antiepileptic activity as compared to the standard (Acetazolamide) for 6O4L is -5.1 kcal/mol. Furthermore, pharmacokinetics and toxicity parameters were within acceptable limits according to ADMET studies.

Conclusion

Results from the binding potential of phytoconstituents aimed at antiepileptic activity were encouraging. It promotes the usage of *Solanum indicum* and offers crucial details on pharmaceutical research and clinical care.

1. INTRODUCTION

Solanum indicum, also known as Birhata, Badi Kateri, or Indian night shade, belongs to the Solanaceae family. It is a common upright undershrub in warmer parts of India, Asia, and Africa that grows up to 1.5 metres in height. Its height ranges from 0.30 to 1.8 metres. Nationally, 500–1000 MT are needed each year. The berries, leaves, roots, seeds, and stems of this plant have all been used in traditional medical systems to treat a wide range of ailments, including bronchitis, asthma, dry cough, rhinitis, dysuria, leucoderma, sexual dysfunction, insomnia, heart weakness, and pruritis.¹

Solanum indicum, which is consumed as a vegetable in some regions of Africa, may prevent cardiovascular diseases. It was exciting to read the studies on how it may be used to treat hypertension. The extract's potent therapeutic and preventative benefits against hypertension may not have been possible without the presence

of chlorogenic acids. The antihypertensive effect might be due to other components. The findings urge further research into the extract as a possible treatment for hypertension.²

However, there are few studies on the phytoconstituents of *Solanum indicum* for the

antiepileptic activity. Thus, keeping the above information in view, the present investigation was designed to identify the potential phytochemicals of *Solanum indicum* against 6O4L using a molecular docking method.

2. MATERIALS AND METHODS

2.1. Platform for molecular docking

The computational docking study of all the phytoconstituents selected as ligands with antiepileptic activity as the target was performed using PyRx software.³

2.2. Protein preparation

The macromolecule is 6O4L, *in silico* analysis of selected phytoconstituents was performed on the 1.85 Å crystal structure of antiepileptic macromolecule with inhibitor, (PDB ID: 6O4L, having resolution Resolution: 1.85 Å, R-Value Free: 0.220, R-Value Work: 0.174, R-Value Observed: 0.176), which was retrieved from the protein data bank (<https://www.rcsb.org>). 6O4L is classified as Crystal Structure of ALDH7A1 mutant E399D complexed with NAD all other molecules, such as co-crystallized water molecules, unwanted chains, and nonstandard residues, were deleted. Using Discovery studio.⁴

2.3. Mechanism of Action

6O4L: Aldehyde dehydrogenase 7A1 (ALDH7A1) is an enzyme that catabolizes lysine, and some loss-of-function mutations in this gene result in pyridoxine-dependent epilepsy (PDE). To understand how the mutations affect NAD⁺ binding, the crystal structures of the mutant enzymes in complex with NAD⁺ were examined. At the tested dose of NAD⁺, these alterations result in less active tetrameric ALDH7A1.⁵

2.4. Ligand preparation

The three-dimensional (3D) structures of all constituents were retrieved using Avogadro software from the PubChem database available on the NCBI website (<https://pubchem.ncbi.nlm.nih.gov/>). However, the drawing of geometrical 2D structure was performed using the ChemSketch program. The two-dimensional (2D) structures were transformed into 3D models using the Avogadro software and the ligand structures were saved in the PDB format. All the chemical structures are shown in Figure 1.

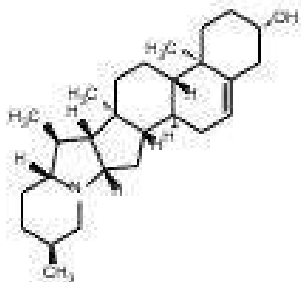
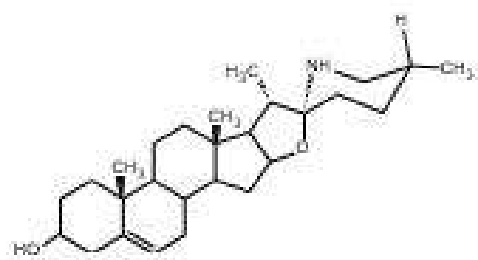
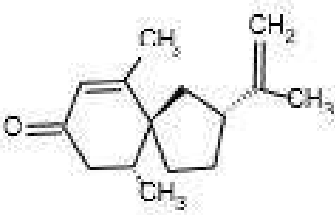
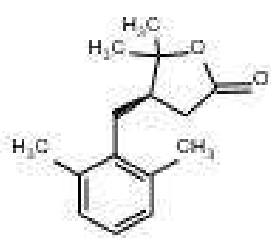
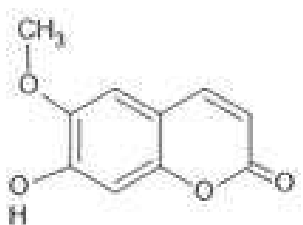
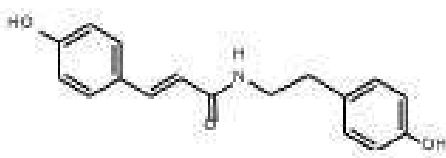
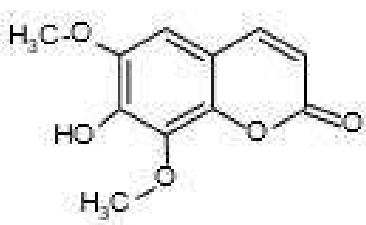

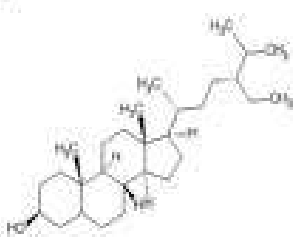
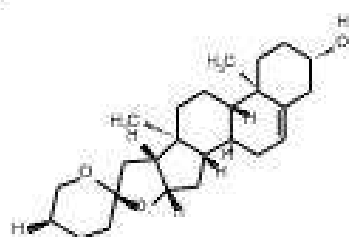
Solanidine 	Solasodine 
Solavetivone 	Solafuranone 
Scopoletin 	N-p-trans-Coumaroyltyramine 
Isotraxidin 	Lauric acid 
β-sitosterol 	Diosgenin 

Fig. 1. Chemical structures of all selected phytoconstituents in the molecular docking studies

2.5. Standard Preparation

The standard is prepared steps such as, the 2D structure of standard drug was made using chem sketch program, then the 2D structure was converted into 3D model using Avogadro Software, it was saved in PDB format.

By using PyRx molecular docking of Acetazolamide was done with 6O4L.

2.6. Molecular docking

Molecular docking evaluates the protein-ligand interactions and estimates the scoring function based on the geometry to predict the binding affinity of the ligand molecule^{6,7}. We applied molecular docking studies to investigate the binding pattern of selected phytoconstituents (Figure 1) and the standard drug, along with the crystal structure of antiepileptic activity macromolecule (PDB ID: 6O4L). The molecular docking study was performed using PyRx software, Binding affinity was explored using the Vina wizard tool. The final results were analysed and visualized using Discovery Studio 2020 Client⁸, with bound ligands as the standard. Visualization of protein ligand interaction reflects the number of interactions and active residues responsible for significant binding at the active site of the target enzyme.

2.7. Absorption, distribution, metabolism, and excretion (ADME) and toxicity prediction

The selected phytoconstituents and standard drug were further checked for drug-likeness properties according to Lipinski's rule. During drug development, it is necessary to predict the tolerability of phytochemicals before being ingested by humans and animal models. The pharmacokinetic profile (ADME) and toxicity predictions of ligands were conducted using SwissADME (<http://www.swissadme.ch>) and pkCSM (an online server database predicting small-molecule pharmacokinetic properties using graph-based signatures, (<http://biosig.unimelb.edu.au/pkcsml/prediction>)). To analyse the toxicological properties of ligands, Simplified Molecular Input Line Entry System (SMILES) notations or PDB files were uploaded, followed by selecting the required models for generating numerous information about structure-related effects^{9,10}.

3. RESULT AND DISCUSSION

The present study aimed to explore the inhibitory potential of the phytoconstituents present in *Solanum indicum* targeting antiepileptic activity. In this study, we performed molecular docking studies of all phytoconstituents found in *Solanum indicum* using AutoDock Vina, followed by a study of interacting amino acid residues and their influence on the inhibitory potentials of the active constituents. Selected phytoconstituents showing the best fit were further evaluated for absorption, distribution, metabolism, excretion, and toxicological (ADMET) properties using SwissADME and pkCSM servers.

3.1 Molecular docking

The docking scores and binding energies of all chemical constituents of *Solanum indicum* targeting antiepileptic activity (PDB ID: 6O4L) and binding interactions with amino acid residues are presented in Table 1 respectively.

Table 1. Binding interaction of ligands from *Solanum indicum* targeting antiepileptic activity (PDB ID:6O4L)

Sr. No.	Chemical constituent	PubChem ID	Docking Score
			6O4L
1.	Solanidine	65727	-10.0

2.	Solasodine	5250	-9.0
3.	Solavetivone	442399	-7.3
4.	Solafuranone	11107208	-7.8
5.	Scopoletin	5280460	-6.5
6.	N-p-trans-Coumaroyltyramine	5372945	-6.7
7.	Isofraxidin	5318565	-6.1
8.	Lauric acid	3893	-3.7
9.	β -sitosterol	222284	-7.1
10.	Diosgenin	99474	-8.1
Standard Drug			
11	Acetazolamide	1986	-5.1

The binding affinities of phytoconstituents ranged from -10.0 to -3.7 kcal/mol. From the docked results, it is evident that the compounds, Solanidine exhibit the most favourable binding affinity (-10.0 kcal/mol) in complex with selected macromolecules (PDB ID: 6O4L) as compared to other docked compounds i.e., Solsodine (-9.0 kcal/mol), Diosgenin (-8.1 kcal/mol), Solafuranone (-7.8 kcal/mol), Solavetivone (-7.3 kcal/mol), Beta sitosterol (-7.1 kcal/mol), N-p-trans-Coumaroyltyramine (-6.7 kcal/mol), Scopoletin (-6.5 kcal/mol), Isofraxidin (-6.1 kcal/mol), Lauric acid (-3.7 kcal/mol). Visual examination of the computationally docked optimal binding poses of phytoconstituents on selected macromolecules (i.e., 6O4L) revealed the significant involvement of various types of interactions, such as hydrogen bonding and hydrophobic interactions, including π - π stacking and π -alkyl and alkyl interactions, in the stability of the binding of the phytoconstituents to 6O4L.

The binding affinity of the standard (Acetazolamide) for 6O4L is -5.1 kcal/mol.

3.1.1. Solafuranone, 6O4L

The number of intermolecular hydrogen bonds, the binding energy of ligand 6O4L stable complexes, and the number of nearest amino acid residues were also determined for selected compound Solafuranone All synthesized derivatives formed complexes with target proteins. Analysis of interactions of the 6O4L protein complex and ligand Solafuranone showed that the ligand molecule is oriented due to Conventional Hydrogen

bond with THR A: 346 amino acid residue and Pi-Pi Stacked interaction with PHE A: 401 amino acid residue were found.

3.1.2. Isofraxidin, 6O4L

An analysis of the interactions between the 6O4L protein complex and the Isofraxidin ligand was also carried out, which showed that the ligand molecule is oriented due to conventional hydrogen bond with the ASP A: 399, THR A: 346, PHE A: 401 amino acid residue and Pi-Alkyl interaction with ALA A: 349 amino acid residue were found.

3.1.3. Acetazolamide, 6O4L

The binding affinity of the standard (Acetazolamide) for 6O4L is -5.1 kcal/mol. the

interactions between the 6O4L protein complex and the Acetazolamide ligand was also carried out, which showed that the ligand molecule is oriented due to conventional hydrogen bond with the PHE A:166, THR A:164 amino acid residue, Carbon hydrogen bond with PRO A:193 amino acid residue, Pi-Sulfur interaction with PHE A:166 amino acid residue, Pi-Cation interaction with LYS A:190 and Pi-Alkyl interaction with ALA A:165, ALA A:192 amino acid residue were found.

Table No. 2. Interactions with amino acid residue.

Sr. No.	Molecule	Binding Energy (kcal/mol)	H bond	Main amino acid interactions	
				Pi-alkyl, alkyl, Pi-S/Pi-Pi, T shaped/halogen/unfavourable donor-donor interactions	Van der Waals interactions
1	Solanidine	-10.0	No interactions	ALA A:192, ALA A: 165, VAL A: 250	No interactions
2	Solasodine	-9.0	GLY A: 226	VAL A: 250, PRO A: 193	No interactions
3	Solavetivone	-7.3	ASN A: 379, ASN A: 46	TYR A: 41	No interactions
4	Solafuranone	-7.8	THR A: 346	PHE A: 401	No interactions
5	Scopoletin	-6.5	THR A: 164, PHE A: 401	CYS A: 302, ALA A: 165	No interactions
6	N-p-trans-Coumaroyltyramine	-6.7	SER A: 460	PHE A: 168, CYS A: 302, TRP A: 175, PHE A: 468	No interactions
7	Isofraxidin	-6.1	ASP A: 399, PHE	ALA A: 349	No interactions
8	Lauric acid	-3.7	PHE A: 292	PRO A: 288, LEU A: 285, PRO A: 458	No interactions
9	β -sitosterol	-7.1	No interactions	TRP A: 31, ALA A: 207, LYS A: 204, LYS A: 208, VAL A: 209, ALA A: 92	No interactions
10	Diosgenin	-8.1	ASN A: 379	TYR A: 41, PHE A: 166	No interactions
11	Acetazolamide	-5.1	THR A: 164, PHE A: 166, PRO A: 193	ALA A: 165, ALA A: 192, LYS A: 190	No interactions

3.2. ADMET study

Pharmacokinetic profile (ADME) and toxicity predictions of the ligands are important attentive parameters during the transformation of a molecule into a potent drug. In the present study, these parameters were assessed using SwissADME and pkCSM. The absorption potential and lipophilicity are characterized by the partition coefficient (Log *P*) and topological polar surface area (TPSA), respectively. For better penetration of a drug

molecule into a cell membrane, the TPSA should be less than 140 Å. However, the value of Log *P* differs based on the drug target. The ideal Log *P* value for various drugs are as follows: oral and intestinal absorption,

1.35 – 1.80; sublingual absorption, > 5; and central nervous system (CNS)¹¹. The aqueous solubility of ligands ideally ranges from – 6.5 to 0.5¹², while the blood brain barrier (BBB) value ranges between – 3.0 and 1.2¹³. In addition, non-substrate P-glycoprotein causes drug resistance¹⁴.

In our study, all the selected ligands followed the TPSA parameter, P-glycoprotein non-inhibition, thereby showing good intestinal absorption and an acceptable range of BBB values. All the compounds showed aqueous solubility values within the range. Further, it was predicted that the selected ligands do not show AMES toxicity, hepatotoxicity, and skin sensitivity. In addition, it did not inhibit hERG-I (low risk of cardiac toxicity). Lipinski's rule violations, *T. pyriformis* toxicity, minnow toxicity, maximum tolerated dose, rat acute oral toxicity, and chronic toxicity are depicted in table.

Table 3. ADME and toxicity predicted profile of ligands with superior docking score

ADMET Properties	Formula	MW (g/mol)	Log P	PSA (Å ²)	HB done r	Hb accept or	Aqueous solubility (Log mol/L)	Human intestinal absorption (%)	Blood Brain Barrier
Solanidine	C ₂₇ H ₄₃ NO	397.647	5.655	23.47 Å ²	1	2	-4.927	92.975	0.695
Solasodine	C ₇ H ₄₃ NO ₂	413.64	5.2869	41.49 Å ²	2	3	-3.809	92.324	0.035
Solavetivone	C ₁₅ H ₂₂ O	218.33	3.9042	17.07 Å ²	0	1	-4.615	95.873	0.635
Solafuranone	C ₁₅ H ₂₀ O ₂	232.323	3.18764	26.30 Å ²	0	2	-3.551	95.523	0.206
Scopoletin	C ₁₀ H ₈ O ₄	192.17	1.5072	59.67 Å ²	1	4	-2.504	95.277	-0.299
N-p-trans-Coumaroyltyramine	C ₁₇ H ₁₇ NO ₃	283.327	2.4699	69.56 Å ²	3	3	-3.165	90.031	-0.552
Isofraxidin	C ₁₁ H ₁₀ O ₅	222.196	1.5158	68.90 Å ²	1	5	-2.458	95.588	-0.377
Lauric acid	C ₁₂ H ₂₄ O ₂	200.322	3.9919	37.30 Å ²	1	1	-4.181	93.379	0.057
β-sitosterol	C ₂₉ H ₅₀ O	414.718	8.0248	20.23 Å ²	1	1	-6.773	94.464	0.781
Diosgenin	C ₂₇ H ₄₂ O ₃	414.63	5.7139	38.69 Å ²	1	3	-5.713	96.565	0.2
Acetazolamide	C ₄ H ₆ N ₄ O ₃ S ₂	222.251	-0.8561	151.66 Å ²	2	6	-2.428	59.043	-0.622

Table 3 Continued

ADMET Properties	P-glyco-protein substrate	Total clearance [Log mL/(min.kg)]	Bioavailability score	AMES toxicity	Max tolerated dose [Log mg/(kg.d)]	hERG I inhibitor	hERG II inhibitor
Solanidine	YES	0.028	0.55	NO	-0.882	NO	YES

Solasodine	YES	0.09	0.55	NO	-0.375	NO	YES
Solavetivone	NO	1.225	0.55	NO	0.044	NO	NO
Solafuranone	NO	1.256	0.55	NO	0.526	NO	NO
Scopoletin	NO	0.73	0.55	NO	0.614	NO	NO
N-p-trans-Coumaroyltyramine	YES	0.265	0.55	NO	-0.213	NO	YES
Isofraxidin	NO	0.713	0.55	NO	0.56	NO	NO
Lauric acid	NO	1.623	0.85	NO	-0.34	NO	NO
β -sitosterol	NO	0.628	0.55	NO	-0.621	NO	YES
Diosgenin	NO	0.328	0.55	NO	-0.559	NO	YES
Acetazolamide	NO	-0.01	0.55	NO	1.263	NO	NO

Table 3 Continued

ADMET Properties	Acute oral rat toxicity. LD50(mol/kg)	Oral rat chronic toxicity (Log mg/kgbw/day)	Hepatotoxicity	Skin sensation	T.Pyriformis toxicity (Log μ g/L)	Minnow toxicity (Log mmol/L)	Lipinski's rule Violation
Solanidine	2.596	1.334	YES	NO	0.378	-0.493	YES (1)
Solasodine	2.489	1.332	YES	NO	0.311	0.381	YES (1)
Solavetivone	1.643	1.19	NO	YES	1.453	0.874	YES (0)
Solafuranone	1.865	1.947	NO	YES	2.151	0.557	YES (0)
Scopoletin	1.95	1.378	NO	NO	0.516	1.614	YES (0)
N-p-trans-Coumaroyltyramine	2.17	1.271	NO	NO	1.008	1.514	YES (0)
Isofraxidin	2.326	1.825	NO	NO	0.431	1.862	YES (0)
Lauric acid	1.511	2.89	NO	YES	0.954	-0.084	YES (0)
β -sitosterol	2.552	0.855	NO	NO	0.43	-1.802	YES (1)
Diosgenin	1.921	1.452	NO	NO	0.399	0.247	YES (1)
Acetazolamide	2.292	2.143	NO	NO	0.239	2.895	YES (0)

3.3. Interaction of Standard Drug (Acetazolamide) with 6O4L

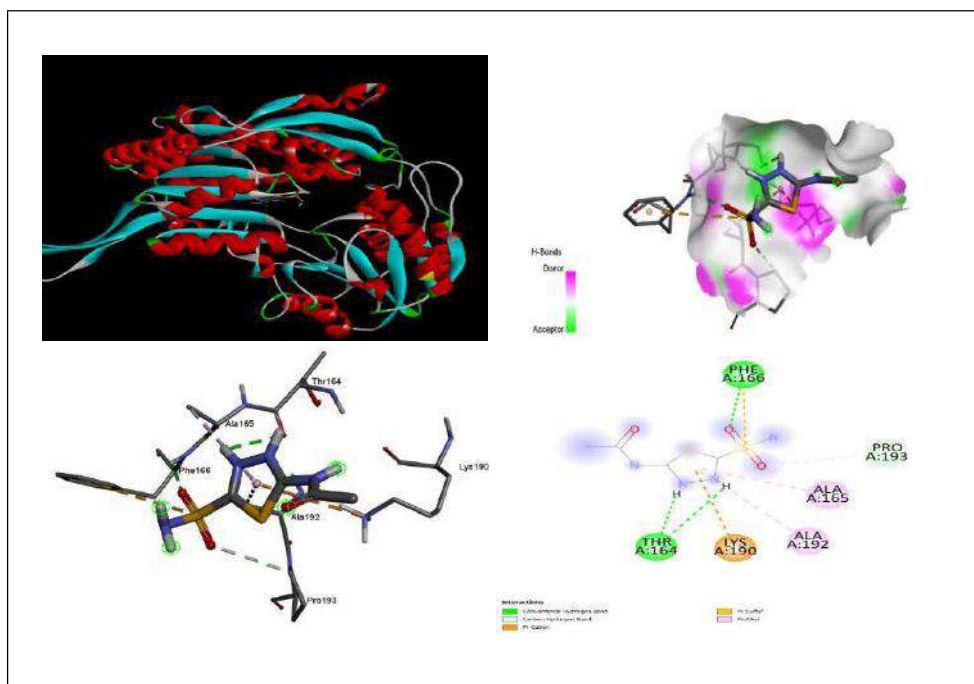
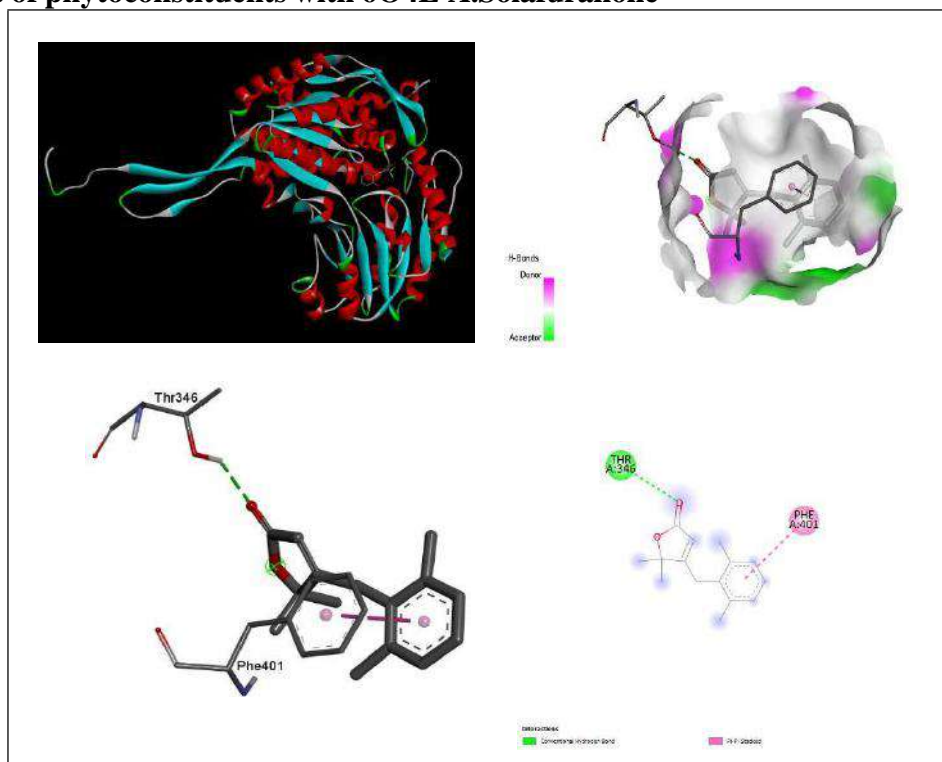


Fig. 2. Docking scores and binding interaction of Acetazolamide (PDB ID: 6O4L). The ligand is shown in line and stick representation along with its 2D diagram and hydrogen bond interaction.

3.4. Interactions of phytoconstituents with 6O4L A.Solafuranone



B.Isofraxidin

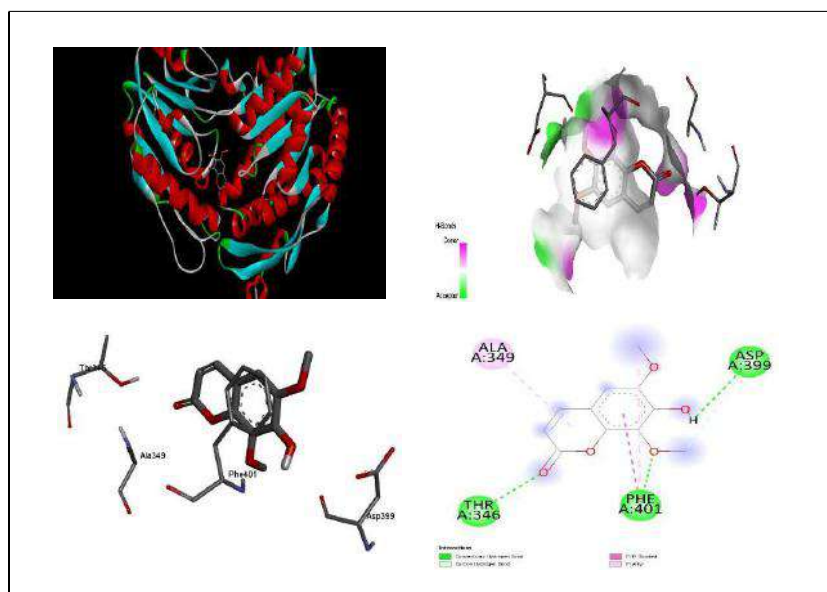


Fig. 3. Docking scores and binding interaction of phytoconstituents (PDB ID: 6O4L). The ligand is shown in line and stick representation along with its 2D diagram and hydrogen bond interaction.

3.5. Boiled Egg

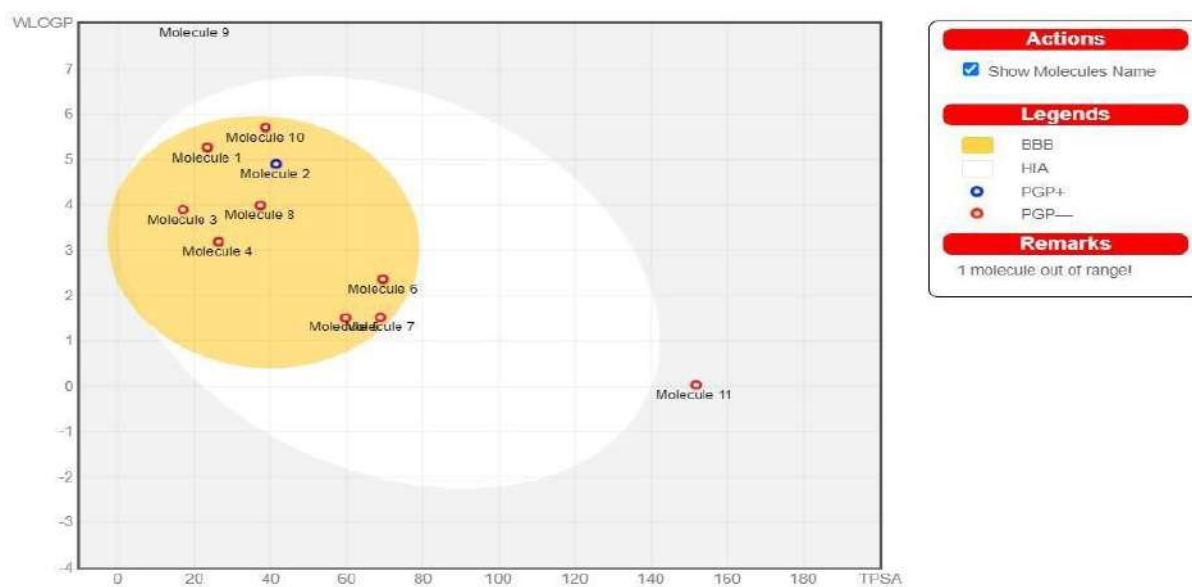


Fig no. 4. Combined Boiled Egg Diagram

Table no. 4. Name of molecules contained in Boiled Egg Diagram

MOLECULE NUMBER	MOLECULE NAME
1	Solanidine
2	Solasodine
3	Solavetivone
4	Solafuranone
5	Scopoletin
6	N-p-trans-Coumaroyltyramine
7	Isofraxidin
8	Lauric acid
9	β -sitosterol
10	Diosgenin
11	Acetazolamide

BOILED means **B**rain **O**r **I**ntestina**L** **E**stimate**D** permeation predictive model. The boiled egg diagram shows two regions white region and yellow region.

The white region is the physicochemical space of molecules with highest probability of being absorbed by the gastrointestinal tract, and the yellow region (yolk) is the physicochemical space of molecules with highest probability to permeate to the brain.

In addition, the points are coloured in blue if predicted as actively effluxed by P-gp (PGP+) and in red if predicted as non-substrate of P-gp (PGP-).

4. CONCLUSION

In this study, we have carried out an *in-silico* screening of the phytoconstituents of *Solanum indicum* plant. This study demonstrated the sixteen compounds from *Solanum indicum* plant, (Solanidine, Solasodine, Solavetivone, Solafuranone, Scopoletin, N-p-trans-Coumaroyltyramine, Isofraxidin, Lauric acid, β -sitosterol, Diosgenin). The selected phytocompounds showed docking scores ranging from -10.0 to -3.7 kcal/mol in 6O4L. Among all, Solafuranone and Isofraxidin gave the highest binding energy (-7.8 kcal/mol) and (-6.1 kcal/mol) in complex with 6O4L, whereas the reference compound, Acetazolamide showed a docking score with a binding energy of -5.1 kcal/mol. Furthermore, these ligands exhibited good ADMET properties. To summarize, phytoconstituents present in *Solanum indicum* possess strong effects against 6O4L and could be further evaluated for their antiepileptic effect, as well as for the development of alternative drugs with fewer side effects for the treatment of epilepsy.

REFERENCES

1. Saxena HO, Parihar S, Pawar G, Choubey SK, Dhar P. Phytochemical screening and HPTLC fingerprinting of different parts of *Solanum indicum* L.: A dashmool species.

- Journal of Pharmacognosy and Phytochemistry. 2021;10(1):1935-41.
2. Bahgat A, Abdel-Aziz H, Raafat M, Mahdy A, El-Khatib AS, Ismail A, Khayyal MT. Solanum indicum ssp. distichum extract is effective against l-NAME-induced hypertension in rats. *Fundamental & clinical pharmacology*. 2008 Dec;22(6):693-9.
 3. Morris GM, Huey R, Lindstrom W, Sanner MF, Belew RK, Goodsell DS, Olson AJ. AutoDock4 and AutoDockTools4: Automated docking with selective receptor flexibility. *Journal of computational chemistry*. 2009 Dec;30(16):2785-91.
 4. Pettersen EF, Goddard TD, Huang CC, Couch GS, Greenblatt DM, Meng EC, Ferrin TE. UCSF Chimera— a visualization system for exploratory research and analysis. *Journal of computational chemistry*. 2004 Oct;25(13):1605-12.
 5. Liles JT, Corkey BK, Notte GT, Budas GR, Lansdon EB, Hinojosa-Kirschenbaum F, Badal SS, Lee M, Schultz BE, Wise S, Pendem S. ASK1 contributes to fibrosis and dysfunction in models of kidney disease. *The Journal of Clinical Investigation*. 2018 Oct 1;128(10):4485-500.
 6. Verdonk ML, Cole JC, Hartshorn MJ, Murray CW, Taylor RD. Improved protein–ligand docking using GOLD. *Proteins: Structure, Function, and Bioinformatics*. 2003 Sep;52(4):609-23.
 7. Leach AR, Shoichet BK, Peishoff CE. Prediction of protein– ligand interactions. Docking and scoring: successes and gaps. *Journal of medicinal chemistry*. 2006 Oct 5;49(20):5851-5.
 8. SAMANT L, Javle V. Comparative docking analysis of rational drugs against COVID-19 main protease.
 9. Arora S, Lohiya G, Moharir K, Shah S, Yende S. Identification of potential flavonoid inhibitors of the SARS-CoV-2 main protease 6YNQ: a molecular docking study. *Digital Chinese Medicine*. 2020 Dec 1;3(4):239-48.
 10. Shah S, Chaple D, Arora S, Yende S, Moharir K, Lohiya G. Exploring the active constituents of Oroxyllum indicum in intervention of novel coronavirus (COVID-19) based on molecular docking method. *Network Modeling Analysis in Health Informatics and Bioinformatics*. 2021 Dec;10:1-2.
 11. Kaloni D, Chakraborty D, Tiwari A, Biswas S. In silico studies on the phytochemical components of *Murraya koenigii* targeting TNF- α in rheumatoid arthritis. *Journal of Herbal Medicine*. 2020 Dec 1;24:100396.
 12. Joshi T, Sharma P, Joshi T, Chandra S. In silico screening of anti-inflammatory compounds from Lichen by targeting cyclooxygenase-2. *Journal of Biomolecular Structure and Dynamics*. 2020 Aug 12;38(12):3544-62.
 13. Nisha CM, Kumar A, Vimal A, Bai BM, Pal D, Kumar A. Docking and ADMET prediction of few GSK- 3 inhibitors divulges 6-bromoindirubin-3-oxime as a potential inhibitor. *Journal of Molecular Graphics and modelling*. 2016 Apr 1;65:100-7.
 14. Tsujimura S, Tanaka Y. Disease control by regulation of P-glycoprotein on lymphocytes in patients with rheumatoid arthritis. *World journal of experimental medicine*. 2015 Nov 11;5(4):225.

33

Deep Discoveries in Chemistry: Unraveling the Mysteries at the Molecular Level

Dr. Prashant R. Mahalle*

Assistant Prof. and Head, Department of Chemistry
Late B. S. Arts, Prof. N. G. Science & A. G. Commerce College, Sakharherda
Email: prashantmahalle2014@gmail.com

Abstract:

This research article delves into the profound discoveries and advancements in the field of chemistry, exploring breakthroughs that have unraveled the mysteries at the molecular level. From the elucidation of complex chemical reactions to the design of novel materials with unprecedented properties, these deep discoveries have significantly impacted various scientific disciplines and technological applications. This article provides an overview of key developments, showcasing the depth and breadth of contemporary research in chemistry.

Key Words: Chemistry Discoveries, Molecular-Level Understanding, Sustainable Practices, Environmental Chemistry, Bottom-Up Nanofabrication etc.

Introduction:

Deep discoveries in science, especially those at the molecular level in fields such as chemistry, play a crucial role in advancing scientific knowledge and driving technological innovation. Deep discoveries provide a fundamental understanding of the underlying principles governing natural phenomena. This knowledge serves as the basis for developing theories and frameworks that explain complex processes at a molecular level¹. Scientific breakthroughs often translate into technological innovations. Discoveries at the molecular level can lead to the development of new materials, processes, and technologies with applications ranging from medicine and electronics to energy and environmental management. Deep discoveries stimulate curiosity² and open up new avenues for research. Discoveries in molecular biology and pharmacology contribute to the development of new drugs and therapies.

Deep discoveries in chemistry contribute to the development of green and sustainable practices. Advances at the molecular level often contribute to the convergence of technologies³. For example, discoveries in nanotechnology, which deals with materials at the nanoscale, have implications not only in material science but also in medicine, electronics, and energy storage. Deep discoveries have the potential to revolutionize entire industries. For example, advancements in molecular electronics may lead to the development of smaller, faster, and more efficient electronic devices, transforming the semiconductor industry. In summary, deep discoveries in science, particularly at the molecular level, are instrumental in shaping the scientific landscape and driving technological progress. They provide the foundation for innovations that have far-reaching implications across diverse fields, contributing to the betterment of society and the advancement of human knowledge.

Objectives and Materials and Methods:

Several discoveries in the field of chemistry have challenged traditional understanding, leading to paradigm shifts and opening new avenues for synthesis. Here are a few notable examples:

1. Molecular Machines and Nanotechnology: The development of molecular machines, such as synthetic molecular motors and switches, challenges traditional notions of static molecular

structures. Researchers have created nanoscale machines capable of controlled movement, enabling potential applications in drug delivery, nanoelectronics, and other fields.

2. Metathesis Reaction: The discovery of metathesis reactions, particularly the development of olefin metathesis by Grubbs⁴, Schrock, and Chauvin, challenged traditional thinking about the limitations of organic synthesis. This groundbreaking discovery provided a powerful tool for creating carbon-carbon double bonds in a controlled manner, revolutionizing the synthesis of complex organic molecules.

3. Click Chemistry: Click chemistry, introduced by K. Barry Sharpless and others, represents a set of highly efficient and selective reactions that challenge traditional synthesis methods. These reactions, characterized by their reliability and simplicity, have found widespread use in various applications, including drug discovery and materials science⁵.

4. Molecular Electronics: The field of molecular electronics challenges traditional semiconductor technology by exploring the use of individual molecules as electronic components. Researchers aim to create electronic devices at the molecular scale, potentially leading to smaller, faster, and more energy-efficient electronics.

5. Green Chemistry Principles: The emergence of green chemistry⁶ challenged traditional chemical practices by emphasizing the importance of designing environmentally friendly processes. This approach considers the environmental impact at every stage of chemical production, leading to the development of more sustainable and less toxic chemical syntheses.

6. C–H Activation: Traditional organic synthesis often involves functionalizing carbon-hydrogen (C–H) bonds, which were once considered unreactive. Recent advancements in C–H activation chemistry challenge this convention, allowing chemists to directly functionalize C–H bonds, streamlining synthetic routes and reducing the number of steps required for complex molecule synthesis.

7. Supramolecular Chemistry: Supramolecular chemistry challenges traditional views by focusing on non-covalent interactions to create complex, hierarchical structures. The field explores the assembly of molecules into larger, functional structures, leading to applications in materials science, drug delivery⁷, and catalysis.

8. Chemoselective Reactions: Discoveries in chemoselective reactions challenge traditional chemical methods by enabling the selective modification of one functional group in the presence of others. This has profound implications in the synthesis of complex molecules, where multiple functional groups may be present.

9. Metal-Organic Frameworks (MOFs): The development of metal-organic frameworks⁸ challenges traditional notions of solid-state chemistry. MOFs are porous materials with high surface areas, and their design and synthesis have opened up new possibilities for gas storage, catalysis, and separation processes.

10. Directed Evolution of Enzymes: The directed evolution of enzymes challenges the traditional concept that enzymes have fixed structures and functions. Through directed evolution, researchers can engineer enzymes with enhanced or entirely new functionalities, leading to applications in pharmaceuticals, biofuels, and more.

These examples illustrate how breakthrough discoveries in chemistry have questioned established norms, prompting researchers to explore novel avenues for synthesis and innovation. These paradigm shifts contribute to the continuous evolution and advancement of the field.

Conclusion:

From the above points of informative aspects, deep discoveries represent a journey into the unknown, reshaping our understanding of the molecular world and propelling technological advancements. They underscore the dynamic nature of science, where each revelation not only expands our knowledge but also sparks innovation that has far-reaching consequences for society. As we continue to unravel the mysteries at the molecular level, the transformative impact on both scientific understanding and technological applications will undoubtedly persist, driving the evolution of science and technology.

References:

1. Cramer, R. E., & Truhlar, D. G. (2009). A universal approach to solvation modeling. *Accounts of Chemical Research*, 42(6), 841-850. DOI: 10.1021/ar800249u.
2. Whitesides, G. M. (2015). Is the focus of most chemistry journals too narrow? *ACS Central Science*, 1(1), 16-18. DOI: 10.1021/acscentsci.5b00029.
3. Nørskov, J. K., Bligaard, T., Rossmeisl, J., & Christensen, C. H. (2009). Towards the computational design of solid catalysts. *Nature Chemistry*, 1(1), 37-46. DOI: 10.1038/nchem.121.
4. Grubbs, R. H. (2003). *Handbook of metathesis*, Wiley.
5. Chhowalla, M., Shin, H. S., Eda, G., Li, L. J., Loh, K. P., & Zhang, H. (2013). The chemistry of two-dimensional layered transition metal dichalcogenide nanosheets. *Nature Chemistry*, 5(4), 263-275. DOI: 10.1038/nchem.1589.
6. Anastas, P. T., & Warner, J. C. (1998). *Green chemistry: Theory and practice*. Oxford University Press.
7. MacArthur, E. H., & Warren, W. S. (2003). Ultrashort pulse lasers in medicine. *Lasers in Surgery and Medicine*, 32(4), 283-305. DOI: 10.1002/lsm.10150.
8. Yaghi, O. M., & Li, H. (1995). Hydrothermal synthesis of a metal-organic framework containing large rectangular channels. *Journal of the American Chemical Society*, 117(34), 10401-10402. DOI: 10.1021/ja00141a008.

Synthesis, Characterization of (3-Chloro-benzylidene) – (4-Phenyl-thiazol-2-yl) amine and Studied their antioxidant Activity

Ghodile R.D¹, Chaudhari P.S.², Dharamkar R. R³.

¹ Department of Chemistry, S.P.M. Science & Gilani Arts Commerce College, Ghatanji Dist:- Yavatmal-445301 India Email: pravinghodile01@gmail.com

² Department of Chemistry Vitthal Rukhmini College Savana Ta-Mahagaon Dist- Yavatmal (MS) India

³ Department of Chemistry, G. S. Science, Arts, & Commerce College Khamgaon Dist. Buldhana (MS) India

Abstract -

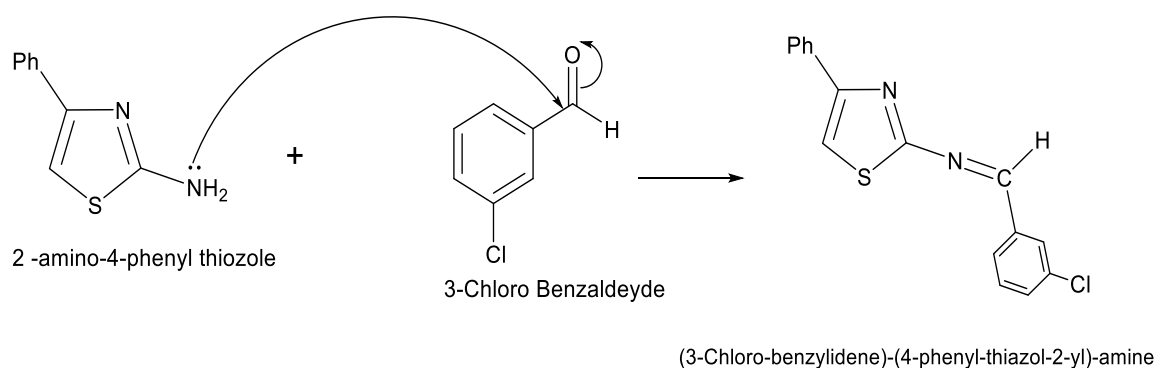
In the current study, substituted aromatic aldehydes (2a-c) were combined with 2- amino-4-phenyl thiazole to create a series of 4-phenyl-thiazolyl substituted Schiff bases (3a-c) derivatives. The IR and ¹H-NMR of all the produced compounds validated their structures and its antibacterial activity was examined. All the title compounds were screened for their antibacterial activity. Most of the compounds exhibited moderate antimicrobial activity.

Keywords: Schiff's base; Aromatic Aldehydes; 3-Chloro-benzylidene) – (4-Phenyl-thiazol-2-yl) amine, Potassium ferricyanide.

Introduction-

In pharmaceutical chemistry, thiazole derivatives have been extremely important. Thiazole have a wide variety of pharmacological properties, including antimicrobial¹⁻⁴, analgesic⁶⁻⁷, anticonvulsant⁸⁻⁹, and antioxidant¹⁰, hypolipidemic¹¹, anti HIV-1¹²⁻¹³, adenosine receptor antagonist¹⁴⁻¹⁵ and osteoporosis inhibitor¹⁶. For the creation of antimalarial drugs, Schiff bases have proven to be intriguing moieties¹⁷⁻¹⁸. As potential antibacterial agents, Schiff bases have been mentioned¹⁹⁻²¹. It is imperative to find and create more powerful antifungal medicines, and several Schiff bases are well-known to be effective ones²².

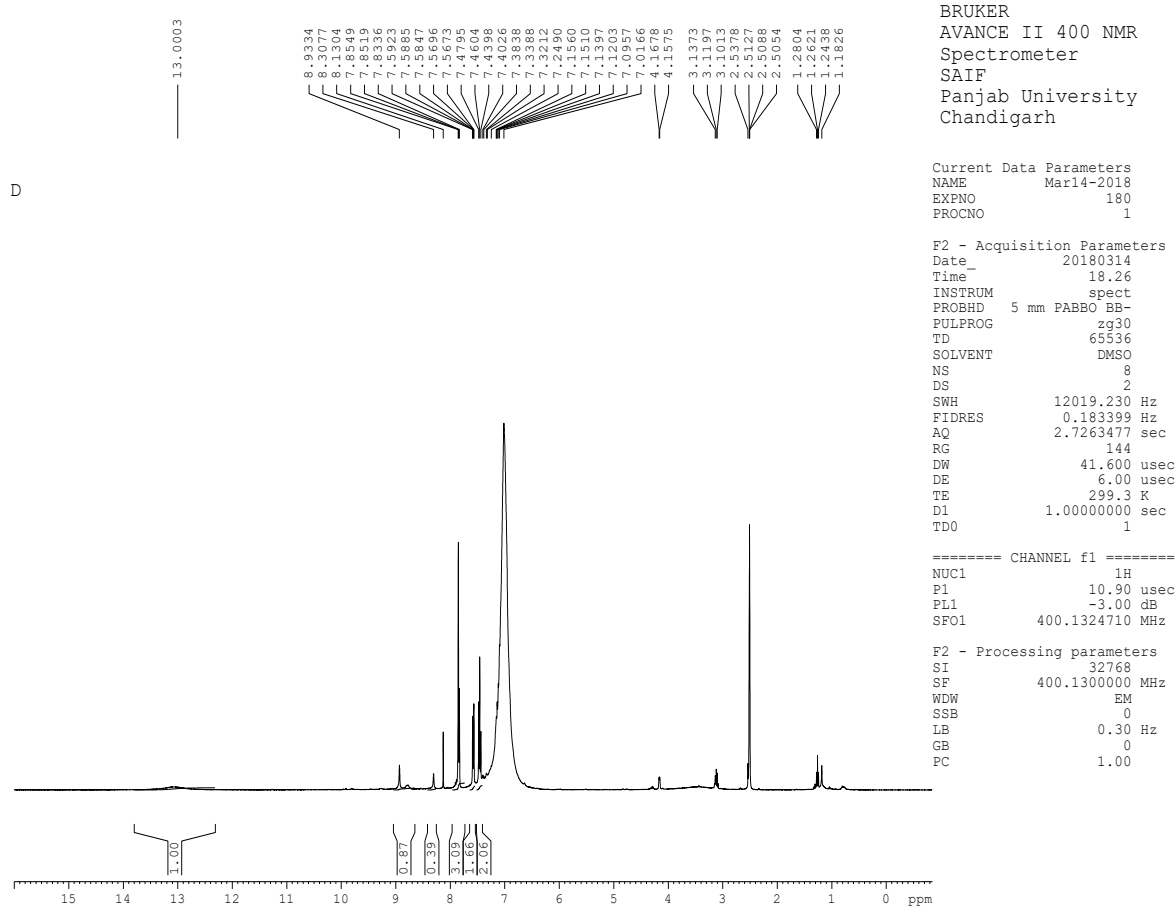
Reaction scheme



Experimental Section

General Conditions: Melting points were discovered using open capillary tubes and are uncorrected. Iodine spotting and TLC were applied to the silica gel-G surface. Nicolet 5ZDXFT-IR spectrometers in the KBr phase and Bruker WP 200 and 500 SY spectrometers in the ¹H NMR phase were used to record the IR spectra. Preparation of [(3-chloro-benzylidene)-4-phenyl-thiazole-2-yl)-amine: general technique (3a) In the presence of HCl, (0.001mole) 2- amino 4- phenyl thiazole and 0.70gm of 3- chlorobenzaldehyde were refluxed for three to four hours. The product, M.P.-150-154⁰C, was obtained from the resultant solid after it had been filtered, cleaned, and recrystallized from ethanol. 3a: ¹HNMR: 2.6 (s,1H, CH3), 7.2-8.7 (m, 10H, Ar-H), IR (KBr): 1575 cm⁻¹ (C=N)

IR Data



Sr. No.	Frequency in cm^{-1}	Assignment	Literature value cm^{-1}
1	3194.26	Ar -H	3300-2900
2	1608.70	C=N stretching	1640-1690
3	1473.68	C=C stretching	1400-1500

Antioxidant

Ferric reducing antioxidant power assay

Reducing power assay method for determination of antioxidant activity/ potential of samples

Procedure:-

Different concentration of the drug (10-50ug/ml) was added to 2.5 ml of 0.2M sodium phosphate buffer (pH 6.6) & @.5ml of 1% potassium ferricyanide [K₃Fe(CN)₆] solution. The reaction mixture was vortexed well & then incubated at 50⁰ C for 20 min using vortex shaker. At the end of the incubation , 2.5 ml of 10% trichloacetic acid was added to the mixture and centrifuged at 3,000 rpm for 10min. The supernatant (2.5ml) was mixed with 2.5 ml of deionized water & 0.5ml of 0.1% ferric chloride. The coloured solution was read at 700nm against the blank with reference to standard using UV Spectrophotometer. Here, ascorbic acid was used as a reference standard.

The percentage of radical scavenging (%) was calculated by the following formula:

$$\% \text{ Free radical scavenging activity} = A_c - A_s / A_c \times 100$$

Where , A_c = Absorbance of control at 720 nm

A_s = Absorbance of sample

The concentration of sample required to scavenge 50% of the DPPH free radical (IC₅₀) was determined from the curve of percent inhibitions plotted against the respective concentration.

Experimental

Absorbance should increase with increase in concentration. Results confirm the reducing power of samples which increased with increasing concentration. Higher value absorbance of the reaction mixture indicated greater reducing power. The reducing power was found to be in order Br>NO₂.

Table 1 Ferric Reducing Antioxidant Power Assay

Standard Observation - (Ascorbic acid) (720nm)

Concentration(ug/ml)	Absorbance 1	Absorbance 2	Absorbance 3
10ug/ml	0.002	0.006	0.061
20ug/ml	0.395	0.251	0.029
30ug/ml	0.941	0.775	0.499
40ug/ml	1.451	1.350	1.036
50ug/ml	2.000	2.000	2.000

Control Absorbance - 0.812 (720nm)

Sample Observation- (720nm)

Formula –

$$\text{Scavenged}(\%) = (A_{\text{cont}} - A_{\text{test}}) / (A_{\text{cont}}) \times 100$$

Table2 (% Scavenged of DPPH free radical)

Sample name	Concentration	Absorbance	%Scavenged
4a (H)	a) 30ug/ml	0.121	72.1 %
	b) 50ug/ml	0.305	
4b (OCH ₃)	c) 30ug/ml	0.213	68.2 %
	d) 50ug/ml	0.504	
4c (NO ₂)	a) 30ug/ml	0.068	62.9%
	50ug/ml	0.463	

4d (Br)	e) 30ug/ml	0.171	17.1%
	f) 50ug/ml	0.629	
4e (Cl)	a) 30ug/ml	0.058	21.2%
	b) 50ug/ml	0.102	

Results and Discussion

Several five member aromatic systems having three hetero atoms at symmetrical position 1,3,4-thiadiazole had been studied because of their interesting physiological properties. Specifically substituted benzaldehyde or naphthaldehyde were combined with 2-amino-5-diethylamino-pentane in an equal amount of methanol to produce the desired Schiff-base phenols or Schiff base naphthalene ligands for evaluation ¹⁹. Furthermore, by reducing their corresponding Schiff-base counterparts with KBH₄ at 80°C for 3 hours, substituted amine phenol or amine naphthalene ligands were also produced ²⁰.

All compounds underwent standard analytical procedure purification and characterization. The spectral and analytical data for digits 1 through 7 agreed with the suggested formulation. By measuring the incorporation of 3 H hypoxanthine, we assessed 1-7's capacity to prevent the formation of trophozoites in intraerythrocytic culture [21]. A more accurate way to quantify parasite development is through the inhibition of hypoxanthine incorporation, which correlates well with direct blood smear counts. Unfortunately, neither the CQ-sensitive (HB3) nor the CQ-resistant (Dd2) strains were significantly affected by compounds 1, 2, 3, 4, and 6. The moderate half-maximal inhibitory concentration (IC₅₀) values for the active compounds 5 and 7 against CQ-sensitive lines, respectively, were 5.53 and 6.38 M. However, compound 7 was found to be twice as effective as compound 5 against CQ-resistant Dd2 lines (IC₅₀, 3.5 M for compound 5; 1.7 M for compound 7).

The structural differences of compounds 5 and 7 may be responsible for their varied biological actions. The quinoline ring of the CQ, which lacks chlorine at position 7 and the quinonyl basic nitrogen, has a simple substituted aromatic ring in position 5, but the quinoline ring of the 7 contains a naphthalene ring. Furthermore, it has been demonstrated previously that nitrogen atoms of side chain in chloroquine and aromatic ring assist in accumulation of the drug within the digestive vacuole of the parasite (Vydac) employing an eluent mixture of methanol and water (100% water for first 5 minutes, followed by a change to 50 : 50 (Water : MeOH) for the next 5-20 minutes, and finally 100% MeOH for the next 20-25 minutes). The retention times (Rt) are given for selected compounds.

Absorbance should increase with increase in concentration. Results confirm the reducing power of samples which increased with increasing concentration. Higher value absorbance of the reaction mixture indicated greater reducing power. The reducing power was found to be in order Br>NO₂.

Acknowledgment:

The Authors are very thankful to the Department of Chemistry S. P. M. Science and Gilani Arts, Commerce College Ghatanji and Shri Shivaji Science College Amravati for provide the necessary facilities in the laboratory. Words of gratitude are also expressed for SAIF/RSIC Chandigarh for IR and NMR spectral data.

References:

1. P M Bonilla, A P Cardena, E Q Marmol, J L Tellez & G L M Rejon, *Heteroatom. Chem.*, 17(2006)254.
2. K A Parmar, B G Suthar & S. Parajapati, *Bull. Korean. Chem. Soc.*, 31 (2010) 793.
3. N C Desai, N B Bhatt, H C Somani, & A R Trivedi, *Eur. J. Med. Chem.*, 67 (2013).
4. A Idhayadulla, R S Kumar, A J A Naseer, *J. Mexican. Chem. Soc.*, 55 (2011) 218.

5. A K Prajapati & V P Modi, *J. Chil. Chem. Soc.*, 55 (2010) 240.
6. G Saravanan, V Alagarasamy & C R Prakash, *Asian J Res. Pharm. Sci.* 1 (2011) 134.
7. N Siddiqui & W Ahsan, *Eur. J. Med. Chem.*, 45 (2010) 1536.
8. N Siddiqui & W Ahsan, *Med. Chem. Res.*, 20 (2011) 261.
9. A Geronikaki, D H Litina, C. Chatziopoulos & G. Soloupsis, *Molecules*, 8 (2003), 472.
10. S N Mokale, P T Sanap & D B Shinde, *Eur. J. Med. Chem.*, 45(2010) 3096.
11. P Vicini, A Geronikaki, M Incerti & B. Busonera, *Bioorg. Med. Chem.*, 11 (2003) 4785.
12. W Fathalla, *Arkivoc*, 12 (2008) 245.
13. P Bhattacharya, J T Leonard & K. Roy, *Bioorg. Med. Chem.*, 13 (2005) 1159.
14. A B Scheiff, S G Yerrande & El Tayeb, *Bioorg. Med. Chem.*, 18 (2010) 2195.
15. ChSanjeeva Reddy*^a, M VaniDevia, M Sunithaa, B Kalyania & A Nagarajb. Synthesis and antibacterial activity of diheteryl substituted [1,2,4]triazolo[3,4-b][1,3,4]thiadiazoles. *Indian journal of chem.* vol. 55B May 2016 pp. 590-597.
16. PramillahSah* & VasudhaKaul. Synthesis and in-vitro biological evaluation of some quinazolin of chem. Vol. 49B Oct 2010 pp. 1406-1412.
17. Kanti Sharma* & RenukaJain. Synthesis, reaction and anthelmintic activity of 1-[benzimidazol-2-yl]-4-formyl-3-[2'(- substituted phenyl) indole-3-yl]pyrazoles. *Indian journal of chem.* Vol. 51B Oct 2012 pp. 1462-1469.
18. K. Taguchi, F. H. Westheimer, *J Org Chem*, Volume 36, Issue 11, 1971, pp. 1570-1572
19. Welles, T. *Science*, 2002, 298, 124.
20. Sharma, V. *Mini Rev. Med. Chem.*, 2005, 5, 337.
21. Ocheskey, J.; Harpstrite, S.; Oksman, A.; Goldberg, D.; Sharma, V. *Chem. Commun.*, 2005, 1622

Synthesis and Characterization of Schiff Bases Using Different Amines and their Biological Activities

Priyadarshani N Deshmukh

SSES Amt's Science College, Nagpur
preetiingole@gmail.com

Nowadays, the research field dealing with Schiff base chemistry has expanded enormously. The importance of Schiff base for bioinorganic chemistry, biomedical applications, supramolecular chemistry, catalysis and material science, separation and encapsulation processes, and formation of compounds with unusual properties and structures has been well recognized and reviewed. They also serve as a back bone for the synthesis of various heterocyclic compounds. Schiff bases have been utilized as synthons in the preparation of a number of industrial and biologically active compounds like formazans, 4-thiazolidinines, benzoxazines, and so forth, via ring closure, cycloaddition, and replacement reactions. Schiff base are organic compounds possessing azomethine group which resulted from condensation of amine with aldehyde or ketone. Schiff base derived from aromatic amine and aromatic aldehydes have a wide variety of application such as biological activity, catalytic activity and also used as ligands to obtain metal complexes because of their excellent abilities of this type of Schiff base are widely used as anticorrosion for different metals in different media. The synthesis and characterization of transition metal complexes of schiff bases containing nitrogen and oxygen donors atoms has increased manifold in the recent past. The Schiff base ligands are considered to be good chelating agents [3], Schiff bases are a special class of ligands with a variety of donor atoms exhibiting interesting coordination modes towards transition metals, and azomethine linkage is responsible for the biological activities. The Schiff bases derived from various amines have been widely investigated and find applications in biomimetic catalytic reactions, materials chemistry and industry. Schiff base complexes have also gained attention as stereo chemical models in transition metal coordination chemistry due to their structural variety.

Key Word:- Synthesis, Schiff Bases, Biological Activity.

MATERIALS AND METHOD

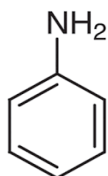
Preparation of Schiff Base by using different substituted aromatic amines with substituted aromatic benzaldehyde. Following materials and method is included.

MATERIALS

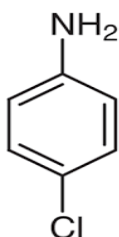
Materials Required are -

Substituted Aromatic Amines such as Aniline, p-chloro Aniline,

ANILINE-Aniline appears as a yellowish to brownish oily liquid with a musty fishy odor. melting point -6°C ; boiling point 184°C ; flash point 158°F . Denser than water (8.5 lb/gal) and slightly soluble in water. Vapours heavier than air. Toxic by skin absorption and inhalation. Produces toxic oxides of nitrogen during combustion. Used to manufacture other chemicals, especially dyes, photographic chemicals, agricultural chemicals and others.

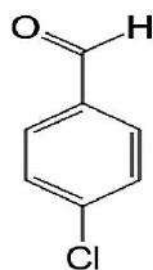


P-CHLORO ANILINE-4-Chloro aniline is a chloroaniline in which the chloro atom is para to the aniline amine group. It is a member of monochlorobenzenes. P-chloroaniline appears as a white or pale yellow solid. Melting Point is 69.5°C.



Substituted Aromatic Benzaldehydes such as 4-chloro Benzaldehyde

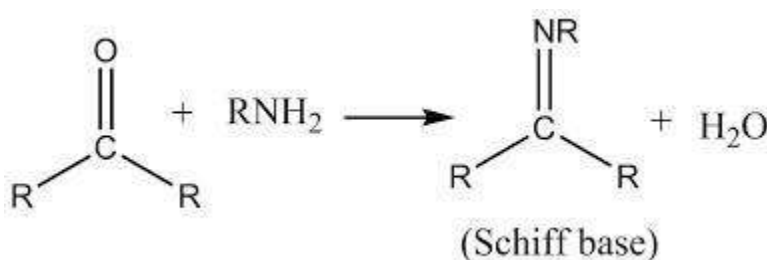
4-CHLOROBENZALDEHYD



4-Chloro Benzaldehyde appears as colourless to yellow powder or white crystalline solid. It has a pungent odour.

GENERAL METHOD FOR PREPARATION OF SCHIFF BASE-

The mixture of different substituted aromatic amines and substituted aromatic benzaldehyde was dissolved in methanol. This solution was acidified and refluxed for about 5-6 hrs. The excess of solvent was removed under pressure. The resulting compound was washed, dried and crystallized.



ANTIMICROBIAL ACTIVITY OF SCHIFF BASE

The synthesized schiff bases were screened in vitro for their antibacterial activities against *Escherichia coli* (*E.coli*) and *Bacillus subtilis* (*B. subtilis*) bacterial strains using well diffusion method. The bacterial cultures were incubated at $30 \pm 0.1^\circ\text{C}$ for 24 hours by inoculation into nutrient agar. Schiff bases were stored dry at room temperature and 3ml ethanol. Antibacterial activities of each compound were evaluated by the agar disc diffusion method. Muller hinton agar media (15 cm^3) kept at 45°C was poured in the petri dishes and allowed to solidify poured petri plates were streaked with culture media wells formed prepared schiff bases ($100\mu\text{l}$) were applied on the solid agar media by pressing tightly. The petri plates were placed at 37°C for 24 hours. At the end of period the inhibition zones formed on media were measured with zone reader millimeters.

<u>SAMPLE</u>	Conc. ($\mu\text{g/ml}$)	GRAM POSITIVE <i>E. coli</i>	GRAM NEGATIVE <i>B. subtilis</i>
N-(4-CHLOROBENZYLIDENE ANILINE) (1C)	100 μL	10mm	12mm
	100 μl	-	13mm
N-(4-CHLORO BENZYLIDENE)-4-CHLORO ANILINE (2C)	100 μl	10mm	16mm
	100 μl	-	14mm

Antibacterial activities against Schiff compound at concentration 100 $\mu\text{l/ml}$.

REFERENCES

1. Pouralimardan, O; Chamayou, A. C; Janiak, C; Monfared, H. H, Inorg. Chim.Act. 360,2007, 1599.
2. Krishnapriya, K. R.; Kandaswamy, M.; Polyhedron, 2005, 24, 113.
3. ooyseena, I. N.; Maikooa, S.; Akermana, M. P.; Xulua, B.; Munro, O. J. Coord.Chem., 2013, 66(20), 3673.
4. Chandra, S; Jain, D; Sharma, A. K; Sharma, P, Molecules 2009, 14, 174.
5. Sinha, D.; Tiwari, A. K; Singh, S; Shukla, G; Mishra, P; Chandra, H.; Mishra, A. K. Eur. J. Med. Chem. 2008, 43, 160.
6. Ansary, E.; Soliman, A. L.; Sherif, A.A.; Ezzat, J. A. Synth. React. Inorg.MetOrg.Chem.,2002,32(7).1301.
7. Celik,C.;Tumer,M.;Serin,S.Synth.React.Inorg. Met-Org.Chem.,2002,32(10)1839.
8. Biswas,C.;Drew,M.G.B.;Figuerola,V.;GomezCoca,S.;Ruiz,E.;Tangoulis,V.;Ghos h,A.; Inorg.Chim.Act.,2010,363,846.
9. Schiff,H.Justus Liebig's Ann. Chem.1864,131,118.
10. R.HernandezMolina,A.Medros,ComprehensiveCoordinationChemistry II,2003,411-446.
11. Patai S. The Chemistry of the carbonnitrogen double bond, John Wiley & Sons Ltd., London,1970.
12. Arora K. and Harma K. P. Synth. React. Inorg. Met.-Org. Chem. 2003, 32, 913.
13. Nimitsirwat, N.; Vernon, C. J Am Chem Soc 2004, 32,126.
14. Mirkin, M.V. and Bard, A.J. J. Anal. Chem. 1991, 63, 532.
15. Kratz, F.; Beyer, U.; Schutte, M. T. Crit. Rev. Ther. Drug 1999, 16, 245.
16. Saito, H.; Hoffman, A. S.; Ogawa, H. I. J. Bioact. Compat. Polym. 2007, 22, 589
17. Dhar DN, Taploo CL. J Sci Ind Res. 1982, 41, 501.
18. Przybylski P, Huczynski A, Pyta K, Bartl, B. Curr. Org. Chem. 2009, 13,124.

36

Physico-Chemical Assessment of Soil Sample in Jarud Region in Amravati District of Maharashtra (India)**¹Dr. Priyanka U. Belsare and ²Ku Tejashri M. Ghotkar.**¹Department of Chemistry, Mahatma Fule Arts, Commerce and Sitaramji Chaudhari Science Mahavidyalaya, Warud. Dist. Amravati-444906 (M.S.) India.²Department of Chemistry, Art's and Commerce College, Jarud. Dist. Amravati (M.S.) India.Corresponding author: priyankabelsare45@gmail.com¹**ABSTRACT**

Soil is a natural body of mineral and organic material differentiated into horizons, which differ among themselves as well as from underlying materials in their morphology, physical make-up, chemical composition and biological characteristics. In the present research work, studies on soils with physical properties, chemical properties and micronutrients of soils have been done. Soil samples were collected from two different locations covering Jarud, in Warud Tahsil in Amravati District (Maharashtra) India. The soil parameters like soil colour, moisture, pH, Carbon, Nitrogen, Copper, Potassium, Phosphorous, Zinc, Boron, Copper and Sulphur content, were analyzed in the month of March 2022. The values of pH indicated that all samples of the soils are alkaline, all samples were containing moderate amount of available micronutrients.

Keywords: Physico-Chemical analysis, Parameters, Jarud Village, Plants Nutrients.

INTRODUCTION

To improve soil, plant health and soil balance to optimize production, it's important to identify the soil's biological, mineral, chemical and physical requirements. When evaluating the soil analysis, we look for synergies and approach mineral and microbe plant and pest management holistically to provide the formula for nutrient, trace elements and biological inputs to achieve true soil balance. The soil analysis report provides the information necessary to set nutrient application targets, which are used to calculate manure and fertilizer application rates. Test results from regular field sampling (particularly from benchmark sites) allow monitoring and detection of changes in soil parameters (e.g., nutrients, pH, and salinity) with time.

Soil analysis provides us the background knowledge on soil available nutrient status along with some physico-chemical and biological properties; that we need in order to take specific decisions on balanced and integrated nutrient management for healthy soils and crops. The quality and health of soil determine agricultural sustainability and environmental quality which jointly determines plant, animal and human health. The status of available micronutrients in soils and their relationship with various physico-chemical properties have been attempted by several investigators (1-2). Considerable research work has been done regarding the study of Nutrients and Physico-Chemical assessment of various types of soil in Maharashtra as well as in India (3-4) but the investigation of nutrients and parameters of soil of Jarud village in Amravati district in Maharashtra.

Physico-chemical characteristics of some samples of soil from some farms of nearby villages of Kannad taluka, Dist. Aurangabad (5). Abhishek Jangir et. al. (6) evaluates the major and micronutrient status of Kelapur block, Yavatmal district, Maharashtra. Wodaje Addis et. al. (7) carried out assessment of some selected physicochemical parameters in soil samples collected from four agricultural areas of East Gojjam Zone (Debre Markos, Dejen, Bichena

and Debre (Werk), Ethiopia. Perveen et. al. (8) has studied micronutrient status of soils and their relationship with various physico-chemical properties. Khadke et. al. (9) reported soil analysis and its environmental impact on Nanded city of Maharashtra State. The impacts of industrial pollution on the ground water soil and plant have also been reported in our country and abroad (10). Investigation of some parameter and Nutrients from Soil samples of Rice field by Jadhav et.al. (11). Geeta Tewari et. al. (12) carried out the physico-chemical properties of soils from different land use systems viz. agriculture, oliculture and two dominant forest types.

R. Zornoza et al (13) studied the Soil quality (SQ) assessment has long been a challenging issue, since soils present high variability in properties and functions. K. Senthilarasan et. al. (14) worked on soil analysis to study physical properties and micronutrients of soils. Soil samples were collected from five different locations covering Nagapattinam district (south) in tamilnadu. Joshi et al. concluded that India Soil salinity greatly affects growth and development of vegetation (15), but the investigation of nutrients and parameters of Soil of Jarud village in Warud Tahsil of Amravati district in Maharashtra, India was still lacking.

EXPERIMENTAL

Study Area

Mauja Jarud (part2) is a small village in Warud Tahsil of Amravati District (Maharashtra State). This area is well known for orange, cotton and Toor. The sources of water for this area are of well. Relative to its geographical location, the study area enjoys a tropical type of climate.

Collection of Samples

Soil samples were collected randomly at 0 to 15 cm and 15 to 30 cm depths with five plots (field), five samples from each plot (field) respectively, in well sterilized polythene pouches. Soil sample were collected from following Farmers fields.

1) Sample 1 (TMG-1) was collected from Mr. Manikrao Sitaramji Ghotkar field.

2) Sample 2 (TMG-2) was collected from Mr. Raju Devrao dathe field.

Table-1: Nutrients and Physico-Chemical assessment of Soil Samples.

Analysis of Parameters			
Sr.No.	Parameters	TMG-1	TMG-2
1	Colour	Black	Whitish Black
2	pH	7.41	7.42
3	Organic Carbon (%)	0.46	0.45
4	Nitrogen	210	200
5	Phosphorous (kg/hect.)	28	31
6	Potassium (kg/hect.)	340	350
7	Mn (ml/gm/kg)	8	7
8	Fe (ml/gm/kg)	39	39
9	Zinc (ml/gm/kg)	3.1	3.1
10	Boron	1.5	1.5
11	Copper	8	9
12	Sulphur	59	59
13	Salinity	0.2	0.2

Determination of Physical Parameters

Reagents used for this research work were AR grade and chemicals other than reagent are LR grade manufactured by S.D. fine, LOBA and Merck. The soil samples were dried for about 24 hr. and grinded more finely. In this work about thirteen physico-chemical parameters and nutrients of two soil samples were determined and results were also recorded. During collection, temperature of the sample was recorded.

Following methods were used for estimation of various parameters are:

- i. Determination of Moisture: by Weighting Method.
- ii. Determination of pH: by Digital pH Meter
- iii. Determination of Organic Carbon: by Titration Method
- iv. Determination of Copper (Cu): by Atomic Adsorption Spectroscopy.
- v. Determination of Nitrogen (N): by Titration Method
- vi. Determination of Phosphorous (P): by Titration Method
- vii. Determination of Potassium (K): by Flame Photometry
- viii. Determination of Color of Soil: by Viewing soil

RESULTS AND DISCUSSION

Colour

The soil sample TMG-1 was black in colour and sample TMG-2 was whitish black in colour.

Moisture

Moisture content value ranges from 1% - 4%. It is clear from the result that Soil sample TMG-1 and TMG-2 has 2.5 and 3.7% moisture respectively.

pH

pH was medium quantity in the ranges 7.41 to 7.42. To dig drains, to make out flows, sowing green crops, cow manure to bury plant wastes, to supply necessary amount of water, use of gypsum is need.

Organic carbon

Organic carbon contents were recorded in the range 0.46-0.45 %. The soil sample TMG-1 and TMG-2 has medium organic carbon.

Nitrogen

Available Nitrogen quantity ranged from 200– 210 Kg/hect. The soil sample TMG-1 and TMG-2 has less Nitrogen content.

Phosphorous

Available Phosphorous was medium quantity ranged from 28-31kg/hect. The soil sample TMG-1 have less Phosphorous as compared to TMG-2.

Potassium

Available Potassium quantity ranged from 340-350 kg/hect. The soil sample observed value for potassium was medium.

Zinc

The Zinc was less in quantity in both TMG-1 and TMG-2 i.e 3.1 ml/kg.

Copper

Copper content in soil sample ranges from 8-9. It has been seen that in soil sample TMG-1 and TMG-2 has approximate quantity of copper.

Boron

It has been seen that in soil sample TMG-1 and TMG-2 has 1.5 ml/gm/kg of Boron. Both the soil sample contains approximate Boron quantity.

Sulphur

It has been seen that in soil sample TMG-1 and TMG-2 has 59 ml/gm/kg of Sulphur. Both the soil sample contains approximate Sulphur quantity.

CONCLUSION

In the soil sample TMG-1 and TMG-2, the pH becomes middle alkali and to increase the pH of this soil suggested the use of compost manure. Then recommendation of to dig drains, to make out flows, sowing green crops, cow manure to bury plant wastes, to supply necessary amount of water, use of gypsum. In the soil sample TMG-1 and TMG-2, Zinc becomes less, then recommendation zinc sulphate 10 kg / hectare. In the soil sample TMG-1 and TMG-2 the potassium become medium, then recommendation Potash 400gm / hectare. In the soil sample TMG-1 and TMG-2 the phosphorous is middle. To increase the crop quality phosphorous will be given through fertilizer 2000 gm /hectare. In the soil sample TMG-1 and TMG-2, Boron becomes approximate. Organic fertilizer from goat manure resulted in the highest yield per hectar in groundnut and total biomass in palm oil plant. In the soil sample TMG-1 and TMG-2 sulphur become approximate. In the soil sample TMG-1 and TMG-2 medium organic carbon and nitrogen. So, to increase more yield of crop by using carbon and nitrogen to soil in the form of compost manure.

ACKNOWLEDGEMENT

The authors are thankful to Dr. G. N. Chaudhari, Principal, Mahatma Fule Art's, Commerce and Sitaramji Chaudhari Science Mahavidyalaya, Warud, Dist. Amravati and Non-teaching staff for providing necessary laboratory facility during this work. Also thankful to Soil testing Lab, Kisan foundation Warud, Amravati for their valuable suggestions.

REFERENCES

1. **M. Kumar and A. L. Babel**, *Indian Journal of Agricultural Science*, 3, 97 (2011).
2. **Rajesh P. Ganorkar, Harshali A. Hole and Dinesh A. Pund**, *Rasayan J. Chem.*, 10(2), 429-433(2017)
3. **R. P. Ganorkar and P. G. Chinchmalatpure**, *Int. J. Chemical, Env. And Pharmaceutical Research*, 4(2&3), 46(2013).
4. **R. P. Ganorkar and N.H. Khan**, *International Journal of Chemical and Pharmaceutical Analysis*, 1(4), 190(2014).
5. **Dhananjay Vyankat Bondar** Physico-chemical analysis of soil (2022).
6. **Abhishek Jangir, R.P. Sharma, G. Tiwari, D. Vasu, S. Chattaraj, B. Dash, L.C. Malav, P. Chandran, S.K. Singh, H. Kuchankar and S. Sheikh** issn: 022-457x ,241-245, (2019)
7. **Wodaje Addis and Alemayehu Abebaw** ISSN: 2226-7522 Science, Technology and Arts Research Journal Sci Technol. Arts Res. J., (2014)
8. **S. Perveen, M. Tariq, J. K. Farmanullah and A. Hamid**, *Journal of Agriculture*, 9(5), 467, (1993).
9. **Khadke P. A., Bhosle A.B. and Yennawar V. B**, *Research Front*, 1(1) (2013)73.
10. **Maliwal, G.L. et al**, *Poll. Res.*, 23(1), (2004)169.
11. **Jadhav S.D, Sawant R.S. and Godghate A.G.**, *Res. J. Agriculture and Forestry Sci.*, 1(4) (2013)24.
12. **Geeta Tewari, Deepti Khati, Lata Rana, Poonam Yadav, Chitra Pande, Sunita Bhatt, Vinod Kumar, Neeta Joshi and Prasoon K. Joshi**, *J. Chem. Eng. Chem. Res.* Vol. 3, No. 11, 2016, pp. 1114-1118, (2016)
13. **R. Zornoza et al.** *SOIL*, Vol. 1, 173–185, (2015).
14. **K. Senthilarasan, P. Sakthivel, A. Jenifer, T. Susmitha, G. Janakiaman**, Volume 5, Issue 4, ISSN-2349-5162 (2018).
15. **V. D. Joshi, N. P. Narhari, & P. R. Rachh**, *Int. Jr. of chemical Reserch*, 1(3), 709 – 713, 2009.

Synthesis ,Characterization And Antimicrobial Study Of Co(II),Cu(II) and Fe(III) Complexes Of Substituted 4,4'- Dimethoxybenzoinhydrazones

P.M.Dahikar

Department of Chemistry

J.D.Patil Sangludkar Mahavidyalaya Daryapur, Dist.- Amravati E-mail: pushpadahikar@gmail.com

Abstract: Metal benzoinhydrazone complexes have been synthesized from substituted benzoinhydrazone were carried out by the known literature method. The structure of all the synthesized compounds were justified on the basis of chemical characterized by elemental and spectral analysis. The Physico-Chemical data suggest octahedral geometry for Co(II) & Cu(II) complexes. The synthesized complexes were screened for antimicrobial activity at a concentration of 1000µgm/ml. Which was serially diluted to determine their MIC values.

Keywords:- Metal complexe, 4,4'-Dimethoxybenzoinhydrazones, sodiumhydroxide DMF-Water(80%) medium, Antimicrobial Activity , spectral analysis.

Introduction:-

The complex formation of benzoinhydrazone with copper(II) and nickel(II) , were synthesized by scherbakov¹ .Prasad² , studied by the synthesis of Novel(II) complexes with now ligand derived from hydrazone of isoniazid and their magnetic-spectral, electrochemical, thermal and antimicrobial investigation. Benzoinhydrazone are well known for their biological activity coordination compounds containing ONS as donor atoms are reported to antimicrobial activity³. Synthesis, spectral and biological studies of Co(II), Ni(II), Zn(II), Cu(II) and Cd(II) complex with benzyl salicyladehyde acyldihydrazone were carried out by singh⁴. The simultaneous spectroscopic determination of palladium and osmium with salicyladehyde hydrazone was carried out by Ray⁵. The synthesis and structural characterization of three new co-ordination complexes of Co(II), Mn(II) and Cu(II) with N,N,O- donor hydrazine ligands were carried out by shit⁶. The coordination chemistry of hydrazones is an intensive area of study and numerous transition metal complexes of these ligands have been investigated⁷. Synthesis and characterization of some copper(II) complexes with N,S,O-donor thiohydrazones were carried out by Dey⁸. The important reactions of carbonyl with hydroxylamine, semicarbazide and various hydrazines were briefly studied in presence of strong base in ethanol medium.⁹⁻¹⁴. While furoinbenzoinoximes, furoinbenzoin hydrazone, furoinphenyl hydrazone and furoinbenzoin semicarbazone were synthesized by the interaction of furoinbenzoin with hydroxylamine hydrochloride, hydrazine hydrate, phenyl hydrazine and semicarbazide hydrochloride in presence of aqueous sodium hydroxide in DMF-Dioxane-water (80%) medium respectively.

Experimental:-

The 4,4'-Dimethoxybenzoinhydrazones was prepared by refluxing substituted benzoine with hydrazine hydrate in presence of alkaline medium for 3-4 hours this reaction mixture was kept overnight. This solid products formed were isolated and washed several times with water alcohol mixture the purity was checked by TLC paper. Their structural details were confirmed on the basis of elemental and spectral analysis. In order to Synthesize the complexes the equimolar mixture of each of the ligand(0.01M) and metal salts(0.01M) were refluxed on a water bath for 6,8 hours in presence of sodium acetate in ethanol . The reaction mixtures was kept overnight. The product formed were isolated washed several times with cold water ethanol

mixture. The characterization of synthesized complexes was made with elemental analysis, IR and UV-VIS spectra.

Result and Discussion

TABLE-1
THE METAL COMPLEXES COMPOUND, MOLECULAR WEIGHT, COLOUR AND
ELEMENTAL ANALYSIS OF VARIOUS METAL IONS

Complexes	Colour	Molecular wt	Elemental analysis Found/(calculated)%			
			C	H	N	M
4,4'-DMBH-Co(II)	Pale	682.93	55.30 (56.22)	4.93 (5.85)	8.19 (8.19)	7.71 (8.62)
4,4'-DMBH-Cu(III)	Brown	687.54	54.90 (55.84)	4.87 (5.81)	8.14 (8.14)	8.30 (9.24)
4,4'-DMBH-Fe(III)	Brown	627.84	60.24 (61.16)	4.86 (5.73)	8.91 (8.91)	7.96 (8.89)

TABLE-2

IR SPECTRAL DATA OF LIGANDS AND ITS METAL COMPLEXES

Ligands and its Complexes	$\nu(\text{O-H})$	$\nu(\text{C=N})$	$\nu(\text{C-O})$	$\nu(\text{M-O})$	$\nu(\text{M-N})$
4,4'-DMBH	3388	1634	1362	-	-
4,4'-DMBH-Co(II)	3351	1614	1308	466	578
4,4'-DMBH-Cu(II)	3327	1618	1317	520	585
4,4'-DMBH-Fe(III)	3378	1610	1249	471	565

The IR spectra of ligand shows a strong band at 1634 cm^{-1} due to (C=N) group broad band around 3388 cm^{-1} in the spectra of complexes is assignable of water. 4,4'-DMBH-Co(II) shows band at 3388 (O-H). Which decreases 3351 cm^{-1} indicating that attached to oxygen. However 1634 (C=N) significantly decrease to 1614 cm^{-1} showing linkage through azido nitrogen. The $\nu(\text{M-O})$ & $\nu(\text{M-N})$ vibration are verified to existing by the appearance of new weak bands in the spectra of complexes at 578 & 565 respectively.

TABLE-3
ELECTRONIC SPECTRAL DATA, MAGNETIC MOMENT AND LIGAND
FIELD PARAMETER OF THE METAL COMPLEXES

Complexes	μ_{eff} (B.M.)	λ_{max} (cm ⁻¹)	Dq	B	CFSE	% Cova	$(\Lambda_M)\Omega^{-1}$ Cm ² Mol ⁻¹
4,4'-DMBH-Co(II)	4.72	13604,19018, 23023	1492	0.737	205	26.03	9.5
4,4'-DMBH-Cu(II)	1.79	13698,18587, 22984	1492	0.737	205	26.29	10.8
4,4'-DMBH-Fe(III)	5.67	13888,17979, 22471	1514	0.646	346	35.04	11.4

The electronic spectrum of Co(II) complexes exhibits three bands at 13604,19018 and 23023 cm⁻¹ which may be assigned to ${}^4A_{2g} \rightarrow {}^4T_{2g}$ (F), ${}^4A_{2g} \rightarrow {}^4T_{1g}$ (F) and ${}^4A_{2g} \rightarrow {}^4T_{1g}$ (P), transition, respectively for an octahedral stereochemistry¹¹. The magnetic moment value of 4.72 B.M for Co(II) complex is consistent with octahedral geometry around metal centre. Fe(III) Complexes three bands are observed in case of Fe(III) complexes at 13888,17979,22471 cm⁻¹ which may be assigned to ${}^6A_{1g} \rightarrow {}^4T_{1g}$ (F), ${}^6A_{1g} \rightarrow {}^4T_{2g}$ (F) and ${}^6A_{1g} \rightarrow {}^4E_g$, belongs to transition respectively, indicating octahedral geometry of Fe(III) complexes¹²⁻¹³. The value of 5.67 B.M. would suggest high spin six coordination for Fe(III) complexes. The values of various ligand field parameters 10Dq, B, λ_{max} , CFSE and conductance respectively favoring in octahedral geometry for this complex.

ANTIMICROBIAL ACTIVITY OF COMPLEXES

The compounds were assayed for their antimicrobial activities¹⁴ against four test organisms E.coli, S. aureus, Ps.aeruginosa, B. subtilis at a concentration of 1000 µgm/ml by agar well technique¹⁵. Further their MIC value against these organisms were determined by serial dilution method using DMF as a solvent. The results obtained are given in table-5

TABLE-5
MIC VALUES IN µgm/ml OF COMPOUNDS

Complexes	E.coli	S.aureus	P. aeruginosa	B.Subtilis
4,4'-DMBH-Co(II)	125	250	125	125
4,4'-DMBH-Cu(III)	125	63	63	63
4,4'-DMBH-Fe(III)	125	250	125	125

On the basis of MIC values, 4,4'-DMBH-Cu(II) is found to be most effective antimicrobial agent followed by 4,4'-DMBH-Co(II) and 4,4'-DMBH-Fe(III). The enhanced antimicrobial activity in case of the compounds. 4,4'-DMBH-Cu(II) showed the lowest MIC values (i.e. 63 µg/ml) against maximum number of microorganisms.

Acknowledgement

The authors are thankful to the SAIF, CDRI, Lucknow for IR SAIF Chandigarh. Department of Physics, SGBAU, Amravati for magnetic measurements of the compounds respectively.

References

1. I.N. Shcherba, I.D. Popov, S.I. LEVCHENKOV, A.N. Kogan, A.D. Vikrishchuk, Russian J. of chem: Vol. 79, No. 4, pp. 826-832, 2009
2. S. Prasad and R.K. Agrawal, Research letters in Inorganic Chem: 10, 1-4, 2008
3. (Miss) K. Shrivastava and J.K. Mehrota, J. Ind. chem. soc., 38(12), 1015-1017, 1961
4. V.P. Singh; P. Gupta; N. Lal. Russian J. Co-ordination chem.; 34(4), 270-277, 2008
5. (Miss) Hil. RAY; B.S. Garg; R.P. Singh J. IND chem. soc. LVI, 975-976, 1979
6. S. Shit, J. Chakraborty; B. SAMANATA; A.M.Z. Salwin, V. Gramlich; S. Mitra, Struct Chem; 20, 633-642
7. S.M. Sondhi, M. Dinodia and A. Kumar, Bioorg. med. chem., 14; 4657, 2006
8. K. Dey, and K. Chakraborty, Indian J. Chem., 39A; 1140
9. A.G. Starikov, V.A. Kogan, V.V. Lukov, V.J. Minkin and R.M. Minyaev, Russian J. Co-ordination Chem., 35(8), 616-620, 2009
10. Kedar, Ph.D. Thesis S.G.A.V. Amravati.
11. D. Pavia, G. Lampman and G. Kriz, Introduction to Spectroscopy, Thomson Asia Pvt. Lit. Singapore, 3rd Ed., 2004.
12. J.C. Hegde, N.S. Raj & Balkrishna, J. Chem. Sci. III, 9(4), 2007.
13. A. Hassan, A. Fetout, M. Kamal, H.A. Shraf, Molecules, 10, 2005.
14. R.M. Silverstein, G.C. Bassler, T.C. Morrill, Spectroscopic Identification of Organic Compounds, 4th Ed., John Wiley and Sons, INC, New York.
15. S. Chandra, and Anil Kumar, J. Saudi Chem. Soc; Vol. No. 2; pp 299-309, 2007

Study of Extraction and Chemical Screening of *T. cordifolia* (Guduchi) Stem & Leaves

Ramesh Tukaram Parihar¹, S A Quazi², Shaikh Farah T³

¹Department of Chemistry, Vidnyan Mahavidyalaya Malkapur Dist. Buldhana Maharashtra-44310

²Department of Chemistry, Bapumiya Sirajoddin Patel Arts, Commerce and Science College, Pimpalgaon kale, Tq- Jalgaon Jamod, Dist-Buldhana

³Department of Botany, Bapumiya Sirajoddin Patel Arts, Commerce and Science College, Pimpalgaon kale, Tq- Jalgaon Jamod, Dist-Buldhana

Abstract:

The water & ether extracts of *T. cordifolia* Stem & leaves were prepared- the total ash found to be 6.861. The leaves show dark yellow fluorescent colour with picric acid the extracts were tested for some phytochemicals. *T. cordifolia* commonly named as "Guduchi" is known for its immense application in the treatment of various diseases in the traditional ayurvedic literature. Recently the discovery of active components from the plant and their biological function in disease control has led to active interest in the plant across the globe. Encompasses (i) the genetic diversity of the plant and (ii) active components isolated from the plant and their biological role in disease targeting. The future scope of the review remains in exploiting the biochemical and signaling pathways affected by the compounds isolated from *Tinospora* so as to enable new and effective formulation in disease eradication.

Keyword: *T. Cordifolia*, Fluorescent Test, Ether Extraction, Water Extraction, Antimicrobial activity.

INTRODUCTION:

The possibility of outbreak of severe acute respiratory syndrome (SARS) and Bird Flu Virus continuing spread of HIV/AIDS and emergence of resistant pathogenic strains against current medication compel investigators to look for new protective measure against these threats. Immune activation is an effective as well as protective approach against emerging infection disease ⁽¹⁾. *T. cordifolia* commonly known as guduchi, heart-leaved moonseed and giloya is a herbaceous vine of the family Menispermaceae, is a glabrous climbing succulent shrub. It is native to India, easily in the tropical region. It is widely used in Ayurvedic medicine in India as well as tonicizer and as a remedy for diabetes mellitus and metabolic disorders, ⁽²⁾ the fundamental role of innate immunity in host defense is becoming clearer as analysis of human genome continues to identify new genes serving innate immune function. Innate immune activations immune response antigen- specific T & B lymphocytes ^(3, 4) Cytokines play crucial roles in regulating various aspect of immune response. Among cytokines interleukin IL-12 plays a central role in co-ordinating innate and cell mediated adaptive immunity, ⁽⁵⁾ Immune stimulation can provide both prophylactic as well as postexposure protection ⁽⁶⁾. Dementia is a syndrome of failing memory and other intellectual functions with little or no disturbance in consciousness. Degeneration of the cerebral neurons is one of the commonest and vital causes for dementia with increasing age, thereby leading to deterioration in quality of life in elderly. Hence a greater research is required in early diagnosis of the condition and development of newer effective drugs to prevent or halt the progression of the disease. This is possible by basic understanding of learning and memory process ⁽⁷⁾. Medicines derived from plants have played a pivotal role in health care of ancient and modern cultures. Ayurveda, the Indian system of medicine mainly uses plant based drugs or formulations to treat various ailments including cancer. Recent surveys suggest that one in three Americans uses dietary supplements daily and the rate of usage is much higher in cancer patients, which may be up to 50% of patients treated

in cancer centers ⁽⁸⁾. Many synthetic or natural agents have been investigated in the recent past for their efficacy to protect against radiation damage. Among the natural radioprotective agents compounds, cystine, cysteamine, 5-hydroxytryptophan, 5-hydroxytryptamine, glutathione, and vitamins like A, C, and E2 have been extensively studied. Important synthetic molecules include amino-ethyl-isothiuronium bromide hydrobromide (AET), WR-272 1. However, the inherent toxicity of these agents at the radioprotective concentration warranted further search of a safer and effective radioprotector. To reduce toxicity, a strategy of combining radioprotective molecules working through different modes of action has also been attempted. Three in fact, no radioprotective agent now available, either singularly or in combination, meets all the requisites of an ideal radioprotector. Four recently several isolated plant products and crude extracts that may have a natural combination of several bio-active molecules capable of giving radioprotection through different mechanisms, have been investigated ⁽⁹⁾.

EXPERIMENTAL: - Fresh healthy leaves and stem of *T.cordifolia* were collected. They were washed thoroughly with distilled water and dried in shade for seven day followed by grinding to make powder of the same size and stored in air tight bottles.

Total Ash: About 10 g of powdered leaves & stem was accurately weighed and taken in a silica crucible, which was previously ignited and weighed. The powder was spread as a fine, even layer on the bottom of the crucible. The crucible was incinerated gradually by increasing temperature to make it dull red hot until free from carbon. The crucible was cooled and weighed. The procedure was repeated to get constant weight.

Acid Insoluble Ash: The ash obtained as described above was boiled With 25 ml of 2N HCl for five minutes. The insoluble ash was collected on an ash less filter paper m and washed with hot water. The insoluble ash was transferred into a silica crucible, ignited and weighed. The procedure was repeated to get a constant weight

Water Soluble Ash: The ash obtained as described in e determination of total ash was boiled for 5 minutes with 25 ml of water. The insoluble matter was collected on ash less filter paper and washed with hot water. The insoluble ash was transferred into silica crucible, ignited for 15 minutes, and weighed. The procedure was repeated to get a constant weight. The weight of insoluble matter was subtracted from the weight of the total ash. The difference of weight was considered as water-soluble ash the result of total ash, acid insoluble ash, water soluble ash and other physical Para meters of *T.cordifolia* leaves are summarized in Percentage of ash and Chemical Screening.

Antimicrobial Activity: Antimicrobial activity of *T.cordifolia* plant was determined against bacterial strain, salmonella typhimurium, Escherichia Coli, Staphylococcus aureus, Bacillus subtilis by well diffusion assay on agar plate. The bacterial culture were grown on nutrient broth for 24 hrs. The activity grown cultures were spread on nutrient agar plates by spread plate method well were prepared by brose sample was poured in the well. Streptomycin antibiotic is used as standard 100 mg 1 ml concentration.

WATER EXTRACTION: 10 gm of sample (*Tinospora* plant) was taken in round bottom flask. 35ml of distilled water was added. Water condenser was arranged. Refluxed for 3 hrs after complete heating the water extract was cooled. Solution was filtrated through whatman paper No. 42 Residue was dried and weight was took and water soluble compound was calculated.

ETHER EXTRACTION: 10 gm of leaves & stem sample was taken *Tinospora* plant (10 gm each) was extracted using Round bottom flask, soxhlet apparatus was arranged. The extracts

were too dried to yield crude residue. The extracts were auto-calved and stored at 5⁰c until further use. Ether soluble compound was calculated.

RESULT & DISCUSSION :In study of three crude extracts of leaves and stem of T.Condifolia have been investigatged, aqueous either and water extraction were tested for their total Fluonaid contents microbial activity performed by using assay of reducing powder of Tinospora plant.

Percentage of ash

Sr. No.	Sample (ash)	Percentage
1.	Total Ash	5.78%
2.	Water Soluble	28.03%
3.	Acid Insoluble	59.00%

Chemical Screening

Sr. No.	Chemical Screening	Water Extraction	Ether Extraction
1.	Tannins	+ve	-ve
2.	Saponins	-ve	+ve
3.	Phenols	+ve	+ve
4.	Flavonoids	-ve	-ve
5.	Alkaloids	-ve	+ve

REFERENCE:

1. P.K. Raveendra Nair, Sonia Rodriguez, Reshma Ramachandran, Arturo Alamo, Steven J. Melnick, Enrique Escalon & Pedro I, *Immune stimulating properties of a novel polysaccharide from the medicinal plant Tinospora Cordifolia*. International Immunopharmacology, 4,(2004),1645-1659.
2. P. Stanely, Mainzen Prince & Venugopal P. Menon, *Hypoglycaemic and other related actions of Tinospora conrdifolia roots in alloxan-induced diabetic rats*. Journal of Ethnopharmacology, 70,(2000) ,9-15.
3. Salah. M. EL Naggar, Botany Dept. *Pollen Morphology of Egyptian Malvaceae: Abutlion pannosum* .28,(2004),227-240.
4. Anup A. Arbat, *Pharmacognostic Studies Stem of Tinospora Plant*, BioscienceDiscovery,3 (3),(2012),317-320.
5. Survase S.A., B.P. Sarwade and D.P. Chavan *Antimicrobail Activity of various extracts of Tinospora Plant*, African Journal of Plant Science. 7 (4),(2013),128-130.
6. Walker P.S., Scharton-Kersten T., Krig A.M., Homant, Rowton E.D. & Udey M.C. at *Immunostimunity oligodeox-yucdeotide s. protective immunity and provide systemic terepy for leishmaniasi*, IL-12 and IF N - gamma depend + mechanism .96,(1999),6970-6957.
7. Ashutosh Agarwal, S. Malini, K.L. Bairy, Muddanna S.Rao. *Effect of Tinospora Cordifolia on Learning and Memory in Normal and Memory Deficit Rats*. Indian Journal of Pharmacology . 34,(2002),339-349.
8. Ganesh Chandra Jagetia and Shaival Kamalaksha Rao, *Evaluation of the Antineoplastic Activity of Guduchi (Tinospora Cordifolia) in Ehrlich Ascites Carcionma Bearing Mice*. Biol. Pharm, Bull 29,(3),(2006) ,460-166 .
9. Harish Chandra Goel, Jagadish Prasad, Surinder Singh, Ravinder Kumar Sagar, Paban Kumar Agrawala, Madhu Bala, Auran Kumar and Ruchi Dogra, *Radioprotective Potendial of an Herbal Extract of Tinospora Cordifolia*, 45, (2004), 61-68.

In-silico QSAR-based virtual screening recognition of novel anaphylactic lymphoma kinase inhibitor

Rahul D. Jawarkar^{1*}, Praveen Sharma¹, Sachin Kumar Jain¹

¹Faculty of Pharmacy, Oriental University, Indore 453555, Madhya Pradesh, India;

*Contact: rahuljawarkar@gmail.com; Mobile: +91 7385178762.

Abstract: The goal of this work is to find a new treatment option that blocks ALK tyrosine kinase. We used drug repositioning and a QSAR-based virtual screening method together in this work to find a new lead drug candidate that might be able to stop ALK tyrosine kinase receptors. Molecular docking, MD modelling, and MMGBSA studies were used to look into how the new FDA-approved drugs interact with each other. To make sure the results we got online were correct, we used the A549 lung cancer cell line to do an in vitro MTT test. The usual method suggested by the OECD is used in this study. It includes QSARINS GA-MLR models, QSAR-based virtual screening of about 1652 FDA chemicals, MD simulation, and MMGBSA analysis using Desmond software. The MTT test confirmed what was found in the computer model. The QSAR model that was made meets a number of validation standards, such as $R^2 = 0.79$, $Q^2_{\text{LOO}} = 0.78$, $Q^2_{\text{LMO}} = 0.78$, $R^2_{\text{ex}} = 0.77$, and $\text{CCC}_{\text{ex}} = 0.87$. Using QSAR-based virtual screening, we also found 12 FDA drugs that were hits in the computer. Some of these substances could be used as ALK-TK inhibitors in clinical settings because their docking values ranged from -7.10 to -10.57 kcal/mol. The A549 cancer cell line was used in the MTT test to support the results that were found in a computer programme. The QSAR-based virtual screening indicated that the new molecule ZINC000150338819 would have a pIC_{50} of 9.18 M. This drug has both wild-type and mutant ALK-TK. The molecule got a docking score of -10.57 kcal/mol and an RMSD of 1.54 Å as well. The ZINC000150338819-ALK TK complex is stable, and it includes both wild-type and mutant ALK TK. This was proven by MD modelling and MMGBSA tests that lasted 200 ns. To confirm the results from the computer simulation, the MTT test shows that Ledipasvir had more inhibition than ceritinib. It is suggested in this study that the chemical ZINC000150338819 could be used as an ALK TK inhibitor in the drug development field.

Keywords: OECD; GA-MLR; MD simulation; MMGBSA; X-Ray.

1 Introduction

In 1991, researchers discovered a membrane-bound tyrosine kinase receptor called anaplastic lymphoma kinase (ALK). Abnormal forms of ALK, such as fusion proteins, point mutations that activate ALK, and gene amplification, are found in cancer. Abnormal ALK expression is linked to the development of many types of cancer [1]. The human ALK gene is located in the chromosomal region 2p23.2p23.1. This 26-exon gene encodes the ALK protein, which is 1620 amino acids long. The full-length ALK protein has a transmembrane region, a ligand-binding region, and an intracellular tyrosine kinase region consisting of 561 amino acids[2,3]. The 3-tyrosine motif (Tyr1278, Tyr1282, and Tyr1283), where autophosphorylation for kinase activity occurs, is also found in other members of the same family of kinases (See fig.1).

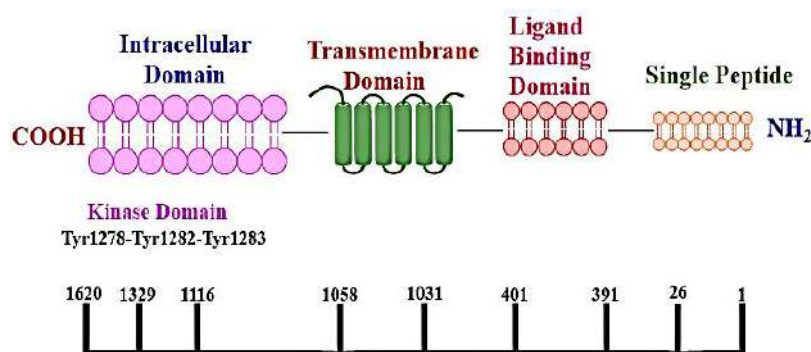


Figure 1 Structure of ALK, showing a polypeptide of 1620 amino acids. The full-length form of ALK resembles other receptor tyrosine kinases. Kinase activity is regulated by a 3-tyrosine motif (Tyr1278, Tyr1282, and Tyr1283), which is located in an intracellular tyrosine kinase domain.

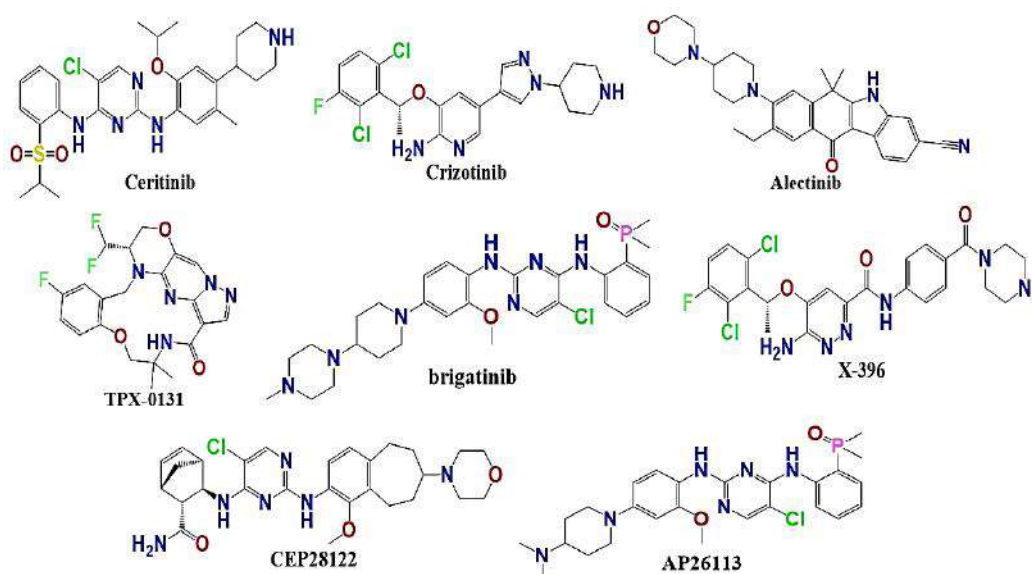


Figure 2 Some of the ALK tyrosine kinase discovered till date and available in clinical practice.

Several research studies have revealed that TKIs' ability to inhibit ALK kinase activity has a substantial anticancer effect [4-11]. Moreover, numerous potent and selective ALK-TKIs have been designed to inhibit fusion proteins and activate ALK variants[12-22]. Targeted therapy using the epidermal growth factor receptor (EGFR) has been discovered as a treatment for NSCLC patients with ALK activation mutations. However, most patients who receive targeted treatment relapse due to genetic changes that confer resistance[12,23]. Many ALK TKIs are available for cancer therapy in different regions. The FDA has approved several ALK inhibitors for cancer therapy, including ceritinib, brigatinib, crizotinib, alectinib, TPX-0131, GSK1838705, CEP28122, AP26113, and X-396 (See fig. 2).

In the present work, we used a QSAR-based virtual screening approach combined with drug repositioning to find a unique lead drug candidate that might effectively inhibit ALK tyrosine kinase receptors. The interactions between the newly discovered FDA drugs were investigated using molecular docking, MD modelling, and MMGBSA studies. To corroborate the results obtained virtually, we conducted an in vitro MTT experiment using the A549 lung cancer cell line.

2 Material and Method

2.1 QSAR Methodology

The current study adheres to the conventional technique advised by the OECD and other scholars for doing QSAR analysis[24-26]. All tools were used with their default values; however, certain settings were altered, and these are detailed in the documentation, in order to generate a robust QSAR model with an equilibrium of predictive capacity and mechanistic understanding.

Step 1: Data collection and curation:

To start, the Binding DB (<https://www.bindingdb.org/bind/index.jsp>; last accessed: 12/24/2021) was used to get a large dataset with 1806 IC₅₀ values for experimentally proven ALK-TK inhibitors. Data quality, and suitable curation before further processing have a significant impact on QSAR analysis[25,27-29]. After that, we filtered the data[30], which included eliminating duplicates, organometallic compounds, salts, molecules with ambiguous IC₅₀ values, and so on. This resulted in a reduction of the dataset's molecules from 1807 to 1328. In spite of the reduced size of the dataset, it still included molecules with experimental IC₅₀ (nM) values between 0.3 and 83,000 nM and the occurrence of different scaffolds such as heterocyclic rings, positional isomers, stereoisomers, etc., all of which widened the chemical space and increased the model's applicability. Table 1 (See Table 1 in the Supplementary Materials) contains the SMILES (Simplified Molecular Input Line Entry System) nomenclature for all of the compounds used in this investigation, together with their experimental IC₅₀ and pIC₅₀ (=log₁₀IC₅₀).

Table 1 shows a few representative values for IC₅₀ (nM) and pIC₅₀ (M) in the SMILES format, along with some examples of the most and least active compounds.

Table 1. SMILES notation, IC₅₀ (nM), and pIC₅₀ (M) values for the five most and least active compounds in the selected data set.

Id	SMILES	IC ₅₀	
		in nm	pIC ₅₀
25	<chem>CCc1cc2C(=O)c3c([nH]c4cc(ccc34)C#N)C(C)(C)c2cc1N1CCC(CC1)N1CCC(O)CC1</chem>	0.3	9.523
33	<chem>C[C@H]1Oc2nc(cnc2N)-c2cc(ccc2CN(C)C(=O)c2ccc(F)cc12)S(C)(=O)=O</chem>	0.34	9.469
35	<chem>COc1cc(ccc1Nc1ncc(Cl)c(Nc2ccccc2P(C)(C)=O)n1)N1CCC(O)CC1</chem>	0.36	9.444
36	<chem>COc1cc(ccc1Nc1ncc(Cl)c(Nc2ccccc2P(C)(C)=O)n1)N1CCC(CC1)N1CCN(C)CC1</chem>	0.37	9.432
37	<chem>CCN1CCCc2cc(Nc3ncc(Cl)c(Nc4ccccc4S(=O)(=O)C(C)C)n3)c(OC)cc2C1</chem>	0.38	9.42
1791	<chem>CN1CCN(CC1)c1ccc(Nc2ncc3ccc(-c4ccccc4C(N)=O)n3n2)cc1</chem>	726	6.139
1793	<chem>COc1ccccc1C#Cc1ccnc2[nH]c3ccc(cc3c12)-c1ccc(cc1)N1CCN(C)CC1</chem>	750	6.125
1800	<chem>CN1CCN(Cc2ccc(cc2)C(=O)Nc2nc(cs2)-c2ccc(C)c(c2)C#Cc2ccc(C)cc2)CC1</chem>	83000	4.081
1803	<chem>CC1(C)c2[nH]c3cc(ccc3c2C(=O)c2ccc(OC[C@H](O)CO)cc12)-c1ccn[nH]1</chem>	770	6.114
1805	<chem>CC(C)S(=O)(=O)c1ccccc1Nc1nc(Nc2nc3CCN(C)CCc3s2)ncc1Cl</chem>	773	6.112

Step-2 Second, we utilised the default settings for OpenBabel 2.4[31] and MOPAC 2012 (openmopac.net, obtained on March 5, 2022) to generate SMILES notations for the optimum 3D structures of the compounds (semi-empirical PM3 technique).

Step 3: If enough molecular descriptors are generated and subsequently pruned to limit the chance of overfitting from redundant noisy descriptors, then a QSAR model may strike a satisfactory balance between mechanistic interpretation and predictive ability[32]. Then, molecular descriptors were generated from 1D to 3D for every molecule. For this objective, we used PyDescriptor [33], which can calculate over 40,000 molecular descriptors for a given

molecule. To reduce the number of molecular descriptors in the descriptor pool, we used QSARINS 2.2.4 to eliminate duplicates and variables with strong correlation ($|R| > 0.95$ or $> 98\%$) [34]. This resulted in a reduction from 40,000 to 2,376, but still covered a broad spectrum of molecular descriptors.

2.2 Subjective Feature Selection (SFS) involves separating the dataset into a training set and an external set

Splitting the dataset into a training set and an external set (also known as a prediction set or test set) is essential for developing and validating a reliable QSAR model [25,27-29]. In order to exclude any possible bias, we divided the dataset into a training set of 1062 molecules (80%) and an external collection of 266 molecules (20%) for this study. The only purpose served by the external set was model validation (predictive QSAR), whereas the molecular descriptors were selected from the training set to determine how many parameters were desired. QSARINS 2.2.4 was used to develop the model through multi-linear regression (MLR) and the Genetic Algorithm (GA). With a fitness function of Q^2_{LOO} and 10,000 iterations. Determining the right number of molecular descriptors to use in a model's creation is an important step in quantitative structure-activity relationship (QSAR) modelling. Until the value of Q^2_{LOO} rose beyond a certain threshold, the heuristic search had to construct a large number of models, beginning with a univariate model and progressing to a multivariate model as additional molecular descriptors were included.

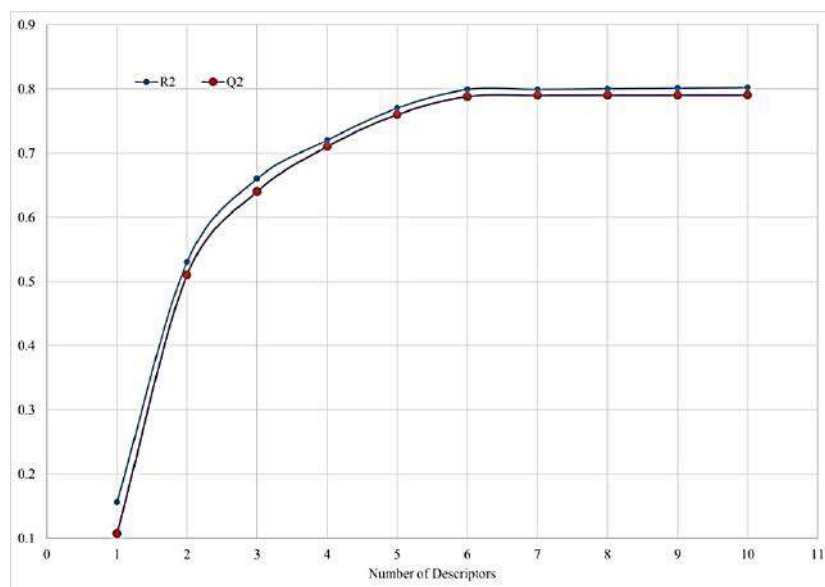


Figure 3 Graph for the number of descriptors vs. leave-one-out Coefficient. Q^2_{LOO} for optimal descriptor count.

Figure 27 is a two-dimensional graph showing the correlation between the Q^2_{LOO} values and the number of chemical descriptors employed by the models. Adding more molecular descriptors did not increase the model's statistical performance; hence, this threshold was used to determine the ideal number of variables to include in the model. The investigation established critical values for six independent variables[35,36] (See Fig. 3). This meant that the QSAR models with more than six descriptors had to be rejected.

2.3 Constructing a Valid Regression Model and its validation

Several validation methods, such as cross-inter validation, external validation, Y-randomization analysis, and the applicability domain (William's plot), can be used to test how

accurate and reliable a QSAR model is. A well-validated QSAR model is very helpful for virtual screening, lead/hit optimisation, decision-making, and other activities. Several types of validation—cross-inter, external, Y-randomization, and applicability domain (William's plot)—can be used to approximate the robustness and wide application of a QSAR model[25,37-40].

The following are the typical criteria for assessing QSAR models, together with their corresponding threshold values for validation parameters[35,36]. There have been several successful model generation efforts using GA-MLR. The best possible model was selected using the following stringent parameters and criteria: $R^2_{tr} \geq 0.6$, $Q^2_{loo} \geq 0.5$, $Q^2_{LMO} \geq 0.6$, $R^2 > Q^2$, $R^2_{ex} \geq 0.6$, $RMSE_{tr} < RMSE_{cv}$, $K \geq 0.05$, $CCC \geq 0.80$, $Q^2-Fn \geq 0.60$, $r^2_m \geq 0.5$, $(1-r^2/ro^2) < 0.1$, $0.9 \leq k \leq 1.1$, or $(1-r^2/r'o^2) < 0.1$, $0.9 \leq k' \leq 1.1$, $|ro^2-r'o^2| < 0.3$, $RMSE_{ex}$, MAE_{ex} , R^2_{ex} , Q^2_{F1} , Q^2_{F2} , Q^2_{F3} , and low R^2_{Yscr} , $RMSE$ and MAE .

Validation of quantitative structure-activity relationship (QSAR) models entails establishing the model's applicability. We used a Williams plot to determine the extent to which the QSAR model was reliable. (Table 2 in the supplemental materials lists the computed descriptors used to create the QSAR model.) Table 3 of the supplementary materials provides the formulas for determining these statistical features.

2.4 QSAR-Based Virtual Screening for Drug Repositioning (Repurposing)

Due to the rising need for novel anticancer treatments, drug repurposing has fascinated the cancer research community. Even though there are many ways to treat cancer, such as chemotherapy and targeted therapies, cancer is defined by its inability to respond to current medicines and drugs. Because of this, studying potential novel cancer treatments is a thriving field of study[41-43]. Nowadays, drug repositioning is an emerging area of study; therefore, we utilised this information to conduct a QSAR-based virtual screening using the zinc database and its 1615 FDA compounds. Since then, QSAR-based VS has used 1615 FDA substances. Before doing molecular descriptor calculations, the 3D structures of molecules were constructed in the same way as a modelling set. The ALK-TK inhibitory action of 1615 FDA-approved drugs was predicted using a completely validated six-parameter quantitative structure-activity relationship (QSAR) model, which was derived using estimated chemical descriptors. The chemical details and predicted IC_{50} values for the zinc FDA 1615 compounds are included in Table 4 of the supplemental materials.

2.5 Molecular Docking Analysis

The ALK TK wild type (pdb-4cmu) and mutant (pdb-4clj) Protein Data Bank (pdb) data were obtained from the protein data bank[44]. The pdb:4cmu and 4clj were chosen on the basis of X-ray resolution and completion of amino acid sequences. Ramachandran's plot was used to determine the protein's health before running docking simulations. The protein, after optimisation, passes muster for docking studies. Both PDB files had their native ligands removed before docking analysis could begin. To facilitate comparison between the wild-type (4cmj) and mutant (4clj) strains, all 12 hit molecules from the QSAR-based virtual screening were docked into the active sites of both. For convenience, we've included the docking position of Ledipasvir, the most active molecule.

Molecular docking analysis was performed in NRGSuite software package [45]. This is an open-access tool that is available at no cost as a plugin for the PyMOL software (www.pymol.org as of March 9, 2022). FlexAID can help you find cavities on protein surfaces to ensure that it can be utilised in docking simulation targets[46]. Covalent docking, conformational search using a genetic algorithm, and the mobility of ligands and side chains are all modelled. For optimal performance in this study, NRGsuite was run with the following flexible-rigid docking with default parameters: Input Method for Boundary Sites: HET groups

contain water molecules; have a van der Waals permeability of 0.1; have gone through 1000 generations; use the share fitness metric; reproduce using the population explosion model; have five TOP complexes; have a cylindrical form (diameter: 19); have a three-dimensional grid spacing of 0.367; have no side-chain mobility; be ligand-adaptable; not have a ligand posture for comparison; have no constraints; and so on. For both the wild-type and mutant strains, the accuracy of molecular docking was tested using two molecules: PF-06463922 and (10R) -7-amino-12-fluoro-1, 3, 10, 16-tetramethyl-16, 17-dihydro-1H-8, 4-(metheno) pyrazole (4, 3-) (2, 5, 11). ((10R) -7-amino-12-fluoro-2,10,16-trimethyl-15-oxo-10,15,16-tetrahydro-2H-8) 4-(metheno) pyrazole (4, 3-h) (2,5,11) is a well-characterised inhibitor of ALK TK that was used to verify the docking method.

2.6 Molecular dynamics (MD) simulations

Molecular dynamics and simulation (MDS) methods were used to look into how stable and convergent the interaction between ledipasvir and ALK TK was. This study examined both wild (pdb-4cmu) and mutant (pdb-4clj) strains for their stability. The system builder was used to construct intricate systems for the strains of Ledipasvir-wild, Ledipasvir-mutant, Ceritinib-wild, and Ceritinib-mutant. This action was undertaken in order to facilitate the execution of simulations. The system used the OPLS-2005 force field and included an explicit solvent model using SPC water molecules[47,48]. The baseline parameters for the explicit SPC water model's orthorhombic box measuring 7.0 x 7.0 x 7.0 metres were established using Desmond 2018-4[49]. The neutralisation of both wild-type and mutant ALK-TK complexes was achieved by introducing NaCl salt at a concentration of 0.15 M Na⁺ ions. In the Desmond system builder panel, the neutralise option has been selected to introduce a predetermined quantity of counterions. In the molecular dynamics simulation approach, 18 sodium (Na) ions and 15 chloride (Cl) ions were included. After using the ASL module to choose certain residues of the ligand and protein molecules, the Desmond default relaxation technique was employed to improve the performance of the resulting systems. To learn more about each complex, we conducted molecular dynamics (MD) simulations. In the previous production run, we kept the temperature and pressure (NPT) constant and ran a molecular dynamics simulation (MDS) for 200 ns. The Nosé-Hoover chain coupling method was used to create the NPT ensemble, and the final simulation was run at 300 K with a relaxation period of 1 ps throughout the whole dynamics [49,50]. With a relaxation time of just 2 picoseconds[51], pressure was controlled using a barostat based on the Martyna Tuckerman-Klein chain coupling system. The Desmond simulation used the isotropic Martyna-Tobias-Klein barostat and the Nose-Hoover thermostat to regulate the pressure at 1 atmosphere and the temperature at 300 Kelvin. The NPT ensemble was used in all runs, with a temperature of 300 K and a pressure of 1 bar. We successfully estimated the bonding interactions by utilising a time step of 2 femtoseconds and the RESPA integrator. Using the particle mesh Ewald method, and keeping the radius for Coulomb interactions at 9 [52], we were able to calculate the long-range electrostatic interactions between the particles. This investigation describes the remaining possible setups. After finishing the last simulation run, the simulated trajectories of the wild-type and mutant Ledipasvir strains were analysed. Root-mean-square deviation (RMSD), root-mean-square fluctuation (RMSF), and hydrogen-bond formation were the primary areas of study in this examination. Binding energies for the complexes were estimated using the MM-GBSA technique, which was applied to 200 individual 1 ns trajectories. Standard deviations and mean binding energies were calculated from the data so obtained.

2.7 Molecular Mechanics: Generalised Borne Surface Area

Docked complexes of ledipasvir and ceritinib were analysed to determine their binding free energy (G_{bind}) with the help of the MM-GBSA module. During molecular dynamics (MD) simulations, the ALK complex was attached to both natural (4cmu) and mutant (4clj) strains,

allowing for this estimate to be made. The New York-based Schrodinger Suite, LLC, version 2023–24, was used to run the simulations. Binding free energy was determined using a rotamer search and calculated with the OPLS 2005 force field and the VSGB solvent model [53]. After an MD experiment was completed, a time window of 10 ns was used to choose the frames of the trajectories. By using Equation 1, the comprehensive free energy of binding was successfully determined.

$$\Delta G_{\text{bind}} = G_{\text{complex}} - (G_{\text{protein}} + G_{\text{ligand}}) \quad (1)$$

Where,

ΔG_{bind} = binding free energy,

G_{complex} = free energy of the complex,

G_{protein} = free energy of the target protein,

and G_{ligand} = free energy of the ligand.

The trajectories of the MMGBSA results were analysed to learn more about the structural changes that occurred after the dynamics were applied.

2.8 In-Vitro Evaluation of Anticancer Activity by MTT Assay

The A549 lung cancer cell line, at passage 68, was purchased from NCCS, Pune, India. F-12K medium, antibiotic-antimycotic solution, HEPES solution, and 10% foetal bovine serum were used to cultivate the cells after they were frozen. The experiment used the 3(4,5-dimethyl-thiazol-2-yl)-2,5-diphenyl tetrazolium bromide (MTT) assay to assess mitochondrial function. This assay relies on the reducing properties of MTT, which lead to the formation of insoluble formazan crystals specifically inside viable mitochondria. In summary, 1×10^4 A549 cells were seeded into each well of a 96-well plate, and the plate was then incubated for 24 hours at 37°C in 5% CO₂. Following removal of the medium, the cells were treated with Ceritinib (5 M), Posaconazole (10 M), Ledipasvir (20 M), and Ledipasvir (40 M) for 24 hours in triplicate. The chemical ceritinib was used as a standard. Each well was given a media volume of 300 l. After 24 hours of treatment, 25 L of MTT solution (5 mg/mL) was added to each well, and the cells were incubated for 4 hours at 37°C in a 5% CO₂ atmosphere. Following the dissolution of the formazan crystals in a volume of 100 litres of dimethyl sulfoxide (DMSO), the absorbance was then determined at a wavelength of 570 nanometers using an Epoch Microplate Spectrophotometer manufactured by Biotek Instrument. The IC₅₀ values were calculated using GraphPad Prism (version 7) software. Examining a nonlinear plot of the percentage of cell inhibition against the logarithm of concentration enabled this. The calculation of cell growth inhibition percentage was performed using the below formula:

$$\% \text{ Cell Viability} = (AT / AU) \times 100$$

Where; AT = Absorbance of Treated Cells (Drug)

AU = Absorbance of Untreated Cells, % Cell Inhibition = 100 - % Cell Viability

3 Results and Discussion

This work used molecular docking and quantitative structure-activity relationship analysis to identify ALK-TK inhibitory structural components. A QSAR paradigm combines structural characteristics to basic chemical descriptors. The six-parametric GA-MLR model's structural interpretation and clear molecular descriptors make it a good external predictor. IC₅₀ values of molecules in the dataset can explain the effect of a specific descriptor, but the combined or

inverse effect of unknown factors or other molecular descriptors could have a significant impact on a molecule's IC₅₀ value (See figure 4).

QSAR Model

$pIC_{50} = 5.577 (\pm 0.087) + 1.21 (\pm 0.102) * \text{aroC_sumpc} + 0.086 (\pm 0.006) * \text{ringC_plaN_6B} + 0.221 (\pm 0.029) * \text{fnotringNsp3C4B} + -0.269 (\pm 0.027) * \text{faroNC8B} + 1.059 (\pm 0.103) * \text{fdonnotringN5B} + -0.595 (\pm 0.061) * \text{fnotringNringN4B} +$

$R^2: 0.7909$, $R^2_{adj}: 0.7897$, $R^2 - R^2_{adj}: 0.0012$, LOF: 0.2544, K_{xx}: 0.3058, Delta K: 0.0661, RMSE_{tr}: 0.4987, MAE_{tr}: 0.4215, RSS_{tr}: 264.3315, CCC_{tr}: 0.8832, s: 0.5003, F: 665.6663, Q^2_{loo} : 0.7882, $R^2 - Q^2_{loo}$: 0.0027, RMSE_{cv}: 0.5019, MAE_{cv}: 0.4242, PRESS_{cv}: 267.7734, CCC_{cv}: 0.8817, Q^2_{LMO} : 0.7885, R^2_{Yscr} : 0.0056, Q^2_{Yscr} : -0.0076, RMSEAV_{Yscr}: 1.0874, RMSE_{ext}: 0.5285, MAE_{ext}: 0.4460, PRESS_{ext}: 74.0260, R^2_{ext} : 0.7710, Q^2_{F1} : 0.7708, Q^2_{F2} : 0.7690, Q^2_{F3} : 0.7651, CCC_{ext}: 0.8739, r^2_m aver.: 0.6744, r^2_m delta: 0.1472, R^2 : 0.7882, R^2_o : 0.7334, k': 0.9956, Clos': 0.0695, r^2_m : 0.6038. Pred(x) vs. Exp(y): R^2 : 0.7882, R^2_o : 0.7882, k: 1.0000, Clos: 0.0000, r^2_m : 0.7869, Exp(x) vs. Pred(y): R^2 : 0.7710, R^2_o : 0.7223, k': 0.9998, Clos': 0.0632, r^2_m : 0.6008, R^2 : 0.7710, R^2_o : 0.7701, k: 0.9951, Clos: 0.0012, r^2_m : 0.7480.

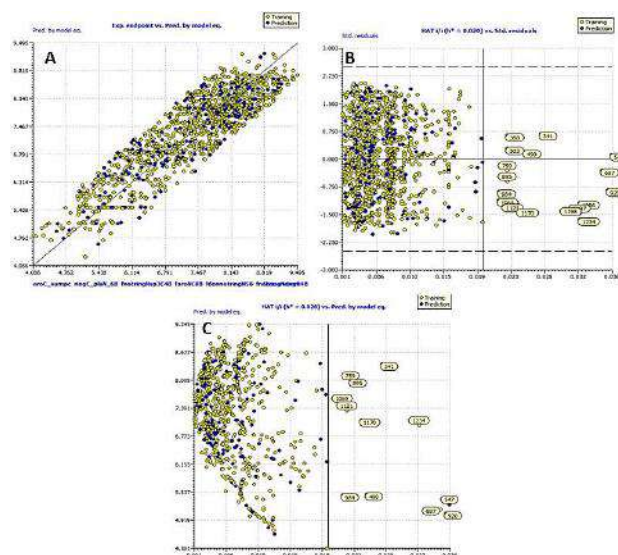


Figure 4 QSAR model development and accompanying graphs (a) A scatter plot contrasting the expected and experimental pIC₅₀ values (b) a portrayal of a Williams plot to assess the model's applicability domain; and (c) a presentation of an Insubria plot.

3.1 QSAR Mechanistic Interpretation

The significance of the sum of partly charged carbon atoms in aromatic fragments is shown by **aroC_sumpc**. It is one of the variables that exhibit a positive correlation in the constructed QSAR model. These descriptions highlight the charges, both complete and partial, that are linked to carbon atoms with aromatic and fragrant properties. The presence of a positive coefficient for this descriptor suggests that there is a direct relationship between a greater activity profile and a higher aroC_sumpc score. The evaluation involves analysing the following pair of molecules: 502 (502, IC₅₀=4.67 nM, aroC_sumpc=0.65, ringCplus_sumpc=0.97) and 1030 (1030, IC₅₀=19.05 nM, aroC_sumpc=0.49, ringCplus_sumpc=0.85) (see fig 5).

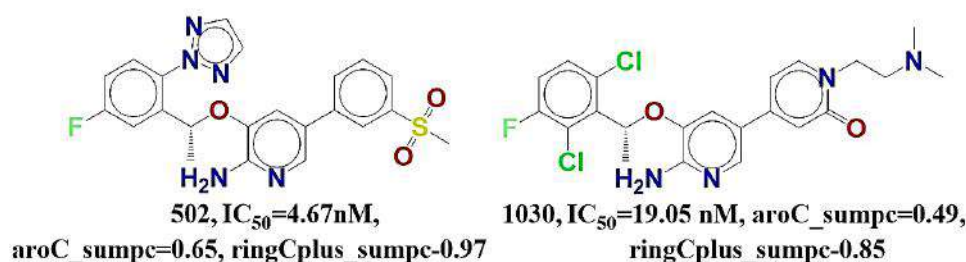


Figure 5 The molecular descriptor aroC_sumpc, shown exclusively for molecules 502 and 1030.

Ring carbon and planar nitrogen were found to be important for TK ALK to work as an inhibitor (**ringC_plaN_6B**). It shows that there are ring carbons in the six bonds of the flat nitrogen atoms. It's much better for TK-ALK to stop a reaction when the positive factor number for this trait in the QSAR model goes up. One way to show this is to compare molecule 1065 (1065, $IC_{50} = 21.38\text{ nM}$, $\text{ringC_plaN_6B} = 20$, $\text{C_plaN_5B} = 26$, $\text{aroC_plaN_6B} = 16$) to molecule 1778 (1778, $IC_{50} = 69183\text{ nM}$, $\text{ringC_plaN_6B} = 16$, $\text{C_plaN_5B} = 16$, $\text{aroC_plaN_6B} = 12$) (See Fig. 6)

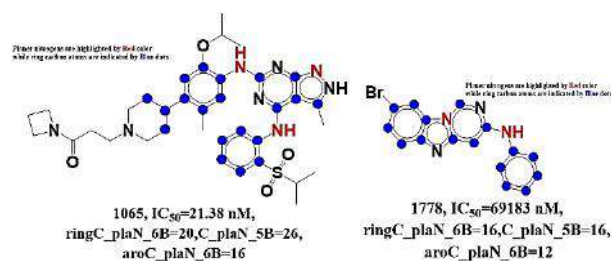


Figure 6. For molecules 1065 and 1778, the molecular descriptor ringC_plaN_6B is shown.

fnotringNsp3C4B: The abbreviation fnotringNsp3C4B describes how often Sp^3 -hybridized carbon atoms are found within 4 bonds of acyclic or non-ring nitrogen atoms. Since it has a positive coefficient, the value of the molecular marker fnotringNsp3C4B goes up as the activity profile does. The fnotringNsp3C4B is not worked out if the same sp^3 hybrid carbon atom is three or five bonds away from the carbon atom. This is clear when you look at the molecule 135 ($IC_{50} = 1\text{ nM}$, $\text{fnotringNsp3C4B} = 2$, $\text{fnotringNnotringC4B} = 2$, $\text{fplaNsp3C4B} = 2$) next to the molecule 1670 ($IC_{50} = 371.5\text{ nM}$, $\text{fnotringNsp3C4B} = 1$, $\text{fnotringNnotringC4B} = 1$, $\text{fplaNsp3C4B} = 1$) (See fig. 7).

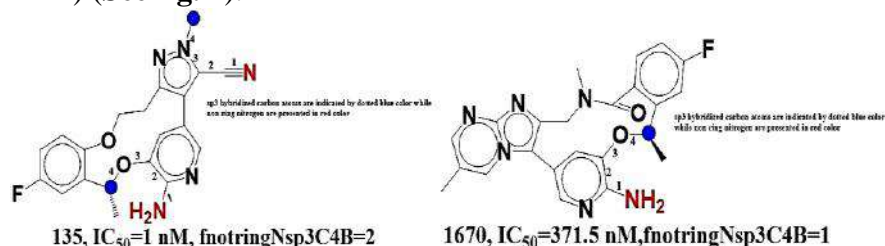


Figure 7: For molecules 135 and 1670, the fnotringNsp3C4B molecular descriptor is shown.

fdonnotringN5B (The chance of a nitrogen atom that is not in a ring is exactly 5 bonds away from the source atoms.) This trait has a positive coefficient in the standard QSAR model. This means that as its value goes up, ALK-TK suppression goes up as well. It can be seen that between molecules 245 ($IC_{50} = 2.13\text{ nM}$, $\text{fdonnotringN5B} = 1$) and 1449 ($IC_{50} = 812.8\text{ nM}$, $\text{fdonnotringN5B} = 0$). This might explain the differences in inhibitory activity of ALK TKs (See Figure 8).

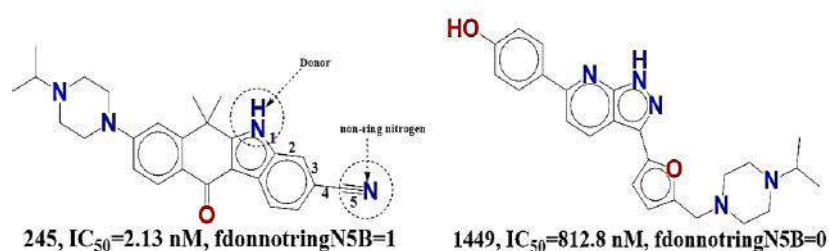


Figure 8 For molecules 245 and 1449, the molecular descriptor fdonnotringN5B is shown.

The abbreviation **faroNC8B** shows how often aromatic nitrogen atoms with carbon atoms connected in exactly 8 bonds are found. The suggested QSAR model shows that this trait has a negative coefficient. Increasing its value would make ALK TK even less effective at blocking it. To make ALK TK as good at stopping cell growth as possible, more changes should be made to the molecule that lower the value of faroNC8B. This remark can be explained by comparing molecule 1168 ($IC_{50} = 107.1$ nM, faroNC8B = 2) to molecule 1118 ($IC_{50} = 81.8$ nM, faroNC8B = 1) (see fig. 9).

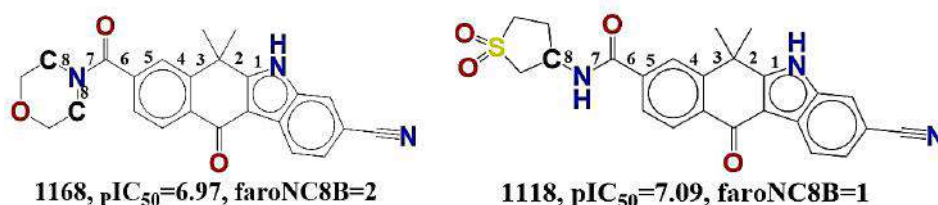


Figure 9 Illustration of the molecular descriptor faroNC8B for the molecules 1168 and 1118.

fnotringNringN4B (frequency of occurrence of a ring nitrogen atom exactly at 4 bonds from a non-ring nitrogen atom) As the value of the descriptor goes up in the QSAR model that was made, negative coefficients of the descriptor make the inhibitor less active. This can be demonstrated by comparing molecule 192 ($pIC_{50} = 8.77$, fnotringNringN4B = 0) with molecule 1343 ($pIC_{50} = 6.43$, fnotringNringN4B = 1) (see fig. 10).

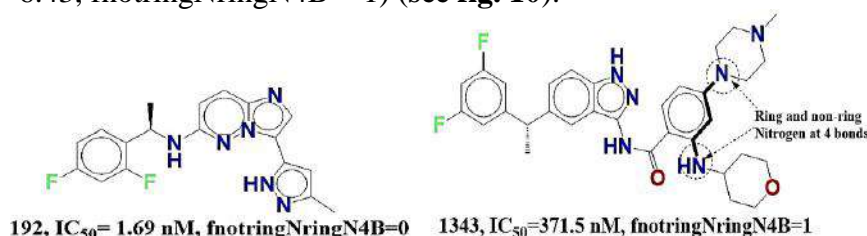


Figure 10 The fnotringNringN4B molecular descriptor is presented only for molecules 192 and 1343.

3.2 Drug Repositioning and QSAR Based Virtual Screening

After making the QSAR model, we used it to predict the ALK-TK inhibitory activity of 1650 FDA molecules through a QSAR-based virtual screening. The 12 hit molecules were obtained as repurposed drug candidates against the ALK-TK receptor. Based on its pIC_{50} , the molecule ZINC000150338819 (Ledipasvir) was chosen as a major hit among the top hit molecules.

3.4 Applicability domain study of the Identified hit molecules

To see how widely our QSAR model could be used, we used a collection of 1329 molecules for training and a set of 12 hit molecules for forecast. Twelve molecules were found through QSAR-based virtual screening and were then described. As you can see in **Fig. 11**, the hit molecules ZINC000150338819, ZINC000150588351, ZINC000203686879, and

ZINC000068204830 are on the edge of the application domain in the Williams plot. This means that the leverage value is low.

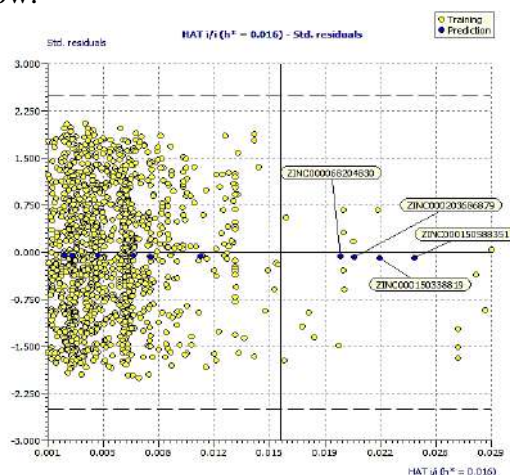


Figure 11 The 12 hit molecules from the QSAR-based virtual screening are shown in a Williams plot for their potential applicability domain (blue dots represent the hit molecules).

3.5 Molecular Docking analysis

All reported hit compounds were docked to ALK TK wild (pdb-4cum wt) and mutant strains (pdb-4clj mutant) to analyse the binding relationships. The QSAR-based virtual screening anticipated several FDA compounds' ALK-TK inhibitory activity. The docking scores and predicted activity (PIC₅₀) of the 12 hit molecules for the wild-type ALK TK and the mutant L1196M TK are shown in Tables 1 and 2, respectively. The QSAR-based virtual screening showed that all antiviral drugs had a greater pIC₅₀ against both wild and mutant ALK TK strains than the clinically proven ALK TK inhibitors (See Tables 2 and 3).

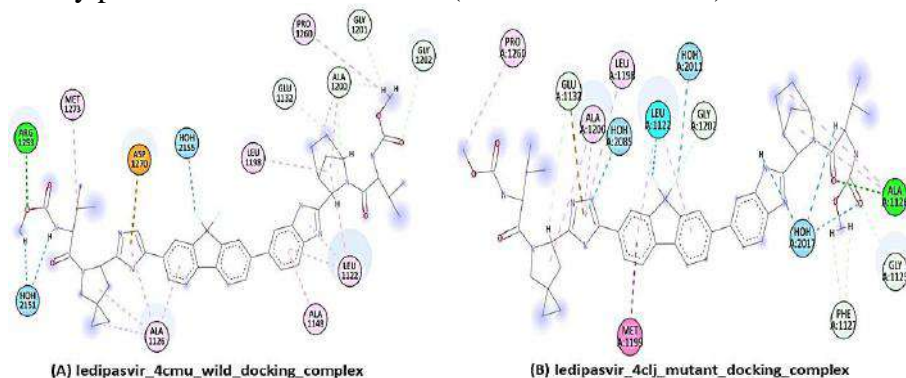


Figure 12 Depiction of 2D interaction) of ZINC000150338819 (Ledipasvir) with ALK TK wild strain (A) and mutant strain(B).

Table 2 Depiction of the Docking Results of the 12 hits for ALK TK (pdb-4cmu, wild strain)

SN	ZINC I.D. hit molecules	pIC ₅₀ by QSAR VS	Docking Score kcal/mol	RMSD Å	Binding free energy
1	ZINC000150338755 (Venetoclax)	9.36	-9.90	1.64	-38.63
2	ZINC000150338819 (Ledipasvir)	9.18	-10.57	1.54	-55.19
3	ZINC000150588351 (Elbasvir)	9.02	-9.93	2.37	-61.26
4	ZINC000066166864 (Alectinib)	8.67	-7.65	1.96	-34.99
5	ZINC000203686879 (Velpatasvir)	8.58	-10.08	2.10	-51.97

6	ZINC000148723177(Brigatinib)	8.53	-8.45	1.78	-29.96
7	ZINC000096272772(Ceritinib)	8.28	-8.17	1.58	-38.64
8	ZINC000028639340	8.25	-8.94	2.65	-50.07
9	ZINC000003938482(Posaconazole)	8.25	-9.70	1.59	-49.49
10	ZINC000072316335(Ribociclib)	8.20	-7.48	1.12	-34.62
11	ZINC000068204830(Daclatasvir)	8.14	-10.10	2.15	-49.15
12	ZINC000003787097(Besifloxacin)	8.03	-7.10	0.99	-32.95

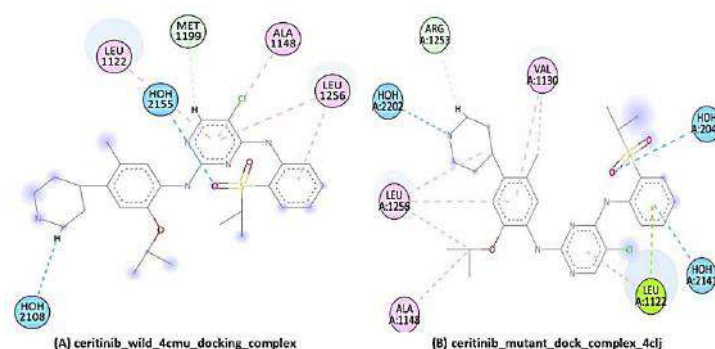


Figure 13 Depiction of 2D interaction) of ZINC000096272772 (Ceritinib) with ALK TK wild strain (A) and mutant strain(B).

Table 3 Depiction of the docking Results of 12 hits for ALK TK (pdb-4clj, mutant strain).

sn	ZINC I.D.	pIC ₅₀ by QSAR VS	Docking Score kcal/mol	RMSD A0	Binding energy	free
1	ZINC000150338755 (Venetoclax)	9.36	-8.87	2.28	-46.77	
2	ZINC000150338819(Ledipasvir)	9.18	-8.52	2.09	-37.33	
3	ZINC000150588351(Elbasvir)	9.02	-8.95	4.25	-39.68	
4	ZINC000066166864 (Alectinib)	8.67	-7.70	1.47	-32.47	
5	ZINC000203686879 (Velpatasvir)	8.58	-9.35	1.70	-31.60	
6	ZINC000148723177(Brigatinib)	8.53	-8.33	1.70	-40.17	
7	ZINC000096272772(Ceritinib)	8.28	-8.36	1.60	-34.64	
8	ZINC000028639340	8.25	-7.07	2.19	-23.41	
9	ZINC000003938482(Posaconazole)	8.25	-8.29	3.46	-44.94	
10	ZINC000072316335(Ribociclib)	8.20	-7.93	3.70	-39.19	
11	ZINC000068204830(Daclatasvir)	8.14	-8.43	4.77	-41.96	
12	ZINC000003787097(Besifloxacin)	8.03	-7.27	1.89	-30.17	

It has a strong preference for Ledipasvir because the ALK TK mutant strain reacts with it in a way that is less water-friendly than the normal ALK TK. Arg1253 formed a normal hydrogen bond with Ledipasvir, and water formed hydrogen bonds with HOH2151, HOH2155, and HOH2151. It takes -0.33 kcal/mol of energy for ledipasvir to bind to Met1199 in the active "DFG-in" shape of wild-type ALK TK. It needs -0.88 kcal/mol in the mutant strain. This shows that Ledipasvir has a stronger attraction for the mutant ALK TK strain compared to the wild strain, even though the contact distance between the two strains was only 3.88. The gap between Gly1202 and fluorine atoms that made touch was found to be 4.14. In the wild ALK TK, which was shaped like a boat, no similar contact was found between Gly1202 and fluorine atoms. Also, the way the fluorine atoms are arranged in the hydrophobic pocket brings them

closer to the Asn1254 residue of the mutant ALK-TK. This improves the interactions between molecules and keeps its chair-shaped shape. Along the same lines, this is like how fluorine atoms are oriented towards the Asn1254 residue of the pdb-4clj binding. The difference in binding free energy between the two strains could be because Ledipasvir has different shapes when it comes to normal and mutant ALK TK. Also, the wild ALK TK had a fluorine atom arrangement with a dihedral angle of 52.2 degrees. The mutant ALK TK, on the other hand, had an angle of 70 degrees, which means it rotated 18 degrees differently. This shows that the mutant ALK TK goes through big changes in its shape that affect its capacity to attach to Ledipasvir (see **fig 112 and 13**).

3.6 Molecular dynamics (MD) simulations

The apo-ALK tyrosine kinase (TK) was stable throughout the 200-nanosecond simulation, except for a 60–85 nanosecond variation. The c-alpha atoms' root mean square deviation (RMSD) varied from 2.0 to 2.2 angstroms at this time. The system converged at 2.27 angstroms RMSD. The apo-ALK tyrosine kinase (TK) showed larger variations in the back area (RMSD = 2.3 Å) and sidechain region compared to the C- and backbone regions (RMSD = 3.2) (see figure 1(B)). Figure 1 indicates that the wild type A-loop RMSD converged to 1.8 after 40 ns of simulation. In the L1196 mutant, the A-loop RMSD reached 2.4 at 40 ns and varied between 40 and 50 ns. The value dropped to 2.4 between 100 and 110 ns after reaching 3.1 between 80 and 90 ns. The MD simulation ended with it rising from 2.6 to 2.8. This suggests that the L1196 mutant's A-loop is more flexible than the normal type (see **fig. 14**).

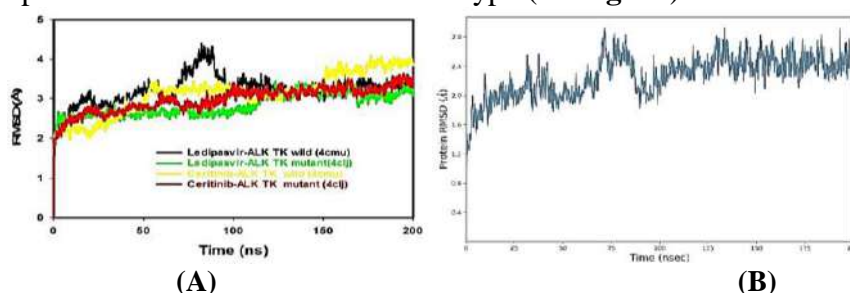


Figure 14. (A) Root Mean Square Deviation (RMSD) analysis of MD simulation trajectories for (i) wild (4cmu) Ledipasvir-ALK TK, (ii) mutant (green, yellow) (4clj) Ledipasvir-ALK TK, (iii) wild (4cmu) Ceritinib-ALK TK, and (iv) mutant (red, 4clj) Ceritinib-ALK TK. (B) RMSD plot for the Apo-4cmu (non-complex) ALK TK protein.

Figure 19 demonstrates that the wild type A-loop RMSD converged to 1.8 after 40 ns of simulation. The A-loop RMSD of the L1196 mutant increased to 2.4 at 40 ns and ranged from 40 to 50 ns. Between 80 and 90 ns, it hit 3.1 before dropping to 2.4 between 100 and 110 ns. Later in the MD simulation, it rose from 2.6 to 2.8. The L1196 mutant's A-loop is more flexible than the normal kind.

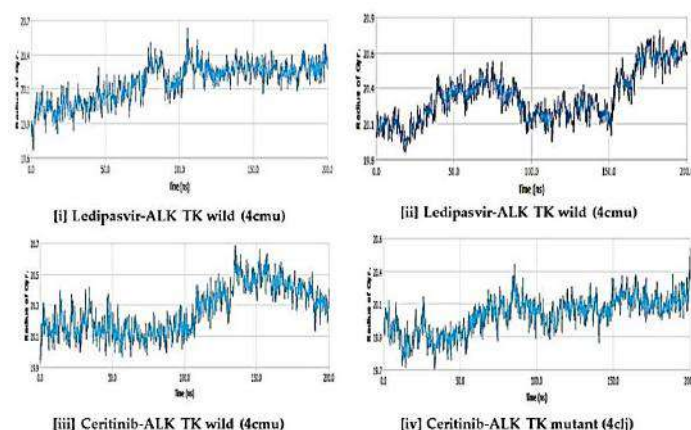


Figure 15. Radius of gyration (R_g) trajectory study using MD simulations for [i] wild (4cmu) and [ii] mutant (4clj) Ledipasvir-ALK TK, [iii] wild (4cmu) and [iv] mutant (4clj) Ceritinib-ALK TK.

In **figure 15**, the C-backbone of ALK TK wild-type coupled to Ledipasvir has the least compactness because its R_g plot fluctuates from 20.1 to 20.7, with a mean of 20.3 over 200 ns. However, the C backbone of the ALK-TK mutant bound to Ledipasvir gyrated at 8.5 with minor modifications. A reduction in R_g indicates a well-bound protein-ligand combination. Mutant ALK-TK complexes with Ledipasvir were substantially more stable than wild-type ones. Throughout the simulation, the RMSF plot showed each amino acid residue in its most stable configuration. The amino acid residues in the ledipasvir-bound wild-type and mutant ALK TK complex were least likely to alter (see **fig. 16**).

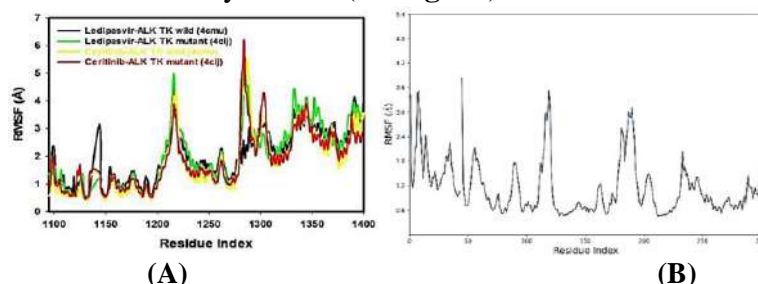


Figure 16. (A) Root Mean Square Fluctuations (RMSF) in MD simulations of [i] wild (4cmu) and [ii] mutant (4clj) Ledipasvir-ALK TK, [iii] wild (4cmu) and [iv] mutant (4clj) Ceritinib-ALK TK. (B) Root Mean Square Fluctuations (RMSF) in MD simulations of Apo-ALK TK (non-complexed ALK TK).

Global quality study of RMSD and R_g demonstrates that ledipasvir significantly affects the stability of wild-type and mutant ALK TK targets in the binding cavities. Root mean square fluctuation (RMSF) plots with a time function of 200 nanoseconds indicated considerable RMSF at particular residues in both wild-type and mutant ALK-TK proteins. In contrast, apo-ALK TK fluctuated less.

3.7 Molecular Mechanics Generalised Born Surface Area (MMGBSA)

MMGBSA is mostly used to measure ligand-protein binding. Ledipasvir-ALK TK wild-type (4cmu) and mutant (4clj) complexes' binding free energies, ceritinib-ALK TK complexes' binding free energies, and other non-bonded interaction energies were assessed. The Ledipasvir ligand bound to the wild-type (4cmu) and mutant (4clj) ALK TK complexes at -47.77 and -61.68 kcal/mol, respectively. Table 5 shows the average binding energies of the wild-type (4cmu) and mutant (4clj) ceritinib-ALK TK complexes, -58.49 and -51.31 kcal/mol. Unlike

ceritinib, ledipasvir bound to mutant ALK TK more strongly than native ALK TK. Gbind is governed by non-covalent interactions such GbindCoulomb, GbindCovalent, GbindHbond, GbindLipo, GbindSolvGB, and GbindvdW. GbindLipo and GbindCoulomb contributed less energy than GbindvdW, but all three energies affected the binding affinity between wild-type and mutant ALK TK and ceritinib. A key role for GbindvdW in drug receptor interactions has been discovered. In contrast, GbindSolvGB and Gbind covalent energies had the least effect on mean binding energies (see **table 4**).

Table 4 Presentation of the MMGBSA results for the ledipasvir and ceritinib wild and mutant ALK TK strains.

Energies (kcal/mol) *	Ledipasvir- ALK-TK wild (4cmu)	Ledipasvir- ALK-TK mutant(4clj)	Ceritinib- ALK-TK wild (4cmu)	Ceritinib-ALK TK-mutant (4clj)
ΔG_{bind}	-47.77 ± 6.95	-61.68 ± 8.16	-58.49 ± 4.42	-51.31 ± 6.29
$\Delta G_{bindLipo}$	-17.98 ± 1.95	-22.92 ± 2.55	-19.20 ± 1.46	-17.51 ± 2.01
$\Delta G_{bindvdW}$	-52.58 ± 6.71	-66.37 ± 5.71	-54.49 ± 3.75	-54.21 ± 5.77
$\Delta G_{bindCoulomb}$	-17.51 ± 15.17	9.10 ± 13.51	10.96 ± 10.63	11.57 ± 3.17
$\Delta G_{bindHbond}$	-0.85 ± 0.47	-0.93 ± 0.53	-0.95 ± 0.50	-0.60 ± 0.35
$\Delta G_{bindSolvGB}$	9.98 ± 13.37	14.32 ± 12.01	-1.40 ± 9.36	5.82 ± 3.12
$\Delta G_{bindCovalent}$	6.86 ± 3.59	5.59 ± 2.66	6.59 ± 3.12	3.64 ± 2.17

The wild-type and mutant ledipasvir and ceritinib-ALK TK complexes formed stable hydrogen bonds with amino acid residues. Their GbindHbond interaction values showed this. Both GbindSolvGB and GbindCovalent showed negative energy contributions for each molecule, indicating binding resistance. Ledipasvir and ceritinib have transformed from curved to straight in the binding pockets of wild-type and mutant ALK-TK proteins (200 ns). Changes in conformation improve contact between the binding pocket and residues, increasing stability and binding energy.

3.8 MTT Assay (In-Vitro Cell line study)

Ledipasvir and posaconazole, our most active hits, were tested in vitro on A549 cell lines for anticancer activity. Ledipasvir and posaconazole were selected for in vitro cell line research because they are in or near the QSAR model's applicability region.

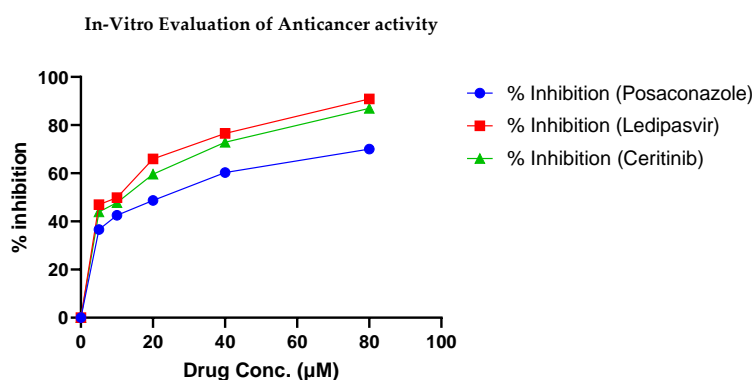


Figure 17: Depiction of in-vitro evaluation of anticancer activity.

Our study of in vitro anticancer activity on the A549 lung cancer cell line found that our acquired hit, Ledipasvir, had a slightly higher inhibition rate than the standard reference molecule, Ceritinib (see figure 17). The findings match computer predictions, indicating that the same mechanism that reduced A549 lung cancer cells may inhibit ALK TK. However, we believe further enzyme tests are needed to provide greater information.

4 Conclusion

A six-descriptor QSAR model was created for 1328 drugs exhibiting TK-ALK inhibitory activity (IC₅₀). The robust and predictive QSAR model meets all threshold values, including $R^2 = 0.79$, $Q^2_{\text{LOO}} = 0.78$, $Q^2_{\text{LMO}} = 0.78$, $R^2_{\text{ex}} = 0.77$, $\text{CCC}_{\text{ex}} = 0.87$, etc. The model discovered many hidden pharmacophoric features, including the sum of aromatic carbon partial charges, sp³-hybridized carbons within 4 bonds of non-cyclic carbons, and planer nitrogen within 6 bonds of the ring carbon atom. The Quantitative Structure-action Relationship (QSAR) research showed that the aromatic or ring carbon atom, ring nitrogen atom, or non-ring nitrogen atom significantly affected ALK TK's inhibitory action. As with other TK ALK inhibitors like crizotinib and brigatinib, X-ray-resolved structures confirmed the mix of revealed and hidden structural features. Additionally, QSAR-based virtual screening and drug repositioning identified ledipasvir as an FDA-approved compound with a clinical trial IC₅₀ of 0.65 nM (pIC₅₀–9.18 M). Ledipasvir outperformed ceritinib in molecular docking, scoring -10.57 kcal/mol against the ALK TK wild strain (pdb-4cmu) and -8.5286303 against the mutant strain (pdb-4clj, mutant). Ledipasvir has a greater binding energy than ceritinib (-38.64 kcal/mol against natural ALK TK and -34.64 against mutant ALK TK) and other ALK TK inhibitors, according to docking research. Ledipasvir had a high affinity because the ALK-TK mutant strain established more hydrophobic contact with it than the natural strain. The MD simulation and MMGBSA analysis showed that the drug-receptor complex was stable beyond 200 ns and had high binding energy. The mutant ALK TK-ledipasvir combination was much more stable than the natural complex. Thus, MD simulation trajectories and binding energy docking data validated MM-GBSA predictions. Additionally, the MTT test showed that ledipasvir had somewhat stronger anticancer activity against the lung cancer cell line A549 than ceritinib. The in-silico investigation confirms the in vitro anticancer effectiveness. These results may help design a novel ALK-TK chemotherapy treatment.

References

1. Morris SW, Kirstein MN, Valentine MB, et al. Sequence Correction. *Science*. 1995;267(5196):316-317.
2. Morris SW, Naeve C, Mathew P, et al. ALK, the chromosome 2 gene locus altered by the t(2;5) in non-Hodgkin's lymphoma, encodes a novel neural receptor tyrosine kinase that is highly related to leukocyte tyrosine kinase (LTK). *Oncogene*. 1997;14(18):2175-2188.
3. Iwahara T, Fujimoto J, Wen D, et al. Molecular characterization of ALK, a receptor tyrosine kinase expressed specifically in the nervous system. *Oncogene*. 1997;14(4):439-449.
4. Sakamoto H, Tsukaguchi T, Hiroshima S, et al. CH5424802, a Selective ALK Inhibitor Capable of Blocking the Resistant Gatekeeper Mutant. *Cancer Cell*. 2011;19(5):679-690.
5. Guan J, Tucker ER, Wan H, et al. The ALK inhibitor PF-06463922 is effective as a single agent in neuroblastoma driven by expression of ALK and MYCN. *Disease Models & Mechanisms*. 2016.
6. Lu J, Guan S, Zhao Y, et al. The second-generation ALK inhibitor alectinib effectively induces apoptosis in human neuroblastoma cells and inhibits tumor growth in a TH-MYCN transgenic neuroblastoma mouse model. *Cancer Letters*. 2017;400:61-68.
7. Gettinger SN, Bazhenova LA, Langer CJ, et al. Activity and safety of brigatinib in ALK-rearranged non-small-cell lung cancer and other malignancies: a single-arm, open-label, phase 1/2 trial. *The Lancet Oncology*. 2016;17(12):1683-1696.

8. Infarinato NR, Park JH, Krytska K, et al. The ALK/ROS1 Inhibitor PF-06463922 Overcomes Primary Resistance to Crizotinib in ALK-Driven Neuroblastoma. *Cancer Discovery*. 2016;6(1):96-107.
9. Zhang S, Anjum R, Squillace R, et al. The Potent ALK Inhibitor Brigatinib (AP26113) Overcomes Mechanisms of Resistance to First- and Second-Generation ALK Inhibitors in Preclinical Models. *Clinical Cancer Research*. 2016;22(22):5527-5538.
10. Carneiro BA, Pamarthy S, Shah AN, et al. Anaplastic Lymphoma Kinase Mutation (ALK F1174C) in Small Cell Carcinoma of the Prostate and Molecular Response to Alectinib. *Clinical Cancer Research*. 2018;24(12):2732-2739.
11. Friboulet L, Li N, Katayama R, et al. The ALK Inhibitor Ceritinib Overcomes Crizotinib Resistance in Non-Small Cell Lung Cancer. *Cancer Discovery*. 2014;4(6):662-673.
12. Choi YL, Soda M, Yamashita Y, et al. EML4-ALK Mutations in Lung Cancer That Confer Resistance to ALK Inhibitors. *New England Journal of Medicine*. 2010;363(18):1734-1739.
13. Heuckmann JM, Hölzel M, Sos ML, et al. ALK Mutations Conferring Differential Resistance to Structurally Diverse ALK Inhibitors. *Clinical Cancer Research*. 2011;17(23):7394-7401.
14. Doebele RC, Pilling AB, Aisner DL, et al. Mechanisms of Resistance to Crizotinib in Patients with ALK Gene Rearranged Non-Small Cell Lung Cancer. *Clinical Cancer Research*. 2012;18(5):1472-1482.
15. Katayama R, Shaw AT, Khan TM, et al. Mechanisms of Acquired Crizotinib Resistance in ALK-Rearranged Lung Cancers. *Science Translational Medicine*. 2012;4(120).
16. Shaw AT, Kim D-W, Mehra R, et al. Ceritinib in ALK-Rearranged Non-Small-Cell Lung Cancer. *New England Journal of Medicine*. 2014;370(13):1189-1197.
17. Katayama R, Friboulet L, Koike S, et al. Two Novel ALK Mutations Mediate Acquired Resistance to the Next-Generation ALK Inhibitor Alectinib. *Clinical Cancer Research*. 2014;20(22):5686-5696.
18. Ou S-HI, Ahn JS, De Petris L, et al. Alectinib in Crizotinib-Refractory ALK-Rearranged Non-Small-Cell Lung Cancer: A Phase II Global Study. *Journal of Clinical Oncology*. 2016;34(7):661-668.
19. Rotow J, Bivona TG. Understanding and targeting resistance mechanisms in NSCLC. *Nature Reviews Cancer*. 2017;17(11):637-658.
20. Gainor JF, Dardaei L, Yoda S, et al. Molecular Mechanisms of Resistance to First- and Second-Generation ALK Inhibitors in ALK-Rearranged Lung Cancer. *Cancer Discovery*. 2016;6(10):1118-1133.
21. Holla VR, Elamin YY, Bailey AM, et al. ALK: a tyrosine kinase target for cancer therapy. *Molecular Case Studies*. 2017;3(1).
22. Rashda S, Gerber DE. A crowded, but still varied, space: brigatinib in anaplastic lymphoma kinase-rearranged non-small cell lung cancer. *Translational Cancer Research*. 2017;6(S1):S78-S82.
23. Engelman JA, Jänne PA. Mechanisms of Acquired Resistance to Epidermal Growth Factor Receptor Tyrosine Kinase Inhibitors in Non-Small Cell Lung Cancer. *Clinical Cancer Research*. 2008;14(10):2895-2899.
24. Dearden JC, Cronin MTD, Kaiser KLE. How not to develop a quantitative structure-activity or structure-property relationship (QSAR/QSPR). *SAR and QSAR in Environmental Research*. 2009;20(3-4):241-266.
25. Cherkasov A, Muratov EN, Fourches D, et al. QSAR Modeling: Where Have You Been? Where Are You Going To? *Journal of Medicinal Chemistry*. 2014;57(12):4977-5010.
26. Huang J, Fan X. Why QSAR Fails: An Empirical Evaluation Using Conventional Computational Approach. *Molecular Pharmaceutics*. 2011;8(2):600-608.
27. Muratov EN, Bajorath J, Sheridan RP, et al. QSAR without borders. *Chemical Society Reviews*. 2020;49(11):3525-3564.
28. Golbraikh A, Muratov E, Fourches D, et al. Data Set Modelability by QSAR. *Journal of Chemical Information and Modeling*. 2014;54(1):1-4.
29. Martin TM, Harten P, Young DM, et al. Does Rational Selection of Training and Test Sets Improve the Outcome of QSAR Modeling? *Journal of Chemical Information and Modeling*. 2012;52(10):2570-2578.
30. Fourches D, Muratov E, Tropsha A. Trust, But Verify: On the Importance of Chemical Structure Curation in Cheminformatics and QSAR Modeling Research. *Journal of Chemical Information and Modeling*. 2010;50(7):1189-1204.
31. O'Boyle NM, Banck M, James CA, et al. Open Babel: An open chemical toolbox. *Journal of Cheminformatics*. 2011;3(1).
32. Tetko IV, Sushko I, Pandey AK, et al. Critical Assessment of QSAR Models of Environmental Toxicity against *Tetrahymena pyriformis*: Focusing on Applicability Domain and Overfitting by Variable Selection. *Journal of Chemical Information and Modeling*. 2008;48(9):1733-1746.
33. Masand VH, Rastija V. PyDescriptor : A new PyMOL plugin for calculating thousands of easily understandable molecular descriptors. *Chemometrics and Intelligent Laboratory Systems*. 2017;169:12-18.
34. Gramatica P, Chirico N, Papa E, et al. QSARINS: A new software for the development, analysis, and validation of QSAR MLR models. *Journal of Computational Chemistry*. 2013;34(24):2121-2132.
35. Zaki MEA, Al-Hussain SA, Bukhari SNA, et al. Exploring the Prominent and Concealed Inhibitory Features for Cytoplasmic Isoforms of Hsp90 Using QSAR Analysis. *Pharmaceutics*. 2022;15(3).

36. Zaki MEA, Al-Hussain SA, Masand VH, et al. Mechanistic and Predictive QSAR Analysis of Diverse Molecules to Capture Salient and Hidden Pharmacophores for Anti-Thrombotic Activity. *International Journal of Molecular Sciences*. 2021;22(15).
37. Gramatica P. Principles of QSAR Modeling. *International Journal of Quantitative Structure-Property Relationships*. 2020;5(3):61-97.
38. Gramatica P. On the Development and Validation of QSAR Models. *Computational Toxicology. Methods in Molecular Biology* 2013. p. 499-526.
39. Chirico N, Gramatica P. Real External Predictivity of QSAR Models: How To Evaluate It? Comparison of Different Validation Criteria and Proposal of Using the Concordance Correlation Coefficient. *Journal of Chemical Information and Modeling*. 2011;51(9):2320-2335.
40. Gramatica P. Principles of QSAR models validation: internal and external. *QSAR & Combinatorial Science*. 2007;26(5):694-701.
41. Pushpakom S, Iorio F, Eyers PA, et al. Drug repurposing: progress, challenges and recommendations. *Nature Reviews Drug Discovery*. 2018;18(1):41-58.
42. Sleire L, Førde HE, Netland IA, et al. Drug repurposing in cancer. *Pharmacological Research*. 2017;124:74-91.
43. Eid AH. Drug Repurposing in Cancer: Now and Beyond. *Current Medicinal Chemistry*. 2021;28(11):2083-2084.
44. Johnson TW, Richardson PF, Bailey S, et al. Discovery of (10R)-7-Amino-12-fluoro-2,10,16-trimethyl-15-oxo-10,15,16,17-tetrahydro-2H-8,4-(metheno)pyrazolo[4,3-h][2,5,11]-benzoxadiazacyclotetradecine-3-carbonitrile (PF-06463922), a Macrocyclic Inhibitor of Anaplastic Lymphoma Kinase (ALK) and c-ros Oncogene 1 (ROS1) with Preclinical Brain Exposure and Broad-Spectrum Potency against ALK-Resistant Mutations. *Journal of Medicinal Chemistry*. 2014;57(11):4720-4744.
45. Gaudreault F, Morency L-P, Najmanovich RJ. NRGsuite: a PyMOL plugin to perform docking simulations in real time using FlexAID. *Bioinformatics*. 2015;31(23):3856-3858.
46. Gaudreault F, Najmanovich RJ. FlexAID: Revisiting Docking on Non-Native-Complex Structures. *Journal of Chemical Information and Modeling*. 2015;55(7):1323-1336.
47. Bowers KJ, Sacerdoti FD, Salmon JK, et al. Molecular dynamics---Scalable algorithms for molecular dynamics simulations on commodity clusters. *Proceedings of the 2006 ACM/IEEE conference on Supercomputing - SC '06* 2006.
48. Shivakumar D, Williams J, Wu Y, et al. Prediction of Absolute Solvation Free Energies using Molecular Dynamics Free Energy Perturbation and the OPLS Force Field. *Journal of Chemical Theory and Computation*. 2010;6(5):1509-1519.
49. Jorgensen WL, Chandrasekhar J, Madura JD, et al. Comparison of simple potential functions for simulating liquid water. *The Journal of Chemical Physics*. 1983;79(2):926-935.
50. Martyna GJ, Tobias DJ, Klein ML. Constant pressure molecular dynamics algorithms. *The Journal of Chemical Physics*. 1994;101(5):4177-4189.
51. Martyna GJ, Klein ML, Tuckerman M. Nosé-Hoover chains: The canonical ensemble via continuous dynamics. *The Journal of Chemical Physics*. 1992;97(4):2635-2643.
52. Di Pierro M, Elber R, Leimkuhler B. A Stochastic Algorithm for the Isobaric-Isothermal Ensemble with Ewald Summations for All Long Range Forces. *Journal of Chemical Theory and Computation*. 2015;11(12):5624-5637.
53. Piao L, Chen Z, Li Q, et al. Molecular Dynamics Simulations of Wild Type and Mutants of SAPAP in Complexed with Shank3. *International Journal of Molecular Sciences*. 2019;20(1).

40

Synthesis, characterization and biocidal study of some novel 2-hydroxy 4,6-disubstituted phenyl pyrimidines bearing 4-bromo phenol moiety**Rajendra M. Pathade*, Pravin. S. Bodkhe**Department of chemistry, Vidyabharati Mahavidyalaya, Amravati. * Email: rmpathade@gmail.com**ABSTRACT**

In the present research work a series of 2-Hydroxy 4,6-disubstituted phenyl Pyrimidine derivatives was synthesized from 4-bromo phenol as a precursor. The compound 4-bromo phenol react with acetic anhydride to obtained 4-bromo phenyl acetate (1) then it follows Fries' rearrangement reaction to form 5-bromo,2-hydroxy acetophenone(2).The compound(2) allowed to react with different benzoic acids to give corresponding substituted 2-benzoyloxy acetophenone (3a-d) which follow B.V.T. rearrangement reaction to obtained propan1,3-diones(4a-d) and then it reacts with Urea to yield 2-hydroxy 4,6-disubstituted phenyl pyrimidine derivatives (5a-d).The newly synthesized compounds are characterized by IR, ^1H NMR, Mass spectral and elemental analysis. These compounds were also screened for their biocidal study i.e., antibacterial, antifungal, anti-oxidant and anti-inflammatory activities.

KEYWORDS: 4-bromo phenol, Urea,2-Hydroxy 4,6-disubstituted phenyl Pyrimidine, antibacterial, antifungal, anti-oxidant and anti-inflammatory activities.

INTRODUCTION

Heterocyclic compounds are abundant in nature and it have great significance to life. The natural heterocyclic compounds such as vitamins, hormones, antibiotics etc. These heterocyclic compounds containing nitrogen play an important role in medicinal chemistry and also contribute to the society. Pyrimidine is a six-member heterocyclic compound which contains two nitrogen atoms at positions 1 and 3. Pyrimidine derivatives are known to be biologically active compounds and substituted pyrimidines have shown wide range of biological activities like Anticancer [1,2], antibacterial [3-6], antifungal [7], antioxidant [8,9], anti-inflammatory [10,11],anti-HIV [12],antitumor [13], antiparasitic [14],anti-Alzheimer's agent [15], anti-diabetic agent [16].In addition to the diverse biological activities of pyrimidines play an essential role in several biological processes and have a considerable chemical and pharmacological importance. In the present research work some novel 2-hydroxy 4,6-disubstituted phenyl pyrimidine(5a-d) compounds have been synthesized and studies their structural characterization, antibacterial, antifungal, antioxidant and anti-inflammatory activities.

EXPERIMENTAL SECTION**Materials and Methods**

All the solvents and chemicals were of research grade and highest purity. The IR spectrum was recorded by using Shimadzu IR affinity-1FTIR instrument, ^1H NMR spectra were recorded on Bruker advance II 400 MHz spectrometer, Mass spectra were recorded on ESI and Melting point were determined by open capillary tube method which are uncorrected.All the synthesized compounds were purified by recrystallization and purity of the compound was checked by TLC and elemental analysis.

General procedure for the Synthesis of 2-hydroxy 4,6-disubstituted phenyl Pyrimidine derivatives (5a-d)

The synthesis involves the following steps.

Synthesis of 4-bromo phenyl acetate (1)

Take 4-bromo phenol (0.05M) fused with acetic anhydride(5ml) and sodium acetate. The mixture was refluxed for 1hr. then cooled for 15 min. and poured in ice water. Acetate layer was separate out by separating funnel. The product was obtained 4-bromo phenyl acetate (1).

Synthesis of 5-bromo,2-hydroxy acetophenone (2)

Place aluminum chloride (120 g) in kjeldal flask and add compound (1)(40 ml) drop wise. Heat the reaction mixture in oil bath for 60 min at 120°C. It was cooled and add in to acidified ice crushed water to get crude product of 5-bromo,2-hydroxy acetophenone (2).

Synthesis of 2-substituted benzoyloxy 5-bromo acetophenone (3a-d)

A mixture of compound (2)(0.05M) and substituted benzoic acid (0.05M) were dissolved in dry pyridine at 0°C. Then add POCl₃ dropwise with constant stirring below 10°C. The reaction mixture was allowed to stand for overnight at room temperature. Then it was poured in ice cold 10% HCl. Then the product was wash by 10% NaHCO₃ and water. Recrystallized the product by ethanol to obtained a series of 2- substituted benzoyloxy 5-bromo acetophenone (3a-d).

Synthesis of substituted propane 1,3-diones (β-diketones) (4a-d)

Take compound (3a-d) (0.05M) was dissolved in dry pyridine. The reaction mixture was heated up to 60°C with pulverized KOH slowly with constant stirring. After 5-6 hr. the reaction mixture was acidified by dil. HCl in ice cold water. The crude product was filtered, washed it with NaHCO₃ (10%) and water. Recrystallized the product from ethanol-acetic acid mixture to get substituted propane 1,3-diones (4a-d).

Synthesis of 2-hydroxy-4,6-disubstituted phenyl pyrimidine derivatives (5a-d)

A mixture of compound (4a-d) (0.02 M) and urea (0.02 M) dissolved in DMF solvent. It was refluxed on water bath at 75°C for 1hr. then mixture was cooled and pour in ice cold water. The product was recrystallized by aq. alcohol to obtained a series of 2-hydroxy-4,6-disubstituted phenyl pyrimidine derivatives (5a-d)

General reactions scheme is given below.

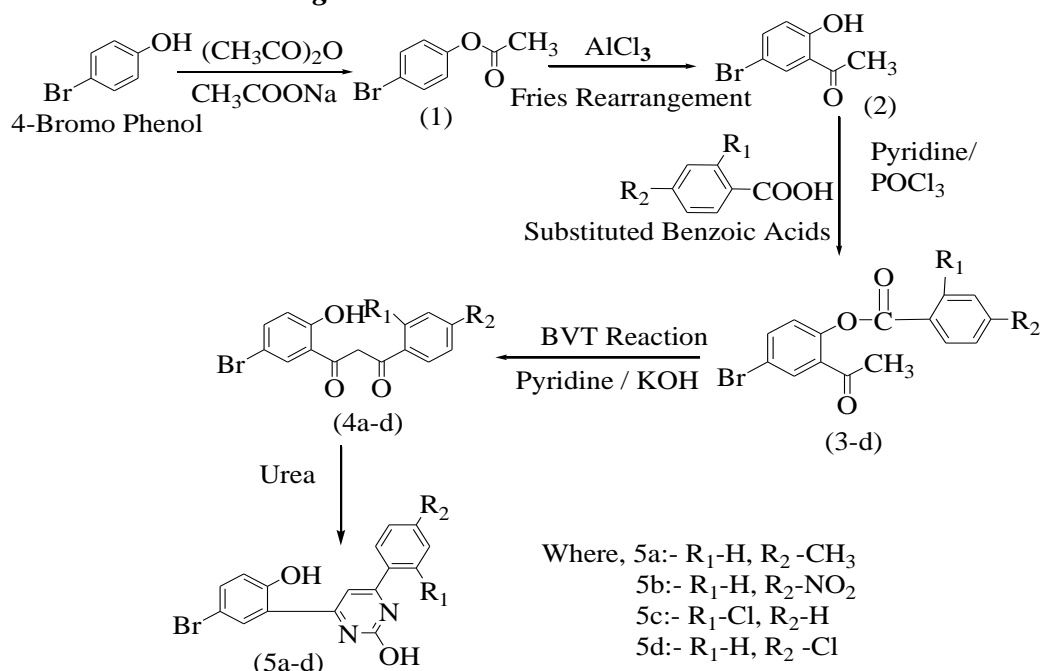


Figure-1-The general reaction scheme for the synthesis of 2-hydroxy-4,6-disubstituted phenyl pyrimidines (5a-d)

Table No.1: Physical data of 2-hydroxy-4,6-disubstituted phenyl Pyrimidines (5a-d)

Code	Compound Name	M.F./ M.W.	Rf value	M.P. (⁰ C)	Yield (%)
5a	2-hydroxy-4-(4-methyl phenyl)-6-(2-hydroxy-5 bromo phenyl) pyrimidine	C ₁₇ H ₁₃ BrN ₂ O ₂ / (357.20)	0.72	80 - 86	58%
5b	2-hydroxy-4-(4-nitro phenyl)-6-(2-hydroxy-5 bromo phenyl) pyrimidine	C ₁₆ H ₁₀ BrN ₃ O ₄ / (388.17)	0.68	116 - 122	71%
5c	2-hydroxy-4-(2-chloro phenyl)-6-(2-hydroxy-5 bromo phenyl) pyrimidine	C ₁₆ H ₁₀ BrClN ₂ O / (377.96)	0.66	74 - 78	61%
5d	2-hydroxy-4-(4-chloro phenyl)-6-(2-hydroxy-5 bromo phenyl) pyrimidine	C ₁₆ H ₁₀ BrClN ₂ O / (377.96)	0.70	112- 116	65%

Antimicrobial Activity

The in-vitro anti-microbial screening of newly synthesized 2- hydroxy -4,6-disubstituted phenyl pyrimidines (5a-d) was carried out against bacteria *staphylococcus aureus* (gram +ve), *Salmonella typhus* (gram-ve) and fungi *Candida albicans* and *aspergillus niger* by disc diffusion method [17,18] and compared with that of the standard drugs Oxacillin (2 µg) and Fluconazole (25 µg) respectively of each drug was defined as the lowest concentration of an antimicrobial that will inhibit the visible growth of microorganism after incubation time. Muller Hinton Agar was used as basal medium for test of bacteria and fungi respectively. The compounds tested at concentration of 50 µg/ml, 100 µg/ml and 250 µg/ml for bacterial and fungal growth in DMSO solvent it was added to the wells made on culture medium. After 24 hrs. of incubation at 37⁰C for antibacterial activity and after 24 hrs. at room temp. for antifungal activity, record the zone of inhibition was compared with the standard drug Oxacillin and Fluconazole.

Anti-Inflammatory Activity

Take 10 mg of Ibuprofen as a reference drug was added to 10 ml of distilled water. Serial dilution from above stock solution takes 0.1 ml, 0.2 ml, 0.3 ml and prepare 10 ppm, 20 ppm and 30 ppm and also it was performed for sample 2- hydroxy -4,6-disubstituted phenyl pyrimidines (5a-d) extract. The reaction mixtures were prepared using 2.8 ml of phosphate-buffered saline (pH 6.4) and 0.2 ml of egg albumin. Then take 2 ml of extract from each different concentration were mixed gently with reaction mixtures. A similar procedure was used for reference drug ibuprofen. The absorbance of these solutions was determined by using spectrophotometer at wavelength of 660 nm. The % denaturation of the protein (% inhibition) was determined. [19]

Anti-Oxidant Activity

Stock solution of DPPH (2,2-diphenyl-1-picrylhydrazyl) was prepared by dissolving 1.083 mg in 10 ml of ethanol. Stock solution of sample 2-hydroxy-4,6-disubstituted phenyl pyrimidines (5a-d) take 100 µg/ml was prepared by dissolving 1 ml of sample in 10 ml of ethanol. From this stock solution, further dilutions were prepared of concentrations 10, 20, 30, 40 and 50 µg/ml using ethanol. Similarly, stock solution of standard ascorbic acid was prepared by dissolving 10 mg ascorbic acid in 10 ml ethanol. From this stock solution further dilutions of concentrations 1, 2, 3, 4 and 5 µg/ml were prepared. Absorbance of blank (5 ml ethanol + 1 ml DPPH solution) as a positive control was recorded using colorimeter at 517 nm. Similarly, the absorbance of

sample and comparative standard ascorbic acid was taken at 517 nm. The % scavenging activity was determined.[20]

RESULTS AND DISCUSSION

Spectroscopic characterization data

(5a) 2-hydroxy-4-(4-methyl phenyl)-6-(2-hydroxy-5 bromo phenyl) pyrimidine

Solid, yellow, IR (cm⁻¹): 3200 (Ar-OH), 3058 (Ar-C-H), 2928 (Ar-CH₃), 1613 (C=N), 1458 (C=C), 640 (C-Br), 1280 (C-O); ¹H-NMR (δ ppm): δ 7.90-7.98 (m, 8H of Ar-H), δ 7.36-7.40 (s, 1H of -OH), δ 2.38 (s, 3H of -CH₃); MASS (m/z, %): 358 (M⁺); C, H, N, O % Calculated (Found) C: 57.16 (56.86), H: 3.67 (3.61), N: 7.84 (7.62), O: 8.96 (8.17).

(5b) 2-hydroxy-4-(4-nitro phenyl)-6-(2-hydroxy-5 bromo phenyl) pyrimidine

Solid, yellow, IR (cm⁻¹): 3379 (Ar-OH), 3096 (Ar-C-H), 1605 (C=N), 1456 (C=C), 705 (C-Br), 1207 (C-O), 1345 (-NO₂); ¹H-NMR (δ ppm): δ 7.2-8.4 (m, 8H of Ar-H), δ 6.85 (s, 1H of Ar-OH); MASS (m/z, %): 388.99 (M⁺); C, H, N, O % Calculated (Found): C: 49.51 (48.29), H: 2.60 (2.13), N: 10.83 (10.01), O: 16.49 (15.59).

(5c) 2-hydroxy-4-(2-chloro phenyl)-6-(2-hydroxy-5 bromo phenyl) pyrimidine

Solid, brown, IR (cm⁻¹): 3076 (Ar-OH), 2927 (Ar-C-H), 1637 (C=N), 1459 (C=C), 529 (C-Br), 1275 (C-O), 757 (C-Cl); ¹H-NMR (δ ppm): δ 7.31-8.19 (m, 8H of Ar-H), δ 6.69 (s, 1H of Ar-OH); MASS (m/z, %): 377.97 (M⁺); C, H, N, O % Calculated (Found): C: 50.89 (50.02), H: 2.67 (2.13), N: 7.42 (7.15), O: 8.47 (7.98).

(5d) 2-hydroxy-4-(4-chloro phenyl)-6-(2-hydroxy-5 bromo phenyl) pyrimidine

Solid, yellow, IR (cm⁻¹): 3188 (Ar-OH), 3088 (Ar-C-H), 1610 (C=N), 1465 (C=C), 527 (C-Br), 1274 (C-O), 641 (C-Cl); ¹H-NMR (δ ppm): δ 7.90-7.98 (m, 8H of Ar-H), δ 7.36-7.40 (s, 1H of Ar-OH); MASS (m/z, %): 379 (M⁺); C, H, N, O % Calculated (Found): C: 50.89 (50.12), H: 2.67 (1.99), N: 7.42 (6.76), O: 8.47 (8.17).

BIOCIDAL STUDY

Table No.2- Antibacterial activity of 2-hydroxy 4,6-disubstituted pyrimidines (5a-5d)

Compound code	Zone of inhibition in mm							
	<i>Salmonella typhi</i> (gram -tive)				<i>Staphylococcus aureus</i> (gram +tive)			
	Concentrations µgm/ml				Concentrations µgm/ml			
	50	100	250	Standard Ofloxacin 2 mcg	50	100	250	Standard Ofloxacin 2 mcg
5a	++	++	++	++	++	+++	+++	+++
5b	++	++	++	-	-	-	-	-
5c	-	-	-	-	++	+++	+++	-
5d	-	-	-	-	-	++	++	-
Highly active+++ = 13-24, Moderate active++ = 7-12, Less active+ = 1-6, No zone of inhibition-								

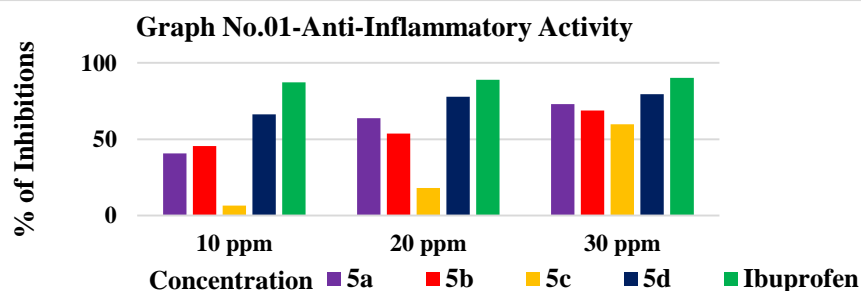
Table No.3- Antifungal activity of 2-hydroxy 4,6-disubstituted pyrimidines (5a-5d)

Compound code	Zone of inhibition in mm							
	<i>Candida albicans</i>				<i>Aspergillus niger</i>			
	Concentrations µgm/ml				Concentrations µgm/ml			
	50	100	250	Standard Fluconazole 25 µgm	50	100	250	Standard Fluconazole 25 µgm
5a	-	-	-	+++	-	-	-	+++
5b	-	-	++	-	-	++	++	-
5c	-	++	+++	-	-	-	++	-
5d	-	-	-	-	-	-	-	-
Highly active+++ = 13-24/Moderate active++ = 7-12/Less active+ = 1-6/No zone of inhibition-								

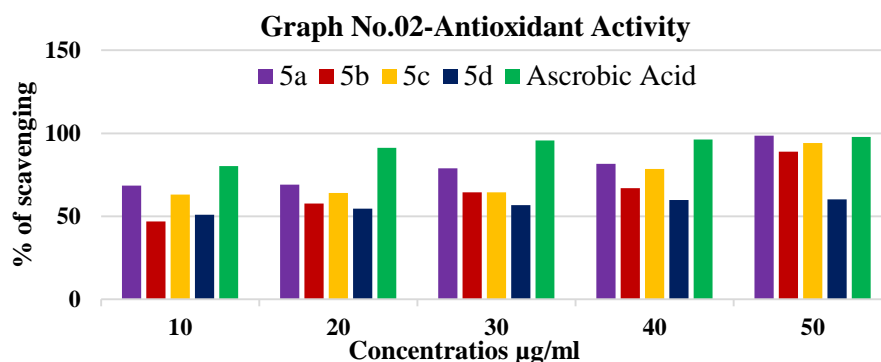
The antibacterial activity results revealed that compounds showed significant activity against gram +ve organisms. The compound 5a and 5b showed moderate activity against *Salmonella typhi* and compounds 5a and 5c shows highly activity and 5d shows moderate activity against *Staphylococcus aureus*. The compounds 5c and 5d does not showed any zone of inhibition against the gram -ve organism. In the antifungal activity, compound 5b and 5c showed moderate to weak activity against *Candida albicans* and *Aspergillus niger*. The compounds 5a and 5d does not showed any zone of inhibition in fungal activity at different concentration.

Table No.4-Anti-inflammatory activity of 2-hydroxy 4,6-disubstituted pyrimidines(5a-d)

Sr. No.	Compound Code	% Inhibition		
		Concentration of compound in ppm		
		10 ppm	20 ppm	30 ppm
1	5a	40.67	63.68	73.06
2	5b	45.47	53.75	68.76
3	5c	6.34	17.88	59.71
4	5d	66.33	77.81	79.41
5	Ibuprofen	87.36	88.90	90.23

**Table No.5- Anti-oxidant activity of 2-hydroxy 4,6-disubstituted pyrimidines(5a-d)**

Sr. No.	Compound Code	% scavenging activity				
		Concentration of compound in µg/ml				
		10 µg/ml	20 µg/ml	30 µg/ml	40 µg/ml	50 µg/ml
1	5a	68.43	69.08	78.95	81.58	98.46
2	5b	46.93	57.68	64.48	66.89	88.82
3	5c	63.16	64.04	64.48	78.51	94.08
4	5d	50.88	54.61	56.80	59.87	60.09
5	Ascorbic Acid (Standard)	80.26	91.22	95.61	96.27	97.80



CONCLUSION

In the present work newly synthesized 2-hydroxy 4,6-disubstituted phenyl Pyrimidines containing 4-bromo phenol moiety involves different steps to get good yield. The structure of synthesized compound was elucidated on the basis of ¹H-NMR, IR and Mass spectra. In antibacterial activity compound 5a and 5b shows moderate activity against *Salmonella typhi* and the compound 5a, 5c and 5d shows highly active to moderate zone of inhibition against *Staphylococcus aureus*. In antifungal activity compound 5b and 5c showed moderate to weak activity against *Candida albicans* and *Aspergillus niger* at concentration 100 µgm and 250 µgm. Also compounds **5a, 5b, 5c** and **5d** exhibited significant anti-inflammatory activity by using albumin denaturation technique at 30 ppm concentration. Antioxidant activity as indicated by absorbance of compounds 5a-5d increased with increasing concentration. Higher value of absorbance of the reaction mixture indicated greater reducing power. The reducing power was found to be in order of **5a>5c>5b>5d**

ACKNOWLEDGEMENT

The author is thankful to the Principal, Vidyabharati Mahavidyalaya, Amravati for providing the laboratory facilities and Director, SAIF Panjab University, Chandigarh for providing NMR, IR and Mass spectra analysis. Also thankful to Prof. Dr. Sharda Deore Government Pharmacy college, Amravati for Pharmacological activity and Dr. S. R. Gulhane, Microbiology Diagnostic Lab, Amravati for biocidal activity.

REFERENCES

- [01] Zhao A., Gao X., Wang Y., Ali J., Wang Y., Chen Y. *et al.* 'Discovery of novel c-Met kinase inhibitors bearing a thieno [2,3-*d*] pyrimidine or Furo[2,3-*d*] pyrimidine scaffold' *Bioorgan Med Chem*, **2011**, 19:3906-3918.
- [02] Shaaban MA, Mohamed KO, Hegazi ME, Montaser A. Shaykoon, Yaseen AMM Elshaier 'Synthesis of Some Pyrimidine and Fused Pyrimidine Derivatives with Antimicrobial and Anticancer Activities' *Der Pharma Chemica*, **2018**; 10(7):180-200.
- [03] Liu, Yu; Sun, Xiao; Yin; Da; Yuan, Fang, 'Syntheses and biological activity of chalcones -imidazole derivatives' *Research on Chemical Intermediates*, **2013**, Vol.39, pp.1037-1048.
- [04] Abdel Gawad MA. Synthesis and antibacterial evaluation of new azo-pyrimidine derivatives. *J Appl Pharm Sci.* **2019**; 9(1):9-16
- [05] Sebastin V. *et al.*, "Synthesis and Antibacterial Activity of Pyrimidine Derivatives of 1,3-Dihydropyrimidine" *Am. J Pharm Tech Res.* **2017**; 7(5):24-29
- [06] Binani *et al.* "synthesis, characterization and in vitro antimicrobial evaluation of novel 2-mercapto-4,6-disubstituted phenyl pyrimidine derivatives" *int j pharm pharm sci*, vol 6, issue 1, **2014**, 461-463, ISSN- 0975-1491.
- [07] Y. M. Zohny *et al.* *Pharmacophore* **2015**, Vol. 6 (6), 255-266.
- [08] K. Elumalai, M. A. Ali, M. Elumalai, K. Eluri, S. Srinivasan, *J Acute Disease*, **2013**, 316-321.
- [09] T. N. Doan, D. T. Tran. *Pharmacol. Pharm.*, **2011**, 2, 282-288.
- [10] C. M. Bhalgat, M. I. Ali, B. Ramesh, G. Ramu, *Ara J Chem.*, **2011**, 1-8.
- [11] Bhalgat CM., *et al.* "Novel pyrimidine and its triazole fused derivatives: Synthesis and investigation of antioxidant and anti-inflammatory activity" *Arabian Journal of Chemistry* 7.6, **2014**, 986-993.
- [12] Kashyap, S. J. *et al.* *J. Adv. Sci. Res.* **2011**, 2, 18-24.
- [13] Li Q., *et al.* "Synthesis and biological activity of fused furo [2,3-*d*] pyrimidinone derivatives as analgesic and antitumor agents" *Research on Chemical Intermediates* 42.2, **2016**, 939-949.
- [14] Azas, N.; Rathelot, P.; Djekou, S.; Delmas, F.; Gellis, A.; Giorgio, C. D.; Vanelle, P.; Timon-David, P. *Farmaco* **2003**, 58, 1263-1270.
- [15] Elmegeed G. A., Ahmed H. H., Hashash M. A., Abd-Elhalim M. M., El-kady D. S. "Synthesis of novel steroidal curcumin derivatives as anti-Alzheimer's disease candidates: evidences-based on *in vivo* study Steroids". **2015**, 101:78-89.
- [16] Barakat A. *et al.* "Synthesis and structure investigation of novel pyrimidine-2,4,6-trione derivatives of highly potential biological activity as anti-diabetic agent", *Russian Journal of Bioorganic Chemistry* 41, **2015**, 192-200.
- [17] Sambhaji P. Vartale *et al.* 'Synthesis and antimicrobial evaluation of pyrimido pyrimidine derivatives', *IJRPC* **2015**, 5(1), 208-214 ISSN: 2231-2781.
- [18] Vijay V. Dabholkar and Ashish S. Sanghvi. *Indian Journal of Heterocyclic Chemistry*, **2006**, 16:105.
- [19] Monica Kachroo *et al.* "Synthesis and Biological Activities of Some New Pyrimidine Derivatives From Chalcones" *Der Pharma Chemica*, **2014**, 6(2), 352-359.
- [20] Reşat Apak *et al.* *J. Agric. Food Chem.* **2016**, 64, 997-1027, DOI: 10.1021/acs.jafc.5b04739.

Investigation of antimicrobial Activities of Dihydropyrazines

Manish Fukate^a, Sheryil Malvilayils^a, Roshan Jaiswal^b, Swati Bawiskar^b

^a G H Raisonni University Amravati ^a G H Raisonni University Amravati

^b G H Raisonni University Saikheda ^b G H Raisonni University Saikheda

corresponding author manish.fukate@raisonni.net

Abstract

Seven Dihydropyrazines **4a–g** are screened for their antibacterial activity against *Staphylococcus aureus*, *Escherichia coli*, *Klebsiella pneumoniae*, *Pseudomonas aeruginosa*, *Salmonella typhi* and antifungal activity against *Candida albicans*, *Aspergillus flavus*, *Rhizopus* and *Mucor*. Ciprofloxacin is used for the standard for antibacterial and Amphotericin B is used for the standard for antifungal studies. Compounds **4b**, **4c**, **4f** and **4g** exhibited excellent *in vitro* antibacterial activity against all the tested organisms. Whereas the same set of compounds exerted potent *in vitro* antifungal activity against *Candida albicans*, *Aspergillus flavus* and *Rhizopus*.

Keywords: Dihydropyrazines, Antibacterial activity, antifungal activity, Ciprofloxacin, Amphotericin B.

1. INTRODUCTION

The biological and physical roles of dihydropyrazines (DHPs) such as DNA cleavage [1], growth inhibition of *Escherichia coli* [2], Cyclooxygenase inhibitory activity [3] and NPY antagonists [4] are well documented. Dihydropyrazines are universal in the human body [5] however, there is little reported concerning the biological and physiological roles of DHPs. Yamaguchi *et al.* [1] reported generation of free radicals from dihydropyrazines with DNA strand-

Breakage activity. Takechi *et al.* [6] reported the growth inhibition and mutagenesis induced in *Escherichia coli* by dihydropyrazines with DNA strand-cleaving activity. 2-cyanopyrazine derivatives show anticancer, anti-inflammatory and analgesic activities [7]. Pyrazine derivatives exhibit a tuberculostatic activity [8]. It also exhibits antimicrobial [9] and biological [10] activities. Alkyl substituted pyrazines are found in the growth medium of the polymyxin-producing bacterium *Paenibacillus polymyxa* [11].

The above observations place new emphasis on the need of as well as search for alternative new and more effective antimicrobial agents with a broad spectrum.

The aim of this study was to evaluate the biological activities of dihydropyrazines **4a–4g**. The results of the antibacterial and antifungal activities are discussed in this paper. To perceive structure-activity relationship well, numbering of the target compound is shown below **Fig. 1**.

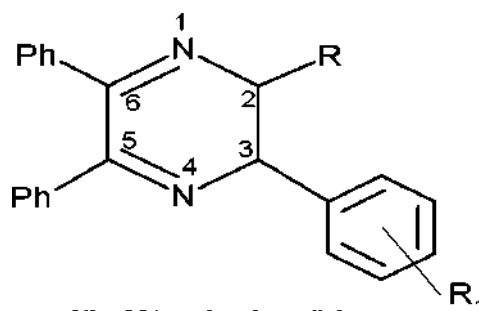


Fig.1 Numbering of **4a–g**

2. MATERIALS & METHODS

2.1 Materials

All the bacterial strains namely *Staphylococcus aureus*, *Escherichia coli*, *Klebsiella pneumoniae*, *Pseudomonas aeruginosa*, *Salmonella typhi* and fungal strains namely *Candida albicans*, *Aspergillus flavus*, *Rhizopus* and *Mucor* were obtained

2.2 Methods

The compounds were synthesized by the following literature procedure.¹² The *in vitro* antimicrobial activities of the compounds were tested in Sabouraud's dextrose broth (SDB, Hi-media, Mumbai) for fungi and nutrient broth (NB, Hi-media, Mumbai) for bacteria by the twofold serial dilution method.¹³

The test compounds were dissolved in dimethyl sulfoxide (DMSO) to obtain 1 mg/ml stock solutions. Seeded broth (broth containing microbial spores) was prepared in NB from 24 h old bacterial cultures on nutrient agar (Hi-media, Mumbai) at 37 ± 1 °C while fungal spores from 24 h to 7-day-old Sabouraud's agar slant cultures were suspended in SDB. The colony forming units (cfu) of the seeded broth were determined by the plating technique and adjusted in the range of 10^4 – 10^5 cfu/ml. The final inoculum size was 10^5 cfu/ml for the antibacterial assay and 1.1 – 1.5×10^2 cfu/ml for the antifungal assay. Testing was performed at 7.4 ± 0.2 . Exactly 0.2 ml of the solution of test compound was added to 1.8 ml of seeded broth to form the first dilution. One ml of this was diluted with a further 1 ml of the seeded broth to give the second dilution and so on until six such dilutions were obtained. A set of assay tubes containing only seeded broth was kept as control and likewise solvent controls were also run simultaneously. The tubes were incubated in biochemical oxygen demand (BOD) incubators at 37 ± 1 °C for bacteria and 28 ± 1 °C for fungi. The minimum inhibitory concentrations (MICs) were recorded by visual observations after 24 h (for bacteria) and 72–96 h (for fungi) of incubation. Ciprofloxacin was used as a standard for the bacterial study while Amphotericin B was used as a standard for the fungal study.

3. RESULT & DISCUSSION

Physical data of the compounds **4a–4g** are given in the **Table 1**.

Table 1. Physical data of the compounds **4a–4g**

Compound	R	Yield (%)	Melting Point °C
4a	H	96	242- 243
4b	4-Cl	98	211 - 212
4c	2-Cl	92	235- 236
4d	4-CH ₃	96	254- 255
4e	4-OCH ₃	98	208- 209
4f	4-NO ₂	94	284 - 285
4g	4-F	96	236 - 237

In vitro antibacterial and antifungal activity

Compounds **4a–4g** were tested for their antibacterial activity *in vitro* against *Staphylococcus aureus*(SA), *Escherichai coli* (EC), *Klebsiella pneumonia*(KP), *Pseudomonas aeruginosa*(PA) and *Salmonella typhi* (ST). Ciprofloxacin was used as standard drug. Minimum inhibitory concentration (MIC) in µg/ml values shown in **Table 2**.

Table 2. In vitro antibacterial activity of compounds **4a–g**

Compound	Minimum Inhibitory Concentration (MIC) in µg/ml				
	SA	EC	KP	PA	SA
4a	100	200	200	200	100
4b	25	25	50	25	25
4c	25	25	50	25	25
4d	50	100	100	100	50
4e	50	100	100	50	50
4f	6.25	6.25	6.25	12.5	6.25
4g	3.13	3.13	6.25	3.13	3.13
Ciprofloxacin	25	25	12.5	25	25

All the 3,4-dihydropyrimidin-2(1H)-ones **4a–4g** exerted potent antibacterial activity *in vitro* against the tested bacterial strains. Moreover, compounds **4b**, **4c**, **4f** and **4g** exerted excellent antibacterial activities against *S. aureus*, *E. coli*, *K. pneumoniae*, *P. aeruginosa* and *S. typhi*. A comparative study of minimum inhibitory concentration for the compounds **4a–4g** using standard Ciprofloxacin *versus* bacterial strains given in **Fig. 2**.

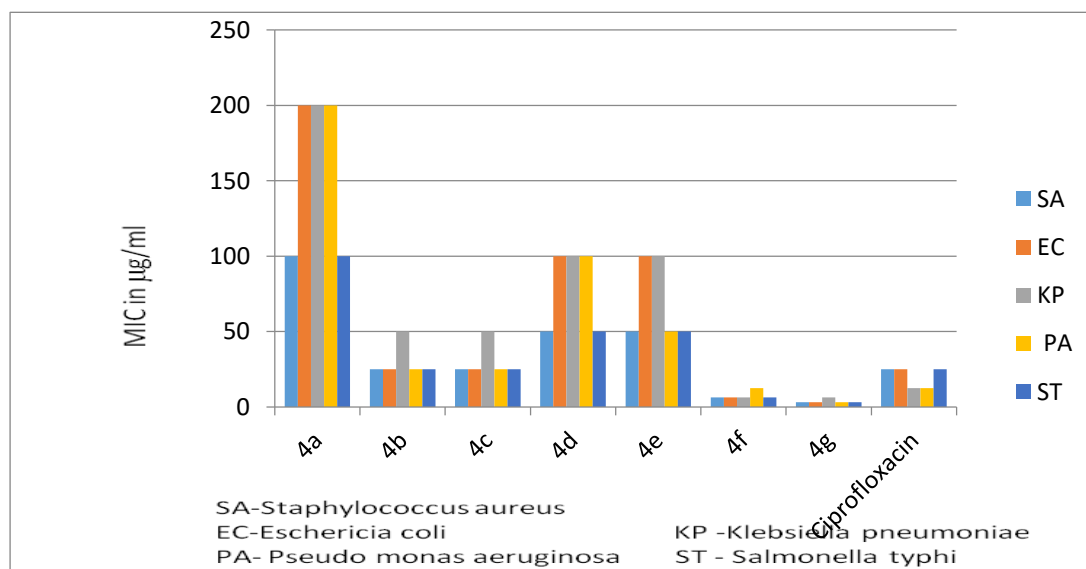


Fig. 2. Comparison of minimum inhibitory concentration of compounds **4a–g** with Ciprofloxacin (as standard) against bacterial strains from serial dilution method.

The *in vitro* antifungal activity of the synthesized compounds **4a–4g** was studied against the fungal strains viz., *Candida albicans* (CA), *Aspergillus flavus* (AF), *Rhizopus* and *Mucor*. Amphotericin B was used as a standard drug. Minimum inhibitory concentration (MIC) in µg/ml values is shown in **Table 3**.

Table 3. In vitro antifungal activity of compounds **4a–g**

Compound	Minimum Inhibitory Concentration (MIC) in $\mu\text{g/ml}$			
	CA	AF	<i>Rhizopus</i>	<i>Mucor</i>
4a	100	200	200	200
4b	25	50	25	25
4c	25	50	25	25
4d	50	100	50	50
4e	50	100	100	50
4f	6.25	6.25	12.5	6.25
4g	3.13	3.13	6.25	3.13
Amphotericin B	25	25	50	25

Compounds **4b**, **4c**, **4f** and **4g** exhibited excellent antifungal activities against all the tested fungal strains except *Mucor*. Minimum inhibitory concentration of compounds **4a–4g** were compared with standard Amphotericin B against fungal strains shown in **Fig 3**.

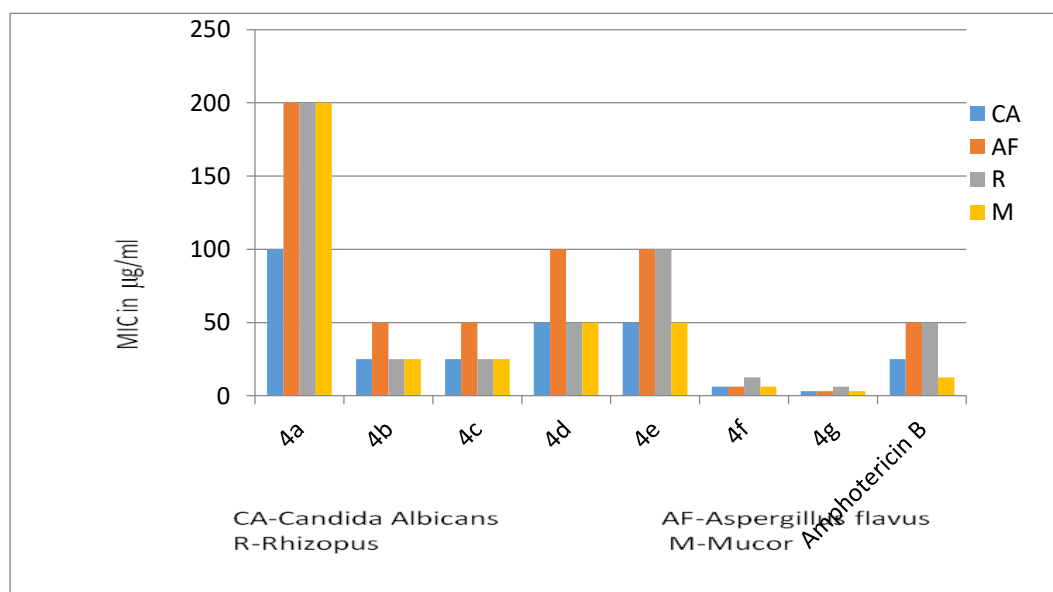


Fig. 3. Comparison of minimum inhibitory concentration of compounds **4a–g** with Amphotericin B (as standard) against fungal strains from serial dilution method.

4. Conclusion

Results of this study show that compounds **4b**, **4c**, **4f** and **4g** which contain chloro, nitro and fluoro moieties exerted excellent antimicrobial activities against the tested organisms. Further development of this group of 3,4-dihydropyrimidinones may lead to compounds with better pharmacological profile than standard drugs and serve as templates for the construction of better drugs to come to blows bacterial and fungal infections.

References

- [1] Yamaguchi T, Matsumoto S, Watanabe K. Generation of free radicals from dihydropyrazines with DNA strand-breakage activity. *Tetrahedron Lett.* 1998; 39: 8311 - 8312.
- [2] Takeda O, Takechi S, Katoh T, Yamaguchi T. The role of dihydropyrazines in accelerated death of *Escherichia coli* on addition of copper(II). *Biol Pharm Bull.* 2005; 28: 1161 - 1164.
- [3] Singh S K, Saibaba V, Ravikumar V, Rudrawar S V, Daga P, Rao C S, Akhila V, Hegde P, Rao Y K. Synthesis and biological evaluation of 2,3-dihydropyrazines and quinoxalines as selective COX-2 inhibitors. *Bioorg Med Chem.* 2004; 12: 1881 - 1893.
- [4] Sit S Y, Huang Y, Antal-Zimanyi I, Ward S, Poindexter G S. Novel dihydropyrazine analogues as NPY antagonists. *Bioorg Med Chem.* 2007; 12: 337 – 340.
- [5] Yamaguchi T, Nomura H, Matsunaga K, Ito S, Takata J, Karube Y. The behavior of dihydropyrazine with DNA strand-breakage activity in vivo. *Biol Pharm Bull.* 2003; 26: 1523 - 1527.
- [6] Takechi S, Yamaguchi T, Nomura H, Minematsu T, Nakayama T. Growth inhibition and mutagenesis induced in *Escherichia coli* by dihydropyrazines with DNA strand-cleaving activity. *Mutation Res.* 2004; 560: 49 - 55.
- [7] Sondhi S M, Singh N, Rajvanshi S, Johar M. Synthesis, hydrolysis over silica column, anticancer, anti-inflammatory and analgesic activity evaluation of some pyridine and pyrazine derivatives. *Indian J Chem.* 2005; 44B: 387 – 399.
- [8] Foks H, Trapkowska I, Janowiec M, Zwolska Z, Augustynowicz-Kopec E. Synthesis, reactions and tuberculostatic activity of pyrazinyl-substituted derivatives of hydrazinocarbodithioic acid. *Chem Heterocyclic Compd.* 2000; 40: 1185 – 1193.
- [9] Farghaly A R, El-Kashef H. Pyrazoles and pyrazolo [4,3-e] pyrrolo [1,2-a] pyrazines, I. Synthesis and antimicrobial activity. *Monatshefte Fiir Chemie.* 2005; 136: 217 - 227.
- [10] El-Kashef H S, El-Emary T I, Gasquet M, Timon-David P, Maldonado J, Vanelle P. New pyrazolo [3,4-b] pyrazines: synthesis and biological activity. *Pharmazie.* ,2000; 55: 572 - 576.
- [11] Beck H C, Hansen A M, Lauritsen F R. Novel pyrazine metabolites found in polymyxin biosynthesis by *Paenibacillus polymyxa*. *FEMS Microbiol Lett.* 2006; 220: 67 – 73.
- [12] Baliah V, Lakshmanan M R, Pandiarajan K. Synthesis of some 1,2-ethanediamines. *Indian J Chem, Vol.* 1990; 16B: 72-73.
- [13] Dhar M H, Dhar M M, Dhawan B N, Mehrotra B N. Screening of Indian plants biological activity Part I. 1968; 6: 232-247.

Synthesis and Spectral Characterization of Novel 1,2,4-Dithiazole Derivatives

Mr Ramdas N Ingole¹, Dr Siddharth S Waghmare¹ and Dr Pravin S Bodkhe²

¹Research Center, Department of Chemistry, Ghulam Nabi Azad Arts, Commerce and Science College
Barshitakli District Akola 444401 (M.S.), India.

²Research Center, Department of Chemistry, Vidya Bharti Mahavidyalaya, Amaravti.
e-mail:dasingole@gmail.com

Abstract

A single step synthesis of N-(5-(substitutedimino)-5H-1,2,4-dithiazol-3-yl)benzo[d]thiazol-2-amine (II a-d) was carried out by oxidative cyclisation of 2-(5-substituted-2,4-dithiobiureto) benzothiazole (I a-d) using liquid bromine in chloroform medium as an oxidizing agent. The products were isolated, characterized and justified on the basis of conventional chemical characteristics and spectral studies.

Key-words: Benzothiazole, oxidative cyclization, dithiazoles, oxidizing agent.

Introduction

Organic compounds containing thiadiazole as the heterocycles in their structure are identified for their biological activities, pharmaceutical activities, industrial applications, agricultural purposes and in medicinal sciences. Basically structure of thiadiazole is five membered nitrogen and sulphur containing heterocyclic compound. Presence of sulphur and nitrogen in its structure enhances the biological potential of the thiadiazole. Recently reported some newer thiadiazole along with pyridine for the anti-bacterial activities¹⁻² and effect of germination pattern of jowar, Bhagwatkar³ synthesized and reported the thiadiazole based triazine for the antibacterial activities and some different substituent's attached thiadiazole directly or indirectly shows effect directly in their biological, pharmaceutical and agricultural applications⁴⁻⁵. The benzothiazole based heterocycles are five membered heterocycles containing sulphur and nitrogen as a heteroatom were created its own background in the synthetic organic chemistry⁶⁻¹⁰. The biological as well as industrial applications of benzothiazole get enhanced, due the presence of the thiadiazole nucleus in their structure. Trusting the literature ideas in mind it is decided to design such organic moiety should contain thiadiazole along with the benzothiazole; to synthesize such series of benzothiazole based five member heterocycle containing sulphur and nitrogen as a heteroatom¹¹⁻¹⁷.

As a part of research work presently it has been planned to design and synthesize novel series of N-(5-(substitutedimino)-5H-1,2,4-dithiazol-3-yl)benzo[d]thiazol-2-amine (II a-d) in this laboratory with the easiest and cheaper method by oxidative cyclisation of 2-(5-substituted-2,4-dithiobiureto) benzothiazole (I a-d) with liquid bromine in chloroform medium. The present method utilized somewhat suitable, convenient, cheaper, more practical utility and only a single step direct method for the synthesis of (IIa-d).

Experimental Section

Materials:

All chemicals used were of Mercks Millipore (Indian made). 2-(5-substituted-2,4-dithiobiureto) benzothiazole (I a-d) were prepared by known literature method³.

Method:

Method employed in the present experiments for the synthesis of series 1,2,4-dithiazole based benzothiazole is conventional refluxing under water bath for different hours for different experiments. The melting points of synthesized compounds were recorded using hot paraffin

bath and uncorrected. IR spectra were recorded on Perkin Elmer spectrometer in the range 4000-400 cm^{-1} in KBr pellets. PMR spectra were recorded on BRUKER AIIANCE II 400 NMR spectrometer with TMS as an internal standard using CDCl_3 and DMSO-d_6 as a solvent. The purity of the compounds was checked on silica gel – G plates by TLC with layer thickness of 3mm.

General Procedure:

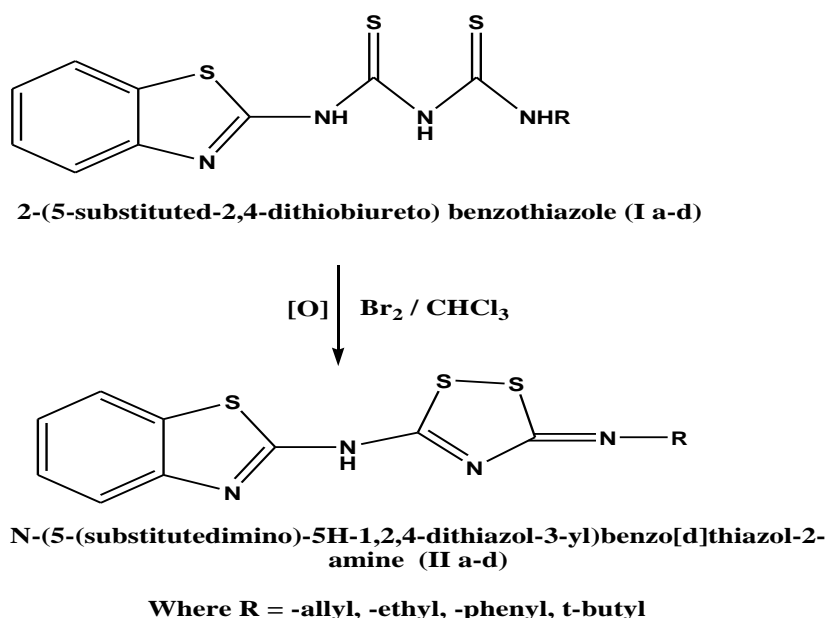
Experiment No. 1

Synthesis of N-(5-(allylimino)-5H-1,2,4-dithiazol-3-yl)benzo[d]thiazol-2-amine (IIa):

The pest of 2-(5-allyl-2,4-dithiobiureto) benzo[d]thiazole (Ia) was prepared in chloroform in a clean china dish and liquid bromine in chloroform was added with constant stirring at room temperature. During the addition of bromine in chloroform solution to the pest of (Ia), firstly the colour of bromine disappear, further addition of bromine in chloroform colour of bromine appears and persists. Such solution of bromine in chloroform and (Ia) kept for 4 hours at room temperature. Basification of the reaction mixture with dilute ammonium hydroxide solution gives the formation bright cream yellow coloured product (IIa). Recrystallization of the product was done using ethanol. Yield 89%, M. P. 172°C .

Similarly, N-(5-(ethylimino)-5H-1,2,4-dithiazol-3-yl)benzo[d]thiazol-2-amine (IIb), N-(5-(phenylimino)-5H-1,2,4-dithiazol-3-yl)benzo[d]thiazol-2-amine(IIc), N-(5-(t-butylimino)-5H-1,2,4-dithiazol-3-yl)benzo[d]thiazol-2-amine (IId) were synthesized from the oxidative cyclisation of 2-(5-ethyl-2,4-dithiobiureto) benzo[d]thiazole (Ib), 2-(5-phenyl-2,4-dithiobiureto) benzo[d]thiazole (Ic), 2-(5-t-butyl-2,4-dithiobiureto) benzo[d]thiazole (Id) with liquid bromine in chloroform medium respectively by the above mentioned method in Experiment No. 1 to 4 and the data obtained by the characterization of synthesized compound in a series (IIa-d) is given result section.

Reaction Scheme:



Results and Discussion:

Spectral data obtained from the present research support the formation of designed or target products. Spectral characterizations of all the synthesized compounds are also given below:

Data Analysis:

N-(5-(allylimino)-5H-1,2,4-dithiazol-3-yl)benzo[d]thiazol-2-amine (IIa):

Cream Yellow solid, $C_{13}H_{11}N_3S_3$, Yield-89 %, M.P. 272, **FTIR (KBr) ν cm**-3085.89-3004.89 (Ar C-H stretching), 574.75(S-S stretching), 1587.31 (S-C=N stretching), 794.62-761.83 (C-S stretching); **1H NMR (400 MHz $CDCl_3$ δ ppm)**, doublet of 2H of $-CH_2$ at δ 2.00 ppm, singlet of 1H of NH at δ 4.00ppm, pentate of 1H, doublet 2H and doublet of 2H of allyl at δ 5.70ppm, 4.97ppm and 5.0ppm respectively and multiplet of 7H of Ph at δ 7.55-8.23ppm; Mol. Wt.:305.

N-(5-(ethylimino)-5H-1,2,4-dithiazol-3-yl)benzo[d]thiazol-2-amine (IIb)

Dark Yellow solid, $C_{11}H_{10}N_4S_3$, Yield-92%, M.P. 168 $^{\circ}C$, **FTIR (KBr) ν cm**-3085.89-3004.89(Ar-H Stretching), 574.75(S-S stretching), 1587.31(-C=N stretching), 794.62-761.83(C-S stretching); **1H NMR (400 MHz $CDCl_3$ δ ppm)**, triplet of 3H, $-CH_3$ at δ 0.90ppm, quartate of 2H of $-CH_2$ at δ 1.4ppm, multiplet of 7H, Ph at δ 6.52-8.01ppm, singlet of 1H, NH at δ 4.35ppm ; Mol. Wt.: 294.

N-(5-(phenylimino)-5H-1,2,4-dithiazol-3-yl)benzo[d]thiazol-2-amine(IIc)

Yellow, $C_{15}H_{10}N_4S_3$, Yield-88%, M.P. 174 $^{\circ}C$, **FTIR (KBr) ν cm**- 3056.96-3004.89 (Ar-H Stretching), 592.11 (S-S stretching), 1587.31 (-C=N stretching), 794.62-761.83 (C-S stretching); **1H NMR (400 MHz $CDCl_3$ δ ppm)**, multiplet of 12H, Ph at δ 6.11-8.02ppm and singlet of 1H, $-NH$ at δ 4.34ppm; ESI-MS (m/z) gives base at m/z+=226.98, 74.90, 359.93 and molecular ion i.e. molecular weight is 342.

In the present work is best cheaper and less time consuming method of cyclisation of organic compound. Route of mechanism of the present synthesis is due to the conjugation of amido-H with thionyl Sulphur. Among all the synthesised of compounds (IIa-IId), percentage of yield of compound (IIb) is highest i.e. 92%.. However (IIa) and (IId) shows comparable yield with the (IIb).

Conclusion

In all the synthesized compounds, maximum yield of (IIb) displays ethyl group is electrometrically donating group on nitrogen in 2,4-dithiobiurets with increases the rate of reaction by giving its electrons.

References

- [1] PP Pathe, MW Ambekar, NM Nimdeokar, MG Paranjpe; Indian J. Chem., 1982, 59, 670.
- [2] AK Bhagwatkar; Synthesis and antimicrobial analysis of substituted 1,3,5-triazin-6-ylsubstitutedamidinothiocarbamides and their cyclisation into 1,3,5-thiadiazines and 1,3,5-triazines', Ph.D. Thesis, SGBAU, Amravati, 2013.
- [3] AKSingh, G Mishra and K Jyoti; Journal of App. Pharm. Science, 2011, 1(5), 44-49.
- [4]J Tao, ZW Duo and HC Ling; J Chinese Chem Soc., 2010, 57,1077-80.
- [5] NV Madhav, AS Nayak, AJ Rao, and M Sarangapani; J Pharm Res., 2011, 4(5), 1396-97.
- [6] D Patel and A Singh; -Jour Chem., 2009, 6(4), 1017-1022.
- [7] PR Mahalle and SP Deshmukh; Int. J. of Pharmacy and Pharmaceutual Science, 2011, 3(4), 277-279.
- [8] MA Saleh, Sulfur letters, 2002, 25, 235-245.
- [9] F Sansone, E Chierci, A Casanti and R Ungaro; Org. Bio. Mol. Chem, 20031, 1802-1803.
- [10]PR Mahalle and SP Deshmukh, Int. J. of Carbohydrate Research, 2012, 1(1), 1-3.
- [11]KM Heda and SP Deshmukh, Rasayan J. Chem., 2012, 5(1), 24-27.
- [12]K Willi, B Helmut, K Wolfgang, M Edger and R Peter; Chem. Abstr., 1978, 88, 152668.
- [13]CJ Cavalito, CM Martini and FC Nachod; Journal of American Chemical Society, 1951, 73, 2354.
- [14]N Siddiqui and A Hussain; Indian Journal of Pharmacology, 2001, 33, 382-383.
- [15]CW Pouton ; Euro.J.Pharma.Sci., 2006, 29, 278-287.
- [16]DJ Faulkner ; Tetrahedron Lett., 1993, 38, 21-25.
- [17]JJ Bhatt, BR Shah, PB Trivedi, NK Undavia and NC Desai, Ind. J. Chem, 1994, 33(B), 189-192.

Synthesis of Substituted Flavanones and their Impact on Seed Germinations

S. P. Rathod^{1*}, R.T.Parihar², A.P.Mitake³, T.M.Bhagat⁴ and
S. B. Waghmare⁵

1. Department of Chemistry, G. S. G. College, Umarkhed (MS) India.

2. Department of Chemistry, Vidnyan college, Malkapur (M.S) India.

3. Department of Chemistry, G. S. G. College, Umarkhed (MS) India.

4. Department of Chemistry, G. S. G. College, Umarkhed (MS) India

5. Department of Chemistry, G. S. G. College, Umarkhed (MS) India

E-mail – rathodsp.gsg@gmail.com

ABSTRACT:

As a part of systematic investigation, spectral analysis and morphology (root and shoot elongation) of a several chlorosubstituted flavanones from diketones, gives various series by using different aldehydes. As in series, 3-methoxy-8-chlorobenzoylflavanone, 3-chlorobenzoyl-8-chloroflavanone, 3-benzoyl-8-chloroflavanone.

KEYWORDS:- Diketones, flavanones, root and shoot elongation.

INTRODUCTION:

Flavanones are group of common natural polyphenolic compound that are widely found in plant kingdom. It consists of two aromatic ring links through three Carbon bridge with a carbonyl function. Actually these are the class of Flavanoids, which can be subdivided into several classes such as chalcone, flavanones, isoflavanones, aurones etc. The flavanones are mainly distributed in citrus fruits. In present study, various chlorosubstituted flavanones were synthesized from chlorosubstituted diketones and screened for their morphology (i.e. root and shoot elongation) against some crop plants. Flavanones and their analogues having attracted considerable attention because they possess antioxidant effect, cytotoxic, antimicrobial. Antinflammatory activities etc.

Larget R et.al.¹ reported substituted flavanone & studied as neuroprotective agents. Venkatramn et.al.² synthesized the flavanone from chalcone by dehydrogenation with SeO₂. Yoigtandes et.al.³ reported the flavanone from flavanone by heating with I₂. Patill⁴ synthesized flavanone from by using F₂/DMSO as a dehydrogenating agent. Mayer A.M.et.al.⁵ synthesized cumarine and their role as growth regulators in several plants.. Korade D.L. et.al.⁶ reported the effect of Anthracenes on seed germination of *Lolium multiflorum* plants. Gibba Z. et.al.⁷ studied the effect of nitric oxide on germination of *Empress tree* seeds. Majumdar, G. p.⁸ reported studied the cambial activities of root habit and shoot development in some plants.

The reaction of diketones with various aldehydes gives various flavanones these reactions carried out in presence of ethanol as energy transfer medium in aq.KOH.

It has been well established that, the presence of chlorosubstituted ketones present in flavanones, with the hope that the resulting molecules would exhibit promising root and shoot elongation as shown in table and graph.

EXPERIMENTAL METHODS:

All the glassware's used in the present work were of Pyrex quality. Melting points were determined in open capillary and are uncorrected. Purity of compounds was monitored on silica gel coated TLC plate. I.R. spectra were recorded on SHIMADZU Spectrophotometer in KBr

palates. The analytical data of compounds were highly satisfactory. All the chemicals used were of analytical grade. All the solvents used were purified by standard methods. Physical characterization data of all the compounds are given in Table 1.

Result and discussion

The synthetic methods used in present work are given below along with their, IR data.

Acetylation of P- Chlorophenol:

P – Chlorophenol 50 ml was mixed with acetic anhydride 60 ml & anhydrous sodium acetate 5 gm the mixture was refluxed for about 1 hrs. it was cooled and poured into cold water. Acetated layer was separated & washed with water several times finally it was purified by distillation and the distillate of compound was collected at about 232°C. Yield 75%, B.P. 232°C

2 – Hydroxy 5 – chloro-acetophenone:

When Phenyl acetate (50ml) was mixed with anhydrous AlCl_3 (120gm) & heated at 120°C for 45 min on oil bath. The reaction mixture was decomposed with ice cold water containing little hydrochloric acid to get crude ketone. It is purified by dissolving in acetic acid & allowing the solution to fall drop by drop into cold water with stirring. A slightly yellow powder was obtained having M.P. = 86°C, Yield = 72%

2 – Benzoyloxy 5 - chloroacetophenone:

2 – Hydroxy 5- Chloroacetophenone (0.04 mol) & (8.59 ml) Benzoyl Chloride (0.05 mol) were dissolved in NaOH (10 %) (30 ml). The reaction mixture was shaken for about 45 min. The product thus separated filtered, washed with water followed by sodium bicarbonate (10%) again with water. The solid product was crystallized from ethanol to obtain. 2 – benzoyloxy 5-chloroacetophenone white crystal is obtained having M.P. - 87°C, Yield - 80%.

1 – (2-hydroxyl Phenyl) 5 – Chloro- 3 – Phenyl – 1, 3 – Propanedione:

2 – Benzoyloxy 5 - chloroacetophenone (1.5 gm) was dissolved in (40 ml) dry Pyridine. The solution was warmed up to 60°C pulverized KOH (15gm) was added slowly with constant stirring. After 4 hours of heating then reaction mixture was acidified by adding ice cold HCl (1 : 1). The brownish yellow solid product thus separated was filtered, washed with sodium bicarbonate solution (10%) and finally again with water. It was then crystallized from ethanol-acetic acid mixture to get 1 – (2-hydroxyl phenyl) 5 – Chloro -3 – Phenyl – 1, 3 – Propanedione. M.P:121°C, Yield – 75 %.

3 – benzoyl - 8 – chloro flavanone:

A mixture of 1 – (2-hydroxyl phenyl)- 5 – Chloro 3 – Phenyl – 1, 3 – Propanedione (0.01 mol) (3 gm) & Benzaldehyde (0.12 mol) (1 ml) was refluxed in ethanol (25 ml) and KOH (1 gm) for 15 – 20 min described to get compound M.P. - 230°C, Yield - 79%.

3 – Methoxy – 8-chloro benzoyl flavanone:

A mixture of 1 – (2-hydroxyl phenyl)-3 – phenyl – 1, 3 – propanedione (0.01 mol) (3 gm) & anisaldehyde (0.12 mol.) (1 ml) was refluxed in ethanol (25 ml) & KOH (1 gm) for 15 -20 min. & process as described to get compound, 3 – methoxy-8 – chloro benzoyl flavanone. M.P. - 251°C, Yield – 72 %.

Table (1): Characterization data of synthesized new compound

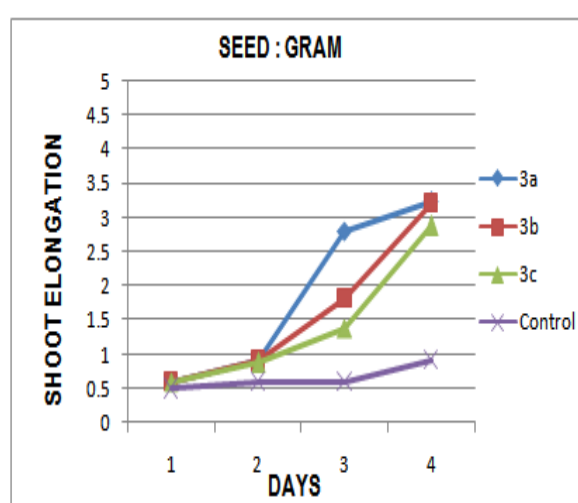
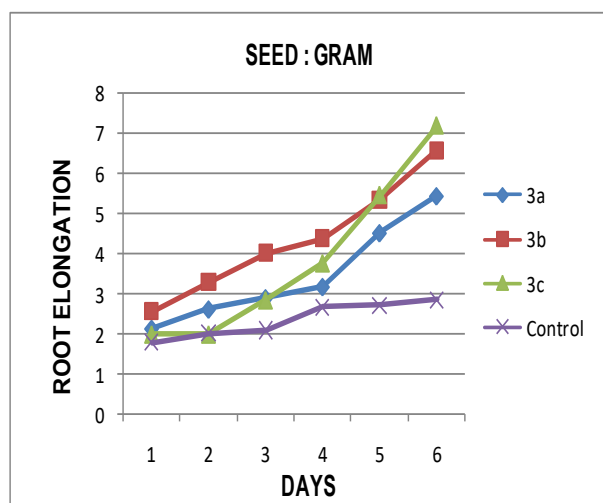
Compound	Molecular Formula	M.P. (°C)	Yield (%)	Rf
3a	C ₂₁ H ₁₃ O ₃ Cl	230	79	0.76
3b	C ₂₂ H ₁₆ O ₄ Cl	251	75	0.78
3c	C ₂₁ H ₁₄ O ₃ Cl ₂	240	75	0.79

TABLE NO. 1 : SEEDS - GRAM

Sr. No.	Comp.	% of germination					Average length of root in cm.						Average length of shoot in cm.					
		Day					Day						Day					
		2	4	6	8	10	2	4	6	8	10	12	2	4	6	8	10	12
1	3a	80%	100%				1	2	2.4	3.2	3.5	4			0.6	0.9	2.8	3.2
2	3b	80%	100%				1	1.5	2	2.7	3.2	3.9			0.6	0.9	1.8	3.2
3	3c	100%	100%				2	2.4	2.6	3.4	3.7	4			0.6	0.9	1.4	2.9
4	Control	80%	90%				0.5	1.2	1.4	2	2.5	2.7			0.5	0.6	0.6	0.9

TABLE NO. 2 : SEEDS - Black Eyed Beans (Chawali)

Sr. No.	Comp.	% of germination					Average length of root in cm.						Average length of shoot in cm.					
		Day					Day						Day					
		2	4	6	8	10	2	4	6	8	10	12	2	4	6	8	10	12
1	3a	80%	100%				2.1	2.6	2.9	3.2	4.5	5.4			0.6	0.9	2.8	3.2
2	3b	80%	100%				2.6	3.3	4.0	4.4	5.4	6.6			0.6	0.9	1.8	3.2
3	3c	80%	100%				2.6	3.3	4.0	4.4	5.4	6.6			0.6	0.9	1.8	3.2
4	Control	80%	90%				1.8	2	2.1	2.7	2.7	2.9			0.5	0.6	0.6	0.9



Conclusion

The present study was aimed at investigating the impact of newly synthesized substituted flavanone on some crop plants viz: *Gram* and , *Black Eyed Been (Chawali)*. The choice of these crops was based on their enormously vast utility and also the indispensability for the survival of the human race, all across the globe.

The efforts have been made to investigate and analyze the convergence and divergence effect of test compounds on the morphology of plants under investigation. It was interesting to note that, all the treated seeds exhibited remarkable roots and shoots elongation as compared to untreated ones.

When the growth of all the treated plants were compared among themselves, it was distinctly observed that, the change which is dominant while applying the treated compound i.e. chlorosubstituted flavanones in *Gram*, *Black Eyed Been (Chawali)*. In the initial stage vegetative growth was not significance but after 2nd interval it gradually increases and after 12 days roots and shoots elongation were dominant to a considerable extent. Thus there has been fair amount of satisfaction in crying out the present study. The encouraging results have surely contributed to the enthusiasm of the author. But honestly, this is just the beginning. There is a much scope for further study, and there is a long way to go.

ACKNOWLEDGEMENT

The authors are thankful to G.S.G.College, Umarkhed affiliated by S.G.B.Amaravati University (M.S.) for providing all the facilities to carry out the work.

References:

1. Larget R, , B, Renard P, Bioorg med. Chem. Left 10(8) : 835-38, **April 2000**.
2. ., Venkataramn K, Mahal H.S, : Curr.Sci27, (**1933**), 124
3. Yoigtande, H.W., and Haertner : Arch. P(harm (YYeinneim Ger.) 316(3), (**1983**), 219-22.
4. Patil K.N., Ph.D. Thesis "Synthesis and rection of 3-aroylechloroflavanoneides." Amravati University (**1993**).
5. Mayer A.M., Poljakotta A, *Amer Lowa Univ. Press* 735-749, **1993**.
6. Korade D.L. & Fulekan M.H., *Biology and Medicine, Vol 1(1)* : 28-34, **2009**.
7. Gibba Z., Grubisic D., Todorovic S. *Plant Growth Regulation* 26, 175-181, **1998**.
8. Majumdar, G.P. Hetero-archic roots in Enhydra fluctuans Laour. *J. Indian bot. Soc. (11)*, 225-227; **1932**.
9. Rathod S.P.,Rajput P.R.,*Rasayan J.Chem.*4(3),660-665:**2011**.
10. Osman A.M.,Hasan K,*Indian J.Chem.*14B,282: **1954**.
11. Rajora J.,Yadav J, Kumar R, *Indian J.Chem.*49B,989-993: **2010**.
12. Kaliranjan R., Rathore S., *Indian J.Chem.*50B,1794-1799: **2011**.

Antimicrobial Resistance : A Global Challenge

Reshal Deshmukh

Department of Chemistry, Shri Shivaji Science College, Congress Nagar Nagpur
Email reshaldeshmukh@rediffmail.com

ABSTRACT

Decades after the first patients were treated with antibiotics, bacterial infections have again become a threat because of the rapid emergence of resistant bacteria. Multidrug resistant urinary tract infection is a most problematic infection and it is very difficult to doctors to manage the patient by using appropriate antibiotics due to development of multidrug resistant strains of bacteria. MDR strains shows resistant to maximum number of antibiotics and sensitive to very few antibiotics.

Keywords : Urinary tract infection , multidrug resistant , antibiotic , bacteria

INTRODUCTION:

The bacterial associated Urinary Tract infection is most common infection found in all ages and both the genders offering antibiotic resistance in most of the cases of infection. Now a day's antibiotic resistance has becomes major public health problem leads to increase resistant to huge number of antibiotics from few years. The antibiotics are also responsible to develop multidrug resistant strain due to resistance genes of resistant bacteria. The rapid emergence of antibiotic resistant transfer genes among uro-pathogens are important cause of development of antibiotic resistance. The increased antibiotic resistant suggest that the choice of antibiotic should be guided by culture and sensitivity assay. In past decades many kind of resistant strains are discovered.

PRINCIPLE OF ANTIMICROBIAL THERAPY

The objective of antibacterial therapy is to eliminate the bacterial growth in the urinary tract and the antibiotics used are efficacious, safe, and cost effective. The basic treatment starts with the antibiotics which are number of choices available in market. The resolution of infection is dependent on the susceptibility of the bacteria to the concentration of the antibiotic achieved in urine. Antibiotics should eliminates the bacterial growth in urinary tract when proper antibiotics are used which is able to achieve level in urine and the duration that this level remains above the minimum inhibitory concentration (MIC) of microorganism that attack on urinary tract. (Hooton TM, 1991). An effective antibacterial usually achieved MIC both in serum and urine of healthy adults, the urinary level often many folds greater than serum level. However the serum levels are critical in patients with uro-sepsis and urinary tract infection involving renal parenchyma. (Jacobson SH, 1991)

Resistance to B-Lactams

Urinary bacteria may develop several mechanisms of resistance to Blactams which is most efficient method of resistance to these agents in Gramnegatives is the synthesis of B-lactamases. B- lactamases have presumably evolved to fight natural B-lactams, produced by bacteria such as Streptomyces, Lysobacter , penicillium or Acremonium. (Brakhage AA,

2005). However the widespread administration of antibiotics is influenced the development of B- lactamases mediated resistance. Since B- lactam antibiotics came into clinical use, B- lactamases are evolved with them. The emergence of MBL mediated resistant among enterobacteriaceae has also becomes serious health concern. More ever the increase in international travel is likely to be contributory factor for the ascendancy of mobile MBL genes as much as the mobility among individual bacteria.

Resistance to Colistin

Colistin belongs to the antimicrobial class of polymyxin and acts by binding to the lipid moiety of the bacterial lipopolysaccharide and subsequently disintegrating the bacteria membrane. Resistance to colistin associated with lipopolysaccharide modification leading to a high level of antibiotic non-susceptibility

Resistance to Tigecycline

Tigecycline is first glycylcycline to be approved by the FDA, may lose its activity against MDR strains, particularly when low drug concentration are attained in the serum during treatment. Resistance develops when the MIC of the targeted pathogen exceed the C_{max} of the drug, which is almost the rule for all targeted *A. baumannii* strains. According to molecular studies efflux pumps seem to be the most important mechanism of resistance to tigecycline both in enterobacteriaceae and non-fermenting rods.

Resistance to Fluoroquinolone

Fluoroquinolone such as ciprofloxacin with bactericidal activity against gram negative pathogens. Fluoroquinolone act by binding to the nuclear enzyme DNA gyrase and topoisomerase IV. In spite of particular targets, resistance mechanisms both chromosomal and plasmidic have been developed. Chromosomal resistance mechanism includes target mutation and augmented expression of efflux pumps.

CONCLUSION:

Antibiotic therapy is a choice of treatment for the bacterial infections , but due to development of multidrug resistant strains the antibiotics are not effective as a treatment to patient. New antibiotic developed which may be the used as a antibiotic therapy in future in resistant cases. The present review is helpful to know few multidrug resistant pathogens are sensitive to particular antibiotics and the proper antibiotic has been administrated to patient for rapid cure of infection.

REFERENCES :

- Brakhage AA, Al-Abdallah Q, Tuncher A, Sprote P. Evolution of B- lactam biosynthesis genes and recruitment of transacting factors . *Phytochemistry*,2005 , 66(11),1200-1210.
- Dozzo P, Moser HE. New aminoglycoside antibiotics.*Expert Opin. Ther. Path.* ,2008 , 20(10), 1321-1341.
- Drlica K, Malik M,. Fluroquinolones : action and resistance. 2003 , *Curr. Top. Med. Chem.* 3(3) ,249-282.
- Falagas ME,Rafailidis PI ,Mathaiou DK. Resistance to polymyxin genes : Mechanisms , frequency and treatment option. *Drug resist. Update* , 2010 , 13(4-5),132-138.
- Hooton TM , Stamm WE. Management of acute uncomplicated urinary tract infection in adults. *Med Clin North Am.* 1991; 75:339-357.
- Jacobson SH . A five year prospective followup of women with non-obstructive pyelonephritic renal scarring. *Scand J Urol Nephrol.* ,1991;25:51-5
- Rawat D, Nair D. Extended spectrum B-lactamases in gram-negative bacteria. *J Glob.infect Dis.* ,2010,2(3) ,263-274

Wings across Reservoirs: Understanding and Safeguarding the Migration Patterns of Insectivorous Birds in Anthropogenic Landscapes

Dr. Chandrashekhar R. Kasar*, Ku. Revati Kishor Lonkar**

*Associate professor and Head, Department of Zoology, S.P.M. Gilani College, Ghatanji, Dist. – Yavatmal
Email – chandrashekharkasar8954@gmail.com

** Research Student, Department of Zoology, S.P.M. Gilani College, Ghatanji, Dist. – Yavatmal
Email – Rewati.lonkar96@gmail.com

ABSTRACT:

The migration patterns of insectivorous birds in reservoir dams play a vital role in ecosystem dynamics, influencing insect populations and contributing to overall biodiversity. This research investigates the intricacies of bird migration in the specific context of reservoir dams, focusing on insectivorous species and their seasonal movements. The study aims to understand the routes, patterns, and ecological implications of bird migration in these anthropogenic environments. The research delves into the ecological role of insectivorous birds in reservoir dams. Preliminary analyses suggest a substantial impact on insect populations, with potential cascading effects on the broader ecosystem. Understanding these ecological dynamics is crucial for effective reservoir dam management and conservation. The study's findings have implications for reservoir dam management, emphasizing the need for conservation strategies that consider the ecological importance of these birds in maintaining ecosystem balance.

Keywords: Bird migration, insectivorous birds, reservoir dams, ecosystem dynamics.

INTRODUCTION:

Bird migration, a phenomenon deeply ingrained in the evolutionary tapestry of avian species, plays a pivotal role in ecological systems worldwide. The intricate journeys undertaken by birds across vast distances are essential for maintaining biodiversity, influencing insect populations, and contributing to ecosystem resilience. In this context, our research focuses specifically on the migration patterns of insectivorous birds within the unique environment of reservoir dams.

1.1 Background: Reservoir dams, man-made structures designed primarily for water storage, have become integral components of the human landscape. These environments, often shaped by anthropogenic influences, present a distinctive ecosystem where wildlife, particularly avian species, adapts to novel challenges. Insectivorous birds, a diverse group with varied migratory behaviors, find themselves navigating these artificial landscapes.

1.2 Importance of Studying Bird Migration in Reservoir Dams: Understanding bird migration in reservoir dams is not merely an academic pursuit but a necessity for effective environmental management. Reservoir dams, with their altered landscapes and proximity to human activities, pose unique challenges to avian species. Insectivorous birds, reliant on specific habitats and food sources, become crucial indicators of the ecological health of these environments.

As reservoir dams serve multifaceted roles, from water supply to energy production, their impact on local ecosystems extends beyond their primary function. Our study recognizes the need to explore how these human-altered landscapes influence the migratory behaviors of insectivorous birds, species that contribute significantly to pest control and ecosystem balance.

1.3 Specific Focus on Insectivorous Birds: The choice to concentrate on insectivorous birds stems from their ecological significance. These avian species, characterized by their diet primarily consisting of insects, fulfill essential roles in regulating insect populations. As they traverse vast distances during migration, their interactions with the environment become intricate ecological narratives. By studying the migration patterns of insectivorous birds, we aim to unravel the complexities of their journeys and comprehend their contribution to the ecological equilibrium of reservoir dam ecosystems.

1.4 Research Question and Objectives: At the heart of this study lies the fundamental question: How do insectivorous birds navigate and contribute to ecosystem dynamics in the context of reservoir dams? To address this question, our research objectives are as follows:

- To identify the insectivorous bird species inhabiting reservoir dam environments.
- To analyze the migration routes and patterns of these bird species.
- To investigate the influence of environmental factors, such as climate and food availability, on the migration behaviors of these birds.
- To assess the ecological consequences of alterations in migration patterns within reservoir dams.

This research seeks not only to enhance our understanding of bird migration in anthropogenic landscapes but also to provide valuable insights for conservation strategies tailored to the unique challenges presented by reservoir dam environments.

LITERATURE REVIEW:

2.1 Bird Migration Studies: Bird migration, a phenomenon studied for centuries, has been a subject of fascination and scientific inquiry. Classical migration studies often focused on well-known flyways, such as the East Atlantic Flyway or the East Asian-Australasian Flyway, tracking the movements of waterfowl and shorebirds. While these studies have significantly contributed to our understanding of long-distance migration, the dynamics of migration within human-altered landscapes, such as reservoir dams, remain relatively understudied.

2.2 Migration in Anthropogenic Environments: The impact of human activities on bird migration patterns has gained attention in recent decades. Urbanization, deforestation, and climate change have altered the traditional routes and behaviors of migratory birds. However, the specific influence of reservoir dams, with their unique combination of altered habitats and human activities, merits closer examination. Some studies have explored how artificial water bodies affect bird migration, but the focus on insectivorous species within reservoir dams remains limited.

2.3 Significance of Insectivorous Birds in Ecosystems: Insectivorous birds, a diverse group encompassing species from various families, play crucial roles in maintaining ecological balance. Their diet primarily consists of insects, making them natural regulators of pest populations. In agricultural landscapes, insectivorous birds contribute to integrated pest management, reducing the need for chemical interventions. However, the extent of their contribution in reservoir dam ecosystems and the potential consequences of altered migration patterns remain underexplored.

2.4 Environmental Factors Influencing Bird Migration: Numerous environmental factors influence bird migration, including climate conditions, food availability, and habitat changes. Climate change, in particular, has been identified as a significant driver of alterations in migration patterns. Understanding how these factors intersect within the context of reservoir

dams is crucial for predicting and mitigating potential ecological disruptions. The literature review seeks to identify key studies that have examined the interplay between environmental factors and bird migration in both natural and artificial environments.

2.5 Gaps in Current Knowledge: Despite the wealth of information available on bird migration, there is a noticeable gap in literature concerning insectivorous birds in reservoir dams. Existing studies often focus on waterfowl or larger species, neglecting the ecological nuances associated with insectivorous behaviors. This literature review underscores the need for targeted research that specifically addresses the migration patterns, behaviors, and ecological roles of insectivorous bird species within reservoir dam environments.

METHODOLOGY:

3.1 Study Sites Selection: The choice of study sites is a critical aspect of our methodology. Reservoir dams selected for this research are characterized by diverse ecological settings, representing different climatic zones and geographic regions. This diversity ensures a broad understanding of how insectivorous birds adapt to various environmental conditions within reservoir dams.

3.2 Field Observations and Behavioral Analysis: Continuous field observations will complement the technological aspects of our methodology. Researchers will spend extended periods at the selected study sites, documenting bird behaviors, feeding patterns, and interactions with the reservoir dam environment. Behavioral analysis will focus on understanding how insectivorous birds adapt to the altered habitats presented by reservoir dams, including changes in foraging behavior and nesting preferences.

3.3 Climate and Habitat Analysis: Environmental factors, such as climate conditions and habitat changes, are integral components of our study. Climatic data will be collected to correlate with bird migration patterns, exploring the influence of temperature, precipitation, and seasonal variations on migration behaviors. Habitat analysis involves assessing the availability of insect prey, vegetation cover, and water quality within reservoir dams.

3.4 Data Analysis: The collected data will undergo rigorous analysis. Statistical methods will be applied to identify migration hotspots, determine seasonal variations in bird populations, and assess correlations between environmental factors and migration behaviours. Geospatial tools will aid in mapping migration routes and stopover locations.

3.5 Ethical Considerations: All aspects of the research adhere to ethical standards and prioritize the well-being of the studied birds. Bird handling follows established protocols to minimize stress and potential harm. The research team has obtained necessary permits and approvals from relevant wildlife conservation authorities, ensuring compliance with legal and ethical guidelines.

3.6 Community Engagement: Recognizing the importance of community involvement, our methodology includes outreach programs to engage local communities residing near the selected reservoir dams. Workshops, awareness campaigns, and citizen science initiatives aim to foster a sense of shared responsibility for the conservation of insectivorous birds and their habitats.

3.7 Limitations: While our methodology is comprehensive, certain limitations are inherent in avian migration studies. External factors such as predation, disease, and unforeseen events may impact the reliability of data collected through bird banding and satellite tracking. However, the combination of multiple data sources enhances the robustness of our findings.

CASE STUDIES:

4.1 Case Study 1: The Warbler's Journey *Species:* Black-and-white Warbler (*Mniotilta varia*) *Migration Route:* Northeastern study site to Central America *Key Findings:* This case study reveals a remarkable migratory journey of Black-and-white Warblers navigating from a northeastern reservoir dam to their wintering grounds in Central America. Satellite tracking data indicated distinct stopover points in areas with abundant insect populations, emphasizing the critical role of reservoir dam habitats in supporting migratory journeys.

4.2 Case Study 2: Navigating Urban Reservoirs *Species:* Common House Martin (*Delichon urbicum*) *Migration Route:* Urban reservoir dams in European settings *Key Findings:* In contrast to traditional rural habitats, this case study explores the migratory patterns of Common House Martins within urban reservoir dams. These insectivorous birds demonstrated adaptive behaviors, utilizing artificial structures for nesting and displaying adjusted migration routes influenced by urban landscape features.

CONSERVATION STRATEGIES:

5.1 Habitat Restoration and Enhancement: Implementing habitat restoration initiatives within reservoir dams involves reestablishing native vegetation, maintaining suitable nesting sites, and creating insect-rich environments. This strategy aims to ensure that migratory birds find optimal conditions for feeding, resting, and breeding.

5.2 Climate-Responsive Conservation: Given the influence of climate on bird migration, conservation efforts must be adaptive to changing climatic conditions. Integrating climate-responsive strategies involves monitoring climate trends, understanding their impact on bird behavior, and adjusting management practices accordingly.

5.3 Community-Based Conservation: Engaging local communities in the conservation process is paramount. By fostering awareness, providing education, and involving communities in citizen science initiatives, a sense of shared responsibility is cultivated. Local support contributes to sustainable conservation practices and the protection of reservoir dam ecosystems.

5.4 Sustainable Development Practices: Promoting sustainable development around reservoir dams ensures the coexistence of human activities and wildlife conservation. Implementing regulations that minimize disturbances, control pollution, and prioritize ecosystem health contributes to the long-term viability of insectivorous bird populations.

CONCLUSION:

This research has delved into the intricate world of insectivorous bird migration within reservoir dams, uncovering diverse patterns, adaptive behaviors, and ecological interactions. The case studies underscore the importance of these avian species in maintaining ecological balance and pest control within human-altered landscapes.

The conservation strategies proposed emphasize a holistic approach that integrates habitat restoration, climate-responsive measures, community engagement, and sustainable development practices. Preserving the migratory routes of insectivorous birds is not only vital for their well-being but also contributes to the overall health and resilience of reservoir dam ecosystems.

As we navigate an era marked by rapid environmental changes, understanding and safeguarding the migratory journeys of insectivorous birds become imperative. This research serves as a stepping stone towards comprehensive avian conservation strategies, bridging the

gap between scientific knowledge and on-the-ground initiatives. The journey of these birds, intertwined with the ecosystems of reservoir dams, unveils a narrative of adaptation, resilience, and the delicate balance between human activities and the natural world.

WORKS CITED:

1. Ahmed, N., Khan, M. S., & Rahman, K. U. (2018). "Biodiversity Assessment of Birds in Urban Reservoirs of Karachi, Pakistan." *Pakistan Journal of Zoology*, 50(3), 1019-1027.
2. Alerstam, T., Hedenström, A., & Åkesson, S. (2003). "Long-distance migration: evolution and determinants." *Oikos*, 103(2), 247-260.
3. BirdLife International. (2021). "Delichon urbicum (amended version of 2020 assessment)." *The IUCN Red List of Threatened Species*.
4. Gill, R. E., Douglas, D. C., & Handel, C. M. (2001). "Long-term tracking of arctic terns: new global information on migration pathways and breeding grounds." *The Condor*, 103(2), 428-440.
5. Newton, I. (2008). "The Migration Ecology of Birds." Academic Press.
6. Robinson, R. A., Learmonth, J. A., & Hutson, A. M. (2003). "Atlas of Bird Migration: Tracing the Great Journeys of the World's Birds." Random House UK.
7. Runge, C. A., Martin, T. G., Possingham, H. P., Willis, S. G., & Fuller, R. A. (2014). "Conserving mobile species." *Frontiers in Ecology and the Environment*, 12(7), 395-402.
8. Saini, J., & Khera, N. (2017). "Assessment of Water Quality in Reservoirs of Shimla Hills Using CCME Water Quality Index." *Journal of Scientific Research & Reports*, 14(3), 1-14.
9. Sanderson, F. J., Donald, P. F., Pain, D. J., Burfield, I. J., & van Bommel, F. P. (2006). "Long-term population declines in Afro-Palearctic migrant birds." *Biological Conservation*, 131(1), 93-105.
10. Wang, Y., Zhu, W., Zhang, Y., & Ma, M. (2020). "Impacts of Urban Reservoirs on the Distribution and Diversity of Wintering Waterbirds." *Water*, 12(1), 176.
11. Zalles, J. I., & Bildstein, K. L. (2000). "Raptor Watch: A Global Directory of Raptor Migration Sites." BirdLife International.

46

Synthesis and Characterization of Pyrazolone and its derivatives.**Mr. R. N. Gaikwad**

Maharashtra Udayagiri Mahavidyalaya, Udgir Dist. Udgir 413517

Abstract:

The synthesis of pyrazolone and its derivatives is achieved by a clean, one-pot, multi-component condensation reaction combining ethyl acetoacetate, hydrazine hydrate, aromatic aldehyde in catalytic amount of MSA. This approach has numerous benefits, including a quick reaction time and an easy work-up process. Compounds were identified via mass spectral analysis, NMR, IR, and chemical transformation.

Keywords: aryl aldehyde, ethyl acetoacetate, hydrazine hydrate, MSA, pyrazolone etc.

Introduction

Pyrazolone are a class of organic compounds that feature a five-membered ring containing three carbon atoms and two nitrogen atoms. The molecular formula of pyrazolone is $C_3H_3N_2$. This heterocyclic ring structure imparts unique chemical and pharmacological properties to pyrazolone, making them significant in various fields such as chemistry and medicine. Pyrazolone also exhibit interesting coordination chemistry, forming complexes with various metal ions. This property makes them relevant in coordination chemistry and catalysis. The chemical, pharmaceutical, and agrochemical industries are very interested in pyrazolone derivatives^{1,2}. Considered an active scaffold with pharmacological importance, pyrazolone and its derivatives exhibit nearly all pharmacological activity. The pyrazolone moiety's pharmacological potential has been demonstrated by the nucleus's presence in pharmacological agents belonging to various therapeutic categories, including rimonabant, difenamisole, an analgesic; fezolamide, an antidepressant; and celecoxib, a potent anti-inflammatory and antipsychotic.³ Because of their many characteristics and uses, pyrazolones are a class of chemicals that have been studied. These include pyrazol-3-ol and pyrazolin-5-one. Sulfamazone, propyphenazone, and nifenazone⁴ are a few of the exploratory small compounds containing pyrazolone that have been considered as potential therapeutic possibilities. Derivatives of pyrazolone are a significant class of heterocyclic chemicals found in numerous medications and synthetic goods. Based on a review of the literature, pyrazolone derivatives exhibit a range of pharmacological actions, including, anti-tubercular⁵, anti-fungal,^{6,7} anti-bacterial,⁸ anti-inflammatory,⁹ anti-tumor,¹⁰ anti-microbial.¹¹

In this study, we have created a sophisticated, effective, simple, and straightforward method for the synthesis of pyrazolone and its derivatives. We do this by employing ethanol as a solvent together with hydrazine hydrate, ethyl acetoacetate, and substituted aryl aldehydes in a catalytic quantity of MSA. In terms of environmentally friendly procedures, the combination of the green technique and the catalyst results in an outstanding product yield. This approach offers many important benefits, including reduced reaction time, solvent-free conditions, atom economy, using a green catalyst, and a more pleasant workup process.

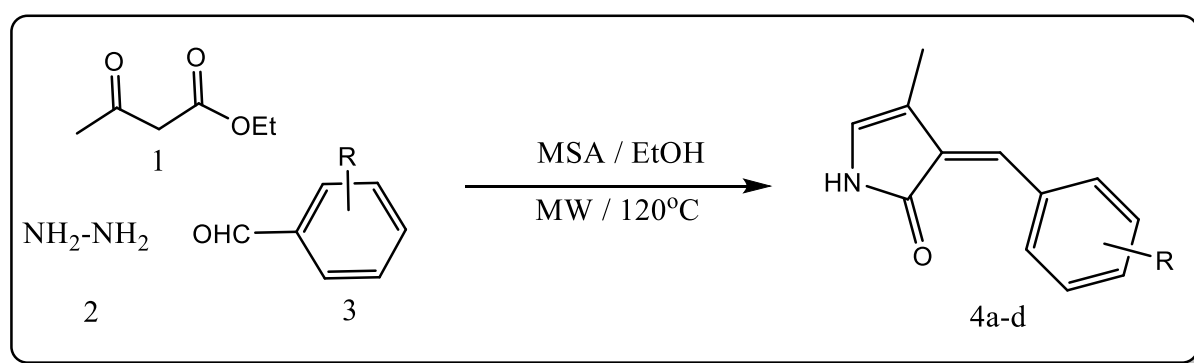
Experimental**General**

The digital melting point device (Veego-VMD) was used to record the uncorrected melting point of the produced chemical. A.R. Grade chemicals were used. Every chemical employed was of A.R. Grade, and it wasn't purified further. Microwave irradiation was carried out in a Microwave Oven, Model No. MS2079 DB DB1QILN (2450 MHz, 1050 W) equipped with

Erlenmeyer flask. The compound's melting point was measured in an open capillary tube and might not be accurate. Using an FT-IR spectrophotometer made by Perkin-Elmer, IR spectra were recorded. KBR Pellet. Using chloroform as a solvent, the ^1H NMR spectra and mass were recorded using a Perkin-Elmer spectrophotometer. The chemical shift value was reported in parts per million (ppm) with respect to TMS, which served as an internal standard.

General Procedure for the synthesis of Pyrazolone and its Derivatives

The combination of **1**ethyl acetoacetate (0.01mmol), **2**hydrazine hydrate (0.01mmol), and **3**aryl aldehyde (0.01mmol) in catalytic amount of Methane sulphonic acid (MSA) in an Erlenmeyer flask and irradiated until completion of the reaction in microwave oven. The reaction mixture was poured in crushed ice and filtered, washed with ethyl acetate, the product was recognized as 3-methyl-4-arylidene pyrazolone (4a-d). The crude product was collected and recrystallized in ethanol and dried. The entire product was characterized by physical constant and spectroscopic techniques and compared with the standard method.



Scheme 1

Result and Discussion

As indicated in the scheme 1, we reported a direct method for the synthesis of pyrazolone and its derivatives by one pot condensation of aromatic aldehyde, hydrazine hydrate, and ethyl-acetoacetate. The yield was really high. In order to assess the extent and constraints of the methodology, the reactions were conducted in the absence of a catalyst, and the structures of all newly synthesized pyrazolone derivatives were established using chemical transformation, NMR, IR, and mass analysis.

Table1: Synthesis of pyrazolone & its derivatives catalyzed by MSA under M.W. (120oC/300W)

Product	Name of compound	% yield	Melting Point in $^{\circ}\text{C}$
4a	(Z)-3-benzylidene-4-methyl-1,3-dihydro-2H-pyrrol-2-one	94%	122 $^{\circ}\text{C}$
4b	(Z)-3-(4-chlorobenzylidene)-4-methyl-1,3-dihydro-2H-pyrrol-2-one	89%	215 $^{\circ}\text{C}$
4c	(Z)-4-methyl-3-(3-nitrobenzylidene)-1,3-dihydro-2H-pyrrol-2-one	87%	195 $^{\circ}\text{C}$
4d	(Z)-3-(4-hydroxybenzylidene)-4-methyl-1,3-dihydro-2H-pyrrol-2-one	92 %	197 $^{\circ}\text{C}$

Table 2. Optimization of catalyst concentration of (4b) under M.W. Irradiation

Entry	Catalyst mol %	Time, min	Yields %
1	No catalyst	9	-
2	1	8	76
3	2	7	89
4	3	3	95
5	4	5	85
6	5	8	70

Initially, the mixture of Ethyl acetoacetate, Hydrazine hydrate and substituted aryl aldehydes, (0.01 mol each) was taken in an 50 mL vessel and subjected to microwave irradiation under neat conditions in the absence of catalyst and solvent, and the reaction was failed to get the product under this condition. The reaction was repeated in the presence of catalyst in the range 1-5 mol %. We have optimized the amount of catalyst for the synthesis of (**4b**, Table 1) under microwave irradiation and excellent yield was obtained in only 3 minutes when 3 mol % catalysts are introduced (**Table 2**, entry 4).

Spectroscopic characterization.

4c) (Z)-4-methyl-3-(3-nitrobenzylidene)-1,3-dihydro-2H-pyrrol-2-one

Solid: - Melting point = 195°C

IR (KBr, cm^{-1}): 1354, 1260, 1500, 1607, 670.

^1H NMR (400 MHz, DMSO-d_6): δ 7.2(1H,s), 1.18 (1 H, s), 6.93 (1 H, s), 8.10-8.12 (4H, m).

4d) (Z)-3-(4-hydroxybenzylidene)-4-methyl-1,3-dihydro-2H-pyrrol-2-one

Solid: - Melting point = 197°C

IR (KBr, cm^{-1}): 1354, 1260, 1500, 1607, 670.

^1H NMR (400 MHz, DMSO-d_6): δ 7.45(1H,s), 6.89 (1 H, s), 9.81 (1 H, s), 5.0(1H,s), 6.93 (4H, m).

Conclusion

We have been able to offer an effective method for the synthesis of pyrazolone derivatives in the presence of MSA in our current study. All of the recently synthesized compounds' structures were determined via mass spectral analysis, NMR, IR, and chemical transformations.

Condensation-enhanced pyrazolone synthesis and its derivatives provide high yields of pyrazolone in good quality and purity at a low cost.. This approach has the noteworthy advantages of being catalyst-free and having an easy workup procedure. The synthesis process used to create these molecules is very easy to use, clean, economical, green, and environmentally friendly.

References :

1. S. Mert, R. Kashmogullari, Postdoc, 2, 450, 2014.
2. G.Mariappan, B.Saha, Journal of pharmacy research, 3, 2856, 2010.
3. P. Gupta, K.Halve, International journal of pharmaceutical sciences and research, 4, 2291, 2015.
4. Z. Zhao, X. Dai, Eur.J.Med.Chem, 186, 1118, 93, 2020.
5. K. Karrouchi, S. Radii, Y. Ramli, Molecule, 23, 45, 2018.
6. M.Radii, V. Bernardo, B. Bechi, D. Castagnoio, Tetrahedron letters, 50, 6572, 2009.
7. P. Mitra, A.Mitra, Indian Chem. Soc., 58, 695, 1981.
8. B.Singh, Indian Chem. Soc., 68, 165, 1991.
9. M. Ruoqun, J. Zhu, J. Liu, L.Chem, X. Shen, H. Jiang, Molecule, 15, 3593, 2010.
10. R. Prajuli, J.Banerjee, H. Khanal, Oriental journal of chem., 31, 540, 2015.
11. M. Nashwa El- Metwaly, G. Marwa, A. Thoraya, M. Abelaua, Biogenetic chemistry and applications, 3, 654, 2018.
12. British Pharmacopici Vol. 2, Her Mejestis Stationary Office, London,12,(1980)British Pharmacopeia's Pharmaceutical press London,(1953)796.
- 13.Bary A.I., *The antimicrobial susceptibility test*, Principle and Practices Illusia and Febiger, Philadelphia, PA, USA, 180.
- 14.Cavangh F., *Analytical Microbiology* Academic Press New York, (1963) 126.

Preliminary Phytochemical analysis of Leaves extract of the plant *Justicia Adhatoda*

Swapnil D. Bhagat^{1*}, Sopan D. Ingole¹, Varun A. Mahale², Nandkishor S. Thakare¹ & Chandrakant U. Dhanwad¹

¹Department of Chemistry, M.S.P. Arts, Science & K.P.T. Commerce College, Manora, Maharashtra, INDIA

²Department of Chemistry, S.S.S.K.R. Innani Mahavidyalaya Karanja (Lad), INDIA

Email.-swapnil9388@gmail.com

Mobile No. 9595197970

Abstract:

The well-known Indian medicinal herb *Justicia adhatoda* is known for its pharmacopoeia. This plant has been used commonly in the ayurvedic system of medicine. This plant's root, bark, leaf and flower are used to heal many types of infection. In the present study, we have done the phytochemical screening of its leaves for glycoside, flavonoids, tannin, alkaloid, phenols, terpenoids and steroids and in the prepared hydroalcoholic extracts using Soxhlet extraction method

Key Words: Phytochemical Analysis, *Justicia Adhatoda* plant.

Introduction:-

Justicia adhatoda is a member of family Acanthaceae which is a small evergreen herbal plant. This plant is distributed all over the India. All the parts of this plant has been used for their curative effects from ancient times¹. *J. adhatoda* is a widely used plant medication in Unani and Ayurvedic medicine². *Justicia adhatoda* produces vasicine, which is used to treat a variety of illnesses, primarily respiratory tract conditions. In Sweden *J. adhatoda* is classified as a natural remedy and some preparations based on protocols against cough containing an extract of *J. adhatoda* are accessible³.

It is used by Ayurvedic physicians and possesses some medicinal properties. It has been used to treat a wide range of illnesses, most notably those affecting the respiratory system. As a result, it is one of the main herbs in the Ayurvedic system and is used to treat asthma, bronchitis, cough, and cold symptoms⁴. It has been used to control both internal and external bleeding such as peptic ulcers, hemorrhoids, bleeding gums and also used for a multitude of disorders including; leprosy, blood disorders, heart troubles, fever, vomiting, loss of memory, leucoderma, jaundice, tumors, mouth troubles, sore-eye and gonorrhea. In Sri Lanka, the plant is used to cure menorrhagia and profuse phlegm⁵. It is also used for the treatment of bleeding piles⁶, impotence and sexual disorders⁷.

In order to prepare the respiratory tracts for the rigorous breathing exercises, chewing the leaf buds alone or with a small amount of ginger root is a common yogic practice. Many leaf preparations are used in Southeast Asia to treat leprosy, bleeding, haemorrhage, skin conditions, wounds, and headaches^{8,9}. The bruised fresh leaves are used for snake-bites in India and Sri Lanka¹⁰.

Methods and Materials:

The plant leaf extract was prepared by using 25 gm of fresh leaves collected from the local areas. Fresh leaves were washed extensively with water followed by final wash twice thrice with distilled water to remove all the dust and unwanted visible particle. The leaves were cut in to small pieces and then shade dried for 2-3 days. Leaves were homogenized to a fine coarse powder using mortar and pestle and then stored in fine air tight container for further process.

Preparation of Plant Extract:

The powdered dried plant leaves were taken in a round bottom flask and extracted (25g) exclusively with 100 ml each of acetone, methanol, ethyl acetate, chloroform and diethyl ether in a soxhlet extractor for 4 hrs. and few porcelain pieces were added in to it to avoid bumping. After heating gently removed the solvent from sample by evaporation extract remains in round bottom flask used for phytochemical test.

Phytochemical Analysis:

Phytochemical analysis was carried out using standard methods^{11,12,13,14}.

1) Test for Carbohydrates :**Test for Starch:**

Procedure: Plant extract + 5 ml 5% KOH

Observation: A canary colouration.

2) Test for Glycosides :**i. 10% NaOH test:**

Procedure: 1 ml dil. H₂SO₄+0.2 ml extract+ boiled for 15 min + allowed cooling+ neutralize with 10%NaOH + 0.2 ml feeling solution A and B.

Observation: A brick red precipitate.

ii. Concentrate H₂SO₄ test:

Procedure: 5ml extracts solution + 2 ml Glacial acetic acid + a drop of 5% FeCl₃ + Con. H₂SO₄

Observation: A brown ring is observed

3) Test for Proteins and Amino acids :**Xanthoproteic test:**

Procedure: Plant extract + few drops of Con. nitric acid.

Observation: Yellow colored solution.

4) Salkowski's Test (Detection of Phytosteols):

Procedure: plant extract with chloroform + few drops of Conc. H₂SO₄, (Shake well and allowed to Stand).

Observation: Formation of Brown Color ring.

5) Salkowski's Test (Detection of Terpinoids):

Procedure :Plant extract + Chloroform + few drops of Conc. H₂SO₄, Shake well and allowed to Stand.

Observation: Reddish brown coloration (at bottom).

6) Test for Alkaloids:**i. Wagner's Test:**

Procedure: 1 ml Plant extract + 2ml Wagner's reagent (Solution of Iodine in Potassium Iodide)

Observation: Brown colored ppt. is formed

ii. Mayer's test:

Procedure: 1 ml plant extract with dil HCL +1-2 drops of mayer's reagent (Potassium mercuri iodide solution) Along the side of test tube.

Observation: yellow precipitate formed

7) Test for Flavonoids:**Lead acetate Test:**

Procedure: Plant extract is dissolved in 5 ml of distilled water + 3 ml of 10% lead acetate solution

Observation: A White ppt is formed

8) Test for Phenol:

Iodine test:- Procedure: 1 ml extract+ few drops of dil. Iodine solution.

Observation: A red colour present

9) Test for Saponin:

Foam test Procedure : 0.5 gm plant extract+ 2 ml water (vigorously shaken)

Observation: Persistent foam for 10 min

Result and Discussion:

The results for the phytochemical analysis of *Justicia adhatoda* plant was shown in Table no.1

Sr. No.	Test		Inference
1.	Test for Carbohydrates (Test For Starch)		+ve
2.	Test for Proteins	Xanthoproteic test	+ve
3.	Test for Phytosterols	Salkowski's Test	+ve
4.	Test for Terpenoids	Salkowski's Test	+ve
5.	Test for Alkaloids	Wagner's Test	+ve
		Mayer's test	+ve
6.	Test for Glycosides	NaOH test	+ve
		Conc. H ₂ SO ₄ test	+ve
7.	Test for Flavonoids	Lead acetate test	+ve
8.	Test for Phenol	Iodine Test	+ve
9.	Test for Saponin	Foam Test	+ve

The result from table no.1 shows that among the analyzed phytochemicals are Carbohydrates, Proteins, Phytosterols, Terpenoids, Alkaloids, Flavonoids, Saponin and Phenols were found present in the ethanolic extract of leaves of *Justicia adhatoda* plant. The medicinal properties of the plants are due to the presence of different phytochemicals which are present in the leaves of the plant.

Conclusion:

From the result, it is concluded that extract of leaves of *Justicia adhatoda* plants contains many active phytochemicals. Therefore the extract of these plants can be used as a drug. Further studies on isolation, purification, and characterization of phytochemicals are suggested for the development of new plant base pharmaceuticals having lesser side effects.

References:

1. Atal CK. Chemistry and Pharmacology of vasicine (1980): A new Oxytocin and abortifacient. Indian Drugs.; 15: 15-18.
2. Claeson UP, Malmfors T, Wikman G, Bruhn JG (2000). *Adhatoda vasica*: A critical review of ethnopharmacological and toxicological data. J. Ethnopharmacol., 72: 1-20
3. Farnlof A Naturalakemedel and Naturmedel.Halsokas-TradetsForlog. Stockholm, (1998) pp. 109-132,

4. Karthikeyan A, Shanthi V, Nagasathya A (2009). Preliminary Phytochemical and antibacterial screening of crude extract of the leaf of *Adhatoda vasica* (L). Int. J. Green Pharm., 3: 78-80.
5. Kirtikar KR, Basu BD .Indian medicinal plants (second Ed.) Bishen Singh Mahendra Pal Singh, Delhi, 3: 1899-1902, (1975)
6. Ahmad S, Garg M, Ali M, Singh M, Athar MT, Ansari SH (2009). A phyto-pharmacological overview on *Adhatoda zeylanica*. Medic. Syn. *A. vasica* (Linn.) Nees. Nat. Prod. Rad., 8: 549-554.
7. Pushpangadan P, Nyman U, George V (1995). Glimpses of Indian Ethnopharmacology. Tropical Botanic Garden and Research Institute, Kerala, pp. 309-383.
8. Adnan M, Hussain J, Shah MT, Ullah F, Shinwari JK, Bahadar A, Khan AL (2010). Proximate and nutrient Composition of Medicinal Plants of Humid and Sub-humid regions in Northwest Pakistan. J. Med. Plant Res., 4: 339-345
9. Atta-Ur-Rahman, Said HM, Ahmad VU (1986). Pakistan Encyclopaedia Planta Medica. Hamdard Foundation Press, Karachi, 1: 181-187.
10. Roberts E (1931). Vegetable materia medica of India and Ceylon. Plate Limited, Colombo, pp. 16-17.
11. Handayani R. Harahap U., Karsono (2017): Hypoglycemic Activity of Nano Particles from Temuru Leaves and Temuru(*Murraya koenigii* (L.) Spreng.) Leaf Extract on Alloxan Induced rats and Antioxidant Activity International Journal of ChemTech Research,10(2): 108-114.
12. Doughari JH (2012): Phytochemicals:extraction methods, basic structures andmode of action as potentialchemotherapeutic agents, phytochemicalsA global perspective of their role innutrition and health, In Tech, Rijeka,Croatia.
13. JB (1998): Phytochemical methods. Aguide to modern techniques of plantanalysis. (3rdedn) eds. Chapman and Hall.
14. Trease GE, Evans WC (1989):Pharmacology, (11thed) Bailliere TindallLtd, London.

***In-Silico* Prediction of Phytoconstituents From *Solanum Indicum* for Antistress Activity Targeting Ask 1 Inhibitor**

Sakshi Mude*, parimala Katolkar, Pradeep Raghatate, Jagdish Baheti

Kamla Nehru College of Pharmacy, Butibori, Nagpur 441108 (MS), INDIA

*Email:sakshi28mude@gmail.com

ABSTRACT

Objective Stress in psychology is defined as tension or pressure on emotion. Natural products and their active principles as sources for new drug discovery and treatment of diseases have attracted considerable attention of researchers. Compounds found in medicinal plants have been the source of many conventional medications. *In-silico* testing of *Solanum indicum* phytoconstituents on ASK 1 inhibitor for antistress efficacy was a part of our investigation.

Methods

Utilizing Discovery studio, molecular docking is done to assess the pattern of interaction between the phytoconstituents from the plant *Solanum indicum* and the crystal structure of the ASK 1 inhibitor (PDB ID: 3VW6). Later, SwissADME and pkCSM were used to screen for toxicity as well as the pharmacokinetic profile. Further, interaction between proteins by STRING network analysis was also evaluated.

Results

The docked results suggest that Solafuranone (-8.4 kcal/mol), Isofraxidin (-6.9 kcal/mol) for 3VW6 macromolecule has best binding towards antistress activity as compared to the standard (Fluvoxamine) for 3VW6 is -6.6 kcal/mol. Furthermore, pharmacokinetics and toxicity parameters were within acceptable limits according to ADMET studies.

Conclusion

Targeting ASK 1 inhibitor against the stress by phytomolecules from *Solanum indicum* can serve as a rational approach for designing future antistress drugs.

KETWORDS: *In-silico*, *Solanum indicum*, anti-stress activity, 3VW6, Discovery studio.

1. INTRODUCTION

The plant *Solanum indicum*, is a member of the Solanaceae family and is also known as Byakur, Guta started, Kata began and Indian Night Shade. *Solanum indicum*, also known as Badi Bhatkataiya in Hindi and "Brihati" in Sanskrit, is a plant used either alone or in combination with other drugs in the Ayurvedic medicinal system. The use of seeds, roots, leaves, and berries can be used to treat a variety of illnesses, including bronchitis, asthma, dry cough, rhinitis, dysuria, leucoderma, sexual dysfunction, insomnia, weak heartbeat, and pruritis.¹

A prickly perennial under shrub that can reach a height of 1 m and is mostly found in warmer areas of India up to a height of 1500 m, *Solanum indicum*, sometimes known as poison berries in English, is recognised for its poisonous berries-like fruit. This important medicinal plant is frequently used to treat poisonous affections, skin diseases, ulcers, breathing difficulties, abdominal pain, cough, and dyspepsia in folk and traditional Indian systems of medicine. Siddha and Ayurveda both use it.²

However, there are few studies on the phytoconstituents of *Solanum indicum* for the antistress activity. Thus, keeping the above information in view, the present investigation was designed to identify the potential phytochemicals of *Solanum indicum* against 3VW6 using a molecular docking method.

2. MATERIALS AND METHODS

2.1. Platform for molecular docking

The computational docking study of all the phytoconstituents selected as ligands with antistress activity as the target was performed using PyRx software.³

2.2. Protein preparation

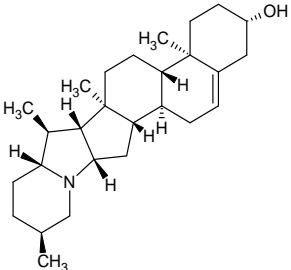
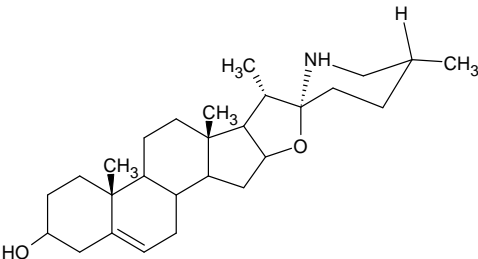
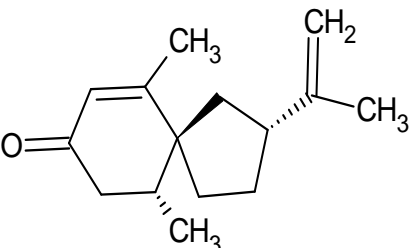
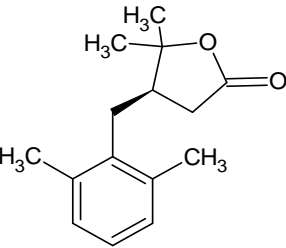
The macromolecule is 3VW6, *in silico* analysis of selected phytoconstituents was performed on the 2.40 Å crystal structure of antistress macromolecule with inhibitor, (PDB ID: 3VW6, having resolution Resolution: 2.40 Å, R-Value Free: 0.252, R-Value Work: 0.213, R-Value Observed: 0.215), which was retrieved from the protein data bank (<https://www.rcsb.org>). 3VW6 is classified as Crystal structure of human apoptosis signal-regulating kinase 1 (ASK1) with imidazopyridine inhibitor all other molecules, such as co-crystallized water molecules, unwanted chains, and nonstandard residues, were deleted. Using Discovery studio.⁴

2.3. Mechanism of Action

3VW6: Apoptosis signal-regulating kinase 1 (ASK1) was originally identified as a member of the mitogen-activated protein kinase (MAP3K) family that activates both p38 MAP kinase and c-Jun N-terminal kinase (JNK) pathways ASK1 is stimulated by various cell stressors including cytotoxic cytokines, reactive oxygen species (ROS), and endoplasmic reticulum stress. Recent studies revealed that ASK1 contributes not only to the regulation of cell death, but also to cytokine responses, cell differentiation, and immune regulation. Therefore, ASK1 inhibitors are thought to have potential for the protection of cells from various stresses in wide-ranging pathological situations such as autoimmune disease, diabetes, cardiovascular disease, neurodegenerative disorders, and inflammatory disorders.⁵

2.4. Ligand preparation

The three-dimensional (3D) structures of all constituents were retrieved using Avogadro software from the PubChem database available on the NCBI website (<https://pubchem.ncbi.nlm.nih.gov/>). However, the drawing of geometrical 2D structure was performed using the ChemSketch program. The two-dimensional (2D) structures were transformed into 3D models using the Avogadro software and the ligand structures were saved in the PDB format. All the chemical structures are shown in Figure 1.

<p>Solanidine</p> 	<p>Solasodine</p> 
<p>Solavetivone</p> 	<p>Solafuranone</p> 

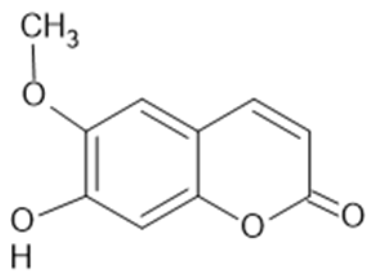
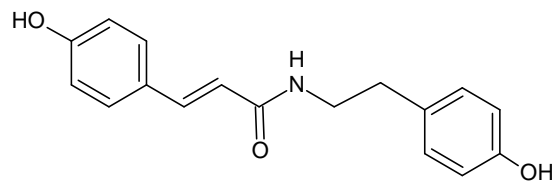
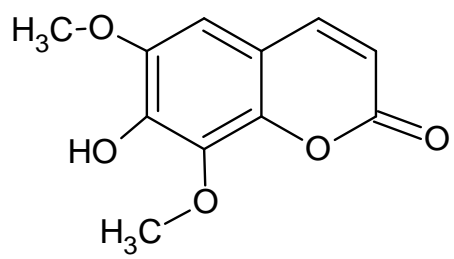
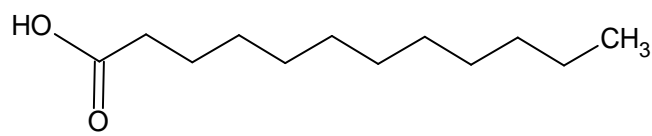
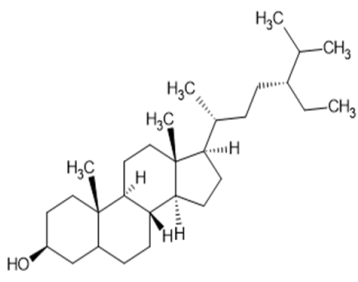
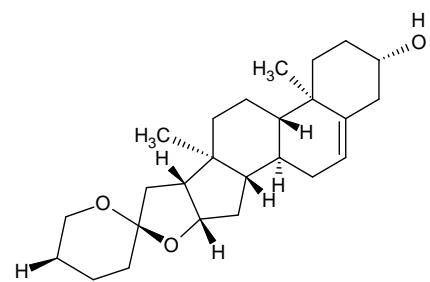
<p>Scopoletin</p> 	<p>N-p-trans-Coumaroyltyramine</p> 
<p>Isofraxidin</p> 	<p>Lauric acid</p> 
<p>β-sitosterol</p> 	<p>Diosgenin</p> 

Fig. 1. Chemical structures of all selected phytoconstituents in the molecular docking studies

2.5. Standard Preparation

The standard is prepared steps such as, the 2D structure of standard drug was made using chem sketch program, then the 2D structure was converted into 3D model using Avogadro Software, it was saved in PDB format.

By using PyRx molecular docking of Fluvoxamine was done with 3VW6.

2.6. Molecular docking

Molecular docking evaluates the protein-ligand interactions and estimates the scoring function based on the geometry to predict the binding affinity of the ligand molecule^{6,7}. We applied molecular docking studies to investigate the binding pattern of selected phytoconstituents (Figure 1) and the standard drug, along with the crystal structure of antistress activity macromolecule (PDB ID: 3VW6). The molecular docking study was performed using PyRx software, Binding affinity was explored using the Vina wizard tool. The final results were analysed and visualized using Discovery Studio 2020 Client⁸, with bound ligands as the

standard. Visualization of protein ligand interaction reflects the number of interactions and active residues responsible for significant binding at the active site of the target enzyme.

2.7. Absorption, distribution, metabolism, and excretion (ADME) and toxicity prediction

The selected phytoconstituents and standard drug were further checked for drug-likeness properties according to Lipinski's rule. During drug development, it is necessary to predict the tolerability of phytochemicals before being ingested by humans and animal models. The pharmacokinetic profile (ADME) and toxicity predictions of ligands were conducted using SwissADME (<http://www.swissadme.ch>) and pkCSM (an online server database predicting small-molecule pharmacokinetic properties using graph-based signatures, (<http://biosig.unimelb.edu.au/pkcsml/prediction>)). To analyse the toxicological properties of ligands, Simplified Molecular Input Line Entry System (SMILES) notations or PDB files were uploaded, followed by selecting the required models for generating numerous information about structure-related effects^{9,10}.

3. RESULT AND DISCUSSION

The present study aimed to explore the inhibitory potential of the phytoconstituents present in *Solanum indicum* targeting antistress activity. In this study, we performed molecular docking studies of all phytoconstituents found in *Solanum indicum* using AutoDock Vina, followed by a study of interacting amino acid residues and their influence on the inhibitory potentials of the active constituents. Selected phytoconstituents showing the best fit were further evaluated for absorption, distribution, metabolism, excretion, and toxicological (ADMET) properties using SwissADME and pkCSM servers.

3.1 Molecular docking

The docking scores and binding energies of all chemical constituents of *Solanum indicum* targeting antistress activity (PDB ID: 3VW6) and binding interactions with amino acid residues are presented in Table 1 respectively.

Table 1. Binding interaction of ligands from *Solanum indicum* targeting antistress activity (PDB ID:3VW6)

Sr. No.	Chemical constituent	PubChem ID	Docking Score
			3VW6
1.	Solanidine	65727	-9.1
2.	Solasodine	5250	-7.4
3.	Solavetivone	442399	-6.9
4.	Solafuranone	11107208	-8.4
5.	Scopoletin	5280460	-6.7
6.	N-p-trans-Coumaroyltyramine	5372945	-7.0
7.	Isofraxidin	5318565	-6.9
8.	Lauric acid	3893	-3.7
9.	β -sitosterol	222284	-7.4
10.	Diosgenin	99474	-8.5
Standard Drug			
11	Fluvoxamine	5324346	-6.6

The binding affinities of phytoconstituents ranged from -9.1 to -3.7 kcal/mol. From the docked results, it is evident that the compounds, Solanidine exhibit the most favourable binding affinity (-9.1 kcal/mol) in complex with selected macromolecules (PDB ID: 3VW6) as compared to other docked compounds i.e., Diosgenin (-8.5 kcal/mol), Solafuranone (-8.4 kcal/mol), Solasodine (-7.4 kcal/mol), Beta sitosterol (-7.4 kcal/mol), N-p-trans-

Coumaroyltyramine (−7.0 kcal/mol), Isofraxidin (−6.9 kcal/mol), Solavetivone (−6.9 kcal/mol), Scopoletin (−6.7 kcal/mol), Lauric acid (−3.7 kcal/mol). Visual examination of the computationally docked optimal binding poses of phytoconstituents on selected macromolecules (i.e., 3VW6) revealed the significant involvement of various types of interactions, such as hydrogen bonding and hydrophobic interactions, including π – π stacking and π –alkyl and alkyl interactions, in the stability of the binding of the phytoconstituents to 3VW6.

The binding affinity of the standard (Fluvoxamine) for 3VW6 is -6.6 kcal/mol.

3.1.1. Solafuranone, 3VW6

The number of intermolecular hydrogen bonds, the binding energy of ligand-3VW6 stable complexes, and the number of nearest amino acid residues were also determined for selected compound Solafuranone. All synthesized derivatives formed complexes with target proteins. Analysis of interactions of the 3VW6 protein complex and ligand Solafuranone showed that the ligand molecule is oriented due to Pi-alkyl interactions with LEU A: 810 amino acid residues Conventional Hydrogen bond with LYS A: 709 and Pi-Sigma interaction with LEU A: 686 amino acid residue were found.

3.1.2. Isofraxidin, 3VW6

An analysis of the interactions between the 3VW6 protein complex and the Isofraxidin ligand was also carried out, which showed that the ligand molecule is oriented due to conventional hydrogen bond with the amino acid residue LYS A: 688 and SER A: 821 and Pi-Alkyl and Alkyl interaction with ALA A:707, LUE A:686 and LUE A: 810, Pi-Sigma interaction with VAL A: 694 amino acid residue were found.

3.1.3. Fluvoxamine, 3VW6

The binding affinity of the standard (Fluvoxamine) for 3VW6 is -6.6 kcal/mol. the interactions between the 3VW6 protein complex and the Fluvoxamine ligand was also carried out, which showed that the ligand molecule is oriented due to conventional hydrogen bond with the ASP A:803, ARG A:767, SER A:821 amino acid residue, Pi-Alkyl and Alkyl interaction with ALA A:7047, MET A:754, LEU A:810, VAL A:694 amino acid residue and Salt bridge with ASP A:822 amino acid residue were found.

Table No. 2. Interaction with amino acid residue.

Sr. No.	Molecule	Binding Energy (kcal/mol)	H bond	Main amino acid interactions	
				Pi-alkyl, alkyl, Pi-S/Pi-Pi, T shaped/halogen/unfavourable donor-donor interactions	Van der Waals interactions
1	Solanidine	-9.1	No interaction	PHE A: 782, TRP A: 770	No interaction
2	Solasodine	-7.4	ASN A: 702, ASP A: 699	LEU A: 741, VAL A: 704, ARG A: 705	No interaction

3	Solavetivone	-6.9	No interaction	LEU A: 810, VAL A: 694	No interaction
4	Solafuranone	-8.4	LYS A: 709	LEU A: 810, LEU A: 686	No interaction
5	Scopoletin	-6.7	VAL A: 757, GLU A: 755, LYS A: 709	MET A: 754, LEU A: 810, VAL A: 694, ALA A: 707, LEU A: 686	No interaction
6	N-p-trans-Coumaroyltyramine	-7.0	VAL A: 757	GLY A: 759, VAL A: 694, MET A: 754	No interaction
7	Isofraxidin	-6.9	LYS A: 688, SER A: 821	ALA A: 707, LEU A: 686, LEU A: 810, VAL A: 694	No interaction
8	Lauric acid	-3.7	GLN A: 756	LEU A: 810	No interaction
9	β -sitosterol	-7.4	No interaction	LEU A: 686, ALA A: 707, MET A: 754, LEU A: 810, VAL A: 738, VAL A: 694, VAL A: 685, LYS A: 688	No interaction
10	Diosgenin	-8.5	ASN A: 702	ARG A: 705, VAL A: 704	No interaction
11	Fluvoxamine	-6.6	ASP A: 803, ARG A: 767, SER A: 821	ASP A: 822, VAL A: 694, LEU A: 810, MET A: 754, ALA A: 707	No interaction

3.2. ADMET study

Pharmacokinetic profile (ADME) and toxicity predictions of the ligands are important attentive parameters during the transformation of a molecule into a potent drug. In the present study, these parameters were assessed using SwissADME and pkCSM. The absorption potential and lipophilicity are characterized by the partition coefficient (Log *P*) and topological polar surface area (TPSA), respectively. For better penetration of a drug molecule into a cell membrane, the TPSA should be less than 140 Å. However, the value of Log *P* differs based on the drug target. The ideal Log *P* value for various drugs are as follows: oral and intestinal absorption, 1.35 – 1.80; sublingual absorption, > 5; and central nervous system (CNS)¹¹. The aqueous solubility of ligands ideally ranges from – 6.5 to 0.5¹², while the blood brain barrier (BBB) value ranges between – 3.0 and 1.2¹³. In addition, non-substrate P-glycoprotein causes drug resistance¹⁴.

In our study, all the selected ligands followed the TPSA parameter, P-glycoprotein non-inhibition, thereby showing good intestinal absorption and an acceptable range of BBB values. All the compounds showed aqueous solubility values within the range. Further, it was predicted that the selected ligands do not show AMES toxicity, hepatotoxicity, and skin sensitivity. In addition, it did not inhibit hERG-I (low risk of cardiac toxicity). Lipinski's rule violations, *T. pyriformis* toxicity, minnow toxicity, maximum tolerated dose, rat acute oral toxicity, and chronic toxicity are depicted in table.

Table 3. ADME and toxicity predicted profile of ligands with superior docking score

ADMET Properties	Formula	MW (g/mol)	Log P	TPSA (\AA^2)	HB donor	Hb acceptor	Aqueous solubility (Log mol/L)	Human intestinal absorption (%)	Blood Brain Barrier
Solanidine	$\text{C}_{27}\text{H}_{43}\text{NO}$	397.647	5.655	23.47 \AA^2	1	2	-4.927	92.975	0.695
Solasodine	$\text{C}_7\text{H}_{43}\text{NO}_2$	413.64	5.2869	41.49 \AA^2	2	3	-3.809	92.324	0.035
Solavetivone	$\text{C}_{15}\text{H}_{22}\text{O}$	218.33	3.9042	17.07 \AA^2	0	1	-4.615	95.873	0.635
Solafuranone	$\text{C}_{15}\text{H}_{20}\text{O}_2$	232.323	3.18764	26.30 \AA^2	0	2	-3.551	95.523	0.206
Scopoletin	$\text{C}_{10}\text{H}_8\text{O}_4$	192.17	1.5072	59.67 \AA^2	1	4	-2.504	95.277	-0.299
N-p-trans-Coumaroyltyramine	$\text{C}_{17}\text{H}_{17}\text{NO}_3$	283.327	2.4699	69.56 \AA^2	3	3	-3.165	90.031	-0.552
Isofraxidin	$\text{C}_{11}\text{H}_{10}\text{O}_5$	222.196	1.5158	68.90 \AA^2	1	5	-2.458	95.588	-0.377
Lauric acid	$\text{C}_{12}\text{H}_{24}\text{O}_2$	200.322	3.9919	37.30 \AA^2	1	1	-4.181	93.379	0.057
β -sitosterol	$\text{C}_{29}\text{H}_{50}\text{O}$	414.718	8.0248	20.23 \AA^2	1	1	-6.773	94.464	0.781
Diosgenin	$\text{C}_{27}\text{H}_{42}\text{O}_3$	414.63	5.7139	38.69 \AA^2	1	3	-5.713	96.565	0.2

Fluvoxamine	$C_{15}H_{21}F_3N_2O_2$	318.339	3.2015	56.84 Å ²	1	4	-3.641	90.686	-0.312
-------------	-------------------------	---------	--------	----------------------	---	---	--------	--------	--------

Table 3 Continued

ADMET Properties	P-glyco-protein substrate	Total clearance [Log mL/(min.kg)]	Bioavailability score	AME S toxicity	Max tolerated dose [Log mg/(kg.d)]	hERG I inhibitor	hERG II inhibitor
Solanidine	YES	0.028	0.55	NO	-0.882	NO	YES
Solasodine	YES	0.09	0.55	NO	-0.375	NO	YES
Solavetivone	NO	1.225	0.55	NO	0.044	NO	NO
Solafuranone	NO	1.256	0.55	NO	0.526	NO	NO
Scopoletin	NO	0.73	0.55	NO	0.614	NO	NO
N-p-trans-Coumaroyltyramine	YES	0.265	0.55	NO	-0.213	NO	YES
Isofraxidin	NO	0.713	0.55	NO	0.56	NO	NO
Lauric acid	NO	1.623	0.85	NO	-0.34	NO	NO
β -sitosterol	NO	0.628	0.55	NO	-0.621	NO	YES
Diosgenin	NO	0.328	0.55	NO	-0.559	NO	YES
Fluvoxamine	NO	0.589	0.55	NO	0.213	NO	YES

Table 3 Continued

ADMET Properties	Acute oral rat toxicity. LD50(mol/kg)	Oral rat chronic toxicity (Log mg/kgbw/day)	Hepatotoxicity	Skin sensation	T.Pyriformis toxicity (Log µg/L)	Minnow toxicity (Log mmol/L)	Lipinski's rule Violation
------------------	---------------------------------------	---	----------------	----------------	----------------------------------	------------------------------	---------------------------

Solanidine	2.596	1.334	YES	NO	0.378	- 0.493	YES (1)
Solasodine	2.489	1.332	YES	NO	0.311	0.381	YES (1)
Solavetivone	1.643	1.19	NO	YES	1.453	0.874	YES (0)
Solafuranone	1.865	1.947	NO	YES	2.151	0.557	YES (0)
Scopoletin	1.95	1.378	NO	NO	0.516	1.614	YES (0)
N-p-trans-Coumaroyltyramine	2.17	1.271	NO	NO	1.008	1.514	YES (0)
Isofraxidin	2.326	1.825	NO	NO	0.431	1.862	YES (0)
Lauric acid	1.511	2.89	NO	YES	0.954	- 0.084	YES (0)
β -sitosterol	2.552	0.855	NO	NO	0.43	- 1.802	YES (1)
Diosgenin	1.921	1.452	NO	NO	0.399	0.247	YES (1)
Fluvoxamine	3.311	1.314	NO	NO	1.183	0.841	YES (0)

3.3. Interaction of Standard Drug (Fluvoxamine) with 3VW6

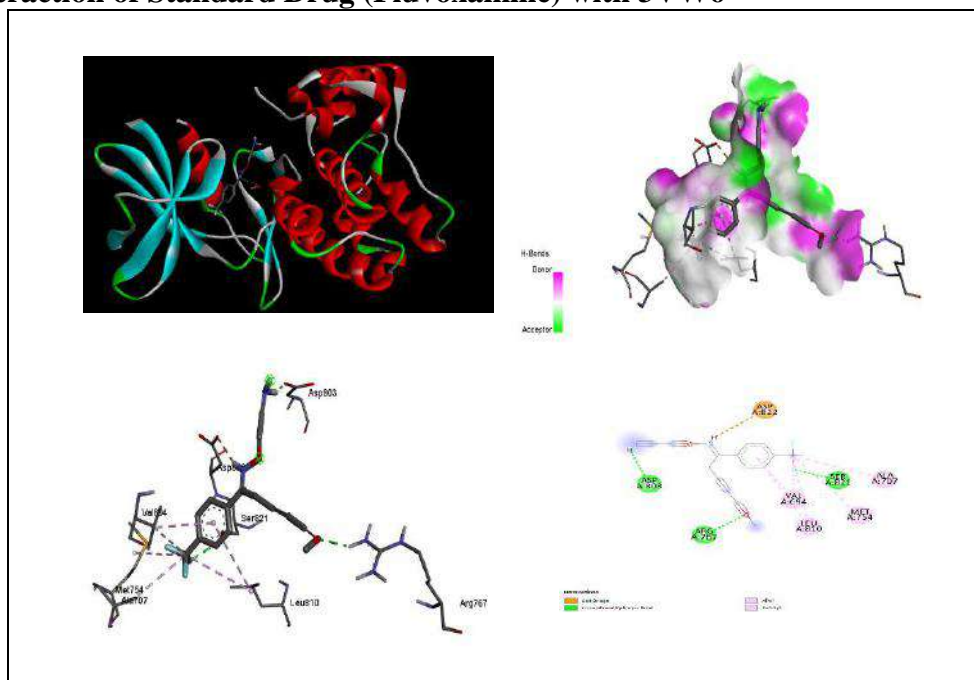
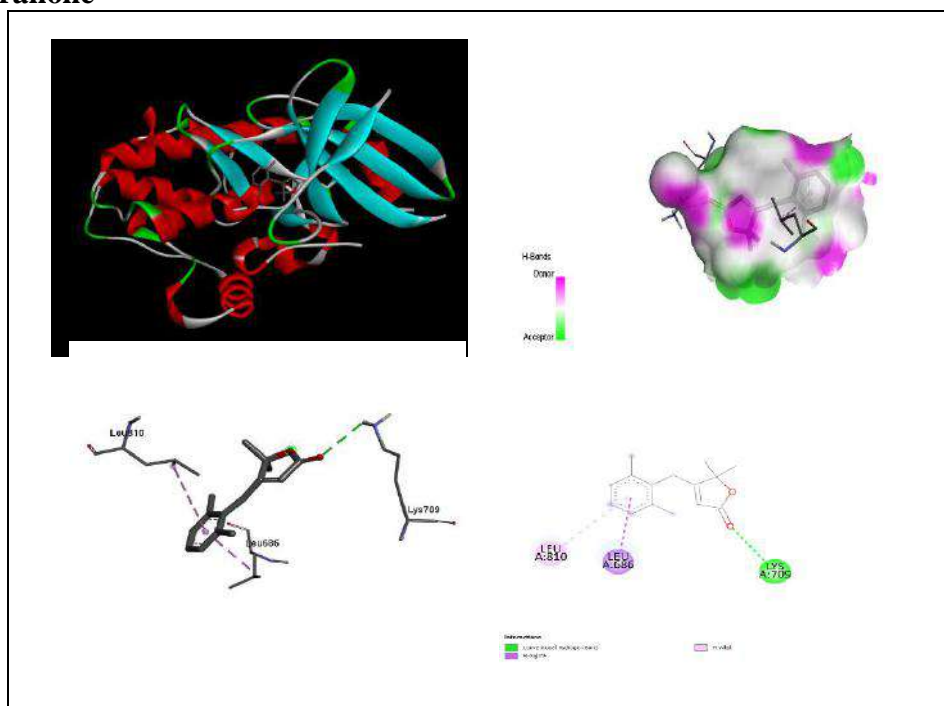


Fig. 2. Docking scores and binding interaction of Fluvoxamine (PDB ID: 3VW6). The ligand is shown in line and stick representation along with its 2D diagram and hydrogen bond interaction.

3.4. Interactions of phytoconstituents with 3VW6

A.Solafuranone



B.Isofraxidin

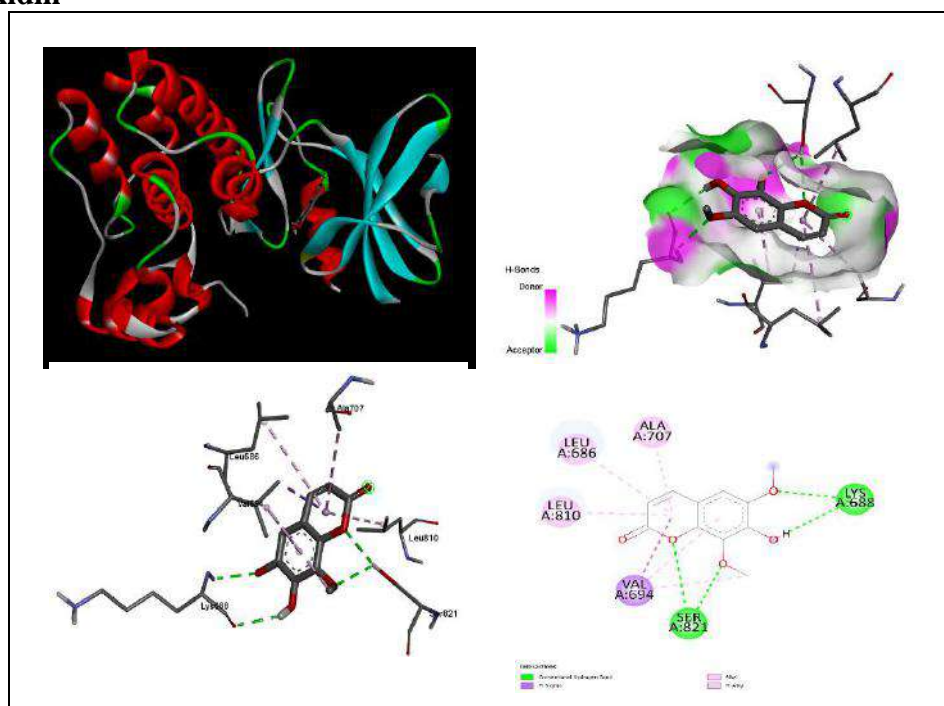


Fig. 3. Docking scores and binding interaction of phytoconstituents (PDB ID: 3VW6). The ligand is shown in line and stick representation along with its 2D diagram and hydrogen bond interaction.

3.5. Boiled Egg

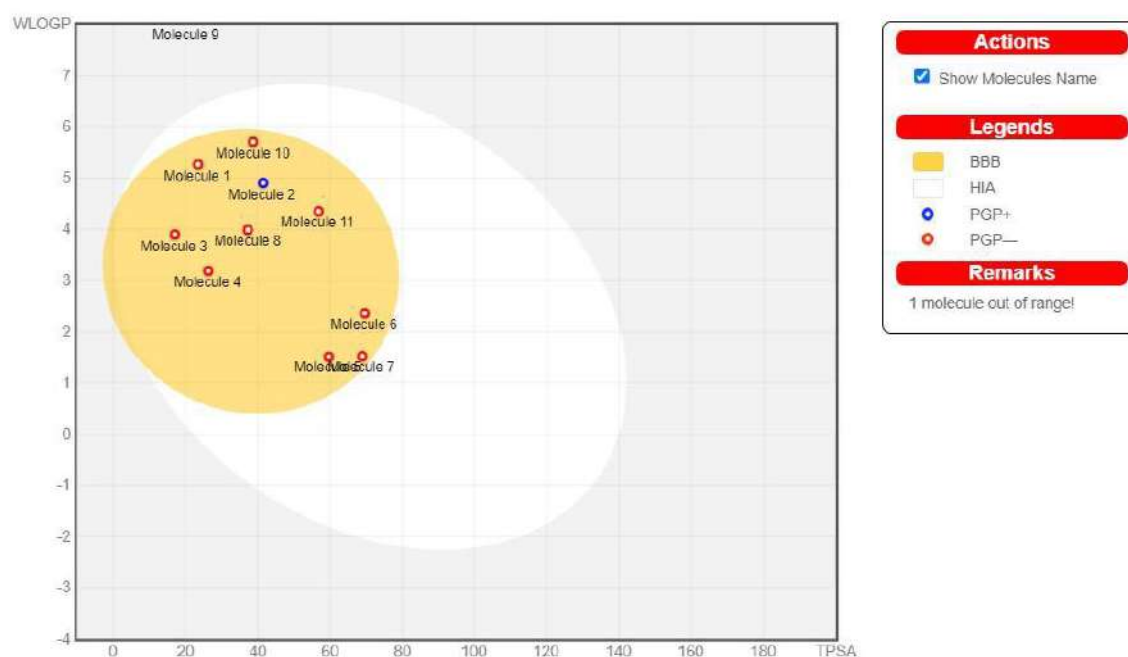


Fig no. 4. Combined Boiled Egg Diagram

Table no. 4. Name of molecules contained in Boiled Egg Diagram

MOLECULE NUMBER	MOLECULE NAME
1	Solanidine
2	Solasodine
3	Solavetivone
4	Solafuranone
5	Scopoletin
6	N-p-trans-Coumaroyltyramine
7	Isofraxidin
8	Lauric acid
9	β -sitosterol
10	Diosgenin
11	Fluvoxamine

BOILED means **B**rain **O**r **I**ntestina**L** **E**stimated permeation predictive model. The boiled egg diagram shows two regions white region and yellow region.

The white region is the physicochemical space of molecules with highest probability of being absorbed by the gastrointestinal tract, and the yellow region (yolk) is the physicochemical space of molecules with highest probability to permeate to the brain.

In addition, the points are coloured in blue if predicted as actively effluxed by P-gp (PGP+) and in red if predicted as non-substrate of P-gp (PGP-).

4. CONCLUSION

In this study, we have carried out an *in-silico* screening of the phytoconstituents of *Solanum indicum* plant. This study demonstrated the sixteen compounds from *Solanum indicum* plant, (Solanidine, Solasodine, Solavetivone, Solafuranone, Scopoletin, N-p-trans-Coumaroyltyramine, Isofraxidin, Lauric acid, β -sitosterol, Diosgenin). The selected phytocompounds showed docking scores ranging from -9.1 to -3.7 kcal/mol in 3VW6. Among all, Solafuranone and Isofraxidin gave the highest binding energy (-8.4 kcal/mol) and (-6.9

kcal/mol) in complex with 3VW6, whereas the reference compound, Fluvoxamine showed a docking score with a binding energy of -6.6 kcal/mol. Furthermore, these ligands exhibited good ADMET properties. To summarize, phytoconstituents present in *Solanum indicum* possess strong effects against 3VW6 and could be further evaluated for their antistress effect, as well as for the development of alternative drugs with fewer side effects for the treatment of stress.

REFERENCES

1. Sharma V, Hem K, Seth A, Maurya SK. *Solanum indicum* Linn.: An ethnopharmacological, phytochemical and pharmacological review. *Curr. Res. J. Pharm. Allied Sci.* 2017;1:1-9.
2. Jayanthi A, Maurya A, Verma SC, Srivastava A, Shankar MB, Sharma RK. A brief review on pharmacognosy, phytochemistry and therapeutic potential of *Solanum indium* L. used in Indian Systems of Medicine. *Asian Journal of Research in Chemistry.* 2016;9(3):127-32.
3. Morris GM, Huey R, Lindstrom W, Sanner MF, Belew RK, Goodsell DS, Olson AJ. AutoDock4 and AutoDockTools4: Automated docking with selective receptor flexibility. *Journal of computational chemistry.* 2009 Dec;30(16):2785-91.
4. Pettersen EF, Goddard TD, Huang CC, Couch GS, Greenblatt DM, Meng EC, Ferrin TE. UCSF Chimera—a visualization system for exploratory research and analysis. *Journal of computational chemistry.* 2004 Oct;25(13):1605-12.
5. Yu YN, Han Y, Zhang F, Gao Z, Zhu T, Dong S, Ma M. Design, synthesis, and biological evaluation of imidazo [1, 2-a] pyridine derivatives as novel PI3K/mTOR dual inhibitors. *Journal of Medicinal Chemistry.* 2020 Feb 18;63(6):3028-46.
6. Verdonk ML, Cole JC, Hartshorn MJ, Murray CW, Taylor RD. Improved protein–ligand docking using GOLD. *Proteins: Structure, Function, and Bioinformatics.* 2003 Sep;52(4):609-23.
7. Leach AR, Shoichet BK, Peishoff CE. Prediction of protein– ligand interactions. Docking and scoring: successes and gaps. *Journal of medicinal chemistry.* 2006 Oct 5;49(20):5851-5.
8. SAMANT L, Javle V. Comparative docking analysis of rational drugs against COVID-19 main protease.
9. Arora S, Lohiya G, Moharir K, Shah S, Yende S. Identification of potential flavonoid inhibitors of the SARS-CoV-2 main protease 6YNQ: a molecular docking study. *Digital Chinese Medicine.* 2020 Dec 1;3(4):239-48.
10. Shah S, Chaple D, Arora S, Yende S, Moharir K, Lohiya G. Exploring the active constituents of *Oroxylum indicum* in intervention of novel coronavirus (COVID-19) based on molecular docking method. *Network Modeling Analysis in Health Informatics and Bioinformatics.* 2021 Dec;10:1-2.
11. Kaloni D, Chakraborty D, Tiwari A, Biswas S. In silico studies on the phytochemical components of *Murraya koenigii* targeting TNF- α in rheumatoid arthritis. *Journal of Herbal Medicine.* 2020 Dec 1;24:100396.
12. Joshi T, Sharma P, Joshi T, Chandra S. In silico screening of anti-inflammatory compounds from Lichen by targeting cyclooxygenase-2. *Journal of Biomolecular Structure and Dynamics.* 2020 Aug 12;38(12):3544-62.
13. Nisha CM, Kumar A, Vimal A, Bai BM, Pal D, Kumar A. Docking and ADMET prediction of few GSK-3 inhibitors divulges 6-bromoindirubin-3-oxime as a potential inhibitor. *Journal of Molecular Graphics and modelling.* 2016 Apr 1;65:100-7.
14. Tsujimura S, Tanaka Y. Disease control by regulation of P-glycoprotein on lymphocytes in patients with rheumatoid arthritis. *World journal of experimental medicine.* 2015 Nov 11;5(4):225.

Design, Synthesis, Spectral Characterisation and Antibacterial Screening of Some Novel 4-Substitutedimino-1,3,5-Dithiazine Along With Pyrimidine Nucleus

S. B. Sarkate^{a*}, S. A. Waghmare^b, K. U. Dongare^c, R. N. Ingole^d

^{a,b,c}Department of Chemistry, Ghulam Nabi Azad Arts, Commerce and Science College Barshitakli Dist. Akola 444401 (M.S.), India.

^dDepartment of Chemistry, Shri Vitthal Rukhmini College, Sawana, Mahagaon, Dist. Yavatmal, (M.S.) India

*Corresponding author- swapnilsarkate1991@gmail.com

ABSTRACT

In recent times in the laboratory, synthesis of 2-(2-Phenylimino-4-substitutedimino-1,3,5-dithiazino) aminopyrimidine (**IIIa-e**) were synthesized by refluxing 2-(5-phenyl-2,4-dithiobiureto) pyrimidine (**I**) with alkyl/aryl isocyanodichlorides (**IIa-e**) in acetone-ethanol medium in 1:1 molar proportion. The structures of all the synthesized compounds were acceptable on the basis of chemical characteristics, elemental analysis, spectral studies and their antibacterial screening against the gram positive and gram negative bacteria such as *S. typhi*, *E. coli*, *S. aureus*, *A. Aerogenes*, *B. Subtilis* and *B. Megatherium*. etc.

INTRODUCTION

Heterocycles containing organic molecules are more fascinating, because they are convenient in a variety of applications, a multitude of uses are included by the heterocycles' size and heteroatom diversity. These compound nitrogen, oxygen and sulphur are composed of six member¹⁻⁵, five member⁶⁻⁷ fused heterocycles with aromatic rings. Particularly noteworthy are the numerous biological and industrial uses for heterocycles that combine sulphur and nitrogen in one ring. Six member two sulphur and one nitrogen atom prepare 1,3,5-dithiazine. It is one of the six member heterocycles that functions as a strong medication in the sectors of medicine, agriculture, and industry⁹⁻⁸.

Tayade¹⁰, Pathe¹¹ and Mur¹² Synthesized numerous heterocycles containing 1,3,5-dithiazines as main nucleus. Each 1,3,5-dithiazino moiety has different applications according to the substituent attached to the basic nucleus of the 1,3,5-dithiazine. It has been also observed during literature study that, 1,3,5-dithiazino nucleus and its derivatives possesses biological and medicinal effective properties¹³⁻¹⁴.

Substituted isocyanodichlorides were used by researchers to synthesise 1,3,5-dithiazines in the laboratory. This 1,3,5-dithiazine synthesis technique is quicker, less complicated, less expensive and requires less time.

MATERIAL AND METHOD

Material

All the chemical used were of loba chemie (AR grade).

Method

In the present experiment for the synthesis of different substituted 1,3,5-dithiazino aminopyrimidine is conventional refluxing under electronic water bath for different hours for different experiment.

EXPERIMENTAL

All the chemicals used for the synthesis were purified. After refluxing the purity of the compounds were checked by TLC (aluminium TLC) with thin layer thickness of 200 μ m. The melting points of all synthesized compounds will be recorded using hot paraffin bath. The carbon and hydrogen analysis were carried out on Carlo-Ebra-1106 analyser Nitrogen estimation were carried out with colmon-N-analyzer-29. IR spectra were recorded with Bruker spectrometer in

the range 4000-400 cm⁻¹. PMR spectra were recorded on VARIAN 400 MHz spectrometer with TMS as internal standard using CDCl₃ and DMSO Solvent.

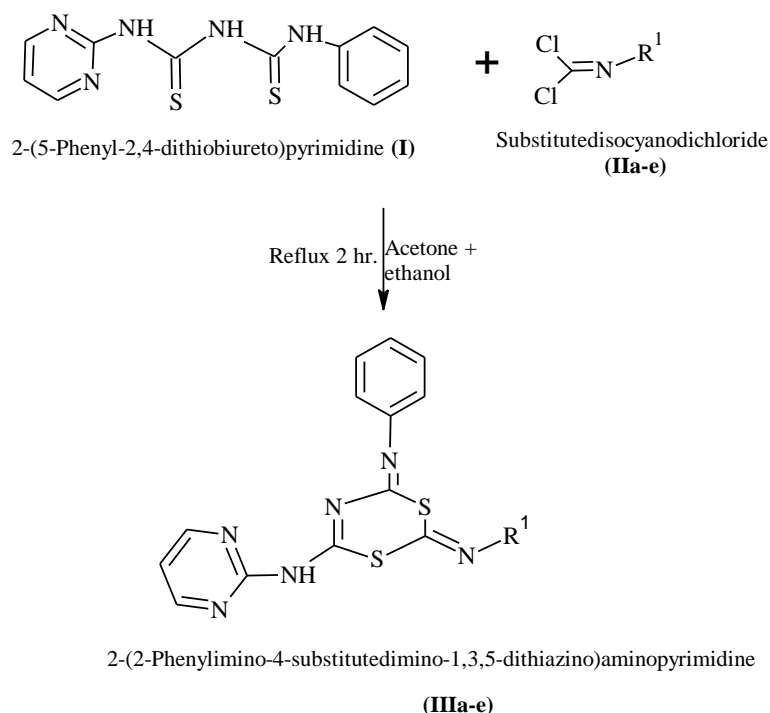
GENERAL PROCEDURE

A reaction of 2-(5-phenyl-2,4-dithiobiureto)pyrimidine (**I**) and substitute disocyanodichloride (**IIa-e**) in 1:1 molar ratio refluxed on water bath in acetone-ethanol medium for 2 hours. The evolution of the hydrochloride gas was clearly observed during refluxion. After distillation of excess solvent orange product isolated which on basification with dilute ammonium hydroxide orange crystalline products obtained.

Similar, procedure was adopted for the synthesis of all the derivatives in the series.

The tentative reaction for the formation of product is depicted below,

Reaction



Similarly, 2-(5-phenyl-2,4-dithiobiureto)pyrimidine (**I**) were react with phenylisocyanochloride (**IIa**), ethylisocyanodichloride (**IIb**), tertbutylisocyanodichloride (**IIc**), P-tolylisocyanodichloride (**IId**) and 4-chlorophenhyisocyanodichloride (**IIe**) by the above mentioned method to isolate 2-[2,4-di(phenylimino)-1,3,5-dithiazino] aminopyrimidine (**IIIa**), 2-(2-phenylimino-4-ethylimino-1,3,5-dithiazino) aminopyrimidine(**IIIb**), 2-(2-phenylimino-4-*tert*-butylimino-1,3,5-dithiazino) aminopyrimidine (**IIIc**), 2-[2-phenylimino-4-(4-methylphenylimino)-1,3,5-dithiazino]aminopyrimidine (**IIId**) and 2-[2-phenylimin-4-(4-chlorophenylimino)-1,3,5-dithiazino]aminopyrimidine (**IIIe**).

RESULT AND DISCUSSION

Spectral characterization results for all the synthesized compounds are given below

Spectral Characterization

1. 2-(2,4-diphenylimino-1,3,5-dithiazino)aminopyrimidine (**IIIa**)

Colour-Yellow solid, **Molecular formula**- C₁₅H₁₄N₆S₂, **Yield** 85%, **M.P.** 162^oC, **% Composition found (calculated)** C-52.90 , H-4.83 , N-25.20, S-23.21 , **FTIR (Kbr) vcm**- 3245.22 N-H stretching, 3051.47 (C-H Ar Stretching), 3187.38 (N-H Amido), 1950.37 (C-H Ar Bending,), 1185.99 (C=S Stretching), 670.04(=C-H bending); **¹H NMR (400MHz CDCl₃ δ ppm)**, 8.4ppm (2H, double, CH) of pyrimidine, 7.2ppm (2H, CH, doublet) of pyrimidine, 7.2

ppm (2H, , doublet CH) of phenyl, 3.4 ppm (1H, singlet NH), 4.6 ppm 1H singlet, 7.39 1H triplet CH benzene, 1H triplet CH benzene 2.2 ppm 2H quartet, 2.3 ppm 3H triplet **Mass m/z** 390.30

2. 2-(2-phenylimino-4-ethylimino-1,3,5-dithiazino)aminopyrimidine (IIIb)

Colour-Yellow solid, **Molecular formula**- $C_{15}H_{14}N_6S_2$, **Yield** 86%, **M.P.** 170°C, % **Composition found (calculated)** C-52.90 , H-4.83 , N-25.20, S-23.21 , **FTIR (Kbr) vcm**- 3245.22 N-H stretching, 3051.47 (C-H Ar Stretching), 3187.38 (N-H Amido), 1950.37 (C-H Ar Bending,), 1185.99 (C=S Stretching), 670.04(=C-H bending); **¹H NMR (400MHz CDCL₃ δ ppm)**, 8.4ppm (2H, double, CH) of pyrimidine, 7.2ppm (2H, CH, doublet), 7.2 ppm (2H, , doublet CH) of phenyl, 3.4 ppm (1H, singlet NH), 4.6 ppm 1H singlet, 7.39 1H triplet CH benzene, 1H triplet CH benzene 2.2 ppm 2H quartet, 2.3 ppm 3H triplet **Mass m/z** 342.30

3. 2-(2-phenylimino-4-tertbutylimino-1,3,5-dithiazino)aminopyrimidine (IIIc)

Colour-Yellow solid, **Molecular formula**- $C_{17}H_{18}N_6S_2$, **Yield** 90%, **M.P.** 158°C, % **Composition found (calculated)** C-55.90 , H-4.83 , N-23.20, S-17.21 , **FTIR (Kbr) vcm**- 3245.22 N-H stretching, 3045.47 (C-H Ar Stretching), 3140.38 (N-H Amido), 1995.37 (C-H Ar Bending,), 1164.99 (C=S Stretching), 710.04(=C-H bending); **¹H NMR (400MHz CDCL₃ δ ppm)**, 8.2ppm (2H, double, CH), 7.2ppm (2H, CH, doublet), 7.1ppm (2H, , doublet CH), 3.5 ppm (1H, singlet NH), 4.5 ppm 1H singlet, 7.40 1H triplet CH benzene, 2.4 9H singlet **Mass m/z** 370.50

4. 2-(2-phenylimino-4-tolylimino-1,3,5-dithiazino)aminopyrimidine (IIId)

Colour-Yellow solid, **Molecular formula**- $C_{20}H_{16}N_6S_2$, **Yield** 82%, **M.P.** 167°C, % **Composition found (calculated)** C-55.90 , H-4.83 , N-23.20, S-15.21 , **FTIR (Kbr) vcm**- 3200.22 N-H stretching, 2901.47 (C-H Ar Stretching), 316038 (N-H Amido), 1960.37 (C-H Ar Bending,), 1167.99 (C=S Stretching), 745.04(=C-H bending); **¹H NMR (400MHz CDCL₃ δ ppm)**, 8.2 ppm (2H, double, CH) of pyrimidine, 7.3ppm (2H, CH, doublet), 7.2 ppm (2H, , doublet CH), 3.5 ppm (1H, singlet NH), 4.7 ppm 1H singlet, 7.39 1H triplet CH benzene, 3.4 ppm 3H singlet. **Mass m/z** 404.60

5. 2-(2-phenylimino-4-p-chlorophenylimino-1,3,5-dithiazino)aminopyrimidine (IIIe)

Colour-Yellow solid, **Molecular formula**- $C_{19}H_{13}N_6S_2$, **Yield** 80%, **M.P.** 145°C, % **Composition found (calculated)** C-53.90 , H-3.83 , N-20.20, S-15.21Cl-8.45 , **FTIR (Kbr) vcm**- 3263.22 N-H stretching, 3051.47 (C-H Ar Stretching), 3216.38 (N-H Amido), 1966.37 (C-H Ar Bending,), 1165.99 (C=S Stretching), 720.04(=C-H bending); **¹H NMR (400MHz CDCL₃ δ ppm)**, 8.4 ppm (2H, double, CH) of pyrimidine, 7.03ppm (2H, CH, doublet), 7.4 ppm (2H, , doublet CH), 3.5 ppm (1H, singlet NH), 4.6 ppm 1H singlet, 7.39 1H triplet CH benzene, **Mass m/z** 424.80.

CONCLUSION

In the present work is cheaper and less time consuming method for synthesis of organic compound (IIIa-e). In all the synthesized compounds give the maximum yield of product (III a-e). A variety of pyrimidine based 1,3,5-dithiazine derivative can be synthesized for their antimicrobial activities adopting the method.

PHARMACOLOGICAL STUDIES

Antimicrobial activity

All the synthesized compounds (III-a) to (III-e) were screened for antibacterial activity against *S. typhi*, *E. coli*, *S. aureus*, *A. Aerogenes*, *B. Subtilis* and *B. Megatherium*. by disc diffusion method was performed using mueller hinton agar as well as nutrient agar medium. Each and every compound was tested at conc. 50 µg/ml in ethanol. The zone of inhibition of all the synthesized compounds were measured after 24 hour incubation at 37 °C. Standard drug used for comparison the activity was Ciprofloxacin.

Table 1: Synthesized compound **IIIa-e** activity against Gram +ve and Gram -ve bacteria

Table No. 1.1 - Antibacterial activity of synthesized compound against bacteria (Zone of inhibition in mm) (after 24 hrs at 37 °C temp)							
SR No.	Compd.	Gram positive			Gram negative		
		<i>S. aureus</i>	<i>B. subtilis</i>	<i>B. megatherium</i>	<i>S. typhi</i>	<i>E. coli</i>	<i>A. aerogenes</i>
1	SBS-IIIa	18	12	16	14	18	11
2	SBS-IIIb	11	12	14	14	11	12
3	SBS-IIIc	11	11	12	11	11	11
4	SBS-IIId	10	12	12	12	11	11
5	SBS-IIIE	14	12	14	12	16	12
6	Std Ciprofloxacin	18	16	20	18	20	14

REFERENCE

- Zhang, D. H., Zhang, Z., & Shi, M. (2012). Transition metal-catalyzed carbocyclization of nitrogen and oxygen-tethered 1, n-enynes and diynes: synthesis of five or six-membered heterocyclic compounds. *Chemical Communications*, 48(83), 10271-10279.
- Larrosa, I., Romea, P., & Urpí, F. (2008). Synthesis of six-membered oxygenated heterocycles through carbon-oxygen bond-forming reactions. *Tetrahedron*, 64(12), 2683-2724.
- Sanu, M. C., Joseph, J., Chacko, D., Vinod, B., & Daisy P., A. (2021). Review on six membered nitrogen containing heterocyclic compounds with various biological activities. *International Journal of Pharmaceutical Sciences Review and Research*, 69(2), 64-68.
- Walton, J. C. (2016). Synthetic strategies for 5-and 6-membered ring azaheterocycles facilitated by iminyl radicals. *Molecules*, 21(5), 660.
- Huh, D. N., Cheng, Y., Frye, C. W., Egger, D. T., & Tonks, I. A. (2021). Multicomponent syntheses of 5-and 6-membered aromatic heterocycles using group 4–8 transition metal catalysts. *Chemical Science*, 12(28), 9574-9590.
- Sergey P., Vladimir N., Andrey, E., & A. Pimerzin, E. Vishnevskaya E., Thermodynamic analysis of strain in the five-membered oxygen and nitrogen heterocyclic compounds. *The Journal of Physical Chemistry*, 115(10), 1992–2004.
- Kaur, N., Yadav, N., & Verma, Y. (2023). Acetamidine in heterocycle synthesis. *Synthetic Communications*, 53(9), 577-614.
- Gujjar, K. N., & Narasimha S M., (2023). A Review: Important applications of Heterocyclic Compounds. *Europeam Chemical Bulletin*, 12(12), 625-630.
- Sharma, P. K., Amin, A., & Kumar, M. (2020). A review: Medicinally important nitrogen sulphur containing heterocycles. *The Open Medicinal Chemistry Journal*, 14(1), 49-64.
- Tayade, D. T., & Padhen, S. S. (2016). Synthesis and Characterization of 1-Phenyl-3- [4-(2-Substitutedimino-4-Substitutedimino-1,3,5-Dithiazino) Aminophenyl]- Prop-2-Ene-1-Ones. *International Journal of Pharmacy and Pharmaceutical Research*, 7 (1), 53-58.
- Pathe, P. P., & Paranjpe, M. G. (1984). Preparation of 5-aryl-4- arylimino-6-benzylimino-2-phenylimino-1,3,5-dithiazine. *Indian chemical society*, 15(43), 149-150.
- Mur, V. I. (1964). 2, 4, 6-trichloro-1, 3, 5-triazine (cyanuryl chloride) and its future applications. *Russian Chemical Reviews*, 33(2), 92-103.
- Panpaliya, K. S., Tayade, D. T., Shaikh, R. S., & Thakare, A. N. (2017). Synthesis of 1-phenyl-3-substituted- 2,6-dithio-4- amino-[(2-phenylthiocarbamido)- 1,3-benzothiazolo]- 1,3,5-triazine and their effects on germination pattern of sorghum vulgare. *Online International Interdisciplinary Research Journal*, 1, 6-9.
- Deohate, P. P., & Berad, B. N. (2005). Synthesis and antimicrobial activity of 1, 3, 5-thiadiazines and their isomerism into 1, 3, 5-triazines. *Indian journal of Chemistry*, 44B, 638-642.

Comparative Account of Partial Molar Volumes and Compressibilities of Aqueous-(L-Arginine + Glucose/Lactose) Solutions at 310.15 K

R. V. Dudhate¹, H. N. Pawar¹, B. R. Bhosle¹, S. D. Deosarkar¹, S. D. Deshmukh², and P. S. Bodkhe³

¹School of Chemical Sciences, Swami Ramanand Teerth Marathwada University, Nanded

²College of Engineering and Technology, Akola

³Vidya Bharati Mahavidyalaya, Camp Amravati

Abstract: Partial molar volumes and compressibilities of aqueous-(L-Arginine + Glucose/Lactose) solutions have been determined from measured densities and ultrasonic velocities at 310.15 K. The measured, calculated and graphically determined properties viz. densities and ultrasonic velocities, apparent molar volumes and compressibilities and partial molar volumes and compressibilities and have been interpreted in terms of different interactions in studied solutions. Effect of Glucose/Lactose on structural orientation, hydration behavior and different interactions including hydrogen bonding has been evaluated. Study has importance in amino acid-sugar interactions.

Introduction:

L-Arginine is an essential basic amino acid found in protein rich food and strongly interacts with organic acids as well as carbohydrates through hydrogen bonding and hydrophilic/hydrophilic interactions. Glucose is a most abundant monosaccharide sugar [1-2]. Lactose (milk sugar) is a disaccharide sugar used in the food industry [3].

Numbers of researchers have carried out molecular interaction studies of L-Arginine in aqueous and various cosolutes including drug [4-8] solutions. These interactions lead to the perturbation of structure and orientation of aqueous L-Arginine. Sugar interactions with amino acid specifically L-Arginine through volumetric and ultrasonic studies in solution is lacking. In view of importance of these studies in this short communication, we report comparison of partial molar volumes and compressibilities of these solutions at 310.15 K.

Experimental:

L-Arginine (Himedia, 174.2 g/mol) solutions in water and aqueous Glucose (Himedia, 180.16 g/mol)/Lactose (Himedia, 342.30 g/mol) were prepared in double distilled water. Details of experimental work (measurement of densities and ultrasonic velocities) are explained in our previous papers [9-11]. Apparent and partial molar volume and compressibility and corresponding transfer properties are determined using standard relations [12-17].

Results and discussion:

It is seen from Figure 1 and 2 that the measured densities (ρ) and ultrasonic velocities u increase with increase in the concentration of L-Arginine as well as increase in the concentration of cosolutes (Figure 1 A and C, 2 A and C). The apparent molar volumes ($V_{2,\phi}$) and compressibilities ($\kappa_{2,\phi}$) increase with increase in concentration L-Arginine as well as increase in cosolute concentration (Figure 1 B and C, 2 B and D). However these values are larger in Lactose solution compared to Glucose solution. This is attributed to the more number of -OH groups in Lactose compared to Glucose which makes loose structure, expansion in volume of hydration with more compression in Lactose.

The partial molar properties, partial molar volumes ($V_{2,\phi}^o$) and partial molar compressibilities ($\kappa_{2,\phi}^o$) are determined from straight line equations as an intercept of lines using Masson's and Gucker's equations and solute-solute interaction parameters (S_v and S_k) are determined as a slope of these lines and are listed in Table 1 and 2. Partial molar properties and transfer properties ($\Delta V_{2,\phi}^o$ and $\Delta \kappa_{2,\phi}^o$) of L-Arginine increases on addition of cosolutes and further increases with their concentration. This is due

to the overlap of cospheres of solute and cosolute and release of water molecules into the bulk solution (Scheme 1).

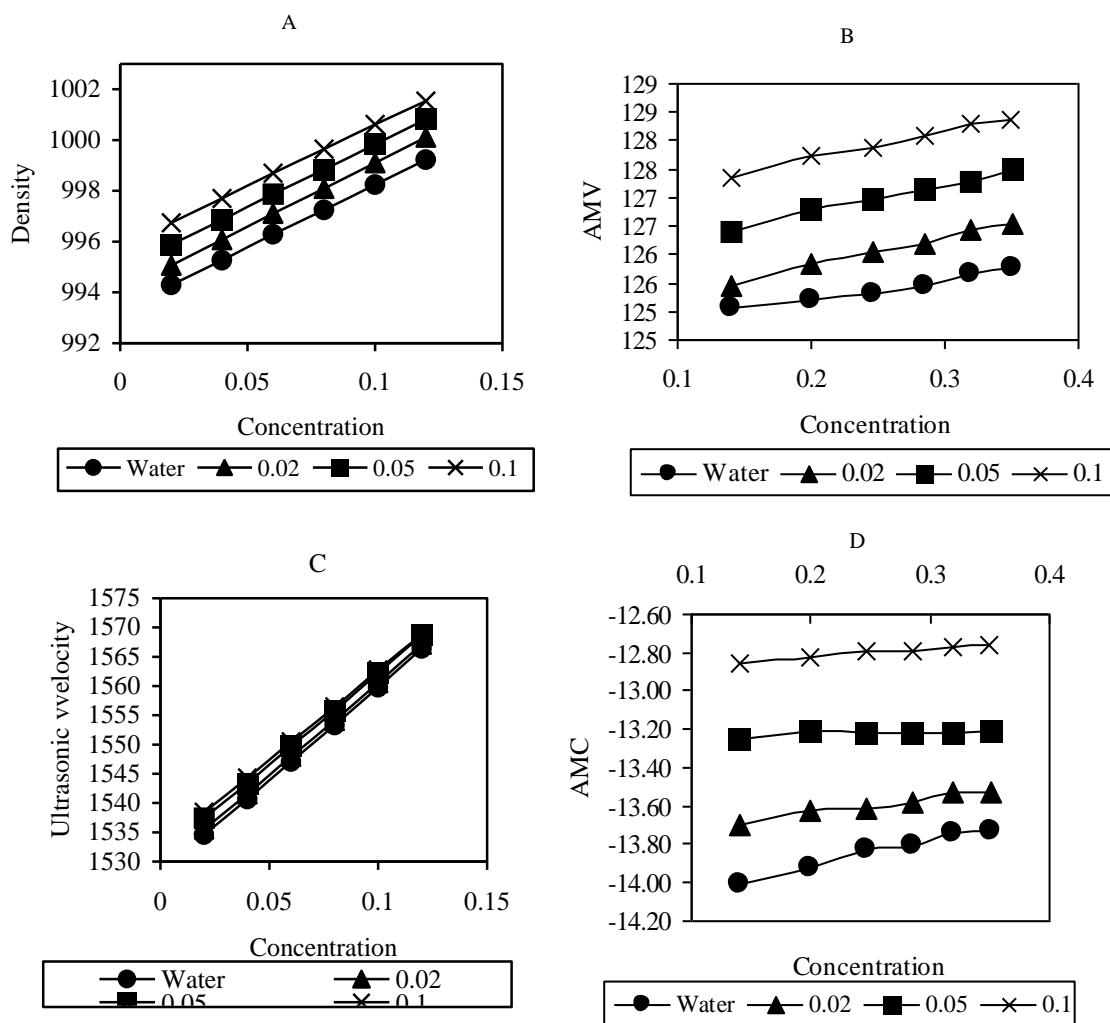
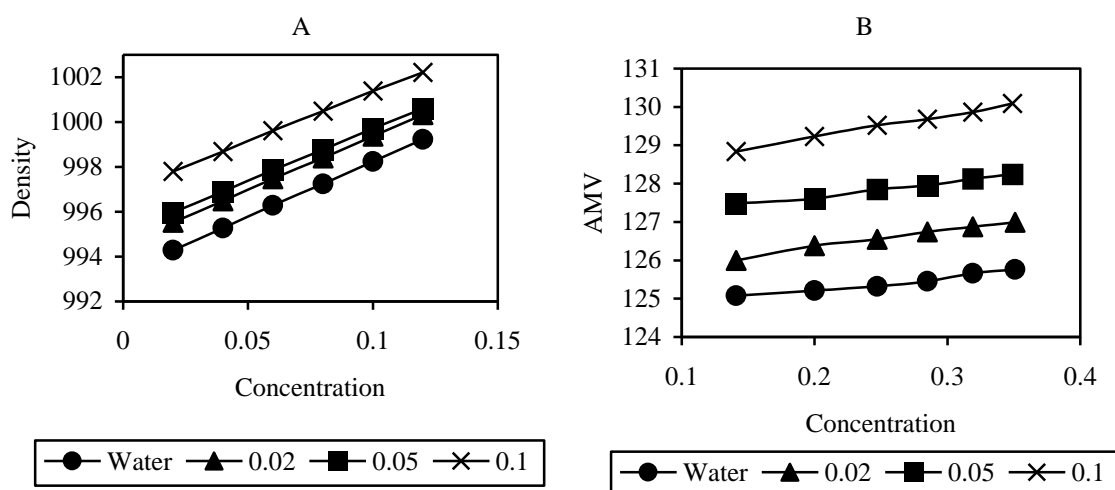


Figure 1 A-D. The, ρ , $V_{2,\phi}$ and u , $\Delta\kappa_{2,\phi}$ values of (Aq. L-Arginine + Glucose) at 310.15 K



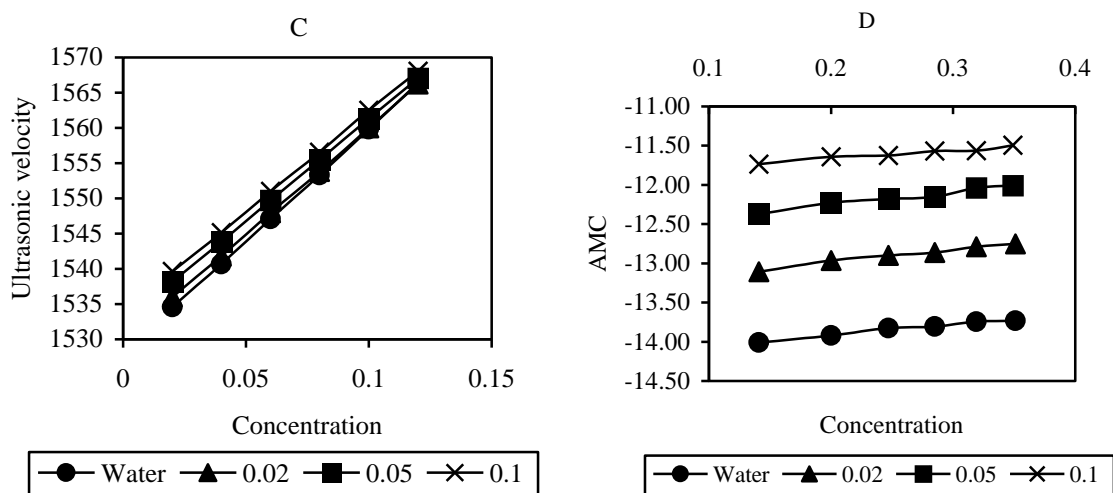


Figure 2 A-D. The, ρ , $V_{2,\phi}$ and u , $\Delta\kappa_{2,\phi}$ values of (Aq. L-Arginine + Lactose) at 310.15 K

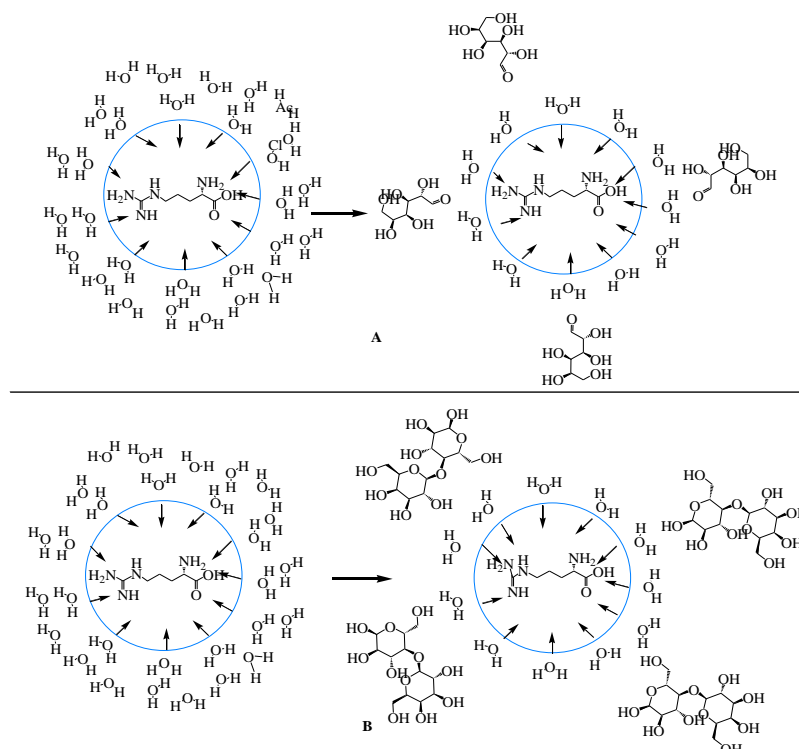
Table 1. The $V_{2,\phi}^0$, S_v , $\Delta V_{2,\phi}^0$ and $\kappa_{S,2,\phi}^0$, $\Delta\kappa_{S,2,\phi}^0$ values of (Aq. L-Arginine + Glucose) at 310.15 K

System/property	$V_{2,\phi}^0$	S_v	$\Delta V_{2,\phi}^0$
Water	124.56	3.307	0.000
0.02M aq. Glucose	124.73	5.267	0.170
0.05M aq. Glucose	125.73	4.954	1.170
0.10 M aq. Glucose	126.69	4.894	2.130
System	$\kappa_{S,2,\phi}^0$	S_k	$\Delta\kappa_{S,2,\phi}^0$
Water	-14.190	1.361	0.000
0.02M aq. Glucose	-13.797	0.781	0.393
0.05M aq. Glucose	-13.256	0.146	0.934
0.10 M aq. Glucose	-12.908	0.426	1.282

Table 2. The $V_{2,\phi}^0$, S_v , $\Delta V_{2,\phi}^0$ and $\kappa_{S,2,\phi}^0$, $\Delta\kappa_{S,2,\phi}^0$ values of (Aq. L-Arginine + Glucose) at 310.15 K

System/property	$V_{2,\phi}^0$	S_v	$\Delta V_{2,\phi}^0$
Water	124.56	3.307	0.000
0.02M aq. Lactose	125.40	4.624	0.840
0.05M aq. Lactose	126.91	3.769	2.350
0.10 M aq. Lactose	128.05	5.801	3.490
	$\kappa_{S,2,\phi}^0$	S_k	$\Delta\kappa_{S,2,\phi}^0$
Water	-14.190	1.361	0.000
0.02M aq. Lactose	-13.318	1.643	0.872
0.05M aq. Lactose	-12.596	1.687	1.594
0.10 M aq. Lactose	-11.873	1.047	2.317

Foot Note: $V_{2,\phi}^0 = \text{cm}^3 \cdot \text{mol}^{-1}$, $S_v = \text{cm}^3 \cdot \text{mol}^{-3/2} \cdot \text{kg}^{1/2}$, $\kappa_{S,2,\phi}^0 = \times 10^{-14} \text{ m}^3 \cdot \text{mol}^{-1} \cdot \text{Pa}^{-1}$, $S_k = \times 10^{-14} \text{ m}^3 \cdot \text{mol}^{-3/2} \cdot \text{kg}^{1/2} \cdot \text{Pa}^{-1}$, $\Delta V_{2,\phi}^0 = \text{cm}^3 \cdot \text{mol}^{-1}$, $\Delta\kappa_{S,2,\phi}^0 = \times 10^{-14} \text{ m}^3 \cdot \text{mol}^{-1} \cdot \text{Pa}^{-1}$.



Scheme 1. Hydration of L-Arginine in presence of A) Glucose and B) Lactose

The study has implications in protein-sugar interactions in solution which discloses size of hydration sphere, specific interactions and solution behavior of amino acids in specific and proteins in general. The observations in present systems reveals that the hydrogen bonding and hydrophilic-hydrophilic interactions occurs in L-Arginine and Glucose//Lactose with dominance of these interactions in Lactose solution.

Conclusion:

Hydration structure of L-Arginine affects in presence of cosolutes glucose and Lactose as a result of hydrogen bonding and other interactions in solution. The cosolute causes increase in the volume and compression and weakening of solute-solvent interactions as a cosphere overlap. This effect is dominant in Lactose solutions.

References:

1. Domb, Abraham J.; Kost, Joseph; Wiseman, David (1998-02-04). CRC Press. 275. ISBN 978-1-4200-4936-7.
2. Kamide, Kenji (2005). Amsterdam: Elsevier. ISBN 9780080454443.
3. Gerrit M. Westhoff; Ben F.M. Kuster; Michiel C. Heslinga; Hendrik Pluim; Marinus Verhage (2014). ISBN 978-3-527-30673-2.
4. Anil Kumar Nain, J. Mol. Liq. 113736 (2020).
5. V. D. Umare, Int. J. Res. Appl. Sci. Engg. Tech., 8 (2020).
6. E. Jasmine Vasantha Rani, K. Kannagi, Padmavathy Rajasekaran, N. Radha, Ind. J. Pure Appl. Sci. 52(3):155–161 (2014).
7. R. Palani, S. Balakrishnan and G. Arumugam, J. Phy. Sci. 22(1), 131–141, (2011).
8. Sonu R. Dhumane, Nita S. Ramteke and K. C. Patil, Int. J. Res. Bio. Agri. Tech. 38–41 (2016).
9. Deosarkar, S.D., Arsule, A.D., Kalyankar, T.M. Coll. Surf. A 613, 126052 (2021).
10. Arsule, A.D., Sawale, R.T., Kalyankar, T.M., Deosarkar, S.D., J. Solut. Chem. 49(1), 83–99 (2020).
11. A.D. Arsule, R.T. Sawale, S.D. Deosarkar, J. Mol. Liq. 266 413–424 (2018).
12. Ivanov, E.V., Lebedeva, E.Y., J. Mol. Liq. 222, 1164–1171 (2016).
13. Chauhan, S., Chauhan, M.S., Jyoti, J., Rajni, J. Mol. Liq. 148, 24–28 (2009).
14. Kumar, K., Chauhan, S., Thermochim. Acta 606, 12–24 (2015).
15. Pal, A., Chauhan, N.: J. Mol. Liq. 162, 38–44 (2011).
16. Kumar, K., Chauhan, S., Thermochim. Acta 606, 12–24 (2015).
17. Pal, A., Chauhan, N., J. Mol. Liq. 162, 38–44 (2011).

Studies in the Synthesis of 5-(3-Substitutedthiocarbamido) Aminoindole by Microwave Technique

M. B. Shahakar^{1*}, R.D. Isankar¹, P.V. Raut²

¹Department of Chemistry, Government Vidarbha Institute of Science and Humanities Amravati, MH-444604, India.

²Department of Chemistry, Radhabai Sarda Arts, Commerce and Science College, Anjangaon Surji, Amravati, MH-444705, India.

*Corresponding author E-mail monaliraut78876@gmail.com

Abstract: We reported synthesis of 5-(3-thiocarbamido)aminoindol, 5-(3-allylthiocarbamido) aminoindole, 5-(3-*o*-nitrophenylthio- carbamido)aminoindol, 5-(3-*p*-nitrophenylthiocarbamido)aminoindol, 5-(3-*m*-chloro- phenylthiocarbamido)aminoindole by interacting 5-chloroindol with thiourea, allyl thiourea, *o*-nitrophenylthiourea, *m*-chlorophenylthiourea respectively. Ethanol was taken and kept in microwave oven and irradiation was carried out for 2 minutes at 50 °C. The justification and determination of structures of synthesized molecules were done on the basis of elemental analysis, chemical characterizations, IR, ¹H-NMR, ¹³C-NMR studies. This green synthetic method increases yield of products by maintaining the purity of the products this is the novelty of the research work.

Key words: 5-chloroindole, substituted thiourea, green synthesis, microwave technique.

INTRODUCTION

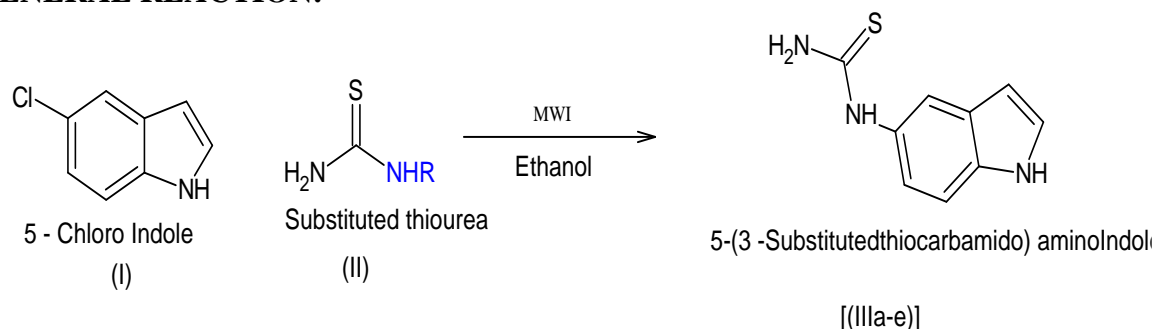
Indole nucleus containing heterocycles created their own identity due to these applications in life, pharmaceutical, medical, and agricultural sciences. Indoles showed anticancer, anti-inflammatory, antioxidant activities¹⁻³.

Indole based heterocycles are well known recognised for their antimicrobial, anti-micotic and inhibition of chemical mediator's release⁴, anti-inflammatory⁵⁻⁷, anti-asthma⁸, anti-vascular⁹, antifungal¹⁰, activities. At the same time thiocarbamido nucleus showed antioxidant, anticancer, anti-inflammatory antitubercular activities. Majority of alkaloids contain indole nucleus which exhibits excellent biological activities i.e. antiviral, antitumor, antiplasmodial, antibacterial and neurochemicals melatonin and serotonin are more complex bisindole natural products vincristine and vinblastine these are the key structural component of many effective synthetic pharmaceuticals⁴⁻⁵. Amino acid tryptophans, the biogenic amines serotonin, tryptamine and the mammalian hormone melatonin are broadly known indole derivatives play an significant role in lively activity of humans and animals¹¹.

Synthetic applications of cynoguanidine and 1, 3- diformamido-thiocarbamide had been briefly explored¹². Synthesis of nitrogen, sulphur and nitrogen and sulphur containing heteroacycles and heterocycles the interactions of cynoguanidine with various thiourea and isothiocyanates have been investigated in sufficient details¹³⁻¹⁸. Some of these compounds showed remarkable pharmaceutical and biological activities¹⁹⁻²⁰. As a wider programme of this research laboratory we have decided to synthesize a novel series of 5-(3-substituted thiocarbamido) aminoindole by interacting 5-chloroindole (I) with thiourea (IIa), allyl thiourea (IIb), *o*-nitro-phenyl thiourea (IIc), *p*-nitro-phenyl thiourea (IId), *m*-chloro-phenyl thiourea (IIe) in presence of ethanol by using microwave technique. Structure determination and

identification of the synthesized product is done on the basis of chemical characteristics, elemental analysis and spectral data.

GENERAL REACTION:-



Where R = -H, -allyl, -*o*-nitrophenyl, -*p*-nitrophenyl, *m*-chlorophenyl

1. EXPERIMENTAL

The melting point of the all synthesized compounds was recorded using hot paraffin bath. The carbon and hydrogen analysis were carried out on Carlo-Ebra 1106 analyzer. Nitrogen estimation was carried out on Colman-N-analyzer-29. IR spectra were recorded on Perkin Elmer Spectrometer in range $4000\text{--}400\text{cm}^{-1}$ in KBr pellets. The purity of compound was checked by TLC plate. All chemicals used were of AR-grade.

2.1 5-(3-Thiocarbamido) Amino Indole (IIIa)

A mixture of 5-chloroindole (I) (0.1M, 0.392 gms) and thiourea (0.1M, 0.152 gms) in ethanol was kept in microwave used to synthesis 5-(3-thiocarbamido) amino indole (IIIa) (1 gm, 97.35%), melting point 160°C . (D)

RESULTS AND DISCUSSION

Properties of (IIIa): It is pale yellow colour crystalline solid having melting point 160°C (D). It gave positive test for nitrogen and sulphur. Desulphurised with alkaline plumbite solution. It forms picrate, melting point 120°C . Elemental analysis C {(found 67.58%) calculated 68.30%}, H {(found 5.17%) calculated 5.33%}, N {(found 14.86%) calculated 14.94 %}, S {(found 11.24%) calculated 11.38%}.

IR Spectra

FTIR Spectrum was recorded using KBr-pellets and is reproduced. Important absorption can be correlated as (cm^{-1}): N-H stretching at 3387.00cm^{-1} ($3500\text{--}3000\text{cm}^{-1}$), Ar-H stretching at 2690.70cm^{-1} ($3000\text{--}2500\text{cm}^{-1}$), Ar-C=C stretching at 1612.49cm^{-1} ($1600\text{--}1500\text{cm}^{-1}$), C-N stretching at 1085.92cm^{-1} ($1200\text{--}1000\text{cm}^{-1}$), N-C=S stretching at 1462.04cm^{-1} ($1550\text{--}1250\text{cm}^{-1}$), NN>C=S stretching at 1400.89cm^{-1} ($1400\text{--}1200\text{cm}^{-1}$).

NMR

This spectrum distinctly displayed signals at (δ ppm): signal at 7.2646-7.1726 ppm is due to Ar-H, signal at 4.2911-4.4564 ppm is due to N-H in aromatic ring, signal at 3.1402-2.2160 ppm is due to NH_2 and -NH protons. ^{13}C Spectrum: This spectrum distinctly displayed signals due to C=S carbon at δ 181.76 ppm, Ar-C carbon at δ 155.58-112.58 ppm, $-\text{CH}_2$ carbons at δ 79.04-78.38 ppm, $-\text{CH}_3$ carbons at δ 40.12-38.87 ppm.

2.2 5-(3-Allylthiocarbamido) Amino Indole (IIIb)

A mixture of 5-chloroindole (I) (0.1 M, 1.56 gm) and allyl thiourea (IIb) (0.1 M, 0.68 gm), in ethanol was kept in microwave used to synthesis 5-(3-allylthiocarbamido) amino indole (IIIb) (2 gm, 90%), melting point 186⁰C.(D)

RESULTS AND DISCUSSION

Properties of (IIIb): It is lemon yellow colour crystalline solid having melting point 186⁰c (D). It gave positive test for nitrogen and sulfur. Desulphurized with alkaline plumbite solution. It forms picrate, melting point 110⁰c. Elemental analysis C {(found 68.58%) calculated 69.27%}, H {(found 5.11%) calculated 5.35%}, N {(found 15.86%) calculated 16.64 %}, S {(found 11.34%) calculated 11.48% }.

IR Spectra

The IR spectra was carried out in KBr pellets and the important absorptions can be correlated as, (cm⁻¹) 3312 (N-H stretching), 1197 (C-N stretching), 3012 (Ar-H stretching), 1736 (N=C-N stretching), 1512 (Ar-C=C), 1487 (N-C=S) Bending.

NMR

Ar-H protons (6.8720-6.8991 ppm), N-H protons (5.0417-5.0471 ppm), N-H of five membered ring (4.2921-4.5564 ppm), -CH₃ protons (3.4386-3.8638 ppm).

2.3 5-(3-*o*-nitro-phenyl thiocarbamido) Amino Indole (IIIc)

A mixture of 5-chloroindole (I) (0.1 M, 1.17 gm) and *o*-nitro-phenyl thiourea (IIc) (0.1 M, 1.212 gm), in ethanol was used to synthesis 5-(3-*o*-nitro-phenylthiocarbamido) amino indole (IIIc) (3 gm, 94%), melting point 192⁰C.(D)

RESULTS AND DISCUSSION

Properties of (IIIc)-It is orange colour crystalline solid having melting point 192⁰c (D). It gave positive test for nitrogen and sulphur. Desulphurisd with alkaline plumbite solution. It forms picrate, melting point 120⁰c. Elemental analysis C {(found 63.58%) calculated 64.27%}, H {(found 5.91%) calculated 6.35%}, N {(found 15.06%) calculated 16.64 %}, S {(found 11.34%) calculated 11.48% }.

IR Spectra

The IR spectra was carried out in KBr pellets and the important absorptions can be correlated as, (cm⁻¹) 3312 (N-H stretching), 1197 (C-N stretching), 3012 (Ar-H stretching), 1736 (N=C-N stretching), 1512 (Ar-C=C), 1487 (N-C=S) Bending.

NMR

Ar-H protons (6.8720-6.8291 ppm), N-H protons (5.0417-5.0471 ppm), N-H of five membered ring (4.2920-4.5565 ppm).

2.4 5-(3-*p*-nitro-phenyl thiocarbamido) Amino Indole (IIId)

A mixture of 5-chloroindole (I) (0.1 M, 1.16 gm) and *o*-nitro-phenyl thiourea (IIId) (0.1 M, 1.26 gm), in ethanol was used to synthesis 5-(3-*p*-nitro-phenylthiocarbamido) amino indole (IIIId) (2.9 gm, 94%), melting point 194⁰C.(D)

RESULTS AND DISCUSSION

Properties of (IIIId)-It is pale orange colour crystalline solid having melting point 194⁰c (D). It gave positive test for nitrogen and sulphur. Desulphurisd with alkaline plumbite solution. It forms picrate, melting point 130⁰c. Elemental analysis C {(found 63.98%) calculated 64.57%}, H {(found 4.91%) calculated 5.59%}, N {(found 15.26%) calculated 16.97 %}, S {(found 11.34%) calculated 11.78%}.

IR Spectra

The IR spectra was carried out in KBr pellets and the important absorptions can be correlated as, (cm⁻¹) 3612 (N-H stretching), 1097 (C-N stretching), 3092 (Ar-H stretching), 1796 (N=C-N stretching), 1572 (Ar-C=C), 1447 (N-C=S) Bending.

NMR

Ar-H protons (6.8420-6.8491 ppm), N-H protons (5.0417-5.0471 ppm), N-H of five membered ring (4.2960-4.5566 ppm).

2.5 5-(3-*m*-chloro-phenyl thiocarbamido) Amino Indole (IIIe)

A mixture of 5-chloroindole (I) (0.1 M, 1.36 gm) and *m*-chloro-phenyl thiourea (IIe) (0.1 M, 1.09 gm) in ethanol was used to synthesis 5-(3-*m*-chloro-phenylthiocarbamido) amino indole (IIIe) (2.4 gm, 95%), melting point 193⁰C.(D)

RESULTS AND DISCUSSION

Properties of (IIIe)-It is ivory colour crystalline solid having melting point 193⁰c (D). It gave positive test for nitrogen and sulphur. Desulphurisd with alkaline plumbite solution. It forms picrate, melting point 180⁰c. Elemental analysis C {(found 62.98%) calculated 63.57%}, H {(found 4.31%) calculated 5.89%}, N {(found 14.26%) calculated 15.97 %}, S {(found 11.24%) calculated 11.94%}.

IR Spectra

The IR spectra was carried out in KBr pellets and the important absorptions can be correlated as, (cm⁻¹) 3412 (N-H stretching), 1037 (C-N stretching), 3192 (Ar-H stretching), 1996 (N=C-N stretching), 1672 (Ar-C=C), 1457 (N-C=S) Bending.

NMR

Ar-H protons (6.9420-6.8491 ppm), N-H protons (5.0417-5.0461 ppm), N-H of five membered ring (4.2760-4.5596 ppm).

ACKNOWLEDGMENTS

Author is very much thankful to Dr. R. D. Isankar, Assistant Professor dept. of chemistry Govt. Vidarbha Institute of Science and Humanity Amravati, Also thankful to Dr.

D. T. Tayade, professor dept. of chemistry Govt. Vidarbha Institute of science and Humanity Amravati, for valuable help during this work.

References

1. R. D. Isankar, D. T. Tayade, *Journal of medicinal chemistry and drug discovery*, 02, **2017**, 541-545.
2. P.S. Bodkhe A.B. Wadekar, R.D. Isankar and D.T. Tayade, *Journal of chemistry and chemical sciences*, 9(2), **2019**, 45-48.
3. K. D. Tayade, D. A.Pund, R.D.Isankar, S.U.Patil, *Journal of Medicinal chemistry and Drug discovery*, 1, **2016**, 15-19.
4. Cimanga, T., De Bruyne L., Pieters, M., Claeys A. V., *Tet. Lett.*, 37, **1996**, 1703-1706.
5. Radwan M.A. Ragab E.A., Sabri N.M., El-Shenaw., *Bioorg. Med. Chem. Lett.*, 15, **2007**, 3832-3841.
6. Palomba M., Paua A., Boattoa G., Aspronia B., Auzzasa L., Cerria R.*Archive. Pharm. Med. Chem.*, 14, **2000**, 17-33.
7. Rani P., Srivastava V.K., Kumar A., *Eur. J. Med. Chem.*, 39, **2004**, 449-452.
8. Stanton J.L., Ackerman M.H. *J. Med. Chem.*, 26, **1983**, 986-989.
9. Ryu C.K., Lee J.Y., Jeong S.H., Nho J.H., *Bioorg. Med. Chem. Lett.*, 19, **2009**, 146-148.
10. Archana, Sachin Saini, Synthesis and anticonvulsant studies, *Drug Res*, 69 (08), **2019**, 445- 450.
11. Kumar and Ritika, *Future Journal of pharmaceutical sciences*, 6, **2020**, 121.
12. Syed Muhammad Umer, Mehwish Solangi, Khalid Mohammad Khan, *Molecules*, 27, **2022**, 7586.
13. Richard P. Nugent, Scot Pounds, Crist N. Filer, *Applied Radiation and Isotopes*, 69, **2011**, 423-425.
14. BugaenkoDmiry I., Karchava Alexander V., Yurovskaya Marina A., *Russ. Chem.*, 88 (2), **2019**, 99-159.
15. Tayade D. T. Ph.D Thesis Amravati University,Amravati **1996**.
16. Tayade D.T., Raghuwanshi M.R., Bhagwatkar R.A., *International Journal of Chemistry Canada*, 3(2), **2011**, 74-78.
17. Bhagwatkar R.A., Tayade D.T., Orbital Elec. J.Chem., *Campo Grande Brazil*, 3(1), **2011**, 53-56.
18. Tayade D.T., Bhagwatkar R.A, Panpalia R.C., *International Journal of Chemistry Canada*, 2(2), **2010**, 41-43.
19. Tayade D.T., Pund D.A., Bhagwatkar R.A., Rathod D.B., Bhagwatkar N.A., *International Journal of Chemistry Canada*, 3(1), **2011**, 36-41.
20. Raut P. V., Waghmare S. A., Tayade D. T., *JETIR*7(2), **2020**, 437-439.

Understanding the Role of Lipophilicity and Pharmacophore Elements in Pyrimidinedione based BCAT1 Inhibitory Activity

S. R. Deshmukh^a, P.P. Nalawade^{*b}, V. H. Masand^b, S. D. Thakur^c, P. S. Navale^b

^a Department of Chemistry, PRMIT&R College, Badnera-Amravati, Maharashtra, India

^b Department of Chemistry, Vidya Bharati Mahavidyalaya, Amravati, Maharashtra, India

^c Department of Chemistry, RDIK and NKD College, Badnera-Amravati, Maharashtra, India

Abstract:

This paper presents the findings from pharmacophore-oriented studies on BCAT1 inhibitors. Understanding the role of lipophilicity and pharmacophore elements is paramount in elucidating the inhibitory activity of pyrimidinedione-based compounds targeting BCAT1. This study investigated a novel structural class of BCAT1 inhibitors, specifically (trifluoromethyl)pyrimidinediones, identified through high-throughput screening. The research emphasized the significance of lipophilicity, demonstrated by the increased BCAT1 inhibitory action resulting from the substitution of lipophilic groups in the molecular structure. Pharmacophore modeling revealed crucial elements, including hydrogen bond acceptors and donors, influencing the BCAT1 inhibitory activity. The examination of potent inhibitors, such as BAY-069, shed light on the cellular activity and selectivity of these compounds. The study contributes to a comprehensive understanding of the intricate relationship between lipophilicity, pharmacophore features, and the effectiveness of pyrimidinedione-based BCAT1 inhibitors.

Keywords: Pharmacophore modeling, Pymol, BCAT1 Inhibitors, Pyrimidinedione,

Introduction:

The pursuit of effective cancer treatments has long been at the forefront of medical research, prompting the exploration of innovative therapeutic avenues¹. Among the promising targets for cancer therapy are the branched-chain amino acid transaminase enzymes (BCAT1 and BCAT2), which play a crucial role in the metabolic reprogramming of cancer cells. These enzymes facilitate the catabolism of branched-chain amino acids (BCAAs), such as leucine, isoleucine, and valine, leading to the generation of key metabolic intermediates necessary for tumor growth and survival².

In recent years, significant attention has been directed towards the development of BCAT1/2 inhibitors as potential anticancer agents. Among these, the pyrimidinedione-based inhibitors have emerged as a particularly promising class of compounds with potent inhibitory activity against BCAT1 and BCAT2 enzymes³.

The overexpression of BCAT1 and BCAT2 has been observed in various cancer types, including breast, prostate, lung, and pancreatic cancers. Their upregulation has been associated with aggressive tumor behavior, metastasis, and resistance to standard cancer therapies. Consequently, targeting these enzymes represents a rational and attractive strategy to disrupt cancer cell metabolism, impair tumor growth, and enhance the efficacy of existing treatments⁴. Pyrimidinedione-based BCAT1/2 inhibitors offer several advantages over traditional anticancer agents. Their unique chemical structure confers a high degree of specificity towards BCAT1 and BCAT2 enzymes, minimizing off-target effects and reducing potential toxicity to normal cells. Moreover, their distinct mode of action disrupts the intricate metabolic networks within cancer cells, creating an environment detrimental to cancer cell survival⁵.

Pharmacokinetic profiling plays a pivotal role in drug development, guiding the understanding of how a compound is absorbed, distributed, metabolized, and excreted in the body. This study focuses on the pharmacokinetic profiling of innovative pyrimidinedione-based BCAT1 inhibitors, aiming to unravel essential aspects related to their bioavailability, tissue distribution, and metabolic fate⁶. The investigation explores how these novel compounds interact within the

biological system, with a specific emphasis on their potential implications for optimal drug delivery and therapeutic efficacy. By elucidating the pharmacokinetic behavior of these BCAT1 inhibitors, this research aims to provide valuable insights that can inform the design of effective drug formulations, dosing regimens, and administration routes, ultimately advancing their translational potential in the realm of cancer therapeutics.

Methodology:

1. Selection of Dataset: The consensus pharmacophore model was developed using a dataset of 43 molecules⁷. The molecules were screened for their activity and selectivity for BCAT1 inhibitors. The activity values (IC_{50} expressed as nM) were used to find most active molecules. The Table 1 contains top active molecules and least active molecules which are used for model building.

Table 1. SMILES notations and activity values IC_{50} (nM) of four highly reactive molecules and least active molecule used for alignment

S.N.	SMILES	IC_{50} (nM)
1	<chem>Cc1cccc1Oc2cc(N3C(=O)NC(=CC3=O)C(F)(F)F)c4cccc4c2Cl</chem>	31
2	<chem>COc1cc(C#N)c(Oc2cccc2C)cc1N3C(=O)NC(=CC3=O)S(=O)(=O)c4cccc4</chem>	60
3	<chem>COc1cc(C#N)c(Oc2cccc2C)cc1N3C(=O)NC(=CC3=O)C(F)(F)F</chem>	162
4	<chem>COc1cc(C#N)c(Oc2cccc2C)cc1N3C(=O)NC(=CC3=O)C(F)(F)C(F)(F)F</chem>	792
5	<chem>Cc1cccc1Oc2ccc(F)c(c2)N3C(=O)NC(=CC3=O)C(F)(F)F</chem>	50000

2. Compound Representation, Geometry Optimization & File Format Conversion with Open Babel::

- Chemical structures were drawn using Chem Draw ensuring accurate depiction of bond types, stereochemistry, and relevant functional groups.
- Optimized the 3D structures of the compounds using Chem Draw or a molecular mechanics tool to refine bond angles and minimize steric clashes
- Identified key pharmacophoric features (e.g., hydrogen bond donors/acceptors, hydrophobic regions) using Chem Draw.
- Annotated each feature with relevant distances and angles.
- Converted the optimized 3D structures to a common format (e.g., MOL) using Open Babel for compatibility with PyMOL.⁸

3. Pharmacophore Alignment and Visualization with PyMOL:

- Loaded the converted structures into PyMOL for molecular visualization.
- Aligned the structures based on common pharmacophoric features using PyMOL's alignment tools.
- Visualized and refined the pharmacophore model in PyMOL, considering spatial arrangements.⁹

4. Validation and Refinement & Export Pharmacophore Features:

- Validated the pharmacophore model against known ligand-receptor interactions.
- Refined the model iteratively based on experimental data or additional computational analyses.

- Exported the refined pharmacophore features from PyMOL for further analysis or virtual screening.

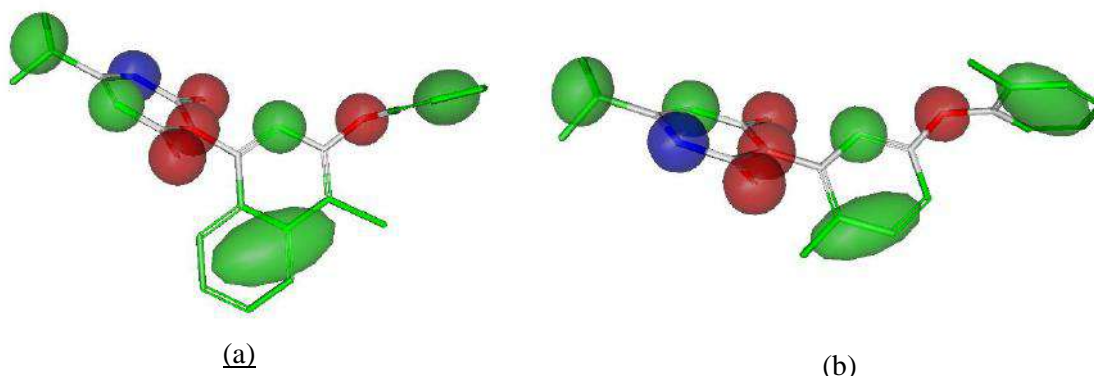


Figure 1. Consensus pharmacophore model (a)Most active Molecule ($IC_{50}=31nm$) (b) Most active molecule ($IC_{50}=5000nm$) showing contours for different regions (Green: Lipophilic, Blue: H-Bond donor and Red: H-Bond acceptor region)

Result and Discussions:

The current pharmacophore-oriented research reveals a strong association between the BCAT1 inhibitory activity of the compounds chosen for this investigation and five lipophilic, one H-Bond donor, and four H-bond acceptor groups. However, as the pharmacophore modeling of the other most active compounds listed in the above table shows, the mere presence of a given number of lipophilic, donar, and acceptor regions does not immediately correlate with the level of their activity against BCAT1 enzyme.

Increased lipophilicity of the molecules caused by the substitution of lipophilic groups for the original molecule is thought to be the probable cause of the increased BCAT1 inhibitory action. One nitrogen atom function as a donor and the other two oxygen atoms on the pyrimidinedione ring as H-bond acceptors. According to published research, these medicinal compounds' ability to bind BCAT1 inhibitors is directly impacted by regions that are more lipophilic.

Figure 1 examination demonstrates that the lipophilic character of the bicyclic and aromatic rings of pyrimidinedione-based BCAT1 inhibitors is responsible for the BCAT1 inhibitory activity of BAY-069 derivatives.

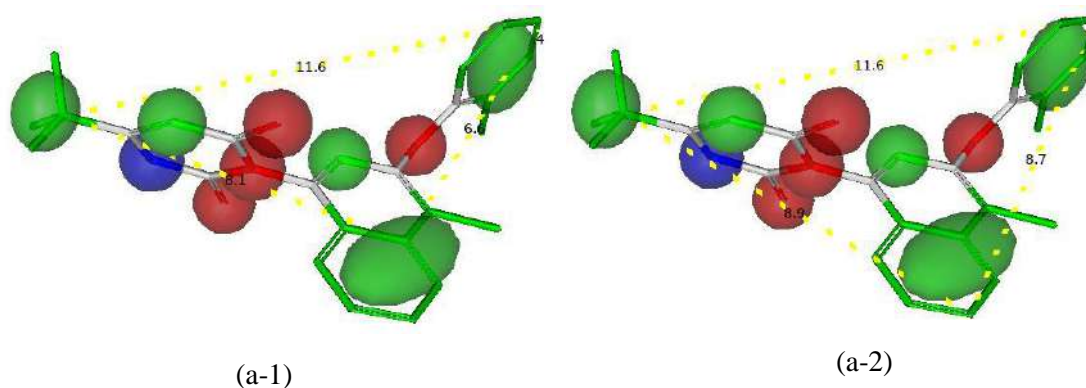


Figure 2: Intramolecular distances (pm) of lipophilic region

Based on pharmacophore-oriented study, the selected compounds have five lipophilic, one H-bond donor, and four H-bond acceptor groups, all of which are positively correlated with BCAT1 inhibitory action. Yet, as previous highly active molecules have demonstrated, the

fixed number of these regions alone does not directly correlate with the strength of BCAT1 inhibitory activity¹⁰.

Increased lipophilicity brought about by molecule replacement with lipophilic groups is thought to be the cause of the increased BCAT1 inhibitory action. Increased lipophilic surfaces affect the intramolecular distances of lipophilic regions, H-bond donors, and H-bond acceptors, which in turn affects how certain BCAT1 amino acids interact (Figure 2).

Conclusions: The pharmacophore-oriented exploration of BCAT1 inhibitory activity reveals a nuanced connection between molecular characteristics and compound efficacy. While the presence of lipophilic, donor, and acceptor groups correlates positively with BCAT1 inhibition, this relationship is not solely dictated by their fixed quantity. Pharmacophore modeling of highly active compounds underscores the influence of additional factors on overall BCAT1 enzyme activity. Enhanced lipophilicity, achieved through substituting lipophilic groups, significantly contributes to heightened BCAT1 inhibitory effects. This involves the introduction of lipophilic moieties, increasing relevant surfaces, impacting intramolecular distances, and influencing interactions with BCAT1 amino acids. The nitrogen and oxygen atoms on the pyrimidinedione ring, serving as H-bond donor and acceptors, respectively, emphasize the crucial role of these structural elements. In conclusion, this research underscores the intricate interplay of molecular features in BCAT1 inhibitory activity, stressing the need for a comprehensive understanding beyond the mere presence of specific pharmacophoric elements. Future BCAT1-targeted drug design should consider quantitative aspects, spatial arrangements, and interactions for potent inhibitor development.

References:

- ¹ "Targeted Therapy Drug List by Cancer Type - NCI," cgvArticle, December 20, 2023, nciglobal,ncicenterprise, <https://www.cancer.gov/about-cancer/treatment/types/targeted-therapies/approved-drug-list>.
- ² Kassidy Lee and Cynthia Blanton, "The Effect of Branched-Chain Amino Acid Supplementation on Cancer Treatment," *Nutrition and Health* 29, no. 4 (December 2023): 621–35, <https://doi.org/10.1177/02601060231153428>.
- ³ Judith Günther et al., "BAY-069, a Novel (Trifluoromethyl)Pyrimidinedione-Based BCAT1/2 Inhibitor and Chemical Probe," *Journal of Medicinal Chemistry* 65, no. 21 (November 10, 2022): 14366–90, <https://doi.org/10.1021/acs.jmedchem.2c00441>.
- ⁴ Mohammad Hassan Baig et al., "Enzyme Targeting Strategies for Prevention and Treatment of Cancer: Implications for Cancer Therapy," *Seminars in Cancer Biology*, Current Vision on Target Enzymes for Cancer Therapy, 56 (June 1, 2019): 1–11, <https://doi.org/10.1016/j.semcancer.2017.12.003>.
- ⁵ Jennifer A. Borthwick et al., "Structurally Diverse Mitochondrial Branched Chain Aminotransferase (BCATm) Leads with Varying Binding Modes Identified by Fragment Screening," *Journal of Medicinal Chemistry* 59, no. 6 (March 24, 2016): 2452–67, <https://doi.org/10.1021/acs.jmedchem.5b01607>.
- ⁶ Teresa Kaserer et al., "Pharmacophore Models and Pharmacophore-Based Virtual Screening: Concepts and Applications Exemplified on Hydroxysteroid Dehydrogenases," *Molecules* 20, no. 12 (December 19, 2015): 22799–832, <https://doi.org/10.3390/molecules201219880>.
- ⁷ Günther et al., "BAY-069, a Novel (Trifluoromethyl)Pyrimidinedione-Based BCAT1/2 Inhibitor and Chemical Probe."
- ⁸ "Open Babel - the Chemistry Toolbox — Open Babel Openbabel-3-1-1 Documentation," accessed January 25, 2024, <https://openbabel.org/>.
- ⁹ "PyMOL | Pymol.Org," accessed January 27, 2024, <https://pymol.org/2/>.
- ¹⁰ Günther et al., "BAY-069, a Novel (Trifluoromethyl)Pyrimidinedione-Based BCAT1/2 Inhibitor and Chemical Probe."

Use of Formic Acid as Co Surrogates in Palladium Catalyzed Carbonylation Reaction

Shoeb R. Khan*, Pratik E. P. Michael*, Mayur V. Khedkar*

Department Of Chemistry, Hislop College, Nagpur-440001 (M.S), India

E-mail: mvkhedkar@gmail.com; 9096312458

ABSTRACT:

Carbonylation is the process of utilizing carbon monoxide (CO) as a highly effective building block in organic transformations. Nevertheless, managing this hazardous and environmentally impactful CO gas poses a significant challenge for chemists. To address this concern, toxic carbon monoxide gas has been substituted with alternative CO sources referred to as CO surrogates. Formic acid and formaldehyde have proven to be highly applicable in organic synthesis and are consequently utilized as non-gaseous CO surrogates. This article outlines recent advancements in the exploration of formic acid as a CO surrogate in transition-metal catalyzed carbonylation reactions.

Keywords: Carboxyboronate, Carbon building block, C-C coupling, Carbonylation

INTRODUCTION:

Transition-metal-catalyzed carbonylations represents an important class of reactions for the effective preparation of range of carbonyl-containing compounds (Cornils 2009). The Carbonylation reaction allows one step insertion of CO to a substrate therefore much efforts has been made to explore the new carbonylative transformations (Wang 2010). The first carbonylation reaction catalyzed by transition metal using gaseous carbon monoxide (CO) was demonstrated Heck and co-workers in 1974 (Schoenberg 1974). This discovery set milestone in use of gas phase reaction.

There is a major drawback with a carbonylation reaction is that in most cases, the highly toxic, tasteless, odorless, and colorless gas carbon monoxide is required, and it is often exploited in large excess and in many instances at higher pressure than the atmospheric (Cao, 2017). The laboratories also need special CO detectors and possibly high pressure reactors limit the use of this CO gas (Khedkar, 2011). As a result of the physical properties of carbon monoxide, its use in the fine chemical industry and academia is limited. Thus in context of solving this problem, carbonylations without the use of CO gas become better alternative for synthetic organic chemists.

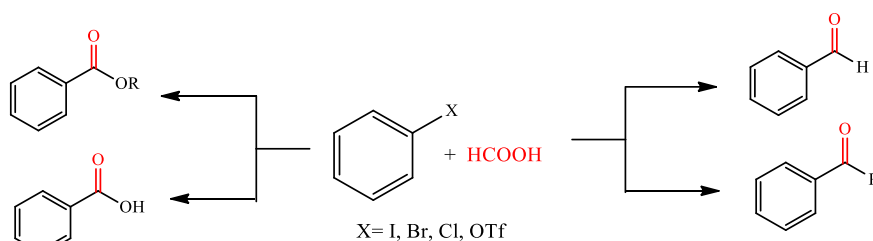
In this respect, in 2004 Morimoto and Kakiuchi explored the CO surrogates for Pauson–Khand reactions, carbonylation reactions by using aromatic halides, and sometime applied for alkenes. (Morimoto, 2004) Since then, many research projects have addressed new strategies and new carbonyl sources. (Park, 2010)

M. Larhed and co-workers reviewed the molybdenum hexacarbonyl as a solid surrogate for the carbonylative insertion reactions (Odell, 2012). Beller et al. summarized different carbonylation reactions using alkenes as a substrate with CO surrogates (Wu, 2014). Use of formic acid derivatives like phenyl formate and N-formylsaccharin as CO surrogates was demonstrated by Konishi and Manabe (Konishi 2014). Bhanage and co-workers focused on alkynes, arenes and aryl halides as a substrate for carbonylation reaction catalyzed by

transition-metal using CO surrogates (Gautam, 2015). Use of COgen (9-methylfluorene-9-carbonyl chloride) and SilaCOgen (methyldiphenylsilacarboxylic acid) was explored by Skrydstrup and co-workers (Friis, 2016). Unlike these CO surrogates, formic acid and there salt also found to be an excellent source of CO. However, formic acid (HCOOH) was successful applied carbonylation reactions. Hence present article address the recent updates in use formic acid and there salt in CO free carbonylation reactions.

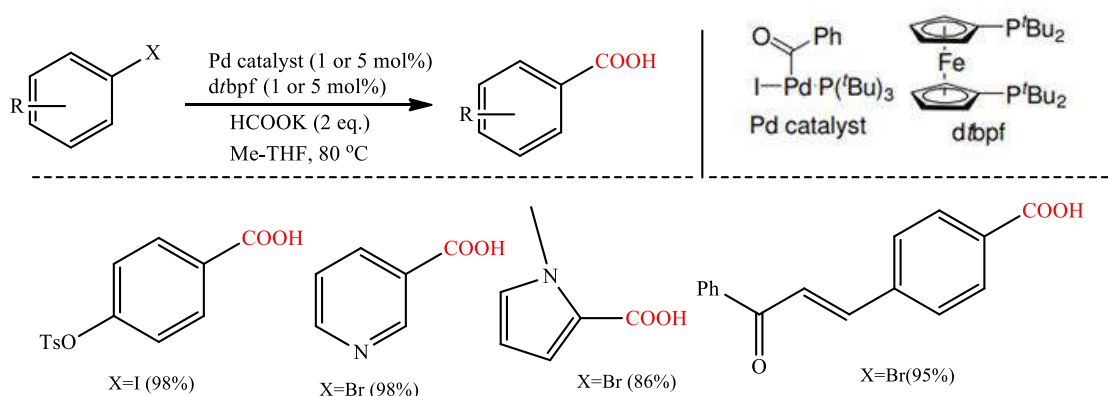
Use of Formic Acid in Palladium-Catalyzed Carbonylation reactions

Thus in search of new safer CO surrogates, for the first time Simonato discovered use of formic acid as a CO source (Simonato, 2003). After this discovery first palladium catalysed Carbonylation reaction using formic acid as alternative to CO was explored by Cacchi and co-workers (Scheme 1) (Cacchi, 2003). They studied the hydroarylation reactions of alkynes with aryl halides catalyzed by palladium by employing formate anions as reducing agents. They found that in the presence of acetic anhydride, formate anion can act as CO surrogate. They also projected a mechanism which comprising the formation of formic acetic anhydride from formate anion and acetic anhydride. The reaction proceed with the thermal decomposition to generate acetic acid and carbon monoxide, which underwent in-situ palladium-catalyzed hydroxycarbonylation.



Scheme 1:- Palladium catalyzed carbonylation reaction using formic acid as a CO source.

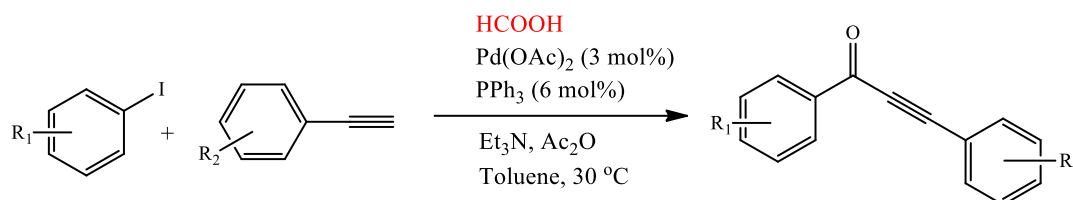
Bessmernykh and Caille et al explored the combination of palladium(II) acetate with 1,1'-bis(diphenylphosphino)ferrocene(dppf) as a catalytic combination for hydroxycarbonylation of aryl and vinyl bromides (Scheme 2) (Berger, 2006).



Scheme 2:- Palladium catalyzed hydroxycarbonylation using formic acid as a CO source.

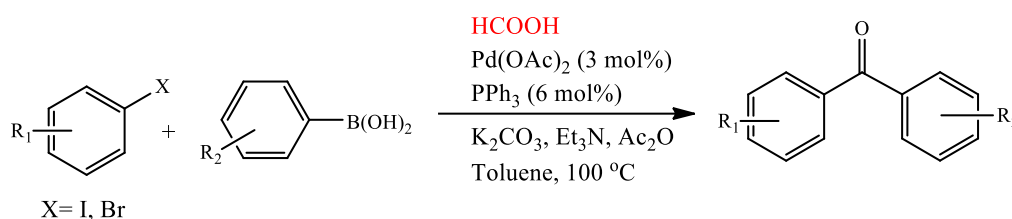
Skrydstrup and co-workers discovered use potassium salt of formic acid (HCOOK) as CO source for carbonylation reaction (Korsager, 2013). An acyl Pd(II) complex was employed as a pre-catalyst with dtpbf as ligand. The reaction condition was tested for different substrates.

The cross-coupling reaction involving CO is a powerful carbon-carbon bond formation process which leads to synthesis of range of useful carbonyl compounds like ketones, Amides or esters etc. Carbonylative Coupling of alkyne with aryl iodide i.e Sonogashira coupling using formic acid as carbon monoxide surrogates has been reported by Wu and co-workers (Scheme 3). (Qi, 2015)



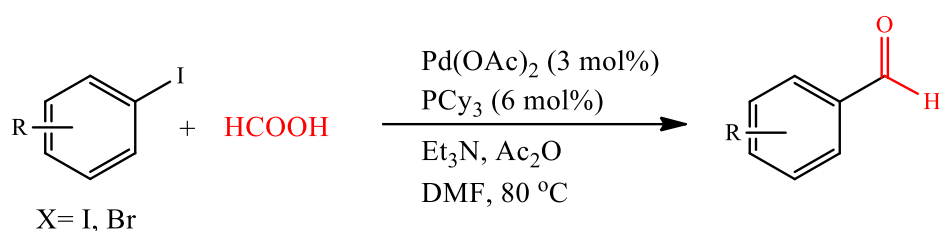
Scheme 3:- Palladium catalyzed Sonogashira coupling employing formic acid as CO surrogates.

Carbonylative Suzuki coupling employing reaction of aryl halides and arylboronic acids in occurrence of formic acid was published by Qi et al. (Scheme 4). (Qi, 2015) Same group further reported synthesis of ester using Palladium catalysed Alkoxy carbonylation under Formic acid (Qi, 2016)



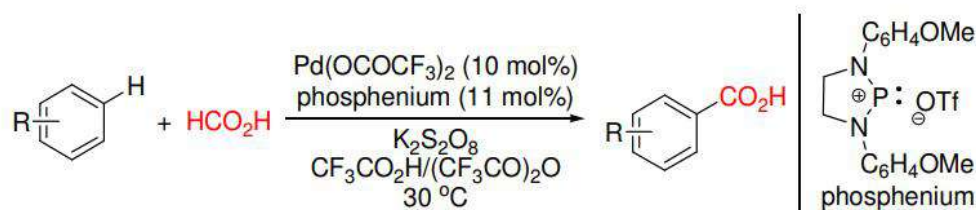
Scheme 4:- Palladium catalyzed Suzuki coupling with formic acid as CO surrogates.

Wu and co-workers explored Palladium-catalyzed reductive carbonylation of aryl iodides with formic acid as the formyl source. This protocol gave direct access to wide range of Aromatic aldehyde in single step (Scheme 5). (Wu 2016)



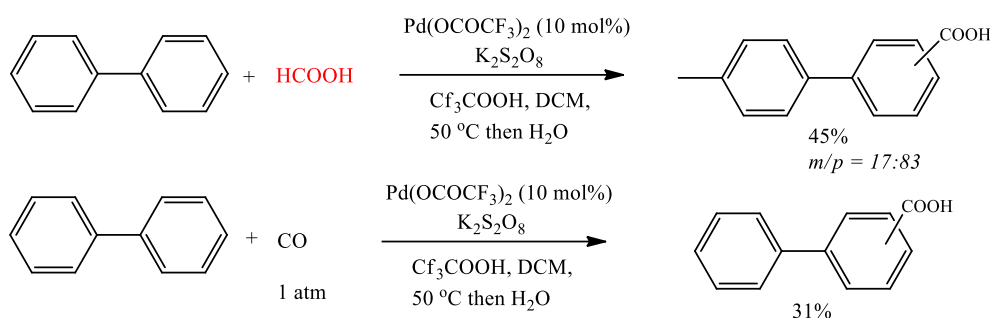
Scheme 5:- Reductive carbonylation of aryl iodides with formic acid by sing Palladium

Nozaki and co-workers developed Palladium-catalyzed hydroxycarbonylation of arenes via aromatic C–H bond activation using formic acid as a source of carbonyl (Shibahara, 2004). During this Surprisingly, they found that, simultaneously hydroxylation and carboxylation of biphenyl to give 4'-hydroxy-4-biphenylcarboxylic acid in the presence of formic acid, whereas with carbon monoxide gas instead of formic acid, the reaction only give hydroxycarbonylation product (Scheme 6).



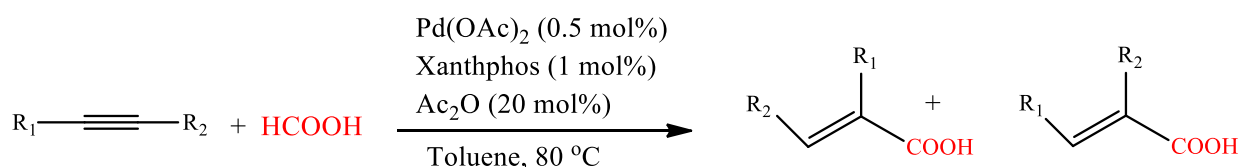
Scheme 6:- Hydroxycarbonylation of arenes via aromatic C-H bond activation using formic acid.

Shi and group developed hydrocarboxylation of olefins with HCOOH and HCOOPh catalyzed by palladium. In this reaction HCOOPh was used in catalytic amount. Using same reaction condition lactones and β -amino acid derivatives were also prepared (Scheme 7) (Wang, 2014)



Scheme 7:- Hydroxycarbonylation of arenes via aromatic C-H bond activation using formic acid.

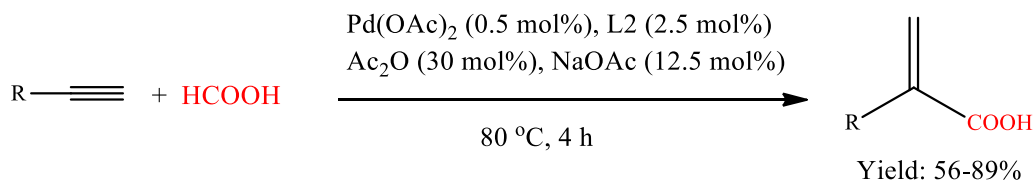
In 2015, Zhou and co-workers proposed hydrocarboxylation of alkynes and formic acid catalyzed by palladium and xantphos. The reaction circumvents a novel method for the synthesis of acrylic acids under mild carbonylation deprived of external CO gas. A catalytic amount of acetic anhydride was utilized for release of carbon monoxide (Scheme 8) (Hou, 2015).



Scheme 8:- Hydrocarboxylation reaction of alkynes and formic acid with Palladium Xantphos.

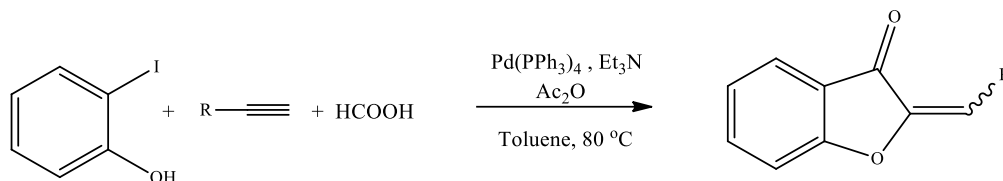
Fu et al. further promoted Nickel catalysed hydrocarboxylation of various alkynes with HCOOH, in which 1,2-bis(diphenylphosphino)-benzene (dppbz) or *cis*-1,2 bis(diphenylphosphino)ethylene (dppen) was used as ligand (Scheme 14) (Fu, 2016)

In 2018 selective palladium-catalyzed alkoxy carbonylation of all kinds of alkenes with formic acid (HCOOH, FA) was described Sang et al (Sang, 2018). Different alkenes including terminal, di-, tri-, and tetra-substituted olefins were transformed into linear esters with very good yields and regioselectivity. Very recently hydrocarboxylation of terminal alkynes with formic acid was reported by Liu and group (Liu, 2022) different α,β -unsaturated carboxylic acids with excellent branched regioselectivity were prepared in one step (Scheme 9).



Scheme 9:- Terminal alkynes with formic acid for Hydrocarboxylation reaction

Xinxin Qi et al. first reported the synthesis of aurone using Formic acid as a CO source.[Qi, 2016] In this strategy, in situ CO was generated using formic acid and acetic anhydride which then employed in carbonylation of 2-iodophenol with terminal alkynes. They also screen different Pd catalyst, solvents, and bases for optimization (Scheme 10).



Scheme 10:- Synthesis of aurone using Formic acid as a CO source.

CONCLUSION

This review highlights the recent advancements in carbonylation reactions, with a particular focus on formic acid as a substitute for CO. The shift from toxic CO gas to a cost-effective, readily accessible, and convenient CO source such as formic acid has garnered considerable attention in recent times. The literature reveals diverse approaches, including cross-coupling reactions of organic halides, hydroxycarbonylation, reductive carbonylation, and carbonyl insertion into C-H bonds, showcasing the versatility and widespread application of formic acid in these processes.

Reference

1. CORNILS, B.; HERRMANN, W.A.; RASCH, M. OTTO ROELEN, (1994) Pioneer in Industrial Homogeneous Catalysis. *Angew. Chem. Int. Ed. Engl.*, 33(21), 2144-2163.
2. WANG, Z. (2010) *Comprehensive Organic Name Reactions and Reagents*. John Wiley & Sons: Reppe Carbonylation., pp. 2352-2357.
3. SCHOENBERG, A.; BARTOLETTI, I.; HECK, R.F. (1974) Palladium-catalyzed carboalkoxylation of aryl, benzyl, and vinylic halides. *J. Org. Chem.*, 39, 3318-3326.
4. CAO, J.; ZHENG, Z.; XU, Z.; XU L. (2017,) Transition-Metal-Catalyzed Transfer Carbonylation with HCOOH or HCHO as a Non-Gaseous C1 Source. *Coord. Chem. Rev.*, 336, 43-53.
5. KHEDKAR, M. V.; KHAN, S. R.; SAWANT, D. N.; BAGAL, D. B.; BHANAGE, B.M. (2011) Palladium on carbon: An efficient, heterogeneous and reusable catalytic system for carbonylative synthesis of N-substituted phthalimides. *Adv. Synth. & Cat.*, (18), 3415-3422.
6. SCHOENBERG, A.; BARTOLETTI, I.; HECK, R.F. (1974,) Palladium-catalyzed carboalkoxylation of aryl, benzyl, and vinylic halides. *J. Org. Chem.* 39, 3318-3326.
7. MORIMOTO T., KAKIUCHI K., (2004) Evolution of Carbonylation Catalysis: No Need for Carbon Monoxide, *Angew. Chem.* 43, 5580 – 5588.
8. PARK, J. H., CHO, Y., CHUNG, Y. K., (2010) Rhodium-Catalyzed Pauson-Khand-Type Reaction Using Alcohol as a Source of Carbon Monoxide, *Angew. Chem. Int. Ed.*, 30, 5264-5267.
9. SIMONATO, J.-P., (2003) New efficient catalytic system for hydroxycarbonylation without CO gas, *J. Mol. Catal. A* 197, 61-64.

10. ODELL, L., RUSSO, F., LARHED, M., (2012) Molybdenum Hexacarbonyl Mediated CO Gas-Free Carbonylative Reactions, *Synlett* 23, 685-698.
11. WU, L., LIU, Q., JACKSTELL, R., BELLER, M., (2014) Carbonylations of Alkenes with CO Surrogates *Angew. Chem. Int. Ed.* 53, 6310-6320.
12. KONISHI, H., MANABE, K., (2014) Formic Acid Derivatives as Practical Carbon Monoxide Surrogates for Metal-Catalyzed Carbonylation Reactions, *Synlett* 25, 1971-1986.
13. GAUTAM, P., BHANAGE, B. M., (2015) Recent advances in the transition metal catalyzed carbonylation of alkynes, arenes and aryl halides using CO surrogates *Catal. Sci. Technol.* 5, 4663-4702.
14. FRIIS, S. D., LINDHARDT, A. T., SKRYDSTRUP, T., (2016) The Development and Application of Two-Chamber Reactors and Carbon Monoxide Precursors for Safe Carbonylation Reactions *Acc. Chem. Res.* 49, 594-605.
15. CACCHI, S., FABRIZI, G., GOGGIAMANI, A., (2003) Palladium-Catalyzed Hydroxycarbonylation of Aryl and Vinyl Halides or Triflates by Acetic Anhydride and Formate Anions *Org. Lett.* 5, 4269-4272.
16. BERGER, P., BESSMERNYKH, A., CAILLE, J.-C., MIGNONAC, S., (2006) Palladium-Catalyzed Hydroxycarbonylation of Aryl and Vinyl Bromides by Mixed Acetic Formic Anhydride, *Synthesis* 3106-3110.
17. KORSAGER, S., TAANING, R. H., SKRYDSTRUP, T., (2013) Effective Palladium-Catalyzed Hydroxycarbonylation of Aryl Halides with Substoichiometric Carbon Monoxide, *J. Am. Chem. Soc.* 135, 2891- 2894.
18. QI, X., JIANG, L.-B., LI, C.-L., LI, R., WU, X.-F. (2015) Inside Cover: Palladium-Catalyzed One-Pot Carbonylative Sonogashira Reaction Employing Formic acid as the CO Source, *Chem. Asian J.* 10, 1802-1802.
19. QI, X., LIA, R., WU, X.-F. (2016) Selective palladium-catalyzed carbonylative synthesis of aurones with formic acid as the CO source *RSC Adv.* 6, 62810-62813.
20. QI, X., LI, C.-L., JIANG, L.-B., ZHANG, W.-Q., WU, X.-F. (2016) Palladium-catalyzed alkoxy carbonylation of aryl halides with phenols employing formic acid as the CO source, *Catal. Sci. Technol.* 6, 3099-3107.
21. QI, X., LI, C.-L., WU, X.-F. (2016) A Convenient Palladium-Catalyzed Reductive Carbonylation of Aryl Iodides with Dual Role of Formic Acid, *Chem. Eur. J.* 22, 5835-5838.
22. SHIBAHARA, F., KINOSHITA, S., NOZAKI, K., (2004) Palladium(II)-Catalyzed Sequential Hydroxylation-Carboxylation of Biphenyl Using Formic Acid as a Carbonyl Source, *Org. Lett.* 6, 2437-2439.
23. WANG, H., DONG, B., WANG, Y., LI, J., SHI, Y., (2014) A Palladium-Catalyzed Regioselective Hydroesterification of Alkenylphenols to Lactones with Phenyl Formate as CO Source; *Org. Lett.* 16 186-189.
24. HOU, J., XIE, J.-H., ZHOU, Q. L., (2015) Palladium-Catalyzed Hydrocarboxylation of Alkynes with Formic Acid, *Angew. Chem. Int. Ed.* 54, 6302-6304.
25. FU, M. C., SHANG, R., CHENG, W. M., FU, Y., (2016) Nickel-Catalyzed Regio- and Stereoselective Hydrocarboxylation of Alkynes with Formic Acid through Catalytic CO Recycling, *ACS Catal.* 6, 2501-2505.
26. SANG, R., KUCMIERCZYK, P., DONG, K., FRANKE, R., NEUMANN, H., JACKSTELL, R., BELLER M., (2018), Palladium-Catalyzed Selective Generation of CO from Formic Acid for Carbonylation of Alkenes, *J. Am. Chem. Soc.* 140, 15, 5217-5223.
27. LIU, L., YAO, Y., CHEN, X., GUO, L., LU, Y., ZHAO, X., LIU, Y., (2022) Hydrocarboxylation of alkynes with formic acid over multifunctional ligand modified Pd-catalyst with co-catalytic effect. *Journal of Catalysis* , 405 , 322-332.

In-Silico Prediction of Phytoconstituents From Solanum Indicum for Antianxiety Activity

Shweta Dhole*, Parimal Katolkar, Pradeep Raghatate, Jagdish Baheti

Kamla Nehru College of Pharmacy, Butibori, Nagpur 441108 (MS), INDIA

*Email: shwetadhole4@gmail.com

ABSTRACT

Objective Anxiety is a common reaction to stress, and it may even be beneficial in certain situations. It can alert us to potential dangers and help with planning and focus. Instead of the usual sensations of apprehension or anxiety, there is excessive fear or anxiety when anxiety disorders are present. Compounds found in medicinal plants have been the source of many conventional medications. *In-silico* testing of *Solanum indicum* phytoconstituents for antianxiety efficacy was a part of our investigation.

Methods Utilizing Discovery studio, molecular docking is done to assess the pattern of interaction between the phytoconstituents from the *Solanum indicum* plant and the crystal structure of the stress proteins (PDB ID: 5XVG). Later, SwissADME and pkCSM were used to screen for toxicity as well as the pharmacokinetic profile.

Results The docked results suggest that Solafuranone (-8.1 kcal/mol) and Isofraxidin (-6.8 kcal/mol) for 5XVG macromolecule has best binding towards antianxiety activity as compared to the standard (Gabapentin) for 5XVG is -5.1 kcal/mol. Furthermore, pharmacokinetics and toxicity parameters were within acceptable limits according to ADMET studies.

Conclusion

Results from the binding potential of phytoconstituents aimed at antianxiety activity were encouraging. It promotes the usage of *Solanum indicum* and offers crucial details on pharmaceutical research and clinical care.

1. INTRODUCTION

In traditional Chinese medicine, the plant *Solanum indicum* is used to treat wounds and reduce inflammation because it contains special dioscins, or indiosides. Our earlier research showed that a number of synthetic indiosides derived from *Solanum indicum* has strong anticancer properties, whereas other compounds have CNS depressing properties.¹

Solanum indicum is a plant that is eaten as a vegetable in some parts of Africa, and folk medicine experts claim that it may fend off cardiovascular conditions. The research on how it can be utilised to treat hypertension was fascinating. The presence of chlorogenic acids may only have served as a supportive role in the extract's strong therapeutic and preventive effects against hypertension. Other ingredients could be responsible for the antihypertensive impact. Future investigation into the extract as a potential therapy for hypertension is encouraged by the results.²

However, there are few studies on the phytoconstituents of *Solanum indicum* for the antianxiety activity. Thus, keeping the above information in view, the present investigation was designed to identify the potential phytochemicals of *Solanum indicum* against 5XVG using a molecular docking method.

2. MATERIALS AND METHODS

2.1. Platform for molecular docking

The computational docking study of all the phytoconstituents selected as ligands with antianxiety activity as the target was performed using PyRx software.³

2.2. Protein preparation

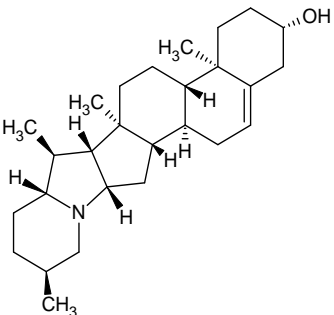
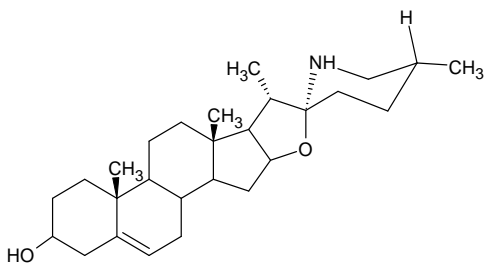
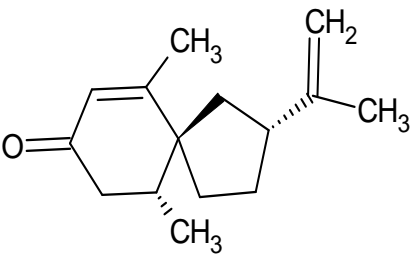
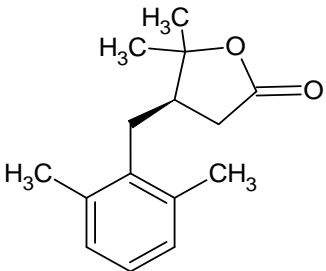
The macromolecule is 5XVG, *in silico* analysis of selected phytoconstituents was performed on the 2.15 Å crystal structure of antianxiety macromolecule with inhibitor, (PDB ID: 5XVG, having resolution Resolution: 2.10 Å, R-Value Free: 0.235, R-Value Work: 0.181, R-Value Observed: 0.184), which was retrieved from the protein data bank (<https://www.rcsb.org>). 5XVG is classified as crystal structure of PAK4 in complex with the inhibitor CZH226 all other molecules, such as co-crystallized water molecules, unwanted chains, and nonstandard residues, were deleted. Using Discovery studio.⁴

2.3. Mechanism of Action

5XVG: DI-1859 is a potent, selective and covalent DCN1 inhibitors. Mass spectrometric analysis and co-crystal structures reveal that this compound employ a unique mechanism of covalent bond formation with DCN1. The p21-activated kinases (PAKs) are serine/threonine (Ser/Thr) protein kinases that have been identified as downstream signaling effectors of Rho-family GTPases. PAK4 is the most studied group II PAK member, and it has a place at critical nodal points in multiple signaling pathways that are associated with cell growth, cytoskeletal dynamics, cell polarity, survival, and development. PAK4 is particularly highly expressed in prostate, testis, lung, heart, brain, and liver.⁵

2.4. Ligand preparation

The three-dimensional (3D) structures of all constituents were retrieved using Avogadro software from the PubChem database available on the NCBI website (<https://pubchem.ncbi.nlm.nih.gov/>). However, the drawing of geometrical 2D structure was performed using the ChemSketch program. The two-dimensional (2D) structures were transformed into 3D models using the Avogadro software and the ligand structures were saved in the PDB format. All the chemical structures are shown in Figure 1.

<p>Solanidine</p> 	<p>Solasodine</p> 
<p>Solavetivone</p> 	<p>Solafuranone</p> 

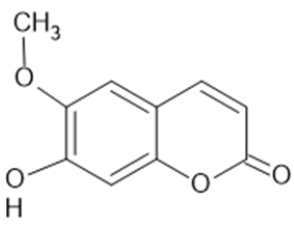
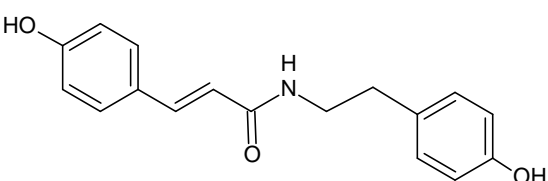
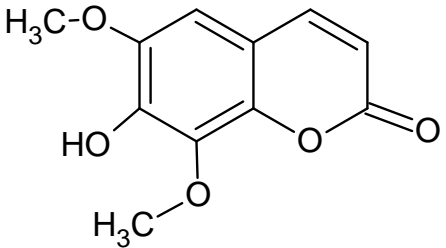
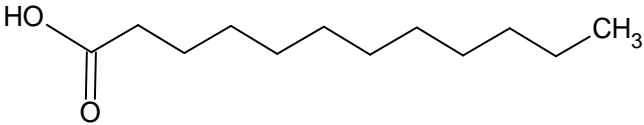
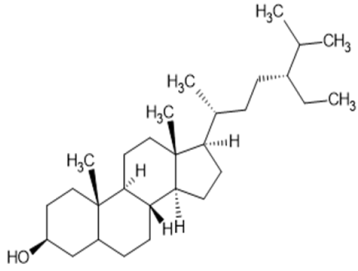
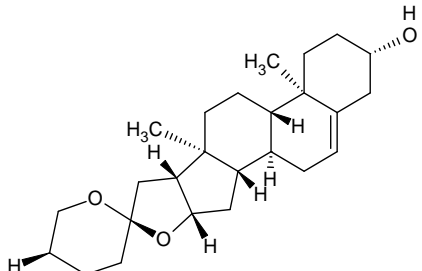
<p>Scopoletin</p> 	<p>N-p-trans-Coumaroyltyramine</p> 
<p>Isofraxidin</p> 	<p>Lauric acid</p> 
<p>β-sitosterol</p> 	<p>Diosgenin</p> 

Fig. 1. Chemical structures of all selected phytoconstituents in the molecular docking studies

2.5. Standard Preparation

The standard is prepared steps such as, the 2D structure of standard drug was made using chem sketch program, then the 2D structure was converted into 3D model using Avogadro Software, it was saved in PDB format.

By using PyRx molecular docking of Gabapentin was done with 5XVG.

2.6. Molecular docking

Molecular docking evaluates the protein-ligand interactions and estimates the scoring function based on the geometry to predict the binding affinity of the ligand molecule^{6,7}. We applied molecular docking studies to investigate the binding pattern of selected phytoconstituents (Figure 1) and the standard drug, along with the crystal structure of antianxiety activity macromolecule (PDB ID: 5XVG). The molecular docking study was performed using PyRx software, Binding affinity was explored using the Vina wizard tool. The final results were analysed and visualized using Discovery Studio 2020 Client⁸, with bound ligands as the standard. Visualization of protein ligand interaction reflects the number of interactions and active residues responsible for significant binding at the active site of the target enzyme.

2.7. Absorption, distribution, metabolism, and excretion (ADME) and toxicity prediction

The selected phytoconstituents and standard drug were further checked for drug-likeness properties according to Lipinski's rule. During drug development, it is necessary to predict the tolerability of phytochemicals before being ingested by humans and animal models. The pharmacokinetic profile (ADME) and toxicity predictions of ligands were conducted using SwissADME (<http://www.swissadme.ch>) and pkCSM (an online server database predicting small-molecule pharmacokinetic properties using graph-based signatures, (<http://biosig.unimelb.edu.au/pkcsml/prediction>)). To analyse the toxicological properties of ligands, Simplified Molecular Input Line Entry System (SMILES) notations or PDB files were uploaded, followed by selecting the required models for generating numerous information about structure-related effects^{9,10}.

3. RESULT AND DISCUSSION

The present study aimed to explore the inhibitory potential of the phytoconstituents present in *Solanum indicum* targeting antianxiety activity. In this study, we performed molecular docking studies of all phytoconstituents found in *Solanum indicum* using AutoDock Vina, followed by a study of interacting amino acid residues and their influence on the inhibitory potentials of the active constituents. Selected phytoconstituents showing the best fit were further evaluated for absorption, distribution, metabolism, excretion, and toxicological (ADMET) properties using SwissADME and pkCSM servers.

3.1 Molecular docking

The docking scores and binding energies of all chemical constituents of *Solanum indicum* targeting antianxiety activity (PDB ID: 5XVG) and binding interactions with amino acid residues are presented in Table 1 respectively.

Table 1. Binding interaction of ligands from *Solanum indicum* targeting antianxiety activity (PDB ID:5XVG)

Sr. No.	Chemical constituent	PubChem ID	Docking Score
			5XVG
1.	Solanidine	65727	-8.0
2.	Solasodine	5250	-8.3
3.	Solavetivone	442399	-6.3
4.	Solafuranone	11107208	-8.1
5.	Scopoletin	5280460	-6.7
6.	N-p-trans-Coumaroyltyramine	5372945	-6.7
7.	Isofraxidin	5318565	-6.8
8.	Lauric acid	3893	-4.2
9.	β -sitosterol	222284	-7.4
10.	Diosgenin	99474	-8.0
Standard Drug			
11	Gabapentin	3446	-5.1

The binding affinities of phytoconstituents ranged from -8.3 to -4.2 kcal/mol. From the docked results, it is evident that the compounds, Solasodine exhibit the most favourable binding affinity (-8.3 kcal/mol) in complex with selected macromolecules (PDB ID: 5XVG) as compared to other docked compounds i.e., Solafuranone (-8.1 kcal/mol), Solanidine (-8.0 kcal/mol), Diosgenin (-8.0 kcal/mol), , Beta sitosterol (-7.4 kcal/mol), Isofraxidin (-6.8 kcal/mol), Scopoletin (-6.7 kcal/mol), N-p-trans-Coumaroyltyramine (-6.7 kcal/mol), Solavetivone (-6.3 kcal/mol), Lauric acid (-4.2 kcal/mol). Visual examination of the

computationally docked optimal binding poses of phytoconstituents on selected macromolecules (i.e., 5XVG) revealed the significant involvement of various types of interactions, such as hydrogen bonding and hydrophobic interactions, including π - π stacking and π -alkyl and alkyl interactions, in the stability of the binding of the phytoconstituents to 5XVG.

The binding affinity of the standard (Gabapentin) for 5XVG is -5.1 kcal/mol.

3.1.1. Solafuranone, 5XVG

An analysis of the interactions between the 5XVG protein complex and the Solafuranone ligand was also carried out, which showed that the ligand molecule is oriented due to Pi-Sigma interaction with LEU A:447 amino acid residue and Pi-Alkyl interaction with ALA A:348, VAL A:335 amino acid residue were found.

3.1.2. Isofraxidin, 5XVG

An analysis of the interactions between the 5XVG protein complex and the Isofraxidin ligand was also carried out, which showed that the ligand molecule is oriented due to Pi-Sigma interaction with VAL A: 335, LEU A: 447 amino acid residue and Alkyl and Pi-Alkyl interaction with ALA A: 348, MET A: 395, LYS A: 350 amino acid residue Conventional Hydrogen bond with LEU A: 398, ASP A: 458 amino acid residue and Carbon hydrogen bond with GLU A: 329 amino acid residue were found.

3.1.3. Gabapentin, 5XVG

The binding affinity of the standard (Gabapentin) for 5XVG is -5.1 kcal/mol. the interactions between the 5XVG protein complex and the Gabapentin ligand was also carried out, which showed that the ligand molecule is oriented due to conventional hydrogen bond with the ASP A:444, SER A:443, GLU A:507 amino acid residue and attractive charge interaction with LYS A:442 amino acid residue were found.

Table No. 2. Interactions with Amino acid residue

Sr. No.	Molecule	Binding Energy (kcal/mol)	H bond	Main amino acid interactions	
				Pi-alkyl, alkyl, Pi-S/Pi-Pi, T shaped/halogen/unfavourable donor-donor interactions	Van der Waals interactions
1	Solanidine	-8.0	GLY A: 452	PRO A: 578, ALA A:423, ALA A: 419	No interactions
2	Solasodine	-8.3	No interactions	PRO A: 479, TYR A: 480, PHE A: 516	No interactions
3	Solavetivone	-6.3	VAL A: 454, ASN A: 377	PRP A: 578, LEU A: 422	No interactions
4	Solafuranone	-8.1	No interactions	VAL A: 335, ALA A: 348, LEU A: 447	No interactions
5	Scopoletin	-6.7	LEU A: 398	MET A:395, ALA A: 402, VAL A: 335, ALA A: 348, LEU A: 447	No interactions

6	N-p-trans-Coumaroyltyramine	-6.7	GLU A: 329, ASP A:440	ASP A: 458, SER A: 331, ILE A: 327	No interactions
7	Isofraxidin	-6.8	LEU A: 398, ASP A: 458, GLU A: 329	LEU A: 447, ALA A: 348, VAL A: 335, MET A: 395, LYS A:350	No interactions
8	Lauric acid	-4.2	PHE A: 304, SER A: 300	ILE A: 369, VAL A: 368, PHE A: 364	ARG A: 360
9	β -sitosterol	-7.4	No interactions	VAL A: 335, LEU A: 447, ALA A: 348, ILE A: 327, ILE A: 337	No interactions
10	Diosgenin	-8.0	No interactions	PRO A: 578	No interactions
11	Gabapentin	-5.1	ASP A: 444, SER A: 443, GLU A: 507	TRP A: 481	LYS A: 442

3.2. ADMET study

Pharmacokinetic profile (ADME) and toxicity predictions of the ligands are important attentive parameters during the transformation of a molecule into a potent drug. In the present study, these parameters were assessed using SwissADME and pkCSM. The absorption potential and lipophilicity are characterized by the partition coefficient ($\log P$) and topological polar surface area (TPSA), respectively. For better penetration of a drug molecule into a cell membrane, the TPSA should be less than 140 Å. However, the value of $\log P$ differs based on the drug target. The ideal $\log P$ value for various drugs are as follows: oral and intestinal absorption, 1.35 – 1.80; sublingual absorption, > 5; and central nervous system (CNS)¹¹. The aqueous solubility of ligands ideally ranges from – 6.5 to 0.5¹², while the blood brain barrier (BBB) value ranges between – 3.0 and 1.2¹³. In addition, non-substrate P-glycoprotein causes drug resistance¹⁴. In our study, all the selected ligands followed the TPSA parameter, P-glycoprotein non-inhibition, thereby showing good intestinal absorption and an acceptable range of BBB values. All the compounds showed aqueous solubility values within the range. Further, it was predicted that the selected ligands do not show AMES toxicity, hepatotoxicity, and skin sensitivity. In addition, it did not inhibit hERG-I (low risk of cardiac toxicity). Lipinski's rule violations, *T. pyriformis* toxicity, minnow toxicity, maximum tolerated dose, rat acute oral toxicity, and chronic toxicity are depicted in table.

Table 3. ADME and toxicity predicted profile of ligands with superior docking score

ADMET Properties	Formula	MW (g/mol)	Log P	TPSA (Å ²)	HB donor	Hb acceptor	Aqueous solubility (Log mol/L)	Human intestinal absorption (%)	Blood Brain Barrier
Solanidine	C ₂₇ H ₄₃ N ₇ O	397.647	5.655	23.47 Å ²	1	2	-4.927	92.975	0.695

Solasodine	C ₇ H ₄₃ N O ₂	413.64	5.2869	41.49 Å ²	2	3	-3.809	92.324	0.035
Solavetivone	C ₁₅ H ₂₂ O	218.33	3.9042	17.07 Å ²	0	1	-4.615	95.873	0.635
Solafuranone	C ₁₅ H ₂₀ O ₂	232.32 3	3.1876 4	26.30 Å ²	0	2	-3.551	95.523	0.206
Scopoletin	C ₁₀ H ₈ O ₄	192.17	1.5072	59.67 Å ²	1	4	-2.504	95.277	-0.299
N-p-trans-Coumaroyltyramine	C ₁₇ H ₁₇ N O ₃	283.32 7	2.4699	69.56 Å ²	3	3	-3.165	90.031	-0.552
Isofraxidin	C ₁₁ H ₁₀ O ₅	222.19 6	1.5158	68.90 Å ²	1	5	-2.458	95.588	-0.377
Lauric acid	C ₁₂ H ₂₄ O ₂	200.32 2	3.9919	37.30 Å ²	1	1	-4.181	93.379	0.057
β-sitosterol	C ₂₉ H ₅₀ O	414.71 8	8.0248	20.23 Å ²	1	1	-6.773	94.464	0.781
Diosgenin	C ₂₇ H ₄₂ O ₃	414.63	5.7139	38.69 Å ²	1	3	-5.713	96.565	0.2
Gabapentin	C ₉ H ₁₇ N O ₂	171.24	1.3703	63.32 Å ²	2	2	-2.778	93.257	-0.178

Table 3 Continued

ADMET Properties	P-glyco-protein substrate	Total clearance [Log mL/(min.kg)]	Bioavailability score	AMES toxicity	Max tolerated dose [Log mg/(kg.d)]	hERG I inhibitor	hERG II inhibitor
Solanidine	YES	0.028	0.55	NO	-0.882	NO	YES
Solasodine	YES	0.09	0.55	NO	-0.375	NO	YES
Solavetivone	NO	1.225	0.55	NO	0.044	NO	NO
Solafuranone	NO	1.256	0.55	NO	0.526	NO	NO
Scopoletin	NO	0.73	0.55	NO	0.614	NO	NO
N-p-trans-Coumaroyltyramine	YES	0.265	0.55	NO	-0.213	NO	YES
Isofraxidin	NO	0.713	0.55	NO	0.56	NO	NO
Lauric acid	NO	1.623	0.85	NO	-0.34	NO	NO
β-sitosterol	NO	0.628	0.55	NO	-0.621	NO	YES
Diosgenin	NO	0.328	0.55	NO	-0.559	NO	YES
Gabapentin	NO	0.525	0.55	NO	0.789	NO	NO

Table 3 Continued

ADMET Properties	Acute oral rat toxicity. LD50(mol/kg)	Oral rat chronic toxicity (Log mg/kgbw/day)	Hepatotoxicity	Skin sensation	T.Pyriformis toxicity (Log µg/L)	Minnow toxicity (Log mmol/L)	Lipinski's rule Violation
Solanidine	2.596	1.334	YES	NO	0.378	-0.493	YES (1)
Solasodine	2.489	1.332	YES	NO	0.311	0.381	YES (1)
Solavetivone	1.643	1.19	NO	YES	1.453	0.874	YES (0)
Solafuranone	1.865	1.947	NO	YES	2.151	0.557	YES (0)
Scopoletin	1.95	1.378	NO	NO	0.516	1.614	YES (0)
N-p-trans-Coumaroyltyramine	2.17	1.271	NO	NO	1.008	1.514	YES (0)
Isofraxidin	2.326	1.825	NO	NO	0.431	1.862	YES (0)

Lauric acid	1.511	2.89	NO	YES	0.954	-0.084	YES (0)
β -sitosterol	2.552	0.855	NO	NO	0.43	-1.802	YES (1)
Diosgenin	1.921	1.452	NO	NO	0.399	0.247	YES (1)
Gabapentin	1.871	2.857	NO	NO	0.265	1.698	YES (0)

3.3. Interaction of Standard Drug (Gabapentin) with 5XVG

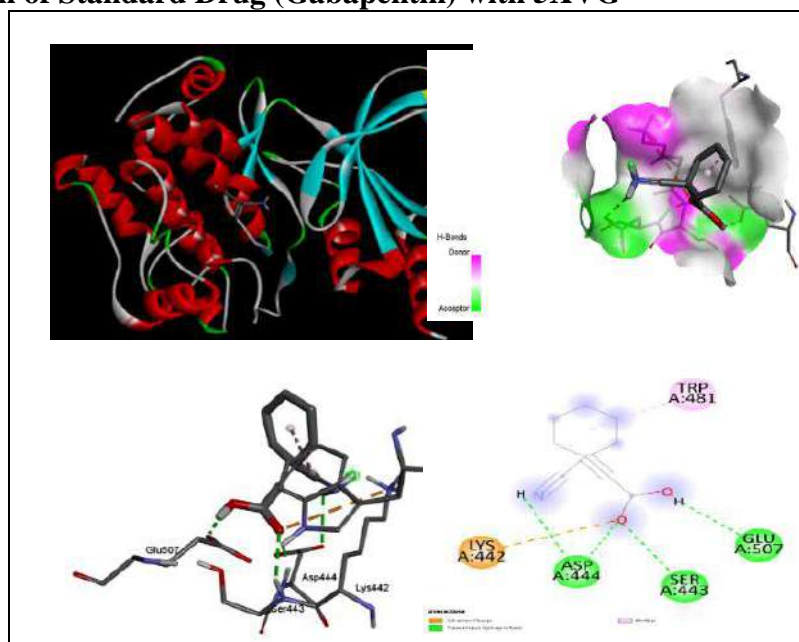
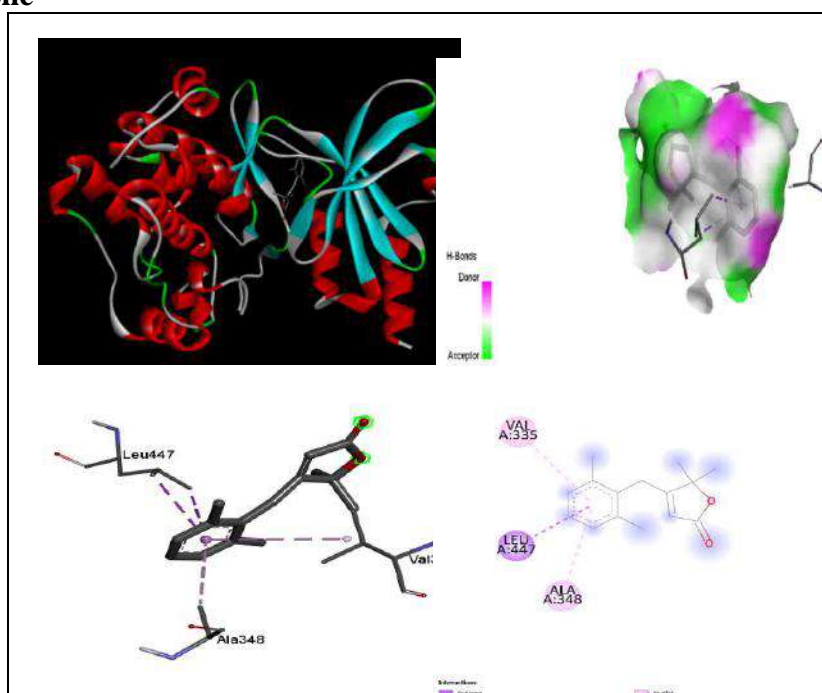


Fig. 2. Docking scores and binding interaction of Gabapentin (PDB ID: 5XVG). The ligand is shown in line and stick representation along with its 2D diagram and hydrogen bond interaction.

3.4. Interactions of phytoconstituents with 5XVG

A.Solafuranone



B.Isofraxidin

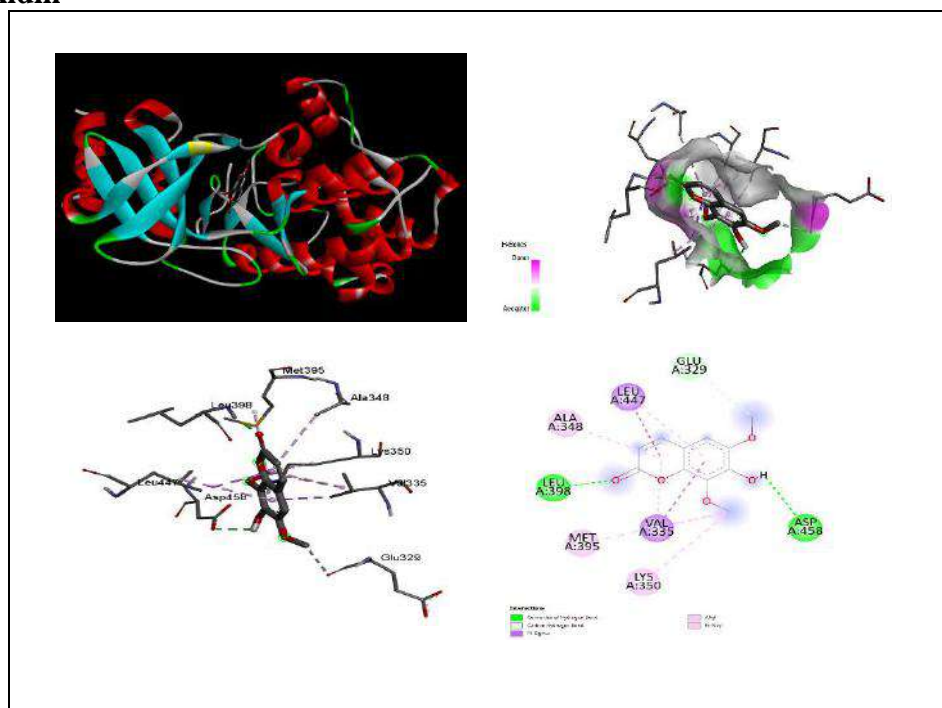


Fig. 3. Docking scores and binding interaction of phytoconstituents (PDB ID: 5XVG). The ligand is shown in line and stick representation along with its 2D diagram and hydrogen bond interaction.

3.5. Boiled Egg

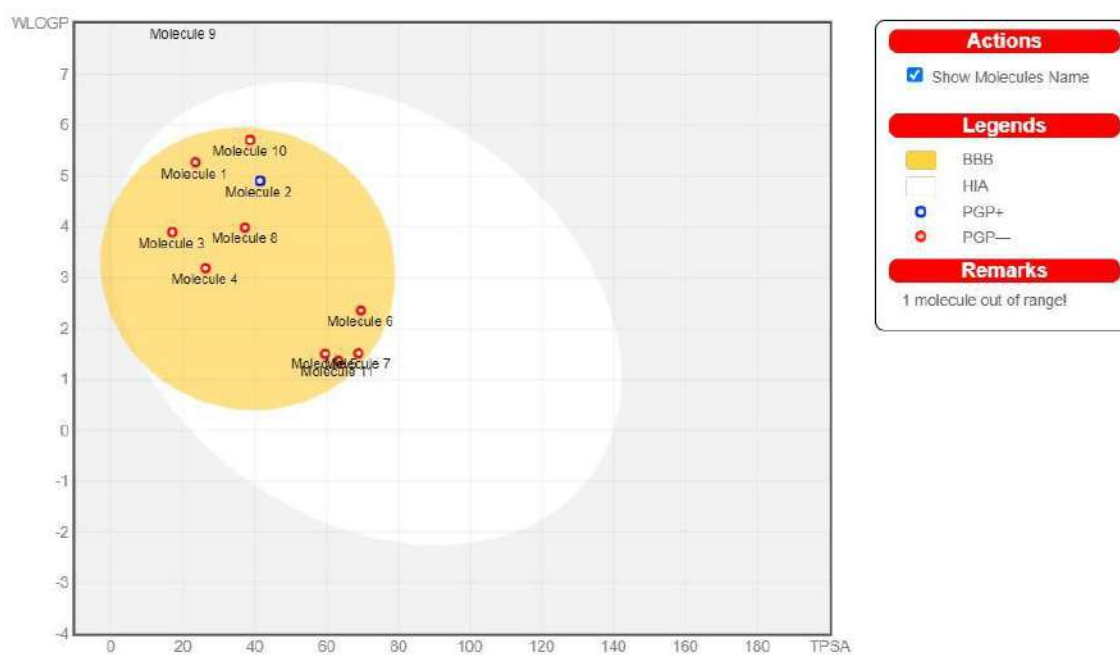


Fig no. 4. Combined Boiled Egg Diagram

Table no. 4. Name of molecules contained in Boiled Egg Diagram

MOLECULE NUMBER	MOLECULE NAME
1	Solanidine
2	Solasodine
3	Solavetivone
4	Solafuranone
5	Scopoletin
6	N-p-trans-Coumaroyltyramine
7	Isofraxidin
8	Lauric acid
9	β -sitosterol
10	Diosgenin
11	Gabapentin

BOILED means **B**rain **O**r **I**ntestinal **E**stimated **D** permeation predictive model. The boiled egg diagram shows two regions white region and yellow region.

The white region is the physicochemical space of molecules with highest probability of being absorbed by the gastrointestinal tract, and the yellow region (yolk) is the physicochemical space of molecules with highest probability to permeate to the brain.

In addition, the points are coloured in blue if predicted as actively effluxed by P-gp (PGP+) and in red if predicted as non-substrate of P-gp (PGP-).

4. CONCLUSION

In this study, we have carried out an *in-silico* screening of the phytoconstituents of *Solanum indicum* plant. This study demonstrated the sixteen compounds from *Solanum indicum* plant, (Solanidine, Solasodine, Solavetivone, Solafuranone, Scopoletin, N-p-trans-Coumaroyltyramine, Isofraxidin, Lauric acid, β -sitosterol, Diosgenin). The selected phytocompounds showed docking scores ranging from -8.3 to -4.2 kcal/mol in 5XVG. Among all, Solafuranone and Isofraxidin gave the highest binding energy (-8.1 kcal/mol) and (-6.8 kcal/mol) in complex with 5XVG, whereas the reference compound, Gabapentin showed a docking score with a binding energy of -5.1 kcal/mol. Furthermore, these ligands exhibited good ADMET properties. To summarize, phytoconstituents present in *Solanum indicum* possess strong effects against 5XVG and could be further evaluated for their antianxiety effect, as well as for the development of alternative drugs with fewer side effects for the treatment of stress.

REFERENCES

1. Ma P, Cao TT, Gu GF, Zhao X, Du YG, Zhang Y. Inducement effect of synthetic indiosides from *Solanum indicum* L. on apoptosis of human hepatocarcinoma cell line Bel-7402 and its mechanism. *Ai Zheng= Aizheng= Chinese Journal of Cancer*. 2006 Apr 1;25(4):438-42.

2. Bahgat A, Abdel-Aziz H, Raafat M, Mahdy A, El-Khatib AS, Ismail A, Khayyal MT. *Solanum indicum* ssp. *distichum* extract is effective against l-NAME-induced hypertension in rats. *Fundamental & clinical pharmacology*. 2008 Dec;22(6):693-9.
3. Morris GM, Huey R, Lindstrom W, Sanner MF, Belew RK, Goodsell DS, Olson AJ. AutoDock4 and AutoDockTools4: Automated docking with selective receptor flexibility. *Journal of computational chemistry*. 2009 Dec;30(16):2785-91.
4. Pettersen EF, Goddard TD, Huang CC, Couch GS, Greenblatt DM, Meng EC, Ferrin TE. UCSF Chimera—a visualization system for exploratory research and analysis. *Journal of computational chemistry*. 2004 Oct;25(13):1605-12.
5. Hao C, Zhao F, Song H, Guo J, Li X, Jiang X, Huan R, Song S, Zhang Q, Wang R, Wang K. Structure-based design of 6-chloro-4-aminoquinazoline-2-carboxamide derivatives as potent and selective p21-activated kinase 4 (PAK4) inhibitors. *Journal of Medicinal Chemistry*. 2018 Jan 11;61(1):265-85.
6. Verdonk ML, Cole JC, Hartshorn MJ, Murray CW, Taylor RD. Improved protein–ligand docking using GOLD. *Proteins: Structure, Function, and Bioinformatics*. 2003 Sep;52(4):609-23.
7. Leach AR, Shoichet BK, Peishoff CE. Prediction of protein– ligand interactions. Docking and scoring: successes and gaps. *Journal of medicinal chemistry*. 2006 Oct 5;49(20):5851-5.
8. SAMANT L, Javle V. Comparative docking analysis of rational drugs against COVID-19 main protease.
9. Arora S, Lohiya G, Moharir K, Shah S, Yende S. Identification of potential flavonoid inhibitors of the SARS-CoV-2 main protease 6YNQ: a molecular docking study. *Digital Chinese Medicine*. 2020 Dec 1;3(4):239-48.
10. Shah S, Chaple D, Arora S, Yende S, Moharir K, Lohiya G. Exploring the active constituents of *Oroxylum indicum* in intervention of novel coronavirus (COVID-19) based on molecular docking method. *Network Modeling Analysis in Health Informatics and Bioinformatics*. 2021 Dec;10:1-2.
11. Kaloni D, Chakraborty D, Tiwari A, Biswas S. In silico studies on the phytochemical components of *Murraya koenigii* targeting TNF- α in rheumatoid arthritis. *Journal of Herbal Medicine*. 2020 Dec 1;24:100396.
12. Joshi T, Sharma P, Joshi T, Chandra S. In silico screening of anti-inflammatory compounds from Lichen by targeting cyclooxygenase-2. *Journal of Biomolecular Structure and Dynamics*. 2020 Aug 12;38(12):3544-62.
13. Nisha CM, Kumar A, Vimal A, Bai BM, Pal D, Kumar A. Docking and ADMET prediction of few GSK-3 inhibitors divulges 6-bromoindirubin-3-oxime as a potential inhibitor. *Journal of Molecular Graphics and modelling*. 2016 Apr 1;65:100-7.
14. Tsujimura S, Tanaka Y. Disease control by regulation of P-glycoprotein on lymphocytes in patients with rheumatoid arthritis. *World journal of experimental medicine*. 2015 Nov 11;5(4):225.

Computational Insight on the Argentophilic Interactions of Axially Chiral Ag-NHC Complex of *R*-BINOL Scaffold via TD-DFT

Sonali Ramgopal Mahule*

ASAS, Amity University Mumbai, Panvel, India 410206

Abstract

A fascinating interaction between the closed shells of many organometallic or inorganic compounds of d^8 , d^2 , and d^{10} systems is interestingly recognized as an important determinant of solid-state structures and a potential source of useful material properties. This work presents such kind of intramolecular metallophilic interactions in the X-ray diffraction structures of bimetallic Ag-NHC complex **1e**. The structural studies revealed that the geometry around the metal centers has M...M interactions. Time-dependent density functional theory (TD-DFT) experiments were done for complex **1e** to insight into the M...M and metal-ligand interactions in them. The results of computational and experimental studies of these complexes showed a good agreement with each other. This attracting feature of closed-shell metallophilic interactions is becoming extremely popular in a variety of materials including nanomaterials for their applications that include rewritable phosphorescent paper for use as color-switchable luminescent materials, phosphorescent organogels for reversible RGB-color switching, luminescence chemosensors to optoelectronic 'on-off' devices, etc.

Introduction

The new chiral ligand framework has been derived from inexpensive and readily available, enantiopure *R*-BINOL. This study uncovered some interesting cage-like structural features in the molecular structure of the silver complex that have potential applications in important domains like asymmetric catalysis and molecular recognition. Herein, we studied the intramolecular M...M interactions in the chiral bimetallic silver(I) NHC complex. In pursuing this work we followed similar steps and concepts which were conspicuously studied and reported in the literature for the silver(I) and gold(I) complexes of N/O-functionalized N-heterocyclic ligand exhibiting closed-shell $d^{10}...d^{10}$ intermolecular argentophilic and aurophilic interactions.^{1,2} Whereas, this work differs from the reported one, and includes investigations of the intramolecular argentophilic interactions in chiral NHC complexes of axially chiral scaffolds containing amido functions. This property of metallophilic interaction in materials is very much popular because of their various applications for *eg.* in chiral recognition, for the development of chiral polymeric materials,^{3,4} in preparation of luminescent sensors^{5,6} etc. Thus, the closed-shell metallophilic interactions by their subtle but significant influence have aroused interest in recent years and have made an impact in frontline application-oriented research.

Results and Discussion

Time-dependent density functional theory (TD-DFT) studies

As the molecular structure of the complex $[L(L'\text{-NHC})_2]\text{Ag}_2$ ($L = 2,2\text{-dioxo-binaphthyl}$, $L' = \text{phenyl-acetamido}$) (**1e**) is determined by X-ray diffraction studies (Figure 1) showed that these are monomeric-bimetallic in nature and exhibit close M...M contact of 3.3011(9) Å which is shorter than twice the *van der Waals* radii of the corresponding silver (3.44 Å), there by indicating the presence of closed shell $d^{10}...d^{10}$ argentophilic interaction. Though numerous N-heterocyclic carbene complexes of silver are known in literature are examples of structurally characterized discrete dimeric $\{(\text{NHC})\text{MX}\}_2$ ($M = \text{Ag, Au}$; $X = \text{halide}$)^{7,8} type. But the

monomeric-bimetallic-*bis*-NHC complexes of type (Figure 1) exhibiting similar metallophilic interaction⁸⁴ are surprisingly not known to the best of our knowledge.

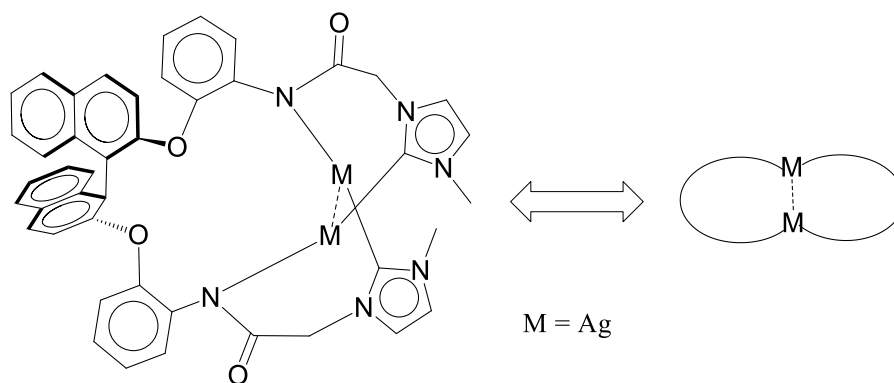
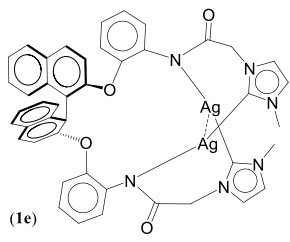


Figure 1. Monomeric chiral bis-M-NHC type of complex showing M...M interaction.

The geometry around the **1e** [C1–Ag1–N1] = 164.09(10)° for **1e**, [C1–Ag1–N3] = 167.5° is consistent with the linear geometries often observed for two-coordinated d^{10} metals.⁹ Quite interestingly, a direct consequence of presence and absence of M...M (M = Ag) interaction occurring through the central metal atom (Ag1) in the monomeric-bimetallic complex is evidenced by the slightly bent angle [C1–Ag1–N1] = 164.09(10)° at silver(I) in [L(L'-NHC)₂]Ag₂ (L = 2,2-dioxo-binaphthyl, L' = phenyl-acetamido)¹⁰ (**1e**) and these results suggest the presence of *argentophilic* interaction in complex **1e**. The effect is very weak as these frameworks are laid quite away from the metal binding sites of the ligands.

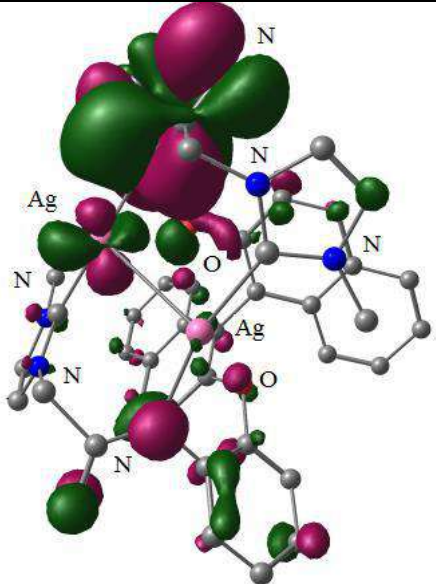
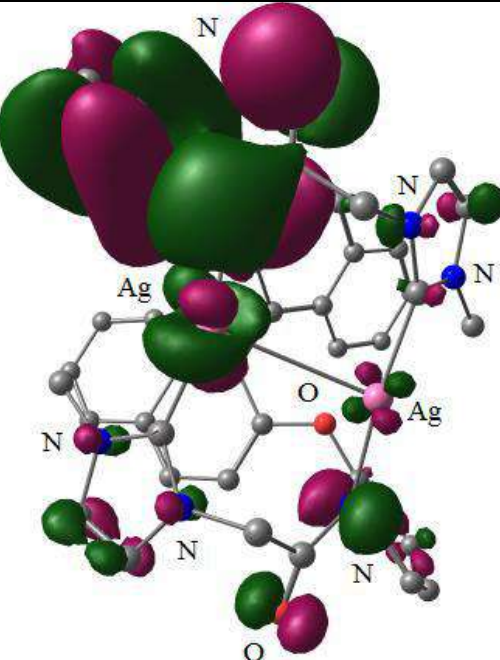
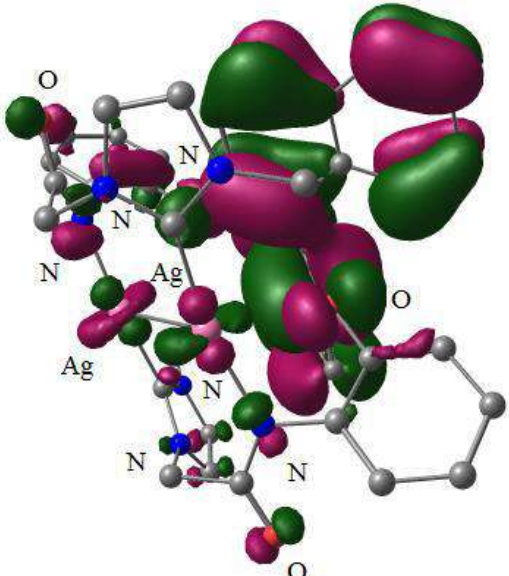
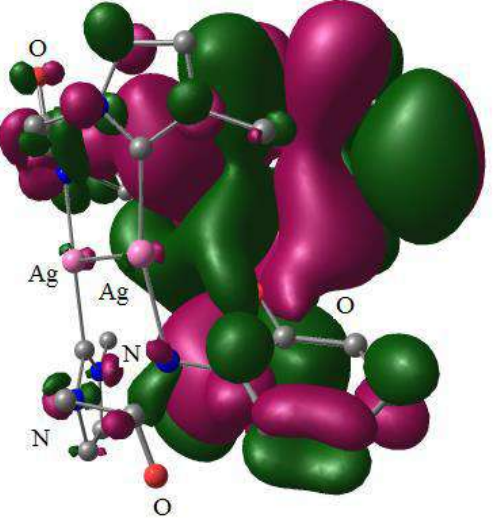
Table 1. Singlet excitation energies computed for complexes L(L'-NHC)₂]Ag₂ (L = 2,2-dioxo-binaphthyl, L' = phenyl-acetamido) (**1e**) and L(L'-NHC)₂]Ag₂ (L = 2,2-dioxo-binaphthyl, L' = phenyl-acetamido) **3e** at B3LYP/SDD, 6-31G* level of theory with an output are shown.

Complex	Excitation Wavelength (nm)	Oscillator strength	$\Psi_o-\Psi_v$	Transition coefficient	Type of transition
 (1e)	347.15	0.0905	HOMO→LUMO+1	0.6941	MLCT ($\pi\rightarrow\pi^*$)
	339.43	0.0061	HOMO→LUMO+2	0.7002	MLCT ($\pi\rightarrow\pi^*$)
	329.09	0.0064	HOMO→LUMO+3	0.6986	MLCT ($\pi\rightarrow\pi^*$)

Furthermore, to gain a better understanding about the interactions in the silver **1e** complex, and to obtain a deeper insight on the nature of NHC-metal interactions in these complexes, detailed density functional theory studies were carried using coordinates of the X-ray diffraction structure as an input data. In particular, the M...M bond order (Wiberg Indices) was computed using B3LYP/SDD, 6-31G(d) level of theory with the objective of estimating the strength of the closed-shell metallophilic interaction present in the complex. The computed bond order (Wiberg Indices) for the M...M interaction in the silver complex **1e** (0.1247) complex were approximately in the order of about a fourth of a single covalent thus supporting the evidence obtained from the X-ray diffraction analysis. The vertical transitions of the singlet excitation

energies obtained using TD-DFT calculations at the B3LYP/SDD, 6-31G(d) level of theory gives three transitions peaks for complex **1e** (347 nm, 339 nm, 329 nm) which coincides with the experimental results of UV-visible spectrum for **1e** and showed absorption at 340 nm.

Table 2. Selected molecular orbitals of the complex $L(L'-NHC)_2Ag_2$ ($L = 2,2$ -dioxo-binaphthyl, $L' =$ phenyl-acetamido) (**1e**) are shown.

	
HOMO Orbital # 203	HOMO Orbital # 204
	
HOMO Orbital # 205	LUMO Orbital # 206

TD-DFT study was performed on the geometry optimized computed structure, there can be a change in positions of transitions wavelengths, when the same experiments will be performed using X-ray crystallographic coordinates of the same complex. The number of transitions can also be increase by increasing the number of microstates in the experiment for the detailed study. These transitions obtained by the TD spectrum in **1e** complex has been assigned to the HOMO→LUMO $\pi \rightarrow \pi^*$ MLCT transitions based on the comparison of intensities of the observed transitions and the comparable computed transitions along with their oscillatory

strength values¹⁰ (Table 1). Different molecular orbitals which are associated with transitions of HOMO→LUMO for Ag-NHC complex **1e** (Table 2) are both ligand and metal in character.

Conclusions

Silver(I) complex **1e** showed mild range of metallophilic interactions in its structure. DFT studies performed on the complex **1e** showed good agreement with that of the experimental studies of the complex. These studies further followed by TD-DFT studies which enabled to determine the metal–metal and metal-ligand interactions, that also show different types of HOMO→LUMO transitions.

References

1. Ray, L.; Shaikh, M. M.; Ghosh, P. *Inorg. Chem.* **2008**, *47*, 230.
2. Samantaray, M. K.; Pang, K.; Shaikh, M. M.; Ghosh, P. *Inorg. Chem.* **2008**, *47*, 4153.
3. Mercks, L.; Albrecht, M. *Chem. Soc. Rev.* **2010**, *39*, 1903.
4. Sluch, I. M.; Miranda, A. J.; Elbjeirami, O.; Omary, M. A.; Slaughter, L. M. *Inorg. Chem.* **2012**, *51*, 10728.
5. Cui, Y.; Yue, Y.; Qian, G.; Chen, B. *Chem. Rev.* **2012**, *112*, 1126.
6. Brandys, M.-C.; Jennings, M. C.; Puddephatt, R. J. *J. Chem. Soc., Dalton Trans.* **2000**, 4601.
7. de Frémont, P.; Scott, N. M.; Stevens, E. D.; Ramnial, T.; Lightbody, O. C.; Macdonald, C. L. B.; Clyburne, J. A. C.; Abernethy, C. D.; Nolan, S. P. *Organometallics* **2005**, *24*, 6301.
8. Wang, H. M. J.; Chen, C. Y. L.; Lin, I. J. B. *Organometallics* **1999**, *18*, 1216.
9. Cotton, F. A.; Wilkinson, G.; Murillo, C. A.; Bochmann, M. *Advanced Inorganic Chemistry*, 6th ed. **1999**, p 1085.
10. Mahule, S.R.; Gangwar, M. K.; Vishnoi P. *ChemistrySelect*, **2018**, *3* (14), 4023.

Agricultural Influence and application of Mn(III), Fe(III) and VO(IV) Schiff base metal Complexes

S. R. Kelode

Department of Chemistry, Arts, Commerce and Science College, Maregaon
e-mail: sandipkelode14@gmail.com

Abstract:

The newly synthesized complexes of Mn(III), Fe(III) and VO(IV) with Schiff base derived from 2-hydroxy-5-methyl acetophenone and 4-(p-hydroxyphenyl)-2-aminothiazole have been synthesized and characterized on the basis of elemental analysis, Infrared, ¹HNMR, molar conductance and magnetic susceptibilities. The Schiff base acts as a monobasic bidentate ligand commonly coordinates through the oxygen atom of phenolic -OH group and the nitrogen atom of azomethine group, which is confirmed by IR spectral data. Agricultural influence and application of Schiff base metal complexes.

Keywords: Schiff base, Magnetic susceptibility and Agricultural application

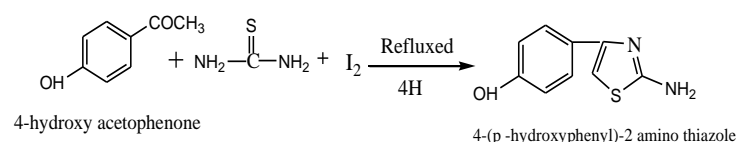
Introduction:

Schiff bases are considered to be the most versatile ligands as they form complexes with the metal atoms. Recent Advances in year 2023 the chiral Schiff Base Compounds¹ There is synthesis, characterization and biological activities of new Schiff Base Compound and its lanthanide complex². Antifungal Activity of Some Mixed Ligand Complexes Incorporating Schiff Bases³ The aim of present investigation is to synthesize Mn(III), Fe(III) and VO(IV) metal complexes of Schiff base derived by the condensation of 2-hydroxy-5-methyl acetophenone and 4-(p-hydroxyphenyl)-2- aminothiazole and to check their potency towards various agricultural influence and application of Schiff base metal complexes.

Experimental:

All the chemicals were of A.R. grade and used as received. 2-hydroxy-5-methyl acetophenone (HMA) and 4-(p-hydroxyphenyl)-2 amino thiazole was prepared by known methods.⁴⁻⁷ The solvents were purified by standard methods.⁸

Synthesis of 4-(p hydroxyphenyl)-2 amino thiazole; A mixture of p-hydroxy acetophenone (12g), thiourea (15.2g), iodine (25g), and 60ml distilled water was taken in a 250ml R.B. flask. The mixture was refluxed for about 4h and poured into crushed ice to get the solid which is basify with sodium hydroxide. The product was filtered and crystallized from 70% ethanol, after several minutes the golden coloured product of 4-(p-hydroxyphenyl)-2 amino thiazole was separated out.⁵⁻⁷ Yield: 10g (83.33%), m.p.: 216⁰C



Synthesis of 2-hydroxy-5-methyl acetophenone 4-(p-hydroxyphenyl)-2 imino thiazole [HMA]: A solution of 4-(p-hydroxyphenyl)-2 imino thiazole (0.02M) in 25ml of ethanol was added to an ethanolic solution(25ml) of 2-hydroxy-5-methyl acetophenone (0.02M) and the reaction mixture was refluxed on a water bath for 4h. After cooling a pale yellow coloured crystalline solid was separated out. It was filtered and washed with ethanol, crystallized from

DMF and dried under reduced pressure at ambient temperature. The purity of ligand was checked by elemental analysis and m.p. It was also characterized by IR and ^1H NMR spectral studies.

Yield: 60%; m.p. 310°C

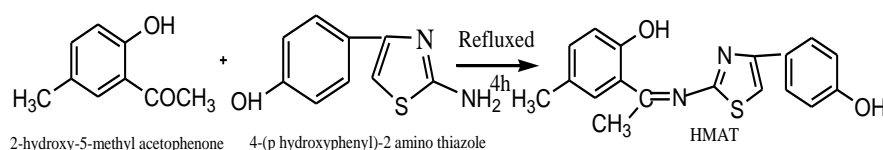


Table 1. Analytical data of the Ligands.

Sr. No.	Ligand	Molecular Formula	Formula Weight	Colour and nature	Elemental Analysis		
					C% found (Cal.)	H% Found (Cal.)	N% Found (Cal.)
1.	HMAT	$\text{C}_{18}\text{H}_{16}\text{N}_2\text{O}_2\text{S}$	324.16	Yellow Crystalline	66.64 (66.75)	04.69 (04.93)	08.60 (08.63)

Preparation of complexes: All the metal complexes were prepared in a similar way by following method. To a hot solution of ligand HMAT (0.02M) in 25ml of ethanol a suspension of respective metal salts was added drop wise with constant stirring. The reaction mixture was refluxed on a water bath for 3-6 h. The precipitated complexes were filtered, washed with ethanol followed by ether and dried over fused calcium chloride. Yield: 45-55%

The complexes are soluble in DMSO and DMF but insoluble in water and common organic solvents. The metal chloride content of complexes were analyzed by standard methods.⁹

The ^1H NMR spectra of ligand was recorded and obtained from RSIC Chandigarh. IR spectra of the compounds were recorded on Perkin Elmer 842 spectrophotometer in the region $400\text{--}4000\text{cm}^{-1}$. Carbon, Hydrogen and Nitrogen analysis were carried out at RSIC, Punjab University, Chandigarh. The molar conductance of the complexes at 10^{-3}M dilution in DMF were determined using equiptronic digital conductivity meter EQ-660 with a cell constant 1.00cm^{-1} at room temperature. The magnetic moment measurement were made on a Gouy balance at room temperature using $[\text{HgCo}(\text{SCN})_4]$ as the calibrant.

Table 2. Analytical data and molar conductance of the compounds.

Compounds	Colour	Mol. wt.	Analysis % Found (calc.)					μ_{eff} B.M.	Λ_{M} ($\Omega^{-1}\text{cm}^2\text{mol}^{-1}$)
			M	C	H	N	Cl		
$[\text{MnL}_2(\text{OAc})] \cdot 2\text{H}_2\text{O}$	Brown	796.1	6.73 (6.89)	57.10 (57.27)	4.52 (4.64)	7.00 (7.03)	—	4.3	22.2
$[\text{FeL}_2(\text{H}_2\text{O})\text{Cl}] \cdot \text{H}_2\text{O}$	Brown	773.6	7.14 (7.22)	55.74 (55.84)	4.31 (4.39)	7.14 (7.23)	4.49 (4.58)	5.3	24.8
$[\text{VOL}_2]$	Green	713.2	7.11 (7.15)	60.45 (60.57)	4.09 (4.20)	7.76 (7.85)	—	1.55	10.8

Result and Discussion:

The ligand and its complexes have been characterized on the basis of ^1H NMR, IR spectral data, elemental analysis, molar conductance and magnetic susceptibility measurements data.

All these values and analytical data is consistent with proposed molecular formula of ligand. All the compounds are coloured solid and stable in air. They are insoluble in water but soluble

in coordinating solvents like DMF and DMSO. The molar conductance values in DMF(10^{-3} M) solution at room temperature (Table 2) shows all the complexes are non electrolytes.

The ^1H NMR spectra of the ligand shows signals at δ 12.03, (1H, s phenolic OH), δ 9.00 (1H, s, phenolic OH), δ 6.83, 6.82, 6.81 and 6.80 (4H, m, phenyl) δ 7.58, 7.53, and 7.52 (3H, s Phenyl), 6.49 (1H s thiophene), and 2.92(3H, s, methyl) 2.58 (3H, s, methyl)¹⁰⁻¹³. The IR spectral data of the ligand and its metal complexes are given in Table 3. The IR spectrum of the free ligand exhibits a broad band at 3119 cm^{-1} which is ascribed to $\nu(\text{O-H})$ vibration lowered due to intramolecular $\text{O-H}\cdots\text{N}$ hydrogen bonding. The absence of C=O band at around $1700 - 1750\text{ cm}^{-1}$ indicates the Schiff base formation.¹⁴⁻¹⁷ The other bands at 1620, 1513 and 1121 are assignable to $\nu(\text{C=N})$, $\nu(\text{C-O})$ (phenolic) and $\nu(\text{C-S})$. In the spectra of all the complexes the $\nu(\text{C=N})$ band is lowered by $25\text{-}40\text{ cm}^{-1}$ indicating the involvement of azomethine nitrogen in coordination. Also, the band due to $\nu(\text{O-H})$ of the ligand disappeared indicating the coordination of phenolic oxygen to metal ion via deprotonation. This is also supported by the shift in $\nu(\text{C-O})$ (phenolic) mode. IR spectrum of Mn(III) complex display two bands near 1616, 1446 cm^{-1} assigned to $\nu_{\text{asy}}(\text{OCO})$ and $\nu_{\text{sym}}(\text{OCO})$ respectively, indicating monodentate nature of the coordinated acetate group. The strong IR bands around 960, 1156 and 910 in the spectrum of VO(III), are assigned to $\nu(\text{V=O})$ $\nu(\text{Zr-OH})$ $\nu(\text{O=U=O})$ vibrations.

Table 3. IR spectra of ligand and metal complexes:

Compound	$\nu(\text{O-H})$ hydrogen bonded	$\nu(\text{C=N})$ Imine	$\nu(\text{C-O})$ phenolic	$\nu(\text{M-O})$	$\nu(\text{M-N})$
HMAT	3119	1620	1513	-	-
$[\text{MnL}_2(\text{OAc})] 2\text{H}_2\text{O}$	—	1560	1450	500	425
$[\text{FeL}_2(\text{H}_2\text{O})\text{Cl}] \text{H}_2\text{O}$	—	1590	1502	520	455
$[\text{VOL}_2]$	—	1594	1508	515	450

Agricultural Influence and application of metal complexes: A ploughshare is an cobalt Copper and nickel metal complexes used in agriculture to increase the production of crops. They are used prior to the seedling stage to loosen up the soil. Essential observed that cobalt (Co), copper (Cu), iron (Fe), manganese (Mn), molybdenum (Mo), nickel (Ni), and zinc (Zn) complexes with schiff base plays a beneficial role in plant growth and development. **Synthetic Action on Insecticides:** Schiff base ligand was derived from the condensation of thiazole and 2-hydroxy-5-chloro-3-nitro acetophenone. Their metal complexes show high activity against insects¹⁸. 2-amino-4-phenylthiazole acts as intermediate in synthesis of photostable pyrthriod insecticides¹⁹. Flourination on aldehyde part of Schiff base increases insecto acracicidal activity²⁰. Schiff bases and their metal complexes with Mn(III), Fe(III) and VO(IV) show insecticidal activities against bollworm ²¹. Most metals complexes cause environmental and atmospheric pollution, and may be lethal to humans. Heavy metals can become strongly toxic by mixing with different environmental elements, such as water, soil, and air, and humans and other living organisms can be exposed to them through the food chain. Arsenic, cadmium, chromium, copper, nickel, lead and mercury are the most common metals which can pollute the environment. They are not all equally important but all play a role in plant growth. The heavy metals Mn(III), Fe(III) and VO(IV) are micronutrients or trace elements for plants. They are essential for growth and stress resistance as well as for biosynthesis and function of different biomolecules such as carbohydrates, chlorophyll, nucleic acids, growth chemicals, and secondary metabolites. Nitrogen (N) containing Schiff base metal complexes is made

available to the plant from the air and soil. But most of the needed elements that are nutrients for plants come from the soil.

Conclusions: The Schiff bases ligand and their metal complexes shows more activity towards the agricultural Influence and applicable for plant growth.

References:

1. T. China, N. Daisuke and A. Takashiro, *Molecules*, 28, 7990 (2023).
2. Y. Abu, A.A Abduh, M.S. Saghir and S.A.M Al-Gabri, *J Pharma* 15, 454, (2022).
3. M. Miloud, M. El-ajaily, Al-noor and N.S. Al-barki. *J Bact Mycol.* 7(1),1122 (2020).
4. A. S. Aswar, P.Bahad, A.Pardhi and N.Bhave, *J. Poym. Mater.* 5, 232 (1988).
5. S.Pattan, M.Ali, J.Pattan, S.Purohit, V.Reddy and B.Nataraj, *Indian J.Chem.*, 45B, 1929. (2006).
6. D.Khrustalev, A.Suleimenova .and S.Fazylov, *Russian J. App. chem.*, 81(5), 900 (2008).
7. H.Maradiya, and V.Patel, *J. Fibers and poly.*, 3(1), 43 (2002).
8. B.Furniss, A.Hannaford, P.Smith & A.Tatchell, *Vogel's practical organic chemistry* 5thEd. (Logman Scientific Technical, John Wiley and Sons), (1989).
9. Vogel AI, "A Text book of quantitative inorganic chemistry" 3thEd., (ELBS,London,1961).
10. S.Sadigova, A.Magerramov and M.Allakhverdiev, *Russian J. Org. chem.*, 81(5), 900 (2008).
11. E.Campbell and S.Nguyen, *J. Tetrahedron*, 42, 1221 (2001).
12. P.Pietikainen and A.Haikarainen *J. Mole. Catalysis.*, 180, 59 (2002).
13. M.Kidwai, P.Podar and k.Singhal, *Indian J. Chem.*, 48B, 59 (2009).
14. S.Sonwane, S.Srivastava and S.Srivastava, *Indian J. Chem.*, 47B, 633 (2008).
15. K.Patel and A.Mehata, *E. J. Chem.*, 3(13), 267 (2006).
16. R.Maurya, D.Antony, S.Gopinathan, V.Puranic, S.Tavale &C.Gopinathan, *Bull.Chem. Soc.*, 68,2847 (1995).
17. D.Boghaei and S.Mohebi *J. Tetrahedron*, 58, 5357 (2002).
18. D.A. Laidler, D.J Milner, *J. Organomet Chem.*, 1984 270, 121-129.
19. N. S. Kozlow, G.P. Korotyshova and N.G. Rozhkova, E.I.Andreeva. *Chem Abstr.* 106, 155955, (1987).
20. L. Zhu, N Chen , .F. Li H, Song, X. Zhu, *Chem Abstr.*, 2004,141, 374026, (2004).
21. S. Huneck, K. Schreiber, H.D. Grimmecke , *J Plant Growth Regul.* 3,75,(1984).

Recent Applications of Deep Eutectic Solvent (DES), a Greener Media in Organic Synthesis

Suchita B. Wankhede*

Department of Chemistry, Amolakchand Mahavidyalaya, Yavatmal 445001 (Maharashtra) India

*Email – suchita333wankhede@gmail.com

Mobile Number - 9421770305

Abstract: A modern era of research mainly focused on study of use of solvent in organic transformation, with its advantageous as environmental benign, cost effectiveness and in a simple and sophisticated practical term. In the search of safe, non-toxic, cheap, biorenewable and biodegradable solvents, deep eutectic solvents (DESs) get the prominent position. DES acts as a valuable alternative which overcome the limitations of use of traditional volatile organic compound (VOCs) solvents. This review paper aims to inspire scientists, work in organic field to study the potential of DES. From understanding of the different aspects like effect of temperature, concentration, addition of water etc. would provide knowledge for deciding the scheme of organic synthesis. Review paper includes study of various organic reactions from literature using DESs as catalyst and solvent media in a tabular form. It also includes recycling and reuse of DESs in organic reactions. Convenient reaction set-up, simple separation and purification built impact of DESs in laboratory and industry in near future.

Keywords: Deep eutectic solvent, catalyst and solvent media, green/ecofriendly solvent, organic transformation, recycle and reuse.

1. Introduction

“Protecting our common environment” is the key objective given in Millenium Declaration adopted by United Nations in 2000. From the last decades when we throw a light on our changing lifestyle which becomes more demanding in different fields like drugs, plastic, polymer etc. These demand causes damage and exploitation of natural resources like water, petroleum, air, minerals etc and the question was arises ‘*Why is chemical manufacture becoming unsustainable?*’[1]. Now it becomes needed to make balance between increasing demand in production of chemical compounds with safe and clean environment. Amongst three states of matter, the most convenient reaction media is solvent (liquid state). Most common volatile organic compound (VOCs) solvents, due to their high cost, high toxicity, high inflammability, non-biodegradability and causing negative impact on environment[2], there is need to develop a new concept of “*ideal green solvent*”. In search of ideal solvents, water, supercritical carbon dioxide (SCD) [3] supercritical water (SCW)[4], and ionic solvents [5] are discovered but due to their disadvantages under different reaction conditions make them unsuitable solvent as reaction media for industrial purpose. Abbott in 2003 [6] first introduced a new generation of safe, nontoxic, cheap, biorenewable and biodegradable, sustainable designer solvent [7] termed as “*Deep Eutectic Solvent*” (DES). They exhibit similar properties like ILs as they work on similar molecular base but still more superior than Ionic liquids. As a designer and environmentally benign solvent, DES has numerous applications in various fields. There are many reviews to study organic reactions based on greener approach using DESs as reaction media. That encourages us to study organic reactions using greener solvent DES.

This review article includes general introduction of DESs, classification and types of DESs, applications in various fields and study of various organic reactions using DESs as

catalyst and solvent media. This review also discussed optimized reactions with recycling and reuse of DESs in organic reactions from literature published in between the session 2020-2023.

2. Deep Eutectic Solvents (DESs)

Deep Eutectic Solvents (DESs), also known as *Deep Eutectic Ionic Liquids (DEILs)*[8], *Low Melting Mixtures (LMMs)* or *Low Transition Temperature Mixtures (LTTMs)*[9] in the literature. The first reported DES was a mixture of choline chloride and urea (1:2), with a melting temperature of 12 °C, much lower than those of the starting materials, 302 °C and 133 °C, respectively [10]. DES is generally defined as a binary mixture of an ionic components, one is a hydrogen bond acceptor (HBA) like chloride ion and the other a hydrogen bond donor (HBD), such as an alcohol, amide or carboxylic acid. Simply DES is a neoteric solvent [11] which are able to form a new eutectic phase (which is a liquid below 100 °C) through hydrogen-bond-promoted self-association and no covalent compounds are formed between them, hence the term 'Deep' is used [12,13].

3. Types and Classification of DESs

DESs are broadly classified as Hydrophilic and Hydrophobic DESs. Main difference between them is their melting point depression. Hydrophilic DESs have deep depression in freezing point due to extensive hydrogen bond interaction eg. choline chloride salt with small alkyl chains, acids, amines etc. While hydrophobic DESs have a large and small depression in freezing point eg. Long hydrocarbon alkyl chain containing salts and acid like Decanoic acid, Dodecanoate sodium salts etc.

DESs are also classified into four types (table 1) from numerous possible combinations of HBD and HBA components. Marcus [14] reported data regarding their molecular mass and their eutectic melting points. Nonionic deep eutectic solvents are the other class of DESs, introduced by Francisco *et al* [15,16] originated from Type –III DES and are characterized by low ionicity, having low electrical conductivity.

Table 1. Types of eutectic mixtures

Types	General formula	Terms	Example
DES I	$\text{Cat}^+\text{X}^- + z\text{MCl}_x$	$\text{M}=\text{Zn, In, Sn, Al, Fe}$	$\text{ChCl} + \text{ZnCl}_2$
DES II	$\text{Cat}^+\text{X}^- + z\text{MCl}_x$	$\text{M}=\text{Cr, Ni, Cu, Fe, Co}$	$\text{ChCl} + \text{CoCl}_2 \cdot 6\text{H}_2\text{O}$
DES III	$\text{Cat}^+\text{X}^- + z\text{RZ}$	$\text{Z}=\text{OH, COOH, CONH}_2$	$\text{ChCl} + \text{urea}$
DES IV	$\text{MCl}_x + z\text{RZ}$	$\text{M}=\text{Zn, Al and Z}=\text{OH, CONH}_2$	$\text{ZnCl}_2 + \text{urea}$

4. Various Organic reactions in four types of deep eutectic solvents

4.1 DES Type I catalysed organic reactions

DES type –I is the combination of quaternary ammonium salts with metal chlorides, eg. quaternary ammonium salts forms eutectic mixtures with zinc and tin chloride to result in freezing points between 13 and 92 °C [17] respectively.

Table 2. DES type I reactions

S. N.	DES used	General reaction and reaction condition	Scope of reaction (% yield)	No. of recycle of DES	References
1.	[CholineCl] [ZnCl ₂] ₃	<p>2-naphthol + R₁CHO + R₂CONH₂ $\xrightarrow{[CholineCl][ZnCl_2]_3 (20mol\%)}$ 1-amidoalkyl naphthol solvent free, 600C, 40-80 min</p>	45-95%	3	[18]
2.	[ChCl][ZnCl ₂]	<p>Substituted Benzaldehyde + N substituted aniline $\xrightarrow{[ChCl][ZnCl_2]}$ Triarylmethane derivatives 4 h, 1300C</p>	30-81%	5	[19]
3.	[ChCl][ZnCl ₂]	<p>Diketone + R₂CHO + NH₄OAc or R₃NH₂ $\xrightarrow{[ChCl][ZnCl_2]}$ Decahydroacridine-1,8diones 1-2 h, 80-900C</p>	75.1-92.6%	3	[20]
4.	[ChCl][ZnCl ₂] ₂	<p>Substituted 2-aminoacetophenone + substituted phenyl acetylene $\xrightarrow{[ChCl][ZnCl_2]_2}$ Quinoline derivatives 80°C, 3 h</p>	63-98%	-	[21]

4.2 DES Type II catalysed organic reactions

DES type II involves organic salts that are easy to handle and overcomes moisture absorption problem in DES type I. Eg. Choline chloride forms a deep eutectic solvent with calcium chloride hexahydrate at several molar ratios, at a 1:2 molar ratio, melting point 2.70 °C [22].

Table 3. DES type II reactions

S. N.	DES used	General reaction and reaction condition	Scope of reaction (% yield)	No. of recycle of DES	References
1.	ChCl.AlCl ₃ .6H ₂ O	<p>Glucose \xrightarrow{DES} putative enediolate intermediate $\xrightarrow{Al_3^+}$ Fructose $\xrightarrow{H^+}$ HMF Path A: Isomerization, Dehydration Path B: Dehydration CH(ChCl) major, CH(AlCl₃.6H₂O, minor) 30 min, 120°C</p>	29-86%	10	[23]

4.3 DES Type III catalysed organic reactions

Type III DESs are very attractive and most investigated class of DES as they are composed of biodegradable and non-toxic HBD's like urea, organic carboxylic acids, polyols. Eg. Tetrabutylammonium chloride forms deep eutectic solvents with ethylene glycol (1:3 mole ratio), glycerol (1:4 mole ratio), and triethylene glycol (1:3mole ratio) with eutectic freezing point -31°C , -13°C and -43°C , respectively [24].

Table 4. DES type III reactions

S. N.	DES used	General reaction and reaction condition	Scope of reaction (% yield)	No. of recycle of DES	References
1.	CholineCl:Urea	<p>4-hydroxycoumarin + aromatic aldehydes + amides $\xrightarrow[\text{90-105 min, } 80^{\circ}\text{C}]{\text{(Choline chloride:urea)}}$ 3-amido-alkyl-4-hydroxycoumarin derivatives</p>	84-92%	4	[25]
2.	EthyltriphenylphosphoniumbromideTHFtetracarboxylic acid.	<p>Aromatic aldehyde + Aromatic amine + beta-ketoester $\xrightarrow[\text{80}^{\circ}\text{C, 1-4 h}]{\text{DES 5mmol}}$ Alkyl 1,2,6-trisubstituted-4-[(hetero)arylamino] 1,2,5,6-tetrahydropyridine-3-carboxylate</p>	60-95%	5	[26]
3.	ChCl:Urea (1:2)	<p>Anthranilic acid derivative + Isocyanate derivative $\xrightarrow[\text{Stirring 1-2 h, MW 1800W 60min, US 60 min}]{\text{DES } 80^{\circ}\text{C}}$ 2-mercaptoquinazolin-4(3H)</p>	Stir.(20-76)MW(12-49)US(17-64%)	4	[27]
4.	[ChCl][Gabapentine]	<p>Aldehyde + C-H activated compounds + Malononitrile $\xrightarrow[\text{75}^{\circ}\text{C, 7-28 min}]{\text{DES 10mol\%}}$ Tetrahydrobenzo[b]pyrane & Pyrano[2,3-d]pyrimidinone(thione)</p>	86-95%	5	[28]
5.	ChCl:Urea (1:2)	<p>2-amino-5-chlorobenzophenone + Substituted aldehyde + Ammonium acetate $\xrightarrow[\text{80}^{\circ}\text{C, 45min}]{\text{DES}}$ quinazoline derivative</p>	84-97%	4	[29]
6.	ChCl:Urea (1:2)	<p>beta-ketodithioesters + Substituted indol-3-carbaldehyde $\xrightarrow[\text{Stirring r.t., 10 min}]{\text{DES}}$ Trisubstituted alkene derivatives</p>	84-90%	5	[30]
7.	Taurine/choline chloride	<p>4-hydroxycoumarin + substituted aldehyde $\xrightarrow[\text{H}_2\text{O, } 90^{\circ}\text{C}]{\text{DES (18 mol\%)}}$ Biscoumarin derivatives</p>	87-95%	4	[31]
		<p>Barbituric acid + Malononitrile + substituted aldehyde $\xrightarrow[\text{H}_2\text{O, } 90^{\circ}\text{C}]{\text{DES (20 mol\%)}}$ Pyrano[2,3-d]pyrimidinone</p>	88-94%		

4.4 DES Type IV catalysed organic reactions

Organic salts used in DES type I, II and III as HBA are now replaced by metal halides in DES type IV. Urea:ZnCl₂ (3.5:1 mole ratio) forms a DES with a melting point of 9 °C [32].

Table 5. DES type IV reactions

S. N.	DES used	General reaction and reaction condition	Scope of reaction (% yield)	No. of recycle of DES	References
1.	CeCl ₃ ·7H ₂ O/ urea (1:5)	<p>unsaturated diketones Aldehydes Xanthenediones</p>	Diketone(80-96%)Xanthenedione (88-97%)	5	[33]
2.	ZrOCl ₂ ·8H ₂ O/ Urea (1:5)	<p>Substituted sulphides Substituted sulfoxide</p>	91-99%	3	[34]
3.	K ₂ CO ₃ /Glycerol (1:4)	<p>Aromatic aldehydes Ethylcyanoacetate Phenyl hydrazine 2,3-dihydro-1H-pyrazole-4-carbonitrile</p>	85-95%	-	[35]
4.	ZrOCl ₂ ·8H ₂ O: Urea (1:5)	<p>Aldehydes Amines Dimethylphosphite alpha-aminophosphonate</p>	88-98%	5	[36]

5. Conclusion

DESs have aroused increasing scientific attention in the field of greener chemistry due to their easy availability and cost effectiveness. Study of organic reactions under four types of DESs, may inspire scientists, who work in organic field to glimpse the potential of DESs. So far, from the study of many reactions, it was observed that reaction in DES along with additional greener methods like microwave irradiation or ultrasonication also helps to increase efficiency and productivity of reactions. It is observed that viscosity plays a very important role in DESs to act as organic solvent. Miracle of DESs in many organic reactions is its recyclability and its reuse, without loss of its activity many times without formation of side products which may affect yield of pure product. Literature study reveals, increase in product yield, higher reaction rates, and reduce reaction time and no need of further purification of product using thin layer chromatography, as compared with the conventional organic synthetic route. On comparison of four types of reactions in DESs media, DESs Type III is mostly used in many organic transformations, while DES Type II is very rarely used as reaction media. Thus still

further research is needed to study mechanism involved in organic transformation involving DESs as reaction solvent. From environmental point of view in an area of organic chemistry, applications of DESs as reaction media, is getting more importance every day and their viewpoint in both laboratory and industry may opens a new era in organic synthesis. But beside of enormous green applications of DESs the next step will be focused on study of its toxicity.

References

- [1] Poliakoff M & Licence P, *Nature*, 450 (2007) 810.
- [2] Amelio A, Genduso G, Vreysen S, Luis P & Van der Bruggen B, *Green Chem.*, 16 (2014) 3045.
- [3] Zhang X, Heinonen S & Levänen E, *RSC Adv.*, 4 (2014) 61137.
- [4] Marcus Y, Biofuels and Biorefineries, Fang Zh, Xu Ch (Eds) (Volume 2||) (*Springer: Dordrecht*) (2014) p.19.
- [5] Marcus Y, Ionic Liquid Properties (*Springer Intl. Publ., Switzerland*) (2016) p.39.
- [6] Abbott A P, Capper G, Davies D L, Rasheed R K & Tambyrajah V, *Chemical Communications*, 1 (2002) 70.
- [7] Xie Y, Dong H, Zhang S, Lu X & Ji X, *Green Energy & Environment*, 1 (2016) 195.
- [8] García-Álvarez J, Technologies for the Environment, (Volume 1186||) (*ACS Symposium Series; American Chemical Society: Washington, DC*) (2014), p.39.
- [9] Francisco M, González A S B, García de Dios S L, Weggemans W & Kroon M C, *RSC Adv.*, 3 (2013) 23553.
- [10] Abbott A P, Boothby D, Capper G, Davies D L & Rasheed R K, *Journal of the American Chemical Society* 126 (2004) 9142.
- [11] Seddon K R, *ChemInform*, 28 (2010).
- [12] Smith E L, Abbott A P & Ryder K S, *Chem. Rev.*, 114 (2014) 11060.
- [13] Martins M A R, Pinho S P & Coutinho J A P, *J. Solut. Chem.*, 48 (2018) 962.
- [14] Marcus Y, Deep eutectic solvents (e-book) Springer, Cham, (*Springer Nature: Switzerland AG*) (2019) p.17.
- [15] Francisco M, Bruinhorst van der A & Kroon C M, *Green Chemistry*, 14 (2012) 2153.
- [16] Francisco M, Bruinhorst van der A & Kroon C M, *Angewandte Chemie*, 52 (2013) 3074.
- [17] Abbott A P, Capper G, Davies D L, Munro H L, Rasheed R K & Tambyrajah V, *Chem. Commun.*, 1 (2001) 2010.
- [18] Nguyen V T, Nguyen H T & Tran P H, *New Journal of Chemistry*, 45 (2021) 2053.
- [19] Zhang L, Hu Z, Chen X, Yan L, Liu Y & Xie Z., *Chinese Journal of Organic Chemistry*, 41 (2021) 4415.
- [20] Xiao L, Liu G, Li Z, Ren P, Ren L & Kong J, (2020). *Chinese Journal of Organic Chemistry*, 40 (2020) 2988.
- [21] Chen G, Xie Z, Liu Y, Meng J & Zhang L..*Chinese Journal of Organic Chemistry*, 40 (2020) 156.
- [22] Shahbaz K, AlNashef I M, Lin R J T, Hashim M A, Mjalli E S & Farid M M, *Solar Energy Mater Solar Cell*, 155 (2016) 147.
- [23] Chen B, Li Z, Feng Y, Hao W, Sun Y, Tang X, Zeng X & Lin L, *ChemSusChem*, 14 (2021) 847.
- [24] Mjalli F S, Naser J, Jibril B, Alizadeh V & Gano Z, *J Chem Eng Data*, 59 (2014) 2242.
- [25] Asadi H, Anaraki-Ardakani H, Torabi P & Taheri N, *Revue Roumaine De Chimie*, 65 (2020) 795.
- [26] Goudarzi H, Habibi D & Monem A, *Scientific Reports*, 13 (2023).
- [27] Komar M, Kraljević T G, Jerković I & Molnar M, *Molecules*, 27 (2022) 558.

-
- [28] Khoshdel M A, Shirini F, Langarudi M S N, Zabihzadeh M & Biglari M, *New Journal of Chemistry*, 45 (2021) 3138.
- [29] Singh R R, Singh T P, Devi T L, Devi T J & Singh O M, *Current Research in Green and Sustainable Chemistry*, 4 (2021) 100130.
- [30] Devi T J, Singh T K, Singh R R, Singh E H & Singh O M, *ChemistrySelect*, 5 (2020) 13351.
- [31] Biglari M, Shirini F, Mahmoodi N O, Zabihzadeh M, Langarudi M S N & Khoshdel M A, *Polycyclic Aromatic Compounds*, 42 (2020) 1452.
- [32] Abbott A P, Barron J C, Ryder K S & Wilson D, *Chem. Eur. J.*, 13 (2007) 6495.
- [33] Shaibuna M, Hiba K & Theresa L V, *New Journal of Chemistry*, 44 (2020) 14723.
- [34] Dutta A, Garg A, Borah J, Borah R P & Sarma D, *Current Research in Green and Sustainable Chemistry*, 4 (2021) 100107.
- [35] Zwain A A, Ahmad I, Khalaf Jebur Ali R, Kahtan M, Khdyair Hamad A, Abdulgader Hassan E, Asiri M, Ridha B M and Alsalamy A, *Front. Mater.*, 10 (2023) 1196583.
- [36] Machingal S & Krishnapillai S, *Beilstein Arch*, (2020) 202097.

Synthesis, Characterization and Pharmacological Evaluation of Some New Functionalized Flavone Derivatives From B-Diketones

Sushil K. Pagariya* and Pravin S. Bodkhe

Post Graduate Department of Chemistry, Vidya Bharati Mahavidyalaya, Amravati 444602, India.

*Corresponding author email: sushilpagariya@gmail.com

ABSTRACT: In present work, a series of novel flavone analogues have been synthesized by dehydrative cyclization of 1,3-diketone (β -diketone) derivatives carrying p-chloro-m-cresol moiety under acidic condition and characterized by usual chemical characteristics, elemental analysis, IR, ^1H NMR and Mass spectral data studies for structure assignment. All the newly synthesized compounds were screened for their *in vitro* antimicrobial activities against human pathogenic bacterial and fungal strains by disc diffusion method. Moreover, they have been evaluated for their *in vitro* antioxidant and anti-inflammatory properties by DPPH free radical scavenging and inhibition of protein denaturation methods respectively with reference to standard drugs.

Keywords: Flavone, β -diketone, p-chloro-m-cresol, synthesis, pharmacological evaluation.

INTRODUCTION

Flavonoids (from the Latin word flavus, which means 'yellow') are a large group of natural polyphenolic compounds with low-molecular weight; particularly, they belong to a class of plants secondary metabolites widely found in fruits, vegetables and plants derived beverages such as green tea and wine. Flavonoids are associated with a broad spectrum of health-promoting effects and are an indispensable component in a variety of nutraceuticals, pharmaceuticals, medicinal and cosmetic applications because of their oxidative, anti-inflammatory, anti-mutagenic and anti-carcinogenic properties coupled with their capacity to modulate key cellular enzyme functions. Structurally, flavonoids is 2-phenyl benzo- γ -pyrone (2-phenyl chromone) consists of fifteen basic carbon atoms (C6–C3–C6) with a general formula $\text{C}_{15}\text{H}_{10}\text{O}_2$ and classified into six subclasses on their chemical structure¹ among which flavone is the most prominent class of flavonoids based on the backbone of 2-phenyl-4H-chromen-4-one (2-phenyl-1-benzopyran-4-one). Flavones are heterocyclic polyphenolic compounds ubiquitously present in plant kingdom, especially in seeds, citrus fruits, olive oil, tea and red wine, vegetables, nuts, stems and flowers, honey and are commonly consumed with the human diet. Flavones display a broad spectrum of biological properties, including antibacterial², antifungal³, antiviral⁴, antidiabetic⁵, anti-inflammatory⁶⁻⁷, antioxidant⁸⁻⁹, hepatoprotective¹⁰, anticancer¹¹, anti-tubercular¹², antitumoral¹³, and antimalarial¹⁴ activities, making them an attractive target for synthesis and further study. Number of methods have been developed for the synthesis of flavones and its derivatives¹⁵⁻¹⁷, among them Claisen-Schmidt condensation and Baker-Venkatarman rearrangement (BVT) are traditional methods to make flavones¹⁸. Under Claisen-Schmidt conditions, hydroxychalcones produced from 2-hydroxyacetophenone and benzaldehyde can undergo oxidative cyclization to yield flavone rings. In Baker-Venkatarman approach¹⁹⁻²⁰, 2-hydroxyacetophenones are converted into benzoyl esters, which are rearranged by a base to a 1,3-diphenylpropane-1,3-diones (which exist also in equilibrium with their enolic forms) followed by cyclization under acidic condition to yield flavones.

In view of pharmacological significance of flavones and in continuation of our work on synthesis of derivatives of β -diketone, it was decided to prepare some novel flavone analogues

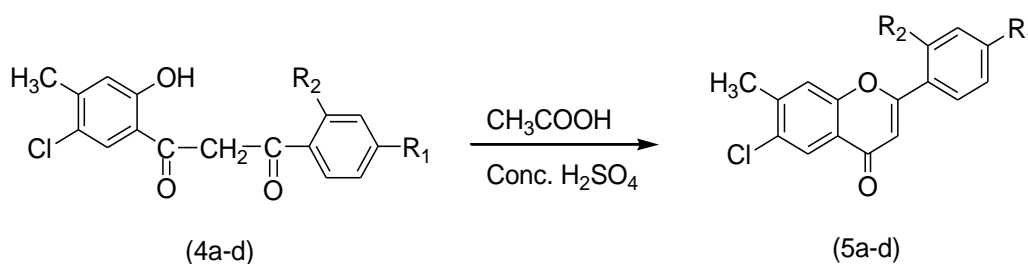
through cyclodehydration of 1,3-diketones (β -diketones) and to study their pharmacological properties. Initially, the 5-chloro-2-hydroxy-4-methylacetophenone (2) was prepared by an acetylation of p-chloro-m-cresol (a) followed by Fries rearrangement of p-chloro-m-cresyl acetate (1) with anhydrous AlCl_3 . Then 2-benzoyloxyacetophenones (3a-d) were synthesized by condensation of 5-chloro-2-hydroxy-4-methylacetophenone (2) with appropriate aromatic carboxylic acids in pyridine using POCl_3 . The required starting materials were prepared via Baker-Venkatarman transformation (BVT) wherein 2-benzoyloxyacetophenones (3a-d) were treated with base (KOH /pyridine) to form β -diketones namely 1-(5'-Chloro-2'-hydroxy-4'-methylphenyl)-3-(substituted phenyl) propane-1,3-diones (4a-d)²¹. In this, all the synthesized diketones containing p-chloro-m-cresol moiety on dehydrative cyclization in glacial acetic acid and H_2SO_4 to yield the titled compounds (5a-d). The success of the synthesis and constitutions of synthesized compounds have been confirmed through their melting point, TLC, elemental analysis, IR, ^1H NMR and Mass spectral studies. Moreover, they have been evaluated for their antimicrobial, antioxidant and anti-inflammatory properties by known literature methods.

MATERIALS AND METHODS

All the chemicals used were of synthetic grade. Melting points were taken in open glass capillaries and were uncorrected. All the compounds were purified by recrystallization and their purity was monitored by TLC using Silica gel (G) plates. Elemental analyses were carried out with a Thermo Scientific (Model FLASH 2000) instrument. IR spectra were recorded on Shimadzu (Model IR Afinity-1CE) spectrophotometer using KBr pellets. A Bruker (Model Avance Neo) FTNMR 500 MHz spectrometer was used to acquire ^1H NMR spectra with DMSO-d_6 as the solvent and TMS as an internal fashionable. Meanwhile, mass spectra were recorded on Waters Micromass (Model Alliance 2795 Q-TOF) spectrometer.

General procedure for the synthesis of flavone derivatives (5a-d)²²

To a solution of 1-(5'-Chloro-2'-hydroxy-4'-methylphenyl)-3-(substituted phenyl) propane-1,3-diones (4a-d) (0.025 M) in glacial acetic acid (30 ml), sulphuric acid (5 ml) was added. The content of reaction mixture was refluxed on water bath for 2 hr followed with occasional stirring. The reaction mixture was allowed to cooled at room temperature and poured into crushed ice to precipitate the product. The separated product was filtered, washed with water followed by sodium hydrogen carbonate (10%) solution and then with sufficient cold water until the washings were neutral to litmus. The dried product was recrystallized from hot ethanol to get shiny yellow crystals of flavones (5a-d) as desired products (Figure-1).



Where, 4a, 5a : $\text{R}_1 = \text{NO}_2$; $\text{R}_2 = \text{H}$ 4c, 5c : $\text{R}_1 = \text{Cl}$; $\text{R}_2 = \text{H}$
 4b, 5b : $\text{R}_1 = \text{Br}$; $\text{R}_2 = \text{H}$ 4d, 5d : $\text{R}_1 = \text{Cl}$; $\text{R}_2 = \text{Cl}$

Figure-1: Scheme for the synthesis of the flavone derivatives (5a-d)

Pharmacological Evaluation
 Antimicrobial activity

All the newly synthesized flavones (5a-d) were screened for their *in vitro* antimicrobial sensitivity against *Escherichia coli* (gram -ve), *Staphylococcus aureus* (gram +ve) bacterial strains and *Aspergillus niger*, *Candida albicans* fungal strains by disc diffusion method²²⁻²⁵. Mueller-Hinton agar (MHA) and Potato Dextrose agar (PDA) plates were employed as culture medium respectively for bacterial and fungal sensitivity and DMSO was used as solvent control. Ofloxacin and amphotericin were used as standard drugs for antibacterial and antifungal activities respectively. The compounds were dissolved in DMSO to give 100 µg/ml, 250 µg/ml, 500 µg/ml solutions. Sterile filter paper discs (Whatmann filter paper No. 40) of 10 mm diameter were dipped in these solutions, dried, and placed on nutrient agar plates spreaded with the bacteria and fungi. The plates were further incubated for 24 hr at 37 °C for antibacterial and 72 hr at 28 °C for antifungal testing and the zones of inhibition were measured in mm using antibiotic zone reader (Hi-Media).

Antioxidant activity

The *in vitro* antioxidant activity of synthesized compounds was performed based on DPPH radical-scavenging assay with free radical scavenging effect of the stable 2, 2-diphenyl-1-picrylhydrazyl (DPPH) with slight modifications²⁶⁻²⁹. A stock solution of DPPH (1.3 mg/ml) was prepared by dissolving 13.0 mg in 10 ml of methanol. The stock solutions of test compounds (5a-d) (100 µg/ml) were prepared and further diluted to prepare solutions of various concentrations (10, 20, 30, 40 and 50 µg/ml). Similarly, a stock solution of standard ascorbic acid (1 mg/ml) was prepared by dissolving 10 mg ascorbic acid in 10 ml of methanol. From this stock solution further dilutions of various concentrations (10, 20, 30, 40, and 50 µg/ml) were prepared. Further, 1 ml of DPPH solution was mixed with 1 ml of different concentration of test solutions and standard (ascorbic acid). These solutions were kept for 30 min in dark and absorbance was measured at 517 nm using methanol (5 ml) with DPPH solution (1 ml) as blank (positive control). The percentage of scavenging activity was calculated by following formula:

$$\% \text{ Scavenging} = [\text{Abs. of control} - \text{Abs. of test sample} / \text{Abs. of control}] \times 100$$

Anti-Inflammatory activity

The *in vitro* anti-inflammatory activity of synthesized compounds was performed by employing inhibition of protein denaturation assay³⁰. Stock solution of NSAID ibuprofen as a reference drug (positive control) was prepared by dissolving 10 mg of ibuprofen in 10 ml of distilled water. Serial dilution from above stock solution takes 0.1 ml, 0.2 ml, 0.3 ml, 0.4 ml, 0.5 ml and prepare 10 ppm, 20 ppm, 30 ppm, 40 ppm, 50 ppm and also it was performed for four sample extract (5a-d). All samples contain 5 ml of total volume. Reaction mixtures were prepared using 2.8 ml of phosphate-buffered saline (pH 6.4) and 0.2 ml of egg albumin. Then take 2 ml of extract from each different concentration were mixed gently with reaction mixtures. A similar procedure was used for reference drug ibuprofen. The absorbance of these solutions was determined by spectrophotometer at wavelength of 660 nm. The percentage inhibition of protein denaturation was calculated by following formula:

$$\% \text{ Inhibition} = [\text{Abs. of blank} - \text{Abs. of test sample} / \text{Abs. of blank}] \times 100$$

RESULTS AND DISCUSSION

Spectral data analysis

The structures of all the newly synthesized flavones (5a-d) were characterized on the basis of melting point, TLC, elemental analysis, IR, ¹H NMR and Mass spectral studies. The IR, ¹H NMR spectra showed expected signals corresponding to various groups present in each of the compounds. The mass spectrum of all the compounds were found to in full agreement with the proposed structures and showed expected peaks which confirms the molecular weights of compounds. The spectral and physical data (Table-1) of all the compounds are shown below:

(5a): 2-(4'-Nitrophenyl)-6-chloro-7-methyl-4*H*-chromen-4-one: IR (cm⁻¹, KBr): 3085 [C-H stretch (aromatic)], 2930 [C-H stretch in -CH₃ (aliphatic)], 1647 (C=O stretch), 1525 [C=C stretch (aromatic)], 1431 [-NO₂ stretch (asym.)], 1345 [-NO₂ stretch (sym.)], 1247 (C-O stretch), 655-691 (C-Cl stretch); ¹H NMR (DMSO-d₆/500 MHz): δ 2.5 ppm (s, 3H of -CH₃), δ 3.38 ppm (s, 1H of -C=CH- of flavone), δ 7.9-8.4 ppm (m, 6H of Ar-H); MS (m/z): 316.04(M⁺).

(5b): 2-(4'-Bromophenyl)-6-chloro-7-methyl-4*H*-chromen-4-one: IR (cm⁻¹, KBr): 3046 [C-H stretch (aromatic)], 2924 [C-H stretch in -CH₃ (aliphatic)], 1632 (C=O stretch), 1434 [C=C stretch (aromatic)], 1244 (C-O stretch), 648 (C-Br stretch); ¹H NMR (DMSO-d₆/ 500 MHz): δ 2.5 ppm (s, 3H of -CH₃), δ 3.4 ppm (s, 1H of -C=CH- of flavone ring), δ 7.8-8.1 (m, 6H of Ar-H); MS (m/z): 348.96/350.96 (M⁺).

(5c): 2-(4'-Chlorophenyl)-6-chloro-7-methyl-4*H*-chromen-4-one: IR (cm⁻¹, KBr): 3043 [C-H stretch (aromatic)], 2922 [C-H stretch in -CH₃ (aliphatic)], 1724 (C=O stretch), 1438 [C=C stretch (aromatic)], 1254 (C-O stretch), 725 (C-Cl stretch); ¹H NMR (DMSO-d₆/ 500 MHz): δ 2.5 ppm (s, 3H of -CH₃), δ 3.4 ppm (s, 1H of -C=CH- of flavone ring), δ 7.6-8.1 ppm (m, 6H of Ar-H); MS (m/z): 305.02 (M⁺).

(5d): 2-(2',4'-Dichlorophenyl)-6-chloro-7-methyl-4*H*-chromen-4-one: IR (cm⁻¹, KBr): 3284 [C-H stretch (aromatic)], 2928 [C-H stretch in -CH₃ (aliphatic)], 1635 (C=O stretch), 1427 [C=C stretch (aromatic)], 1103 (C-O stretch), 628 (C-Cl stretch); ¹H NMR (DMSO-d₆/ 500 MHz): δ 2.5 ppm (s, 3H of -CH₃), δ 3.34 ppm (s, 1H of -C=CH- of flavone ring), δ 7.0-8.1 (m, 5H of Ar-H); MS (m/z): 338.99 (M⁺).

Table-1: Physical and analytical data of synthesized substituted flavones (5a-d)

Compound code	Molecular Formula	Mol.wt (g/mol)	m.p. (°C)	% Analysis: Found (Calcd.)			Yield (%)	Rf value
				C	H	Cl		
5a	C ₁₆ H ₁₀ ClNO ₂	315.71	160-162	61.08 (60.87)	3.06 (3.19)	11.30 (11.23)	80	0.64
5b	C ₁₆ H ₁₀ BrClO ₂	349.61	166-169	55.29 (54.97)	2.79 (2.88)	(9.86) (10.14)	78	0.68
5c	C ₁₆ H ₁₀ Cl ₂ O ₂	305.16	156-158	63.67 (62.97)	3.79 (3.30)	21.99 (23.24)	88	0.70
5d	C ₁₆ H ₉ Cl ₃ O ₂	339.60	170-172	56.77 (56.59)	2.81 (2.67)	(31.16) (31.32)	92	0.69

Pharmacological activity

The antibacterial and antifungal activities of all the newly synthesized compounds were examined *in vitro* tests. The resulting data on antimicrobial activities are depicted in Table-2 and Table-3. They were further subjected for their *in vitro* antioxidant and anti-inflammatory activity whose results are summarized respectively in Table-4 and Table-5 and also shown in Figure-2 and Figure-3 statistically.

Table-2: Antibacterial activity of newly synthesized flavone derivatives (5a-d)

Compound code	Zone of inhibition in mm							
	<i>Escherichia coli</i> (Gram -ve)				<i>Staphylococcus aureus</i> (Gram +ve)			
	Concentration of compounds (µg/ml)				Concentration of compounds (µg/ml)			
	100	250	500	Std.	100	250	500	Std.
5a	NI	NI	NI	20 mm	NI	NI	NI	22 mm
5b	NI	NI	NI		NI	NI	NI	

5c	NI	NI	NI		NI	NI	NI	
5d	10 mm	12 mm	14 mm		10 mm	11 mm	12 mm	
Control	NI	NI	NI		NI	NI	NI	

Note: Standard: Ofloxacin (2 µg/ml); (NI): No Zone of Inhibition; Control: DMSO solvent

Table-3: Antifungal activity of newly synthesized flavone derivatives (5a-d)

Compound code	Zone of inhibition in mm							
	<i>Aspergillus niger</i>				<i>Candida albicans</i>			
	Concentration of compounds (µg/ml)				Concentration of compounds (µg/ml)			
	100	250	500	Std.	100	250	500	Std.
5a	NI	NI	NI	15 mm	NI	NI	NI	14 mm
5b	NI	NI	NI		NI	11 mm	12 mm	
5c	NI	10 mm	11 mm		NI	10 mm	11 mm	
5d	NI	NI	NI		NI	11 mm	12 mm	
Control	NI	NI	NI		NI	NI	NI	

Note: Standard: Amphotericin (50 µg/ml); (NI): No Zone of Inhibition; Control: DMSO solvent

According to the obtained results, compounds 5a, 5b and 5c showed zero zones of inhibition at all the tested concentrations and were found to be inactive against *E. coli* and *S. aureus* while compound 5d showed 10, 12, 14 mm and 10, 11, 12 mm zones of inhibition respectively at 100 µg/ml, 250 µg/ml and 500 µg/ml against *E. coli* and *S. aureus* organisms. Standard ofloxacin (2 µg/ml) showed 20 mm and 22 mm zones of inhibition respectively against bacteria *E. coli* and *S. aureus*. In case of antifungal sensitivity, compounds 5a, 5b and 5d showed no zones of inhibition at all the concentrations and were found to be inactive against *A. niger*, while compound 5c showed 10 and 11mm of zone at 250 µg/ml and 500 µg/ml concentrations respectively against *A. niger*. Standard amphotericin (50 µg/ml) showed 15 mm of zone against *A. niger*. As far as fungus *C. albicans* is concern, compound 5b, 5c, 5d were found to show 11, 12; 10, 11; and 11, 12 mm of zones of inhibition at 250 µg/ml and 500 µg/ml concentrations respectively whereas compound 5a was found to be inactive against *C. albicans* at all the tested concentrations when compared with std. amphotericin drug which showed 14 mm of zone against *C. albicans*.

Table-4: Antioxidant activity of newly synthesized flavone derivatives (5a-d)

Compd. code	% Scavenging of synthesized compounds (5a-d) and std. Ascorbic acid				
	10 µg/ml	20 µg/ml	30 µg/ml	40 µg/ml	50 µg/ml
5a	39.69	45.17	59.42	68.34	79.76
5b	19.51	23.46	24.78	30.33	38.56
5c	26.97	35.96	46.92	60.22	75.09
5d	21.05	35.96	36.84	59.70	71.00
Standard	80.26	91.22	95.61	96.27	97.80

Table-5: Anti-inflammatory activity of newly synthesized flavone derivatives (5a-d)

Compd. code	% Inhibition of synthesized compounds (5a-d) and std. Ibuprofen drug				
	10 µg/ml	20 µg/ml	30 µg/ml	40 µg/ml	50 µg/ml
5a	31.51	59.71	66.72	76.85	85.43
5b	51.65	52.81	54.30	59.95	67.76
5c	39.18	40.17	53.09	60.41	74.38
5d	47.67	52.81	66.39	73.11	81.67
Standard	87.36	88.90	90.23	91.74	93.10

The experimental data on antioxidant activities (Table-4) reveals that, compounds 5a, 5c and 5d showed good scavenging activity while compound 5b showed mild scavenging activity with reference to std. ascorbic acid. Also, one thing is noted that, as the concentration of test compounds increases, their percentage of scavenging also increases. In case of anti-inflammatory activities, we observed that, compounds 5a and 5d showed excellent inhibition to protein denaturation as compared to compound 5b and 5c which showed moderate to good inhibition to protein denaturation with comparison to std. NSAID ibuprofen drug.

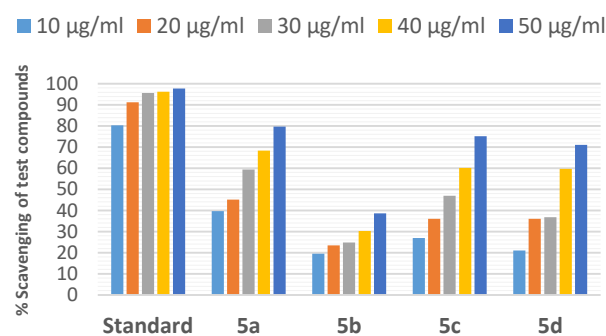


Figure-2: Graph showing percentage of scavenging of test compounds (5a-d)

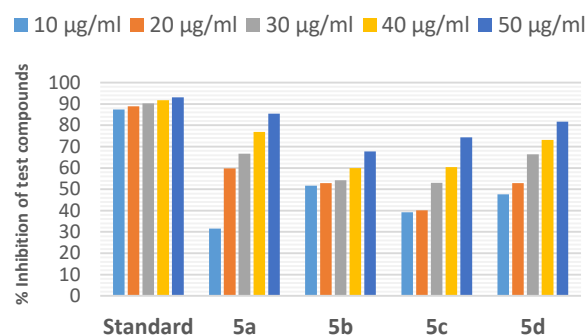


Figure-3: Graph showing percentage of inhibition of test compounds (5a-d)

CONCLUSION

In conclusion, a total four novel flavones viz. 2-(substituted phenyl)-6-chloro-7-methyl-4*H*-chromen-4-one (5a-d) were successfully synthesized by dehydrative cyclization of β -diketones bearing moiety of p-chloro-m-cresol and characterized by spectral studies. All the synthesized compounds were evaluated for their antimicrobial, antioxidant and anti-inflammatory potential *in vitro*. From the results, it was clear that, only the compound 5d was moderately active while compounds 5a, 5b and 5c were found to be inactive against *E. coli* and *S. aureus* as compared to std. antibiotic ofloxacin. Also, it was found that, only the compound 5c was moderately active against *A. niger* while compounds 5a, 5b, 5d do not shown inhibitory action and were found to inactive against *A. niger* when compared with std. amphotericin drug. As far as *C. albicans* is concern, instead of compound 5a, the compounds 5b, 5c, and 5d were found to show moderate to good inhibitory action to growth response of fungus *C. albicans*. The results on antioxidant and anti-inflammatory activities reveals that, among the newer derivatives, compounds 5a, 5c, 5d showed a promising antioxidant activity as well as all the compounds showed notable and excellent anti-inflammatory activities with comparison to std. reference drugs. It is conceivable that these newly synthesized flavones showing *in vitro* scavenging and protein denaturation activity can be further modified to achieve marketable antioxidant and NSAID agents.

ACKNOWLEDGEMENTS

The authors are thankful to Principal, Vidya Bharati Mahavidyalaya, Amravati for providing expensive laboratory facilities. The authors are also grateful to Prof. Dr. S. L. Deore, Govt. College of Pharmacy, Amravati and SAIF, Panjab University, Chandigarh for their help.

REFERENCES

1. Abualhasan, M., Jaradat, N., Al-Rimawi, F., Shahwan, M., Mansour, D., Alhend, Z., Alsoroghli, Y., Mousa, A., *Food Sci. Technol.*, Campinas, 2022, 42, e57122, 1-7.
2. Jayashree, B., Alam, A., Nayak, Y., Kumar, D. V., *Med. Chem. Res.*, 2012, 21 (8), 1991-1996.
3. Cushnie, T.P.T., Lamb, A.J., *Int. J. Antimicrob. Agents*, 2005, 26, 343-356.
4. Wu, J., Wang, X., Yi, Y., Lee, K., *Bioorg. Med. Chem. Lett.*, 2003, 13, 1813-1815.
5. Kunimasa, K., Kuranuki, S., Matsuura, N., Iwasaki, N., Ikeda, M., Ito, A., Sashida, Y., Minaki, Y., Yano, M., Sato, M., Igarashi, Y., Oikawa, T., *Bioorg. Med. Chem. Lett.*, 2009, 19 (7), 2062-2064.
6. Kim, J.Y., Lim H.J., Ryu, J.-H., *Bioorg. Med. Chem. Lett.*, 2008, 18(4), 1511-1514.
7. Mateeva, N., Gangapuram, M., Mazzio, E., Eyunni, S., Soliman, K. F., Redda, K. K., *Med. Chem. Res.*, 2015, 24(4), 1672-1680.
8. Venkatachalam, H., Nayak, Y., Jayashree, B. S., *APCBEE Procedia*, 2012, 3, 209-213.
9. Kaur, R., Kaur, K., Bansal, M., *Asian J. Chem.*, 2016, 28(9), 1921-1924.
10. Liu, Y.-T., Lu, B.-N., Peng, J.-Y., *Food Chem.*, 2011, 125(2), 719-725.
11. Wang, X.-B., Liu, W., Yang, L., Guo, Q.-L., Kong, L.-Y., *Med. Chem. Res.*, 2012, 21(8), 1833-1849.
12. Lin, Y.-M., Zhou, Y., Flavin, M. T., Zhou, L.-M., Nie, W., Chen, F.-C., *Bioorg. Med. Chem.*, 2002, 10(8), 2795-2802.
13. Cardenas, M., Marder, M., Blank, V.C., Roguin, L.P., *Bioorg. Med. Chem.*, 2006, 14 (9), 2966-2971.
14. Auffret, G., Labaied, M., Frappier, F., Rasoanaivo, P., Grellier, P., Lewin, G., *Bioorg. Med. Chem. Lett.*, 2007, 17, 959-963.
15. Pinto, J., Silva, V.L.M., Silva, A.M.G., Silva, A.M.S., *Molecules*, 2015, 20(6), 11418-11431.
16. Chang, M.-Y., Tsai, M.-C., Lin, C.-Y., *RSC Adv.*, 2021, 11, 11655-11662.
17. Bansal, M., Kaur, K., Tomar, J., Kaur, L., *Biomed. J. Sci. Tech. Res.*, 2017, 1(6), 1752-1755.
18. Motghare, A.P., Katolkar, P.P., Chacherkar, P.A., Baheti, J.R., *Asian J. Pharm. Clin. Res.*, 2022, 15(7), 25-34.
19. Pinto, J., Silva, V.L.M., Silva, A.M.G., Silva, A.M.S., *Molecules*, 2015, 20(6), 11418-11431.
20. Doan, T.N., Tran, D.T., *Pharmaco. Pharma.*, 2011, 2(4), 282-288.
21. Pagariya, S.K., Bodkhe, P.S., *Int. J. Curr. Engg. Sci. Res.*, 2019, 6(1), 746-750.
22. Binani, S., Nagamalla, L., Bodkhe, P.S., Joat, R.V., *Int. J. Sci. Engg. Manag.*, 2018, 3(2), 6-9.
23. World Health Organization Expert Committee on Biological Standardization, 1992. Technical report series 822.W.H.O., Geneva.
24. Vaidya, S.R., Shelke, V.A., Jadhav, S.M., Shankarwar, S.G., Chondhekar, T.K., *Archives Appl. Res.*, 2012, 4(4), 1839-1843.
25. Jayaroopa, P., Kumar, G.V., Renuka, N., Nayaka, M.A.H., Kumar, K.A., *Int. J. PharmTech Res.*, 2013, 5(2): 819-826.
26. Li, H.B., Wong, C.C., Cheng, K.W., Chen, F., *LWT-Food Sci. Technol.*, 2008, 41(3), 385-390.
27. Kamble, P., Wadher, S., *Asian J. Pharm. Clin. Res.*, 2018, 11(3), 259-268.
28. Kumar, N., Kumar, S., Gupta, H., Sharma, P.K., *World Res. J. Biochem.*, 2012, 1(1), 1-5.
29. Venkatachalam, H., Nayak, Y., Jayashree, B.S., *Int. J. Chem. Engg. Appl.*, 2012, 3 (3), 216-219.
30. Dharmadeva, S., Galgamuwa, L.S., Prasadine, C., Kumarasinghe, N., *Ayu.*, 2018, 39(4), 239-242.

Design, Synthesis, Spectral Characterisation and Antibacterial Screening of Some Novel 4- Substitutedimino-1,3,5-Dithiazine Along With Pyrimidine Nucleus

S. B. Sarkate^{a*}, S. A. Waghmare^b, K. U. Dongare^c, R. N. Ingole^d

^{a,b,c}-Department of Chemistry, Ghulam Nabi Azad Arts, Commerce and Science College Barshitakli Dist. Akola 444401 (M.S.), India.

^d-Department of Chemistry, Shri Vitthal Rukhmini College, Sawana, Mahagaon, Dist. Yavatmal, (M.S.) India

*Corresponding author- swapnilsarkate1991@gmail.com

ABSTRACT

In recent times in the laboratory, synthesis of 2-(2-Phenylimino-4- substitutedimino-1,3,5-dithiazino) aminopyrimidine (**IIIa-e**) were synthesized by refluxing 2-(5-phenyl-4-dithiobiureto) pyrimidine (**I**) with alkyl/ arylisocyanodichlorides (**IIa-e**) in acetone-ethanol medium in 1:1 molar proportion. The structures of all the synthesized compounds were acceptable on the basis of chemical characteristics, elemental analysis, spectral studies and their antibacterial screening against the gram positive and gram negative bacteria such as *S. typhi*, *E. coli*, *S. aureus*, *A. Aerogenes*, *B. Subtilis* and *B. Megatherium.etc.*

INTRODUCTION

Heterocycles containing organic molecules are more fascinating, because they are convenient in a variety of applications, a multitude of uses are included by the heterocycles' size and heteroatom diversity. These compound nitrogen, oxygen and sulphur are composed of six member¹⁻⁵, five member⁶⁻⁷ fused heterocycles with aromatic rings. Particularly noteworthy are the numerous biological and industrial uses for heterocycles that combine sulphur and nitrogen in one ring. Six member two sulphur and one nitrogen atom prepare 1,3,5-dithiazine. It is one of the six member heterocycles that functions as a strong medication in the sectors of medicine, agriculture, and industry⁹⁻⁸.

Tayade¹⁰, Pathe¹¹ and Mur¹² Synthesized numerous heterocycles containing 1,3,5-dithiazines as main nucleus. Each 1,3,5-dithiazino moiety has different applications according to the substituent attached to the basic nucleus of the 1,3,5-dithiazine. It has been also observed during literature study that, 1,3,5-dithiazino nucleus and its derivatives possesses biological and medicinal effective properties¹³⁻¹⁴. Substituted isocyanodichlorides were used by researchers to synthesise 1,3,5- dithiazines in the laboratory. This 1,3,5-dithiazine synthesis technique is quicker, less complicated, less expensive and requires less time.

MATERIAL AND METHOD

Material

All the chemical used were of loba chemie (AR grade).

Method

In the present experiment for the synthesis of different substituted 1,3,5-dithiazino

aminopyrimidine is conventional refluxing under electronic water bath for different hours for different experiment.

EXPERIMENTAL

All the chemicals used for the synthesis were purified. After refluxing the purity of the compounds were checked by TLC (aluminium TLC) with thin layer thickness of 200 μm . The melting points of all synthesized compounds will be recorded using hot paraffin bath. The carbon and hydrogen analysis were carried out on Carlo-Ebra-1106 analyser Nitrogen estimation were carried out with colmon-N-analyzer-29. IR spectra were recorded with Bruker spectrometer in the range 4000-400 cm^{-1} . PMR spectra were recorded on VARIAN 400 MHz spectrometer with TMS as internal standard using CDCl_3 and DMSO Solvent.

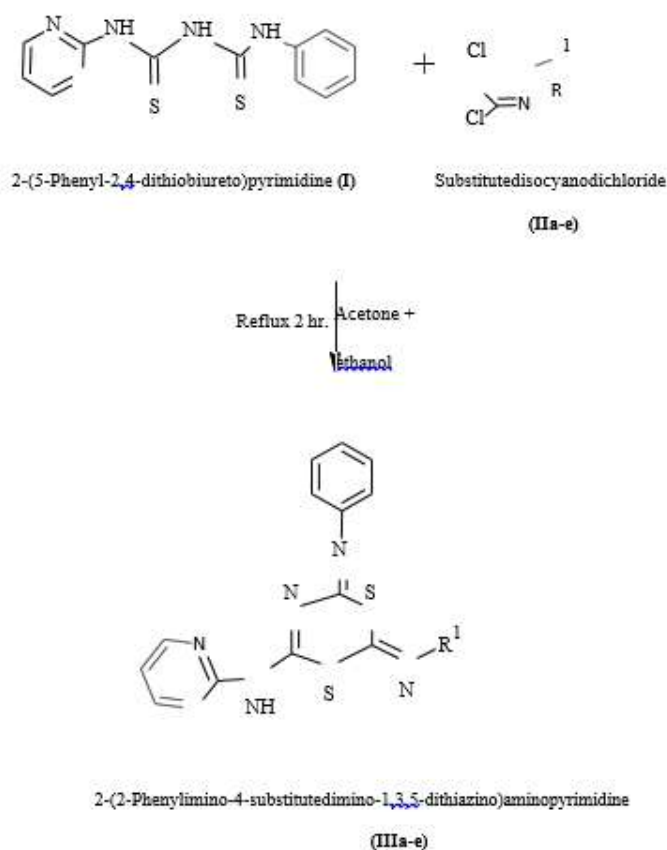
GENERAL PROCEDURE

A reaction of 2-(5-phenyl-2,4-dithiobiureto)pyrimidine (**I**) and substitutedisocyanodichloride (**IIa-e**) in 1:1 molar ratio refluxed on water bath in acetone-ethanol medium for 2 hours. The evolution of the hydrochloride gas was clearly observed during refluxion. After distillation of excess solvent orange product isolated which on basification with dilute ammonium hydroxide orange crystalline products obtained.

Similar, procedure was adopted for the synthesis of all the derivatives in the series.

The tentative reaction for the formation of product is depicted below,

Reaction



Similarly, 2-(5-phenyl-2,4-dithiobiureto)pyrimidine (**I**) were react with

phenylisocyanochloride (**IIa**), ethylisocyanodichloride (**IIb**), tertbutylisocyanodichloride (**IIc**), P-tolylisocyanodichloride (**IId**) and 4-chlorophenylisocyanodichloride (**IIe**) by the above mentioned method to isolate 2-[2,4-di(phenylimino)-1,3,5-dithiazino] aminopyrimidine (**IIIa**), 2-(2-phenylimino-4-ethylimino-1,3,5-dithiazino) aminopyrimidine (**IIIb**), 2-(2-phenylimino-4-tert-butylimino-1,3,5-dithiazino) aminopyrimidine (**IIIc**), 2-[2-phenylimino-4-(4-methylphenylimino)-1,3,5-dithiazino]aminopyrimidine (**IIId**) and 2-[2-phenylimino-4-(4-chlorophenylimino)-1,3,5-dithiazino]aminopyrimidine (**IIIe**).

RESULT AND DISCUSSION

Spectral characterization results for all the synthesized compounds are given below

Spectral Characterization

1. 2-(2,4-diphenylimino-1,3,5-dithiazino)aminopyrimidine (**IIIa**)

Colour-Yellow solid, **Molecular formula**- $C_{15}H_{14}N_6S_2$, **Yield** 85%, **M.P.** 162°C, % **Composition found (calculated)** C-52.90, H-4.83, N-25.20, S-23.21, **FTIR (KBr) vcm**- 3245.22 N-H stretching, 3051.47 (C-H Ar Stretching), 3187.38 (N-H Amido), 1950.37 (C-H Ar Bending), 1185.99 (C=S Stretching), 670.04(=C-H bending); **¹H NMR (400MHz CDCl₃ δ ppm)**, 8.4ppm (2H, double, CH) of pyrimidine, 7.2ppm (2H, CH, doublet) of pyrimidine, 7.2 ppm (2H, , doublet CH) of phenyl, 3.4 ppm (1H, singlet NH), 4.6 ppm 1H singlet, 7.39 1H triplet CH benzene, 1H triplet CH benzene

2.2 ppm 2H quartet, 2.3 ppm 3H triplet **Mass m/z** 390.30

2. 2-(2-phenylimino-4-ethylimino-1,3,5-dithiazino)aminopyrimidine (**IIIb**)

Colour-Yellow solid, **Molecular formula**- $C_{15}H_{14}N_6S_2$, **Yield** 86%, **M.P.** 170°C, % **Composition found (calculated)** C-52.90, H-4.83, N-25.20, S-23.21, **FTIR (KBr) vcm**- 3245.22 N-H stretching, 3051.47 (C-H Ar Stretching), 3187.38 (N-H Amido), 1950.37 (C-H Ar Bending), 1185.99 (C=S Stretching), 670.04(=C-H bending); **¹H NMR (400MHz CDCl₃ δ ppm)**, 8.4ppm (2H, double, CH) of pyrimidine, 7.2ppm (2H, CH, doublet), 7.2 ppm (2H, , doublet CH) of phenyl, 3.4 ppm (1H, singlet NH),

4.6 ppm 1H singlet, 7.39 1H triplet CH benzene, 1H triplet CH benzene 2.2 ppm 2H quartet, 2.3 ppm 3H triplet **Mass m/z** 342.30

3. 2-(2-phenylimino-4-tertbutylimino-1,3,5-dithiazino)aminopyrimidine (**IIIc**)

Colour-Yellow solid, **Molecular formula**- $C_{17}H_{18}N_6S_2$, **Yield** 90%, **M.P.** 158°C, % **Composition found (calculated)** C-55.90, H-4.83, N-23.20, S-17.21, **FTIR (KBr) vcm**- 3245.22 N-H stretching, 3045.47 (C-H Ar Stretching), 3140.38 (N-H Amido), 1995.37 (C-H Ar Bending), 1164.99 (C=S Stretching), 710.04(=C-H bending); **¹H NMR (400MHz CDCl₃ δ ppm)**, 8.2ppm (2H, double, CH), 7.2ppm (2H, CH, doublet), 7.1ppm (2H, , doublet CH), 3.5 ppm (1H, singlet NH), 4.5 ppm 1H singlet,

7.40 1H triplet CH benzene, 2.4 9H singlet **Mass m/z** 370.50

4. 2-(2-phenylimino-4-tolylimino-1,3,5-dithiazino)aminopyrimidine (**IIId**)

Colour-Yellow solid, **Molecular formula**- $C_{20}H_{16}N_6S_2$, **Yield** 82%, **M.P.** 167°C, % **Composition found (calculated)** C-55.90, H-4.83, N-23.20, S-15.21, **FTIR (KBr) vcm**- 3200.22 N-H stretching, 2901.47 (C-H Ar Stretching), 3160.38 (N-H Amido), 1960.37 (C-H Ar Bending), 1167.99 (C=S Stretching), 745.04(=C-H bending); **¹H NMR (400MHz CDCl₃ δ ppm)**, 8.2 ppm (2H, double, CH) of pyrimidine, 7.3ppm (2H, CH, doublet), 7.2 ppm (2H, , doublet CH), 3.5 ppm (1H, singlet NH), 4.7 ppm 1H singlet, 7.39 1H triplet CH benzene, 3.4 ppm 3H singlet. **Mass m/z** 404.60

5. 2-(2-phenylimino-4-p-chlorophenylimino-1,3,5-dithiazino)aminopyrimidine (IIIe)

Colour-Yellow solid, **Molecular formula**- C₁₉H₁₃N₆S₂, **Yield** 80%, **M.P.** 145°C, % **Composition found (calculated)** C-53.90, H-3.83, N-20.20, S-15.21Cl-8.45, **FTIR (KBr)** vcm- 3263.22 N-H stretching, 3051.47 (C-H Ar Stretching), 3216.38 (N-H Amido), 1966.37 (C-H Ar Bending), 1165.99 (C=S Stretching), 720.04(=C-H bending); **¹H NMR (400MHz CDCl₃ δ ppm)**, 8.4 ppm (2H, double, CH) of pyrimidine, 7.03ppm (2H, CH, doublet), 7.4 ppm (2H, , doublet CH), 3.5 ppm (1H, singlet NH), 4.6 ppm 1H singlet, 7.39 1H triplet CH benzene, **Mass m/z** 424.80.

CONCLUSION

In the present work is cheaper and less time consuming method for synthesis of organic compound (IIIa-e). In all the synthesized compounds give the maximum yield of product (III a-e). A variety of pyrimidine based 1,3,5-dithiazine derivative can be synthesized for their antimicrobial activities adopting the method.

PHARMACOLOGICAL STUDIES

Antimicrobial activity

All the synthesized compounds (III-a) to (III-e) were screened for antibacterial activity against *S. typhi*, *E. coli*, *S. aureus*, *A. Aerogenes*, *B. Subtilis* and *B. Megatherium*. by disc diffusion method was performed using mueller hinton agar as well as nutrient agar medium. Each and every compound was tested at conc. 50 µg/ml in ethanol. The zone of inhibition of all the synthesized compounds were measured after 24 hour incubation at 37 °C. Standard drug used for comparison the activity was Ciprofloxacin.

Table 1: Synthesized compound IIIa-e activity against Gram +ve and Gram -ve bacteria

Table No. 1.1 - Antibacterial activity of synthesized compound against bacteria (Zone of inhibition in mm) (after 24 hrs at 37 °C temp)							
SR No.	Compd.	Gram positive			Gram negative		
		<i>S. aureus</i>	<i>B. subtilis</i>	<i>B. megatherium</i>	<i>S. typhi</i>	<i>E. coli</i>	<i>A. aerogenes</i>
1	SBS-IIIa	18	12	16	14	18	11
2	SBS-IIIb	11	12	14	14	11	12
3	SBS-IIIc	11	11	12	11	11	11
4	SBS-IIId	10	12	12	12	11	11
5	SBS-IIIE	14	12	14	12	16	12
6	Std Ciprofloxacin	18	16	20	18	20	14

REFERENCE

1. Zhang, D. H., Zhang, Z., & Shi, M. (2012). Transition metal-catalyzed carbocyclization of nitrogen and oxygen-tethered 1, n-enynes and diynes: synthesis of five or six-membered heterocyclic compounds. *Chemical Communications*, 48(83), 10271-10279.
2. Larrosa, I., Romea, P., & Urpí, F. (2008). Synthesis of six-membered oxygenated heterocycles through carbon-oxygen bond-forming reactions. *Tetrahedron*, 64(12), 2683-2724.
3. Sanu, M. C., Joseph, J., Chacko, D., Vinod, B., & Daisy P., A. (2021). Review on six membered nitrogen containing heterocyclic compounds with various biological activities. *International Journal of Pharmaceutical Sciences Review and Research*, 69(2), 64-68.
4. Walton, J. C. (2016). Synthetic strategies for 5-and 6-membered ring azaheterocycles facilitated by iminyl radicals. *Molecules*, 21(5), 660.
5. Huh, D. N., Cheng, Y., Frye, C. W., Egger, D. T., & Tonks, I. A. (2021). Multicomponent syntheses of 5-and 6-membered aromatic heterocycles using group 4–8 transition metal catalysts. *Chemical Science*, 12(28), 9574-9590.
6. Sergey P., Vladimir N., Andrey, E., & A. Pimerzin, E. Vishnevskaya E., Thermodynamic analysis of strain in the five-membered oxygen and nitrogen heterocyclic compounds. *The Journal of Physical Chemistry*, 115(10), 1992–2004.
7. Kaur, N., Yadav, N., & Verma, Y. (2023). Acetamidine in heterocycle synthesis. *Synthetic Communications*, 53(9), 577-614.
8. Gujjar, K. N., & Narasimha S M., (2023). A Review: Important applications of Heterocyclic Compounds. *Europeam Chemical Bulletin*, 12(12), 625-630.
9. Sharma, P. K., Amin, A., & Kumar, M. (2020). A review: Medicinally important nitrogen sulphur containing heterocycles. *The Open Medicinal Chemistry Journal*, 14(1), 49-64.
10. Tayade, D. T., & Padhen, S. S. (2016). Synthesis and Characterization of 1-Phenyl-3- [4-(2- Substitutedimino-4-Substitutedimino-1,3,5-Dithiazino) Aminophenyl]- Prop-2-Ene-1-Ones. *International Journal of Pharmacy and Pharmaceutical Research*, 7 (1), 53-58.
11. Pathe, P. P., & Paranjpe, M. G. (1984). Preparation of 5-aryl-4- arylimino-6-benzylimino-2- phenylimino-1,3,5-dithiazine. *Indian chemical society*, 15(43), 149-150.
12. Mur, V. I. (1964). 2, 4, 6-trichloro-1, 3, 5-triazine (cyanuryl chloride) and its future applications. *Russian Chemical Reviews*, 33(2), 92-103.
13. Panpaliya, K. S., Tayade, D. T., Shaikh, R. S., & Thakare, A. N. (2017). Synthesis of 1-phenyl-3-substituted- 2,6-dithio-4- amino-[(2- phenylthiocarbamido)- 1,3-benzothiazolo] -1,3,5-triazine and their effects on germination pattern of sorghum vulgare. *Online International Interdisciplinary Research Journal*, 1, 6-9.
14. Deohate, P. P., & Berad, B. N. (2005). Synthesis and antimicrobial activity of 1, 3, 5-thiadiazines and their isomerism into 1, 3, 5-triazines. *Indian journal of Chemistry*, 44B, 638-642.

Colorimetric Phytochemical Analysis of *Tinospora Cordifolia* and FTIR Study of Its Medicinal Sample Giloy Ghanvati

Dr Swaroopa Rani N. Gupta

Professor, Department of Chemistry

Brijlal Biyani Science College, Amravati, Maharashtra India

swargupta@yahoo.com

ABSTRACT

Tinospora cordifolia (common names gurjo, heart-leaved moonseed, guduchi or giloy) is a herbaceous vine of the family Menispermaceae indigenous to tropical regions of the Indian subcontinent. It has been used in Ayurveda to treat various disorders. *Tinospora cordifolia* contains diverse phytochemicals, including alkaloids, phytosterols, glycosides, tinosporide, and other mixed chemical compounds. During the 2020-22 COVID-19 outbreak in India, the Ministry of AYUSH recommended use of Giloy as a home remedy for immune support. Giloy extract was assessed for its phytochemical and antibacterial properties, to find out the bioactive components responsible for such activity.

In Ayurveda, it is said to be the best rejuvenating herb. Acute toxicity studies of aqueous extract of Guduchi reports that it does not produce any toxic effect. The medicinal herb has to be used in an appropriate dose as prescribed by a qualified physician to get medicinal effects. With the wide range of actions and abundant components, Guduchi is a real treasure among herbal drug source. Medicinal applications of Guduchi in countering various disorders and its use as anti-oxidant, anti-hyperglycemic, anti-hyperlipidemic, hepatoprotective, cardiovascular protective, neuroprotective, osteoprotective, radioprotective, anti-anxiety, adaptogenic, analgesic, anti-inflammatory, anti-pyretic, anti-diarrheal, anti-ulcer, anti-microbial, and anti-cancer have been well established.

Present study deals with Colorimetric phytochemical analysis of *Tinospora Cordifolia* (Giloy leaf extract) and FTIR study of its medicinal sample Giloy Ghanvati. Colorimetric phytochemical analysis of *Tinospora Cordifolia* (Giloy leaf extract) involves preparation of standard Giloy Ghanvati solution, Ferric Chloride solution and Giloy leaf Solution. Different systems were prepared. Absorbance of standard Giloy solution was taken at different wavelength. And λ_{max} was calculated. Which was 420 nm. Absorbance of standard Giloy solution of different concentrations were taken at 420 nm and Calibration plot was prepared. Then absorbance of Giloy leaf solutions were taken at 420 nm and concentration of Giloy in Giloy leaf was calculated from calibration plot. *Tinospora cordifolia* which contains diverse phytochemicals, including alkaloids, phytosterols, glycosides, tinosporide, and other mixed chemical compounds reduces ferric ions and production of violet coloration by addition of ferric chloride to dilute solution of Giloy takes place and the concentration of Giloy was investigated colorimetrically. The method is simple, rapid and precise. Interpretation of FTIR Spectra of Giloy Ghanvati medicinal sample shows presence of various functional groups such as O-H stretching - Alcohol, Carboxylic acid, O-H bending - Alcohol, N-H stretching - Amine salt, C=C stretching - α , β - unsaturated ketone and C=O stretching - Conjugated acid.

Keywords: *Tinospora cordifolia*, Giloy, Giloy ghanvati, Colorimetric Phytochemical Analysis, FTIR study

INTRODUCTION

Giloy

Tinospora cordifolia (common names gurjo, heart-leaved moonseed, guduchi or giloy) is a herbaceous vine of the family Menispermaceae indigenous to tropical regions of the Indian subcontinent. It has been used in Ayurveda to treat various disorders, but in spite of clinical investigation, the effectiveness of such treatments remains uncertain. [1] Reddish fruits of *Tinospora cordifolia* is a large, deciduous, extensively-spreading, climbing vine with several elongated twining branches.

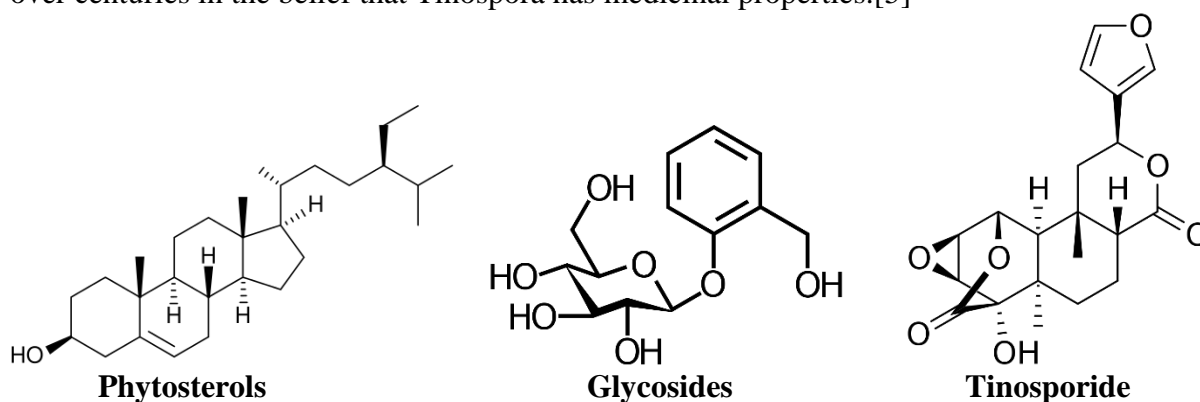


Leaves of *Tinospora cordifolia*



Fruits of *Tinospora cordifolia*

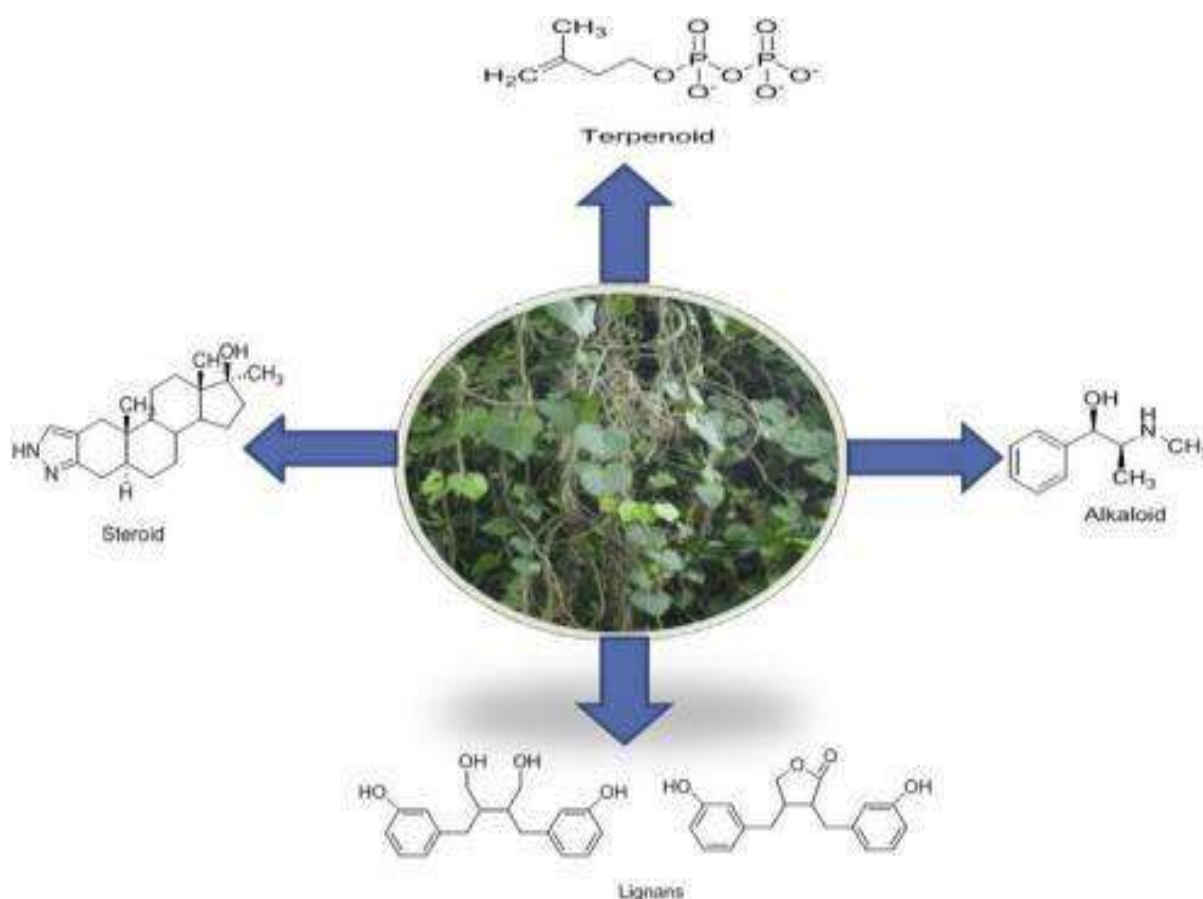
Endophytic fungi colonize the living, internal tissues of their host without causing any harmful effects. A recent study has shown that 29 endophytes belonging to different taxa were present in the samples collected from *Tinospora cordifolia*. [2] Extracts of the endophytic fungus *Nigrospora sphaerica* obtained from *T. cordifolia* were found to have insecticidal properties against the Oriental leafworm moth (*Spodoptera litura*), a polyphagous pest. [3] *Tinospora cordifolia* contains diverse phytochemicals, including alkaloids (Alkaloids are a class of basic, naturally occurring organic compounds that contain at least one nitrogen atom), phytosterols, glycosides, tinosporide, [4] and other mixed chemical compounds. Although used in Ayurveda over centuries in the belief that *Tinospora* has medicinal properties. [5]



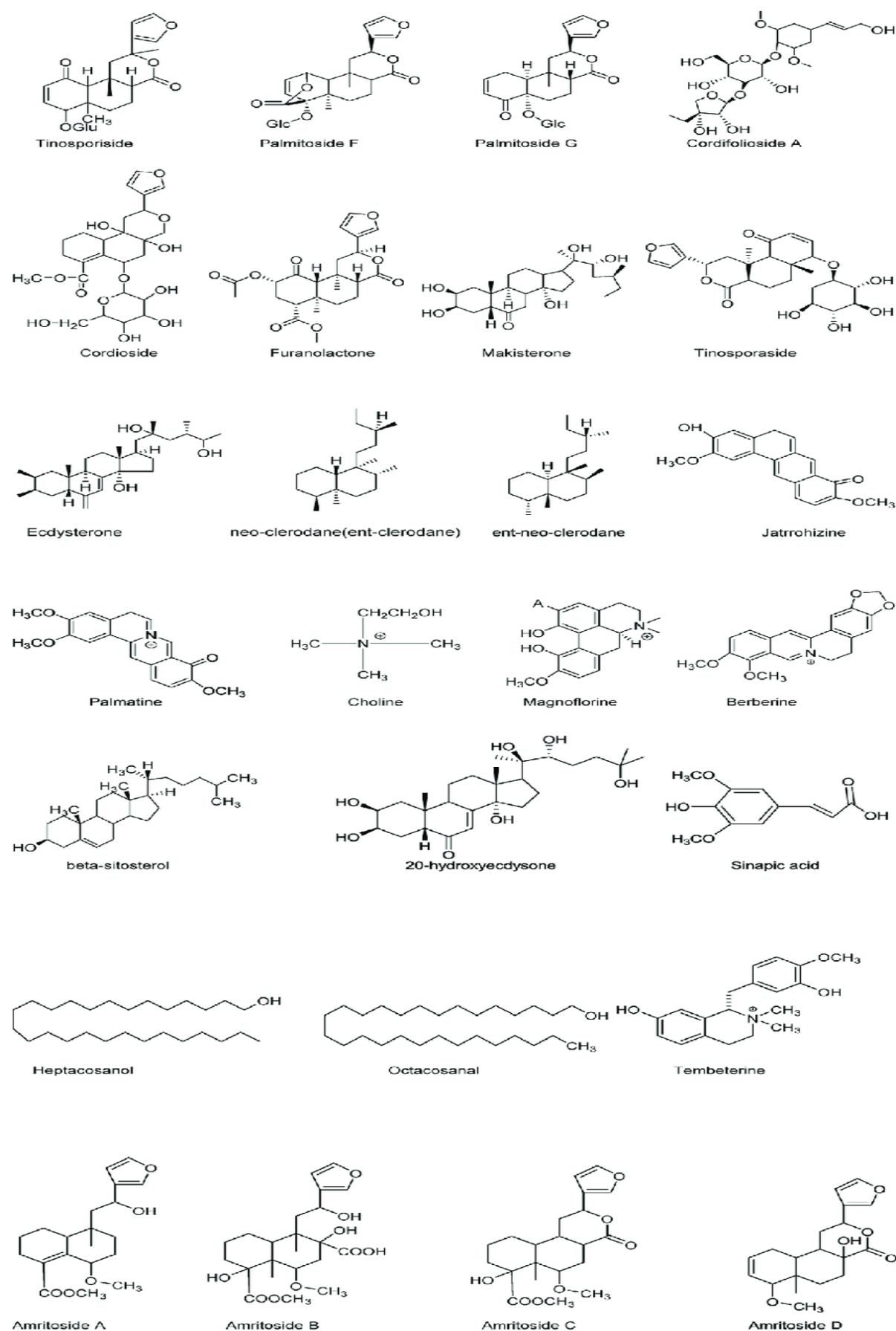
During the 2020-22 COVID-19 outbreak in India, the Ministry of AYUSH recommended use of *T. cordifolia* (Giloy) as a home remedy for immune support, [6] but such a practice appeared

to be associated with hepatitis cases among six people in Mumbai who used boiled or capsule preparations of the plant. [6-9]

Tinospora cordifolia is a popular medicinal plant which is used in several traditional medicines to cure various diseases. The common names are Amrita and Guduchi and belong to the family of Menispermaceae. It is considered an essential herbal plant of Indian system of medicine (ISM) and has been used in the treatment of fever, urinary problem, dysentery, skin diseases, leprosy, diabetes, and many more diseases. The plant is reported to contain chemical compounds including Alkaloids, Terpenoids, Lignans, Steroids and others that establish the phytochemistry and pharmacological activity of *Tinospora cordifolia*. The study highlights the pharmacological importance viz antioxidant activity, antimicrobial activity, antibacterial activity, antifungal activity, anti-diabetic activity, antistress activity, hypolipidaemic effect, hepatic disorder, anticancer anti HIV potential, antiosteoporotic effects, antitoxic effects, wound healing, anticomplementary activity, and immunomodulating activity, systemic infection and Parkinson's disease. [10]



Major constituent of *Tinospora cordifolia*: terpenoid, alkaloid, lignans, steroids. [10]

Structure of the chemical constituent of *T. cordifolia*. [10]

Some of the essential constituents of *T. cordifolia*.

Terpenoids Tinosporide, Furanolactone diterpene, Furanolactone clerodane diterpene, furanoid diterpene, Tinosporaside, ecdysterone makisterone and several glucosides isolated as poly acetate, phenylpropene disaccharides cordifolioside A, B and C, cordifolioside D and E, Tinocordioside, cordioside, palmatosides C and F, Sesquiterpene glucoside tinocordifolioside, Sesquiterpene tinocordifolin. [11-21]

Alkaloids Tinosporine, (S), Magnoflorine, (S), Berberine, (S), Choline, (S), Jatrorrhizine, (S), 1,2-Substituted pyrrolidine(S), Alkaloids, viz. jatrorrhizine, palmatine, beberine, tembeterine, choline. [12-26]

Lignans 3 (a, 4-dihydroxy-3-methoxybenzyl)-4-(4- hydroxy-3-methoxybenzyl), (S) [27]

Steroids Giloinsterol, (S), β -Sitosterol, (S), 20aHydroxy ecdysone, (S). [28-31]

Others Giloin, Tinosporan acetate, Tinosporal acetate, Tinosporidine, Heptacosanol, Octacosanol, sinapic acid, Tinosponone, two phytoecdysones, an immunologically active arabinogalactan. [32-36]

The study planned to prepare antibacterial finish for grey cotton fabric using Giloy stem extract for healthcare applications. The selected grey cotton fabric was pretreated prior to application of the extract. For the extraction of the herb, maceration process was employed and the solution prepared was further subjected to soxhlet extraction to congeal the extract. Giloy extract was assessed for its phytochemical and antibacterial properties, to find out the bioactive components responsible for such activity. [37]

Certain sections of the media have falsely linked again Giloy/Guduchi to liver damage. The Ministry of Ayush reiterates that Giloy/Gudduchi (*Tinospora cordifolia*) is safe and as per available data, Guduchi does not produce any toxic effect. In Ayurveda, it is said to be the best rejuvenating herb. Acute toxicity studies of aqueous extract of Guduchi reports that it does not produce any toxic effect. However, the safety of a drug depends on how it is being used. Dosage is one of the important factors that determine the safety of a particular drug. In a study, lower concentration of Guduchi powder is found to increase the life span of fruit flies (*Drosophila Melanogaster*). At the same time, higher concentration progressively reduced the life span of flies. This clearly indicates that an optimum dosage should be maintained in order to get the desired effects. This infers that the medicinal herb has to be used in an appropriate dose as prescribed by a qualified physician to get medicinal effects. With the wide range of actions and abundant components, Guduchi is a real treasure among herbal drug source. Medicinal applications of Guduchi in countering various disorders and its use as anti-oxidant, anti-hyperglycemic, anti-hyperlipidemic, hepatoprotective, cardiovascular protective, neuroprotective, osteoprotective, radioprotective, anti-anxiety, adaptogenic, analgesic, anti-inflammatory, anti-pyretic, anti-diarrheal, anti-ulcer, anti-microbial, and anti-cancer have been well established.

A special focus has been made on its health benefits in treating various metabolic disorders and its potential as an immune booster. It is used as a major component of therapeutics for ameliorating metabolic, endocrinal, and several other ailments, aiding in the betterment of human life expectancy. It is a popularly known herb for its immense therapeutic applications in traditional systems of medicine and has been used in the management of COVID-19. Considering the overall health benefits, the herb cannot be claimed to be toxic.[38]

During the ongoing COVID-19 pandemic *Tinospora cordifolia* also known as Giloy gained immense popularity and use due to its immunity-boosting function and anti-viral properties. *T. cordifolia* is among the most important medicinal plants that has numerous therapeutic

applications in health due to the production of a diverse array of secondary metabolites. Therefore, to gain genomic insights into the medicinal properties of *T. cordifolia*, the first genome sequencing was carried out using 10x Genomics linked read technology and the draft genome assembly comprised of 1.01 Gbp. This is also the first genome sequenced from the plant family Menispermaceae. The deep sequencing of transcriptome from the leaf tissue was also performed followed by transcriptomic analysis to gain insights into the gene expression and functions. Further, the phylogenetic position of *T. cordifolia* was also determined through the construction of a genome-wide phylogenetic tree using 35 other dicot species and one monocot species as an outgroup species.[39]

Plants produce a diverse range of bioactive molecules, making them a rich source of different types of medicines. A regular and widespread use of herbs throughout the world has increased serious concern over their quality, safety and efficacy. Thus, a proper scientific evidence or assessment has become the criteria for acceptance of herbal health claims. The anti-oxidant effects of leaves of *Tinospora cordifolia* has been examined. [40]

The phytochemical analysis of the plants is very important commercially and has great interest in pharmaceutical companies for the production of the new drugs for curing of various diseases. Phytochemicals have two categories i.e., primary and secondary constituents. Primary constituents have chlorophyll, proteins sugar and amino acids. Secondary constituents contain terpenoids and alkaloids. Medicinal plants have antifungal, antibacterial and anti-inflammation activities. Study involves the qualitative phytochemical analysis of two different medicinal plants: *Tinospora cordifolia* and *Withania somnifera*. Data indicates the presence of flavonoids, alkaloids, proteins, phenolic compounds, cardiac glycosides and tannins. [41]

Tinospora cordifolia is known as Giloe and Guduchi, with significant importance in the traditional medicinal systems. It is dioeciously plant. It is mostly used in Ayurved system. It is also known as a 'Rasayans' of medicinal system, which develops immune system of the body and protect against infection. Study is carried out to analyse the phytochemical compounds in leaves and stem extracts of *T. cordifolia* by using phytochemical screening tests and estimate total flavonoid content (TFC) by using aluminium chloride method in the sample extracts. The leaf and stem extracts of *T. cordifolia* expressed the presence of several phytochemicals viz., flavonoids, amino acids, diterpines, protein, saponins and carbohydrates. The investigation further proposed that the phytochemicals present in stems and leaves of *T. cordifolia*, which can be use as natural antioxidants in medicinal drugs. [42]

The traditional system of medicine in Sri Lanka has shown much better improvement, has fewer side effects, and is less expensive than modern synthetic drugs in the treatment of many diseases. The objective of the was to comparatively evaluate the qualitative and quantitative analysis of phytochemical constituents of leaves of *Murraya koenigii* (L.) Spreng., *Tinospora cordifolia* (Wild) Hook.f., *Enicostemma axillare* (Lam) A. Raynal, and *Gymnema sylvestre* R. Br. were collected from Jaffna District. [43]

Patanjali Giloy Ghanvati

Giloy ghanvati is used as a treatment for general fever and immunity. Useful in generalized debility, fever, skin & urinary disorders. It is also beneficial in general weakness, fever, dengue, chicken guinea. It helps build strength and enhance energy, boosts immunity naturally, offers protection against numerous diseases, alleviates weakness and fatigue. [44]

Patanjali Ayurveda Giloy Ghanvati is an ayurvedic supplement that helps boost immunity and protect from various infections. Its key ingredient is Giloy. It helps build strength and stamina to improve energy levels. The tablets aid in post-illness recovery and manage fever, cough, and cold. Giloy, an active ingredient in the tablet, has an antipyretic activity that helps to reduce fever and recover quickly after an infection or illness. It is known to alleviate the symptoms of the common cold, low immunity, general weakness, and fatigue. This ayurvedic tablet is also known to increase platelet count and reduce dengue fever. It also aids in toxin removal, promoting better skin and skin regeneration by increasing collagen production. It can be used for general weakness and the common cold, Aids in relieving constipation with mucus in the stool, helps to manage cholesterol levels and keep your heart healthy, it is known to lower your risk of recurrent infections, boosts your immune system and prevents immune-deficiency disorders, acts as supportive therapy for individuals with autoimmune disorders, it improves your appetite and aids in overall growth, plays a key role in the treatment of skin conditions, helps deal with urinary problems, including urinary tract infections. [45]

The current severe acute respiratory syndrome disease caused by Coronavirus-2 (SARS-CoV-2) has been a serious strain on the healthcare infrastructure mainly due to the lack of a reliable treatment option. Alternate therapies aimed at symptomatic relief are currently prescribed along with artificial ventilation to relieve distress. Traditional medicine in the form of Ayurveda has been used since ancient times as a holistic treatment option rather than targeted therapy. The practice of Ayurveda has several potent herbal alternatives for chronic cough, inflammation, and respiratory distress which are often seen in the SARS-CoV-2 infection. The aqueous extracts of *Tinospora cordifolia* (willd.) Hook. f. and Thomson in the form of Giloy Ghanvati, as a means of treatment to the SARS-CoV-2 spike-protein induced disease phenotype in a humanized zebrafish model is used. The resultant changes in the disease phenotype were comparable to the group that were given the reference compound, Dexamethasone. These findings correlated well with various phyto-compounds detected in the Giloy Ghanvati and their reported roles in the viral disease phenotype amelioration.[46]

Present study deals with Colorimetric phytochemical analysis of *Tinospora Cordifolia* (Giloy leaf extract) and FTIR study of its medicinal sample Giloy Ghanvati. Colorimetric phytochemical analysis of *Tinospora Cordifolia* (Giloy leaf extract) involves preparation of standard Giloy Ghanvati solution, Ferric Chloride solution and Giloy leaf Solution. Different systems were prepared. Absorbance of standard Giloy solution was taken at different wavelength. And λ_{\max} was calculated. Which was 420 nm. Absorbance of standard Giloy solution of different concentrations were taken at 420 nm and Calibration plot was prepared. Then absorbance of Giloy leaf solutions were taken at 420 nm and concentration of Giloy in Giloy leaf was calculated from calibration plot. *Tinospora cordifolia* which contains diverse phytochemicals, including alkaloids, phytosterols, glycosides, tinosporide, and other mixed chemical compounds reduces ferric ions and production of violet coloration by addition of ferric chloride to dilute solution of Giloy takes place and the concentration of Giloy was investigated colorimetrically. The method is simple, rapid and precise. Interpretation of FTIR Spectra of Giloy Ghanvati medicinal sample shows presence of various functional groups such as O-H stretching - Alcohol, Carboxylic acid, O-H bending - Alcohol, N-H stretching - Amine salt, C=C stretching - α , β - unsaturated ketone and C=O stretching - Conjugated acid.

METHODOLOGY

1. Colorimetric phytochemical analysis of *Tinospora Cordifolia* (Giloy)

Colorimetric phytochemical analysis of *Tinospora Cordifolia* (Giloy leaf extract) involves preparation of standard Giloy Ghanvati solution, Ferric Chloride solution and Giloy leaf Solution. Different systems were prepared. Absorbance of standard Giloy solution was taken at different wavelength. And λ_{max} was calculated. Which was 420 nm. Absorbance of standard Giloy solution of different concentrations were taken at 420 nm and Calibration plot was prepared. Then absorbance of Giloy leaf solutions were taken at 420 nm and concentration of Giloy in Giloy leaf was calculated from calibration plot. *Tinospora cordifolia* which contains diverse phytochemicals, including alkaloids, phytosterols, glycosides, tinosporide, and other mixed chemical compounds reduces ferric ions and production of violet coloration by addition of ferric chloride to dilute solution of Giloy takes place and the concentration of Giloy was investigated colorimetrically. The method is simple, rapid and precise.

Preparation of Standard Giloy Ghanvati solution: Weight of 1 tablet of Giloy Ghanvati was taken and crushed it then 0.1 g powder was dissolved in 100 ml distilled water.

Preparation of Ferric Chloride solution: 1 g Ferric chloride was dissolved in 20 ml distilled water.

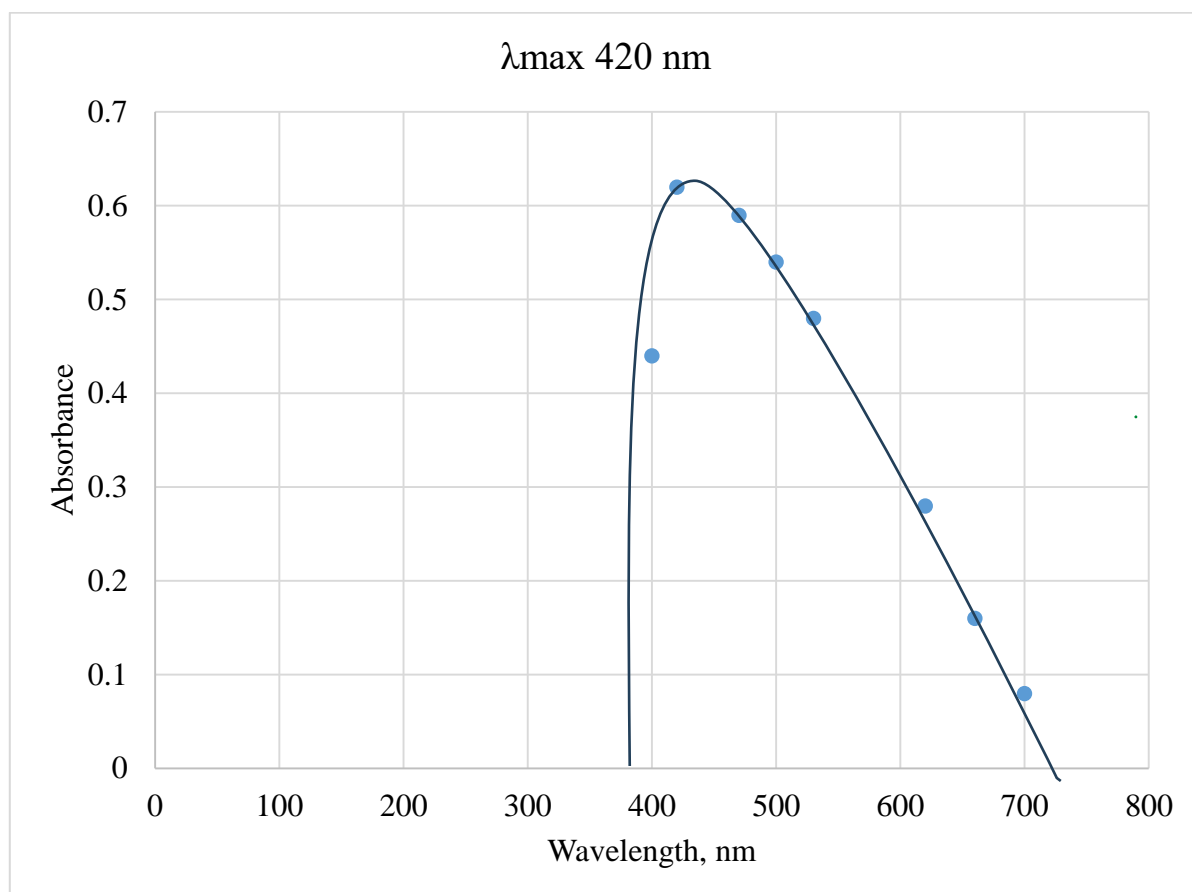
Preparation of Giloy Leaf Solution: 2 Giloy leaf was crushed with the help of distilled water, transferred completely in 100 ml volumetric flask and volume was made up to 100 ml with the help of distilled water.

Following systems were prepared

System No.	Standard Giloy Ghanvati Solution, ml	Giloy Leaf Solution	Ferric Chloride solution, ml	Distilled water
1	1	-	1	8
2	2	-	1	7
3	3	-	1	6
4	4	-	1	5
5	5	-	1	4
6	6	-	1	3
7	-	1	1	8
8	-	2	1	7
9	-	3	1	6
10	-	4	1	5
11	-	5	1	4
12	-	6	1	3

Absorbance of system No 1 taken at different wave length using water as blank. λ_{max} was noted which is 420 nm. Absorbance of system 1 to 6 was taken at λ_{max} 420 nm. Then absorbance of system 7 to 12 was taken at 420 nm wavelength. Calibration plot was prepared between Concentration of Giloy and Absorbance. And from this calibration plot concentration of Giloy from Giloy Leaf sample was calculated.

Wave length, nm	Absorbance of System No. 1	Wave length, nm	Absorbance of System No. 1
400	0.44	530	0.48
420	0.62	620	0.28
470	0.59	660	0.16
500	0.54	700	0.08

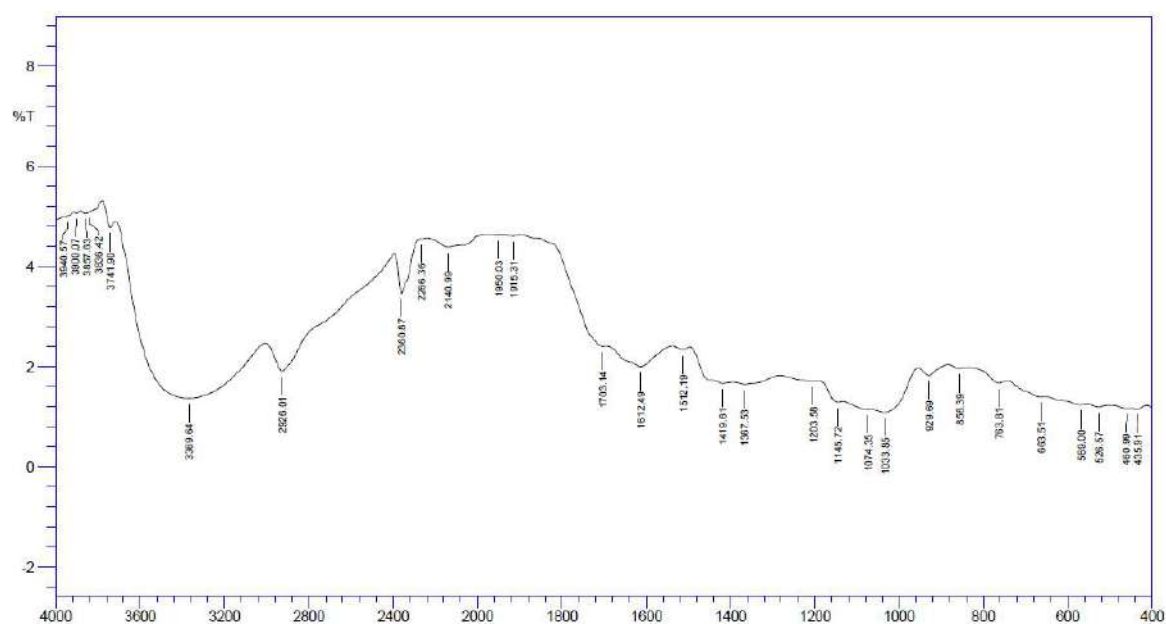


System No.	Absorbance at λ_{max} 420 nm	System No.	Absorbance at λ_{max} 420 nm
1	0.72	7	0.68
2	0.77	8	0.88
3	0.79	9	1.04
4	0.81	10	1.13
5	0.84	11	1.24
6	0.86	12	1.27

2. FTIR study of Giloy Ghanvati medicinal sample

FTIR can be routinely used to identify the functional groups and identification/quality control of raw material / finished products. Spectrum RX-I offers fast throughput and rapid access to reliable and dependable IR results. High signal to noise ratio makes FTIR more useful for difficult samples. It has resolution of 1 cm⁻¹ and scan range of 4000 cm⁻¹ to 250 cm⁻¹. In the normal mode around 10 mg sample is required in the form of fine powder. The sample can be analyzed in the form of liquid, solid and thin films also.

FTIR spectra of Giloy Ghanvati medicinal sample is obtained at room temperature by using an FTIR Spectrophotometer – Perkin Elmer – Spectrum RX-IFTIR. The spectra is collected in a range from 400 to 4000 cm⁻¹.



FTIR spectra of Giloy Ghanvati medicinal sample

RESULTS AND DISCUSSION

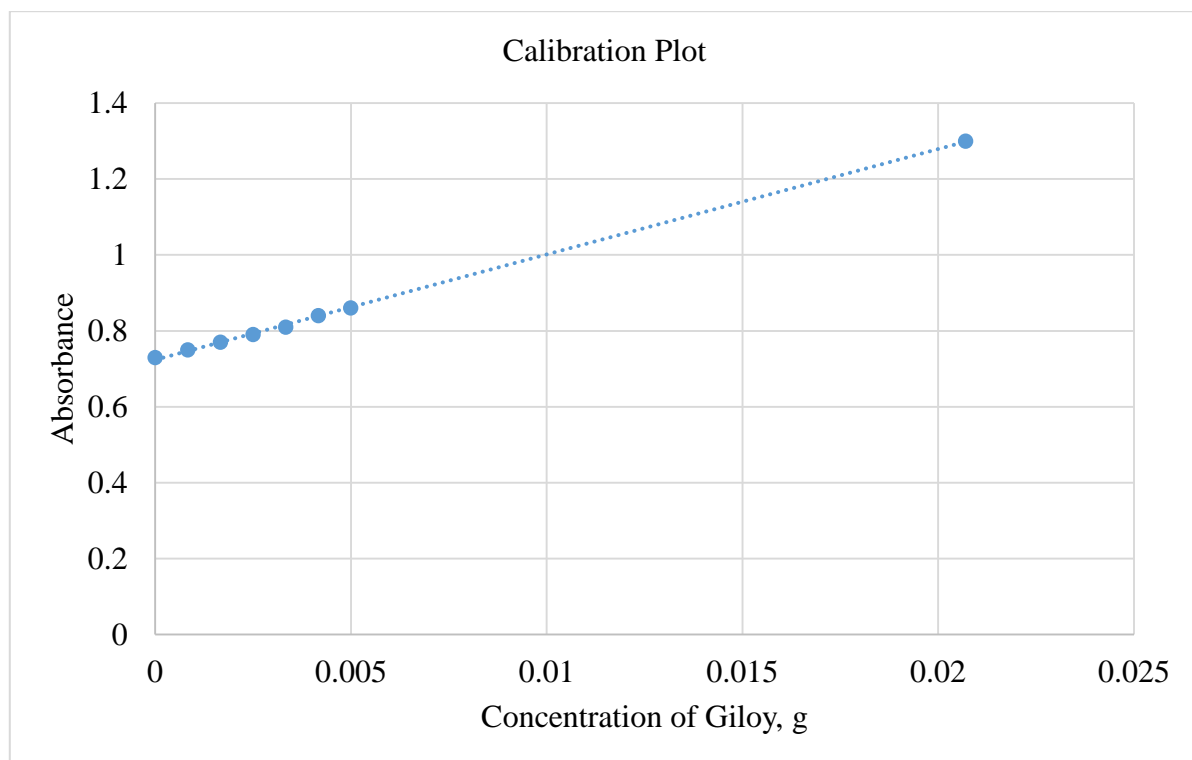
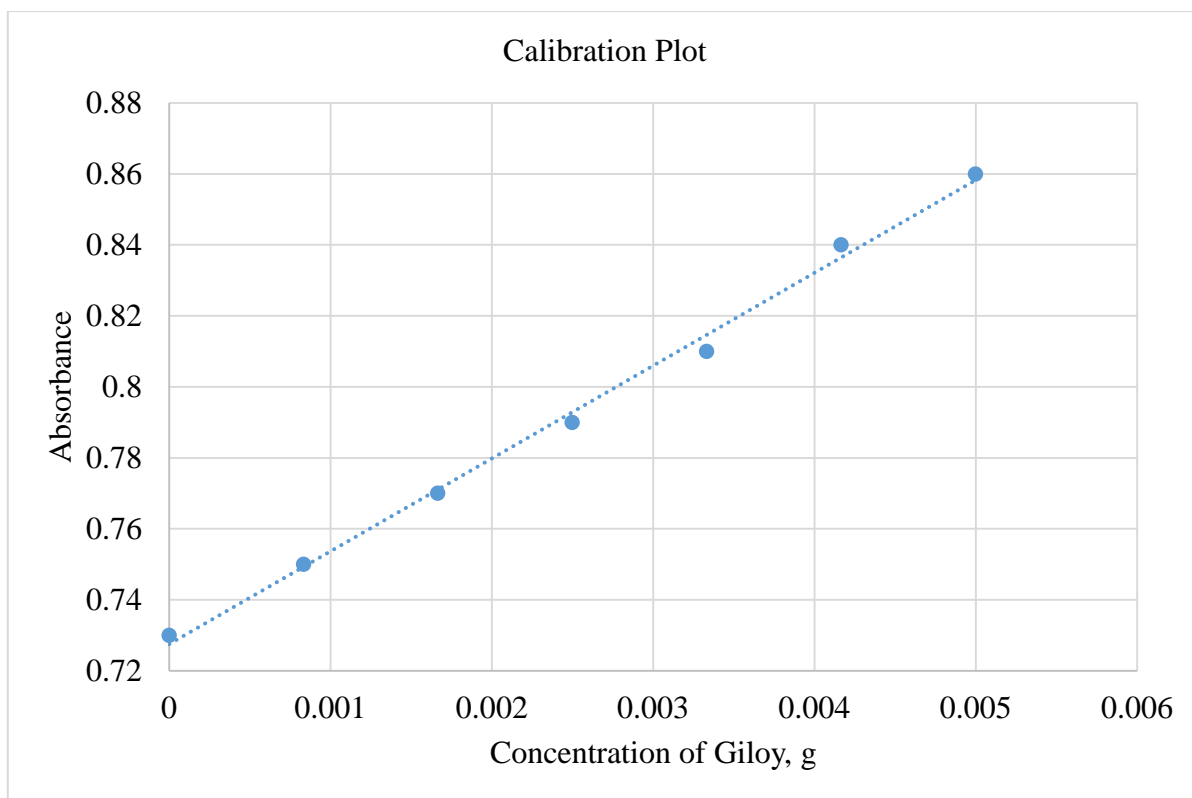
1. Colorimetric phytochemical analysis of *Tinospora Cordifolia* (Giloy)

1 Tablet of Giloy Ghanvati contains 0.5 g Giloy (Quoted value).

Weight of 1 tablet of Giloy Ghanvati was 0.6 g. Hence 0.6 g tablet contains 0.5 g Giloy

0.1 g tablet powder will contains $0.1 \times 0.5 / 0.6 = 0.0833$ g Giloy.

System No	Volume of standard Giloy Ghanvati solution taken, ml	Weight of Giloy, g	Absorbance at 420 nm
1	1	$1 \times 0.0833 / 100 = 0.000833$	0.75
2	2	$2 \times 0.0833 / 100 = 0.001666$	0.77
3	3	$3 \times 0.0833 / 100 = 0.002499$	0.79
4	4	$4 \times 0.0833 / 100 = 0.003332$	0.81
5	5	$5 \times 0.0833 / 100 = 0.004165$	0.84
6	6	$6 \times 0.0833 / 100 = 0.004998$	0.86



Syste m No	Absorb ance at 420 nm	Concentration of Giloy from graph, g	Volume of Giloy leaf solution taken, ml	Concentration of Giloy per100 ml, g	Average concentration of Giloy per 100 ml, g
7	0.68	-	1	-	0.3435
8	0.88	0.0056	2	$100 \times 0.0056 / 2 = 0.28$	
9	1.04	0.0114	3	$100 \times 0.0114 / 3 = 0.38$	
10	1.13	0.0145	4	$100 \times 0.0145 / 4 = 0.3625$	
11	1.24	0.0185	5	$100 \times 0.0185 / 5 = 0.37$	
12	1.27	0.0195	6	$100 \times 0.0195 / 6 = 0.325$	

Hence 100 ml Giloy leaf solution contains 0.3435 g Giloy. Hence 2 Giloy leaf contains 0.3435 g Giloy. Hence 1 Giloy leaf will contain $0.3435 / 2 = 0.1718$ g Giloy i.e., diverse phytochemicals, including alkaloids, phytosterols, glycosides, tinosporide, and other mixed chemical compounds.

2. FTIR study of Giloy Ghanvati medicinal sample

Spectral region wave number cm^{-1}	Pattern and intensity of Band	Bond causing Absorption	Compound Class
3940.57	Broad and low intensity	-	-
3900.07	Broad and low intensity	-	-
3857.63	Broad and low intensity	-	-
3836.42	Broad and low intensity	-	-
3741.90	Broad and low intensity	-	-
3369.64	Broad and strong intensity	O-H stretching	Alcohol
2926.01	Broad and strong intensity	O-H stretching N-H stretching	Carboxylic acid Amine salt
2360.87	Sharp and moderate intensity	-	-
2266.36	-	-	-
2140.99	Broad and low intensity	-	-
1950.03	-	-	-
1915.31	-	-	-
1703.14	Broad and strong intensity	C=O stretching	Conjugated acid
1612.49	Broad and strong intensity	C=C stretching	α , β - unsaturated ketone

1512.19	Broad and low intensity	-	-
1419.61	Broad and moderate intensity	O-H bending	alcohol
1367.53	Broad and moderate intensity	-	-
1203.58	-	-	-
1145.72	Broad and moderate intensity	-	-
1074.35	Broad and moderate intensity	-	-
1033.85	Broad and moderate intensity	-	-
929.69	Broad and low intensity	-	-
856.39	Broad and low intensity	-	-
763.81	Broad and low intensity	-	-
663.51	Broad and low intensity	-	-
569.00	Broad and low intensity	-	-
526.57	Broad and low intensity	-	-
460.99	Broad and low intensity	-	-
435.91	Broad and low intensity	-	-

CONCLUSION

1. Colorimetric phytochemical analysis of *Tinospora Cordifolia* (Giloy)

1 Giloy leaf contains 0.1718 g Giloy i.e., diverse phytochemicals, including alkaloids, phytosterols, glycosides, tinosporide, and other mixed chemical compounds.

2. FTIR study of Giloy Ghanvati medicinal sample

Interpretation of FTIR Spectra of Giloy Ghanvati medicinal sample shows presence of various functional groups such as O-H stretching - Alcohol, Carboxylic acid, O-H bending - Alcohol, N-H stretching - Amine salt, C=C stretching - α , β - unsaturated ketone and C=O stretching - Conjugated acid.

REFERENCES

1. ^ Jump up to:^{a b} "[Tinospora](#)". *Drugs.com*. 15 July 2019. Retrieved 5 September 2019.
2. ^a Mishra, Ashish; Gond, Surendra K.; Kumar, Anuj; Sharma, Vijay K.; Verma, Satish K.; Kharwar, Ravindra N.; Sieber, Thomas N. (2012). "Season and Tissue Type Affect Fungal Endophyte Communities of the Indian Medicinal Plant *Tinospora cordifolia* More Strongly than Geographic Location". *Microbial Ecology*. 64 (2): 388–98. doi:[10.1007/s00248-012-0029-7](#). PMID [22430503](#). S2CID [10738815](#).
3. ^a Thakur, Abhinay; Kaur, Sanjeev; Kaur, Amarjeet; Singh, Varinder (2012). "Detrimental effects of endophytic fungus *Nigrospora* sp. on survival and development of *Spodoptera litura*". *Biocontrol Science and Technology*. 22 (2): 151–61. doi:[10.1080/09583157.2011.646952](#). S2CID [85075708](#).

4. [^] Swaminathan, K.; Sinha, U. C.; Bhatt, R. K.; Sabata, B. K.; Tavale, S. S. (1989). "Structure of tinosporide, a diterpenoid furanolactone from *Tinospora cordifolia* Miers". *Acta Crystallographica Section C*. 45 (Pt 1): 134–136. doi:[10.1107/s0108270188009953](https://doi.org/10.1107/s0108270188009953). PMID [2610955](https://pubmed.ncbi.nlm.nih.gov/2610955/).
5. [^] Kumar, Pradeep; Kamle, Madhu; Mahato, Dipendra K.; Bora, Himashree; Sharma, Bharti; Rasane, Prasad; Bajpai, Vivek K. (2020). "*Tinospora cordifolia* (Giloy): Phytochemistry, Ethnopharmacology, Clinical Application and Conservation Strategies". *Current Pharmaceutical Biotechnology*. 21 (12): 1165–1175. doi:[10.2174/1389201021666200430114547](https://doi.org/10.2174/1389201021666200430114547). PMID [32351180](https://pubmed.ncbi.nlm.nih.gov/32351180/). S2CID [217593876](https://pubmed.ncbi.nlm.nih.gov/217593876/).
6. [^] Jump up to:^{a b} Banjot Kaur (17 February 2022). "[As COVID Surged, India Had a Silent Outbreak of Giloy-Induced Liver Injury](#)". *Science: The Wire*.
7. [^] Nagral, Aabha; Adhyaru, Kunal; Rudra, Omkar S.; et al. (2021-07-02). "[Herbal Immune Booster-Induced Liver Injury in the COVID-19 Pandemic - A Case Series](#)". *Journal of Clinical and Experimental Hepatology*. 11 (6): 732–738. doi:[10.1016/j.jceh.2021.06.021](https://doi.org/10.1016/j.jceh.2021.06.021). ISSN [99736883](https://pubmed.ncbi.nlm.nih.gov/99736883/). PMC [8252698](https://pubmed.ncbi.nlm.nih.gov/8252698/). PMID [34230786](https://pubmed.ncbi.nlm.nih.gov/34230786/).
8. [^] Ray, Kalyan (6 March 2022). "[Ayurvedic drug backed by AYUSH Ministry causes liver damage, says study](#)". *Deccan Herald. The Printers, Mysore*.
9. [^] Kulkarni, Anand V.; Hanchanale, Pavan; Prakash, Vikash; et al. (6 February 2022). "[Tinospora cordifolia \(giloy\)–induced liver injury during the COVID-19 pandemic — Multicenter nationwide study from India](#)". *Hepatology Communications*. 6 (6): 1289–1300. doi:[10.1002/hep4.1904](https://doi.org/10.1002/hep4.1904). PMC [9134809](https://pubmed.ncbi.nlm.nih.gov/9134809/). PMID [35037744](https://pubmed.ncbi.nlm.nih.gov/35037744/).
10. The chemical constituents and diverse pharmacological importance of *Tinospora cordifolia*, Priyanka Sharma, Bharat P. Dwivedee, Dheeraj Bisht, Ashutosh K. Dasha, Deepak Kumar, Heliyon · September 2019. DOI: [10.1016/j.heliyon.2019.e02437](https://doi.org/10.1016/j.heliyon.2019.e02437)
11. M.Q.I. Khuda, A. Khaleque, N. Ray, *Tinospora cordifolia* constituents of plants fresh from the field, *Sci. Res.* 1 (1964) 177–183.
12. J.B. Hanuman, R.K. Bhatt, B.K. Sabata, A diterpenoid furanolactone from *Tinospora cordifolia*, *Phytochemistry* 25 (1986) 1677–1680.
13. R.K. Bhatt, J.B. Hanuman, B.K. Sabata, A new clerodane derivative from *Tinospora cordifolia*, *Phytochemistry* 27 (1988) 1212–1216.
14. J.B. Hanuman, R.K. Bhatt, B. Sabata, A clerodane furano-diterpene from *Tinospora cordifolia*, *J. Nat. Prod.* 51 (1988) 197–201.
15. R.K. Bhatt, B.K. Sabata, A furanoid diterpene glucoside from *Tinospora cordifolia*, *Phytochemistry* 28 (1989) 2419–2422.
16. M.A. Khan, I.A. Gray, P.G. Waterman, Tinosporaside an 18-norclerodane glucoside from *Tinospora cordifolia*, *Phytochemistry* 28 (1989) 273–275.
17. V.D. Gangan, P.P. Arjun, T. Sipahimalani, A. Banerji, A. Cardifolisides, C. B, Norditerpene furon glucoside from *Tinospora cordifolia*, *Phytochemistry* 37 (1994) 781–786.
18. R. Maurya, S.S. Handa, Tinocordifolin, a sesquiterpene from *Tinospora cordifolia*, *Phytochemistry* 44 (1998) 1343–1345.
19. V.D. Gangan, P.P. Arjun, A.T. Sipahimalani, A. Banerji, Norditerpene furon glucoside from *Tinospora cordifolia*, *Phytochemistry* 39 (1995) 1139–1142.
20. V. Wazir, R. Maurya, R.S. Kapil, A clerodane furano diterpene glucoside from *Tinospora cordifolia*, *Phytochemistry* 38 (1995) 447–449.
21. V.D. Gagan, P. Pradhan, A.T. Sipahimalan, A. Banerji, F. Palmatosides C, Diterpene furan glucosides from *Tinospora cordifolia*-structural elucidation by 2D NMR spectroscopy, *Indian J. Chem.* 35B (1996) 630–634.
22. N. Choudhary, M.B. Siddiqui, S. Azmat, S. Khatoon, *Tinospora cordifolia*: ethnobotany, phytopharmacology and phytochemistry aspects, *IJPSR* 4 (2013) 891.
23. N.G. Bisset, J. Nwaiwu, Quaternary alkaloids of *Tinospora* species, *Planta Med.* 48 (1983) 275–279.
24. V.R. Mahajan, C.I. Jolly, K.M. Kundnani, A new hypoglycaemic agent from *Tinospora cordifolia*, *Indian Drugs* 23 (1985) 119–120.
25. D.N.K. Sarma, R.L. Khosa, J.P.N. Chansauria, A.K. Ray, The effect of *Tinospora cordifolia* on brain neurotransmitters in the stressed rat, *Fitoterapia* 66 (1995) 421–422.

26. A.K. Pathak, A.K. Agarwal, D.C. Jain, R.P. Sharma, O.W. Howarth, NMR studies of 20 hydroxyecdysones, a steroid isolated from *Tinospora cordifolia*, Indian J. Chem. 34 (1995) 674–676.
27. J.B. Hanuman, A.K. Mishra, B. Sabata, A natural phenolic lignan from *Tinospora cordifolia* Miers, J. Chem. Soc. (1986) 1181–1185.
28. A.R. Kidwai, K.C. Salooja, V.N. Sharma, S. Siddiqui, Chemical examination of *Tinospora cordifolia*, J. Sci. Indian Res. 8 (1949) 115–118.
29. A. Khaleque, M.A.W. Maith, M.S. Huq, B. K Abul, *Tinospora cordifolia* IV. Isolation of heptacosanol, β sitosterol and three other compounds tinosporine, cordifol and cordifolone, Pakistan J. Sci. Industry Res. 14 (1970) 481–483.
30. S.N. Dixit, R.L. Khosa, Chemical investigations on *Tinospora cordifolia* (wild.) miers, Indian. J. Appl. Chem. 34 (1971) 46–47.
31. A.K. Pathak, D.C. Jain, P.R. Sharma, Chemistry and biological activities of the genus *Tinospora*, Int. J. Pharmacogn. 33 (1995) 277–287.
32. M.Q. Khuda, A. Khaleque, K.A. Basar, M.A. Rouf, M.A. Khan, N. Roy, Studies on *Tinospora cordifolia* II: isolation of tinosporine, tinosporic acid and tinosporol from the fresh creeper, Sci. Res. 3 (1966) 9–12.
33. A. Khaleque, M.A.W. Maith, M.S. Huq, K.A. Tinospora cordifolia III, Isolation of tinosporine, heptacosanol, β sitosterol, Pakistan J. Sci. Industry Res. 14 (1971) 481–483.
34. R. Maurya, V. Wazir, A. Tyagi, R.S. Kapil, Clerodane diterpene from *Tinospora cordifolia*, Phytochemistry 38 (1995) 659–661.
35. P. Pradhan, V.D. Gangan, A.T. Sipahimalani, A. Banerji, Two phytoecdysones from *Tinospora cordifolia*: structural assignment by 2D NMR spectroscopy, Indian J. Chem. 36B (1997) 958–962.
36. G. Chintalwar, A. Jain, A. Sipahimalani, A. Banerji, P. Sumariwalla, R. Ramakrishnan, K. Sainis, An Immunologically active arabinogalactan from *Tinospora cordifolia*, Phytochemistry 52 (1999) 1089–1093
37. Antibacterial and qualitative phytochemical analysis of Giloy extract for application of herbal finish on cotton fabric, K Medhaa, N Aryaa, K Malikb, S Ahlawatc & N Chauhana, Indian Journal of Traditional Knowledge, Vol 20(4), October 2021, pp 944-950
38. <https://pib.gov.in/PressReleasePage.aspx?PRID=1798676>
39. Genome sequencing and assembly of *Tinospora cordifolia* (Giloy) plant, Shruti Mahajan, Abhisek Chakraborty, Titas Sil, Vineet K Sharma, <https://www.biorxiv.org/content/10.1101/2021.08.02.454741v1>
40. Studies on Anti-oxidant activity of *Tinospora cordifolia* (Miers.) Leaves using in vitro models, Ramya Premanath and N. Lakshmidhevi, Journal of American Science, 2010;6(10):736-743.
41. Qualitative phytochemical analysis of *Tinospora cordifolia* and *Withania somnifera*, Iqra Nazir and Rikhi S Chauhan, The Pharma Innovation Journal 2018; 7(10): 333-336
42. Qualitative and quantitative analysis of leaves and stem of *Tinospora Cordifolia* in different solvent extract, Garg Praveen, Garg Rajesh, Journal of Drug Delivery & Therapeutics. 2018; 8(5-s):259-264
43. Comparative Analysis of Qualitative and Quantitative Phytochemical Evaluation of Selected Leaves of Medicinal Plants in Jaffna, Sri Lanka, Gowri Rajkumar, Panambara Arachchilage Harini, Rangana Panambara, Vinotha Sanmugarajah, Borneo Journal of Pharmacy, Vol 5 Issue 2 May 2022, Page 93 – 103
44. <https://www.patanjaliayurved.net/product/ayurvedic-medicine/vati/patanjali-giloy-ghanvati-60-n/624>
45. <https://www.1mg.com/otc/patanjali-ayurveda-giloy-ghanvati-otc324816?wpsrc=Google+Organic+Search>
46. Giloy Ghanvati (*Tinospora cordifolia* (Willd.) Hook. f. and Thomson) Reversed SARS-CoV-2 Viral Spike-Protein Induced Disease Phenotype in the Xenotransplant Model of Humanized Zebrafish, Acharya Balkrishna, Lakshmipathi Khandrika, and Anurag Varshney, Front Pharmacol, 2021; 12: 635510.

Determination of Hydrochloric Acid Neutralizing Capacity of Different Antacid Tablet by Back Titration Method and Its FTIR Analysis

Dr Swaroopa Rani N. Gupta

Professor, Department of Chemistry, Brijlal Biyani Science College, Amravati, Maharashtra India

swargupta@yahoo.com

ABSTRACT

An antacid is a substance which neutralizes stomach acidity and is used to relieve heartburn, indigestion or an upset stomach. Several liquid antacid preparations are marketed. Common liquid preparations include milk of magnesia and magnesium/aluminum combinations. A potential advantage of using a liquid preparation over a tablet is that liquids may provide quicker relief, however this may coincide with a shorter duration of action. Chewable tablets are one of the most common forms of antacids, and are readily available over the counter. Upon reaching the stomach, the tablet powder will dissolve in the stomach acid, allowing the cations to be released and neutralize excess stomach acid. Common salts available in tablet form include those of calcium, magnesium, aluminum, and sodium. Effervescent tablets are tablets which are designed to dissolve in water, and then release carbon dioxide. Common ingredients include citric acid and sodium bicarbonate, which react when in contact with water to produce carbon dioxide. Effervescent antacids may also contain aspirin, sodium carbonate, or tartaric acid. Those containing aspirin may cause further gastric irritation and ulceration due to aspirin's effects on the mucous membrane of the stomach.

Present study deals with determination of Hydrochloric acid neutralizing capacity of an antacid tablets such as ACILOC 150, Athzol-DSR, Gelusil, NEXPRO-40, Omee-D, PAN-L, Pantafol-DSR, Rabesec-20, Rabifeel – LS and Rantac 150 using back titration method and FTIR study of Pantafol-DSR.

Antacid tablets contain bases like calcium carbonate, magnesium carbonate, magnesium hydroxide, sodium bicarbonate etc. The tablet can neutralize the HCl present in stomach and can decrease the acidity. The HCl neutralizing capacity of an antacid tablet can be determined by adding tablet to a known quantity of excess HCl then back titrating the unneutralized acid with standard alkali solution using phenolphthalein indicator. The higher the amount of Hydrochloric acid neutralized by Antacids, the better is the acid neutralizing capacity. The result shows that the tablet Rantac 150 has highest acid neutralizing capacity and PAN_L lowest acid neutralizing capacity. Rantac 150 > Rabifeel – LS > Omee-D > Pantafol-DSR > Rabesec-20 > NEXPRO-40 > Athzol-DSR > ACILOC 150 > Gelusil > PAN-L. The back titration method used in this study is simple, inexpensive and can be used in routine monitoring of the quality of Antacid tablets.

FTIR spectra of Pantafol-DSR is obtained at room temperature by using an FTIR Spectrophotometer – Perkin Elmer – Spectrum RX-IFTIR. The spectra is collected in a range from 400 to 4000 cm^{-1} . Interpretation of FTIR Spectra of Pantafol-DSR shows Presence of various functional groups such as C-H bending - Aromatic compound; O-H stretching – Alcohol, Carboxylic acid, C=O stretching - Conjugated acid, Conjugated aldehyde, C≡C stretching – Alkyne.

Keywords: Hydrochloric Acid Neutralizing Capacity, Antacid Tablet, Back Titration Method, FTIR Analysis

INTRODUCTION

Antacid

An antacid is a substance which neutralizes stomach acidity and is used to relieve heartburn, indigestion or an upset stomach.[1] Some antacids have been used in the treatment of constipation and diarrhea.[2] Marketed antacids contain salts of aluminium, calcium, magnesium, or sodium.[2] Some preparations contain a combination of two salts, such as magnesium carbonate and aluminium hydroxide (e. g. hydrotalcite).[3] Antacids are available over the counter and are taken by mouth to quickly relieve occasional heartburn, the major symptom of gastroesophageal reflux disease and indigestion. Treatment with antacids alone is symptomatic and only justified for minor symptoms.[4] Alternative uses for antacids include constipation, diarrhea, hyperphosphatemia, and urinary alkalization.[5] Some antacids are also used as an adjunct to pancreatic enzyme replacement therapy in the treatment of pancreatic insufficiency.[6] Non-particulate antacids (sodium citrate) increase gastric pH with little or no effect on gastric volume, and therefore may see some limited use in pre-operative procedures. Sodium citrate should be given within 1 hour of surgery to be the most effective.[7] Conventional effervescent tablets contain a significant amount of sodium and are associated with increased odds of adverse cardiovascular events according to a 2013 study.[8] Alternative sodium-free formulations containing magnesium salts may cause diarrhea, whereas those containing calcium or aluminum may cause constipation. Rarely, long-term use of calcium carbonate may cause kidney stones. Long-term use of antacids containing aluminum may increase the risk of developing osteoporosis.[9] In vitro studies have found a potential for acid rebound to occur due to antacid overuse, however the significance of this finding has been called into question.[10][11] When an excess amount of acid is produced in the stomach, the natural mucous barrier that protects the lining of the stomach can degrade, leading to pain and irritation. There is also potential for the development of acid reflux, which can cause pain and damage to the esophagus. Antacids contain alkaline ions that chemically neutralize stomach gastric acid, reducing damage to the stomach lining and esophagus, and relieving pain.[1] Some antacids also inhibit pepsin, an enzyme that can damage the esophagus in acid reflux.[5][12] Antacids do not directly inhibit acid secretion, and thus are distinct from acid-reducing drugs like H₂-receptor antagonists or proton pump inhibitors. Antacids do not kill the bacteria *Helicobacter pylori*, which causes most ulcers.[4] Antacids are known to interact with several oral medications, including fluoroquinolone and tetracycline antibiotics, iron, itraconazole, and prednisone.[13] Metal chelation is responsible for some of these interactions (e.g.fluoroquinolones, tetracyclines), leading to decreased absorption of the chelated drug. Some interactions may be due to the pH increase observed in the stomach following antacid ingestion, leading to increased absorption of weak acids, and decreased absorption of weak bases. Antacids also cause an increase in pH of the urine (alkalization), which may cause increased blood concentrations of weak bases, and increased excretion of weak acids.[14] A proposed method to mitigate the effects of stomach acidity and chelation on drug absorption is to space out the administration of antacids with interacting medications, however this method has not been well studied for drugs affected by urine alkalization.[13] There are concerns regarding interactions between delayed-release tablets and antacids, as antacids may increase the stomach pH to a point at which the coating of the delayed-release tablet will dissolve, leading to degradation of the drug if it is pH sensitive.[14] Antacids may be formulated with other active ingredients such as simethicone to control gas, or alginic acid to act as a physical barrier to acid.[15]

Several liquid antacid preparations are marketed. Common liquid preparations include milk of magnesia and magnesium/aluminum combinations. A potential advantage of using a liquid preparation over a tablet is that liquids may provide quicker relief, however this may coincide

with a shorter duration of action.[16] Chewable tablets are one of the most common forms of antacids, and are readily available over the counter. Upon reaching the stomach, the tablet powder will dissolve in the stomach acid, allowing the cations to be released and neutralize excess stomach acid. Common salts available in tablet form include those of calcium, magnesium, aluminum, and sodium.[13] Some common brand are Tums, Gaviscon chewable tablets, and Maalox chewable tablets.[17] Effervescent tablets are tablets which are designed to dissolve in water, and then release carbon dioxide.[18][19][20] Common ingredients include citric acid and sodium bicarbonate, which react when in contact with water to produce carbon dioxide. Effervescent antacids may also contain aspirin,[21] sodium carbonate, or tartaric acid.[22] Those containing aspirin may cause further gastric irritation and ulceration due to aspirin's effects on the mucous membrane of the stomach.[23] Common brands include Alka-Seltzer, Gaviscon, and Eno.

Study based on the evaluation of acid neutralizing capacity of five different commercial brands of antacid tablets was done. [24] Antacids are commonly used as over - the - counter (OTC) drugs or prescribed medications. Some antacid products may neutralize more acid in the stomach than others. The ability of an antacid to neutralize acid is expressed as its Acid Neutralizing Capacity (ANC). Study was undertaken with the objective of assessing the quality of different brands of antacid tablets. The assessment parameters included the evaluation of uniformity of weight, uniformity of thickness, crushing strength, friability, as well as the ANC (using pH and titrimetric method), which is easy to use, accurate, reproducible, simple, and inexpensive. [25] Study has been evaluated the acid neutralizing and buffering capacities (BC) of nine selected antacid brands ("L1-L9") in Ghana. [26] Gastric acidity is highly prevalent in the Indian Population. People usually take commercially available antacids to alleviate the symptoms. Unfortunately, the use of these over the counter drugs has been so common that they are vastly overused and are taken even for mild heartburn or indigestion, which makes the underlying problem worse. The study aimed at identifying common traditional remedies used in India to treat acidity and to evaluate their acid neutralizing capacity; and compare it with their commercially available counterparts. The acid neutralizing capacities of the traditional remedies were analyzed by Back titration method. [27] The study was aimed to evaluate the acid-neutralizing capacity (ANC) and other properties of antacid drugs marketed in Morocco. Other properties such as price and sodium content were also studied. [28]

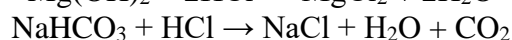
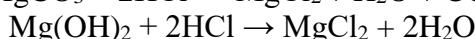
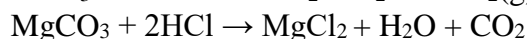
Present study deals with determination of Hydrochloric acid neutralizing capacity of an antacid tablets such as ACILOC 150, Athzol-DSR, Gelusil, NEXPRO-40, Omee-D, PAN-L, Pantafol-DSR, Rabesec-20, Rabifeel – LS and Rantac 150 using back titration method and FTIR study of Pantafol-DSR. Antacid tablets contain bases like calcium carbonate, magnesium carbonate, magnesium hydroxide, sodium bicarbonate etc. The tablet can neutralize the HCl present in stomach and can decreases the acidity. The HCl neutralizing capacity of an antacid tablet can be determined by adding tablet to a known quantity of excess HCl then back titrating the unneutralized acid with standard alkali solution using phenolphthalein indicator. The higher the amount of Hydrochloric acid neutralized by Antacids, the better is the acid neutralizing capacity. The result shows that the tablet Rantac 150 has highest acid neutralizing capacity and PAN_L lowest acid neutralizing capacity value. Rantac 150 > Rabifeel – LS > Omee-D > Pantafol-DSR > Rabesec-20 > NEXPRO-40 > Athzol-DSR > ACILOC 150 > Gelusil > PAN-L. The back titration method used in this study is simple, inexpensive and can be used in routine monitoring of the quality of Antacid tablets. FTIR spectra of Pantafol-DSR is obtained at room temperature by using an FTIR Spectrophotometer – Perkin Elmer – Spectrum RX-IFTIR. The spectra is collected in a range from 400 to 4000 cm^{-1} . Interpretation of FTIR Spectra of Pantafol-DSR shows Presence of various functional groups such as C-H bending - Aromatic

compound; O-H stretching – Alcohol, Carboxylic acid, C=O stretching - Conjugated acid, Conjugated aldehyde, C≡C stretching – Alkyne.

METHODOLOGY

1. Determination of Hydrochloric acid neutralizing capacity of an antacid tablet

Antacid tablets contain bases like calcium carbonate, magnesium carbonate, magnesium hydroxide, sodium bicarbonate etc. The tablet can neutralize the HCl present in stomach and can decrease the acidity. The HCl neutralizing capacity of an antacid tablet can be determined by adding tablet to a known quantity of excess HCl then back titrating the unneutralized acid with standard alkali solution using phenolphthalein indicator.



The above reactions are common reactions between an antacid in which main ingredients are CaCO_3 , MgCO_3 , $\text{Mg}(\text{OH})_2$, NaHCO_3 and stomach HCl



Preparation of 0.1 M Oxalic acid solution: 0.1 M Oxalic acid solution was prepared by dissolving 0.63 g oxalic acid with distilled water in 100 ml volumetric flask and volume was made upto 100 ml mark with distilled water.

Preparation of 0.1 M Sodium hydroxide solution: 0.1 M Sodium hydroxide solution was prepared by dissolving 4 g sodium hydroxide with distilled water in 1 litre volumetric flask and volume was made upto 1litre mark with distilled water.

Preparation of 0.1 M Hydrochloric acid solution: 0.1 M Hydrochloric acid solution was prepared by diluting 8.3 ml of 12 M Hydrochloric acid with distilled water in 1 litre volumetric flask and volume was made upto 1litre mark with distilled water.

Standardization of Sodium hydroxide solution: 10 ml of 0.1 M Oxalic acid solution was taken in 100 ml conical flask to it 3 drops of phenolphthalein indicator was added and solution was titrated with Sodium hydroxide solution until it turns pink which persisted for at least 30 seconds. The volume of Sodium hydroxide solution was recorded. The titration procedure was repeated 2 more times and the constant titre value was recorded.

Standardization of Hydrochloric acid solution: 10 ml of Hydrochloric acid solution was taken in 100 ml conical flask to it 3 drops of phenolphthalein indicator was added and solution was titrated with Sodium hydroxide solution until it turns pink which persisted for at least 30 seconds. The volume of Sodium hydroxide solution was recorded. The titration procedure was repeated 2 more times and the constant titre value was recorded.

Determination of Hydrochloric acid neutralizing capacity of an antacid tablet: One Antacid tablet of Pantafol-DSR, Omee-D, Rabifeel – LS, Rantac 150, Gelusil, Athzol-DSR, PAN-L, Rabesec-20, ACILOC 150 and NEXPRO-40 were crushed in mortal and pestle. 0.5 g crushed tablet was transferred into 250 ml conical flask. To it 75 ml 0.1 N HCl was added and

solution was heated to boil and dissolve the crushed tablet for 5 minutes then cooled and to it 3 drops of phenolphthalein indicator was added and solution was titrated with Sodium hydroxide solution until it turns pink which persisted for at least 30 seconds. The volume of Sodium hydroxide solution was recorded. The titration procedure was repeated 2 more times and the average titre value was recorded. Molarity of HCl in reaction mixture after neutralization with Antacid tablet was calculated. From which difference in Molarity of HCl, weight of HCl neutralized by Antacid Tablet per litre, weight of HCl neutralized by Antacid Tablet per 75 ml and weight of HCl neutralized by 1 g Antacid tablet was calculated.

2. FTIR study of Pantafol-DSR

FTIR can be routinely used to identify the functional groups and identification/quality control of raw material/finished products. Spectrum RX-I offers fast throughput and rapid access to reliable and dependable IR results. High signal to noise ratio makes FTIR more useful for difficult samples. It has resolution of 1 cm⁻¹ and scan range of 4000 cm⁻¹ to 250 cm⁻¹. In the normal mode around 10 mg sample is required in the form of fine powder. The sample can be analyzed in the form of liquid, solid and thin films also.

FTIR spectra of Pantafol-DSR is obtained at room temperature by using an FTIR Spectrophotometer – Perkin Elmer – Spectrum RX-IFTIR. The spectra is collected in a range from 400 to 4000 cm⁻¹.

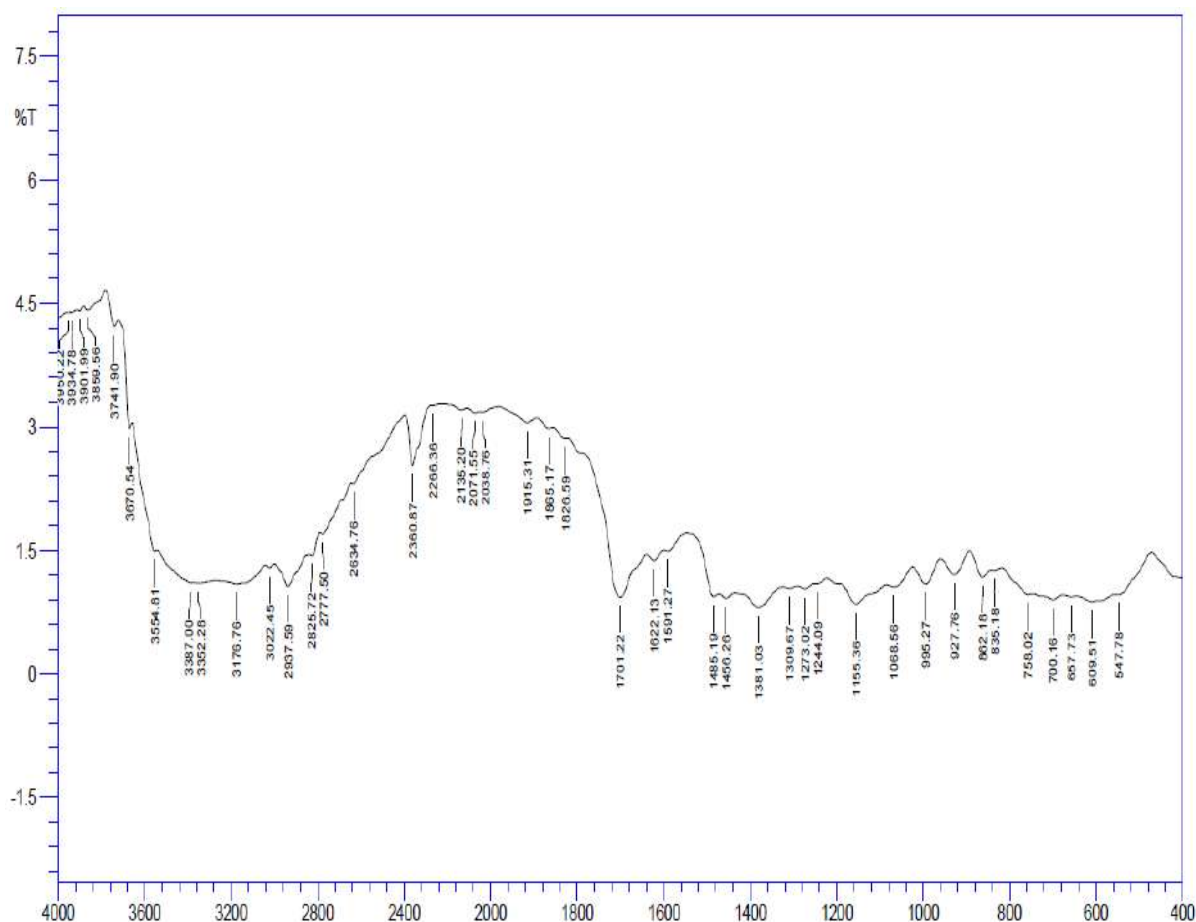


Figure 1. FTIR spectra of Pantafol-DSR

RESULTS AND DISCUSSION

1. Determination of Hydrochloric acid neutralizing capacity of an antacid tablet**Standardization of Sodium hydroxide solution:**

Volume of 0.1 M Oxalic acid solution taken, ml	Volume of Sodium hydroxide solution required, ml	Constant titre value
10	10.0	10.1
10	10.1	
10	10.1	

Standardization of Hydrochloric acid solution:

Volume of Hydrochloric acid solution taken, ml	Volume of Sodium hydroxide solution required, ml	Constant titre value
10	10.0	9.9
10	9.9	
10	9.9	

Determination of Hydrochloric acid neutralizing capacity of an antacid tablet:

Molarity of Oxalic acid = $0.63 \times 10 / 63 = 0.1$

Molarity of Sodium hydroxide solution = $0.1 \times 10 / 10.1 = 0.099$

Molarity of Hydrochloric acid solution = $0.099 \times 9.9 / 10 = 0.098$

Table 1. Determination of Hydrochloric acid neutralizing capacity of an antacid tablet

Name of Antacid Tablet	Constant titre value, ml	Molarity of HCl in reaction mixture after neutralization with Antacid tablet	Difference in Molarity of HCl	Weight of HCl neutralized by Antacid Tablet per liter, g	Weight of HCl neutralized by Antacid Tablet per 75 ml, g	Weight of HCl neutralized by 1 g Antacid tablet, g
ACILOC 150	12	$0.099 \times 12 / 75 = 0.0158$	$0.098 - 0.0158 = 0.0822$	$0.0822 \times 36.5 = 3.0003$	$3.0003 \times 75 / 1000 = 0.2250$	$0.2250 \times 1 / 0.5 = 0.45$
Athzol-DSR	10.5	$0.099 \times 10.5 / 75 = 0.0139$	$0.098 - 0.0139 = 0.0841$	$0.0841 \times 36.5 = 3.0697$	$3.0697 \times 75 / 1000 = 0.2302$	$0.2302 \times 1 / 0.5 = 0.4604$
Gelusil	14.5	$0.099 \times 14.5 / 75 = 0.0191$	$0.098 - 0.0191 = 0.0789$	$0.0789 \times 36.5 = 2.8799$	$2.8799 \times 75 / 1000 = 0.2160$	$0.2160 \times 1 / 0.5 = 0.432$
NEXPRO-40	8.6	$0.099 \times 8.6 / 75 = 0.0114$	$0.098 - 0.0114 = 0.0866$	$0.0866 \times 36.5 = 3.1609$	$3.1609 \times 75 / 1000 = 0.2371$	$0.2371 \times 1 / 0.5 = 0.4742$
Omee-D	2.1	$0.099 \times 2.1 / 75 = 0.0028$	$0.098 - 0.0028 = 0.0952$	$0.0952 \times 36.5 = 3.4748$	$3.4748 \times 75 / 1000 = 0.2606$	$0.2606 \times 1 / 0.5 = 0.5212$
PAN-L	16	$0.099 \times 16 / 75 = 0.0211$	$0.098 - 0.0211 = 0.0769$	$0.0769 \times 36.5 = 2.8069$	$2.8069 \times 75 / 1000 = 0.2105$	$0.2105 \times 1 / 0.5 = 0.421$
Pantafol-DSR	4.8	$0.099 \times 4.8 / 75 = 0.0063$	$0.098 - 0.0063 = 0.0917$	$0.0917 \times 36.5 = 3.3471$	$3.3471 \times 75 / 1000 = 0.2510$	$0.2510 \times 1 / 0.5 = 0.502$

Rabesec-20	6.5	$0.099 \times 6.5 / 75 = 0.0086$	$0.098 - 0.0086 = 0.0894$	$0.0894 \times 36.5 = 3.2631$	$3.2631 \times 75 / 1000 = 0.2447$	$0.2447 \times 1 / 0.5 = 0.4894$
Rabifeel - LS	1	$0.099 \times 1 / 75 = 0.0013$	$0.098 - 0.0013 = 0.0967$	$0.0967 \times 36.5 = 3.5296$	$3.5296 \times 75 / 1000 = 0.2647$	$0.2647 \times 1 / 0.5 = 0.5294$
Rantac 150	0.5	$0.099 \times 0.5 / 75 = 0.0007$	$0.098 - 0.0007 = 0.0973$	$0.0973 \times 36.5 = 3.5515$	$3.5515 \times 75 / 1000 = 0.2664$	$0.2664 \times 1 / 0.5 = 0.5328$

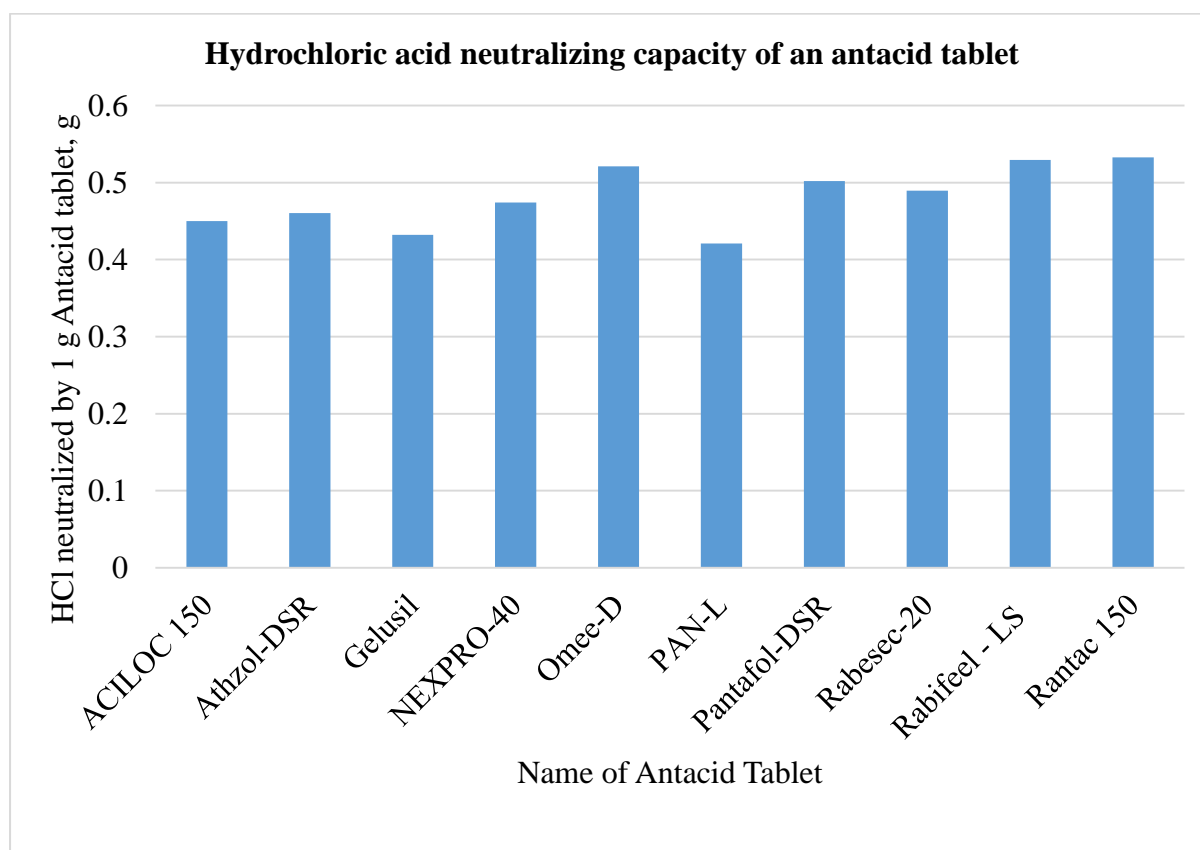


Figure 2 Hydrochloric acid neutralizing capacity of an antacid tablet

Hydrochloric acid neutralizing capacity of commercial antacid tablets are summerized in Table 1 and graphically depicted in Figure 2.

2. FTIR study of Pantafol-DSR

Interpretation of FTIR Spectra of Pantafol-DSR can be done as follows:

Spectral region wave number cm^{-1}	Pattern and intensity of Band	Bond causing Absorption	Compound Class
3950.22	Broad and low intensity	-	-
3934.78	Broad and low intensity	-	-
3901.99	Broad and low intensity	-	-

3859.56	Broad and low intensity	-	-
3741.90	Broad and low intensity	-	-
3670.54	Sharp and moderate intensity	O-H stretching	Alcohol
3554.81	Broad and strong intensity	O-H stretching	Alcohol
3387.00	Broad and strong intensity	O-H stretching	Alcohol
3352.28	Broad and strong intensity	O-H stretching	Alcohol
3176.76	Broad and strong intensity	O-H stretching	Carboxylic acid
3022.45	Broad and strong intensity	O-H stretching	Carboxylic acid
2937.59	Broad and strong intensity	O-H stretching	Carboxylic acid
2825.72	Broad and strong intensity	O-H stretching	Carboxylic acid
2777.50	Broad and strong intensity	O-H stretching	Carboxylic acid
2634.76	Broad and strong intensity	O-H stretching	Carboxylic acid
2360.87	Sharp and moderate intensity	-	-
2266.36	Broad and low intensity	-	-
2135.20	Broad and low intensity	C≡C stretching	Alkyne
2071.55	Broad and low intensity	-	-
2038.76	Broad and low intensity	-	-
1915.31	Broad and low intensity	C-H bending	Aromatic compound
1865.17	Broad and low intensity	C-H bending	Aromatic compound
1826.59	Broad and low intensity	C-H bending	Aromatic compound
1701.22	Broad and strong intensity	C=O stretching C=O stretching	Conjugated acid Conjugated aldehyde
1622.13	Broad and low intensity	-	-
1591.27	Broad and low intensity	-	-
1485.19	Broad and moderate intensity	-	-
1456.26	Broad and moderate intensity	-	-
1381.03	Broad and low intensity	-	-
1309.67	Broad and low intensity	-	-
1273.02	Broad and low intensity	-	-

1244.09	Broad and low intensity	-	-
1155.36	Broad and low intensity	-	-
1068.56	Broad and low intensity	-	-
995.27	Broad and low intensity	-	-
927.76	Broad and low intensity	-	-
862.18	Broad and low intensity	-	-
835.18	Broad and low intensity	-	-
758.02	Broad and low intensity	-	-
700.16	Broad and low intensity	-	-
657.73	Broad and low intensity	-	-
609.51	Broad and low intensity	-	-
547.78	Broad and low intensity	-	-

CONCLUSION

1. Determination of Hydrochloric acid neutralizing capacity of an antacid tablet

The higher the amount of Hydrochloric acid neutralized by Antacids, the better is the acid neutralizing capacity. The result shows that the tablet Rantac 150 has highest acid neutralizing capacity and PAN_L lowest acid neutralizing capacity value. Rantac 150 > Rabifeel – LS > Omee-D > Pantafol-DSR > Rabesec-20 > NEXPRO-40 > Athzol-DSR > ACILOC 150 > Gelusil > PAN-L. The back titration method used in this study is simple, inexpensive and can be used in routine monitoring of the quality of Antacid tablets.

2. FTIR study of Pantafol-DSR

Interpretation of FTIR Spectra of Pantafol-DSR shows Presence of various functional groups such as C-H bending - Aromatic compound; O-H stretching – Alcohol, Carboxylic acid, C=O stretching - Conjugated acid, Conjugated aldehyde, C≡C stretching – Alkyne.

REFERENCES

1. ^ Jump up to:^{a b} *Internal Clinical Guidelines Team. (UK) (2014). Dyspepsia and Gastro-Oesophageal Reflux Disease: Investigation and Management of Dyspepsia, Symptoms Suggestive of Gastro-Oesophageal Reflux Disease, or Both. National Institute for Health and Care Excellence: Clinical Guidelines. London: National Institute for Health and Care Excellence (UK). PMID 25340236.*
2. ^ Jump up to:^{a b} *Salisbury, Blake H.; Terrell, Jamie M. (2020), "Antacids", StatPearls, Treasure Island (FL): StatPearls Publishing, PMID 30252305, retrieved 24 November 2020*

3. [^ "Aluminum hydroxide and magnesium carbonate Uses, Side Effects & Warnings". Drugs.com. Retrieved 24 November 2020.](#)
4. [^ Jump up to:^{a b c} U.S. Department of Health & Human Services. Agency for Healthcare Research and Quality 23 September 2011 \[Consumer Summary – Treatment Options for GERD or Acid Reflux Disease: A Review of the Research for Adults Archived\]\(#\) 11 October 2014 at the \[Wayback Machine\]\(#\)](#)
5. [^ Jump up to:^{a b} Salisbury, Blake H.; Terrell, Jamie M. \(2020\), *"Antacids"*, StatPearls, Treasure Island \(FL\): StatPearls Publishing, \[PMID 30252305\]\(#\), retrieved 23 December 2020](#)
6. [^ Graham, D. Y. \(1982\). *"Pancreatic enzyme replacement: the effect of antacids or cimetidine"*. *Digestive Diseases and Sciences*. 27 \(6\): 485–490. \[doi:10.1007/BF01296725\]\(#\). \[ISSN 0163-2116\]\(#\). \[PMID 6282548\]\(#\). \[S2CID 10640940\]\(#\).](#)
7. [^ Practice Guidelines for Preoperative Fasting and the Use of Pharmacologic Agents to Reduce the Risk of Pulmonary Aspiration: Application to Healthy Patients Undergoing Elective Procedures: An Updated Report by the American Society of Anesthesiologists Task Force on Preoperative Fasting and the Use of Pharmacologic Agents to Reduce the Risk of Pulmonary Aspiration. *Anesthesiology*. 2017 March; 126\(3\).](#)
8. [^ George, J; Majeed, W; Mackenzie, IS; Macdonald, TM; Wei, L \(26 November 2013\). *"Association between cardiovascular events and sodium-containing effervescent, dispersible, and soluble drugs: nested case-control study"*. *BMJ \(Clinical Research Ed.\)*. 347: f6954. \[doi:10.1136/bmj.f6954\]\(#\). \[PMC 3898660\]\(#\). \[PMID 24284017\]\(#\).](#)
9. [^ U.S. Department of Health and Human Services, National Institutes of Health, U.S. National Library of Medicine. Page last updated: 7 November 2014 \[Medline Plus: Taking Antacids\]\(#\)](#)
10. [^ Texter, E. C. \(1989\). *"A critical look at the clinical use of antacids in acid-peptic disease and gastric acid rebound"*. *The American Journal of Gastroenterology*. 84 \(2\): 97–108. \[ISSN 0002-9270\]\(#\). \[PMID 2644821\]\(#\).](#)
11. [^ Hade, J. E.; Spiro, H. \(1992\). *"Calcium and acid rebound: a reappraisal"*. *Journal of Clinical Gastroenterology*. 15 \(1\): 37–44. \[doi:10.1097/00004836-199207000-00010\]\(#\). \[PMID 1500660\]\(#\). \[S2CID 10897187\]\(#\).](#)
12. [^ Bardhan, Karna Dev; Strugala, Vicki; Dettmar, Peter W. \(2012\). *"Reflux Revisited: Advancing the Role of Pepsin"*. *International Journal of Otolaryngology*. 2012: 646901. \[doi:10.1155/2012/646901\]\(#\). \[ISSN 1687-9201\]\(#\). \[PMC 3216344\]\(#\). \[PMID 22242022\]\(#\).](#)
13. [^ Jump up to:^{a b c} Ogawa, Ryuichi; Echizen, Hirotoshi \(2011\). *"Clinically Significant Drug Interactions with Antacids"*. *Drugs*. 71 \(14\): 1839–1864. \[doi:10.2165/11593990-000000000-00000\]\(#\). \[ISSN 0012-6667\]\(#\). \[PMID 21942976\]\(#\). \[S2CID 36875514\]\(#\).](#)
14. [^ Jump up to:^{a b} Patel, Divya; Bertz, Richard; Ren, Song; Boulton, David W.; Någård, Mats \(2020\). *"A Systematic Review of Gastric Acid-Reducing Agent-Mediated Drug–Drug Interactions with Orally Administered Medications"*. *Clinical Pharmacokinetics*. 59 \(4\): 447–462. \[doi:10.1007/s40262-019-00844-3\]\(#\). \[ISSN 0312-5963\]\(#\). \[PMC 7109143\]\(#\). \[PMID 31788764\]\(#\).](#)
15. [^ IFFGD. \[Antacids\]\(#\) Adapted from IFFGD Publication #520 by W. Grant Thompson. Last modified on 12 September 2014](#)
16. [^ Barnett, C. C.; Richardson, C. T. \(1985\). *"In vivo and in vitro evaluation of magnesium-aluminum hydroxide antacid tablets and liquid"*. *Digestive Diseases and Sciences*. 30 \(11\): 1049–1052. \[doi:10.1007/BF01315602\]\(#\). \[ISSN 0163-2116\]\(#\). \[PMID 4053915\]\(#\). \[S2CID 8133980\]\(#\).](#)
17. [^ *"Maalox Antacid Oral: Uses, Side Effects, Interactions, Pictures, Warnings & Dosing"*. WebMD. Retrieved 24 June 2022.](#)

18. [^] [Dubogrey, Ilya \(2013\). "Putting the Fizz into Formulation". European Pharmaceutical Contractor. No. Autumn.](#)
19. [^] [British Pharmacopeia 2003](#)
20. [^] [International Pharmacopoeia 2006. World Health Organization. 2006. pp. 966. ISBN 978-92-4-156301-7. Retrieved 1 July 2013.](#)
21. [^] ["Alka Seltzer Directions of use, Sodium & Aspirin content - Alka Seltzer relief from Headaches, Migraine & Upset stomach". alkaseltzer.ie. Archived from the original on 29 April 2015. Retrieved 17 April 2017.](#)
22. [^] [Blair, G. T.; DeFraties, J. J. \(2000\). "Hydroxy Dicarboxylic Acids". Kirk-Othmer Encyclopedia of Chemical Technology. Kirk Othmer Encyclopedia of Chemical Technology. pp. 1–19. doi:10.1002/0471238961.0825041802120109.a01. ISBN 978-0471238966.](#)
23. [^] [Graham, David Y.; Smith, J. Lacey \(1 March 1986\). "Aspirin and the Stomach". Annals of Internal Medicine. 104 \(3\): 390–398. doi:10.7326/0003-4819-104-3-390. ISSN 0003-4819. PMID 3511824.](#)
24. Evaluation of Neutralizing Capacity of Different Commercial Brands of Antacid Tablets, Abdu, K. and Abbagana, M., Chem Search Journal 6(2): 32 – 34, December, 2015
25. Evaluation of the Acid Neutralizing Capacity of Some Commercially Available Brands of Antacid Tablets in Nigeria, Alalor CA, Avbunudiogba JA , Builders FP, Okpara LO, East African Scholars Journal of Medical Sciences, Volume-2, Issue-1, January-2019, pp 12-16
26. Evaluation of acid neutralizing and buffering capacities of selected antacids in Ghana, Isaac Ayensu, Samuel Oppong Bekoe, Joseph Kwasi Adu, Abena Amponsaa Brobbey, Scientific African Volume 8, July 2020, e00347
27. Evaluation of the Effectiveness of Acid-Neutralizing Property of Traditional Antacids commonly used in India, Divya J.O and Faseela Mohammed Rasheed, Journal of Scientific Research, Volume 65, Issue 4, 2021
28. Evaluation of the acid-neutralizing capacity and other properties of antacids marketed in Morocco, [Mohamed Yafout](#), [Hicham Elhorr](#), [Ibrahim Sbai El Otmani](#), [Youssef Khayati](#), Medicine Pharmacy Reports, 2022 Jan; 95(1): 80–87.

Investigation of Physico-chemical parameters of groundwater from Barshitakli tehsil region, Akola district, Maharashtra, India

Dr. S. S Deshmukh¹, Dr. Tejas R. Patil²

^{1,2}Ghulam Nabi Azad Arts, Commerce and Science College, Barshitakli, Dist. Akola.
Sant Gadge Baba Amravati University, Amravati.
Sanjaydeshmukhakola@gmail.com

ABSTRACT

This investigation determines the ground water quality of regions in Barshitakli tehsil, Akola district in Maharashtra. Samples collected from various bore wells that were used for drinking purposes. The physico-chemical parameters such as Electrical conductivity, pH, Total hardness, Mg hardness, Ca hardness, Mg⁺⁺ ions, Ca⁺⁺ ions and Chloride ion were investigated to determine the present condition of the groundwater quality during the periods from December 2020 to December 2021 (consecutive post monsoon and pre monsoon). Overall ground water quality of Barshitakli tehsil region is unsafe for human being. The groundwater samples of bore well from Alanda and Januna village has the Turbidity beyond prescribed limits of drinking water (IS:10500). The post monsoon sample shows increase in the values of physio-chemical parameters of these two villages were due to higher erosion of soil. The advanced farming and excessive use of chemical fertilizer and pesticides might has resulted in the contamination of ground water.

Keywords: Physico-chemical, groundwater, Electrical conductivity, Turbidity, contamination.

INTRODUCTION

Potable water is also called as life and it has less abundance on the earth. Almost all life processes on earth require water. The 71% of area on the earth's crust is occupied by water but earth's 97% of water is present in the oceans which is too salty for drinking, growing crops and for industrial purposes. The water to be describe as potable, the certain physical, chemical and microbiological standards should be designed so as to ensure the water is potable and safe for drinking (Tebutt, 1993 and Oladipo and Adeboye, 2015). Most of the industries discharge their effluent without proper treatment into nearby open pits or pass them through unlined channels, resulting in the contamination of ground water (Rao and Mamatha, 2004, Mahanta et. al., 2015, Pande et. al., 2010). Potable water should be free from disease causing chemical substances and micro-organisms to health (Ihekoronye and Ngoddy, 1985). The majority of fresh water is existing in the ground in the form of soil moisture and beneath the ground in aquifers.

The aim of present investigation is to study the groundwater samples collected from bore well so as to understand the physico-chemical parameters of water in the Barshitakli tehsil region, Akola district, Maharashtra.

STUDY AREA

Barshitakli is a taluka located in Akola district of Maharashtra. It is one of 7 Talukas of Akola district. There are 159 villages in Barshitakli Taluka. The total area of Barshitakli is 812.97 sq.km with population density of 184 per sq.km.

MATERIAL AND METHODS

The water samples from Barshitakli tehsil were collected from bore wells of ten different villages. Water sample were collected in poly bottle during each consecutive month. Physico-chemical parameters like water temperature, pH and transparency were recorded immediately at the time of sample collection by using thermometer, portable digital pH meter and transparency was measured with the help of Secchi disc respectively. The samples were then transferred to laboratory for further analysis. The Parameters Such as TDS, Hardness and chlorides were estimated in the Laboratory by using standard Methods as prescribed by APHA.

SAMPLE COLLECTION

Ground water samples were collected from ten (10) bore wells at various locations within study area during pre and post monsoon season. Details of sampling locations are along with their co-ordinates illustrated in Table1.

PHYSICO-CHEMICAL ANALYSIS OF GROUND WATER

The collected samples were analyzed for different physico-chemical parameters such as pH, Electrical conductivity, Turbidity, TDS, Total hardness, Ca hardness, Mg hardness, Ca ion, Mg ion, Chloride, and Temperature as per the standard methods (APHA, 1998) and the results were compared with the Indian Standards (IS: 10500) for potable water.

RESULTS AND DISCUSSION

The water quality analysis of different ground water samples has been carried out for pH, Electrical conductivity, TDS, Total hardness, Ca hardness, Mg hardness, Ca ion, Mg ion, Chloride, and Temperature. The status of water quality of these ground water sources is given in table 2.

Table 1: Sampling location and their coordinates

Sampling Location Area Code	Location	Co-ordinates
GW1	Alanda	20.712456, 77.333320
GW2	Barshitakli	20.685510, 77.284157
GW3	Bhendi Mahal	20.666653, 77.268490
GW4	Chincholi Rudrayani	20.832091, 77.544832
GW5	Dagadparwa	20.730045, 77.404649
GW6	Dhaba	20.661896, 77.355489
GW7	Donad BK.	20.654725, 77.302891
GW8	Januna	20.694452, 77.254599
GW9	Kanheri	20.709671, 77.234655
GW10	Mahan	20.700926, 77.321669

Table 2: Showing status of water quality of these ground water sources

Area code	pH		Turbidity (cm)		Conductance (µmhos/cm)		Total Hardness (mg/l)		TDS (mg/l)		Ca Ion (mg/l)		Mg Ion (mg/l)		Chloride (mg/l)		Temp °C	
	Pr	Po	Pr	Po	Pr	Po	Pr	Po	Pr	Po	Pr	Po	Pr	Po	Pr	Po	Pr	Po
GW1	7.3	8.0	11.2	16.5	120	180	170	210	468	450	80	180	72	54	120	140	26	22
GW2	6.7	7.2	5.6	6.5	170	210	180	215	450	509	72	250	74	62	160	164	27	24
GW3	6.9	7.1	3.2	5.2	160	230	210	284	480	450	78	260	68	81	142	155	24	27
GW4	7.3	6.8	4.1	5.6	133	270	210	246	502	457	97	240	87	46	155	190	25	21
GW5	7.2	7.2	2.8	4.3	125	166	240	246	350	605	68	210	72	72	86	120	28	23
GW6	6.3	7.4	3.5	7.1	125	188	250	290	498	544	65	150	64	64	182	20	29	24
GW7	7.2	6.9	3.5	4.7	142	200	270	285	609	807	54	168	68	52	163	190	25	24
GW8	7.1	7.8	8.2	13.2	126	198	286	290	568	402	80	125	64	45	54	144	24	26
GW9	7.5	7.6	4.9	6.1	146	210	244	302	390	512	61	230	81	65	144	203	26	24
GW10	7.4	7.6	7.9	9.5	180	234	246	325	480	562	60	200	54	45	200	256	24	22
Mean	7.225		6.68		175.65		269.3		267.05		136.4		64.5		149.4		23.5	
IS: 10500	6.5- 8.5		5.0-10*		-----		300-600		500-2000*		75-200*		30-100*		250-1000*		--	

Pr- Pre-Monsoon, Po-Post Monsoon

Finding of the present investigation is as follows-

1. The pH value found permissible limit as per IS: 10500 of all samples.
2. Turbidity of samples from Alanda (GW1) and Januna (GW8) found 16.5 and 13.6 respectively which is the not in permissible limits as per IS: 10500.
3. Electrical conductivity varied between 120 to 180 µmhos/cm to 180 to 270 µmhos/cm in pre and post monsoon season.
4. The same trend was observed in the case of total hardness of various ground water sources. It varied from 170 to 280 mg/l and 210 to 325 mg/l in pre and post monsoon respectively.
5. TDS in all the samples were found to be within standard limits (IS:10500). In few samples the ions of calcium have crossed the standard limit (IS: 10500) during post monsoon season.
6. Chloride content of the ground water samples of hand pump were found to be within limit during in the range pre and post monsoon season respectively.
7. Temperature of the various ground water samples were noted to be from 24-29 °C and 21-26 °C during pre and post monsoon season respectively.

CONCLUSION

Overall ground water quality of Barshitakli tehsil region is unsafe for human being. The groundwater samples of bore well from Alanda and Januna village has the Turbidity beyond prescribed limits of drinking water (IS:10500). The post monsoon sample shows increase in the values of physio-chemical parameters of these two villages were due to higher erosion of soil. The advanced farming and excessive use of chemical fertilizer and pesticides might has resulted in the contamination of ground water.

Conflicts of interest: The authors stated that no conflicts of interest.

REFERENCES

- Ihekoronye, A. I., & Ngoddy, P. O. (1985). *Integrated food science and technology for the tropics*. Macmillan.
- Mahanta, C., Enmark, G., Nordborg, D., Sracek, O., Nath, B., Nickson, R. T., ... & Bhattacharya, P. (2015). Hydrogeochemical controls on mobilization of arsenic in groundwater of a part of Brahmaputra river floodplain, India. *Journal of Hydrology: Regional Studies*, 4, 154-171.
- Oladipo, I. C., & Adeboye, O. A. (2015). Physico-chemical and bacteriological analysis of well water used for drinking and domestic purposes in Ogbomosho, Nigeria. *International Journal of Current Microbiology and Applied Sciences*, 4(9), 136-145.
- Pandey, V. P., Chapagain, S. K., & Kazama, F. (2010). Evaluation of groundwater environment of Kathmandu Valley. *Environmental Earth Sciences*, 60, 1329-1342
- Rao, S. M., & Mamatha, P. (2004). Water quality in sustainable water management. *Current science*, 942-947.
- Tebutt, T. H. Y. (1983). Principles of quality control. *Pergalmon, England*, 235.
- .

Identification of confluence of multiple scaffolds required for Aurora Kinase A inhibition

Vijay H. Masand¹, S.D. Thakur², M.M. Rathore¹

¹ Vidya Bharati Mahavidyalaya, Amravati, Maharashtra, India- 444 602

² RDIK and NKD College, Badnera-Amravati, Maharashtra, India.

Abstract:

A vital signaling kinase with a significant function in cell division is Aurora Kinase A (AKA). Therefore, inhibiting AKA is a desirable strategy to reduce cancer. Herein, we report a QSAR (Quantitative Structure-Activity Relationships) analysis based on a set of 892 structurally different AKA inhibitors to explore the features governing AKA inhibition. A QSAR model with high statistical performance was created as per OECD (Organisation for Economic Co-operation and Development) guidelines ($R^2_{tr} = 0.794$, $Q^2_{LOO} = 0.787$, $R^2_{ex} = 0.778$, $CCC_{ex} = 0.880$). Predictive QSAR (external predictive ability) and Mechanistic QSAR (mechanistic interpretations) are well-balanced in the recently developed QSAR model, which is based on a set of eight variables. The present QSAR analysis is successful in identifying not only obscure and obvious structural features, but also the reported and unpublished pharmacophoric characteristics. The present research suggests that non-ring nitrogen atoms in combination with planar nitrogen and non-ring oxygen must exist at a precise distance from one another. Furthermore, the limit for simultaneous existence of sp^2 oxygen with sp^3 carbon and ring oxygen is a new feature identified in the present work.

Introduction:

The mitotic machinery, also known as cell division mechanism, is profoundly regulated[1]. Any abnormality or defect in mitosis produces nondiploid DNA, which eventually leads to cancer. The development of cancer chemotherapy drugs that specifically target centrosome maturation and separation, mitotic spindle assembly, chromosomal segregation, and cytokinesis has therefore attracted the attention of researchers. These processes involve the crucial role of several signaling kinases, such as Aurora[2], Plk (Polo-like kinase), and Cdk (cyclin-dependent kinase), to name a few. The Aurora kinase family of serine/threonine kinases is essential for the reliable accomplishment of mitosis[3]. Therefore, these kinases have drawn a lot of attention since their discovery in 1995 and the early identification of their expression in human cancer tissue in 1998. The present involves QSAR analysis to identify important structural features.

Methodology:

The structures were downloaded from ChEMBL (<https://www.ebi.ac.uk/chembl/>) for further analysis. The next step involves conversion of SMILES notation to 3D-optimized structure using MMFF94 (Cut-off: 0.01). Then, the molecular descriptors were calculated using PyDescriptor[4] and PaDEL[5]. Before actual feature selection, descriptor pruning was accomplished. After getting the reduced pool of descriptor GA-MLR was used for model building. After that, the model was validated using different parameters.

Results and Discussion:

The eight parametric model along with its statistical validation is as following:

Model-A:

	Estimate	Std. Error	t value	Pr(> t)	Conf.Int.(+/-95%)
(Intercept)	7.521	0.0314	239.8884	0	0.0616
fringOH6B	0.334	0.0204	16.3689	0	0.0401
fnotringNplaN3B	1.1305	0.0453	24.9618	0	0.0889
fsp2Osp3C4B	0.4022	0.0338	11.8862	0	0.0664
fnotringOnotringN5B	0.4113	0.0546	7.527	0	0.1073
r_ringO_sp2O	-0.9131	0.0796	-11.4699	0	0.1563
r_sp3C_sp2O	-0.1813	0.0089	-20.431	0	0.0174
KRFPC992	-0.7937	0.0361	-21.9712	0	0.0709
KRFPC3612	-1.7261	0.0679	-25.4162	0	0.1333

Statistical parameters associated with Model-A:

S.N.	Parameter	Value	S.N.	Parameter	Value
1.	R2_tr	0.7941	20.	RMSE_ex	0.5129
2.	Adj-R2	0.7918	21.	PRESS_ex	47.0818
3.	F(8-704)	339.4136	22.	Q2F1	0.7674
4.	RSS_tr	154.2898	23.	Q2F2	0.7661
5.	MSE_tr	0.2164	24.	Q2F3	0.7497
6.	RMSE_tr	0.4652	25.	MAE_ex	0.4328
7.	MAE_tr	0.3911	26.	K	1.0069
8.	s	0.4681	27.	K_prime	0.9881
9.	AIC	952.0537	28.	R2ext	0.7782
10.	BIC	997.7485	29.	CCC_ex	0.8802
11.	CCC_tr	0.8852	30.	r2m_ExPy	0.6736
12.	Q2_cv	0.7872	31.	r2m_EyPx	0.701
13.	RMSE_cv	0.473	32.	R2o	0.7683
14.	MSE_cv	0.2237	33.	R2o_dash	0.7601
15.	PRESS_cv	159.498	34.	Clos_dash	0.0232
16.	MAE_cv	0.3969	35.	Clos	0.0126
17.	R2_Yscr	0.011	36.	r2m_avg	0.6873
18.	MSE_ex	0.263	37.	r2m_delta	0.0273
19.	Training Set Compounds	713	38.	Prediction Set Compounds	179

The details of descriptors are as following:

Descriptor	Details	Software used
fringOH6B	Frequency of occurrence of hydrogen exactly at six bonds from ring oxygen	PyDescriptor
fnotringNplaN3B	Frequency of occurrence of planer nitrogen exactly at three bonds from non-ring nitrogen	PyDescriptor
fsp2Osp3C4B	Frequency of occurrence of sp ³ -hybridized carbon exactly at four bonds from sp ² -hybridized oxygen	PyDescriptor

fnotringOnotringN5B	Frequency of occurrence of non-ring nitrogen exactly at five bonds from non-ring oxygen	PyDescriptor
r_ringO_sp2O	Ratio of ring oxygen to sp ² -hybridized oxygen	PyDescriptor
r_sp3C_sp2O	Ratio of sp ³ -carbon to sp ² -hybridized oxygen	PyDescriptor
KRFPC992	[!#1][NH]c1[cH][cH][cH]c(!#1)[cH]1 Meta-substituted aniline ring	PaDEL
KRFPC3612	Cc1ccn[nH]1 3-substituted pyrazole moiety	PaDEL

Model-A contains eight molecular descriptors covering broad chemical space. Four of the eight descriptors, namely fringOH6B, fnotringNplaN3B, fsp2Osp3C4B, and fnotringOnotringN5B, have positive coefficients in model-A, suggesting that augmenting their value could result in a better inhibition of AKA. The opposite is true for the four remaining descriptors, r_ringO_sp2O, r_sp3C_sp2O, KRFPC992, and KRFPC3612. It is to be noted that every molecular descriptor is a mathematical (or numeric) representation of one or more pharmacophoric features that control the biological profile. Further, the final biological activity (say IC₅₀, K_i, etc.) of a molecule varies with multiple pharmacophore features and not by a single feature. In other words, the biological activity is the result of a confluence of various structural characteristics and some unidentified elements. Some characteristics are in charge of enhancing the desired pharmacological action, while others are responsible for reversing it. It is thought that the biological activity is determined concurrently by two or more pharmacophoric groups (Pharmacophore synergism).

Conclusion:

The present research suggests that non-ring nitrogen atoms in combination with planar nitrogen and non-ring oxygen must exist at a precise distance from one another. Furthermore, the limit for simultaneous existence of sp² oxygen with sp³ carbon and ring oxygen is a new feature identified in the present work. In conclusion, the AKA inhibitory activity is associated with a group of structural features.

References:

1. Du R, Huang C, Liu K, et al. Targeting AURKA in Cancer: molecular mechanisms and opportunities for Cancer therapy. *Molecular Cancer*. 2021;20(1). doi: 10.1186/s12943-020-01305-3.
2. Bavetsias V, Linardopoulos S. Aurora Kinase Inhibitors: Current Status and Outlook. *Frontiers in Oncology*. 2015;5. doi: 10.3389/fonc.2015.00278.
3. Borisa AC, Bhatt HG. A comprehensive review on Aurora kinase: Small molecule inhibitors and clinical trial studies. *European Journal of Medicinal Chemistry*. 2017;140:1-19. doi: 10.1016/j.ejmech.2017.08.045.
4. Masand VH, Rastija V. PyDescriptor : A new PyMOL plugin for calculating thousands of easily understandable molecular descriptors. *Chemometrics and Intelligent Laboratory Systems*. 2017;169:12-18. doi: 10.1016/j.chemolab.2017.08.003.
5. Yap CW. PaDEL-descriptor: An open source software to calculate molecular descriptors and fingerprints. *Journal of Computational Chemistry*. 2010;32(7):1466-1474. doi: 10.1002/jcc.21707.

Synthesis, Characterization and Biological Evaluation of 4-(4-Bromo-1-Hydroxy Naphthalen-2-Yl)-6-(4-Hydroxy Phenyl)-5,6-Dihydropyrimidine-2(1h)-One

Dr. V. M. Sherekar^{*1}, Mr. Nilesh S. Padole²

Assistant Professor, Department of Chemistry, Vinayak Vindhyan Mahavidyalaya Nandgaon (Kh), Dist. Amravati (M.S), India.

Head and Assistant Professor, Department of Chemistry, Vinayak Vidnyan Mahavidyalaya, Nandgaon Khandeshwar, Dist. Amravati (M.S.), India.

ABSTRACT: -

1-(4-Bromo-1-hydroxynaphthalen-2-yl)-ethan-1-one was prepared by refluxing 4-bromonaphthalen-1-ol with glacial acetic acid in presence of fused ZnCl_2 . By condensing 1-(4-bromo-1-hydroxynaphthalen-2-yl)-ethan-1-ones with 4-Hydroxy benzaldehyde, to prepared by 1-(4-bromo-1-hydroxynaphthalen-2-yl)-3-(4-Hydroxy phenyl)-prop-2-en-1-one were synthesized. 1-(4-bromo-1-hydroxynaphthalen-2-yl)-3-(4-Hydroxy phenyl)-prop-2-en-1-one, urea and concentrated HCl in DMF were added and refluxed. Cool and pour in crushed ice. Treat it with cold NH_4OH solution to obtain titled compounds. The compounds thus synthesized have been characterized by physical and spectral data. All of these titled synthesized compounds have been screened for antimicrobial study and are found to possess excellent antimicrobial activities.

KEYWORDS: - antimicrobial activities, cold NH_4OH solution, concentrated HCl in DMF.

INTRODUCTION: -

Dihydropyrimidin-2(1H)-one are classified as hetero-cyclic compound and containing pyrimidine ring which is containing two nitrogen atoms in the six-member ring. Dihydropyrimidine are the most important heterocyclic ring system which play an important role in the synthesis of DNA and RNA. They widely using multi-component reaction like Biginelli reaction. In the field of heterocyclic chemistry dihydropyrimidine-2(1H)-one was synthesized through the one-pot condensation of an aromatic aldehyde and urea in the presence of the basic [1-3]. Dihydropyrimidines are one of the important heterocyclic compounds, which are of interest due to its efficiency towards various pharmacological uses [4]. The synthesis of the dihydropyridine and their derivatives increasing tremendously significant because they generally show diverse medicinal properties [5]. Newly researcher goal dihydropyrimidine derivatives modulated heat shock responses and have neuroprotective responses such like that optimized for their ability to modulate cellular stress responses based on favorable toxicological data [6]. Many aryls substituted dihydropyrimidine-2-one are found to exhibited biological activities [7]. Many reports exploring in Vivo and in Vitro dihydropyrimidine-2-one derivatives show variety of pharmacological activities such as active and safe tumor anti-initiating and multi-potent blocking agent [8], anxiolytic [9], antihypertensive agents [10], anticonvulsant [11], anticancer [12], analgesic activities [13], anti-bacterial [14], channel blockers [15], anti-HIV [16].

Their efforts are quite significant in literature hence considering the scope of dihydropyrimidine derivatives we have synthesized novel 4-(4-bromo-1-hydroxynaphthalen-2-yl)-6-(4-hydroxy phenyl)-5,6-dihydropyrimidine-2(1h)-one from 4-bromonaphthalen-1-ol and studied for their biological activities.

MATERIALS AND METHOD: -

Synthesis of 1-(4-Bromo-1-hydroxynaphthalen-2-yl)-ethan-1-one.

1-(4-Bromo-1-hydroxynaphthalen-2-yl) ethan-1-one was prepared by modified Nenchi's method in which 4-bromo-naphthalen-1-ol was refluxed with glacial acetic acid in presence of fused ZnCl_2 .

Synthesis of 1-(4-Bromo-1-hydroxynaphthalen-2-yl)-3-(4-Hydroxy phenyl)-prop-2-en-1-one.

1-(4-Bromo-1-hydroxynaphthalen-2-yl)-3-(4-Hydroxy phenyl)-prop-2-en-1-one were synthesized from 1-(4-Bromo-1-hydroxynaphthalen-2-yl) ethan-1-one by condensing it with 4-Hydroxy benzaldehyde were added in ethanol solvent and KOH mixture.

Synthesis of 4-(4-Bromo-1-hydroxy naphthalen-2-yl)-6-(4-Hydroxy phenyl)-5,6-dihydropyrimidine-2(1H)-one.

4-(4-Bromo-1-hydroxy naphthalen-2-yl)-6-(4-methoxy phenyl)-5,6-dihydropyrimidine-2(1H)-one were prepared from 1-(4-Bromo-1-hydroxynaphthalen-2-yl)-3-(4-Hydroxy phenyl)-prop-2-en-1-one was reflux with urea and concentrated HCl in DMF. It was then treated with cold NH_4OH .

In present work the compounds under investigation are: -

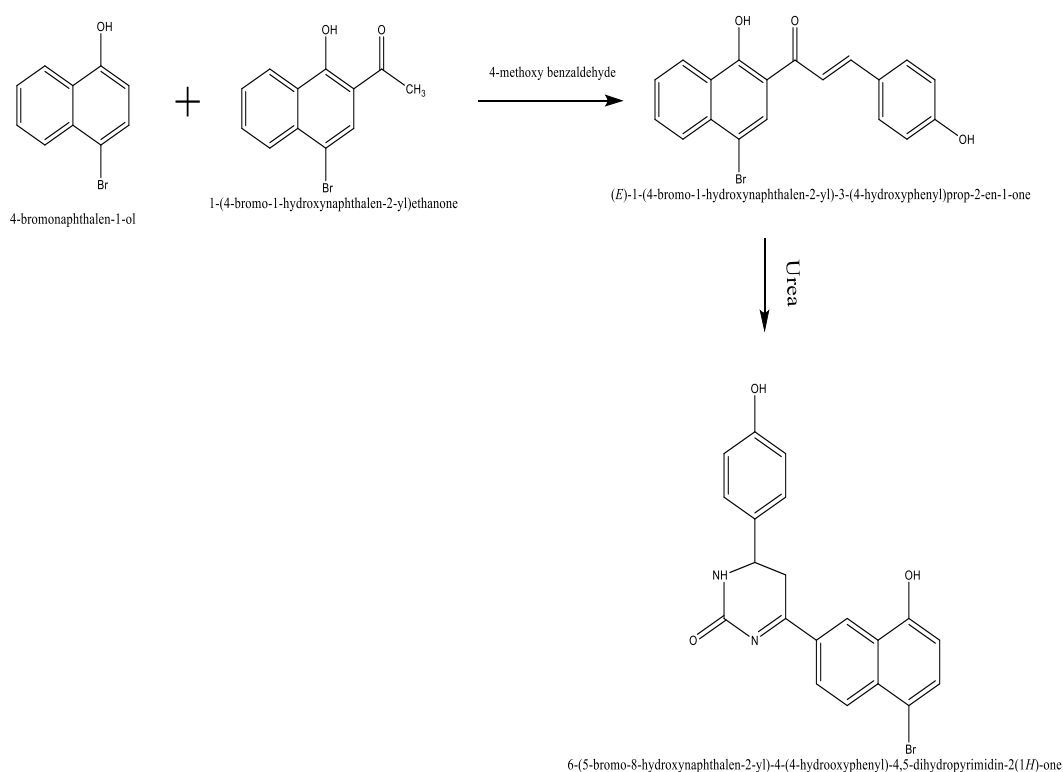
Compound 1: 4-(4-Bromo-1-hydroxy naphthalen-2-yl)-6-(4-hydroxy phenyl)-5,6-dihydropyrimidine-2(1H)-one.

Compound 2: 4-(4-Bromo-1-hydroxy naphthalen-2-yl)-6-(3, 4-hydroxy phenyl)-5,6-dihydropyrimidine-2(1H)-one.

Compound 3: 4-(4-Bromo-1-hydroxy naphthalen-2-yl)-6-(3-Hydroxy phenyl)-5,6-dihydropyrimidine-2(1H)-one.

Compound 4: 4-(4-Bromo-1-hydroxy naphthalen-2-yl)-6-(4-Hydroxy phenyl)-5,6-dihydropyrimidine-2(1H)-one.

SCHEME: -



Sr. no	Compound no	R1	R2	Molecular formula	Melting Point °C	% Yield	% Nitrogen		R.F Value
							Found	Calculated	
1	1	- OCH ₃	-H	C ₁₇ H ₁₇ N ₂ O ₂ Br	259 ⁰ C	45%	6.64	6.61	0.55
2	2	- OCH ₃	OCH ₃	C ₁₇ H ₁₉ N ₂ O ₄ Br	225 ⁰ C	48%	6.21	6.74	0.59
3	3	-H	-OH	C ₁₇ H ₁₅ N ₂ OBr	228 ⁰ C	45%	6.89	6.84	0.55
4	4	-OH	-H	C ₁₇ H ₁₅ N ₂ O ₂ Br	269 ⁰ C	51%	5.84	5.85	0.58

Table 1. PHYSICAL DATA OF SYNTHESIZED COMPOUNDS**SPECTRAL ANALYSIS: -**

IR(vmax) (cm⁻¹): 1624 (C=O, str), 3346 (NH, str), 1568 (C=N), 1171 (C-O-C), 758 (monosubstituted Benzene)

NMR (δ ppm): 1.3-1.8 (m, 2H, -CH₂ of pyrimidine), 10.30 (s, 1H, -OH), 3.61 (s, 3H, -OH), 2.51 (s, 3H, CH₃),

ANTIMICROBIAL STUDIES: -

All above synthesized 4-(4-Bromo-1-hydroxy naphthalen-2-yl)-6-(4-hydroxy phenyl)-5,6-dihydropyrimidine-2(1H)-one have been studied for their antimicrobial activity against *Escherichia coli*, *Proteus mirabilis*, *Staphylococcus aureus*, *Pseudomonas aeruginosa*. The culture of each species was incubated at 37⁰C and the zone of inhibition was measured after 24 hr. Results are tabulated in Table. Most of these compounds were found active

Sr. no	Compound Number	Antimicrobial Activity			
		E-coli	Proteus mirabilis	Staphylococcus aureus	Pseudomonas aeruginosa
1	1	17	18	15	10
2	2	18	10	16	14
3	3	16	13	14	15
4	4	15	14	12	13

Strongly active, range 15-19 Weakly active, range 7-10 mm, moderately active, range 11-14mm, Inactive, -

CONCLUSION: -

Thus, from above results it was observed that these heterocyclic compounds were found effective against *Escherichia coli*, *Proteus mirabilis*, *Staphylococcus aureus*, *Pseudomonas aeruginosa*. So those compounds can be easily be used for the treatment of diseases caused by test pathogens, only when they do not have toxic and other side effects.

REFERENCE: -

1. MF Custodio; CC Allane et al. Z. Kristallogr, 2019, 234 (10), 657-669.
2. P Jain; A Patil. World J. Pharm. Res. 2018, 7(11), 410-427.
3. V Garg; D Jindal; R Singh. TJPLS Journal, 2020, 7, 6, 8-12.
4. A Huseynzada et al; Royal Society of Chemistry, 2021, 11, 11, 6312-6329
5. A Malah; Z Mahmoud; H H Salem; A Abdou; M Soliman; R Hassan. Green Chemistry Letters and Reviews, 2021, 14, 2, 220-232.
6. K Agnes et al. J Alzheimers Dis, 2016, 53 (2), 557-571.
7. VM Sherekar; SE Bhandarkar. Am. J. PharmTech Res. 2016, 6(5), 560-56.
8. VM Sherekar; SE Bhandarkar; World J. Pharm. Res. 2016, 2(6), 275-279.
9. B Padmashali; BN Chidananda; B Govindappa; S Basavaraj. J. Appl. Pharm. Science. 2019, 9(5), 133-140.
10. F Alam; R Amin. IJPSR, 2020, 32, 10, 46-55.
11. V A Adol et al. Material Science Research India, 2020, 17, 1, 13-26.
12. R Al-Saheb et al. Bioscience Reports, 2020, 40, 9, 1-13.
13. R Kaur; S Chaudhary; K Kumar; MK Gupta; RK Rawal. Eur J Med Chem. 2017, 132, 108-134.
14. AY Vargas; HA Rojas; GP Romanelli; JJ Martinez. Green Process Synth. 2017, 6(4), 377-384.
15. R M Keshk; B M Izzularab. Current Organic Synthesis, 2021, 18, 0, 1-10.
16. N Podilla; C Tirthankar. JAOPR, 2018, 6, 1, 11-15.

Efficient Synthesis of Salicylaldehyde-Based Schiff Bases Using Hydrothermal Sonication: A Green Approach

**Vivek Ramkrushna Mate^{a*}, Datta Anandrao Patil^b, Kalpana B. Gawande^c,
Sanjay R. Thakare^c, and Rajkumar Uddhavrao Pokalwal^b**

^a Department of Chemistry, Yashwantrao Chavan College, Mangrulpir, Washim, Maharashtra, India.

^b Department of Chemistry, Degloor College, Degloor, Nanded, Maharashtra, India.

^c Department of Chemistry, Institute of Science, Nagpur, Maharashtra, India.

This study presents a novel, efficient, and environmentally friendly procedure for the synthesis of a series of salicylaldehyde-based Schiff bases utilizing hydrothermal sonication. The procedure involves the condensation of salicylaldehyde with various aromatic amines in water under hydrothermal sonication conditions. Through meticulous selection of the solvent and reaction conditions, the final products are obtained in excellent yields in a single-step procedure. Comparative experiments under thermal conditions yielded lower yields and necessitated more laborious work-up processes. The hydrothermal sonication method demonstrates several advantages, including reduced reaction time, increased conversion, minimized waste production, and favorable yields. The synthesized compounds' structures were confirmed through the analysis of Infrared (IR), Proton Nuclear Magnetic Resonance (¹HNMR and ¹³CNMR), and Mass Spectra data. This research highlights the efficiency and environmental benefits of the hydrothermal sonication method in synthesizing salicylaldehyde-based Schiff bases.

Introduction

The increasing focus on the environmental impact of chemicals has prompted a drive towards cleaner and more eco-friendly synthetic processes. Stringent regulations are geared towards promoting sustainability by minimizing waste generation, eschewing the use of auxiliary substances such as organic solvents and additional reagents, and reducing energy demands. The utilization of water as the reaction medium is particularly advantageous in this context. Firstly, water is cost-effective, nonflammable, non-toxic, and poses minimal safety concerns [1, 3]. Secondly, its distinct physical and chemical properties often augment reactivity or selectivity, which may not be attainable with organic solvents. Lastly, employing water obviates the necessity to dry substrates or reagents prior to use, thereby diminishing or eliminating the consumption of drying agents, energy, and time.

The synthesis of Schiff bases traditionally involves the condensation of a primary amine with an aldehyde, often employing organic solvents such as methanol, tetrahydrofuran (THF), and 1,2-dichloroethane (DCE) [4]. Additionally, solvent-free methods utilizing hydrothermal sonication have been reported for the synthesis of Schiff bases [5]. A comparative analysis of these synthesis methods for simple Schiff bases revealed that hydrothermal sonication irradiation represents the most straightforward approach [6].

The use of Schiff base compounds as ligands is widespread due to their facile formation and diverse coordination chemistry, enabling their application as catalysts in various asymmetric reactions [7, 8]. Notably, Schiff base complexes derived from salicylaldehyde, 2-aminol, and 3,4-thiadiazole have been evaluated for their antibacterial activity against a range of bacterial strains, including *Escherichia coli*, *Staphylococcus aureus*, and *Pseudomonas aeruginosa* [9].

It was observed that the antibacterial efficacy of these Schiff bases was enhanced through chelation/complexation, demonstrating significant activity against the tested bacterial strains and presenting new avenues in combating antibiotic-resistant strains. In light of these discoveries, this manuscript presents the hydrothermal sonication-assisted synthesis of salicylaldehyde-based Schiff bases in aqueous media.

The synthesis of Schiff bases has been extensively documented in the literature [10–13]. However, the reported methods often entail a laborious process utilizing methanol or ethanol as solvents, leading to prolonged reaction times. Typically, the synthesis of Schiff bases through condensation reactions necessitates stringent conditions, including the use of a Dean Stark apparatus, catalysts, elevated temperatures, and extended reaction durations [14]. Notably, the significance of the fluorinated Schiff bases discussed in this manuscript is equally noteworthy. This significance stems from the influence of fluorine substitution on inter- and intramolecular forces, which affect ligand binding and introduce receptor subtype selectivity in biological systems [15, 16]. The breadth and universality of this synthetic process are demonstrated with respect to salicylaldehyde and various fluorinated amines.

In conclusion, we introduce a sustainable and effective approach for synthesizing Schiff bases in aqueous media, as illustrated in Scheme 1. The uncomplicated workup, convenient conditions, swift reaction kinetics, high yields, and reaction specificity collectively enhance the appeal of the current methodology.

Experimental

The purity of the compound was assessed using silica-gel-coated aluminum plates (Merck). Melting points were determined in open capillary tubes. Infrared (IR) spectra were recorded with KBr on a Perkin Elmer Spectrum RX-1 FTIR spectrophotometer. Proton nuclear magnetic resonance (^1H -NMR) and carbon-13 nuclear magnetic resonance (^{13}C -NMR) spectra were acquired on a Jeol JNM-ECX400P instrument operating at 400 MHz. Hydrothermal ultrasonication irradiations were conducted in a hydrothermal sonication synthesizer operating at 37 KHz using Hielscher instrument. All chemicals utilized were of analytical grade.

Conventional Method

Schiff bases were synthesized through the condensation of salicylaldehyde (0.005 mol) with various aromatic amines (a–f) (0.005 mol) in 10 mL of water. The reaction mixture was stirred at ambient temperature, and the progress of the reaction was monitored using thin-layer chromatography (TLC). Upon completion of the reaction, the product was isolated, filtered, dried, and subsequently recrystallized using methanol.

Hydrothermal ultra sonication method

The hydrothermal ultrasonication synthesis method involves subjecting the reactants to high-frequency ultrasound, generating intense sound waves that stimulate chemical reactions. In this sonochemical approach, the reactants are placed in a sonication vessel, exposed to high-frequency ultrasound, leading to localized heating, elevated pressures, and increased concentrations of reactive species, facilitating chemical transformations and yielding the desired Schiff base product.

A mixture comprising salicylaldehyde (0.005 mol) and substituted aromatic amines (2a–f) (0.005 mol) in 10 mL of water was introduced into a hydrothermal sonication tube. The contents underwent hydrothermal sonication irradiation at 37 KHz for a duration of 1 hour. The progress of the reaction was monitored via thin-layer chromatography (TLC). Upon completion

of the reaction, a solid product formed in the reaction mixture, which was subsequently filtered and recrystallized using methanol. The recrystallization process yielded the title compounds in the form of solid crystals.

Results and Discussion

A novel environmentally friendly method utilizing water as a solvent for the synthesis of Schiff bases has been successfully developed, as depicted in the schematic representation in Scheme 1. The optimization of %yield was investigated at various temperatures, revealing an optimal yield at 70 °C. Beyond this temperature, there was no significant change in yield, as summarized in Table 1. The results indicate that at 30 °C, the yield is 5.5%, and with an increase in temperature to 70 °C, the yield significantly improves to 53.5%. This tenfold increase in activity may be attributed to enhanced solubility, increased agitation, and a reduction in intermolecular distances. Consequently, the synthesis of other products (b–f) was carried out under the same reaction conditions, maintaining a temperature of 70 °C. The data suggests that the environmentally friendly method using water as a solvent, particularly at a temperature of 70 °C, significantly enhances the %yield for the synthesis of Schiff bases.

Table 1: Comparison of yield of Schiff base (a) at different temperatures under Hydrothermal ultra sonication.

Compound	Temperature (°C)	% Yield
3a	30	5.5
3a	35	7.5
3a	40	9.5
3a	45	10.0
3a	50	13.6
3a	55	19.5
3a	60	35.4
3a	65	46.2
3a	70	53.5
3a	75	55.1
3a	80	55.5

Reaction Conditions :- Sonication 37 KHz, Time 1 hr, solvent water, and aldehyde : base concentration 1:1 moles.

The impact of different compositions on %yield is detailed in Table 2. A variation in aldehyde and base composition resulted in an increase in %yield from 45.5 to 54.5. This observed increase is likely attributed to the stoichiometric composition of salicylaldehyde and substituted aromatic amines. The optimal %yield of 53.5 was achieved for a composition ratio of 1:1. Consequently, the same composition was adopted for the synthesis of other compounds (b-f). It's clear that the composition ratio of salicylaldehyde and substituted aromatic amines played a significant role in achieving the optimal %yield of 53.5. This information can be valuable for further experiments or scale up applications.

Table 2: Effect of composition of aldehyde and base for the formation of Schiff base (a)

Composition		% Yield
Aldehyde (mole)	Base (mole)	
1	0.75	45.5

1	1.00	53.5
1	1.25	54.1
1	1.50	54.5

Reaction Conditions :- Temperature 70 °C, sonication 37 KHz, Time 1 hr, solvent water.

The comparative result analysis of the hydrothermal ultrasonication method is presented in Table 3. The results obtained with this method were significantly higher, by almost 50%, compared to the conventional hydrothermal method. This suggests that the hydrothermal ultrasonication method, by enhancing the contact time of reactants, leads to a higher %yield. Consequently, this highlights the advantageous nature of the hydrothermal ultrasonication synthesis for the preparation of various Schiff bases. The data indicates that the hydrothermal ultrasonication method is a more effective approach for the synthesis of Schiff bases, resulting in a substantial increase in %yield compared to the conventional hydrothermal method. This insight could be valuable for researchers and practitioners in the field of chemical synthesis.

Table 3: Comparative study of hydrothermal ultra sonication and conventional method.

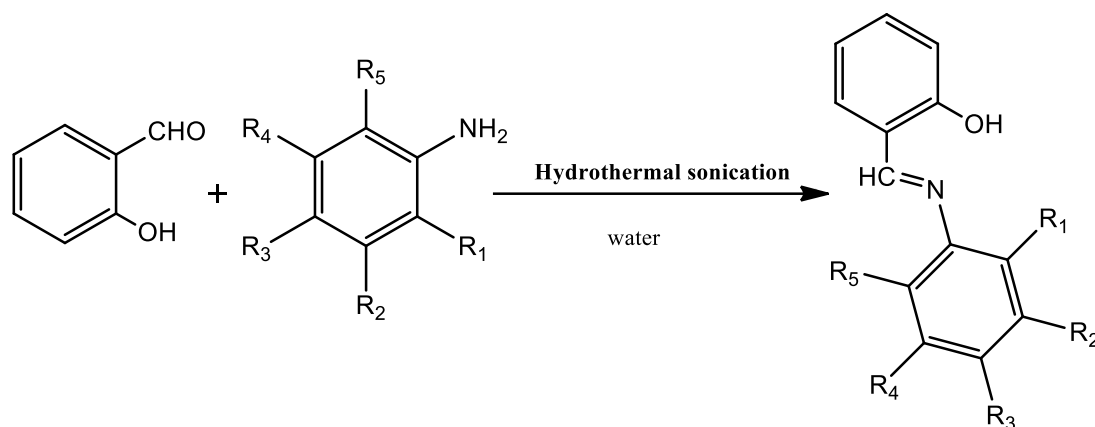
Compound	% Yield	
	Hydrothermal ultra sonication	Conventional
a	53.5	21.0
b	85.6	37.9
c	81.3	37.5
d	80.4	37.5
e	78.4	39.8
f	80.5	32.5

Reaction Conditions :- Temperature 70 °C, sonication 37 KHz, Time 1 hr, solvent water and aldehyde : base concentration 1:1 moles.

Product Characterization Data

- (E)-2-(((2,4-dimethylphenyl)imino)methyl)phenol, colorless solid, M.P. 91- 93°C, IR (KBr, cm^{-1}): 2927.60, 2700, 1615.96, 1490.71, 1282.72, 1144.23, ^1H NMR (400 MHz, CDCl_3) (δ ppm): 8.87 (1CH, s), 7.66 (1H, d), 7.08 (2H, d), 70.2 (1H, s), 7.01 (1H, m), 2.34 (6H, m). ^{13}C -NMR (CDCl_3) (δ ppm): 161.1, 160.0, 132.4, 132.1, 121.4, 120.5, 117.8, 148.1, 132.2, 128.7, 128.7, 127.3, 122.1, 21.6, 18.6, . M/S: 226.12 (M + 1).
- 2-[(4-Chloro-phenylimino)-methyl]-phenol [10]. Yellow solid, M.p. 95–98°C, IR (KBr, cm^{-1}): 2920.94, 1620.86, 1487.51, 1278.31, 1134.17, ^1H NMR (400 MHz, CDCl_3): δ ppm = 13.06 (1CH, s), 8.88 (1H, s), 7.67 (2H, d), 7.57 (1H, m), 7.49 (1H, t), 6.70 (3H, m). ^{13}C -NMR (CDCl_3) (δ ppm): 159.21, 164.71, 163.28, 158.72, 138.09, 134.02, 133.01, 122.08, 120.72, 119.02, 117.41, 112.01, 105.05. M/S: 234.8 (M + 1).
- 2-[(4-Chloro-phenylimino)-methyl]-phenol [11]. Golden solid, M.p. 70–73°C, IR (KBr, cm^{-1}): 2950.53, 1617.09, 1474.16, 1272.73, 841.22, ^1H NMR (400 MHz, CDCl_3): = δ 12.92 (1 H, s), 8.41 (1 H, s), 7.64 (2 H, d), 7.51 (2 H, d), 7.52 (2 H, dd), 7.34 (1 H, d), 7.02 (1 H, t). ^{13}C -NMR (CDCl_3) (δ ppm): 163.07, 162.08, 148.01, 134.01, 133.32, 132.27, 132.18, 129.11, 123.03, 120.07, 119.01, 118.10. M/S: 232.84 (M+ 1).

- (d) 2-[(2,3,4,5-Tetrafluoro-phenylimino)-methyl]-phenol [12]. Greenish solid, M.p. 141–143°C, IR (KBr, cm^{-1}): 2931.04, 1618.71, 1467.17, 1040.21, 775.99. ^1H NMR (400 MHz, CDCl_3): δ ppm = (1H, s), 8.41 (1H, s), 7.34 (2H, dd), 7.16 (1H, d), 6.91 (2H, m). ^{13}C -NMR (CDCl_3) (δ ppm): 164.19, 159.30, 139.25, 134.99, 132.55, 131.72, 129.95, 129.66, 117.83, 117.49, 116.58, 115.61, 101.07. M/S: 270.27 (M + 1).
- (e) 2-[(4-Bromo-phenylimino)-methyl]-phenol [11, 12]. Greenish solid, M.p. 97–99°C, IR (KBr, cm^{-1}): 2911.15, 1616.74, 1480.31, 1271.05, 837.16, 763.41, ^1H NMR (400 MHz, CDCl_3): δ ppm = (1H, s), 8.55 (1H, s), 7.51 (2H, d), 7.49 (2H, m), 7.11 (2H, d), 7.12 (1H, d), 6.97 (1H, t). ^{13}C -NMR (CDCl_3) (δ ppm): 161.99, 161.23, 147.67, 133.48, 132.44, 132.79, 122.19, 120.34, 119.41, 119.50, 117.62. M/S: 276.1 (M + 1).
- (f) 2-[(4-Fluoro-phenylimino)-methyl]-phenol [13]. Yellow solid, M.p. 71–73°C, IR (KBr, cm^{-1}): 2927.88, 1614.71, 1494.00, 1260.05, 830.04, ^1H NMR (400 MHz, CDCl_3): δ ppm= 13.01 (1H, s), 8.58 (1H, s), 7.37 (2H, m), 7.26 (2H, m), 7.12 (2H, m), 7.03 (1H, d), 6.94 (1H, t). ^{13}C -NMR (CDCl_3) δ ppm= 163.40, 161.08, 159.17, 142.01, 131.08, 128.45, 121.02.



- a) :- $\text{R}_1 = \text{CH}_3$, $\text{R}_2 = \text{H}$, $\text{R}_3 = \text{CH}_3$, $\text{R}_4 = \text{H}$, $\text{R}_5 = \text{H}$
 b) :- $\text{R}_1 = \text{F}$, $\text{R}_2 = \text{H}$, $\text{R}_3 = \text{F}$, $\text{R}_4 = \text{H}$, $\text{R}_5 = \text{H}$
 c) :- $\text{R}_1 = \text{H}$, $\text{R}_2 = \text{H}$, $\text{R}_3 = \text{Cl}$, $\text{R}_4 = \text{H}$, $\text{R}_5 = \text{H}$
 d) :- $\text{R}_1 = \text{F}$, $\text{R}_2 = \text{F}$, $\text{R}_3 = \text{F}$, $\text{R}_4 = \text{F}$, $\text{R}_5 = \text{H}$
 e) :- $\text{R}_1 = \text{H}$, $\text{R}_2 = \text{H}$, $\text{R}_3 = \text{Br}$, $\text{R}_4 = \text{H}$, $\text{R}_5 = \text{H}$
 f) :- $\text{R}_1 = \text{H}$, $\text{R}_2 = \text{H}$, $\text{R}_3 = \text{F}$, $\text{R}_4 = \text{H}$, $\text{R}_5 = \text{H}$

Conclusions

In summary, the synthesis of Schiff bases through condensation reactions using both conventional hydrothermal and hydrothermal ultrasonication methods was investigated, with the latter proving to be the more efficient approach. The tenfold increase in activity observed with an increase in temperature from 30 to 70 °C can be attributed to enhanced solubility, increased agitation, and a reduction in intermolecular distances. The highest %yield, reaching 53.5%, was achieved with a composition of salicylaldehyde and the base at a temperature of 70 °C. The optimal composition of salicylaldehyde and substituted aromatic amines was found to be 1:1 for maximum %yield. Subsequently, the synthesis of other products (b–f) was carried out with a composition ratio of 1:1, maintaining a temperature of 70 °C. The data obtained indicates that the hydrothermal ultrasonication method is a more effective approach for the synthesis of Schiff bases, resulting in a substantial increase in %yield compared to the

conventional hydrothermal method. This insight holds significance for researchers and practitioners in the field of chemical synthesis.

References

- 1) S. Bhagat, N. Sharma, and T. Singh Chundawat, "Synthesis of Some Salicylaldehyde-Based Schiff Bases in Aqueous Media" *Journal of Chemistry*, Vol. 2013, Article ID 909217, pp. 1-4. 2013.
- 2) C. J. Li, "Organic reactions in aqueous media with a focus on carbon-carbon bond formations: a decade update," *Chemical Reviews*, vol. 105, no. 8, pp. 3095–3165, 2005.
- 3) H. Yorimitsu, H. Shinokubo, and K. Oshima, "Synthetic radical reactions in aqueous media," *Synlett*, no. 5, pp. 674–686, 2002.
- 4) U. M. Lindstrom, "Stereoselective organic reactions in water," *Chemical Reviews*, vol. 102, no. 8, pp. 2751–2772, 2002.
- 5) A. F. Abdel-Magid, K. G. Carson, B. D. Harris, C. A. Maryanoff, and R. D. Shah, "Reductive amination of aldehydes and ketones with sodium triacetoxyborohydride. Studies on direct and indirect reductive amination procedures," *Journal of Organic Chemistry*, vol. 61, no. 11, pp. 3849–3862, 1996.
- 6) H. J. Yang, W. H. Sun, Z. L. Li, and Z. Ma, "The rapid synthesis of Schiff-base without solvent under microwave irradiation," *Chinese Chemical Letters*, vol. 13, no. 1, pp. 3–6, 2002.
- 7) Z. Yang and P. Sun, "Compare of three ways of synthesis of simple Schiff bas," *Molbank*, vol. 2006, no. 6, Article ID M514, 2006.
- 8) S. C. Gagieva, T. A. Sukhova, D. A. Savinov et al., "New fluorinecontaining bis-salicylideneimine-titanium complexes for olefin polymerization," *Journal of Applied Polymer Science*, vol. 95, no. 5, pp. 1040–1049, 2005.
- 9) A. Patti, S. Pedotti, F. P. Ballistreri, and G. T. Sfrassetto, "Synthesis and characterization of some chiral metal-salen complexes bearing a ferrocenophane substituent," *Molecules*, vol. 14, no. 11, pp. 4312–4325, 2009.
- 10) Z. H. Chohan, M. F. Jaffery, and C. T. Supuran, "Antibacterial Co(II), Cu(II), Ni(II) and Zn(II) complexes of thiadiazoles Schiff bases," *Metal-Based Drugs*, vol. 8, no. 2, pp. 95–101, 2001.
- 11) D. P. Song, Y. G. Li, R. Lu, N. H. Hu, and Y. S. Li, "Synthesis and characterization of novel neutral nickel complexes bearing fluorinated alicylaldiminato ligands and their catalytic behavior for vinylic polymerization of norbornene," *Applied Organometallic Chemistry*, vol. 22, no. 6, pp. 333–340, 2008.
- 12) J. S. Bennett, K. L. Charles, M. R. Miner et al., "Ethyl lactate as a tunable solvent for the synthesis of aryl aldimines," *Green Chemistry*, vol. 11, no. 2, pp. 166–168, 2009.
- 13) W. Qingming, M. Zhu, R. Zhu et al., "Exploration of α -aminophosphonate N-derivatives as novel, potent and selective inhibitors of protein tyrosine phosphatases," *European Journal of Medicinal Chemistry*, vol. 49, pp. 354–364, 2012.
- 14) P. Kathirgamanathan, S. Surendrakumar, J. Antipan-Lara et al., "Novel lithium Schiff-base cluster complexes as electron injectors synthesis, crystal structure, thin film characterisation and their performance in OLEDs," *Journal of Materials Chemistry*, vol. 22, no. 13, pp. 6104–6116, 2012.
- 15) S. Jie and S. Zhang, "2-arylimino-9-phenyl-1,10-phenanthroline-iron, -cobalt and -nickel complexes: synthesis, characterization and ethylene oligomerization behavior," *European Journal of Inorganic Chemistry*, vol. 2007, no. 35, pp. 5584–5598, 2007.
- 16) M. Rowley, D. J. Hallett, S. Goodacre et al., "3-(4-fluoropiperidin-3-yl)-2-phenylindoles as high affinity, selective, and orally bioavailable h5-HT_{2a} receptor antagonists," *Journal of Medicinal Chemistry*, vol. 44, no. 10, pp. 1603–1614, 2001.
- 17) S. Purser, R. M. Peter, S. Swallow et al., "Fluorine in medicinal chemistry," *Chemical Society Reviews*, vol. 37, no. 2, pp. 320–330, 2008.

Viscometric Technique for Evaluation of 1-Phenyl-3-[4-(2-Ethylimino-4-T-Butylimino-1,3,5-Dithiazino)Amino-Phenyl]Prop-2-Ene-1-One in Ethanol-Water Mixture

S.S. Padhen^{1*}, A.B. Wadekar²

1- Department of Chemistry, Rajarshree Shahu Science College Chandur Railway, Dist.-Amravati, 444 904. Maharashtra, India.

2- Department of Chemistry, Shri. Dnyaneshwar Maskuji Burungale Science and Arts College Shegaon Dist. Buldhana, -444 203, Maharashtra, India.

*Email: - sangha0604@gmail.com

ABSTRACT

The evaluation of density and viscometric study of 1-phenyl-3-[4-(2-ethylimino-4-t-butylimino-1,3,5-dithiazino)aminophenyl]prop-2-ene-1-one was recently carried out in our laboratory. In this research work evaluation done at different temperatures by keeping the constant concentration. The experimental data determine the effect of dilution of the solvent and the solute-solvent interaction of drug in current times.

KEYWORDS

Solute-solvent interaction, Viscometric study, 1,3,5-Dithiazino etc.

INTRODUCTION

The chalcones moiety base heterocyclic compounds are very widely distributed in nature. The nitrogen and sulphur containing heterocyclic compounds are very essential to living organisms. In biochemical, agricultural, pharmaceutical, medicinal, and industrial and drug sciences (Solanki A. and Thakur I, 2007) (Saleem F, 2008) viscosity measurements play a crucial role. Liquid have one of the important physical property is viscosity. Due to the shearing effect in the liquid which is the movement of liquid layers over each other hence liquids are viscous in nature (Bhat B.A., 2008). For aqueous and in non-aqueous solution have solute-solute and solute-solvent interaction. This important information provided by measurements of viscometric parameter. Drug behavior like absorption, transmission and its effect will directly relate to its viscosity measurements and solvent interactions in the human framework (Vibhute Y.B. and Bassar M.A., 2008)

Literature review that chalcone derivatives exhibit diverse pharmacological and biochemical activities such as antimicrobial and cytotoxic agents, antiviral, anti-inflammatory, anesthetics, mydriatics. Heterocyclic molecule having 1,3,5-dithiazino nucleus is widely used in medicinal, biochemical, biotechnological and pharmaceutical sciences (Solanki A. and Thakur I, 2007) (Saleem F, 2008) (Bhat B.A., 2008). These compounds showed anti-helminthic, antifungal, antiviral, antibacterial and anti-tuberculostatic properties Vibhute Y.B. and Bassar M.A., 2008). Dithiazines are found to be effective on treatment of cancer (Wan Z.Y., 2005). All these facts consideration a topic of great interest to carry out the viscometric measurements of 1-phenyl-3-[4-(2-ethylimino-4-t-butylimino-1,3,5-dithiazino)aminophenyl]prop-2-ene-1-one by varying temperatures (Jakhar A. and Makrand J.K., 2010) Such kind of study will be helpful to drug effectiveness (Zhang L.X., Zhang A.J., 2003) (Solanki A. and Thakur I, 2007) (Saleem F, 2008).

EXPERIMENTAL

For all type of analysis double distilled water and A.R. grade chemicals were used throughout the evaluation. For compound weight was used Mechaniki Zektady Precyzyjnej Gdansk balance [Poland make (± 0.001 gm)]. For measurement of viscosity of liquid was used Ostwald's viscometer. It was kept in Elite thermostatics water bath and temperature variation was maintained at 29°C (± 0.1) for each measurement. For densities determination bicapillary with a 1 mm internal diameter was used. Viscometer and water bath required sufficient time for maintaining thermal equilibrium.

In this research work viscometric study of 1-phenyl-3-[4-(2-ethylimino-4-t-butylimino-1,3,5-dithiazino)aminophenyl]prop-2-ene-1-one at 0.1M concentration in 60% ethanol-water system separately at varying temperatures. Freshly prepared solutions were used throughout the evaluation. As per the literature given viscometric readings were taken.

OBSERVATIONS AND CALCULATIONS

Molecular interactions in terms of β -coefficient of solute is figured with the help of data obtained in our work. The results obtained are stated in **Table No. 1**. According to Jone's-Dole equation, $(\eta_r - 1)/\sqrt{C} = A + B\sqrt{C}$ at different temperatures keeping the concentration 0.1 M. A and β -coefficient values calculated are enlisted in **Table No.2**.

TABLE No.1
VISCOSITY MEASUREMENTS AT CONSTANT CONCENTRATIONS AND
DETERMINATION OF RELATIVE AND SPECIFIC VISCOSITIES AT DIFFERENT
TEMPERATURES AT 0.1M

MEDIUM - 60% ETHANOL-WATER							
Conc.	Temp. ($^{\circ}\text{C}$)	\sqrt{C}	Time (sec.)	Density $\rho \times 10^3$ (kg.cm^{-3})	η_r	$\eta_{sp} = \eta_r - 1$	$(\eta_r - 1)/\sqrt{C}$ (pa.s)
0.1 M	22	0.314	58	1.0913	0.069341	-0.930659	-2.9638
	24	0.314	51	1.0893	0.067329	-0.932671	-2.9702
	28	0.314	47	1.0676	0.05920	-0.9408	-2.9961
	30	0.314	32	1.0565	0.06453	-0.93547	-2.9792

TABLE No.- 2
A and β Co-Efficient Values from Graphs for 60%.
FOR 1-PHENYL-3-[4-(2-ETHYLIMINO-4-t-BUTYLIMINO-1,3,5-
DITHIAZINO)AMINO- PHENYL]PROP-2-ENE-1-ONE

W-E Mixture(%)	Temp $^{\circ}\text{C}$	Mean "A"	β (Slope "m")
60	24	-2.9702	0.0073

RESULT AND DISCUSSION

The relative viscosity was determined by using following formula

$$\eta_r = D_s \times t_s / D_w \times t_w.$$

While Jone's-Doles equation was used for the analysis of relative viscosities,

$$(\eta_r - 1)/\sqrt{C} = A + B\sqrt{C}$$

Where,

A = Falkenhagen coefficient

B = Jones-Dole coefficient

C = concentration of solutions

Solute-solute interaction was measures by using Falkenhagen coefficient (A) while solute-solvent interaction was measures by using Jones-Dole coefficient (B).

The graph are plotted in between $(\eta_r - 1)/\sqrt{C}$ versus \sqrt{C} . The graph for each system gave linear straight line gave value of β -coefficient.

CONCLUSIONS

In the current work monitor that the density and relative viscosity decreases with increase in temperature. This is supported by the information that as the temperature increases the solute-solvent interaction increases due to which solvation effect increases. Pharmacodynamics and pharmacokinetics study of drug is useful investigation and informative for society.

ACKNOWLEDGEMENT

I am very much thankful to Dr. D. T. Tayade, Professor, GVISH College, and Amravati for kindly cooperation.

REFERENCES

1. Solanki, A. and Thakur, I. (2007). *Indian Journal of Chemistry*. 45(B): 517.
2. Saleem, F. (2008). *Eur. Pot., CHAPPL*. 87: 19.
3. Baldaniya, B.B. and Patel, P.K. (2009). *E-Journal of Chemistry*. 6(3): 673-680.
4. Parajuli, R. and Medhi, C. (2004). *Journal of Chemical Sciences*. 116(4): 235-241.
5. Vibhute, Y.B. and Basser, M.A. (2003). *Ind. J. of Chem*. 42(B): 202-205.
6. Bhat, B.A. Dhar, K.L. Saxena, A.K. and Shanmugavel, M. (2005). *Bio org. and Med. Chem*. 15(3): 177-180.
7. Kalirajan, R. Palanivelu, M. Rajmanickam, V. Vinothapushan, G. and Anandarajagopal, K. (2007). *Int. J. of Chem. Sci*. 5(1): 73-80.
8. Bansal, R.K. (2012). *J.Heterocyclic Chloroic Chemistry*. 8: 12-24.
9. Jakhar, A. and Makrand, J.K. (2010). *J.Chem.Res*. 4(3): 238-240.
10. Wan, Z.Y. Shi, H.X. and Shi, H.J. (2001). *J. Heterocyclic Chloroic Chem*. 38: 335.
11. Zhang, L.X. Zhang, A.J. Hu, M.L. and Lei, X.X. (2003). *Acta Chim.Sinica*. 61(6): 917.
12. Zhang, Y. Qiao, R.Z. and Zhang, Z.Y. (2002). *J.Chin.Chem.Soc*. 49(3): 369.

An Overview on Green Chemistry

Dr. Rupali.S. Talegaonkar

Matoshree Vimalabai Deshmukh Mahavidyalaya, Amravati

E.Mail [-rupaliyeotikar@gmail.com](mailto:rupaliyeotikar@gmail.com)

ABSTRACT

The present review work focuses on the importance and economic development of green chemistry. It is new branch in chemistry dealing with reduction of harmful and toxic chemicals in the synthesis and replacing it with ecofriendly methods. The principle of green chemistry with various benefits have been discussed to understand the basic requirement for replacement of conventional synthetic method with green chemistry synthesis. To describe it the synthetic approach for the synthesis of acetanilide has been discussed and compared.

KEYWORDS: Green Chemistry, Ecofriendly, Conventional, Acetanilide.

1. INTRODUCTION

The accelerated progress in science and technology now a days has led to economic development in world, but such economic development also cause environmental degradation which is manifested by climate change, the issue of ozone holes and accumulation of non-destructive organic pollutant in all parts of biospheres.

So the present situation required the solution to balance the use of natural resources and environmental conservation. From last two decades awareness for environmental protection has increased by using the concept of "Green Chemistry". The new laws and regulations have a Aim to protect the ecosystem from harmful chemicals and develop new compounds by the approach of Green chemistry which are less dangerous to human health and the environment.^[1]

Green chemistry is new branch of chemistry involves pulling together tools and techniques that helps to chemical engineers in research related to the creation of chemical product and processes that reduce or eliminate the use of harmful chemicals as well as reducing harmful and toxic products for the development of more eco-friendly and efficient product with less wastage. Green chemistry is now going to become an essential tool in the field of synthetic chemistry^[2,3].

1.1.Definition of Green Chemistry: According to environmental protection agency, green chemistry is defined as a chemistry that designs chemical products and processes that are harmless to the environment. Chemical products should be made in such a manner that they do not remain in the environment at the end of their application and broken down into components that are harmless to environment.⁴

1.2.History: The term green chemistry was first given by Poul .T. Anastas in 1991 in special program launched by the US environmental Protection Agency (EPA) to implement sustainable development in chemistry ,chemical technology by industry ,academia and government. In 1995 the annual US presidential green chemistry challenge was announced. In 1996 the working party on green chemistry was created, acting within the framework of International Union of Pure and Applied Chemistry. The first book and journals on the subject of green chemistry were introduced in 1990 by the royal society of chemistry. Green chemistry includes a new approach to the synthesis, processing and

application of chemical substances in such a manner to reduce scourge to health and environment like:

- Clean chemistry
- Atom Economy
- Environment begin chemistry ^[5-11]
- Clean Chemistry
- Atom Economy

Twelve principles of Green chemistry have been developed by Poul Anastas, speaks about the reduction of dangerous or harmful substances from the synthesis, production and application of chemical products. When designing a green chemistry process it is impossible to meet the requirements of all twelve principles of the process at the same time, but it attempts to apply as many principles during certain stages of synthesis.^[12,13]

1.3. Principles of Green Chemistry

1.3.1. Pollution Prevention: It is to prevent waste and to treat and clean up waste after it has been created.

1.3.2. Atom Economy: It should be designed to maximize the incorporation of all materials used in process into the final product.

1.3.3. Less Hazardous Chemical Synthesis: The synthetic method should be designed to use and generate substances that process little or no toxicity to human health and the environment.

1.3.4. Designing Safer Chemicals: Chemical product should be designed to affect their desired function while minimizing toxicity.

1.3.5. Safer Solvents and Auxiliaries: The use of auxiliary substances should be made unnecessary wherever possible.

1.3.6. Design for Energy Efficiency: energy requirements of chemical processes should be recognized at low temperature and pressure.

1.3.7. Use of Renewable Feedstock's: A raw material of feedstock should be renewable.

1.3.8. Reduce Derivatives: The unnecessary derivatization like use of blocking groups, protection, deprotection should be avoided whenever impossible.

1.3.9. Catalysis: The catalytic reagents are superior stoichiometric reagents.

1.3.10. Design for Degradation: The chemical products should be designed so that at the end of their function they breakdown into harmless degradation products and do not persist in the environment.

1.3.11. Real-time analysis for Pollution Prevention: Analytical methodologies need to be further developed to allow for real-time, in process monitoring and control prior to the formation of hazardous substances.

1.3.12. Inherently Safer Chemistry for Accident Prevent: The substances used in the chemical process should be chosen to minimize the potential for chemical accidents, explosion and fires. This principle can motivate chemistry at all levels like research, education and public perception.^[14]

1.4. Benefits of Green Chemistry

Benefits for health

- ✓ Cleaner air- less release of hazardous chemicals to air leading to less damage to lungs.
- ✓ Cleaner water- less release of hazardous chemicals waste to water leading to cleaner drinking.
- ✓ Increase safety water for workers in chemical industry, less use of toxic material, less potential for accident

- **Benefits for environment**
 - ✓ Plants and animals suffer less harm from toxic chemicals in environment
 - ✓ Lower potential for Global warming, ozone depletion and smog formation.
- **Economy**
 - ✓ Better performance so that less product is needed to achieve the same function.

REVIEW LITERATURE

2.1. Green chemistry aims to reduce or even eliminates the production of any harmful bi-products and maximizing the desired product without compromising with the environment. The three key developments in green chemistry include use of super critical carbon di oxide as green solvent, aqueous hydrogen peroxide as an oxidizing agent and use of hydrogen in asymmetric synthesis. It also focuses on replacing traditional methods of heating with that of modern methods of heating like microwave radiations so that carbon footprint should be reduces as low as possible.^[15]

2.2. The work focuses to reduce the chemical wastage by applying the concept of green chemistry. Few derivative of acetanilide were synthesized by conventional method as well as by green chemistry method. In conventional method there was wastage of chemicals by the formation of acetic acid molecule but by green synthesis method the formation of byproducts was avoided and the atom economy was calculated on the basis of molecular weight of desired product and it was found to be in the range of 72 to 82% which signify the utility of green synthesis method.^[16]

2.3. Due to technology development the quality of life on earth became much better but harmful effect of chemistry also became pronounced main among them being the pollution of land, water and atmosphere. This is caused mainly due to the use of harmful reactants and effect of by-product of chemical industries, which are being discharge into air, rivers and the land, but by applying the concept of green chemistry these all problems can be reduced.^[17]

2.4. Green chemistry is a term that refers to the production of chemical products and processes that reduce the use of and production of harmful substances^[18]

The green chemistry revolution provides the various numbers of challenges to those who practice chemistry in industry, education and research. It is the modern science of chemistry deals with the application of environment friendly chemical compound in the various area of our life such as industries. The chemical industries supply us a huge variety of essential product, from plastic to pharmaceuticals, these industries has a potential to damage our environment, so green chemistry serves to promote the design and efficient use of chemicals and chemical processes^[19]

3. EXPERIMENTATION

The synthesis of acetanilide by green chemistry has various disadvantages as there is a lot of wastage of acetic acid molecule, which can be minimized by green chemistry.

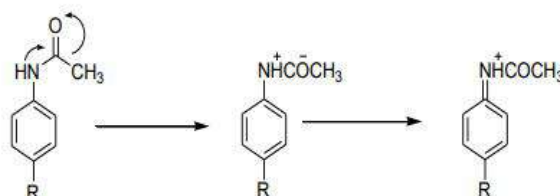
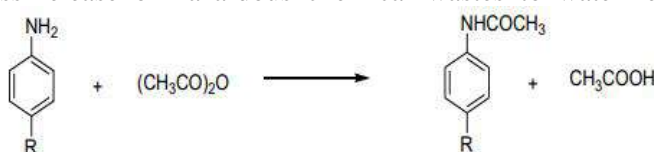
3.1. Synthesis of compounds by conventional method

- In a 250 ml beaker containing 125 ml of water, 4.6 ml of conc. Hydrochloric acid and 5.1
- In a 250 ml beaker containing 125 ml of water, 4.6 ml of conc. Hydrochloric acid and 5.1 g of aniline / substituted anilines were introduced.
- Stirred until all the anilines passes completely into solution.
- To the resulting solution, 6.9 g (6.4ml) of redistilled acetic anhydride was added and stirred until it was dissolved.

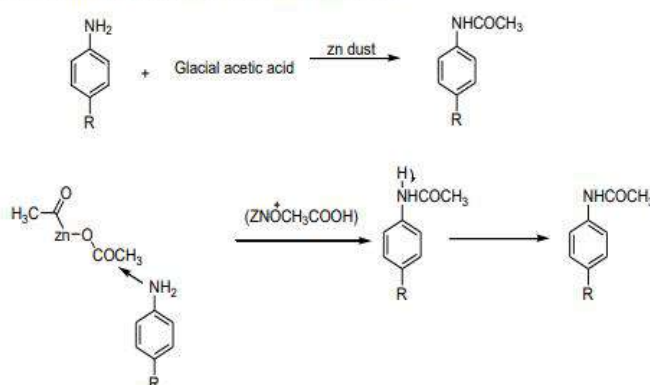
- Poured immediately in a solution of 3.8 g of crystalline sodium acetate in 25 ml of water.
- Stirred vigorously and cooled in ice. Filtered the acetanilide and substituted acetanilide with suction, washed with 10 ml water, drained well and dried upon filter paper. The crude products were recrystallized from boiling water and methylated spirit.
- Non green component: Acetic anhydride leaves one molecule of acetic acid unused.
- Poured immediately in a solution of 3.8 g of crystalline sodium acetate in 25 ml of water.
- Stirred vigorously and cooled in ice. Filtered the acetanilide and substituted acetanilide

3.2. Synthesis of compounds by green chemistry method

- A mixture of aniline / substituted anilines (3.3g) and zinc dust (0.16g) in acetic acid
- A mixture of aniline / substituted anilines (3.3g) and zinc dust (0.16g) in acetic acid (10ml) in 100 ml round bottom flask was heated over a gentle flame using water condenser.
- Heating was continued for about 45 min., the reaction mixture was then carefully poured in cold water (33ml) in 250ml beaker with vigorous stirring.
- The shining crystals of product were separated slowly. After 15 min, crystals were collected by filtration. The solid crystals were washed over the Buchner funnel with water and product was dried and crystallized in boiling water.
- Green context: Minimize waste by-products, avoids use of acetic anhydride
- Benefits for health
- Cleaner air-less release of hazardous chemicals to air leading to less damage to lungs.
- Cleaner water-less release of hazardous chemical wastes to water leading to cleaner



Synthesis and mechanism by conventional method



Synthesis and mechanism by green chemistry method

4. CONCLUSION

This review article will definitely help to understand the importance of green chemistry, conventional methods can be replaced easily by the methods which utilize non toxic and environment friendly techniques for the synthesis of same. One of such approach has been discussed for the synthesis of acetanilide. The approach will definitely help in the synthesis by keeping the environment safe. which is basic requirement in today's pharmaceutical industries. The approach will help to avoid the utilization of the toxic chemicals leading to various hazards in the industry. These

5. REFERENCE

1. Singhal M., Singh A. Khan S.P, Green Chemistry Potential for Past, Present and Future Perspectives, 2012; 3(4).
2. Ahluwalia V.K, Kidwai M., New Trends In Green Chemistry, Anamaya publisher New Delhi, 2nd edition, 2007; 5-18.
3. Ahluwalia V.K, Green chemistry Environmentally Benign Reactions, published by India books, 2nd EDITION, 2006; 1-10.
4. Vojvodic V. Environmental Protection :Green Manufacturing in the pharmaceutical industry and cost reduction, KenInd, 2009; 58(1): 32-33.
5. Anastas. P.T, Warner J.C, Green chemistry Theory and Practice, Oxford University, Press, New York, 1998.
6. Anastas P.T, Hovarth I.T, Innovations and Green Chemistry, Chemistry review, 2007; 107.
7. Ravichandaran S., International Journal, 2010; 2(4): 2191.
8. Trost B.M, Atom economy- A challenge for organic synthesis:Homogeneous catalysis leads the way, 1995; 34: 259.
9. Sheldon R.A, Green solvents for sustainable organic synthesis: State of art, 2005; 7: 267.
10. Bharati V.B, Resonance, 2008; 1041.
11. Ahluwalia V.K and Kidwai M., New Trends in Green Chemistry, Anamaya Publisher, New Delhi, 2004.
12. Anastas P., Warner, Green Chemistry: Theory and Practice, Oxford University Press, Oxford, 1998.
13. Anastas P.T, Heine L.G, Williamson T.V, Green Chemical Synthesis and Processes, American Chemical Society, Washington DC, 2000.
14. Singhal M, Singh A, Khan S.P, Sultan E, Sachan N.K, Green chemistry potential for past present and future perspectives.
15. Gujral. S.S, Sheela. M.A, Khattri S., Singla R.K. A Focus and Review on the Advancement of Green Chemistry, Indo Global Journal of Pharmaceutical Science, 2012; 2(4): 397-408.
16. Redasani V.K, Kumawat V.S, Kabra R.P, Surana S.J, Application Of Green Chemistry in Organic Synthesis, International Journal of Chem Tech Research, 2010.
17. Singhal. M, Singh A., Khan S.P, Green Chemistry Potential for Past, Present and Future Perspectives, International Research Journal of Pharmacy, 2012; 3(4).
18. Ivankovic. A., Dronjic A., Review of 12 Principles of Green Chemistry in Practice, International Journal of Sustainable and Green Energy, 2017; 6(3): 39-48.
19. Chanshetti U., Green Chemistry: Challenges And Opportunities In Sustainable Development, International Journal of Current Research, 2014; 6.

3D Printing Technology for development of Transdermal Drug Delivery Systems

Dr. Amar Deshpande, Dr. Jagdish Baheti

Kamla Nehru College of Pharmacy, Butibori, Nagpur

Abstract:

The innovative approach of three-dimensional printing enables the on-demand production of transdermal drug delivery systems. This technology, already applied in dentistry, orthopedics, and pharmaceuticals, particularly stands out in the latter field. It facilitates the printing of medical devices and diverse formulations of active pharmaceutical ingredients, featuring controlled-release characteristics and varied geometries. This study provides an overview of these pharmaceutical applications, focusing on the 3D printing of transdermal patches. The discussion encompasses different printing technologies and material systems known for their customization capabilities, generating intricate geometries with precise characteristics crucial for transdermal systems, thereby enhancing bioavailability. The study includes case studies, explores advantages and limitations of the technology, and forecasts industry growth, projecting a value exceeding USD 8 Billion by 2025. Despite this potential, the conservative nature of the pharmaceutical industry leans toward cost-effective methods for large-scale production. Nevertheless, 3D printing has the potential to revolutionize the current 'one size fits all' manufacturing approach, becoming an integral part of the drug development timeline.

Keywords: 3D Printing, Inkjet printing, Microneedles, Patches, Transdermal delivery, Pharmaceutics

1. Introduction

The historical application of therapeutic substances, including herbal ointments and various drugs (such as scopolamine, estradiol, fentanyl, rivastigmine), on the human skin serves both medical and cosmetic purposes. Over the past decades, the skin has proven to be an accessible surface for drug administration, making systematic therapy through percutaneous drug absorption feasible (Prausnitz and Langer, 2008; Alkilani et al., 2015; Pastore et al., 2015). The transdermal route emerges as an attractive alternative to traditional methods like oral administration or hypodermic injections. Oral administration may face issues of partial drug absorption, complications related to gastrointestinal metabolism, and slow onset, making it impractical for emergency cases. Hypodermic injections, while effective, are invasive, pose infection risks, require skilled administration, and generate medical waste (Awodele et al., 2016).

Contrarily, transdermal systems offer advantages such as bypassing metabolic systems, ensuring higher bioavailability, and promoting sustained and controlled drug release. Additionally, transdermal drug delivery (TDD) holds promise for vaccinations due to the abundance of dendritic cells in the skin. This patient-friendly approach is noninvasive, contributing to psychological well-being, and provides independence as it doesn't require professional care for repositioning, removal, or replacement.

However, TDD faces limitations, primarily stemming from the skin barrier's nature. The Stratum Corneum, the outermost skin layer, acts as a significant barrier due to its density and low hydration (15–20%). Overcoming this impermeable barrier has been the focus of TDD research, presenting both challenges and opportunities for future progress.

In the current global trend towards personalized patient care, traditional mass-production methods of drug delivery systems are being questioned for their ability to tailor dosages cost-effectively. New technologies, particularly Additive Manufacturing (AM), such as 3D printing, are investigated for their potential in pharmaceutical technology. Initially introduced in the 1980s, 3D printing has gained attention across various industries, contributing to the production of complex structures beyond the capabilities of conventional techniques.

The application of 3D printing in pharmaceuticals is relatively recent, aiming to produce targeted-release and customized drug delivery systems (Goole and Amighi, 2016). In the field of TDD, although studies are limited, they demonstrate the transformative potential of 3D printing. This review explores the existing research on 2D and 3D printing as direct or indirect fabrication methods for TDD systems. The materials and drugs associated with 3D printing in TDD systems are also examined in this context.

2. 3D printing techniques for optimized Transdermal Drug Delivery Systems

Additive Manufacturing (AM), commonly referred to as 3D printing or Solid Freeform Fabrication (SFF), encompasses various techniques that utilize a virtual Computer Aided Design (CAD) model to construct a physical object by depositing consecutive layers. Introduced in the 1980s, 3D printing has revolutionized industrial and scientific sectors, offering fast and precise production of intricate structures beyond the capabilities of traditional methods. The medical field quickly recognized the transformative potential of 3D printing, leading to the creation of customized implants, prosthetics, and ongoing investigations into live tissue printing (Chia and Wu, 2015).

The application of 3D printing in drug delivery has recently gained attention, with the FDA approval of Spritam, the first 3D printed oral administration tablet. This has given rise to the term 'pharmacoprinting' (Prasad and Smyth, 2015; Jacob et al., 2014; Goyanes et al., 2015; Di Prima et al., 2016). While its impact on oral drug delivery is well-established, 3D printing's potential in transdermal drug delivery (TDD) is currently under exploration, with a growing body of relevant studies.

2.1. Inkjet Printing

Inkjet printing, involving the controlled deposition of small droplets, has seen successful applications in medicine but is yet to be extensively explored for TDD. Studies have used inkjet printing for coating microneedles with various agents, demonstrating its potential for controlled and selective deposition on suitable substrates (Boehm et al., 2011, 2013, 2014; Ross et al., 2015; Uddin et al., 2015). While its application for building complex three-dimensional TDD structures remains unexplored, inkjet printing's high resolution and selective deposition make it promising for microneedle coating, enabling personalized dosages with high reproducibility.

2.2. Photopolymerization-based Technologies

A significant group of 3D printing technologies relies on selective polymerization of photo-sensitive polymers through laser emissions or light projections. Techniques like Stereolithography (SLA) and Digital Light Processing (DLP) enable layer-wise polymerization of UV-sensitive polymers. These technologies offer versatility in geometric complexity and resolution, making them suitable for TDD applications. Studies have utilized micro-stereolithography (DLP) to create microneedle arrays indirectly, contributing to the customization of therapeutic approaches (Boehm et al., 2014, 2011, 2012). Photopolymerization-based 3D printing has proven applications in fabricating TDD systems, offering high resolution and flexibility.

2.3. Fused Deposition Modelling (FDM)

Fused Deposition Modelling (FDM), based on the melt-extrusion process, is a versatile 3D printing technique with potential applications in TDD. While FDM's limitations in resolution and sensitivity to process parameters are acknowledged, its ability to produce structures through extrusion without solvents makes it a compelling choice for certain pharmaceutical applications. The combination of FDM with hot-melt extrusion (HME) processes holds promise for producing drug/polymer blends for cost-effective TDD system fabrication.

3. Materials:

In the contemporary landscape, 3D printing technologies possess the capability to manipulate a diverse array of materials, ranging from ceramics and metals to polymers. The categorization of these techniques implies that the choice of a specific technology inherently limits the materials compatible with the corresponding printing apparatus. For instance, SLA or DLP printers exclusively handle photo-cured polymers, while FDM printers utilize thermoplastic filaments. This limitation poses challenges for the widespread adoption of 3D printing as a direct manufacturing technique for Transdermal Drug Delivery (TDD) systems, as the material must meet specific criteria for integration into such systems. (Sharma et al.2011) Essential parameters include stability, biodegradability without toxic by-products, mechanical strength, and non-reactivity with the drug. Material biocompatibility is a critical consideration, as evidenced by studies involving Gantrez, a biocompatible copolymer used in TDD applications. While there's evidence of manufacturing Gantrez biocompatible microneedles using 3D printed molds, the multi-step nature of this approach may hinder mass production scalability. (Boehm et al., 2014, 2011, 2012, Donnelly et al., 2012).

Numerous polymers with biomedical and pharmaceutical applications show promise for integration into 3D printed TDD systems. Polyvinyl alcohol (PVA) and poly lactic acid (PLA) are examples. However, challenges exist, such as PVA's limited biodegradability and PLA's slow degradation rates and poor mechanical properties when employed in FDM technology. Biopolymers, like chitosan and collagen, exhibit favorable attributes for TDD. Bioprinting advancements further expand the possibilities. Yet, ongoing research on materials remains vital for the evolving field of 3D printed TDD. (Economidou et al. 2018)

4. 3D Printed Transdermal Drug Delivery Systems- Future Challenges and Expected Impact:

Transdermal Drug Delivery (TDD) systems, facilitated by 3D printing, hold potential as a user-friendly, personalized pharmaceutical therapy. The layer-by-layer fabrication inherent in 3D printing aligns well with TDD requirements. This technology enables the creation of systems with varying drug concentrations across layers, catering to individual needs. Customization possibilities enhance TDD efficiency, addressing factors like skin hydration and thickness variations among patients. In vaccination, microneedles offer promise, particularly in regions facing challenges with traditional administration methods. 3D printing's role in reducing costs and providing needle-free solutions is crucial for global health initiatives. However, challenges such as limited biomaterial options, dosing constraints, and drug degradation characteristics need resolution. The development of 3D printable materials and improvements in existing technologies could drive the evolution of TDD systems. (Economidou et al. 2018)

5. Regulatory Considerations:

For the commercialization of 3D printed TDD systems, adherence to regulatory requirements is essential. Despite the FDA's approval of the first 3D printed oral tablet, TDD systems face unique regulatory challenges. Microneedle patches, viewed as medical devices, must adhere to Good Manufacturing Practice (cGMP) guidelines. The FDA emphasizes technical

considerations, including the impact of printing parameters, in-situ quality control, design validation, sterilization, and post-process cleaning. A 2017 guidance document provides recommendations for 3D printed medical devices, addressing issues like patient-matched devices and data protection. Sterilization, a regulatory requirement, presents challenges for microneedles. Future success depends on addressing material limitations, improving technology, and establishing specific regulatory frameworks for 3D printed TDD systems. (Economidou et al. 2018)

6. Conclusion:

Since its inception, 3D printing has revolutionized fabrication methods, with potential applications in medicine and pharmaceuticals. Despite being in the early stages, advancements in 3D printed Transdermal Drug Delivery (TDD) systems show promise. Inkjet printing, photopolymerization-based technologies, and FDM have been explored, with inkjet printing successfully depositing films on microneedle surfaces and commercializing 3D inkjet printed microneedles. The integration of elaborate microneedle array systems with precise 3D printing techniques has the potential to reshape modern drug administration. Overcoming engineering, chemistry, and material challenges through interdisciplinary research is crucial. Regulatory considerations, addressed by the FDA, are imperative to ensure the safety and effectiveness of 3D printed TDD systems. Success hinges on resolving material limitations, advancing technology, and establishing specific regulatory frameworks.

References:

1. Alkilani, A.Z., McCrudden, M.T.C., Donnelly, R.F., 2015. Transdermal drug delivery: innovative pharmaceutical developments based on disruption of the barrier properties of the stratum corneum. *Pharmaceutics* 7 (4), 438–470.
2. Awodele, O., Adewoye, A.A., Oparah, A.C., 2016. Assessment of medical waste management in seven hospitals in Lagos, Nigeria. *BMC Public Health* 1–11.
3. Boehm, R.D., Miller, P.R., Hayes, S.L., Monteiro-Riviere, N.A., Narayan, R.J., 2011. Modification of microneedles using inkjet printing. *AIP Adv.* 1 (2), 022139.
4. Boehm, R.D., Miller, P.R., Singh, R., Shah, A., Stafslie, S., Daniels, J., Narayan, R.J., 2012. Indirect rapid prototyping of antibacterial acid anhydride copolymer microneedles. *Biofabrication* 4 (1), 11002.
5. Boehm, R.D., Miller, P.R., Schell, W.A., Perfect, J.R., Narayan, R.J., 2013. Inkjet printing of amphotericin B onto biodegradable microneedles using piezoelectric inkjet printing. *JOM* 65 (4), 525–533.
6. Boehm, R.D., Miller, P.R., Daniels, J., Stafslie, S., Narayan, R.J., 2014. Inkjet printing for pharmaceutical applications. *Mater. Today* 17 (5), 247–252.
7. Chia, H.N., Wu, B.M., 2015. Recent advances in 3D printing of biomaterials. *J. Biol. Eng.* 9 (4).
8. Di Prima, M., Coburn, J., Hwang, D., Kelly, J., Khairuzzaman, A., Ricles, L., 2016. Additively manufactured medical products – the FDA perspective. *3D Print. Med.* 2 (1), 1–6.
9. Donnelly, R.F., Singh, T.R.R., Garland, M.J., Migalska, K., Majithiya, R., McCrudden, C.M., Kole, P.L., Mahmood, T.M.T., McCarthy, H.O., Woolfson, A.D., 2012. Hydrogel forming microneedle arrays for enhanced transdermal drug delivery. *Adv. Funct. Mater.* 22 (23), 4879–4890.
10. Economidou, S. N., Lamprou, D. A., & Douroumis, D., 2018. 3D printing applications for transdermal drug delivery. *International journal of pharmaceutics.* 544(2), 415-424.

11. Gittard, S.D., Miller, P.R., Jin, C., Martin, T.N., Boehm, R.D., Chisholm, B.J., Stafslie, S.J., Daniels, J.W., Cilz, N., Monteiro-Riviere, N.A., Nasir, A., Narayan, R.J., 2011.
12. Goole, J., Amighi, K., 2016. 3D printing in pharmaceuticals: A new tool for designing customized drug delivery systems. *Int. J. Pharm.* 499 (1–2), 376–394.
13. Goyanes, A., Wang, J., Buanz, A., Martinez-Pacheco, R., Telford, R., Gaisford, S., Basit, A.W., 2015. 3D printing of medicines: engineering novel oral devices with unique design and drug release characteristics. *Mol. Pharm.* 12 (11), 4077–4084.
14. Jacob, J., Coyle, N., West, T.G., Monkhouse, T.G., Surprenant, H.L., Jain, M.B., 2014. Rapid Disperse Dosage form Containing Levetiracetam. US 20140271862 A1.
15. Jessen, L., Kovalick, L.J., Azzaro, A.J., 2008. The selegiline transdermal system (Emsam): a therapeutic option for the treatment of major depressive disorder. *Pharm. Ther.* 33 (4), 212–246.
16. Pastore, M.N., Kalia, Y.N., Horstmann, M., Roberts, M.S., 2015. Transdermal patches: history, development and pharmacology. *Br. J. Pharmacol.* 172 (9), 2179–2209.
17. Prasad, L.K., Smyth, H., 2015. 3D printing technologies for drug delivery: a review. *Drug Dev. Ind. Pharm.* 9045 (January), 1–13.
18. Prausnitz, M.R., Langer, R., 2008. Transdermal drug delivery. *Nat. Biotechnol.* 26 (11), 1261–1268.
19. Ross, S., Scoutaris, N., Lamprou, D., Mallinson, D., Douroumis, D., 2015. Inkjet printing of insulin microneedles for transdermal delivery. *Drug Deliv. Transl. Res.* 5 (4), 451–461.
20. Sharma, K., Singh, V., Arora, A., 2011. Natural biodegradable polymers as matrices in transdermal drug delivery. *Int. J. Drug Dev. Res.* 3 (2), 85–103.
21. Uddin, M.J., Scoutaris, N., Klepetsanis, P., Chowdhry, B., Prausnitz, M.R., Douroumis, D., 2015. Inkjet printing of transdermal microneedles for the delivery of anticancer agents. *Int. J. Pharm.* 494 (2), 593–602.

***In-silico* Prediction of Phytoconstituents from *Hymenodictyon excelsum* for Antimalarial Activity Targeting Hypoxanthine-guanine phosphoribosyltransferase (HPRT1)**

Parimal Katolkar*, Jagdish Baheti

Department of Pharmaceutical Chemistry, Kamla Nehru College of Pharmacy, Butibori, Nagpur 441108 (MS), INDIA

**Email: parimal.katolkar@gmail.com*

ABSTRACT

Objective Malaria is referred as a disease caused by parasite. The parasite spread to humans through the infected mosquito bite. People who are infected by malaria feel very sick with high fever and chills. Natural products and their active principles as sources for new drug discovery and treatment of diseases have attracted considerable attention of researchers. Compounds found in medicinal plants have been the source of many conventional medications. *In-silico* testing of *Hymenodictyon excelsum* phytoconstituents on hypoxanthine-guanine phosphoribosyl transferase for antimalarial efficacy was a part of our investigation.

Methods Utilizing Discovery studio, molecular docking is done to assess the pattern of interaction between the phytoconstituents from the *Hymenodictyon excelsum* plant and the crystal structure of the malarial proteins (PDB ID: 4RAC). Later, SwissADME and pkCSM were used to screen for toxicity as well as the pharmacokinetic profile. Further, interaction between proteins by STRING network analysis and bioactivity score analysis using molinspiration tool were also evaluated.

Results The docked results suggest that nardamnanthal (−8.9 kcal/mol), rubiadin (−8.2 kcal/mol) and lucidin (− 8.1 kcal/mol) for 4RAC macromolecule has best binding towards antimalarial activity as compared to the standard (artemisinin) for 4RAC is -7.5 kcal/mol and. Furthermore, pharmacokinetics and toxicity parameters were within acceptable limits according to ADMET studies.

Conclusions Targeting hypoxanthine-guanine phosphoribosyl transferase against malaria by phytoconstituents from *Hymenodictyon excelsum* can serve as a rational approach for designing future antimalarial drugs.

1. INTRODUCTION

About 30 species of flowering plants belong to the genus *Hymenodictyon*, which is part of the Rubiaceae family. The generic name is a combination of the Greek words for membrane and net, hymen and diktyon. It alludes to the wing that envelops every seed. The members in this genus have serrated leaves grouped in opposition, small, clustered blooms, and many seeds capsules. The genus includes widely varying trees and shrubs the majority of them in tropical and subtropical regions of Asia and Africa.¹

Hymenodictyon excelsum Roxb. Wall. syn *H. orixense* Roxb Mobb. belonging to family Rubiaceae, also known as Bhorsal, Kukurkat, Bhaulan, Bauranga, Pottaka, Kusan, and Kadambu (India), Lala (Thailand), and Kuthan (Burma) is a medium to a tall, deciduous tree that typically grows to a height of 10 to 12 metres grey-brown with hints of brown, straight cylindrical bole, rounded crown green, glabrous leaves that are rectangular, ovate, or elliptic in shape, greenish-white, fragrant flowers, and ellipsoid capsules that contain flying seeds Bark

is 10-20 cm long and mostly ruffled, thick, softish scales that exfoliate in irregular shapes. Stipules are approximately 15 mm length, linear to lanceolate to ovate to lanceolate, apex pubescent, acuminate, and deciduous.²⁻⁴

In traditional medical systems all across the world, *H. excelsum*'s bark and leaves are primarily used to cure a variety of illnesses. Bark has a variety of medical benefits. Different plant components have reportedly been used to treat emaciation, a carbuncle, a burning sensation in the chest, as well as problems related to lactation and fever. Additionally, it makes you taste and eat more. Inhalation remedy for diarrhoea.⁵⁻⁶ It has significant *in-vitro* and *in-vivo* antimalarial action since the ethyl acetate extract of *H. excelsum* has showed dose-dependent percentage suppression of *Plasmodium falciparum* schizont formation.⁷

Coumarins⁸ and anthraquinones⁹, two chemical components previously identified as being present in this plant, were detected. The stem bark of the plant contains tannin, the poisonous alkaloid hymenodictine, aesculin, an apioglucoside of scopoletin, and hymexelsin.^{6,10} Additionally isolated from roots are anthraquinones, rubiadin and its methyl ether, lucidin, damnacanthol, nordamnacanthol, 2-benzylanthopurpurin, anthragallol, soranjidol, and Morindone.⁴ Anthragallol, 6-methylalizarin, subiatin, and its 1-methylester, soranjidol, isolated from roots; aesculin (b-methylaescinietin), scopoletin, and hymenodictyonin; alanine, arginine, cystine, glycine, leucine, fruitore, galactose, and glucose,¹¹ acetylenic fatty acids, a novel triglyceride, and 11 recognised chemicals, including ursolic acid, oleaquinic acid, uncarinic acid E, and β -sitosterol, have also been reported in studies.⁸

Malaria is the most common infectious disease in Africa and many Asian nations. Malaria is caused by a microscopic protozoon from the Plasmodium species family, which comprises numerous subspecies. A few Plasmodium species can cause illness.^{12,13}

Five of the 172 Plasmodium species that exist can infect people. These include *P. knowlesi*, *P. vivax*, *P. ovale*, *P. vivax*, *P. malariae*, and *P. falciparum*.¹³⁻¹⁶ Malaria is a disease that is caused by all of the aforementioned Plasmodium species.¹⁷

Female Anopheles mosquitos are the only ones that transmit human malaria. After being bitten by an infected female mosquito, the parasite enters the human blood as a sporozoite and travels on to the hepatocytes after 30 minutes of blood circulation.¹⁸

4RAC Macromolecule: As the only pathway for the synthesis of the purine nucleoside monophosphates necessary for DNA/RNA creation, hypoxanthine, guanine, and [xanthine] phosphoribosyltransferase (HG[X]PRT) is regarded as a crucial target for antimalarial chemotherapy.

In many species, the enzyme hypoxanthine-guanine-[xanthine] phosphoribosyl transferase (HG[X]PRT) plays a vital role. It causes a purine base and a 5'-phospho-D-ribosyl-1-pyrophosphate to combine to generate 6-oxopurine nucleoside monophosphates (PRib-PP).¹⁹ Therefore, replication should stop if this enzyme is inhibited. The Plasmodium falciparum HGXPRT is effectively inhibited by the aza-acyclic nucleoside phosphonates (aza-ANPs) (Pf HGXPRT).

Although it has been hypothesised for a long time that *Plasmodium falciparum* HGXPRT (PfHGXPRT) could be a target for medications intended to treat malaria²⁰, inhibitors have only recently been transformed into substances with antimalarial action.²¹⁻²²

However, there are few studies on the phytoconstituents of *Hymenodictyon excelsum* for the antimalarial activity. Thus, keeping the above information in view, the present investigation was designed to identify the potential phytochemicals of *Hymenodictyon excelsum* against 4RAC using a molecular docking method.

2. MATERIALS AND METHODS

2.1. Platform for molecular docking

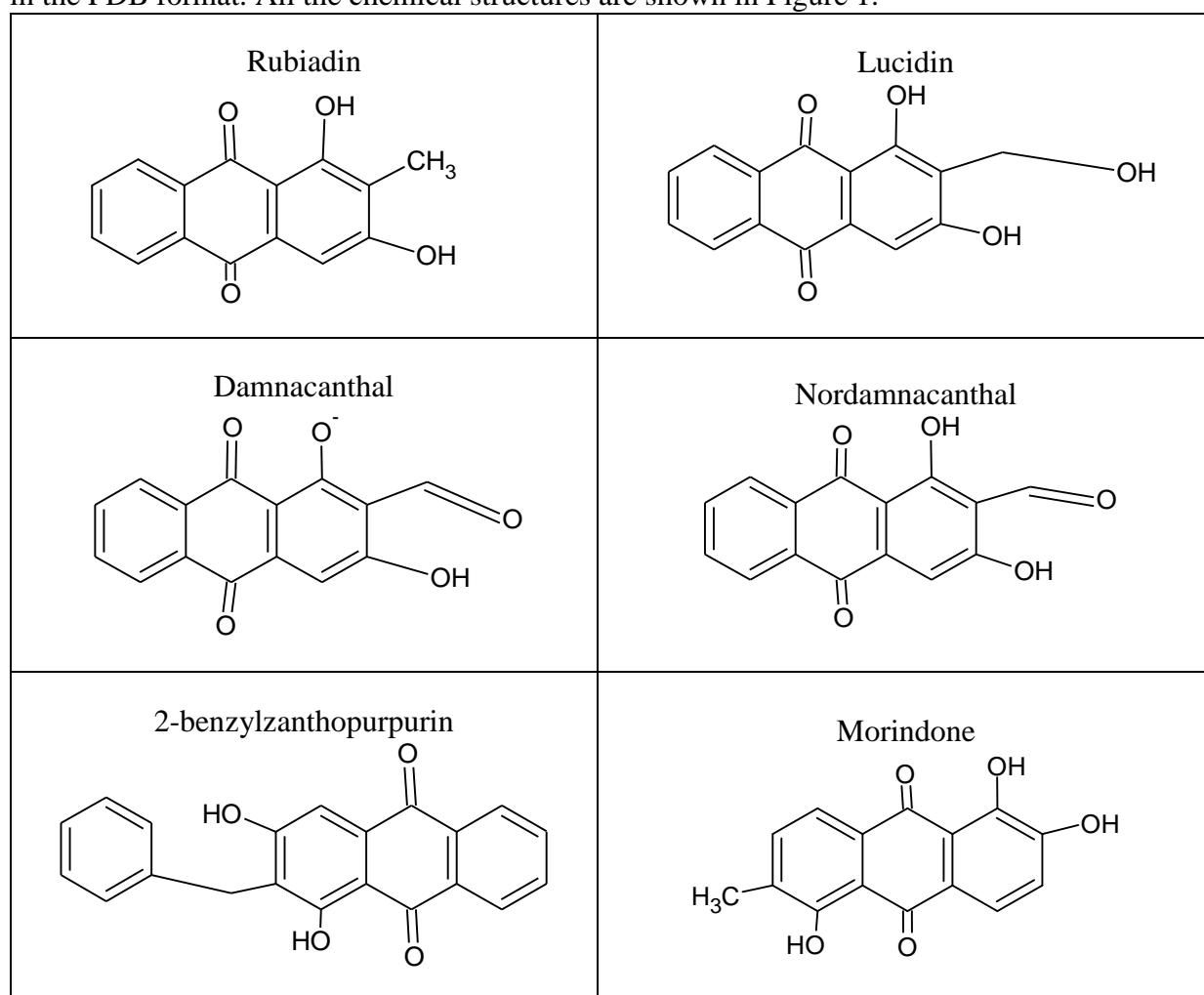
The computational docking study of all the phytoconstituents selected as ligands with antimalarial activity as the target was performed using PyRx software.²³

2.2. Protein preparation

The macromolecule is 4RAC, *in-silico* analysis of selected phytoconstituents was performed on the 2.05 Å crystal structure of antimalarial macromolecule with inhibitor, (PDB ID:4RAC having resolution: 2.05 Å, R-Value Free: 0.244, R-Value Work: 0.194, R-Value Observed: 0.196), which was retrieved from the protein data bank (<https://www.rcsb.org>) 4RAC is classified as Tranferase/Transferase inhibitors. all other molecules, such as co-crystallized water molecules, unwanted chains, and nonstandard residues, were deleted. Using Discovery studio.²⁴

2.3. Ligand preparation

The three-dimensional (3D) structures of all constituents were retrieved using Avogadro software from the PubChem database available on the NCBI website (<https://pubchem.ncbi.nlm.nih.gov/>). However, the drawing of geometrical 2D structure was performed using the ChemSketch program. The two-dimensional (2D) structures were transformed into 3D models using the Avogadro software and the ligand structures were saved in the PDB format. All the chemical structures are shown in Figure 1.



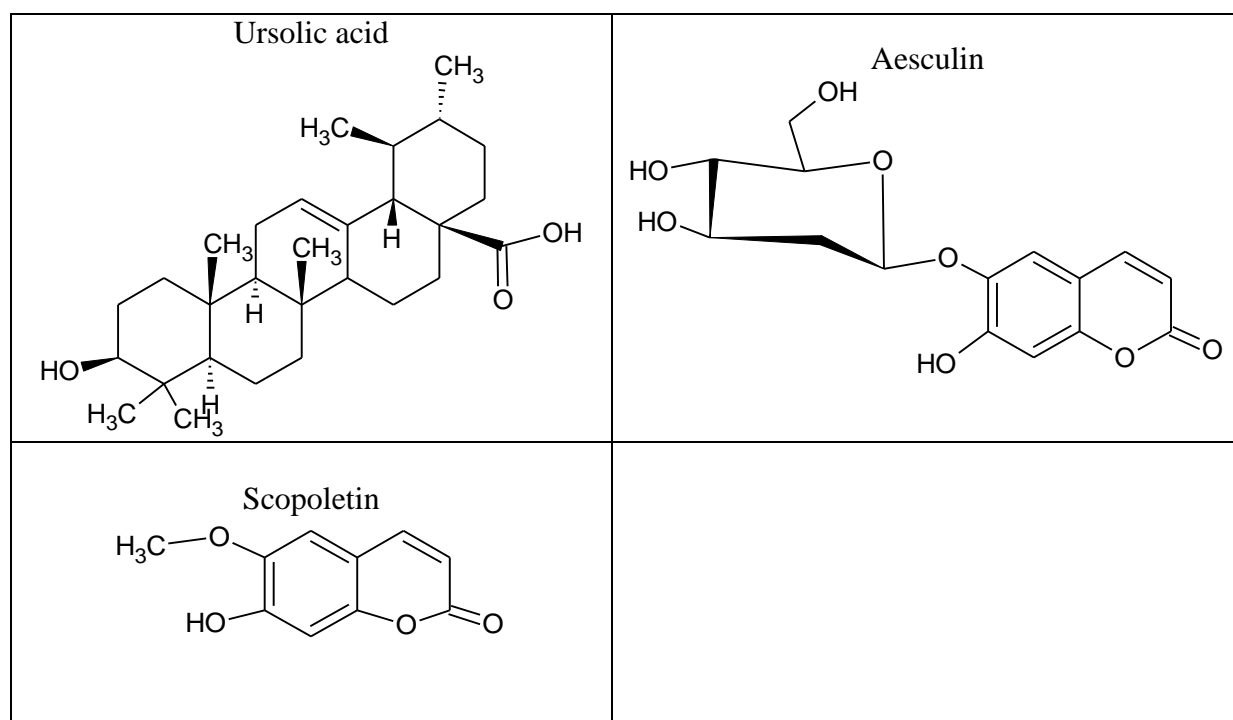


Fig. 1. Chemical structures of all selected phytoconstituents in the molecular docking studies

2.4 Standard Preparation

The standard is prepared steps such as, the 2D structure of standard drug was made using chem sketch program, then the 2D structure was converted into 3D model using Avogadro Software, it was saved in PDB format.

By using PyRx molecular docking of Artemisinin was done with 4RAC.

2.5. Molecular docking

Molecular docking evaluates the protein-ligand interactions and estimates the scoring function based on the geometry to predict the binding affinity of the ligand molecule²⁵⁻²⁶. We applied molecular docking studies to investigate the binding pattern of selected phytoconstituents (Figure 1) and the standard drug, along with the crystal structure of antimalarial activity macromolecule (PDB ID:4RAC). The molecular docking study was performed using PyRxsoftware, Binding affinity was explored using the Vina wizard tool. The final results were analysed and visualized using Discovery Studio 2020 Client²⁷, with bound ligands as the standard. Visualization of protein ligand interaction reflects the number of interactions and active residues responsible for significant binding at the active site of the target enzyme.

2.6. Absorption, distribution, metabolism, and excretion (ADME) and toxicity prediction

The selected phytoconstituents and standard drug were further checked for drug-likeness properties according to Lipinski's rule. During drug development, it is necessary to predict the tolerability of phytochemicals before being ingested by humans and animal models. The pharmacokinetic profile (ADME) and toxicity predictions of ligands were conducted using SwissADME (<http://www.swissadme.ch>) and pkCSM (an online server database predicting small-molecule pharmacokinetic properties using graph-based signatures, (<http://biosig.unimelb.edu.au/pkcsml/prediction>)). To analyse the toxicological properties of ligands, Simplified Molecular Input Line Entry System (SMILES) notations or

PDB files were uploaded, followed by selecting the required models for generating numerous information about structure-related effects²⁸⁻²⁹.

2.7 Interaction between Proteins by STRING Network Analysis

Search Tool for Retrieval of Interacting Genes (STRING) (<https://string-db.org/>) Database predicts and integrates protein–protein interaction to identify functional relationships and interactions between proteins. To seek potential interactions between genes involved in DNA Polymerase λ , the STRING tool was employed. STRING provided a platform that postulated several nodes, edges, average node degrees, protein–protein interaction (PPI) enrichment p-values, and average and local clustering coefficient. STRING provided possible biological processes, molecular function, and cellular components of candidate genes studied.³⁰

2.8 Bioactivity Score Analysis Using Molinspiration Tool

Molinspiration (<http://www.molinspiration.com/cgi-bin/properties>) predicts the drug resemblance properties of the compound dependent on various descriptors. Drugs entering the body should tie to an organic molecule to communicate its movement. Along their path, the bioactivity of compounds was anticipated by utilizing the Molinspiration tool which gave a bioactivity score of the phytocompound against the human receptors like GPCRs, ionic channels, kinases, various receptors, proteases, and proteins. A complex is considered to be dynamic if the bioactivity score is more than 0.0, modestly dynamic if somewhere in the range of –5.0 and 0.0, and idle if under –5.0.³¹

3. RESULTS AND DISCUSSION

The present study aimed to explore the inhibitory potential of the phytoconstituents present in *Hymenodictyon excelsum* targeting antimalarial activity. In this study, we performed molecular docking studies of all phytoconstituents found in *Hymenodictyon excelsum* using AutoDock Vina, followed by a study of interacting amino acid residues and their influence on the inhibitory potentials of the active constituents. Selected phytoconstituents showing the best fit were further evaluated for absorption, distribution, metabolism, excretion, and toxicological (ADMET) properties using SwissADME and pkCSM servers.

3.1 Molecular docking

The docking scores and binding energies of all chemical constituents of *Hymenodictyon excelsum* targeting antimalarial activity (PDB ID:4RAC) and binding interactions with amino acid residues are presented in Table 1 respectively.

Table 1. Binding interaction of ligands from *Hymenodictyon excelsum* targeting antimalarial activity (PDB ID:4RAC)

Sr. No.	Chemical constituent	PubChem ID	Docking Score
			4RAC
1.	Rubiadin	124062	-8.2
2.	Lucidin	10163	-8.1
3.	Damnacanthal	2948	-8.4
4.	Nordamnacanthal	160712	-8.9

5.	2-benzylanthopurpurin	630215	-7.8
6.	Morindone	442756	-8.2
7.	Ursolic Acid	64945	-8.0
8.	Aesculin	5281417	-8.5
9.	Scopoletin	5280460	-6.4
Standard Drug			
10.	Artemisinin	68827	-7.5

The binding affinities of phytoconstituents ranged from – 8.9 to -6.4 kcal/mol. From the docked results, it is evident that the compounds, Nordamnacanthal exhibit the most favourable binding affinity (–8.9 kcal/mol) and in complex with selected macromolecules (PDB ID:4RAC), as compared to other docked compounds i.e. Aesculin (–8.5 kcal/mol), Damnacanthal (–8.4 kcal/mol), Rudiadin(–8.2 kcal/mol), Morindone (–8.2 kcal/mol), Lucidin (–8.1 kcal/mol), 2-benzylanthopurpurin (–7.8 kcal/mol), Scopoletin (– 6.4 kcal/mol). Visual examination of the computationally docked optimal binding poses of phytoconstituents on selected macromolecules (i.e.4RAC) revealed the significant involvement of various types of interactions, such as hydrogen bonding and hydrophobic interactions, including π – π stacking and π –alkyl and alkyl interactions, in the stability of the binding of the phytoconstituents to 4RAC

The number of intermolecular hydrogen bonds, the binding energy of ligand 4RAC stable complexes, and the number of nearest amino acid residues were also determined for selected compound Artemisinin. All synthesized derivatives formed complexes with target proteins. An analysis of the interaction between the 4RAC protein complex and the Artemisinin ligand was also carried out, which showed that the ligand molecule is oriented due to van der Waals interaction with amino acid residue ILE135, ASP137, THR141, LEU101, GLU133, LEU67, VAL66, GLX70, GLY69, LYS68, ARG199, AP193 were also found (Fig. 2).

An analysis of the interactions between the 4RAC protein complex and the Nordamnacanthal ligand was also carried out, which showed that the ligand molecule is oriented due to one Pi–Pi stacked bond with the PHE186 amino acid fragment, conventional hydrogen bonds interactions with ASP193, ARG199, LYS68, GLY69, Pi-sigma interaction with IEL135, Pi-Alkyl interaction with LEU192, Pi-Anion interaction with ASP134. In addition, six van der Waals interactions with amino acid residues VAL187, LYS165, ASP137, THR141, LEU101, LEU67 were also found (Fig. 3a).

Analysis of interactions of the 4RAC protein complex and ligand Rubiadin showed that the ligand molecule is oriented due to one Pi–Pi Stacked bond with the PHE186 amino acid fragment and to Pi-sigma interactions with amino acid residues ILE135, and forming conventional hydrogen bonds with ARG199, ASP193, residues and Pi-Alkyl interaction with LEU192, and Unfavorable Donar interaction with PHE186, and Pi-Anion interaction with ASP134. In addition, seven van der Waals interactions with amino acid residues VAL187, LYS165, ASP137, THR141, LEU101, LUE67, GLX69 were also found (Fig. 3b).

An analysis of the interactions between the 4RAC protein complex and the Lucidin ligand was also carried out, which showed that the ligand molecule is oriented due to one Pi–Pi stacked bond with the PHE186 amino acid fragment, conventional hydrogen bonds interactions with the amino acid residues ASP193, LEU67, GLY69 Pi-sigma interaction with IEL135 Pi Alkyl interaction with LEU192, Unfavorable donar interaction with ARG199, Pi-Anion interaction with ASP134. In addition, eight van der Waals interactions with amino acid residues VAL187, LYS165, ASP137, THR141, LEU101, ARG100, VAL66, LYS68 were also found (Fig. 3c).

Table 2. Binding interactions of ligands with the binding site of Hypoxanthine-guanine phosphoribosyltransferase (HPRT1)

Sr. No	Inhibitors	Binding energy (kcal/mol)	H bond	Main amino acid interaction	
				Pi-alkyl, Pi-Sigma, alkyl, Pi-S/Pi-Pi stacking/Pi-Pi T shaped/halogen/unfavorable donor-donor interactions	van der Waals interaction
1	Rubiadin	-8.2	ARG199, ASP193	PHE186, ILE135, LEU192, PHE186, ASP134	VAL187, LYS165, ASP137, THR141, LEU101, LEU67, GLY69
2	Lucidin	-8.1	ASP193, LEU67, GLY69	PHE186, ILE135, LEU192, ARG199, ASP134	VAL187, LYS165, ASP137, THR141, LEU101, ARG100, VAL66, LYS68
3	Damnacanthal	-8.4	ASP193, ARG199, LYS68	PHE186, ILE135, LEU192, ASP134	VAL187, LYS165, ASP137, THR141, LYS102, LEU101, ARG100, LEU67, GLY69
4	Nordamnacanth al	-8.9	ASP193, ARG199, LYS68, GLY69	ILE135, PHE186, LEU192, ASP134	VAL187, LYS165, ASP137, THR141, LEU101, LEU67
5	2-benzylanthopur purin	-7.8	ASP193	LEU192, ILE113, ILE135, ASP134, THR141	LEU101, LYS102, ASP137, LYS165, VAL187, ARG199, GLY69, LYS68
6	Morindone	-8.2	LEU67, ASP193, ARG199, LYS68, LEU192	PHE186, ASP134	VAL187, LYS165, ASP137, GLY69, ARG100, LEU101
7	Aesculin	-8.5	VAL187, LYS165, ASP193	PHE186, ILE135, LEU192, ASP134	LYS185, LYS102, LEU101, GLU133, LYS68, GLY70, VAL66, GLY69, LEU67, ARG199
Standard Drug					
8	Artemisinin	-7.5	No Interaction	No Interaction	ILE135, ASP137, THR141, LEU101, GLU133, LEU67, VAL66, GLY70, GLY69, LYS68, ARG199, AAP193

3.2. ADMET study

Pharmacokinetic profile (ADME) and toxicity predictions of the ligands are important attentive parameters during the transformation of a molecule into a potent drug. In the present study, these parameters were assessed using SwissADME and pkCSM. The absorption potential and lipophilicity are characterized by the partition coefficient ($\log P$) and topological polar surface area (TPSA), respectively. For better penetration of a drug molecule into a cell membrane, the TPSA should be less than 140 Å. However, the value of $\log P$ differs based on the drug target. The ideal $\log P$ value for various drugs are as follows: oral and intestinal absorption, 1.35 –

1.80; sublingual absorption, > 5; and central nervous system (CNS)³². The aqueous solubility of ligands ideally ranges from – 6.5 to 0.5³³, while the blood brain barrier (BBB) value ranges between – 3.0 and 1.2³⁴. In addition, non-substrate P-glycoprotein causes drug resistance³⁵. In our study, all the selected ligands followed the TPSA parameter, P-glycoprotein non-inhibition, thereby showing good intestinal absorption and an acceptable range of BBB values. All the compounds showed aqueous solubility values within the range. Further, it was predicted that the selected ligands do not show AMES toxicity, hepatotoxicity, and skin sensitivity. In addition, it did not inhibit hERG-I (low risk of cardiac toxicity). Lipinski's rule violations, *T. pyriformis* toxicity, minnow toxicity, maximum tolerated dose, rat acute oral toxicity, and chronic toxicity are depicted in table 3.

Table 3. ADME and toxicity predicted profile of ligands with superior docking scores

ADMET Properties	Formula	MW (g/mol)	Log P	TPSA (Å ²)	HB doner	Hb acceptor	Aqueous solubility (Log mol/L)	Human intestinal absorption (%)	Blood-brain barrier
Rubiadin	C ₁₅ H ₁₀ O ₄	254.24	2.18162	74.60	2	4	-3.243	96.938	0.025
Lucidin	C ₁₅ H ₁₀ O ₅	270.24	1.3655	94.83	3	5	-2.963	70.752	-0.979
Damnacanthal	C ₁₅ H ₇ O ₅	267.21	1.0537	94.50	1	5	-3.04	83.174	-0.288
Nordamnacanthal	C ₁₅ H ₈ O ₅	268.22	1.6857	91.67	2	5	-3.08	92.837	-0.157
2-benzylanthopurpurin	C ₂₁ H ₁₄ O ₄	330.33	3.464	74.60	2	4	-4.133	96.885	0.187
Morindone	C ₁₅ H ₁₀ O ₅	270.24	1.88722	94.83	3	5	-3.093	74.498	-0.707
Ursolic Acid	C ₂₉ H ₄₆ O ₃	442.684	6.6994	57.53	2	2	-4.508	96.081	-0.384
Aesculin	C ₁₅ H ₁₆ O ₈	324.28	-0.2935	129.59	4	8	-2.482	69.689	-1.298
Scopoletin	C ₁₀ H ₈ O ₄	192.17	1.5072	59.67	1	4	-2.467	95.015	-0.309
Standard Drug									
Artemisinin	C ₁₅ H ₂₂ O ₅	282.33	2.3949	53.99	0	5	-3.678	97.543	0.235

Table 3 Continued

ADMET Properties	PGP substrate	Total clearance [Log mL/(min.kg)]	Bioavailability score	AMES toxicity	Max tolerated dose [Log mg/(kg.d)]	hERG I inhibitor	hERG II inhibitor
Rubiadin	YES	0.129	0.55	YES	0.387	NO	NO
Lucidin	YES	0.073	0.55	NO	0.761	NO	NO
Damnacanthal	YES	0.223	0.56	YES	0.077	NO	NO
Nordamnacanthal	YES	-0.024	0.55	NO	0.645	NO	NO
2-benzylanthopurpurin	YES	0.167	0.55	YES	0.199	NO	YES
Morindone	YES	-0.046	0.55	YES	0.556	NO	NO
Ursolic Acid	YES	0.13	0.85	NO	-0.809	NO	NO
Aesculin	YES	0.765	0.55	NO	0.0543	NO	NO
Scopoletin	NO	0.752	0.55	NO	0.292	NO	NO
Standard Drug							
Artemisinin	NO	0.98	0.55	YES	0.065	NO	NO

Table 3 Continued

ADMET Properties	Acute oral rat toxicity, LD50(mol/kg)	Oral rat chronic toxicity (Log mg/kg bw/day)	Hepatotoxicity	Skin sensitisation	T. Pyriformis toxicity (Log µg/L)	Minnow toxicity (Log mmol/L)	Lipinski's rule violations
Rubiadin	2.146	1.554	NO	NO	0.848	0.364	YES (0)
Lucidin	2.283	2.359	NO	NO	0.382	0.457	YES (0)
Damnacanthal	1.998	1.602	NO	NO	0.975	0.678	YES (0)
Nordamnacanthal	1.57	2.389	NO	NO	0.629	2.071	YES (0)
2-benzylanthopurpurin	2.21	1.345	NO	NO	0.298	-0.995	YES (0)
Morindone	2.124	2.215	NO	NO	0.421	1.904	YES (0)
Ursolic Acid	4.018	2.02	YES	NO	0.315	-0.229	YES (1)
Aesculin	2.417	3.255	YES	NO	0.282	2.865	YES (0)
Scopoletin	2.012	1.424	NO	NO	0.453	1.604	YES (0)
Standard Drug							
Artemisinin	2.459	1	NO	NO	0.322	1.406	YES (0)

3.3 String Pathway

Hypoxanthine-guanine phosphoribosyltransferase (HPRT1): Converts guanine to guanosine monophosphate, and hypoxanthine to inosine monophosphate. Transfers the 5-phosphoribosyl group from 5-phosphoribosylpyrophosphate onto the purine. Plays a central role in the generation of purine nucleotides through the purine salvage pathway.

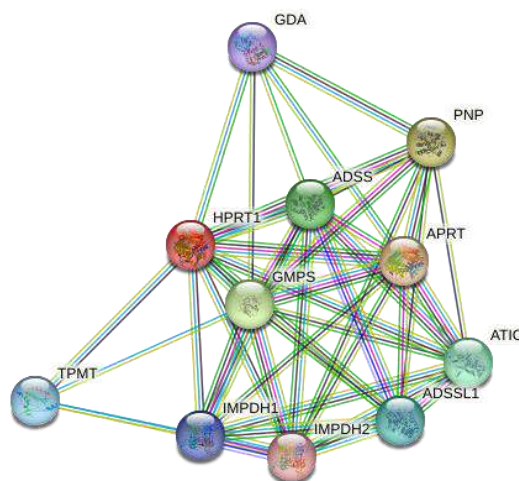


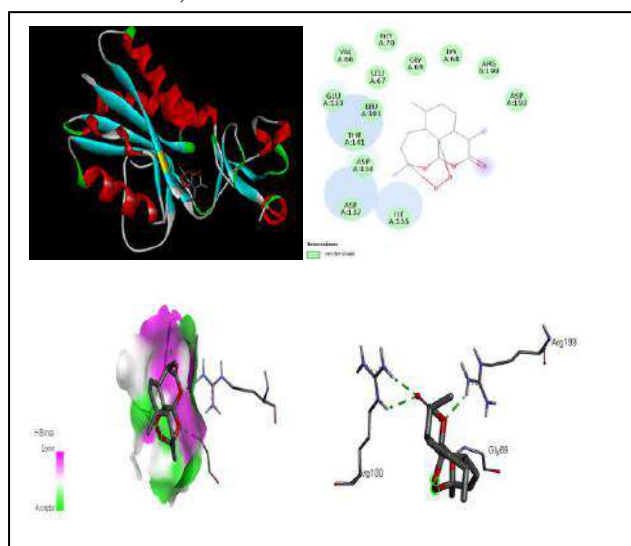
Fig.2. Network formation of HPRT1 using STRING

3.4 Molinspiration

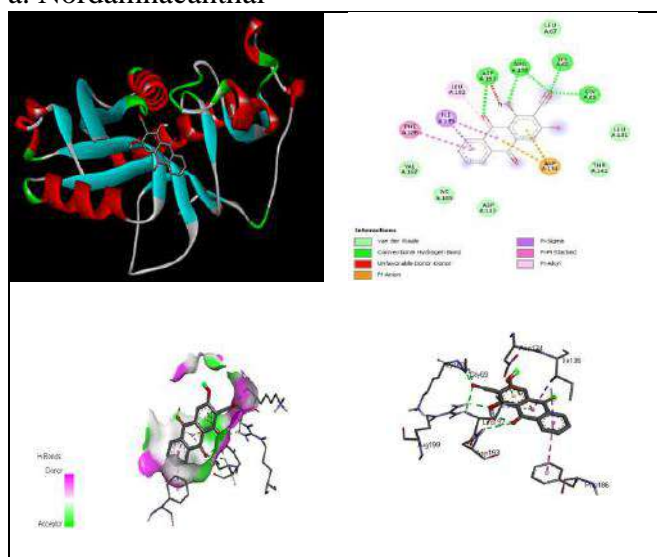
Lastly, we predicted bioactivity scores to identify the potency of Phyto molecules studied (Table 4). Our result showed that nordamnacanthal, rubiadin and lucidin might essentially serve as an interface with Hypoxanthine-guanine phosphoribosyltransferase (HPRT1) as they acted as enzyme inhibitors. Bioactivity scores of phytoconstituents and standard were comparable indicating that these phytocompounds might be utilized as an alternative and in improving treatment to malaria.

Table 4. Summary of predicted Molinspiration bioactivity score for nordamnacanthal, rubiadin and lucidin in comparison to Artemisinin

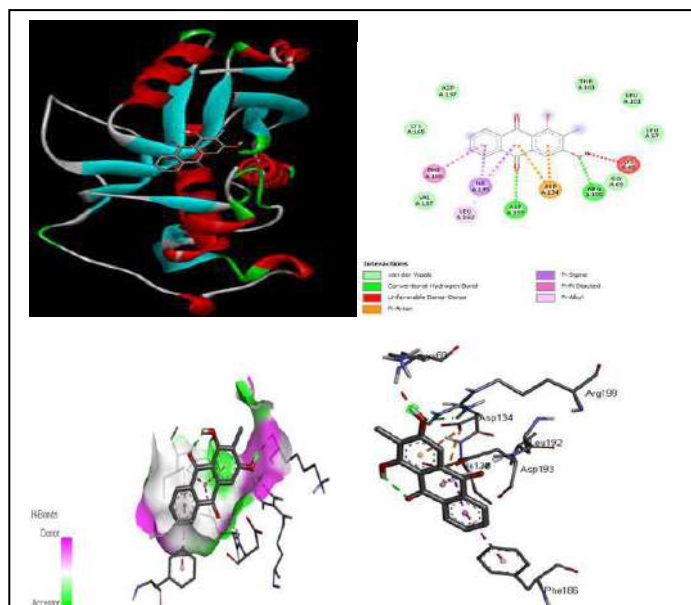
Bioactivity	GPCR ligand	Ion channel modulator	Kinase inhibitor	Nuclear receptor ligand	Protease inhibitor	Enzyme inhibitor
Nordamnacanthal	-0.20	-0.04	0.10	0.15	-0.28	0.22
Rubiadin	-0.20	-0.19	-0.03	0.07	-0.26	0.24
Lucidin	-0.02	0.04	0.13	0.19	-0.02	0.38
Standard Drug						
Artemisinin	-0.17	-0.31	-0.65	-0.00	-0.19	0.39

Standard Drug**1. Artemisinin, 4RAC****Fig. 3. Docking scores and binding interaction of Artemisinin (PDB ID: 4RAC).**

The ligand is shown in line and stick representation along with its 2D diagram and hydrogen bond interaction.

Drugs to be considered**a. Nordamnacanthal**

b. Rubiadin



c. Lucidin

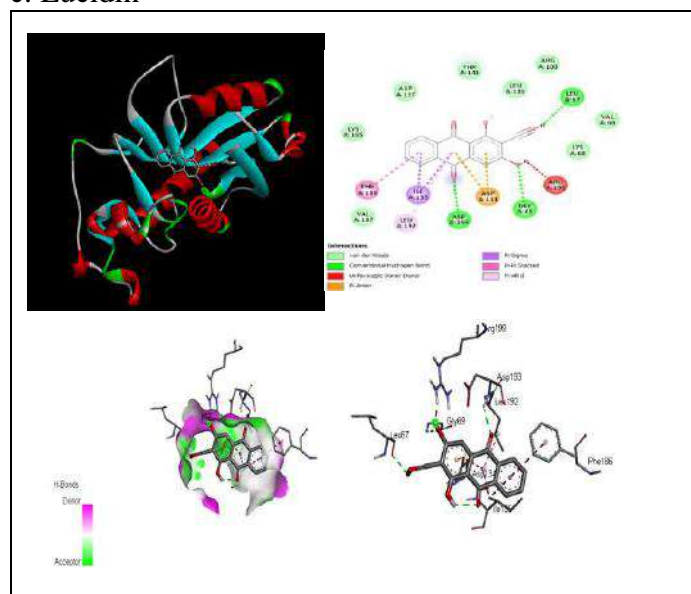


Fig. 4. Docking scores and binding interaction for antimalarial activity (PDB ID: 4RAC). The ligand is shown in line and stick representation along with its 2D diagram and hydrogen bond interaction

Boiled Egg Diagram

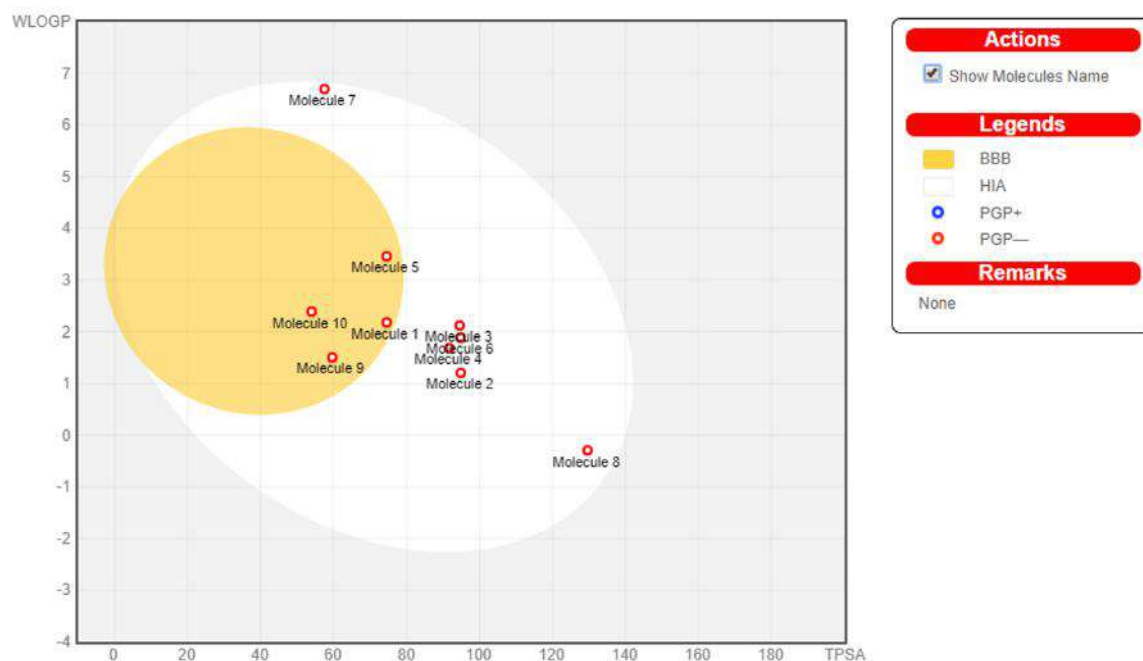


Fig. 5 Combined boiled egg diagram of all phytoconstituents with standard.

Table 5. Molecule names in boiled egg diagram.

MOLECULES NO.	DRUG NAME
1	Rubiadin
2	Lucidin
3	Damnacanthal
4	Nordamnacanthal
5	2-benzylanthopurpurin
6	Morindone
7	Ursolic acid
8	Aesculin
9	Scopoletin
10	Artemisinin

BOILED means **B**rain **O**r **I**ntestina**L** **E**stimate **D** Permeation Predictive model:

The Boiled egg diagram shows two regions white and yellow. The white region is the physiochemical space of molecules with highest probability of being absorbed by the gastrointestinal tract, and the yellow region (yolk) is the physiochemical space of molecules with highest probability to permeate to the brain.

In addition the points are coloured in blue if predicted as activated effluxed by P-gp (PGP+) and in red if predicted as non-substrate of P-gp (PGP-).

CONCLUSION

In this study, we have carried out an *in-silico* screening of the phytoconstituents of *Hymenodictyon excelsum* plant. This study demonstrated the nine compounds from *Hymenodictyon excelsum* plant, (Rubiadin, Lucidin, Damnacanthal, Nordamnacanthal, 2-benzylanthopurpurin, Morindone, Ursolic Acid, Aesculin, Scopoletin). The selected phytocompounds showed docking scores ranging from – 8.9 to -6.4 kcal/mol in 4RAC. Among all, Nordamnacanthal gave the lowest binding energy (– 8.9 kcal/mol) in complex with 4RAC.

whereas the reference compound, Artemisinin, showed a docking score with a binding energy -7.5kcal/mol . Furthermore, these ligands exhibited good ADMET properties. To summarize, phytoconstituents present in *Hymenodictyon excelsum* possess strong effects against 4RAC and could be further evaluated for their anti-malarial effect, as well as for the development of alternative drugs with fewer side effects for the treatment of malaria.

REFERENCE

1. Sylvain GR, Birgitta B (2006) Taxonomic revision of the tribe Hymenodictyeae (Rubiaceae, Cinchonoideae). Botanical Journal of the Linnean Society 152: 331-386.
2. Deb DB (1989) Taxonomic revision of the genus Hymenodictyon (Rubiaceae). Journal of Economic Taxonomy and Botany 13: 673-682.
3. Asolkar LV, Kakkar KK, Chakra OJ (1992) Glossary of Indian Medicinal Plants with Active Principles (Second Supplement) Part-1 (A-K) 1965- 1981. NISC, CSIR, New Delhi, India.
4. Rastogi RP, Mehrotra BN (1993) Compendium of Indian medicinal plants, Vol. 3, edited by Rastogi R.P. Central Drug Research Institute and Publications & Information Directorate New Delhi.
5. Sarin YK (196) Illustrated manual of Herbal Drugs used in Ayurveda, Council of Scientific and industrial Research and Indian council of Medicinal Research New Delhi, India.
6. Ghani A (2003) Medicinal plants of Bangladesh with chemical constituents and uses, 2nd edn, Asiatic Society of Bangladesh, Dhaka.
7. Suruse PB, Duragkar NJ, Deshpande SA (2015) Evaluation of in vitro and in vivo antimalarial activity of Hymenodictyon excelsum bark extracts. Innovations in Pharmaceuticals and Pharmacotherapy (IPP) 3 (1): 554-560.
8. Nareeboon P, Komkhunthot W, Lekcharoen D, Wetprasit N, Piriyaapolsart C, Sutthivaiyakit S. Acetylenic fatty acids, triglyceride and triterpenes from the leaves of Hymenodictyon excelsum. Chemical and Pharmaceutical Bulletin. 2009 Aug 1;57(8):860-2.
9. Brew EJ, Thomason RH. Naturally occurring quinones. Part XIX. Anthraquinones in hymenodictyon excelsum and damnacanthus major. Journal of the Chemical Society C: Organic. 1971:2001-7.
10. Rao PS, Asheervadam Y, Khaleelullah MD, Rao NS, Murray RD. Hymexelsin, an apiose-containing scopoletin glycoside from the stem bark of Hymenodictyon excelsum. Journal of natural products. 1988 Sep;51(5):959-61.
11. Chatterjee A, Pakrashi SC. The Treatise on Indian Medicinal Plants, Vol. 5, National Institute of Science Communication, New Delhi p. 94. Google Scholar. 1997.
12. White NJ, Pukrittayakamee S, Hien TT, Faiz MA, Mokuolu OA, Dondorp AM. Erratum: Malaria (The Lancet (2014) 383 (723-735)). The Lancet. 2014 Jan 1;383(9918).
13. Walker, N.; Nadjm, B.; Whitty, C. Malaria. Medicine **2017**, 42, 52–58.
14. Antinori S, Galimberti L, Milazzo L, Corbellino M. Biology of human malaria plasmodia including Plasmodium knowlesi. Mediterranean journal of hematology and infectious diseases. 2012;4(1).
15. EA A. PyaePhyo 2, Woodrow CJ. Malaria. Lancet. 2018;391(10130):1608-21.
16. Singh B, Daneshvar C. Human infections and detection of Plasmodium knowlesi. Clinical microbiology reviews. 2013 Apr;26(2):165-84.
17. Vuk, I.; Rajic, Z.; Zorc, B. Malaria and antimalarial drugs. Farm Glas**2008**, 64, 51–60.
18. Josling GA, Llinás M. Sexual development in Plasmodium parasites: knowing when it's time to commit. Nature Reviews Microbiology. 2015 Sep;13(9):573-87.
19. Reyes P, Rathod PK, Sanchez DJ, Mrema JE, Rieckmann KH, Heidrich HG. Enzymes of purine and pyrimidine metabolism from the human malaria parasite, Plasmodium falciparum. Molecular and biochemical parasitology. 1982 May 1;5(5):275-90.
20. Ting LM, Shi W, Lewandowicz A, Singh V, Mwakingwe A, Birck MR, Ringia EA, Bench G, Madrid DC, Tyler PC, Evans GB. Targeting a novel Plasmodium falciparum purine recycling pathway with specific immucillins. Journal of Biological Chemistry. 2005 Mar 11;280(10):9547-54.
21. De Jersey J, Holy A, Hocková D, Naesens L, T Keough D, W Guddat L. 6-oxopurine phosphoribosyltransferase: a target for the development of antimalarial drugs. Current topics in medicinal chemistry. 2011 Aug 1;11(16):2085-102.

22. Berg MV, Van der Veken P, Goeminne A, Haemers A, Augustyns K. Inhibitors of the purine salvage pathway: a valuable approach for antiprotozoal chemotherapy?. *Current medicinal chemistry*. 2010 Aug 1;17(23):2456-81.
23. G.M. Morris, R. Huey, W. Lindstrom, *et al.* AutoDock4 and AutoDockTools4: Automated docking with selective receptor flexibility, *Journal of Computational Chemistry*, 30 (16) (2009), pp. 2785-2791.
24. E.F. Pettersen, T.D. Goddard, C.C. Huang, *et al.* UCSF Chimera - a visualization system for exploratory research and analysis, *Journal of Computational Chemistry*, 25 (13) (2004), pp. 1605-1612.
25. M.L. Verdonk, J.C. Cole, M.J. Hartshorn, *et al.* Improved protein-ligand docking using GOLD, *Proteins: Structure, Function, and Bioinformatics*, 52 (4) (2003), pp. 609-623.
26. A.R. Leach, B.K. Shoichet, C.E. Peishoff, Prediction of protein-ligand interactions. Docking and scoring: Successes and gaps, *Journal of Medicinal Chemistry*, 49 (20) (2006), pp. 5851-5855.
27. Biovia DS. Discovery studio modeling environment, Release 2017. San Diego: Dassault Systèmes, 2016.
28. S. Arora, G. Lohiya, K. Moharir, *et al.* Identification of potential flavonoid inhibitors of the SARS-CoV-2 main protease 6YNQ: a molecular docking study, *Digital Chinese Medicine*, 3 (4) (2020), pp. 239-248.
29. S. Shah, D. Chaple, S. Arora, *et al.* Exploring the active constituents of *Oroxylum indicum* in intervention of novel coronavirus (COVID-19) based on molecular docking method, *Network Modeling and Analysis in Health Informatics and Bioinformatics*, 10 (1) (2021), p. 8.
30. zklarczyk D, Franceschini A, Wyder S, Forslund K, Heller D, Huerta-Cepas J, et al. STRING v10: Protein-protein interaction networks, integrated over the tree of life. *Nucleic Acids Res*. 2015;43(Database issue):D447-52.
31. Tariq, M., Sirajuddin, M., Ali, S., Khalid, N., Tahir, M. N., Khan, H., et al. (2016). Pharmacological investigations and Petra/Osiris/Molinspiration (POM) analyses of newly synthesized potentially bioactive organotin(IV) carboxylates. *Journal of Photochemistry and Photobiology B: Biology*, 158, 174-183.
32. D. Kaloni, D. Chakraborty, A. Tiwari, et al. In silico studies on the phytochemical components of *Murrayakoenigii* targeting TNF- α in rheumatoid arthritis *Journal of Herbal Medicine*, 24 (2020), p. 100396.
33. T. Joshi, P. Sharma, T. Joshi, *et al.* In silico screening of anti-inflammatory compounds from Lichen by targeting cyclooxygenase-2 *Journal of Biomolecular Structure and Dynamics*, 38 (12) (2020), pp. 3544-3562.
34. C.M. Nisha, A. Kumar, A. Vimal Docking and ADMET prediction of few GSK-3 inhibitors divulges 6-bromoindirubin-3-oxime as a potential inhibitor *Journal of Molecular Graphics and Modelling*, 65 (2016), pp. 100-10.
35. S. Tsujimura, Y. Tanaka Disease control by regulation of P-glycoprotein on lymphocytes in patients with rheumatoid arthritis *World Journal of Experimental Medicine*, 5 (4) (2015), pp. 225-231.

Spectrophotometric Complexation Study of Cu(II) with 8-Hydroxyquinoline based Azo dye

Santosh M. Chavan¹ Nilesh V. Rathod², Manoj S. More², Chandrakant D. Ghugare¹,
Ravi E. Khadse³, Jayshri S. Jadhao², Akash V. Kubade² Parikshit S. Thakare²,
Arun B. Patil¹

1. Department of Chemistry Phulsing Naik College Pusad MS India-444204

2. Department of Chemistry R.A. Arts Shri. M. K. Commerce and Shri. S.R. Rathi Science College Washim MS India-444505

3. Late Pundlikrao Gawali Arts and Science College Shirpur Jain MS India -444504

Email: Santoshchavan.78@rediffmail.com, nileshrathod3684@gmail.com

Abstract:

In present study Cu(II) and 8-Hydroxyquinoline azo dye (8-HDQ-Cu(II)) were combined to generate a metal complex, which was then examined using IR, UV-Visible and Scanning electron microscopic methods. The complex formation spectroscopic peak is visible at 305 nm. The binding constant and the 1:2 M:L stoichiometry have been ascertained. As a result, the azo dye of 8-hydroxyquinoline is a commonly used indicator in the complexometric method to measure Cu(II).

Keywords: 8-Hydroxyquinoline, Cu(II) metal ion, UV-Visible

Introduction:

Potential applications in industry, technology, and life processes have been identified for coordination complexes containing azo chemicals as ligands[1-4]. Copper complexes have many different and significant applications. Copper complexes find extensive application as fungicides, crop defenders, and polymer additives. Metal complex dyes are essential functional materials that have been incorporated into numerous high-tech applications. The creation of innovative azo dye structures has drawn attention; many of these structures are beneficial for commercial applications such as polyester, polyamide, and polyacrylic, as well as blends with other fibers [5-7]. 8-Hydroxyquinoline (8-HQ), a crucial ligand in this area, is well-known for its potent coordination skills and special capacity to distinguish between various metals [8]. In order to use 8-hydroxyquinoline and its derivatives, the phenolate oxygen and quinoline nitrogen must connect both inside and outside of the cyclic structure. This makes it possible to use it as a metal chelator because it can bind to metals in bidentate and monomeric forms [9].

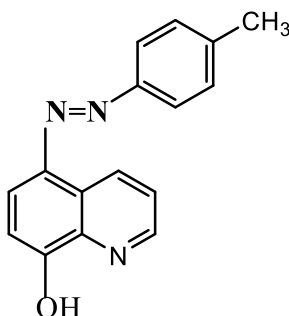


Figure 1: 8-Hydroxyquinoline azo dye

Chemicals and Instruments:

S.D. Fine Chemicals provided all of the chemical substances used in this investigation. A single beam UV-VIS Bio-Era spectrophotometer with a quartz cell (10 mm) was used to measure the electronic spectra, and an IR spectrometer made by Bruker was utilized to get the FT-IR spectra. Additional double-distilled water purification was supplied by Milli-Q. The AR grade of solvents was used. The 8-HDQ dye stock solution contained 2×10^{-4} M, while the metal solutions had 1×10^{-2} M.

Preparation of Ligand and Complex:

The preparation of ligand and its complex was prepared according previously reported literature [10].

UV-Visible Study of ligand and its Cu(II) complex:

The UV-visible spectroscopic approach was used to characterize the study using a UV-visible spectrophotometer with a 10 mm quartz cell. This is the spectrum of an ethanol solution of copper nitrate (5×10^{-4} M) and ligand (5×10^{-5} M) in water after adding some concentrated nitric acid. It was noted from the graph (Fig.2) that the ligand exhibits its greatest absorbance at 305 nm, which is the cause of $n-\pi^*$. However, there is a little shift up to 295 nm that shows the complex formation during complexation with copper metal ion.

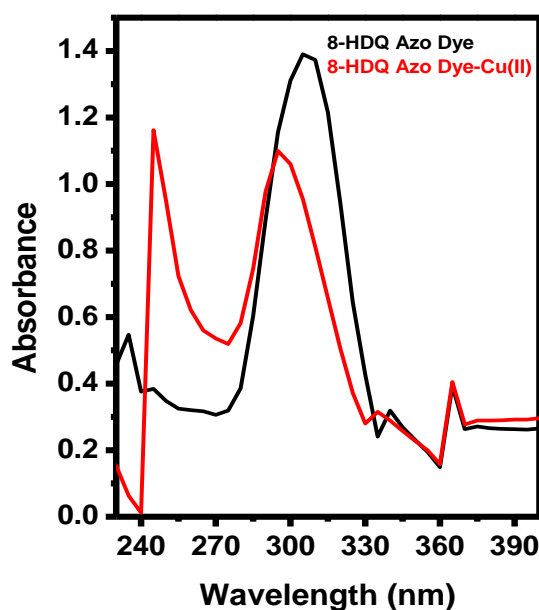


Figure 2: UV-Visible spectra of ligand and its Cu(II) Complex

Metal to ligand stoichiometry:

Cu(II) metal ion solutions and 8-HDQ azo dye were combined in similar mole ratios, with the dye and metal ion concentrations being constant. The complex's stoichiometry was ascertained by measuring the absorbance at a wavelength of 305 nm. The relationship between absorbance and mole fractions is depicted in Figure 3, the resultant absorbance graph. For the 8-HDQ-Cu(II) complexes, the greatest absorbance is observed at a mole ratio of 0.4, indicating that two ligands are bonded to the metal ion in a 1:2 ratio.

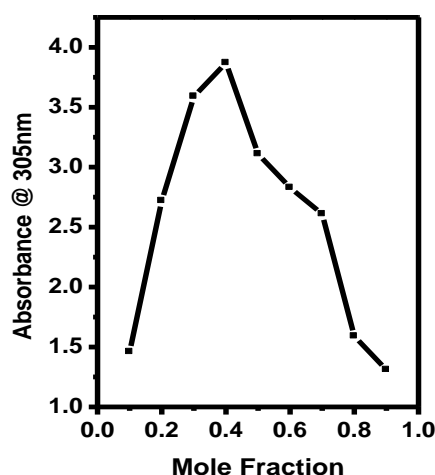


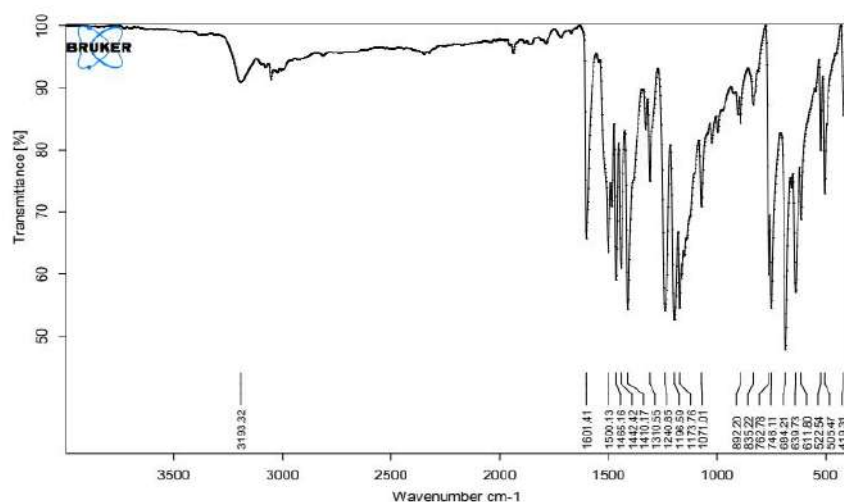
Figure 3: Jobs plot of Complex for the stoichiometry

IR Spectra Study:

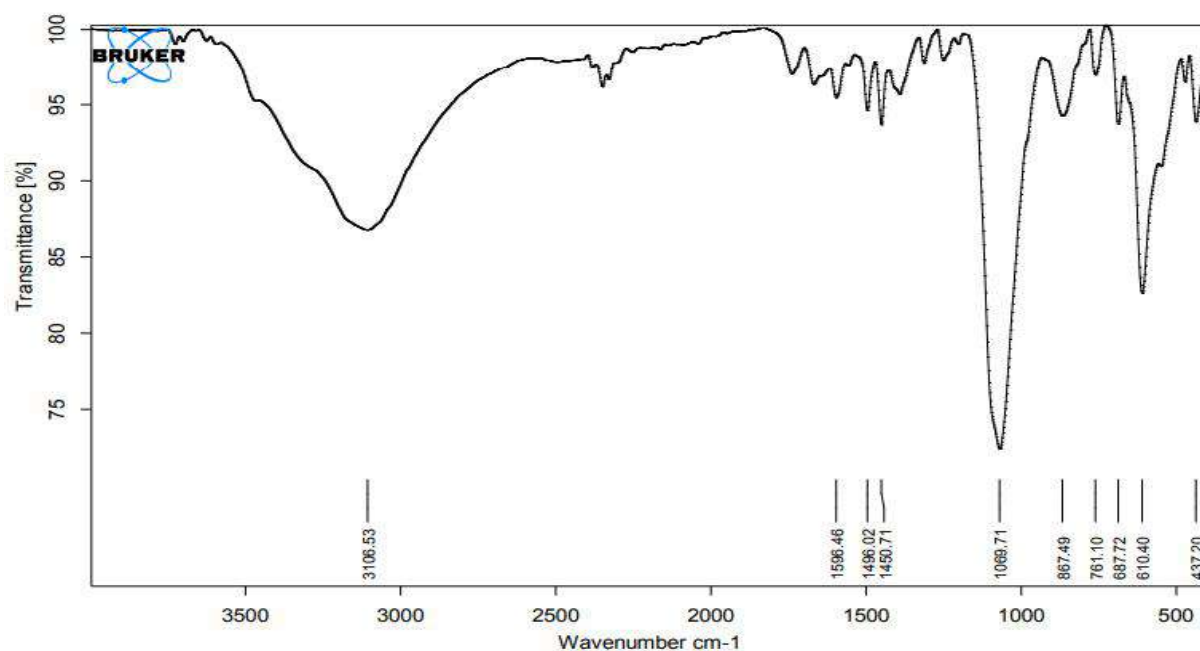
The FTIR spectra of the developed complexes and ligands are shown in Figure 4. Table 1 displays the spectrum data obtained from FTIR spectroscopy. A broad band of moderate intensity was seen on the ligands. The O-H bond of 8-HDQ ligands appeared at 3193 cm^{-1} in the FTIR spectra, however, it moved to 3106 cm^{-1} when the complex formed with the Cu(II) metal ion. In 8-HDQ, a band confirming the presence of the C-O bond was found at 1240 cm^{-1} however, in the complexes, these bands migrated to 1230 cm^{-1} . The vibrational frequencies of the M-O and M-N bonds support the confirmation of the bonding between the ligand and metal ion. These frequencies are roughly 602 cm^{-1} for the former and 437 cm^{-1} for the latter.

Table 1. Infra-red spectral data for 8-HDQ and Co(II) complexes.

Compound	Infra red spectral bands $\bar{\nu}\text{ cm}^{-1}$					
	OH	C-O	C-N	N=N	M-O	M-N
8-HDQ	3193	1240	1310	1465	-	-
8-HDQ-Cu(II)	3106	1230	1305	1450	610	437



(a)



(b)

Figure 4: IR spectra of (a) 8-HDQ (b) 8-HDQ-Cu(II) complex**The stability constant of 8-HDQ-Cu(II) complex:**

The stability constant, sometimes referred to as a binding constant, is the equilibrium constant for complex formation in solution. It serves as an indicator of how well the metal and ligand will bind together to form a complex. The following equation was used to determine the apparent stability constant (K) of the (1:2) Metal: Ligand complex with the use of spectroscopic data.

$$K = 1 - \alpha / 4\alpha^3 c^2 \quad (1)$$

$$\alpha = A_m - A_s / A_m \quad (2)$$

or

$$\alpha = A_s - A_m / A_s$$

where, A_s is the solution's absorption when ligand and metal ions are present in stoichiometric proportions, c is the complex solution's concentration in mol/L, and A is the degree of dissociation. A_m is the quantity of metal absorbed in a solution containing an excess of ligand. The solution's λ_{max} was used to assess the values of A_s and A_m . The values of α , K , A_m , and A_s were tabulated below Table 2, which demonstrates the high value of K , or 2.3×10^5 . This outcome demonstrates the strong binding between Cu(II) metal and 8-HDQ azo dye.

Table 2. The stability constant of 8-HDQ-Cu(II) Complex:

complex	A_s	A_m	α	K_s
[Bi(L) ₂]	2.233	2.595	0.01325	2.3×10^5

Scanning Electron Microscopy Study:

The morphologies of 8-HDQ, and its Cu(II) complexes were investigated in the scanning electron microscopy (SEM) study. The SEM pictures of the ligands exhibit an irregular, rock like morphology with varying lateral diameters, as illustrated in Fig. 5(a,b). It's interesting to note that the complexes' surface shape was significantly changed by metal coordination to the ligand. In particular, the copper complex's SEM micrographs show a noticeably uneven structure that resembles broken ice.

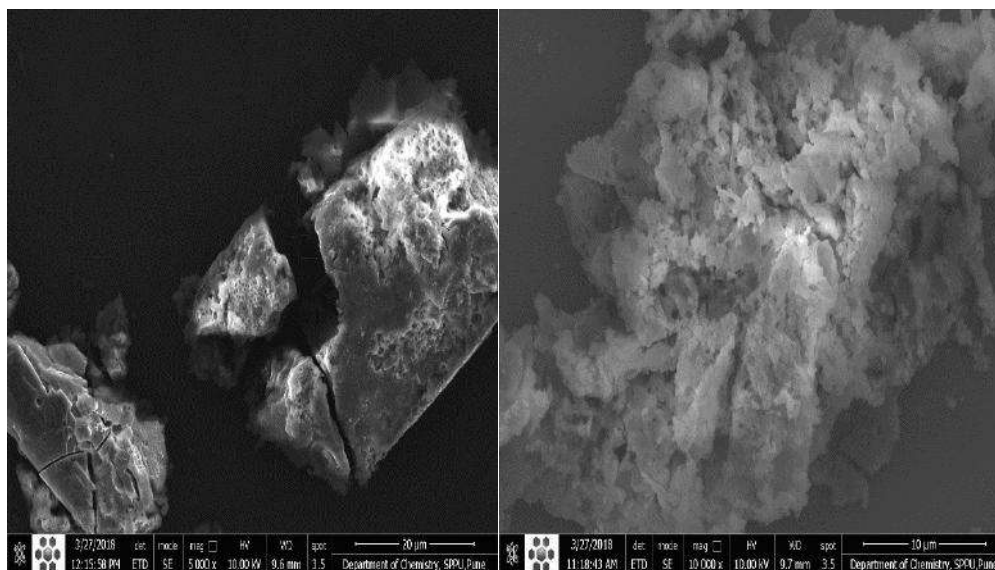


Figure 5: SEM micrograph of (a) 8-Hydroxyquinoline azo dye and (b) 8-HDQ-Cu(II) complex

Conclusion:

In summary, we have effectively created an 8-hydroxyquinoline compound using Cu(II). UV-Vis spectroscopy has been used to study Cu(II) binding with 8-HDQ. After research, the stoichiometry of metal ions and ligands was found to be 1:2. The complex that forms between copper and the azo dye of 8-hydroxy quinoline has a larger stability constant, indicating that it is stable. Additional evidence of the binding relationship between Cu(II) and ligand is provided by SEM studies and IR spectra.

References:

1. B. K. Ghosh and A. Chakravorty, *Coord. Chem. Rev.* 95, 239 (1989).
2. P. K. Santra, T K Misra, D. Das, C. Sinha, A. M. Z. Salwin, J. D. Woollins, *Polyhedron* 18, 2869-2878 (1999).
3. S. S. Kandil, *Trans. Met. Chem.* 23, 461-465 (1998).
4. M. A. Awad, *J. Chem. Biotechnol.* 53, 227(1992).
5. V.H, Patel, M.P. Patel, R.G. patel, 2002. *J. Serb. Chem. Soc* 67 (11) : 727-734.
6. M. Mohorcic, J. Friedrich, and A. Pavko, 2004. *Acta. Chim. Slov* 51(2):619-628.
7. H.R. Maradiya, 2001, *Turk. J. Chem* 25(6): 441-450.
8. M. Albrecht, M. Fiege, O. Osetska, *Coord Chem Rev.* 2008;252(8-9):812-824
9. M. Nguyen, L. Vendier, J.L. Stigliani, B. Meunier, A. Robert Eur. *J. Inorg. Chem.* 2017, 3, 600-608
10. A. El., Nadia, H. F. Wakiel, S.A. Ibrahim, *Appl Organometal Chem*, 31(10), 1-7, (2017)

A Comprehensive Review on Various Method of Synthesis and Biological Activities of Schiff Bases with Heterocyclic Moiety

Rahul P. Rahate

Assistant Professor, Department of Chemistry, Arts, Science and Commerce, College, Chikhaldara, Maharashtra, India, rprascc@gmail.com

Abstract:

Schiff bases are versatile chemical compounds that are becoming more important because of their numerous applications. Schiff bases, which include imines or azomethine functional groups, are formed by the condensation of primary amines with carbonyl compounds or can exist naturally in plants. They are widely used in industry and exhibit a variety of biological activities, such as antibacterial, antifungal, antiviral, and anticancer properties. Researchers are presently focusing on a wide range of biological studies of Schiff bases, which could lead to the discovery of new lead compounds. This review covers discoveries and various methods for synthesising specially Schiff bases with heterocyclic moiety, as well as their biological functions.

Keywords: Schiff bases; Biological activities; Applications; Antifungal; Antiviral; Anticancer

Introduction

Hugo Schiff (1834–1915) (Figure 1) was a German scientist. He discovered some bases and named them Schiff bases [1]. Schiff bases are generated by reacting a primary amine with carbonyl compounds (aldehydes or ketones) under specific conditions. The common structure is $R_1R_2C=NR$ ($R \neq H$), with the main function being the imine or azomethine ($-C=N-$) group (Figure 2) [2].

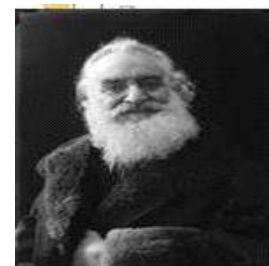


Figure 1.
A portrait of
Hugo Schiff

Schiff bases, particularly those coupled to a heterocyclic moiety, displayed a wide range of pharmacological and biological actions, including antibacterial, cytotoxic, antifungal, antimalarial, anticonvulsant, antioxidant, and anti-inflammatory properties [3–10]. Schiff base used in different field given below in Fig.3.

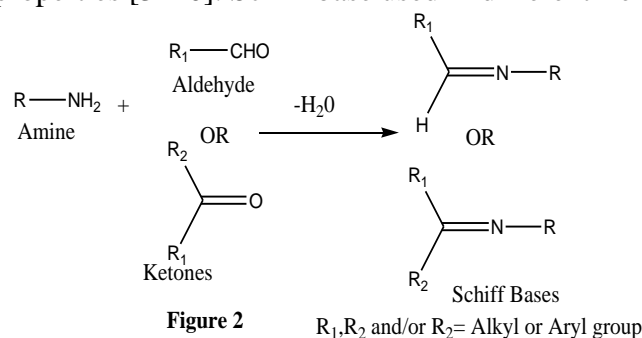
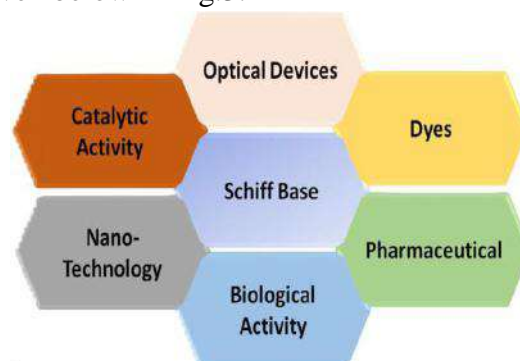


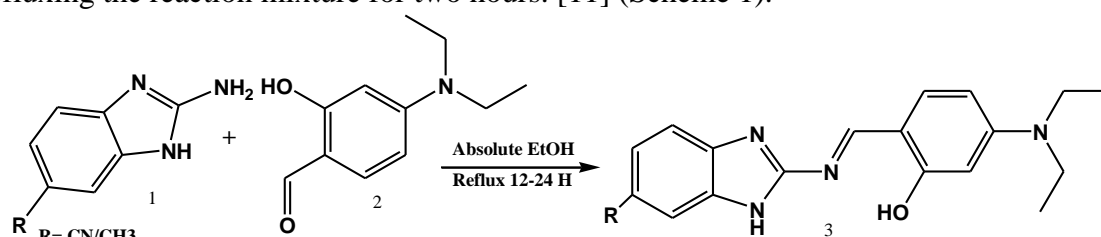
Fig. 3



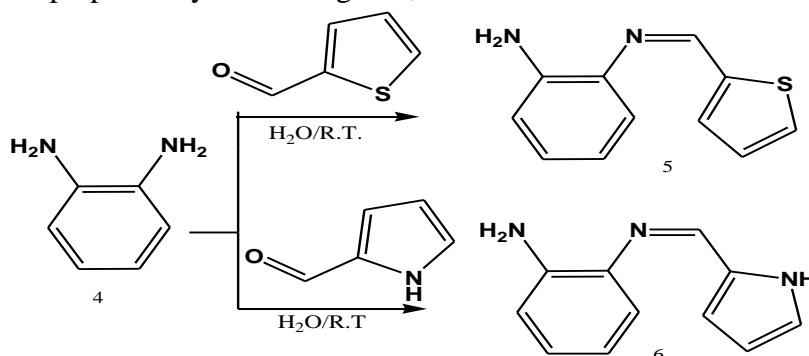
Various Synthesis Methods for Schiff Bases: Schiff bases have been employed in a variety of industries. As a result, many approaches and innovative procedures for the preparation of Schiff bases have been documented, including the following:

i) Conventional or common heating method:

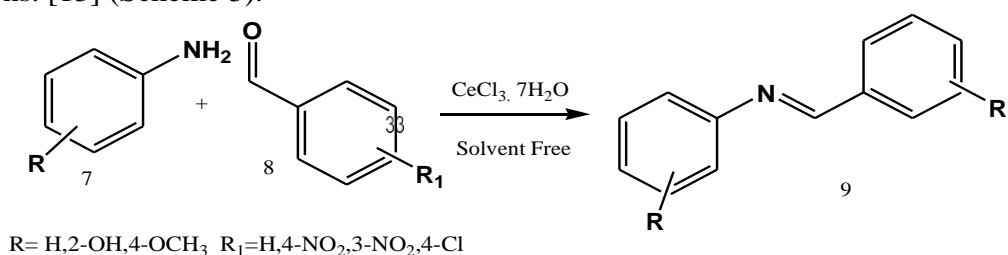
The Schiff base containing benzothiazole moiety **3** was made by reacting 2-amino-6-methylbenzothiazole **1** with 5-bromo-2-hydroxybenzaldehyde **2** in ethanol as a solvent and refluxing the reaction mixture for two hours. [11] (Scheme 1).

**Scheme 1****ii) Using water as a solvent:**

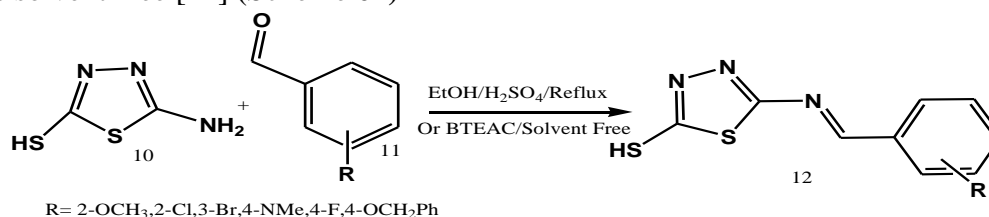
Mono-Schiff bases **5** and **6** were prepared by the stirring of 1,2-diaminobenzene **4** with thiophene-2-carbaldehyde and 1H-pyrrole-2-carbaldehyde, respectively, in H_2O as a solvent. [12]

**SScheme 2****iii) Metal catalyzed:**

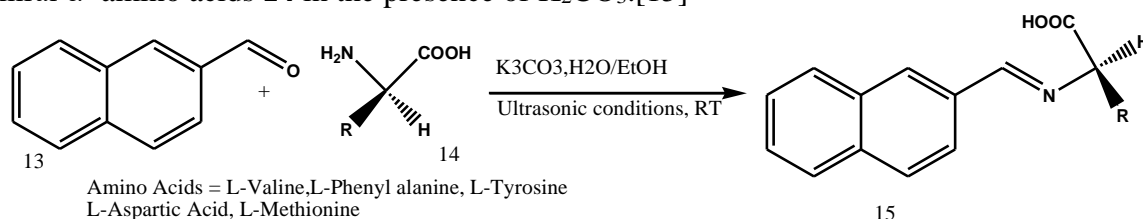
Cerium (III) chloride catalyzed: Schiff base **9** was produced by the reaction of aromatic amines **7** with aldehydes **8** in the presence of $CeCl_3 \cdot 7H_2O$ as a catalyst under solvent-free conditions. [13] (Scheme 3).

**Scheme 3****iv) Acidic and phase transfer catalyst (PTC) conditions:**

The reaction of 2-amino-5-mercapto-1,3,4-thiadiazole **10** with aromatic aldehydes **11** in ethanol in the presence of H_2SO_4 (acidic conditions) produced 1,3,4-thiadiazole Schiff bases **12**. Benzyl triethylammonium chloride (BTEAC) was also used as a catalyst during the process solvent-free [14] (Scheme 04)

**v) Ultrasonic and microwave conditions**

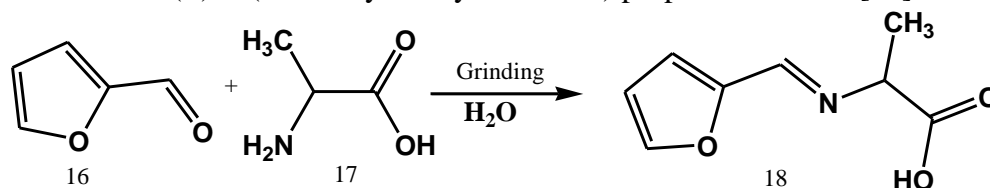
Chiral-Schiff bases **15** were synthesized by ultrasonically reacting 2-naphthaldehyde **13** with chiral α - amino acids **14** in the presence of K_2CO_3 . [15]



Scheme 5

vi) Grinding chemistry technique:

The synthesis of bioactive chemicals was carried out using grindstone technology. Furan-2-carbaldehyde **16** and DL-alanine **17** were reacted in water as a green solvent to produce Schiff base (E)-2-(furan-2-ylmethyleneamino) propanoic acid **18** [16].



Scheme 6

Biological activities of Schiff bases :

Antimicrobial activities:

Triazole-Schiff bases **19** showed strong antibacterial activity against *Escherichia coli*, *Salmonella typhi*, and *Bacillus subtilis*. In addition, they had significant antifungal activity against *Candida albicans*, *Aspergillus flavus*, *Fusarium solani*, and *Candida glabrata*. [17] (**Figure 4**).

Isatin-Schiff base **20** showed significant antibacterial action against *Pseudomonas aeruginosa* (MIC = 6.25 mg/mL) [18] (**Figure 5**).

Acetylenic indole-Schiff base **21** shown antibacterial activity against *Staphylococcus aureus*, with a MIC of 7.81 μ M. Indole-Schiff base **22** showed antifungal efficacy against *Candida krusei*, with a MIC of 15.62 μ M [19] (**Figure 6**).

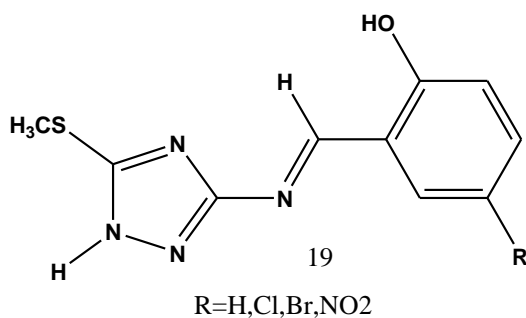
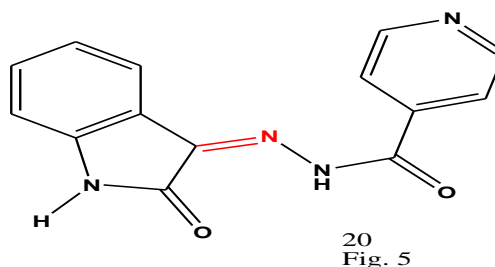


Fig. 4 Triazole-Schiff bases



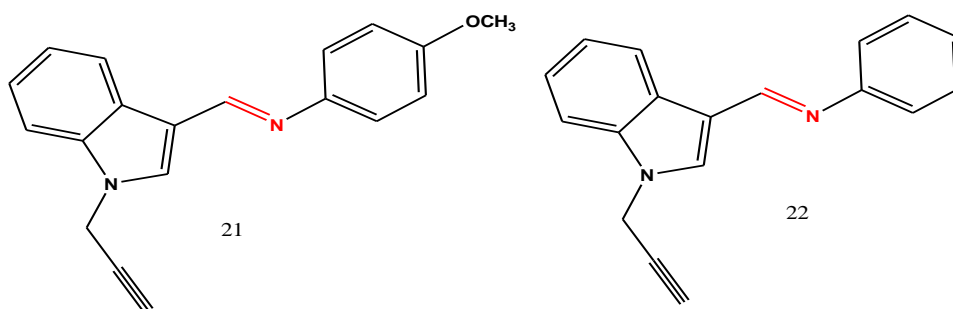


Figure 6. Acetylenic indole-Schiff bases

Piperazine-sulphonamide-linked to Schiff base **23** showed potent antibacterial activity against *Bacillus subtilis* with MIC= 26.1 $\mu\text{g/mL}$ [20] (**Figure 7**).

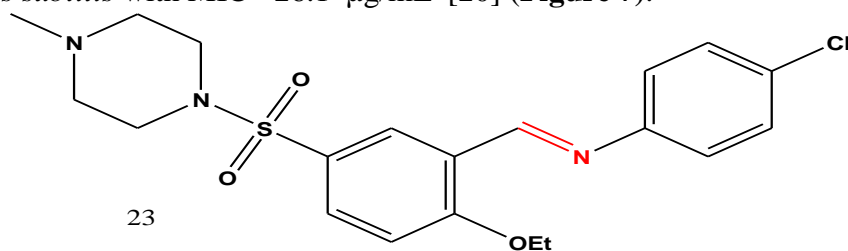


Figure 7 Piperazine-sulphonamide linked to Schiff base 6

Anticancer activities:

1,3,5-Triazine-isatin Schiff base **24** showed anticancer activities against lung (HOP-92), leukemia (CCRF-CEM), and leukemia (SR) cancer cell lines [21] (**Figure 8**).

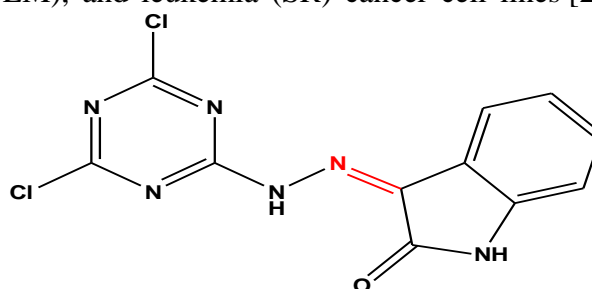


Fig.8 1,3,5-Triazine-isatin Schiff base 24

Anti-inflammatory activities:

Schiff base based on quinazolin-4-one in combination with 1,3,4-oxadiazole moiety **25** showed anti-inflammatory effects [22] (**Figure 9**).

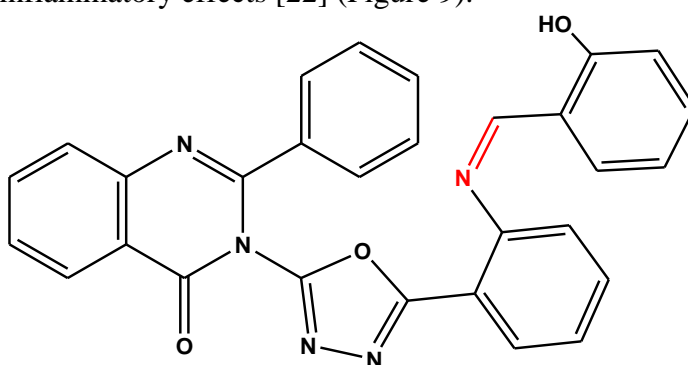


Fig. 9 Schiff base based on quinazolin-4-one with 1,3,4-oxadiazole 25

Analgesic activities: Isatin-Schiff base **26** exhibited good analgesic activity [23] (**Figure 10**).

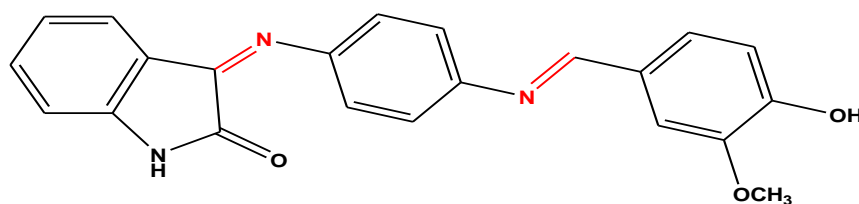


Figure 10 . Isatin-Schiff base 26

Anthelmintic activities:

Antipyrine-coumarin linked to Schiff bases **27** showed excellent anthelmintic activities [24](Figure 11).

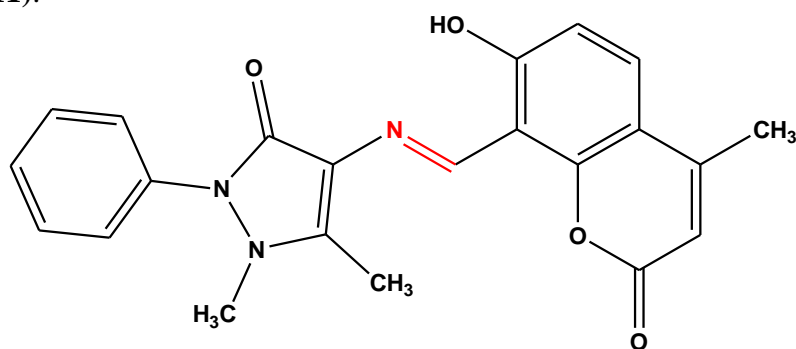


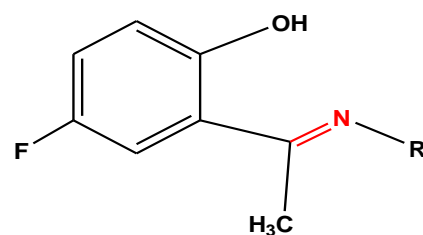
Figure 11 Antipyrine-coumarin linked to Schiff bases 27

Antioxidant activities:

Halogenated Schiff bases **25** showed very low to moderate antioxidant activities [24] (Figure 12).

Conclusion:

Schiff bases were characterized by the presence of the imine or azomethine ($-C=N-$) group. This review focused on some synthesis and biological activities of Schiff bases. From this review, it can be concluded that Schiff bases especially Schiff bases-heterocyclic moiety conjugates display a wide range of pharmacological activities. For that, Schiff bases attracted increasing attention to the scientists for the synthesis of new derivatives for applications in medicinal and in industrial field.



R = C_3H_7 , C_5H_{11} , C_6H_{13} , C_7H_{15}

Figure 12. Halogenated Schiff bases 28

References:

1. Qin, W., Long, S., Panunzio, M., & Biondi, S. (2013). Schiff bases: A short survey on an evergreen chemistry tool. *Molecules*, 18(10), 12264-12289.
2. Ghosh, P., Dey, S. K., Ara, M. H., Karim, K., & Islam, A. B. M. (2019). A review on synthesis and versatile applications of some selected Schiff bases with their transition metal complexes. *Egyptian Journal of Chemistry*, 62(Special Issue (Part 2) Innovation in Chemistry), 523-547.
3. Antony, R., Arun, T., & Manickam, S. T. D. (2019). A review on applications of chitosan-based Schiff bases. *International journal of biological macromolecules*, 129, 615-633.
4. Ledet, I., Alexa, A., Bercean, V., Vlase, G., Vlase, T., Şuta, L. M., & Fuliş, A. (2015). Synthesis and degradation of Schiff bases containing heterocyclic pharmacophore. *International Journal of Molecular Sciences*, 16(1), 1711-1727.
5. Pund, A. A., Saboo, S. S., Sonawane, G. M., Dukale, A. C., & Magare, B. K. (2020). Synthesis of 2, 5-disubstituted-1, 3, 4-thiadiazole derivatives from (2S)-3-(benzyloxy)-2-[(tert-butoxycarbonyl) amino] propanoic acid and evaluation of anti-microbial activity. *Synthetic Communications*, 50(24), 3854-3864.
6. Magalhães, T. F. F., da Silva, C. M., Dos Santos, L. B. F., Santos, D. A., Silva, L. M., Fuchs, B. B., ... & de Fátima, Â. (2020). Cinnamyl Schiff bases: Synthesis, cytotoxic effects and antifungal activity of clinical interest. *Letters in Applied Microbiology*, 71(5), 490-497.
7. Sztanke, K., Maziarka, A., Osinka, A., & Sztanke, M. (2013). An insight into synthetic Schiff bases

- revealing antiproliferative activities in vitro. *Bioorganic & Medicinal Chemistry*, 21(13), 3648-3666.
8. Hassan, A. S., Askar, A. A., Naglah, A. M., Almeshia, A. A., & Ragab, A. (2020). Discovery of new Schiff bases tethered pyrazole moiety: Design, synthesis, biological evaluation, and molecular docking study as dual targeting DHFR/DNA gyrase inhibitors with immunomodulatory activity. *Molecules*, 25(11), 2593.
 9. Morsy, N. M., Hassan, A. S., Hafez, T. S., Mahran, M. R., Sadawe, I. A., & Gbaj, A. M. (2021). Synthesis, antitumor activity, enzyme assay, DNA binding and molecular docking of Bis-Schiff bases of pyrazoles. *Journal of the Iranian Chemical Society*, 18, 47-59.
 10. Murtaza, G., Mumtaz, A., Khan, F. A., Ahmad, S., Azhar, S., Najam-UI-Haq, M., ... & Hussain, I. (2014). Recent pharmacological advancements in schiff bases: A review. *Acta Pol. Pharm*, 71(4), 531-535.
 11. Huda, A. S., Asia, A. S., & Zainab, W. S. (2020). INTERNATIONAL JOURNAL OF RESEARCH IN PHARMACEUTICAL SCIENCES.
 12. Rao, V. K., Reddy, S. S., Krishna, B. S., Naidu, K. R. M., Raju, C. N., & Ghosh, S. K. (2010). Synthesis of Schiff's bases in aqueous medium: a green alternative approach with effective mass yield and high reaction rates. *Green Chemistry Letters and Reviews*, 3(3), 217-223.
 13. Ravishankar, L., Patwe, S. A., Gosarani, N., & Roy, A. (2010). Cerium (III)-catalyzed synthesis of schiff bases: a green approach. *Synthetic Communications®*, 40(21), 3177-3180.
 14. Mobinikhaledi, A., Jabbarpour, M., & Hamta, A. (2011). Synthesis of some novel and biologically active Schiff bases bearing a 1, 3, 4-thiadiazole moiety under acidic and PTC conditions. *Journal of the Chilean Chemical Society*, 56(3), 812-814.
 15. Şendil, K., Tekin, T., Göksu, H., Oğuz, M., Anıl, B., & Gültekin, M. S. (2016). A Novel Method for the Synthesis of Newfangled Asymmetric Schiff Bases from α -amino Acids under Ultrasonic Conditions and in Aqueous Medium. *Journal of the Chinese Chemical Society*, 63(9), 808-817.
 16. Sachdeva, H., Saroj, R., Khaturia, S., & Dwivedi, D. (2012). Operationally simple green synthesis of some Schiff bases using grinding chemistry technique and evaluation of antimicrobial activities. *Green Processing and Synthesis*, 1(5), 469-477.
 17. Chohan, Z. H., & Hanif, M. (2013). Antibacterial and antifungal metal based triazole Schiff bases. *Journal of Enzyme Inhibition and Medicinal Chemistry*, 28(5), 944-953.
 18. Tehrani, K. H. M. E., Hashemi, M., Hassan, M., Kobarfard, F., & Mohebbi, S. (2016). Synthesis and antibacterial activity of Schiff bases of 5-substituted isatins. *Chinese Chemical Letters*, 27(2), 221-225.
 19. Singh, G., Kalra, P., Arora, A., Singh, A., Sharma, G., Sanchita, ... & Verma, V. (2018). Acetylenic Indole-Encapsulated Schiff Bases: Synthesis, In Silico Studies as Potent Antimicrobial Agents, Cytotoxic Evaluation and Synergistic Effects. *ChemistrySelect*, 3(8), 2366-2375.
 20. Patil, R. H., Kalam Khan, F. A., Jadhav, K., Damale, M., Akber Ansari, S., Alkahtani, H. M., ... & Sangshetti, J. N. (2018). Fungal biofilm inhibition by piperazine-sulphonamide linked Schiff bases: Design, synthesis, and biological evaluation. *Archiv der Pharmazie*, 351(3-4), 1700354.
 21. Polovkovych, S. V., Karkhut, A. I., Marintsova, N. G., Lesyk, R. B., Zimenkovsky, B. S., & Novikov, V. P. (2013). Synthesis of New Schiff Bases and Polycyclic Fused Thiopyranothiazoles Containing 4, 6-Dichloro-1, 3, 5-Triazine Moiety. *Journal of Heterocyclic Chemistry*, 50(6), 1419-1424.
 22. Dewangan, D., Nakhate, K. T., Verma, V. S., Nagori, K., & Tripathi, D. K. (2017). Synthesis, Characterization, and Screening for Analgesic and Anti-Inflammatory Activities of Schiff Bases of 1, 3, 4-Oxadiazoles Linked With Quinazolin-4-One. *Journal of Heterocyclic Chemistry*, 54(6), 3187-3194.
 23. Chinnaamy, R. P., Sundararajan, R., & Govindaraj, S. (2010). Synthesis, characterization, and analgesic activity of novel schiff base of isatin derivatives. *Journal of advanced pharmaceutical technology & research*, 1(3), 342.
 24. Manjunath, M., Kulkarni, A. D., Bagihalli, G. B., Malladi, S., & Patil, S. A. (2017). Bio-important antipyrine derived Schiff bases and their transition metal complexes: Synthesis, spectroscopic characterization, antimicrobial, anthelmintic and DNA cleavage investigation. *Journal of Molecular Structure*, 1127, 314-321.
 25. Singh, B. B., Shakil, N. A., Kumar, J., Rana, V. S., & Mishra, A. (2016). Microwave synthesis, characterization, and bio-efficacy of novel halogenated Schiff bases. *Journal of Environmental Science and Health, Part B*, 51(8), 558-570.

Revolutionizing Applications: A Comprehensive Review of Schiff Base Nanoparticles at the Nanoscopic Scale

S. R. Khandekar

Department of Chemistry, Indira Mahavidyalaya, Kalamb, Dist. Yavatmal, (MH) India.

Email – snehalkhandekar11@gmail.com

Abstract

Nanotechnology has emerged as a transformative field with the potential to revolutionize various scientific and technological domains. This chapter delves into the nanoscopic marvels of Schiff base nanoparticles and their applications in advanced technologies. Schiff bases, known for their versatile coordination chemistry, have been harnessed to engineer nanoparticles with unique properties and functionalities. The exploration of these nanoscale wonders encompasses synthesis methodologies, characterization techniques, and their diverse applications in fields such as catalysis, drug delivery, sensing, and imaging. The chapter discusses the tailored design of Schiff base nanoparticles to achieve enhanced performance, stability, and selectivity in various applications. Moreover, it highlights the potential impact of these nanomaterials on advancing technologies and offers insights into future directions for research and development in this rapidly evolving field. The intricate interplay between molecular design, synthesis strategies, and applications underscores the significance of Schiff base nanoparticles as promising candidates for addressing contemporary challenges in nanotechnology.

Keywords: Schiff base nanoparticles, catalysis, drug delivery, nanotechnology.

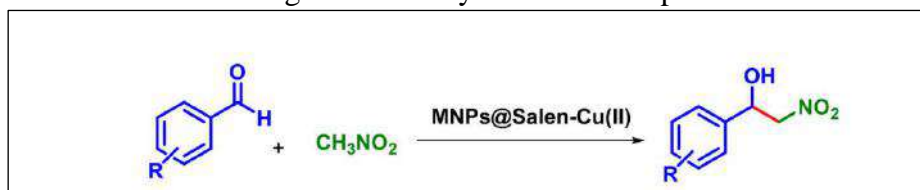
1. Introduction

The imine ($-C=N-$) functional group that results from the interaction of the amine amino group with the aldehyde or ketone carbonyl group defines the Schiff bases class of chemical compounds [1]. The imine functionality of Schiff bases confers significant chemical and biological features, enabling these molecules to coordinate and complexate with metal ions in a variety of chemistry-related domains [2]. Schiff base compounds can function as ligands to produce transition metal Schiff base complexes because of the imine group [3]. Additionally, the imine group ($>C=N-$) of SB ligands stabilizes the nanoparticles by forming bonds with them [4]. The term nanotechnology was first used in 1974 by Japanese scientist Norio Taniguchi and is considered a marvel of science, engineering, and technology [5-7]. The word "nano" comes from the Greek "nanos," which means "small" (10^{-9} m). Nanoparticles (NPs) are essentially very small particulates that range in size from 1 to 100 nm [8]. A higher level of the NPs is ensured by the surface modification, increasing their potential in the disciplines of analysis, electro analytical, catalysis, and biology. SB modified NPs are applied as biosensor, adsorbent, electro catalysis, catalytic dye degradation, and oxidation of different of various organic compounds [9-14]. This chapter delves into the intricate realm of Schiff base nanoparticles, investigating their unique properties and potential applications in various advanced fields.

2. Schiff base complex as a heterogeneous catalyst:

A Cu(II)-Schiff base complex supported on functionalized Fe_3O_4 magnetic nanoparticles (MNPs@Salen-Cu(II)) was firstly prepared by the refluxing it in the toluene solvent for two days. Further this was stirred in ethanol at room temperature with the addition of benzaldehyde and nitromethane. These nanoparticles were employed as effective catalysts in the manufacture of derivatives of nitroaldol through the reaction of nitromethane with aldehydes (Scheme 1). The reaction benefits include selectivity to products, recyclability of the catalysts, simplicity

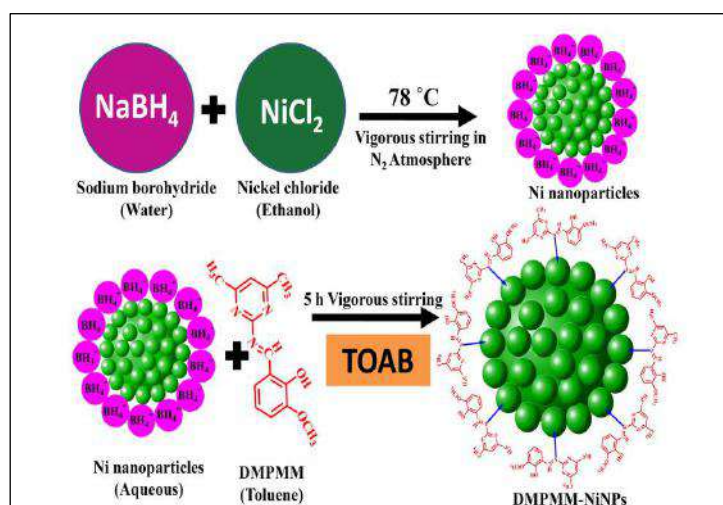
in workup, facile separation, cleanliness, and eco-friendliness. Using VSM, SEM, FT-IR, ^1H NMR, XRD, TGA, and EDX, the produced catalysts were characterized. Using an external magnet, the nanocatalyst may be easily extracted from the reaction mixture and reused 14 times without experiencing a substantial reduction in catalytic activity. Research on the catalyst's leaching revealed that the heterogeneous catalyst's active components do not leach [15].



Scheme 1. Synthesis of nitroaldols by the MNPs@Salen-Cu(II)

3. Exploring the Multifaceted Applications of Nickel Nanoparticles Stabilized by Schiff Base Ligands:

Paulraj Adwin Jose et al. synthesized nickel nanoparticles stabilized by Schiff base ligands derived from pyrimidine derivatives and are verified by using spectroscopic and microscopic, SEM and TEM techniques (Scheme 2). The synthesized compounds exhibited strong DNA binding capability and binding through groove mode. The produced compounds enhanced DNA denaturation and the BSA binding investigations demonstrated the compound's strong BSA interaction. The DMPMM and DMPMM-NiNPs were the subject of antimicrobial investigations using the Agar-Agar well diffusion method. The results of anticancer experiments verified that the produced DMPMM-NiNPs had a specific characteristic of interacting with cancer cells as opposed to normal cells. However the activity rose to a level above that of regular cisplatin when it was capped with metal nanoparticles. The results of tests on antioxidant scavenging demonstrated the strong antioxidant activity of DMPMM-NiNPs [16].

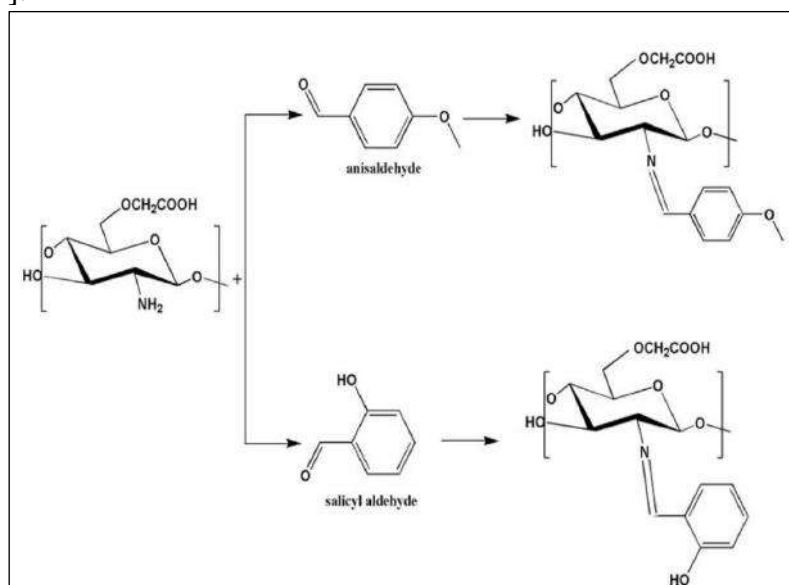


Scheme 2. Synthesis of Schiff base ligand capped nickel nanoparticles (DMPMM-NiNPs).

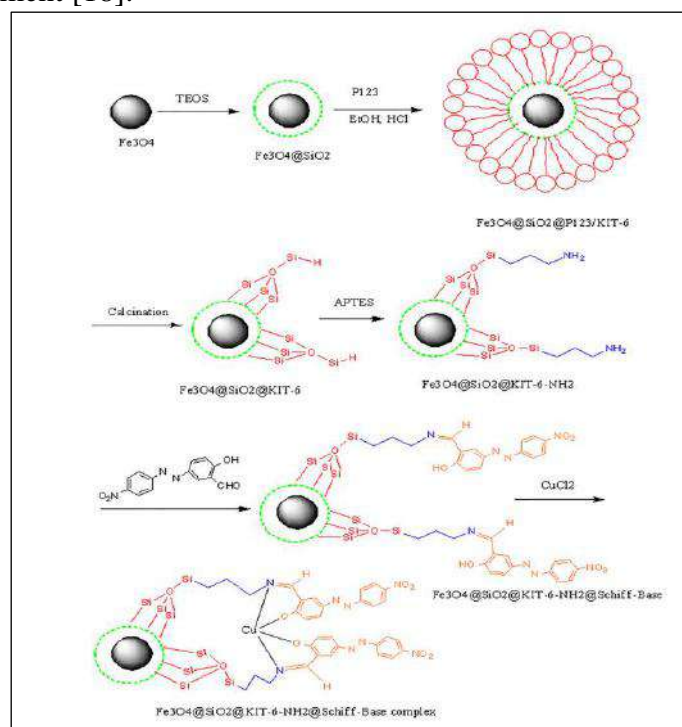
4. Schiff-Bases with Anisaldehyde or Salicylaldehyde in the Presence of Silver Nanoparticles:

Carboxymethyl chitosan-Schiff-bases (CMCs-SB) of anisaldehyde or salicylaldehyde in the absence/presence of silver nanoparticles; with different weight ratios of AgNO_3 (2 and 5% by weight) were prepared by Reham A. Abdel-Monem et al. (Scheme 3) and evaluated as materials with antibacterial efficiencies. The material is characterized by FTIR, SEM, TEM, TGA. The two carboxymethyl chitosan Schiff-bases nanocomposites were found to exhibit inhibitory power against the growth of both Gram +ve and Gram -ve types of bacteria. The antibacterial efficiency of salicylaldehyde/CMCs-SB/AgNPs is higher than that of anisaldehyde/CMCs-SB/AgNPs. The human hepatocellular carcinoma cell line (HEPG2) and

the breast adenocarcinoma (MCF7) were used to test the cytotoxicity of the produced CMC Schiff bases in the presence and absence of AgNPs (2 and 5%). The findings demonstrated that adding AgNPs at weight ratios of 2 and 5 % enhanced the anticancer activity of the produced Schiff bases [17].



Scheme 3. Schematic diagram for the reaction of CMCs with anisaldehyde or salicylaldehyde. Leila Zare Fekri et al. synthesized a copper/Schiff base complex immobilized on amine-functionalized silica MMNPs (Scheme 4). Product is characterized by SEM, TEM, TGA and VSM analysis. The synthesized product is an effective catalyst in a multicomponent reaction involving amine, thioglycolic acid, and aldehyde while stirring. This nanoparticle is a novel mix of organic and inorganic materials. The key benefits of this catalytic process include waste reduction, good selectivity, easy separation and recycling of the magnetic catalyst, outstanding product yields, and low operating complexity. Additionally, this new route is affordable and safe for the environment [18].

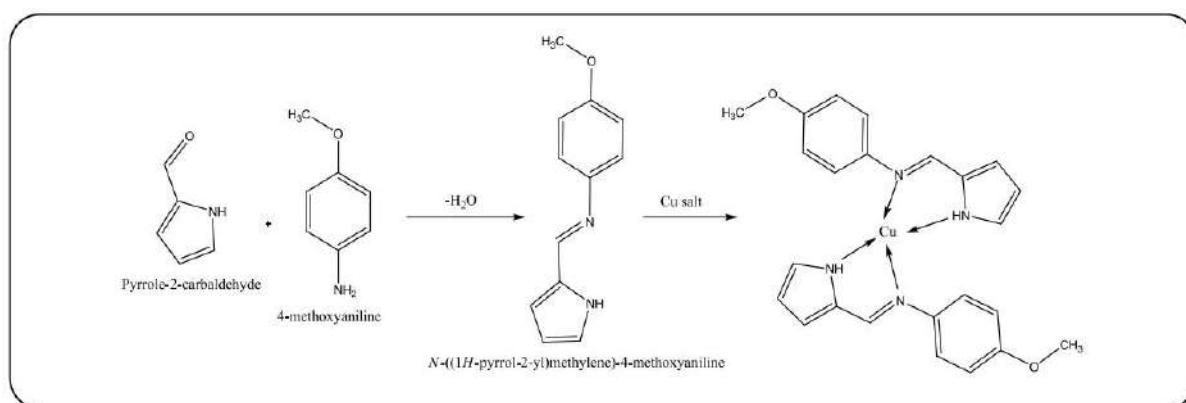


Scheme.4 Synthesis of Fe₃O₄@SiO₂@KIT-6-NH₂@Schiff base complex

5. Exploring Anticancer Potential through DNA Binding by Zn(II) Complex with Schiff Base Ligand:

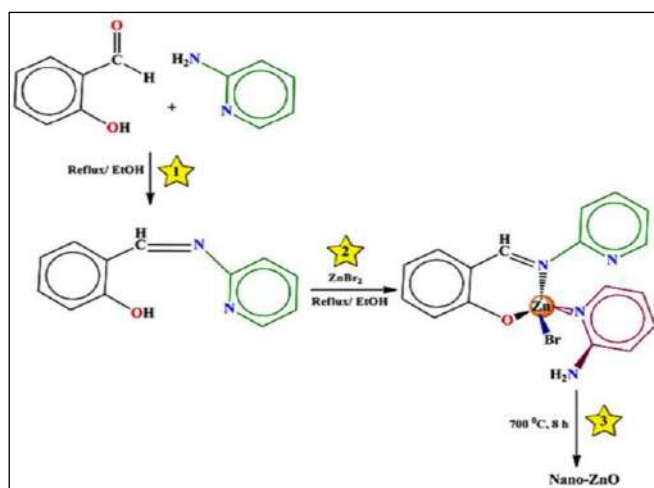
The study involves the synthesis of biologically potent Pt (II) metal ion complexes, characterized by a proposed square planar environment through various physicochemical investigations. These complexes exhibit higher antimicrobial activity compared to the original ligands and demonstrate a strong ability to cleave DNA via the oxidative nuclease pathway, confirmed by band tailing in the DNA spectrum. Additionally, the compounds show significant in vitro anticancer activity against human breast cancer (MCF-7) cell lines, with results compared to the standard drug Cisplatin. The Pt (II) complex induces DNA damage, as evidenced by increased cell cycle depletion of S and G2/M at various concentrations, leading to G1 phase arrest. A notable rise in sub-G1 cells indicates that the complex causes sufficiently high DNA damage, resulting in a large number of cells undergoing apoptosis [19].

Charles, A. et al. synthesized the ZnO film's polycrystalline nature, with its hexagonal wurtzite structure and (002) preferred orientation (Scheme 5). The compound is characterized by Atomic force microscopy (AFM), optical research, and X-ray diffraction (XRD). It was calculated that the grain size was in the nm range. The direct bandgap value of 3.2 eV in the produced films is in close agreement with the stated value of 3.37 eV found in literature. The characterisation studies verify that the deposited ZnO thin films are suitable for use in solar cells and optoelectronic devices [20].



Scheme 5: Synthesis of *N*-((1*H*-pyrrol-2-yl)methylene)-4-methoxyaniline Schiff base (PMMA) and its copper complex $[\text{Cu}(\text{PMMA})_2]\text{Cl}_2 \cdot 2\text{H}_2\text{O}$.

A novel compound of Zn(II) was synthesized and characterized using a metal with a molar ratio of 1:2 and a Schiff base ligand by Masumeh Galini et al. They used FT-IR, ^1H -NMR, UV-Vis X-ray data to determine the structure of the synthesized compound. Furthermore, ZnO nanoparticles of $[\text{ZnL}(2\text{-aminopyridine})\text{Br}]$ using the combustion synthesis method was created. Using FESEM, TEM, FT-IR, and XRD, the shape and crystalline structure of the produced zinc oxide nanoparticles were examined. Additionally, it was shown through the use of molecular docking techniques that the Zn(II) complex binds to the DNA helix's minor groove. $[\text{ZnL}(2\text{-aminopyridine})\text{Br}]$ will function as a tyrosine kinase inhibitor to treat cancer by blocking the receptor for the epidermal growth factor [21].



Scheme 6. Synthetic procedure for the preparation of Schiff base ligand and complex (2:1) and protocol of ZnO nanoparticles.

6. Conclusions

In conclusion, the exploration of Schiff Base Nanoparticles in this review highlights their remarkable potential for advanced applications at the nanoscopic level. The synthesis and characterization of these nanoparticles, with a focus on their unique properties, have paved the way for diverse applications in various fields. From enhanced antimicrobial activity and DNA cleavage capabilities to potent in vitro anticancer effects, Schiff Base Nanoparticles emerge as versatile candidates for innovative biomedical and materials science applications. As we delve into the intricacies of their physicochemical properties and biological activities, it becomes evident that Schiff Base Nanoparticles offer a promising avenue for addressing complex challenges in medicine, materials science, and beyond. The observed cell cycle depletion, G1 phase arrest, and induction of apoptosis underscore their potential as impactful agents in cancer therapeutics. The integration of Schiff Base Nanoparticles into the realm of nanotechnology signifies a frontier in the ongoing pursuit of advanced materials with tailored functionalities. Further research and development in this area are essential to unlock the full spectrum of possibilities and overcome potential challenges. As we embark on this journey, the nanoscopic marvels of Schiff Base Nanoparticles hold immense promise for shaping the future of advanced applications, offering unprecedented solutions for a myriad of scientific and technological endeavors.

References

- [1] Berhanu, A.L.; Gaurav; Mohiuddin, I.; Malik, A.K.; Aulakh, J.S.; Kumar, V.; Kim, K.-H. A review of the applications of Schiff bases as optical chemical sensors. *TrAC Trends Anal. Chem.*, 116, (2019) 74–91.
- [2] Soufeena, P.P.; Nibila, T.A.; Aravindakshan, K. Coumarin based yellow emissive AIEE active probe: A colorimetric sensor for Cu²⁺ and fluorescent sensor for picric acid. *Spectrochim. Acta Part A Mol. Biomol. Spectrosc.*, 223, (2019) 117201.
- [3] Aytac, S.; Gundogdu, O.; Bingol, Z.; Gulcin, I. Synthesis of Schiff Bases Containing Phenol Rings and Investigation of Their Antioxidant Capacity, Anticholinesterase, Butyrylcholinesterase, and Carbonic Anhydrase Inhibition Properties. *Pharmaceutics*, 15, (2023) 779.
- [4] P.A. Jose, M. Sankarganesh, J.D. Raja, G.S. Senthilkumar, R.N. Asha, S.J. Raja, C. D. Sheela, Bio-inspired nickel nanoparticles of pyrimidine Schiff base: In vitro anticancer, BSA and DNA interactions, molecular docking and antioxidant studies, *J. Biomol. Structure, Dynamics* (Pembroke, Ont.) (2021) 1–15
- [5] Y. Wang, A. Chinnathambi, O. Nasif, S.A. Alharbi, Green synthesis and chemical characterization of a novel anti-human pancreatic cancer supplement by silver nanoparticles containing Zingiber officinale leaf aqueous extract, *Arabian Journal of Chemistry* 14 (2021), 103081.

- [6] E.E. Elemike, E.O. Dare, I.D. Samuel, J.C. Onwuka, 2-Imino-(3,4-dimethoxybenzyl) ethanesulfonic acid Schiff base anchored silver nanocomplex mediated by sugarcane juice and their antibacterial activities, *J. App. Res. Tech.* 14 (2016) 38–46.
- [7] K. Kalimuthu, B.S. Cha, S. Kim, K.S. Park, Eco-friendly synthesis and biomedical applications of gold nanoparticles: A review, *Microchemical Journal* 152 (2020) 104296.
- [8] M. Sajida, J.P. Wasyika, Nanoparticles: Synthesis, characteristics, and applications in analytical and other sciences, *Microchemical Journal* 154 (2020), 104623.
- [9] S. Kannaiyan, Easwaramoorthy, K. Kannan, V. Andal, Andal, Synthesis, characterisation, and antimicrobial efficacy of acid fuchsin Schiff base-modified silver nanoparticles, *Nanotech. Russia* 15 (11-12) (2020) 828–836.
- [10] S. Moradinasab, M. Behzad, Removal of heavy metals from aqueous solution using Fe₃O₄ nanoparticles coated with Schiff base ligand, *Desalination, Water Treat.* 57 (9) (2016) 4028–4036.
- [11] R. Mehdaoui, L. Chaabane, E. Beyou, M. Hassen, V. Baouab, Sono-heterogeneous Fenton system for degradation of AB74 dye over a new tetraaza macrocyclic Schiff base cellulose ligand-loaded Fe₃O₄ nanoparticles, *J. Iran. Chem. Soci.* 16 (2019) 645–659.
- [12] J.M. Abad, I. Bravo, F. Pariente, E. Lorenzo, Multi-tasking Schiff base ligand: a new concept of AuNPs synthesis, *Analytical and Bioanalytical Chemistry* 408 (9) (2016) 2329–2338.
- [13] S. Rayati, E. Khodaei, M. Jafarian, A. Wojtczak, Mn-Schiff base complex supported on magnetic nanoparticles: Synthesis, crystal structure, electrochemical properties and catalytic activities for oxidation of olefins and sulfides, *Polyhedron* (2017).
- [14] S.A. Hamrahian, J. Rakhtshah, S.M.M. Davijani, S. Salehzadeh, Copper Schiff base complex immobilized on silica-coated Fe₃O₄ nanoparticles: a recoverable and efficient catalyst for synthesis of polysubstituted pyrroles, *Appli. Organometal. Chem.* (2018) 1–12.
- [15] Niloufar Parandeh-Khoozani and Mohsen Moradian, Synthesis of nitroaldols through the Henry reaction using a copper(II)–Schiff base complex anchored on magnetite nanoparticles as a heterogeneous nanocatalyst, *J Coord Chem* .,74 (12) (2021) 2035–2054.
- [16] P. A. Jose, M. Sankarganesh, J. D. Raja, G. S. Senthilkumar, R. N. Asha, S. J. Raja & C. D. Sheela, Bio-inspired nickel nanoparticles of pyrimidine-Schiff base: In vitro anticancer, BSA and DNA interactions, molecular docking and antioxidant studies, *Journal Of Biomolecular Structure And Dynamics* (Taylor and Francis), 40 (21) (2022) 10715-10729.
- [17] Reham A. Abdel-Monem, Ahmed M. Khalil, Osama M. Darwesh, Ahmed I. Hashim & Samira T. Rabie, Antibacterial properties of carboxymethyl chitosan Schiff-base nanocomposites loaded with silver nanoparticles, *J. Macromol. Sci. A.*, (Taylor and Francis), 57 (2) (2020) 145-155.
- [18] Leila Zare Fekri, Shohreh Zeinali, Copper/Schiff-base complex immobilized on amine functionalized silica mesoporous magnetic nanoparticles under solvent-free condition: A facile and new avenue for the synthesis of thiazolidin-4-ones, *Appl Organometal Chem.* (2020) e5629.
- [19] Bhavana Gupta, Anita Kumari, Savita Belwal, R. V Singh & Nighat Fahmi, Synthesis, characterization of platinum(II) complexes of Schiff base ligands and evaluation of cytotoxic activity of platinum nanoparticles, *Inorganic and Nano-Metal Chemistry*, 50:10, (2020) 914-925.
- [20] Charles, A., Sivaraj, K., Krishnaraj, S., Synthesis of Copper(II) Schiff Base Complex and Its Mixed Thin Layer with ZnO Nanoparticles, *Iran. J. Chem. Chem. Eng.*, 40 (3) (2021) 758-764.
- [21] Masumeh Galini, Mehdi Salehi, Maciej Kubicki, Mehdi Bayat, Rahime Eshaghi Malekshah, Synthesis, structural characterization, DFT and molecular simulation study of new zinc-Schiff base complex and its application as a precursor for preparation of ZnO nanoparticle, *Journal of Molecular Structure*, 1207 (2020) 127715.

Screening Of Antioxidant Property Present In Psidium Guajava Linn

V D Mane & P P Mhasal.

Department of Chemistry,
Shankarlal Khandelwal Arts, Science and Commerce College, Akola.(444 002).
vivekvdm@rediffmail.com

Abstract:

Psidium guajava(Linn) is a member of Myrtaceae family, is a common tropical plant with a long history of traditional usage. *Psidium guajava* have been reported to possess variety of biology activity. Antioxidants both are natural and man-made substance that protects our cell from free radical. In present study we find out the antioxidant and phytochemical property of and water extract of *Psidium guajava* leaves by using DPPH as a free radical scavenger and colorimeter. The activity was evaluated by the decrease in absorbance as the result of DPPH colour change from purple to yellow. The higher the sample concentration used, the stronger was the free radical-scavenging effect. From this study we found that the *Psidium guajava* (linn) has good Antioxidant property. This study revealed that guava leaf extracts comprise effective potential source of natural antioxidants.

Key word: *Psidium guajava* leaves antioxidant property, DPPH.

Introduction

The guava is a small tree with tortuous branches and a smooth trunk. The fruit is a berry with a fleshy yellow or pink pulp and many seeds near the center. Many different varieties have been developed that vary in colour, size and in shape from round to ovoid to pear – shaped. The guava (*Psidium guajava* L.) tree, belonging to the Myrtaceae family, is a very unique and traditional plant which is grown due to its diverse medicinal and nutritive properties. Guava has been grown and utilized as an important fruit in tropical areas like India, Indonesia, Pakistan, Bangladesh, and South America. Different parts of the guava tree, i.e., roots, leaves, bark, stem, and fruits, have been employed for treating stomachache, diabetes, diarrhea, and other health ailments in many countries. Guava leaves (*Psidium guajavae folium*; GL) are dark green, elliptical, oval, and characterized by their obtuse-type apex. Guava leaves, along with the pulp and seeds, are used to treat certain respiratory and gastrointestinal disorders, and to increase platelets in patients suffering from dengue fever. GLs are also widely used for their antispasmodic, cough sedative, anti-inflammatory, antidiarrheic, antihypertension, antiobesity, and antidiabetic properties. Studies on animal models have also established the role of GL isolates as potent antitumor, anticancer, and cytotoxic agents.

Material and method:

The guava leaves were collected and shade dried at room temperature and coarsely powdered using an electric grinder. The coarse powdered materials of leaves were kept in the airtight polythene bag and stored in dry place. The powdered guava leaves were then extracted in distilled water.

Solvent extraction

Preparation of Aqueous extract of guava leaves.

Aqueous extracts of powdered guava leaves was prepared by boiling method. About 10 gram of powder of guava leaves was taken in 50 gram of distilled water and was warmed for about 10 min, and solution was then allowed to cool and filtered through a filter paper. The filtrate then was used for studying the antioxidant activity.

Phytochemical investigation of psidium guajava,linn.

Sr. no	Constituent	Aqueous Extract
1	Carbohydrate	+
2	Tannins	+
3	Saponins	-
4	Flavonoids	+
5	Alkaloids	-
6	Phenols	+
7	Glycosides	+
8	Proteins	-
9	Sterols	+
10	Anthocyanin	-

Study of qualitative antioxidant activity of psidium guajava linn.

Freshly prepared 0.02% of DPPH solution in ethanol was prepared. Single of Aqueous extract of guava leaves was taken on TLC plates, after drying the spots the TLC plates were dipped in DPPH solution and tested for Antioxidant activity.

The aqueous extract of guava showed prominent bleaching of purple colour of DPPH indicating that it has Antioxidant activity.

Qualitative antioxidant activity shown by aqueous extract of Psidium guajava.



Before DPPH.



After DPPH

STUDY OF ANTIOXIDANT ACTIVITY BY DPPH

The antioxidant activity of aqueous extract of guava leaves was assessed on the basis of radical scavenging effect of the stable 1,1- diphenyl 2- picrylhydrazyl (DPPH). The diluted working solutions of the test plant extract was prepared in water. 0.02% DPPH was prepared in ethanol 2 ml of solution having increasing concentration of guava extract, and optical density was measured at 517nm using colorimeter. A blank reading of DPPH was also recorded and % inhibition was calculated using the formula given below.

$$\text{Percentage (\%) Inhibition of DPPH (\% AA)} = \frac{A-B}{A} \times 100$$

Where, A = Blank O.D of DPPH

B = O.D of sample solution.

From this we can calculate IC₅₀ Value of each sample.

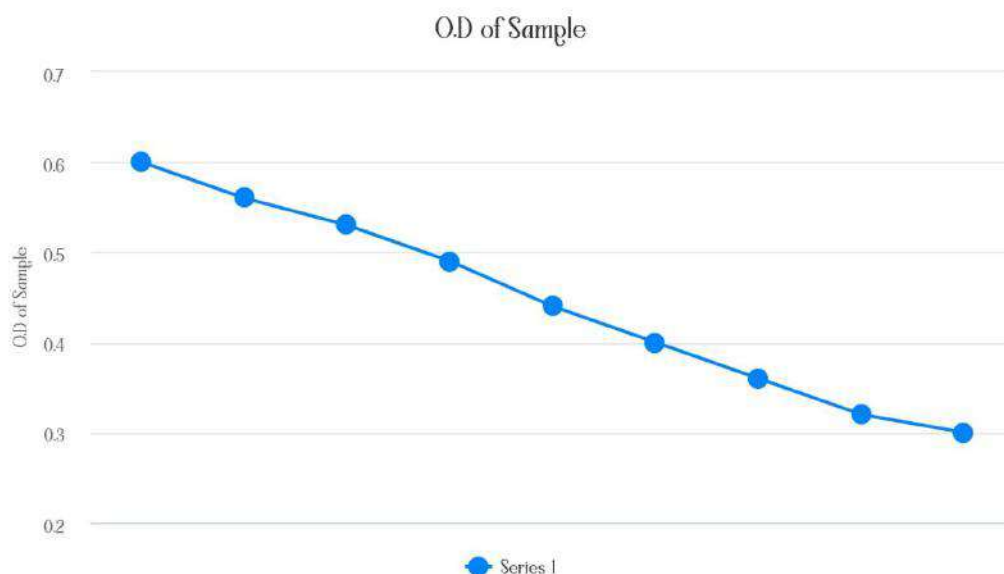
$$\text{IC}_{50} = \text{Max (\% AA)} - 50\% (\text{Max} - \text{Min\% AA})$$

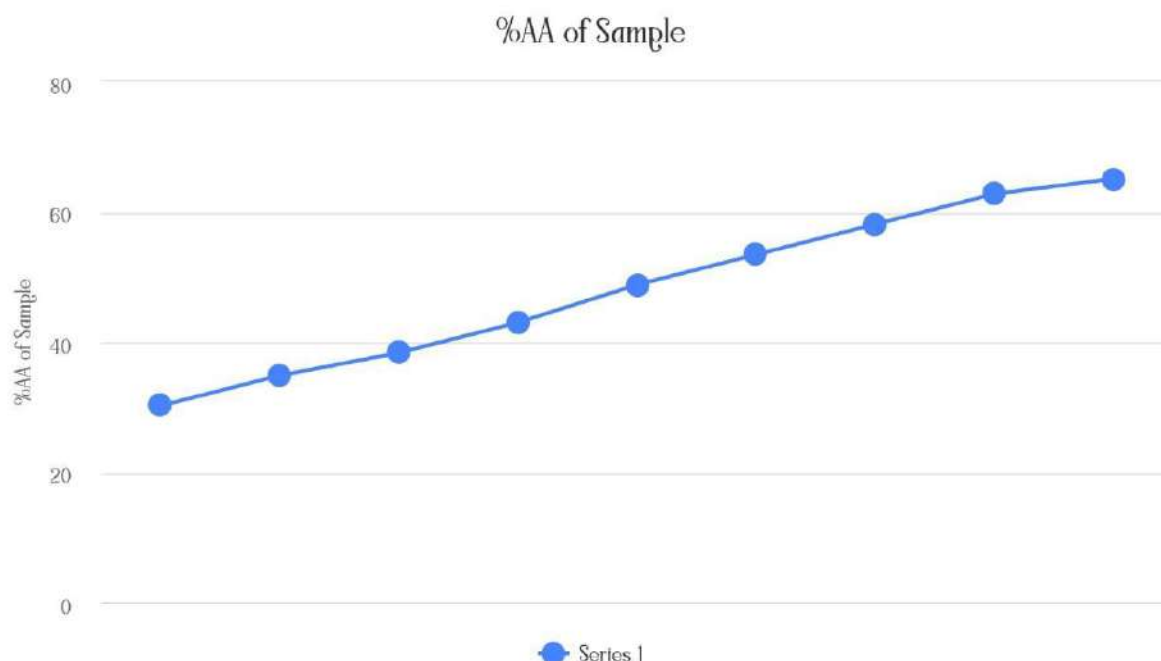
Result and discussion:

Study on Quantitative Antioxidant activity of water extract of guajava leaves.

Table: **Optical density and percent Antioxidant of Aqueous extract of Guava.**

Concentration in mg/ml	0.1	0.2	0.3	0.4	0.5	0.6	0.7	0.8	0.9
O.D of sample	0.60	0.56	0.53	0.49	0.44	0.40	0.36	0.32	0.30
% AA	30.23	34.88	38.37	43.02	48.83	53.48	58.13	62.79	65.11





$$\begin{aligned}
 IC_{50} &= \text{Max } (\%AA) - 50 \% (\text{Max} - \text{Min } \% AA) \\
 &= 65.11 - \frac{1}{2} (65.11 - 30.23) \\
 IC_{50} &= 47.67
 \end{aligned}$$

Conclusion:

The results obtained for the antioxidant assay by DPPH for water extract of leaves *Psidium guajava* plant were reported. The remarkable decrease in O.D value of the test plant samples were observed from the graph, showed antioxidant activity. The IC_{50} value for water extract of leaves of *Psidium guajava* was found to be 47.67mg/ml .

References

- 1) Bipul Biswas, Kimberly Rogers and Anand Yadav. Antimicrobial Activities of leaf extracts of guava. *Int J Microbial*. 2013 : 746165. Doi : 10. 1155/ 2013/ 74165, PMCID: PMC3817707, PMID : 24223039, Oct **2013**.
- 2) Rika Hartati, HashifahI. Nadifan, Irda Fidrianny. Crystal Guava: Evaluation of in Vitro antioxidant capacities and Phytochemical content. *The Scientific World Journal* 2020(3) : 1-7, doi : 10 . 1155/ 9413727, License. CC BY, **2020**.
- 3) Ravi Narayan Venkatachalam, Kanchahlata Singh, ThankamaniMarar. Phytochemical Screening and in Vitro Antioxidant activity of guava. Home / Archives/ Vol. 2, No. 1; *free radical and Antioxidants*. ISSN : 2231 – 2536, **2012**.
- 4) EziucheAmadikeUgbogu, ChibuikeIbe, Emmanuel Dike, Victor ChibuereUde, Celestine NwabuEkweogu. *Arabian Journal of Chemistry*. Volume 15, Issue 5, 103759, May **2022**.
- 5) Larissa Takeda, Lucas Laurindo, ElenGuiguer, AnupamBishayee. *Food Reviews International*. DOI : 10. 1080/ 87559129. 2021. 2023819, Feb **2022**.
- 6) MaryanZahin et al. Antioxidant and antimutagenicpotential of *Psidiumguajava* leaf extracts. *Drug ChemToxicol*. Apr. **2017**.
- 7) N. S. Sampath Kumar, NorizahMhdSarbon, Sandeep Singh Rana, Anjani Devi, Chintagunta et al. Extraction of bioactive compounds from *Psidiumguajava* leaves and

- its utilization in preparation of Jellies. (2021) 11: 36, <https://doi.org/10.1186/513568-021-01194-9>, **2021**.
- 8) R. Manikandan and Vijay Anand. Antioxidant activity of *Psidium guajava*. *Research Journal of Pharmacy and Technology*. 8(3): 339, **2015**.
 - 9) SumraNaseer, Shabbir Hussain, NaureenNaeem, Muhammad Pervaiz and MadhihaRahman. Phytochemical and medicinal value of guava. *Clinical Phytoscience* (Vol. 4, Issue 1), Dec.12, **2018**.
 - 10) N.K. Jain, Zahoor Ahmad Lone. Phytochemical screening of guava. *International journal of innovation in engineering research and management*. ISSN: 2348- 4918, Aug **2022**.
 - 11) Manoj Kumar, RyszardAmarowicz, VivekSaurabh, Surinder Singh, SushilChandan, Mukesh k. Berwal. *Foods*. **2021**, Apr; 10(4) : 752. DOI: 10.3390/foods 10040752, PMCID: PMC8066327.
 - 12) AnumitaBhadra, RattandeepSingh. Phytochemical properties of guava plants. Vol. 11(**2023**) : Ahead of print 1, DOI: <https://doi.org/10.7770/Safer-V11N1-art2385>.
 - 13) Arun K. Verma, V. Rajkumar and ArunK. Das. Guava Powder as an Antioxidant Dietary fibre in Sheep Meat Nuggets. *Asia –Australian Journal of Animal Sciences*. 26(6) : 886 – 895. Doi: 10.5713/ajas. 2012.12671, PMCID : PMC4093245, PMID : 25049864, **2013**.
 - 14) Laily N., Kusumaningtyas R.W., Sukarti I., Rini M.R.D.K. The potency of guava *Psidium guajava* (L.) leaves as a functional immunostimulatory ingredient. *Procedia Chem*. 2015;14:301–307. doi: 10.1016/j.proche.2015.03.042.
 - 15) Chen H.Y., Yen G.C. Antioxidant activity and free radical-scavenging capacity of extracts from guava (*Psidium guajava* L.) leaves. *Food Chem*. 2007;101:686–694. doi: 10.1016/j.foodchem.2006.02.047.
 - 16) . Ashraf A., Sarfraz R.A., Rashid M.A., Mahmood A., Shahid M., Noor N. Chemical composition, antioxidant, antitumor, anticancer and cytotoxic effects of *Psidium guajava* leaf extracts. *Pharm. Biol*. 2016;54:1971–1981. doi: 10.3109/13880209.2015.1137604.
 - 17) . Jiang L., Lu J., Qin Y., Jiang W., Wang Y. Antitumor effect of guava leaves on lung cancer: A network pharmacology study. *Arab. J. Chem*. 2020;13:7773–7797. doi: 10.1016/j.arabjc.2020.09.010.
 - 18) Manoj kumar, Maharish Tomar, Ryzard Amarowicz, Vivek saurabh, M S Naire, Chirag Maheshwari, Minnu sasi, Uma Prajapati, Muzzafar Hasan, Surinder singh, Shushil changan, R K Prajapat, Mukesh Berwal, warsha Satankar, *Foods*. 2021 Apr; 10(4): 752.

In-Silico Prediction of Phytoconstituents From *Solanum Indicum* for Antiepileptic Activity

Pooja.P.Patle*, Parimal Katolkar, Pradeep Raghatate, Jagdish Baheti

Kamla Nehru College of Pharmacy, Butibori, Nagpur 441108 (MS), INDIA

*Email: poojapatle000@gmail.com

ABSTRACT

Objective

A persistent, non-communicable brain disorder is epilepsy. Its distinctive characteristic is recurrent seizures. One or more parts of the body may experience partial or generalised seizures, which are short bursts of uncontrollable movement that can occasionally be followed by loss of consciousness and control over bowel or bladder function. Compounds found in medicinal plants have been the source of many conventional medications. *In-silico* testing of *Solanum indicum* phytoconstituents for antiepileptic efficacy was a part of our investigation.

Methods

Utilizing Discovery studio, molecular docking is done to assess the pattern of interaction between the phytoconstituents from the *Solanum indicum* plant and the crystal structure of the epilepsy proteins (PDB ID: 6O4L). Later, SwissADME and pkCSM were used to screen for toxicity as well as the pharmacokinetic profile.

Results

The docked results suggest that Solafuranone (-7.8 kcal/mol), Isofraxidin (-6.1 kcal/mol) for 6O4L macromolecule has best binding towards antiepileptic activity as compared to the standard (Acetazolamide) for 6O4L is -5.1 kcal/mol. Furthermore, pharmacokinetics and toxicity parameters were within acceptable limits according to ADMET studies.

Conclusion

Results from the binding potential of phytoconstituents aimed at antiepileptic activity were encouraging. It promotes the usage of *Solanum indicum* and offers crucial details on pharmaceutical research and clinical care.

1. INTRODUCTION

Solanum indicum, also known as Birhata, Badi Kateri, or Indian night shade, belongs to the Solanaceae family. It is a common upright undershrub in warmer parts of India, Asia, and Africa that grows up to 1.5 metres in height. Its height ranges from 0.30 to 1.8 metres. Nationally, 500–1000 MT are needed each year. The berries, leaves, roots, seeds, and stems of this plant have all been used in traditional medical systems to treat a wide range of ailments, including bronchitis, asthma, dry cough, rhinitis, dysuria, leucoderma, sexual dysfunction, insomnia, heart weakness, and pruritis.¹

Solanum indicum, which is consumed as a vegetable in some regions of Africa, may prevent cardiovascular diseases. It was exciting to read the studies on how it may be used to treat hypertension. The extract's potent therapeutic and preventative benefits against hypertension may not have been possible without the presence of chlorogenic acids. The antihypertensive effect might be due to other components. The findings urge further research into the extract as a possible treatment for hypertension.²

However, there are few studies on the phytoconstituents of *Solanum indicum* for the antiepileptic activity. Thus, keeping the above information in view, the present investigation was designed to identify the potential phytochemicals of *Solanum indicum* against 6O4L using a molecular docking method.

2. MATERIALS AND METHODS

2.1. Platform for molecular docking

The computational docking study of all the phytoconstituents selected as ligands with antiepileptic activity as the target was performed using PyRx software.³

2.2. Protein preparation

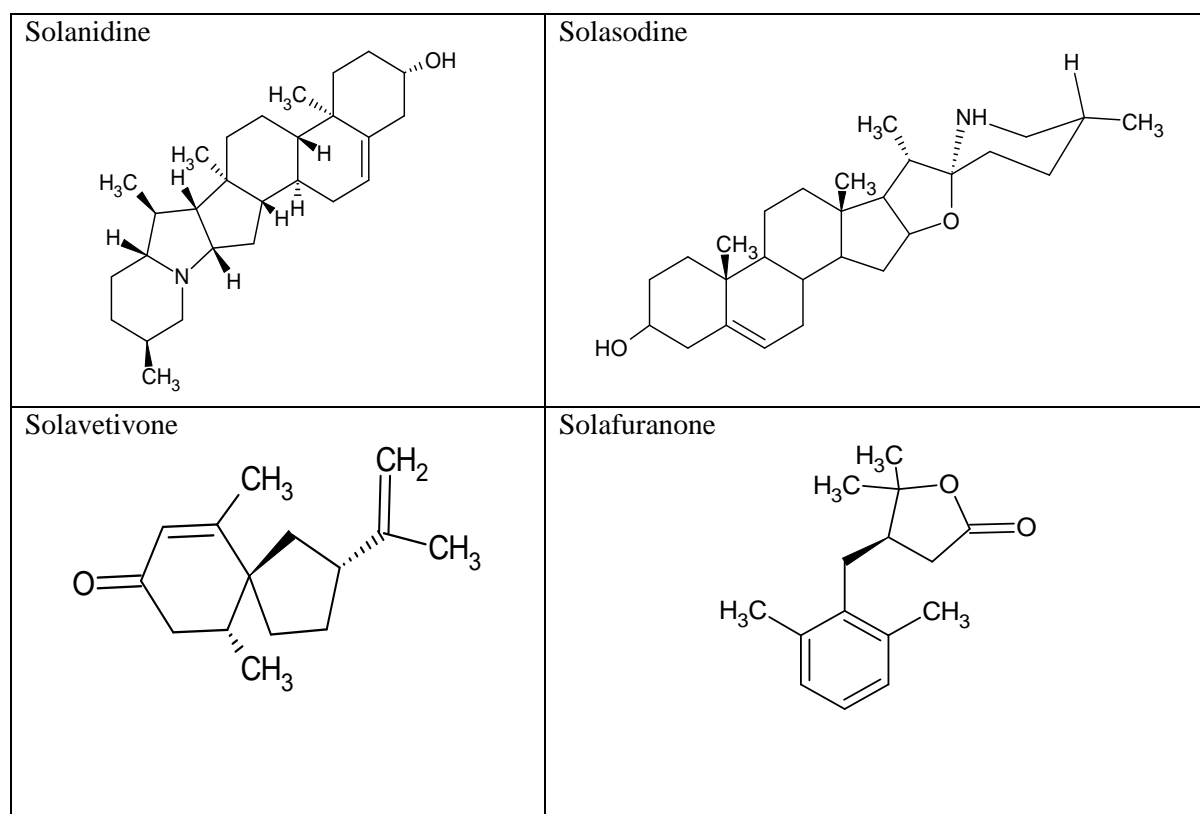
The macromolecule is 6O4L, *in silico* analysis of selected phytoconstituents was performed on the 1.85 Å crystal structure of antiepileptic macromolecule with inhibitor, (PDB ID: 6O4L, having resolution Resolution: 1.85 Å, R-Value Free: 0.220, R-Value Work: 0.174, R-Value Observed: 0.176), which was retrieved from the protein data bank (<https://www.rcsb.org>). 6O4L is classified as Crystal Structure of ALDH7A1 mutant E399D complexed with NAD all other molecules, such as co-crystallized water molecules, unwanted chains, and nonstandard residues, were deleted. Using Discovery studio.⁴

2.3. Mechanism of Action

6O4L: Aldehyde dehydrogenase 7A1 (ALDH7A1) is an enzyme that catabolizes lysine, and some loss-of-function mutations in this gene result in pyridoxine-dependent epilepsy (PDE). To understand how the mutations affect NAD⁺ binding, the crystal structures of the mutant enzymes in complex with NAD⁺ were examined. At the tested dose of NAD⁺, these alterations result in less active tetrameric ALDH7A1.⁵

2.4. Ligand preparation

The three-dimensional (3D) structures of all constituents were retrieved using Avogadro software from the PubChem database available on the NCBI website (<https://pubchem.ncbi.nlm.nih.gov/>). However, the drawing of geometrical 2D structure was performed using the ChemSketch program. The two-dimensional (2D) structures were transformed into 3D models using the Avogadro software and the ligand structures were saved in the PDB format. All the chemical structures are shown in Figure 1.



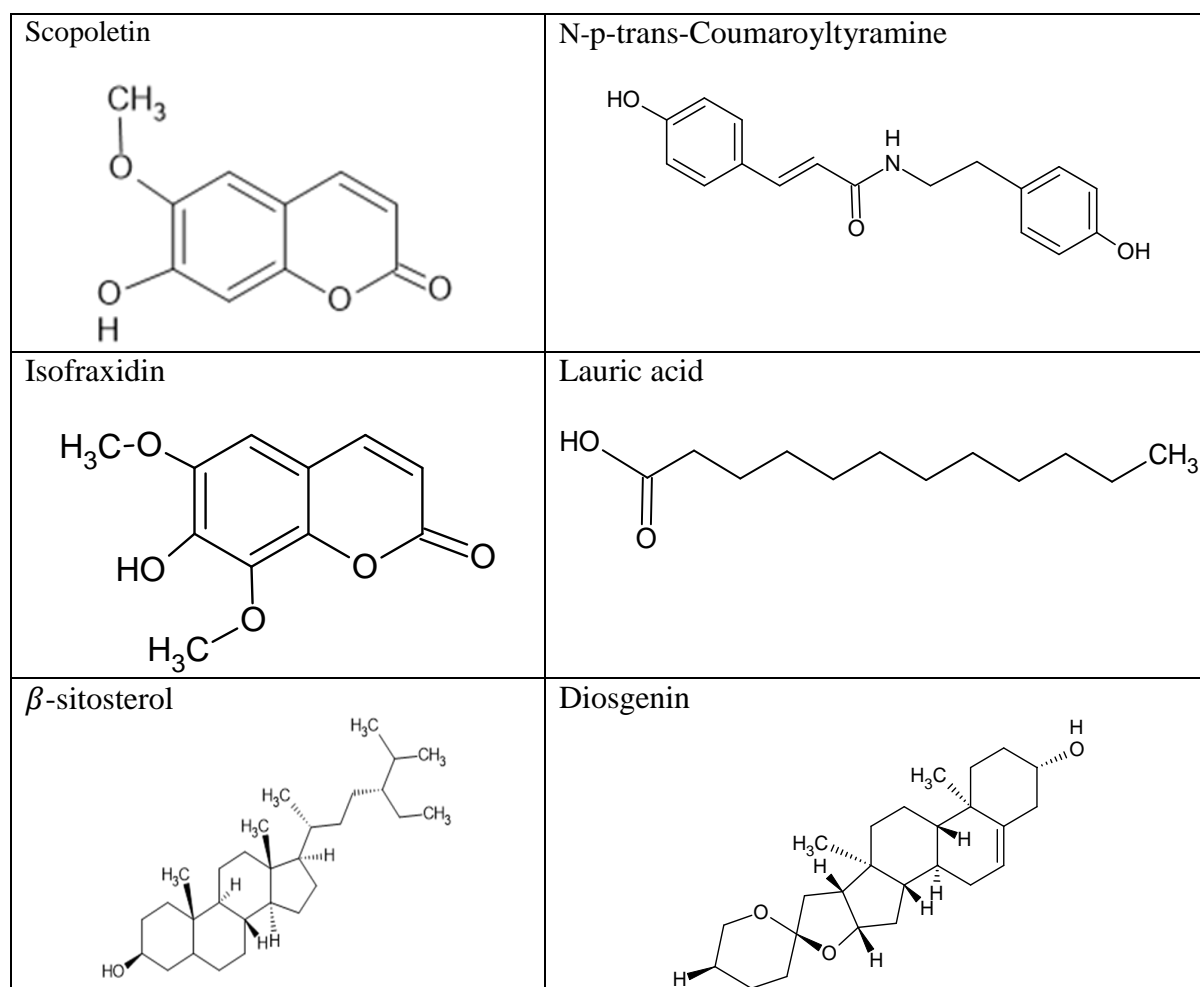


Fig. 1. Chemical structures of all selected phytoconstituents in the molecular docking studies

2.5. Standard Preparation

The standard is prepared steps such as, the 2D structure of standard drug was made using chem sketch program, then the 2D structure was converted into 3D model using Avogadro Software, it was saved in PDB format.

By using PyRx molecular docking of Acetazolamide was done with 6O4L.

2.6. Molecular docking

Molecular docking evaluates the protein-ligand interactions and estimates the scoring function based on the geometry to predict the binding affinity of the ligand molecule^{6,7}. We applied molecular docking studies to investigate the binding pattern of selected phytoconstituents (Figure 1) and the standard drug, along with the crystal structure of antiepileptic activity macromolecule (PDB ID: 6O4L). The molecular docking study was performed using PyRx software, Binding affinity was explored using the Vina wizard tool. The final results were analysed and visualized using Discovery Studio 2020 Client⁸, with bound ligands as the standard. Visualization of protein ligand interaction reflects the number of interactions and active residues responsible for significant binding at the active site of the target enzyme.

2.7. Absorption, distribution, metabolism, and excretion (ADME) and toxicity prediction

The selected phytoconstituents and standard drug were further checked for drug-likeness properties according to Lipinski's rule. During drug development, it is necessary to predict the tolerability of phytochemicals before being ingested by humans and animal models.

The pharmacokinetic profile (ADME) and toxicity predictions of ligands were conducted using SwissADME (<http://www.swissadme.ch>) and pkCSM (an online server database predicting small-molecule pharmacokinetic properties using graph-based signatures, (<http://biosig.unimelb.edu.au/pkcsm/prediction>)). To analyse the toxicological properties of ligands, Simplified Molecular Input Line Entry System (SMILES) notations or PDB files were uploaded, followed by selecting the required models for generating numerous information about structure-related effects^{9,10}.

3. RESULT AND DISCUSSION

The present study aimed to explore the inhibitory potential of the phytoconstituents present in *Solanum indicum* targeting antiepileptic activity. In this study, we performed molecular docking studies of all phytoconstituents found in *Solanum indicum* using AutoDock Vina, followed by a study of interacting amino acid residues and their influence on the inhibitory potentials of the active constituents. Selected phytoconstituents showing the best fit were further evaluated for absorption, distribution, metabolism, excretion, and toxicological (ADMET) properties using SwissADME and pkCSM servers.

3.1 Molecular docking

The docking scores and binding energies of all chemical constituents of *Solanum indicum* targeting antiepileptic activity (PDB ID: 6O4L) and binding interactions with amino acid residues are presented in Table 1 respectively.

Table 1. **Binding interaction of ligands from *Solanum indicum* targeting antiepileptic activity (PDB ID:6O4L)**

Sr. No.	Chemical constituent	PubChem ID	Docking Score
			6O4L
1.	Solanidine	65727	-10.0
2.	Solasodine	5250	-9.0
3.	Solavetivone	442399	-7.3
4.	Solafuranone	11107208	-7.8
5.	Scopoletin	5280460	-6.5
6.	N-p-trans-Coumaroyltyramine	5372945	-6.7
7.	Isofraxidin	5318565	-6.1
8.	Lauric acid	3893	-3.7
9.	β -sitosterol	222284	-7.1
10.	Diosgenin	99474	-8.1
Standard Drug			
11	Acetazolamide	1986	-5.1

The binding affinities of phytoconstituents ranged from -10.0 to -3.7 kcal/mol. From the docked results, it is evident that the compounds, Solanidine exhibit the most favourable binding affinity (-10.0 kcal/mol) in complex with selected macromolecules (PDB ID: 6O4L) as compared to other docked compounds i.e., Solsodine (-9.0 kcal/mol), Diosgenin (-8.1 kcal/mol), Solafuranone (-7.8 kcal/mol), Solavetivone (-7.3 kcal/mol), Beta sitosterol (-7.1 kcal/mol), N-p-trans-Coumaroyltyramine (-6.7 kcal/mol), Scopoletin (-6.5 kcal/mol), Isofraxidin (-6.1 kcal/mol), Lauric acid (-3.7 kcal/mol). Visual examination of the computationally docked optimal binding poses of phytoconstituents on selected macromolecules (i.e., 6O4L) revealed the significant involvement of various types of interactions, such as hydrogen bonding and hydrophobic interactions, including π - π stacking

and π -alkyl and alkyl interactions, in the stability of the binding of the phytoconstituents to 6O4L.

The binding affinity of the standard (Acetazolamide) for 6O4L is -5.1 kcal/mol.

3.1.1. Solafuranone, 6O4L

The number of intermolecular hydrogen bonds, the binding energy of ligand 6O4L stable complexes, and the number of nearest amino acid residues were also determined for selected compound Solafuranone. All synthesized derivatives formed complexes with target proteins. Analysis of interactions of the 6O4L protein complex and ligand Solafuranone showed that the ligand molecule is oriented due to Conventional Hydrogen bond with THR A: 346 amino acid residue and Pi-Pi Stacked interaction with PHE A: 401 amino acid residue were found.

3.1.2. Isofraxidin, 6O4L

An analysis of the interactions between the 6O4L protein complex and the Isofraxidin ligand was also carried out, which showed that the ligand molecule is oriented due to conventional hydrogen bond with the ASP A: 399, THR A: 346, PHE A: 401 amino acid residue and Pi-Alkyl interaction with ALA A: 349 amino acid residue were found.

3.1.3. Acetazolamide, 6O4L

The binding affinity of the standard (Acetazolamide) for 6O4L is -5.1 kcal/mol. the interactions between the 6O4L protein complex and the Acetazolamide ligand was also carried out, which showed that the ligand molecule is oriented due to conventional hydrogen bond with the PHE A:166, THR A:164 amino acid residue, Carbon hydrogen bond with PRO A:193 amino acid residue, Pi-Sulfur interaction with PHE A:166 amino acid residue, Pi-Cation interaction with LYS A:190 and Pi-Alkyl interaction with ALA A:165, ALA A:192 amino acid residue were found.

Table No. 2. Interactions with amino acid residue.

Sr. No.	Molecule	Binding Energy (kcal/mol)	H bond	Main amino acid interactions	
				Pi-alkyl, alkyl, Pi-S/Pi-Pi, T shaped/halogen/unfavourable donor-donor interactions	Van der Waals interactions
1	Solanidine	-10.0	No interactions	ALA A:192, ALA A: 165, VAL A: 250	No interactions
2	Solasodine	-9.0	GLY A: 226	VAL A: 250, PRO A: 193	No interactions
3	Solavetivone	-7.3	ASN A: 379, ASN A: 46	TYR A: 41	No interactions
4	Solafuranone	-7.8	THR A: 346	PHE A: 401	No interactions
5	Scopoletin	-6.5	THR A: 164, PHE A: 401	CYS A: 302, ALA A: 165	No interactions
6	N-p-trans-Coumaroyltyramine	-6.7	SER A: 460	PHE A: 168, CYS A: 302, TRP A: 175, PHE A: 468	No interactions
7	Isofraxidin	-6.1	ASP A: 399, PHE	ALA A: 349	No interactions
8	Lauric acid	-3.7	PHE A: 292	PRO A: 288, LEU A: 285, PRO A: 458	No interactions
9	β -sitosterol	-7.1	No interactions	TRP A: 31, ALA A: 207, LYS A: 204, LYS A: 208, VAL A: 209, ALA A: 92	No interactions
10	Diosgenin	-8.1	ASN A: 379	TYR A: 41, PHE A: 166	No interactions

11	Acetazolamide	-5.1	THR A: 164, PHE A: 166, PRO A: 193	ALA A: 165, ALA A: 192, LYS A: 190	No interactions
----	---------------	------	--	---------------------------------------	--------------------

3.2. ADMET study

Pharmacokinetic profile (ADME) and toxicity predictions of the ligands are important attentive parameters during the transformation of a molecule into a potent drug. In the present study, these parameters were assessed using SwissADME and pkCSM. The absorption potential and lipophilicity are characterized by the partition coefficient (Log *P*) and topological polar surface area (TPSA), respectively. For better penetration of a drug molecule into a cell membrane, the TPSA should be less than 140 Å. However, the value of Log *P* differs based on the drug target. The ideal Log *P* value for various drugs are as follows: oral and intestinal absorption, 1.35 – 1.80; sublingual absorption, > 5; and central nervous system (CNS)¹¹. The aqueous solubility of ligands ideally ranges from – 6.5 to 0.5¹², while the blood brain barrier (BBB) value ranges between – 3.0 and 1.2¹³. In addition, non-substrate P-glycoprotein causes drug resistance¹⁴. In our study, all the selected ligands followed the TPSA parameter, P-glycoprotein non-inhibition, thereby showing good intestinal absorption and an acceptable range of BBB values. All the compounds showed aqueous solubility values within the range. Further, it was predicted that the selected ligands do not show AMES toxicity, hepatotoxicity, and skin sensitivity. In addition, it did not inhibit hERG-I (low risk of cardiac toxicity). Lipinski's rule violations, *T. pyriformis* toxicity, minnow toxicity, maximum tolerated dose, rat acute oral toxicity, and chronic toxicity are depicted in table.

Table 3. ADME and toxicity predicted profile of ligands with superior docking score

ADMET Properties	Formula	MW (g/mol)	Log P	TPSA (Å ²)	HB done r	Hb accepto r	Aqueou s solubilit y (Log mol/L)	Human intestinal absorptio n (%)	Blood Brain Barrie r
Solanidine	C ₂₇ H ₄₃ NO	397.64 ₇	5.655	23.47 Å ²	1	2	-4.927	92.975	0.695
Solasodine	C ₇ H ₄₃ NO ₂	413.64	5.2869	41.49 Å ²	2	3	-3.809	92.324	0.035
Solavetivone	C ₁₅ H ₂₂ O	218.33	3.9042	17.07 Å ²	0	1	-4.615	95.873	0.635
Solafuranone	C ₁₅ H ₂₀ O ₂	232.32 ₃	3.1876 ₄	26.30 Å ²	0	2	-3.551	95.523	0.206
Scopoletin	C ₁₀ H ₈ O ₄	192.17	1.5072	59.67 Å ²	1	4	-2.504	95.277	-0.299
N-p-trans-Coumaroyltyramine	C ₁₇ H ₁₇ NO ₃	283.32 ₇	2.4699	69.56 Å ²	3	3	-3.165	90.031	-0.552
Isofraxidin	C ₁₁ H ₁₀ O ₅	222.19 ₆	1.5158	68.90 Å ²	1	5	-2.458	95.588	-0.377
Lauric acid	C ₁₂ H ₂₄ O ₂	200.32 ₂	3.9919	37.30 Å ²	1	1	-4.181	93.379	0.057
β-sitosterol	C ₂₉ H ₅₀ O	414.71 ₈	8.0248	20.23 Å ²	1	1	-6.773	94.464	0.781
Diosgenin	C ₂₇ H ₄₂ O ₃	414.63	5.7139	38.69 Å ²	1	3	-5.713	96.565	0.2
Acetazolamide	C ₄ H ₆ N ₄ O ₃ S ₂	222.25 ₁	-0.8561	151.66 Å ²	2	6	-2.428	59.043	-0.622

Table 3 Continued

ADMET Properties	P-glyco-protein substrate	Total clearance [Log mL/(min.kg)]	Bioavailability score	AMES toxicity	Max tolerated dose [Log mg/(kg.d)]	hERG I inhibitor	hERG II inhibitor
Solanidine	YES	0.028	0.55	NO	-0.882	NO	YES
Solasodine	YES	0.09	0.55	NO	-0.375	NO	YES
Solavetivone	NO	1.225	0.55	NO	0.044	NO	NO
Solafuranone	NO	1.256	0.55	NO	0.526	NO	NO
Scopoletin	NO	0.73	0.55	NO	0.614	NO	NO
N-p-trans-Coumaroyltyramine	YES	0.265	0.55	NO	-0.213	NO	YES
Isofraxidin	NO	0.713	0.55	NO	0.56	NO	NO
Lauric acid	NO	1.623	0.85	NO	-0.34	NO	NO
β -sitosterol	NO	0.628	0.55	NO	-0.621	NO	YES
Diosgenin	NO	0.328	0.55	NO	-0.559	NO	YES
Acetazolamide	NO	-0.01	0.55	NO	1.263	NO	NO

Table 3 Continued

ADMET Properties	Acute oral rat toxicity. LD50(mol/kg)	Oral rat chronic toxicity (Log mg/kgbw/day)	Hepatotoxicity	Skin sensation	T.Pyrimis toxicity (Log μ g/L)	Minnow toxicity (Log mmol/L)	Lipinski's rule Violation
Solanidine	2.596	1.334	YES	NO	0.378	-0.493	YES (1)
Solasodine	2.489	1.332	YES	NO	0.311	0.381	YES (1)
Solavetivone	1.643	1.19	NO	YES	1.453	0.874	YES (0)
Solafuranone	1.865	1.947	NO	YES	2.151	0.557	YES (0)
Scopoletin	1.95	1.378	NO	NO	0.516	1.614	YES (0)
N-p-trans-Coumaroyltyramine	2.17	1.271	NO	NO	1.008	1.514	YES (0)
Isofraxidin	2.326	1.825	NO	NO	0.431	1.862	YES (0)
Lauric acid	1.511	2.89	NO	YES	0.954	-0.084	YES (0)
β -sitosterol	2.552	0.855	NO	NO	0.43	-1.802	YES (1)
Diosgenin	1.921	1.452	NO	NO	0.399	0.247	YES (1)
Acetazolamide	2.292	2.143	NO	NO	0.239	2.895	YES (0)

3.3. Interaction of Standard Drug (Acetazolamide) with 6O4L

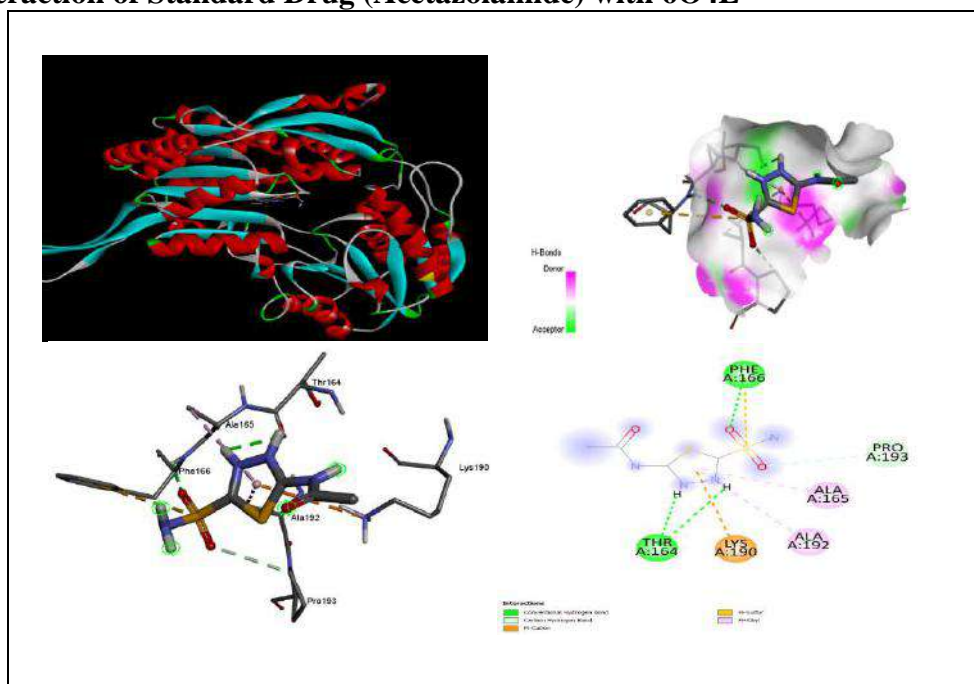
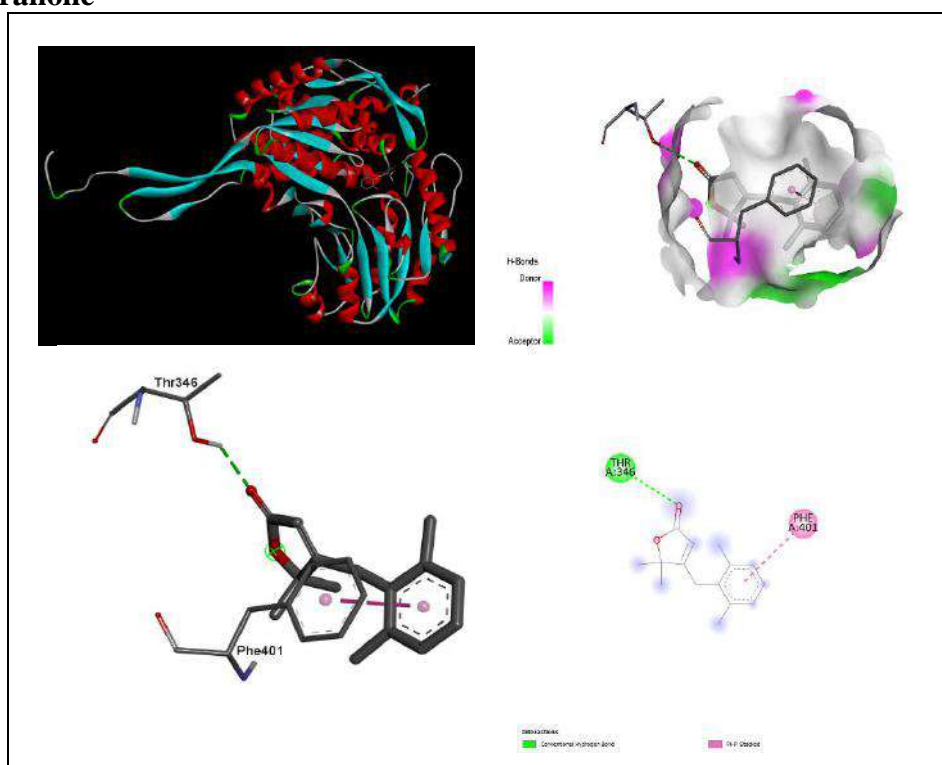


Fig. 2. Docking scores and binding interaction of Acetazolamide (PDB ID: 6O4L). The ligand is shown in line and stick representation along with its 2D diagram and hydrogen bond interaction.

3.4. Interactions of phytoconstituents with 6O4L

A.Solafuranone



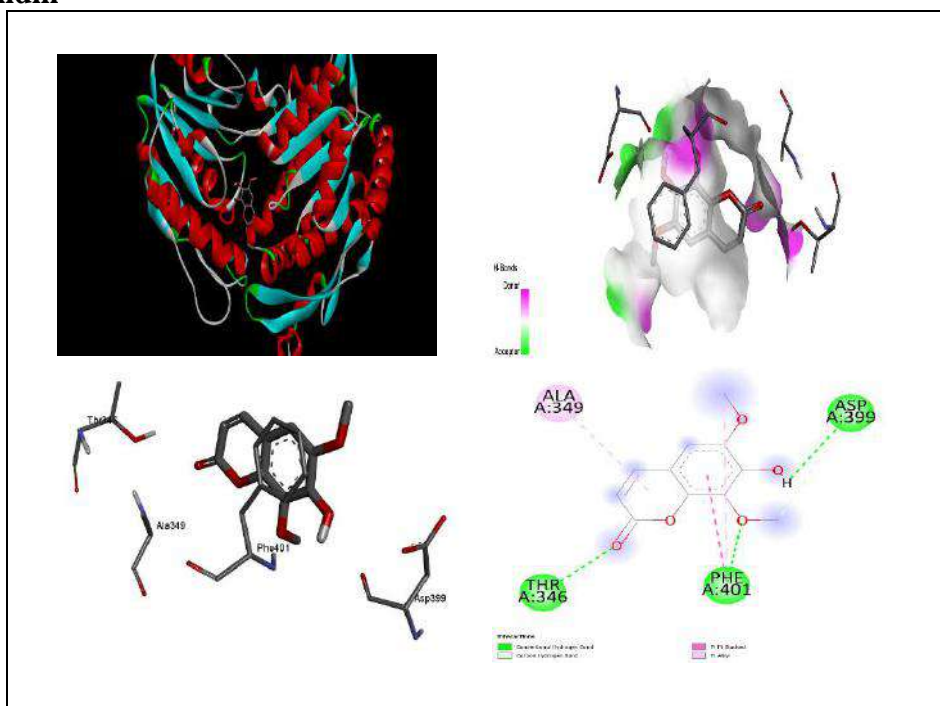
B.Isofraxidin

Fig. 3. Docking scores and binding interaction of phytoconstituents (PDB ID: 6O4L). The ligand is shown in line and stick representation along with its 2D diagram and hydrogen bond interaction.

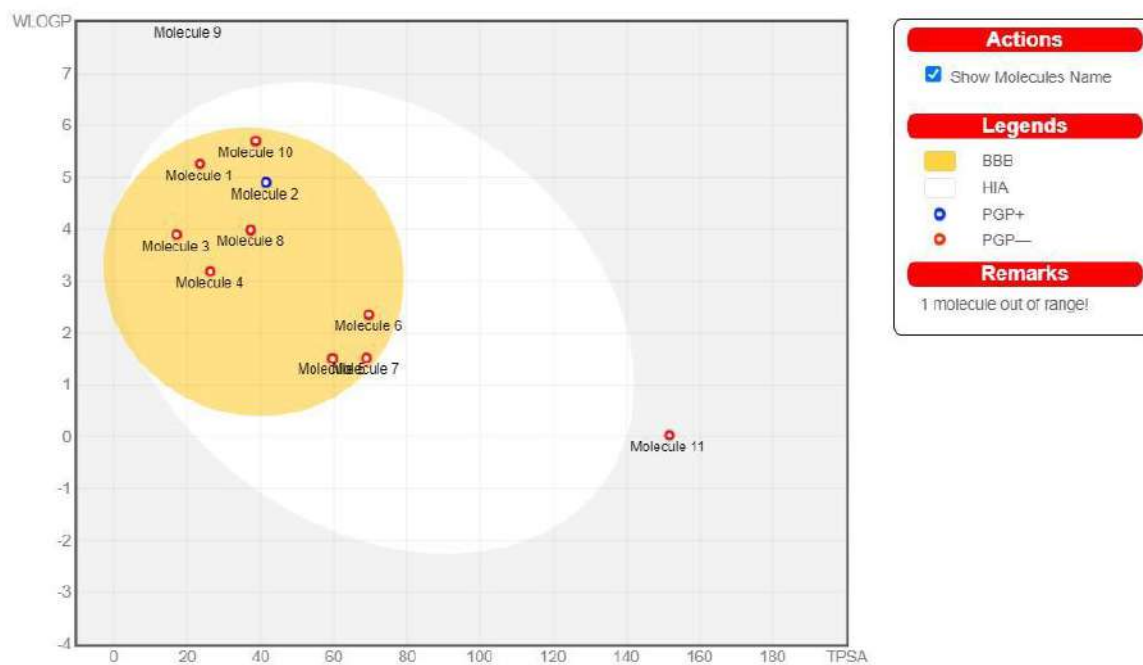
3.5. Boiled Egg

Fig no. 4. Combined Boiled Egg Diagram

Table no. 4. Name of molecules contained in Boiled Egg Diagram

MOLECULE NUMBER	MOLECULE NAME
1	Solanidine
2	Solasodine
3	Solavetivone
4	Solafuranone
5	Scopoletin
6	N-p-trans-Coumaroyltyramine
7	Isofraxidin
8	Lauric acid
9	β -sitosterol
10	Diosgenin
11	Acetazolamide

BOILED means Brain Or Intestinal Estimated permeation predictive model. The boiled egg diagram shows two regions white region and yellow region.

The white region is the physicochemical space of molecules with highest probability of being absorbed by the gastrointestinal tract, and the yellow region (yolk) is the physicochemical space of molecules with highest probability to permeate to the brain.

In addition, the points are coloured in blue if predicted as actively effluxed by P-gp (PGP+) and in red if predicted as non-substrate of P-gp (PGP-).

4. CONCLUSION

In this study, we have carried out an *in-silico* screening of the phytoconstituents of *Solanum indicum* plant. This study demonstrated the sixteen compounds from *Solanum indicum* plant, (Solanidine, Solasodine, Solavetivone, Solafuranone, Scopoletin, N-p-trans-Coumaroyltyramine, Isofraxidin, Lauric acid, β -sitosterol, Diosgenin). The selected phytocompounds showed docking scores ranging from -10.0 to -3.7 kcal/mol in 6O4L. Among all, Solafuranone and Isofraxidin gave the highest binding energy (-7.8 kcal/mol) and (-6.1 kcal/mol) in complex with 6O4L, whereas the reference compound, Acetazolamide showed a docking score with a binding energy of -5.1 kcal/mol. Furthermore, these ligands exhibited good ADMET properties. To summarize, phytoconstituents present in *Solanum indicum* possess strong effects against 6O4L and could be further evaluated for their antiepileptic effect, as well as for the development of alternative drugs with fewer side effects for the treatment of epilepsy.

REFERENCES

1. Saxena HO, Parihar S, Pawar G, Choubey SK, Dhar P. Phytochemical screening and HPTLC fingerprinting of different parts of *Solanum indicum* L.: A dashmool species. *Journal of Pharmacognosy and Phytochemistry*. 2021;10(1):1935-41.
2. Bahgat A, Abdel-Aziz H, Raafat M, Mahdy A, El-Khatib AS, Ismail A, Khayyal MT. *Solanum indicum* ssp. *distichum* extract is effective against l-NAME-induced hypertension in rats. *Fundamental & clinical pharmacology*. 2008 Dec;22(6):693-9.
3. Morris GM, Huey R, Lindstrom W, Sanner MF, Belew RK, Goodsell DS, Olson AJ. AutoDock4 and AutoDockTools4: Automated docking with selective receptor flexibility. *Journal of computational chemistry*. 2009 Dec;30(16):2785-91.
4. Pettersen EF, Goddard TD, Huang CC, Couch GS, Greenblatt DM, Meng EC, Ferrin TE. UCSF Chimera—a visualization system for exploratory research and analysis. *Journal of computational chemistry*. 2004 Oct;25(13):1605-12.

5. Liles JT, Corkey BK, Notte GT, Budas GR, Lansdon EB, Hinojosa-Kirschenbaum F, Badal SS, Lee M, Schultz BE, Wise S, Pendem S. ASK1 contributes to fibrosis and dysfunction in models of kidney disease. *The Journal of Clinical Investigation*. 2018 Oct 1;128(10):4485-500.
6. Verdonk ML, Cole JC, Hartshorn MJ, Murray CW, Taylor RD. Improved protein–ligand docking using GOLD. *Proteins: Structure, Function, and Bioinformatics*. 2003 Sep;52(4):609-23.
7. Leach AR, Shoichet BK, Peishoff CE. Prediction of protein– ligand interactions. Docking and scoring: successes and gaps. *Journal of medicinal chemistry*. 2006 Oct 5;49(20):5851-5.
8. SAMANT L, Javle V. Comparative docking analysis of rational drugs against COVID-19 main protease.
9. Arora S, Lohiya G, Moharir K, Shah S, Yende S. Identification of potential flavonoid inhibitors of the SARS-CoV-2 main protease 6YNQ: a molecular docking study. *Digital Chinese Medicine*. 2020 Dec 1;3(4):239-48.
10. Shah S, Chaple D, Arora S, Yende S, Moharir K, Lohiya G. Exploring the active constituents of *Oroxylum indicum* in intervention of novel coronavirus (COVID-19) based on molecular docking method. *Network Modeling Analysis in Health Informatics and Bioinformatics*. 2021 Dec;10:1-2.
11. Kaloni D, Chakraborty D, Tiwari A, Biswas S. In silico studies on the phytochemical components of *Murraya koenigii* targeting TNF- α in rheumatoid arthritis. *Journal of Herbal Medicine*. 2020 Dec 1;24:100396.
12. Joshi T, Sharma P, Joshi T, Chandra S. In silico screening of anti-inflammatory compounds from Lichen by targeting cyclooxygenase-2. *Journal of Biomolecular Structure and Dynamics*. 2020 Aug 12;38(12):3544-62.
13. Nisha CM, Kumar A, Vimal A, Bai BM, Pal D, Kumar A. Docking and ADMET prediction of few GSK-3 inhibitors divulges 6-bromoindirubin-3-oxime as a potential inhibitor. *Journal of Molecular Graphics and modelling*. 2016 Apr 1;65:100-7.
14. Tsujimura S, Tanaka Y. Disease control by regulation of P-glycoprotein on lymphocytes in patients with rheumatoid arthritis. *World journal of experimental medicine*. 2015 Nov 11;5(4):225.

Development and Characterization of Piroxicam Matrix Based Transdermal Patch

Pragati Hasbe , Zohra Firdous M.S.A*, Pankaj Dhapke, Jagdish Baheti

Kamla Nehru College of Pharmacy, Butibori, Nagpur 441108, Maharashtra, India.

e-mail address: pragatihhasbe2@gmail.com

ABSTRACT:

The present study aims to develop and characterize matrix based transdermal patch for the treatment of dysmenorrhea using the drug Piroxicam, which is a non-steroidal anti-inflammatory drug of oxicam derivative. Matrix-based transdermal patches were prepared using a solvent casting method consisting of polymer (HPMC E5LV) and drug along with PEG 400 (plasticizer) and capsicum oleoresin (penetration enhancer) in a methanol and dichloromethane solution. All F₈ formulation batches prepared were evaluated and optimized. The result shows that the F₃ batch gives consistent results and all the evaluated parameters were within the standard limits. The in-vitro and ex-vivo %CDR of the optimized F₃ batch was found to be 98.76% and 97.65% respectively which indicates that the permeability of the drug through the goat skin within the time period of 2 hours is less than that of the dialysis membrane. The research work concluded that piroxicam matrix based transdermal patch was successfully prepared and evaluated which can provide direct entry of the drug into systemic circulation for immediate action in 2 hours. Therefore, piroxicam matrix based transdermal patches can be used to safely deliver the drug for the treatment of dysmenorrhea while avoiding therapy associated side effects and with good patient compliance.

KEYWORDS: Dysmenorrhea, Piroxicam matrix based transdermal patch, Capsicum oleoresin, HPMC E5LV, PEG 400.

INTRODUCTION

Dysmenorrhea has a negative impact on social, academic, sporting and daily activities. It is the most common problem that can be seen in adolescent and young women all over the world. Worldwide statistics shows that 51% of adolescent girls suffer from dysmenorrhea. Dysmenorrhea can be treated by using non-steroidal anti-inflammatory drugs (NSAIDs). Piroxicam is a non-steroidal anti-inflammatory drug of the oxicam derivative that are used to relieve pain, stiffness, tenderness and swelling by preventing the production of endogenous prostaglandins. This results in inhibition of prostaglandin biosynthesis. It has a role as an analgesic, a COX1 inhibitor, a non-steroidal anti-inflammatory drug, antipyretic, etc. It is used in the treatment of certain inflammatory conditions like primary & secondary dysmenorrhea, rheumatoid and osteoarthritis and postoperative pain. The transdermal drug delivery system (TDDS) is a route of administration where in active ingredients are delivered across the skin for systemic distribution. Transdermal patch is one of the conventional forms of transdermal drug delivery system. TDD is a painless method of delivering drugs systemically by applying a drug formulation onto intact and healthy skin. The drug initially penetrates through the stratum corneum and then passes through the deeper epidermis and dermis without drug accumulation in the dermal layer. When drug reaches the dermal layer, it becomes available for systemic absorption via the dermal microcirculation. Therefore, this work is formulated and evaluated the piroxicam matrix based transdermal patch for the treatment of Dysmenorrhea.

Application of Transdermal Delivery System

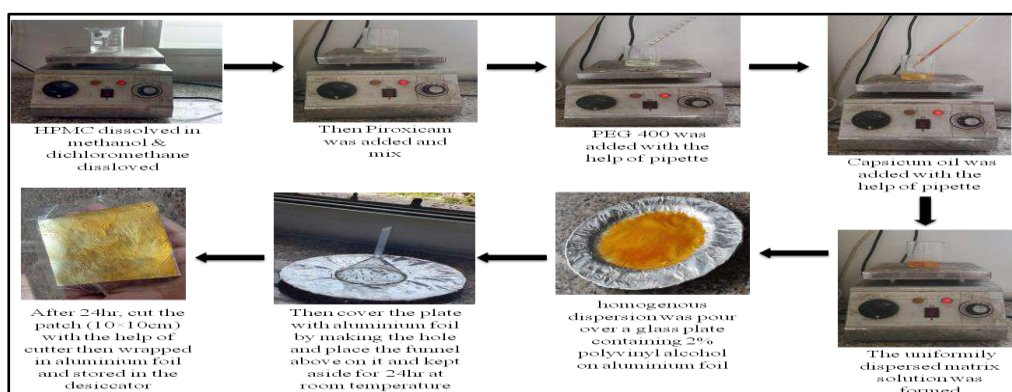
- Transdermal patches adhere to the skin as a way to deliver drugs. They provide a specific, predetermined dose of medication that is absorbed through the skin and penetrates into the bloodstream
- NSAIDs had been in first line of choice for transdermal drug delivery system for a long times due to their improved local effects and possibility to avoid the gastro-irritating effects.
- NSAIDs transdermal patches are most suitable techniques for reducing the adverse effects, increasing the bioavailability by avoiding first-pass hepatic metabolism, elevating the permeability of NSAIDs, and facilitating sustained release of drug for the longer duration of time.
- The drugs such as analgesic, antipyretic, antidepressant, antianginal and NSAIDs can be given by using transdermal drug delivery system.

MATERIALS AND METHODS

Chemicals

Piroxicam was purchased from Yarrow Chem Products, Mumbai, India. HPMC E5 LV was procured from Central Scientific Company, Nagpur, India. PEG 400 and methanol was procured from The Global Marketing, Nagpur, India and dichloromethane were procured from Genex Scientific Company, Nagpur, India. Capsicum oleoresin was purchased from Avi Naturals, Delhi, India. All other chemicals and reagents used in the study were of analytical grade.

Method of preparation of matrix based transdermal patch



RESULTS AND DISCUSSION

Evaluation of Transdermal patches

Physical appearance

The formulated patches were found to be clear, smooth, uniform, flexible and light yellow colour in their physical appearance as shown in figure



***In-vitro* diffusion cell study**

Formulation Code	Thickness (mm)±S.D	Weight Uniformity (mg) ± S.D	Folding Endurance ± S.D	% Moisture Content (%w/w) ± S.D	% Moisture Uptake (%w/w) ± S.D	Drug Content (%) ± S.D
F ₁	0.690 ± 0.051	540.75 ± 0.88	7.67 ± 1.16	2.84 ± 0.57	6.6 ± 0.19	98.8 ± 0.45
F ₂	0.554 ± 0.024	499.5 ± 0.75	6 ± 1	2.53 ± 0.25	4.25 ± 0.21	98.4 ± 0.51
F ₃	0.323 ± 0.007	301.12 ± 0.35	9 ± 1	2.24 ± 0.64	0.15	0.19
F ₄	0.648 ± 0.048	566 ± 0.92	5.67 ± 0.58	4.14 ± 0.31	5.2 ± 0.56	98.18 ± 0.33
F ₅	0.544 ± 0.018	470.37 ± 0.74	6.33 ± 2.31	2.64 ± 0.19	4.6 ± 0.29	94.1 ± 0.70
F ₆	0.615 ± 0.036	520.5 ± 0.80	8 ± 2	4.36 ± 0.04	5.95±0.37	95.8 ± 0.39
F ₇	0.337 ± 0.008	355.75 ± 0.46	6.66 ± 1.53	2.45 ± 0.03	3.77 ± 0.27	97.8 ± 0.79
F ₈	0.450 ± 0.009	388.62 ± 0.51	7.33 ± 1.52	3.03 ± 0.06	5.88 ± 0.20	98.6 ± 0.25

Figure 1: *In-Vitro* diffusion cell study for % Cumulative Drug Release

The % of drug release orders was as follows: F₃ > F₁ > F₈ > F₂ > F₄ > F₇ > F₆ > F₅. The formulation F₃ batch showed a better *in-vitro* drug release profile across the dialysis membrane when compared to the other formulations (figure 12). This might be attributed to the nature of the polymer; plasticizer and the permeation enhancer used. Thus formulation F₃ is considered an optimized formulation

***Ex-vivo* skin permeation study**

The F₃ batch *ex-vivo* skin permeation study was performed. The patch was exposure to the goat skin, 97.65 % of the drug was permeated and 98.76 % of the drug was permeated from *in-vitro* diffusion of optimized F₃ batch as shown in table 12. Thus, the amount of the drug permeated through the goat skin was less than the dialysis membrane. The graph (figure 13) of cumulative drug release, *ex-vivo* skin permeation and *in-vitro* cell study of an optimized batch (F₃)

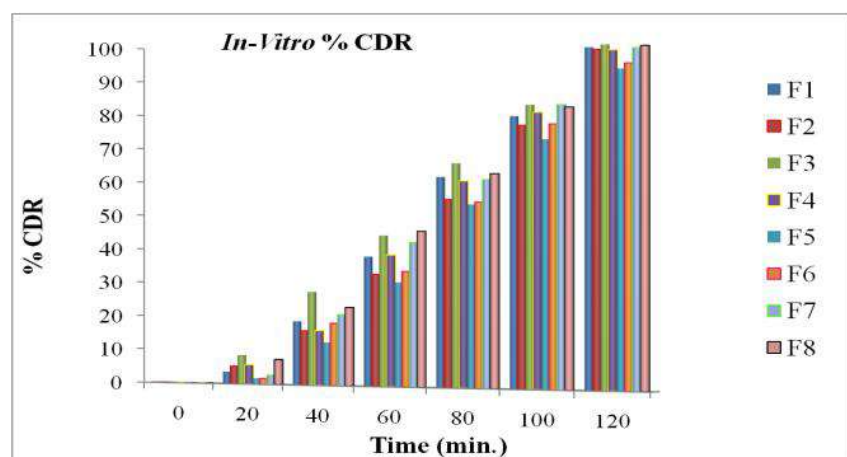


Figure 2: % Cumulative Drug Release *ex-vivo* skin permeation Vs *in-vitro* study of an optimized batch (F₃)

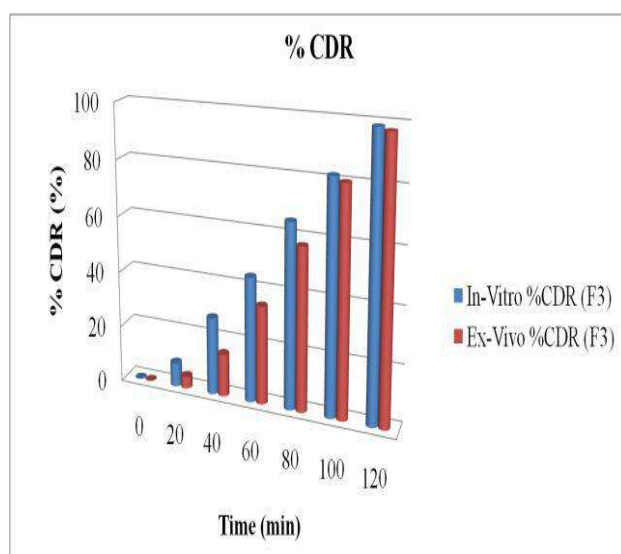
Sr. No.	Time (min.)	<i>In-Vitro</i> %CDR (F ₃) (%)	<i>Ex-Vivo</i> %CDR (F ₃) (%)
1	0	0	0
2	20	8.52 ± 1.16	4.25 ± 1.39
3	40	27.46 ± 1.75	15.12 ± 2.26
4	60	44.19 ± 3.47	34.69 ± 3.96
5	80	65.8 ± 5.34	57.40 ± 1.94
6	100	81.85 ± 5.29	80.06 ± 1.95
7	120	98.76 ± 0.57	97.65 ± 0.65

Stability study of optimized F₃ batch

Stability study was performed for optimized F₃ batch (piroxicam matrix based transdermal patch) was wrapped in aluminium foil by placing in the zip lock bag and kept in stability chambers at 40°C/75% RH for accelerated study of 6 months. Formulation was removed at each time point

(0 day, 1 month, 3 month and 6 month) and evaluated for physical appearance, weight uniformity, thickness, folding endurance and drug contents. The in-vitro & ex-vivo permeation study were also performed. The stability study was completed as shown in table

Time (months)	Appearance	Thickness (mm)	Weight Uniformity (mg)	Folding Endurance	Drug Content (%)	<i>In-Vitro</i> %CDR (F ₃)	<i>Ex-Vivo</i> %CDR (F ₃)
0	Pale light yellow	0.323 ± 0.007	301.12 ± 0.35	9 ± 1	99.17 ± 0.19	98.76 ± 0.57	97.65 ± 0.65
1	Pale light yellow	0.320 ± 0.008	298 ± 0.39	10 ± 1.15	98.95 ± 0.35	98.35 ± 0.71	96.76 ± 0.61
3	Pale light yellow	0.324 ± 0.010	306.1 ± 0.1	12 ± 2.2	98.43 ± 0.5	98.12 ± 1.6	95.98 ± 1.5
6	Pale light yellow	0.319 ± 0.009	299.07 ± 0.37	10 ± 1.05	99 ± 1	98.54 ± 0.8	97 ± 1



CONCLUSION

It is concluded that piroxicam matrix based transdermal patch was successfully formulated and evaluated which may provides direct entry of the drug into the systemic circulation for immediate action in 2 hours. The identification of drug shows pure piroxicam. The prepared matrix based transdermal patch evaluation reveals that the F₃ batch is an optimized batch which shows good uniformity in the evaluation parameters of the patch. Such drugs delivery systems can be used to avoid side effects associated with therapy and safely deliver the drug for the treatment of dysmenorrhea with good patient compliance.

References

1. Azagew AW, Kassie DG, Walle TA. Prevalence of primary dysmenorrhea, its intensity, impact and associated factors among female students' at Gondar town preparatory school, Northwest Ethiopia. *BMC women's health*. 2020;20(1):1-7
2. Singh A, Kiran D, Singh H, Nel B, Singh P, Tiwari P. Prevalence and severity of dysmenorrhea: a problem related to menstruation, among first and second year female medical students. *Indian J Physiol Pharmacol*. 2008;52(4):389-97.
3. Dharshini AV, Sangeetha A, Hemachandrika C. Primary dysmenorrhea and its impact on academic performance among adolescent females—a cross sectional study. *Annals of the Romanian Society for Cell Biology*. 2021:13681
4. Negriff S, Dorn LD, Hillman JB, Huang B. The measurement of menstrual symptoms: factor structure of the menstrual symptom questionnaire in adolescent girls. *Journal of health psychology*. 2009;14(7):899-908.
5. Rafique N, Al-Sheikh MH. Prevalence of primary dysmenorrhea and its relationship with body mass index. *Journal of Obstetrics and Gynaecology Research*. 2018;44(9):1773-8.
6. Speer LM, Mushkbar S, Erbele T. Chronic pelvic pain in women. *Am Fam Phys*. 2016;93:380.
7. Kulkarni A, Deb S. *Dysmenorrhoea obstetrics, gynecology & reproductive medicine*. Elsevier. 2019; 29(10):286-291.
8. Ju H, Jones M, Mishra G. The prevalence and risk factors of dysmenorrhea. *Epidemiologic reviews*. 2014 Jan 1;36(1):104-13.
9. Osayande AS, Mehulic S. Diagnosis and initial management of dysmenorrhea. *Am Fam Physician*. 2014;89(5):341-6.
10. Sultan C, Paris F, Jeandel C, Lumbroso S, Galifer RB, Picaud JC. Ambiguous genitalia in the newborn: diagnosis, etiology and sex assignment. *Pediatric and Adolescent Gynecology*. 2004; 7:23-38.

Analytical Method Development and Validation of Antidiabetic Drugs

Prajakta Sontakke, Disha Dhabarde, Jagdish Baheti

Kamla Nehru College of Pharmacy, Butibori, Nagpur

sontakkeprajakta108@gmail.com

dishamandave20@gmail.com

ABSTRACT

The present study focuses on the analytical method development and validation of antidiabetic drugs by Uv-visible spectrophotometry and High-Performance Liquid Chromatography. Developing single analytical method is challenging task. A simple, rapid, precise and reliable method was developed for the estimation of bulk antidiabetic drugs. The estimation was carried out using an Inertsil-C18 BDS column (250 mm × 4.6 mm, 5 μm) and the mobile phase composed of methanol: H₂O (80:20) at flow rate 1.0ml/min. Detection and Quantification were performed by Uv-visible detection at 230 nm. The retention time of metformin and dapagliflozin was found to be 3.08 and 3.87 minutes respectively. The validated method was successfully applied to the commercially available pharmaceutical dosage form, yielding good and reproducible results.

Keywords: Metformin and Dapagliflozin, Uv-visible spectrophotometry and High-Performance Liquid Chromatography

INTRODUCTION:

Metformin is a biguanide antihyperglycemic agent and first-line pharmacotherapy used in the management of Type II diabetes. Metformin is considered an antihyperglycemic drug because it lowers blood glucose concentrations in Type II diabetes without causing hypoglycemia. It is commonly described as an "insulin sensitizer", leading to a decrease in insulin resistance and a clinically significant reduction of plasma fasting insulin levels.

Dapagliflozin is a sodium-glucose cotransporter 2 (SGLT2) inhibitor, and it was the first SGLT2 inhibitor to be approved, indicated for managing diabetes mellitus type 2. When combined with diet and exercise in adults, dapagliflozin helps to improve glycemic control by inhibiting glucose reabsorption in the proximal tubule of the nephron and causing glycosuria.

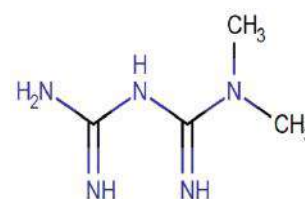


Fig.1

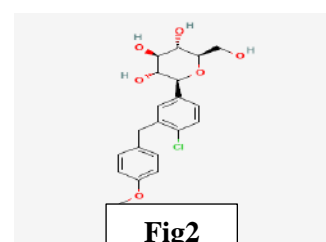


Fig2

Method

Selection of wavelength

Wavelength determination for HPLC analysis involved recording UV spectra (200-400 nm) for individual Metformin and Dapagliflozin solutions. UV spectrum of standard Metformin and Dapagliflozin was observed at 230 nm.

Chromatographic conditions

The developed method employs a reverse-phase C18 column, with a mobile phase consisting of Methanol: H₂O in the ratio of 80:20 v/v. The mobile phase flows at a rate of 1.0 ml/min, and each injection involves 20 μl of the sample. Detection was performed at a wavelength of 230 nm.

Preparation of Standard drug Solution of Metformin and Dapagliflozin

Accurately weighed quantity of 120 mg Metformin diluted to 10 ml of diluent and 24 mg of Dapagliflozin was dissolved in diluent and volume was made up to 100 ml mark by same to obtain 1000 µg/ml. Then further diluted to obtain 100 ppm stock solution. From standard stock solution pipette out 2 ml and dissolved in 20 ml of diluent to obtain 10 µg/ml of solution.

RESULT AND DISCUSSION

Method development

A reverse-phase HPLC method was developed with consideration for key system suitability parameters, including the resolution factor (R_s) between peaks, peak asymmetry (A), number of theoretical plates (N), run time, and cost-effectiveness. In conclusion, the developed method is deemed specific. System precision was evaluated through six replicate injections of the standards mixture at working concentration, revealing a % RSD (Relative Standard Deviation) less than 2 for peak area of both drugs. This signifies acceptable reproducibility and precision within the system.

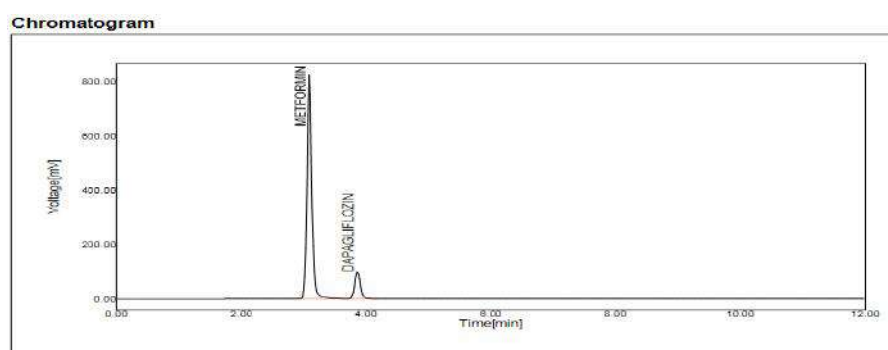


Fig4

Method validation

The HPLC method developed underwent validation following International Conference on Harmonization (ICH) guidelines. The validation included assessments for linearity, accuracy, system precision, intra-day precision, ruggedness, limit of detection (LOD), and limit of quantification (LOQ). Specificity was confirmed by observing peaks only in the standards and sample solutions at working concentrations, with no interference from the blank. The method is considered specific.

System precision was evaluated through six replicate injections of the standards solution at working concentration, showing % RSD (Relative Standard Deviation) less than 2 for peak area of both drugs, indicating acceptable reproducibility and precision.

Method precision was determined by assaying the sample under repeatability conditions (intraday precision) at working concentrations.

System suitability

System suitability is an essential pharmacopeial requirement utilized to assess the reproducibility of a chromatographic system, ensuring its adequacy for accurate analysis

In the study was assessed through recovery studies, involving the addition of standard drug solution to reanalyzed sample solutions at three concentrations: 80%, 100%, and 120% of the spiked levels. The accuracy was determined based on recovery studies conducted using the spiked method, covering the range of 80-120% of the labeled claim.

Linearity

Linearity in analytical methods indicates results directly proportional or following a defined mathematical transformation relative to analyte concentration within a specified range. Assessment involves analyzing samples across the claimed concentration range, creating a graph of area versus analyte concentration, and calculating percentage curve fittings to confirm linearity

Precision

Acceptance criteria require that the Relative Standard Deviation (RSD) should not exceed 2% for the test. The Standard Deviation (SD) and the Relative Standard Deviation (RSD) are calculated from the mean of five injections of the Standard solution and reported for evaluation.

Robustness

Robustness testing of the analytical method aimed to verify its stability against minor variations in optimized parameters. Small changes were introduced in factors such as flow rate, mobile phase composition, and wavelength. Specifically, variations of ± 0.1 ml/min in flow rate, ± 5 in mobile phase composition, and ± 2 nm in wavelength were implemented. The robustness of the method was assessed by calculating the % RSD values to ensure the method's reliability despite these slight variations.

SUMMARY AND CONCLUSION

Name	Preparation	%Assay
1.0 ml/min	Preparation-1	100.27
	Preparation-2	98.86
0.9 ml/min	Preparation-1	98.95
	Preparation-2	99.08
Mean		99.29
SD		0.6595
%RSD (NMT 2)		0.66

An RP-HPLC method was established and applied to pharmaceutical dosage forms for Metformin and Dapagliflozin. A validated simple reverse-phase liquid chromatographic method was developed. A UV-spectrophotometric method has been developed, demonstrating accurate results for estimating drugs in a mixture. The separation method utilized a mobile phase

composed of Methanol, Water, and Trifluoroacetic acid in a ratio of 80:20. Detection was performed using UV-Visible SPD 20 A at 230 nm. The column employed was Hypersil BDS C18 (250 mm \times 4.6 mm, 5 μ m), and the flow rate was set at 1 ml/min.

The retention times for Metformin and Dapagliflozin were determined as 3.08 and 3.87, respectively. The asymmetry factors or tailing factors of 1.17 and 1.10 suggested a symmetrical peak nature at ambient temperature with an injection volume of 20 μ l. The number of theoretical plates was determined as 17196 and 15475, indicating the efficiency performance of the column. Linearity studies were conducted, and specified concentration levels were determined.

The method was validated according to ICH guidelines, demonstrating accuracy, precision, selectivity, and cost-effectiveness. With sharp and well-defined peaks, the method is suitable for the estimation of Metformin and Dapagliflozin in both bulk and pharmaceutical dosage forms.

REFERENCES

1. Chin B. and Anusha M., "Method Development And Validation For Symultaneous Estimation Of Citicoline And Methylcobalamin By Rp-Hplc Method", IPAPR, 2015, 6(10), 342-8.
2. Keval L. and Dilip G., "Rp-Hplc Method For The Estimation Of Epalrestat And Methylcobalamin In Their Combined Dosage Form", Indo American Journal of Pharmaceutical Research, 2014, 4(6), 2697-2705
3. Chatwal A, "Instrumental Method of Chemical Analysis", Himalaya Publishing House, p.no.615-623.
4. Bhardwaj S., Dwivedi K, Agarwal D. A review: HPLC method development and validation. International Journal of Analytical and Bio analytical Chemistry. 2015; 5(4):76-81.
5. Charde M., Welankiwar A.S, Kumar J. Method development by liquid chromatography with validation. International Journal of Pharmaceutical Chemistry. 2014; 4(02):57-61.
6. Murugan S, Elayaraja A, Niranjana Babu M, Chandrakala K, Prathap Naik K, Ramaiah P, Vulchi C. A Review on Method Development and Validation by using HPLC. International journal of novel trends in pharmaceutical sciences. 2013 Oct; 3(3):78-81.
7. Hanif A, Bushra R, Ismail NE, Bano R, Abedin S, Alam S, Khan MA, Arif HM. Empagliflozin: HPLC based analytical method development and application to pharmaceutical raw material and dosage form. Pak. J. Pharm. Sci. 2021 May; 34(3):1081-7.
8. Manoel J, Primieri GB, Bueno LM, Wingert NR, Volpato NM, Garcia CV, Schapoval EE, Steppe M. The application of quality by design in the development of the liquid chromatography method to determine Empagliflozin in the presence of its organic impurities. RSC advances. 2020; 10(12):7313-20.
9. Shirisha V, Krishnaveni B, Illendula S, Rao KN, Dutt HR. A new simple method development, validation and forced degradation studies of Empagliflozin by using Rp-Hplc. International Journal of Pharmacy and Biological Sciences. 2019; 9(1):25-35.
10. 16. Naseef H, Moqadi R, Qurt M. Development and validation of an HPLC method for determination of antidiabetic drug alogliptin benzoate in bulk and tablets. Journal of Analytical Methods in Chemistry. 2018 Sep 24; 2018

Synthesis of colloidal metal oxide using reverse micelle technique and its application in coupling reactions for Benzoxazole formation

Ramesh N. Zade¹, Pravin S. Bodakhe*, Kishor B. Raulkar², Bhupesh M. Mude³

1. Siddharth College of Arts, Science and Commerce, Fort, Mumbai
2. Vidya Bharati Mahavidyalaya, Camp Amravati
3. Vidya Bharati Mahavidyalaya, Camp Amravati
4. Ramanarain Ruia College, Matunga, Mumbai

Abstract:

Metal oxides have profound applications in the various advanced technologies using its catalytic, gas sensing, optoelectronic, ceramic, piezoelectric properties. Physiochemical properties of metal oxides are tuned using various synthetic methods to synthesize particles of various shapes, sizes and geometries. Therefore, focus of the researchers and scientists is to prepare metal oxides nanoparticles using various synthetic routes of Chemical, physical and biological methods. But either these synthetic routes are complicated, energy intensive or producing nanoparticles having potent toxicity which can restrict its long-term use in the various applications and technologies. Potential toxicity of nanoparticles is due to its accumulation in vital organs of the body. Exposure to nanoparticles could trigger the production of reactive oxygen species which subsequently disturb the metabolism as well as damage proteins, enzymes, cell membranes and also DNA. Therefore, for sustainable development of nanotechnology use of nanoparticles in consumer products, environmental benign techniques for the synthesis of metal oxides are to be practiced. Colloidal metal oxides particles have shown promising results in this direction, as colloids are biocompatible in its synthetic ways as well as its application modes. Therefore, in this article, we have focused to prepare copper oxide and nickel oxide using some synthetic methods which successfully lead to synthesize colloidal metal oxides. Characterization of synthesized metal oxide is done for its shape, size, morphology using techniques such as SEM, XRD, FT-IR and BET. These metal oxides subsequently used for reactions which forms the basis of complicated reactions taking place in plant and animal body. These reactions are mainly coupling reactions involving C-N bond and C-O bond formation.

Key words: Metal oxide, nanotechnology, toxicity, reverse micelle, Coupling reactions, Benzoxazole

1. Introduction:

Metal ions are fundamental elements present in plants and animals. Their substantial role in biological systems was recognized a long time ago. They are essential for the maintenance of life and their absence can cause growth disorders, severe malfunction, carcinogenesis or death. They are protagonists as macro or microelements in several structural and functional roles, participating in many biochemical reactions, and arise in several forms. They participate in intra and inter cellular communications, in maintaining electrical charges and osmotic pressure, in photosynthesis and electron transfer processes, in the maintenance of pairing, stacking and the stability of nucleotide bases, and also in the regulation of DNA transcription. They contribute to the proper functioning of nerve cells, muscle cells, the brain and the heart, the transport of oxygen and in many other biological processes up to the point that we cannot even imagine a life without metals.[1]

Heterocyclic moieties play a significant role in the field of drug discovery. C-N and C-O bond formation reactions are the primary synthetic sequence for the generation of heterocyclic molecules. The generation of C-N and C-O bonds involves the use of mostly Pd or Cu

catalysts although other transition metal catalysts are also involved. However, in C–N and C–O bond formation reactions, several problems were faced such as catalytic systems containing costly ligands, lack of substrate scope, lots of waste generation, and high temperature conditions. So it is imperative to uncover new eco-friendly synthetic strategies which provides a short reaction time, tolerance for functional groups, and less waste production. [2, 8, 9]

Microbial organisms possess an incredible capability of fabricating extremely specialized inorganic nanostructures. These magnificent skills of the living creatures have caught the attention of many material scientists towards these biological systems to acquire knowledge and recuperate the skills for the precise formulation of nanostructures. Generally, synthesis of inorganic nanomaterials by living organism has been categorized as biologically controlled and biologically induced synthesis. Biologically controlled synthesis is well-known to occur naturally in a few organisms. During this type of synthesis, the organisms are able to modulate the particle size, composition and surface area of the produced particles. Though biologically controlled synthesis of metal oxide nanoparticles exhibits high control over the morphology and composition of the nanoparticles. [3,4]

The basic idea of the colloidal method is to limit particle growth. As the formation of very small crystals is thermodynamically unfavourable due to the high surface energy of such particles, nanosynthesis must be controlled by kinetics. To achieve this, surfactant molecules are used to limit particle growth. One method uses a non-polar solvent, leading to the formation of reversed micelles. In the polar core of the micelle, a minute amount of water is present in which precipitation of the nanocrystal takes place. The size of the micelles thus determines the size of the particles. [5,6]

Benzoxazoles are an important class of heterocyclic compound that are encountered in a number of natural products and are used in drug and agrochemical discoveries. As a consequence, much effort has been devoted not only to construct basic skeleton of benzoxazole molecules but also to prepare derivatives through C–O or C–N atom bond formation. Hence development of an efficient methodology for the preparation of benzoxazole and its derivatives has gained a lot of importance in current research. [10,11]

2. Synthesis and characterisation of MO:

Cuprous oxide (Cu_2O) is produced by chemical reduction of copper sulphate salts in water-in-oil microemulsion solution using NaBH_4 as a reductant. Water-in-oil (w/o) microemulsions also called reverse micelles are water pools stabilized by surfactants, dispersed in oil phase, that serves as nanoreactors in which nanoparticles form and serve in controlling the size of nanoparticles. The water pools being stabilized by the lipopeptidal surfactant act both as nanoreactors for the process reaction and prevent particle aggregations as the surfactants get adsorbed on the particle surfaces when the particle size approaches the water pool, resulting in fine and uniform particle size distribution. Colloidal particles were then supported on $\gamma\text{-Al}_2\text{O}_3$ are then dried in oven at 80°C for an hour. Characterisation of this colloidal metal oxide is done by FTIR, SEM and XRD.

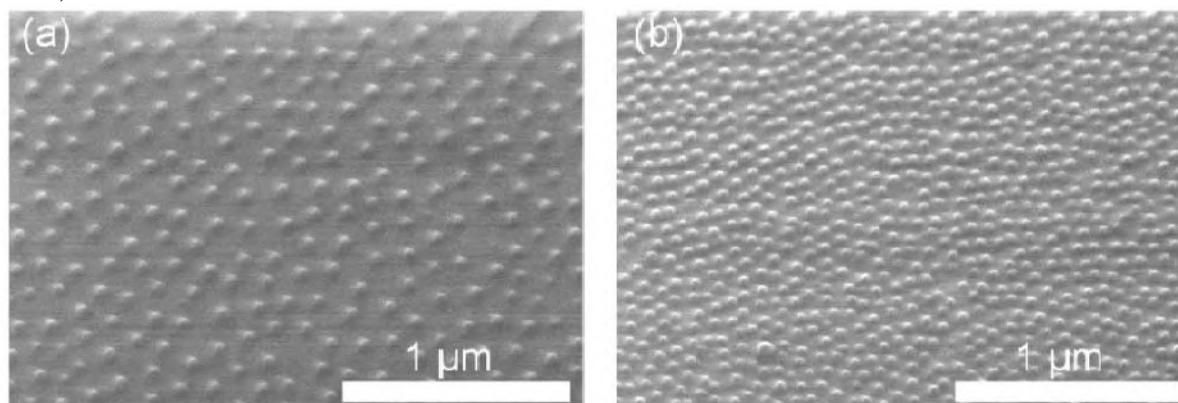


Figure 1 : SEM micrographs at different O/W ratio.

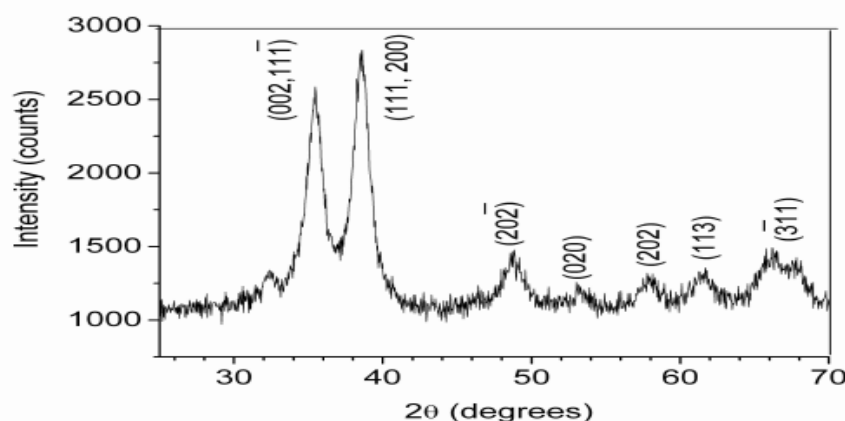


Figure 2: XRD

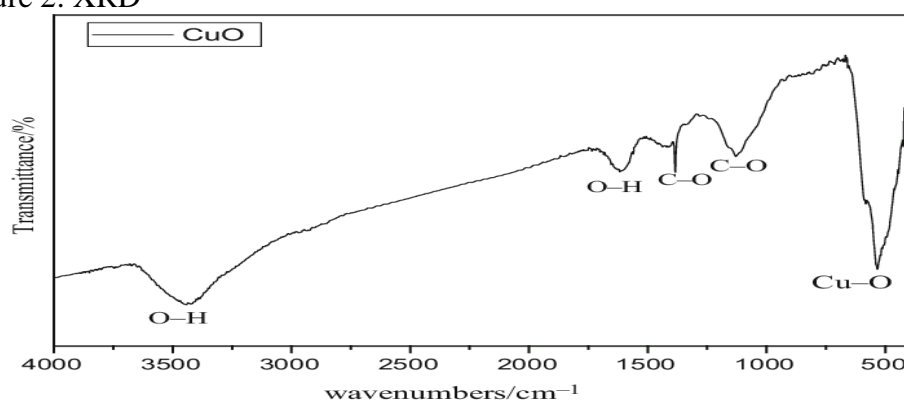
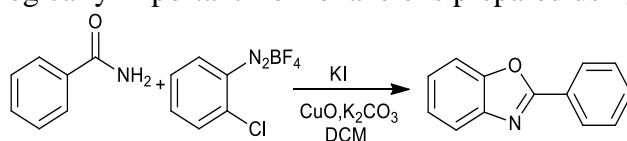


Figure 3: FTIR

3. Application of MO:

CuO prepared is further used as catalyst for coupling reaction in the formation of new C-N and C-O bonds. To illustrate this application following coupling reaction is taken where biologically important Benzoxazole is prepared using amide and aryl diazonium salt.



Conditions of temperature and solvents are optimised at 2 hours of heating and effects of equivalents of CuO is shown below

Sr.No	Equivalents of catalyst	Temperature (°C)	Yield (%)
1	1	110	68
2	2	110	85
3	3	120	85
4	4	120	82

Reaction conditions: amide(1mmol), diazonium salt (1mmol), catalyst (1mol %), solvent (2 mL), KI (1.5mmol), K₂CO₃ (3mmol) 110°C, time 2 Hrs; isolated yield

4. **Result and Conclusion:** Efficient, economical, base free protocol for benzoxazole synthesis has been developed with considerable good yield, high functional group tolerance, cost effective (due to use of diazonium salts). Moreover, CuO NP used is prepared

by reverse micelle which is biocompatible. Therefore, it has prospectus to use in biological systems for diagnose metabolism and also for curative action in case of diseases and deficiencies.

References:

1. Materials (Basel). 2021 Feb; 14(3): 549. Published online 2021 Jan 24. doi: 10.3390/ma14030549 PMCID: PMC7866148 PMID: 33498822 The Role of Metal Ions in Biology, Biochemistry and Medicine, Michael Moustakas
2. Copper Catalyzed Synthesis of Heterocyclic Molecules via C–N and C–O Bond Formation under Microwaves: A Mini-Review Sushovan Jena and Kaushik Chanda
3. Toxicity of metal and metal oxide nanoparticles: a review, Ayşe Busra Sengul & Eylem Asmatulu Environmental Chemistry Letters volume 18, pages1659–1683 (2020)
4. Metal oxide nanoparticles and their applications in nanotechnology Murthy S. Chavali, Maria P. Nikolova Springer Nature Switzerland AG 2019
5. Colloidal synthesis of metal oxide nanocrystals and thin films Fredrik Söderlind, Linköping Studies in Science and Technology Dissertation No. 1182.
6. Colloidal Metal Oxide Nanoparticles Synthesis, Characterization and Applications, Metal Oxides, 8 - Colloidal metal oxides in energy technologies, Sungwook Chung 2020, Pages 183-201
7. Polymer-Metal Oxide Composite (PPy–MoO₃) for Ammonia and Ethanol Gas Sensor, Surendra M. Yenorkar, Ramesh N. Zade, Bhupesh M. Mude, Vijay M. Mayekar, Kushal M. Mude, Kishor B. Raulkar, Ranjeet R. Mistry, A.N. Patange, Macromolecular Symposia Volume 400, Issue 1/2100049, 22 December 2021.
8. ASeung Hwan Cho, Ji Young Kim, Jaesung Kwak and Sukbok Chang* Chem. Soc. Rev., 2011, 40, 5068–5083
9. Xiao-FengWua*, Helfried Neumann , Stephan Neumann , Matthias Beller, Tetrahedron Letters 54 (2013) 3040–3042
10. Sachin A. Sarode, Jeevan M. Bhojane, Jayashree M. Nagarkar*, Tetrahedron Letters 56 (2015) 206–210
11. Russell D. Viirre, GhotasEvindar, and Robert A. Batey*, J. Org. Chem. 2008, 73, 3452–3459

Synthesis, Charecterization and Biological Evaluation of Coumarin – Chalcone Derivatives

Disha M. Dhabarde, Punam B. Rathi, Ashish Telrandhe

ashish0telrandhe@gmail.com

Kamla Nehru College of Pharmacy, Butibori, Dist.-Nagpur, 441122

ABSTRACT –

In the present study, an attempt has been made to synthesize and characterize some coumarin-chalcone derivatives and to evaluate them for their anti-microbial activity. The compounds were prepared as per the reported procedure in literature. The physicochemical characteristic like melting point, percentage yield, R_f value were evaluated. The synthesized compounds were characterized by IR, NMR and Mass spectroscopy. Compounds exhibited good antimicrobial activity when compared with standard. Further, there is a large scope for the development of other derivatives and their pharmacological screening. Since, the synthesized scheme is simple and now well established it would be easy to synthesize other derivatives by incorporating various substitutions and screenings them for other pharmacological activities like Antibacterial, antiviral, anti-tumor, anti-hyperglycemic, analgesic, anti-inflammatory, Moreover the newly synthesized Derivatives can be subjected for QSAR analysis and docking to emphasize the Pharmacophoric requirement and to study drug-receptor interaction and binding for specific target.

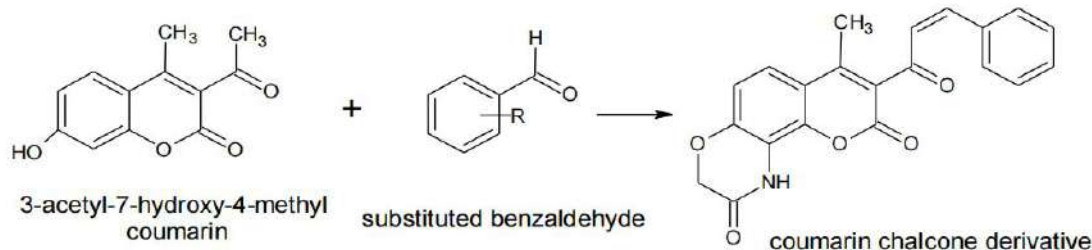
Keywords – Chalcone derivatives, Coumarin, Anti-microbial activity

INTRODUCTION –

Coumarin nucleus is widely distributed in nature in plant kingdom and forms an important class of oxygen heterocycle¹. Over the years, coumarins have been established as well-known naturally occurring oxygen-heterocyclic compounds isolated from various plants². They are the family of lactones containing benzopyrone skeletal framework that have enjoyed isolation from plant as well as total synthesis in the laboratory. The plant extracts containing coumarin-related heterocycles are employed as herbal remedies in traditional systems of medicine. The synthesis of coumarin derivatives has attracted considerable attention of organic and medicinal chemists due to its wide usage in food additives, fragrances, pharmaceuticals and agrochemicals. Given this, coumarins have attracted intense interest in recent years because of their diverse pharmacological properties. Hence, many researchers have reported different biological activities of coumarins derivatives such as antibacterial, antiviral, antitumor, anti-hyperglycemic, analgesic, anti-inflammatory activities and other pharmacological activities³⁻¹¹. Chalcones are α,β -unsaturated ketones which constitute an important group of natural products that serve as precursors for the synthesis of various heterocyclic compounds like pyrimidines, imidazoles, pyrazoles, 2- pyrazoline and flavonoids^{12,13}. Cyclization of chalcones, leading to thiazines, pyrimidines, pyrazoline has been a developing field within the realm of heterocyclic chemistry for the past several years because of their ready accessibility and the broad spectrum of biological activity of the products as antimicrobial, antibacterial, antifungal, antiprotozoal, anti-inflammatory substances¹⁴. With this background it has been thought worth to synthesize some novel heterocyclic compounds comprising of chalcone and coumarin in a single moiety. Also, to evaluate these new compounds for their potency as an anti-microbial agent.

MATERIAL AND METHOD

SYNTHESIS OF COUMARIN CHALCONE DERIVATIVES



A mixture of 3-acetyl-7-hydroxy-9H-benzopyrano-1,4-oxazin-2,9-dione and substituted aromatic aldehyde was stirred for 12 hr. under reflux at temperature 60° C to obtain coumarin chalcone. The compounds were characterized by Infra-red, Mass and NMR Spectroscopy. *In-vitro* antimicrobial activities of synthesized compound were studied by pour plate method using ciprofloxacin as standard for antibacterial and ketoconazole as for antifungal activity respectively. The synthesized compounds were evaluated for their antibacterial activity against *Staphylococcus aureus* and *Escheria coli* and antifungal activity against *Aspergillus Niger*. The activity of synthesized compounds showed that synthesized compounds exhibited good antibacterial activity and antifungal activity.

REFERENCES

1. Cintas P. Activated metals in organic synthesis. CRC Press; 2020 Jan 29;7-10
2. Bhat BA, Dhar KL, Puri SC, Saxena AK, Shanmugavel M, Qazi GN. Synthesis and biological evaluation of chalcones and their derived pyrazoles as potential cytotoxic agents. Bioorganic & medicinal chemistry letters. 2005 Jun 15;15(12):3177-80.
3. Monica Kachroo, Synthesis of some new chalcone derivatives and evaluation of their anticancer activity. Int. J. Drug Dev. and Res, (2013); 5(3):309-315.
4. Mokle SS, Sayeed MA, Kothawar and Chopde. Int. J. Chem. So 2004;2(1):96-100
5. Cheng JH, Hung CF, Yang SC, Wang JP, Won SI, Lin CN. Synthesis and cytotoxic, anti-inflammatory, and antioxidant activities of 2, 5% dialkoxychalcones as cancer chemo preventive agents. Bioorganic & medicinal chemistry. 2008 Aug 1;16(15):7270-6
6. Seema I, Habib et al. Chemical and biological potential of chalcone as a source of Drug: A review. LIPPR, (2018); 11(02):104-118.
7. Rajendra Prasad Yejella et al. Synthesis, antimicrobial, and computational evaluation of novel Isobutyl chalcones as antimicrobial agents, UMC, (2017), 1- 14.
8. Sunny Jalhan et al. Various Biological activities of coumarin and Oxadiazole derivatives. Asian J. Pharm Clin Res, (2017); 10(7):38-43
9. Chapter 5 Synthesis of 7-hydroxy-4-methyl coumarin over Zapo-5 and Lewis acid metal ion-exchanged Zapo-5 molecular sieves 79.90.
10. Antimicrobial Merriam-Webster online dictionary. Archived from the original on (2009).
11. Alivelu Samala et al. Synthesis, characterization of some novel coumarin derivatives and evaluation of their Pharmacological activities. Der Pharma chemical, (2016), 8(12):19-24.
12. Kubba et al. Synthesis and characterization of new coumarin derivatives containing various moieties with antibacterial activities. Int. J. Pharm, Pharm sci, (2015); 7(8):70-74.

Synthesis and Characterization of (3-(3,5-dichloro-2-hydroxyphenyl)-5-(pyridin-2-yl) isoxazol -4-yl)(phenyl) methanone with microwave irradiation.

P. S. Nandurkar¹, M. M Rathore²

¹Department of chemistry, Sant Gadge Baba Amravati University, Amravati

²Department of chemistry Vidyabharati Mahavidyalaya Amravati, Amravati

Abstract:

Isoxazoles¹ is an unsaturated aromatic heterocyclic compound containing three carbon one oxygen and one nitrogen in a ring atom. Isoxazole being an azole with an oxygen atom next to the nitrogen exhibits a broad spectrum of biological activity and also forms a part of various biodynamic agents². A mixture of 3-benzoyl-6,8-dichloro-2-(1-phenylprop-1-en-2-yl)-4H-chromen-4-one (VIa) (0.01 M), hydroxylamine hydrochloride irradiated with DMSO in microwave.

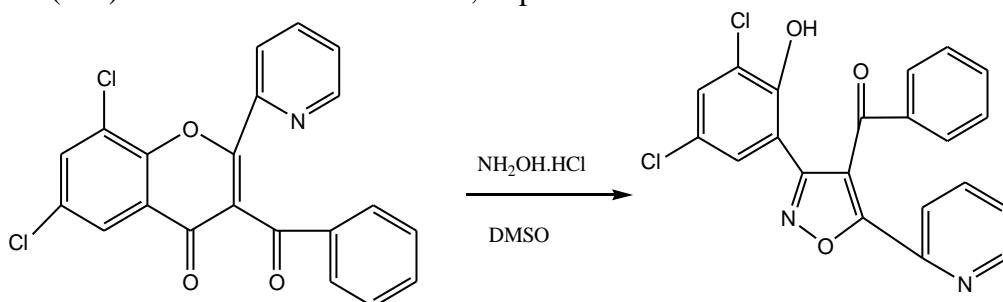
Introduction:

Isoxazole being an azole with an oxygen atom next to the nitrogen exhibits a broad spectrum of biological activity and also forms a part of various biodynamic agents. The substituted isoxazoles are also considered to be important structure due to their versatility toward chemical transformations to useful synthetic intermediates such as 1,3-dicarbonyl, 1,3-iminocarbonyl; and γ -amino alcohols.

The Chlorosubstituted isoxazoles have a wide range of pharmaceutical applications. In most of the skin creams substituted isoxazoles are the main constituents. Various kinds of skin diseases are cured by chlorosubstituted isoxazoles. The healing process of skin specially done by the plant extract found in nature. It is interesting to notice that structure of isoxazole is found in plant extract used for healing process.

Methods of preparation:

A mixture of 3-benzoyl-6,8-dichloro-2-(pyridin-2-yl)-4H-chromen-4-one (VIc) (0.01 mol) and hydroxylamine hydrochloride was irradiated in DMSO (20ml) containing 0.5ml of piperidine for 3 min. 15 sec. in microwave. After cooling the mixture, it was decomposed into the ice and solid product thus obtained crystallized from methanol. The gray coloured crystals of the compound (IXc) were obtained. Yield: 70%, m.p: 191⁰C.



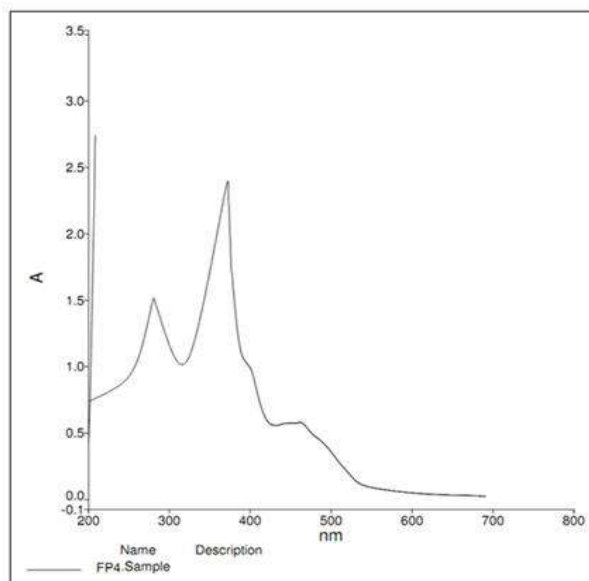
MW, 800 W, time: 3 min. 15 sec., Solvent: DMSO.

Microwave: 3 min. 15 sec, Yield: 70%

Conventional: 1 hour 20 min., Yield: 69%

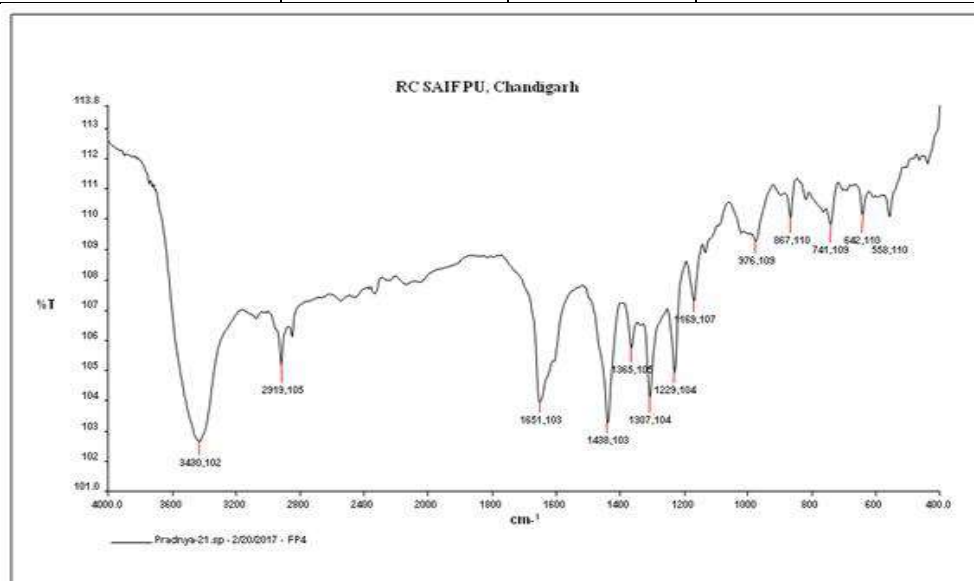
All the synthesized compounds have been characterized on the basis of their chemical properties and spectral data.

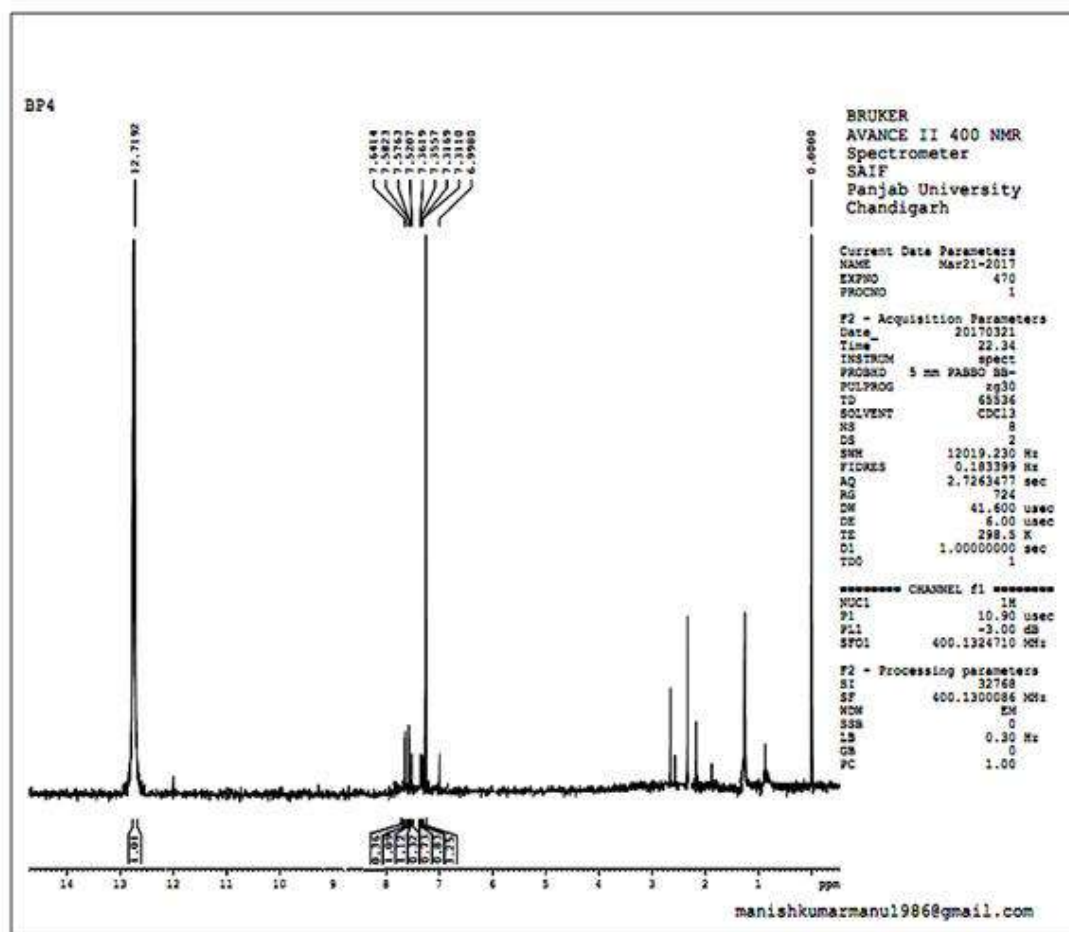
1. The UV-VIS spectrum of the compound **(3-(3,5-dichloro-2-hydroxyphenyl)-5-(pyridin-2-yl) isoxazol -4-yl)(phenyl)methanone** showed λ_{max} value 355 nm respectively corresponding to $n \rightarrow \pi^*$ transition.



2. The IR spectrum (Spectrum No.54) of the compound (Xa) and compound (Xd) (Spectrum No.57) recorded in KBr showed following main absorption bands.

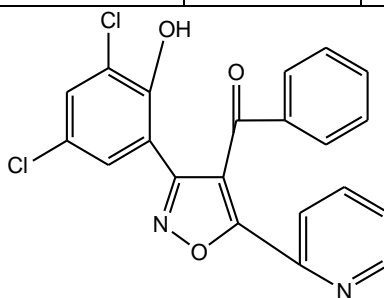
Compound	Frequency (cm^{-1})	Intensity	Correlation
IXd Spectrum No.51	3430	vb	Ar-OH stretch
	2919	vb	Ar C-H stretch
	1651	s	C=O stretch
	1438	s	C=N stretch
	1169	s	C-O stretch
	642	w	C-Cl stretch





- The ^1H PMR spectrum of the compound (II) (Spectrum No.52) recorded in CDCl_3 with TMS as an internal standard. The observed chemical shifts can be correlated as:

Compound (IXd) Spectrum No.52	Chemical shifts δ ppm	Name of peak	No.of protons	Types of protons
	12.71	s	1H	Ar-OH
	6.99 to 7.64	m	9H	Ar-H



(3-(3,5-Dichloro-2-hydroxyphenyl)-5-(pyridin-2-yl)isoxazol-4-yl) (phenyl)methanone

Conclusion and Discussion of the Result

The short reaction time and expanded reaction range were offered by the microwave assisted synthesis. Chlorosubstituted isoxazoles need 6-9 min. exposure to microwaves incomparable to condensation reaction where it takes 2 hours so, it was thought interesting to save time in eco-friendly synthesis of chlorosubstituted isoxazoles.

References:

1. Claisen.; *Ber*, (1891), 24, 3900.
2. Hantzsch; *Ann*, (1888), 130.
3. T. Gilchrist ; *Heterocyclic Chemistry*, (1985), The Bath press.
4. S.Chauhan, Y.Joshi; *Rasayan J. Chem*, (2008), Vol.1, No.3 475-480.
5. V.Mane, D.Mahajan, P. Rajput; *Journal of Medicinal Chemistry and Drug Discovery*, (2017), Issue 03, Vol.02, 590-598.
6. Claisen.; *Ber*, (1891), 24, 3900.
7. Hantzsch; *Ann*, (1888), 130.
8. T. Gilchrist ; *Heterocyclic Chemistry*, (1985), The Bath press.
9. S.Chauhan, Y.Joshi; *Rasayan J. Chem*, (2008), Vol.1, No.3 475-480.
10. V.Mane, D.Mahajan, P. Rajput; *Journal of Medicinal Chemistry and Drug Discovery*, (2017), Issue 03, Vol.02, 590-598.
11. S. Raja, K. Jayaveera, S. Subramanyam, A. S. Reddy and C. Prakash; *IJPSR*, (2016); Vol. 7(6): 2573-2585.
12. P. Kumar, M. Behera, M. Sambaiah, V. Kandula, N. Payili, A. Shree, and S. Yennam; *Hindawi Publishing Corporation Journal of Amino Acids*, (2014) Article ID 721291, 14.
13. M. Maczynski, A. Drynda, B. Obminska-Mrukowicz, S. Ryng; *Immunopharmacology and Immunotoxicology*, 37, (2015), 148-157.
14. J. Shaw, B. Chen, J. Bourgault, H. Jiang, K. Narendra, M. Jayshree, A. Frederick, M. Joe, B. Kevin, P. Halina, E. Matthew and R.Peter; *Am J Biomed Sci.*, (2012), 4(1), 14-25.
15. D. Kashinath, S. Nagaraju, N. Satyanarayana, B. Paplal, A. Vasu, S. Kanvahb; *RSC Adv*, (2015), 5, 81768.
16. N Seelam , S. Shrivastava , S. Prasanthi, S. Gupta; *Journal of Saudi Chemical Society*, (2016), 20, 411–418.
17. E. El-Sawy , A. Mandour, S. Hallouty, K. Shaker, H. Abo-Salem; *Arabian Journal of Chemistry*, (2013), 6,67–78.
18. D. Patel, P. Kumari, N. Patel; *Arabian Journal of Chemistry*, (2017), 10, S3990–S4001.
19. B. Kendre, M. Landge, S. Bhusare; *Arabian Journal of Chemistry*, (2015), doi.org/10.1016/j.arabjc.
20. S. Kobayashi,T. Tanaka,Y. Soeda ,O. Almeid, A.Takashima; *EBioMedicine*, (2017), 20, 120–126.
21. L. Ramdani, O. Talhi, N. Taibi,L. Delort, C. Decombat, A. Silva, K. Bachari,M. vasson, F. caldefie-chezet; *Anticancer research*, (2016), 36: 6399-6408. doi:10.21873/anticancer.11237.
22. L. Bernardes , R. Rosaa, M. Moraesb L. Zimmermanna, E. Paulo, Schenkel, M. Steindel; *European Journal of Medicinal Chemistry*, (2016), doi: 10.1016/j.ejmech.2017.01.029.
23. F. Manetti, A. Santucci, G. Bernardini, D. Braconi, E. Petricci; *J. Med. Chem*, (2017), 60, 4101-4125.
24. R. Hartmann , J. Emmerich, C. Koppen, J. Burkhart,Q. Hu, L. Siebenburger, C. Boerger, C. Scheuer, M. Laschke, M. Menger; *J. Med. Chem*, (2017), 60, 5086-5098.
25. A. Merlo , G. Vilela, T. Fernandes, R. Rosa, S. Kelly, S. Kitney; *Polym. Bull*, (2015). DOI 10.1007/s00289-015-1529-7.

Microbial Examination of Nanoparticle of Tetra-O-acetyl-B-D-Glucosyl-5aryl-4-Dithiobiurets.

Ashish G. Sarap, P.T. Agrawal

Department of Chemistry, Shri R. L. T. College of Science, Akola-444001 (Maharashtra) India

Email: sarap.aashish1@gmail.com, poonamagrawal2575@rediffmail.com

Abstract :-

This discipline focuses on the design, characterization, manufacture, and use of structures, devices, and systems by manipulating form and size at the nanoscale scale. Recent years have seen an increase in the branch of current study known as nanotechnology. Here we screened for their antibacterial and antifungal activities against common pathogens like *Escherichia coli*, *Proteus vulgaris*, *Staphylococcus aureus*, *Pseudomonas aeruginosa*, *Aspergillus niger* and *Penicillium*. Some compounds exhibit less to good activity while some are resistant to the said micro-organisms.

Keywords: TAG Isothiocyanate , Dithiobiurets , Nanoparticles and Antimicrobial Activities.

Introduction :- Carbohydrates are vastly diverse group of organic compounds occurring in all known plants, animal and microbial life. The function of carbohydrate is to provide energy and strength in plants and mammalian tissues they provide a whole variety of specialized functions ranging from cell and organ differentiation to immune protection for new born babies. Antimicrobial agents can be divided into many categories based on how they work and the objectives they serve. Depending on the category of microorganisms impacted, division may be made. Hence, substances that affect bacteria are known as bacteriostatic or bacteriocidal, whereas substances that affect fungus are known as fungistatic or fungicidal¹. The cup plate agar diffusion method²⁻³ provides a simple, convenient reliable test specially applicable in routine clinical bacteriology laboratory.

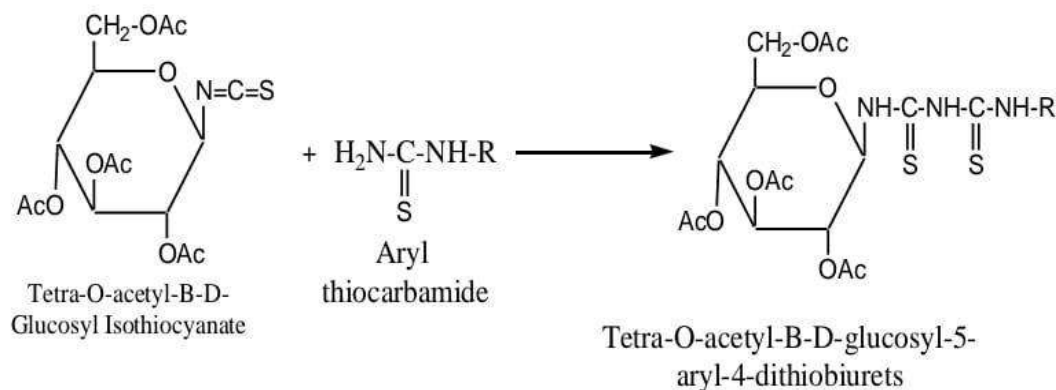
In particular, these substances have been effectively tested against a number of illnesses and have therefore earned medical significance. Chemical substances are used for treatment of diseases and has been known since the 1500's. The chemical substances used for the treatment of infectious diseases and diseases caused by the proliferation of malignant cell are called as chemotherapeutic agents. Antibacterial agents are any chemicals that prevent microorganisms from growing or that kill them. Despite the fact that many different compounds possess these qualities. The phrase is often limited to chemicals that are active at concentrations adequate for practical purposes when it is employed at sufficiently high concentrations.

Carbohydrate represents an important chemical class as many drugs and drug intermediates⁴ are based on carbohydrates chemistry and many drugs such as amino glycoside antibiotics containing carbohydrate structure.

Among all carbohydrates our interest is to synthesized nitrogen linked glucosyl compounds due to its applications in medicinal chemistry and in many other ways⁵⁻⁶. Sugar isocyanate are versatile synthetic intermediate in carbohydrate chemistry. They have attracted considerable interest in synthetic and medicinal chemistry⁷⁻⁸. The glycosides have found use as divertic agent, analgesics, antidiabetic compounds and in many other ways⁹. Methyl β -lactosyl can significantly reduce the formation of tumor colonies in mice¹⁰. To increase its efficiency multivalent β -lactosyl have been synthesized in Roy's group. Heterocyclic derivative of sugars were found to possess anti-tumor and anti-bacterial activity. Besides these and other pharmaceutical applications of glycosyl urecides, they also found to possess applications in paper, textile and food industries

EXPERIMENTAL

The research work presented deals with the study of antimicrobial activities of newly synthesized N-glycosides against pathogenic organisms. Screening of following compounds were carried out against the microbes like *E. coli*, *P. vulgaris*, *S. aureus*, *P. aeruginosa*, *A. niger* and *Penicillium*.



Experiment No. 1:-1-Tetra-O-acetyl- β -D-glucosyl-5-phenyl-4-dithiobiuret. (IIIa)

To a toluene solution of tetra-O-acetyl- β -D-glucosyl isothiocyanate (0.005 M, 1.9g in 20 ml) was added toluene solution of phenyl thiocarbamide (0.005 M, 0.76 g in 10 ml) and reaction mixture was refluxed over boiling water bath for 3hr. Afterwards, solvent was distilled off and sticky mass obtained as residue was triturated several times with petroleum ether afford a white solid. It was crystallized with ethanol-water, m.p. 95°C. [Found: C, 50.30; H, 4.85; N, 7.93; S, 6.19, C₂₂H₂₆O₉N₃S₂. requires; C, 50.38, H, 4.96; N, 8.01, S, 6.10%].

The product was found soluble in ethanol, acetone, chloroform and benzene while insoluble in water and petroleum ether. It charred on heating with conc. sulphuric acid. It was found desulphurisable when boiled with alkaline plumbite solution. It was optically active and its specific rotation was found to be $[\alpha]_D^{32} = -136.94^\circ$ (c, 0.74 in chloroform). The purity of the product was checked by TLC, R_f value 0.69 (CCl₄: EtOAc, 3:2)..

RESULTS AND DISCUSSION:-

The synthesis of N-glycosyl Dithiobiurets is a simple and reliable route. This strategy can be successfully applied to prepare a wide range of glycosyl Dithiobiurets and their derivatives which can be widely used for the preparation of biologically active molecules and good active lead in Medicinal Chemistry. Thus the synthesized novel N-glycosyl Dithiobiurets exhibits antibacterial and antifungal activities against the organisms tested. The method adopted in the synthesis and investigation is simple, efficient and inexpensive in synthesizing pharmacologically important molecule.

Antimicrobial Activity :- These newly synthesized thiocarbamides were screened for their microbial activity against different pathogenic microbes for their antibacterial and antifungal activities using well method¹⁶. The compounds were screened for antibacterial activity against *E. coli*, *P. vulgaris*, *S. aureus*, *P. aeruginosa*, *A. niger* and *Penicillium*. in potato dextrose agar medium. Procedure for antimicrobial screening Media used (Nutrient broth): Peptone – 10 g, NaCl – 10 g and yeast extract 5 g, Agar 20 g in 1000 ml of distilled water. Initially, the stock culture of bacteria were revived by inoculating in broth media and grown at 37 °C for 18 h. The agar plates of the above media were prepared and wells were made in the plate. Each plate was inoculated with 18 h old culture (100 μ L, 10⁴ cfu) and spread evenly on the plate. After 20 min. the wells were filled with different concentrations of samples. The control wells were

filled with Gentamycin. All the plates were incubated at 37 OC for 24 h and the diameter of inhibition zones were noted in mm. The activity was quantitatively assessed on the basis of inhibition zone

Table 1 : Antimicrobial activities of 1-Tetra-O-acetyl- β -D-glucosyl-5-aryl -4 dithiobiurets (I a-g)

Compounds	<i>E.coli</i>	<i>P.vulgaris</i>	<i>S.aureus</i>	<i>P.aeruginosa</i>	<i>A.niger</i>	<i>Penicillium</i>
I-a	+++	+++++	+++	++++	++++	++
I-b	+++	+++	+++	++++	++	+++
I-c	++	++	+++	++++	++	++++
I-d	++	++++	+++	++++	+++	+++
I-e	++	++++	++	++++	+++	++
I-f	--	+++	++++	++	+++	++++
I-g	+++	+++	+++	++++	+++	++

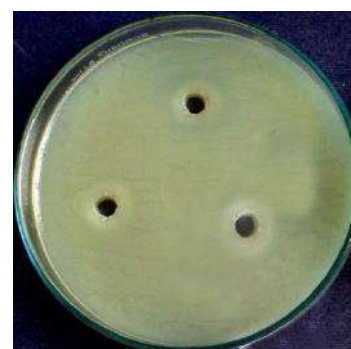
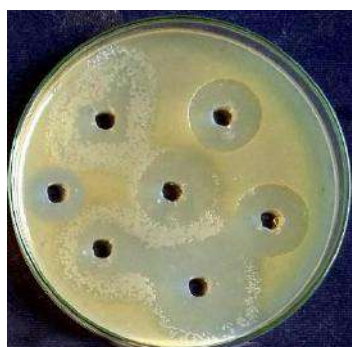
N.B. : ++++ Strongly active (above 20 mm)

+++ Moderately active (15 mm to 20 mm)

++ Weakly active (8 mm – 14 mm)

-- Inactive (below 8 mm)

Bore size = 7 mm



The compounds 1-tetra-*O*-acetyl- β -D-glucosyl-5-aryl-4-dithiobiurets (I-7) showed comparable activity. Compounds 1,2,3 showed strong activity against *P.vulgaris* and *S.aureus* *Penicillium*. Compounds 1-7 showed moderate activity against used microorganisms.

CONCLUSION

Derivatives were synthesized and characterized for their structure elucidation. Various chemical and spectral data supported the structures. Some of the compounds synthesized showed promising antimicrobial activities. The newly synthesized thiocarbamides and thiocarbamates exhibits comparable antibacterial and antifungal activities against the organisms tested. The method adopted in this investigation is simple, efficient and inexpensive and is useful in synthesizing pharmacologically important molecules. The method adopted in the synthesis and investigation is simple, efficient and inexpensive in synthesizing pharmacologically important molecules.

Acknowledgement

Authors are thankful to PDKV Akola for providing the spectral data and also to DR. V. D. Nanoty Principal, Shri R. L. T. College of Science, Akola for providing necessary facilities

Reference :

- [1] **I. Goodman.**;Carbohydrate-urea-phenol-based adhesives: Transient formation of mono- and di-D-glucosylureaAdv. Carbohydr. Chem.,1958 **13**, 215-236
- [2] L.T. Shih, M-C, Cheng, S-H, Wu.,Tetrahedronlett., 2002 **44**, 7921-7923
- [3] Y. Mishikawa, T. Terkeda, S.Shibata, F.Fukuoka., Bull. Chem. Pharma, 1969., **17**, 1910-1916
- [4] A.V. Berenguel, F.O. Caballero, F.Santoya-Gonzalez, J.J.Gracia-Lopez, J.J.Gimenez-Martinez, L.Gracia-fuentes, E.O. Salmeron., J. Eur. Chem., 2002., **8**, 812-827
- [5] Gunawardana, G.P.; Kohmoto, S.; Gunasekera, S.P.; McConnel, O.J.; Koehn, F.E. Dercitine, a new biologically active acridine alkaloid from a deep water marine sponge, *Dercitus* sp. J. Am. Chem. **1988**, *110*, 4856–4858.
- [6] Noel, S.; Cadet, S.; Gras, E.; Hureau, C. The benzazole scaffold: A SWAT to combat Alzheimer's disease. Chem. Soc. Rev. **2013**, *42*, 7747–7762.
- [7] Prajapati, N.P.; Vekariya, R.H.; Borad, M.A.; Patel, H.D. Recent advances in the synthesis of 2- substituted benzothiazoles: A review. RSC Adv. **2014**, *4*, 60176–60208.
- [8] Kok, S.H.L.; Gambari, R.; Chui, C.H.; Yuen, M.C.W.; Lin, E.; Wong, R.S.M.; Lau, F.Y.; Cheng, G.Y.M.; Lam, W.S.; Chan, S.H.; et al. Synthesis and anti-cancer activity of benzothiazole containing phthalimide on human carcinoma cell lines. Bioorg. Med. Chem. **2008**, *16*, 3626–3631.
- [9] Heo, Y.; Song, Y.S.; Kim, B.T.; Heo, J.N. A highly regioselective synthesis of 2-aryl-6- chlorobenzothiazoles employing microwave-promoted Suzuki–Miyaura coupling reaction. Tetrahedron. Lett. **2006**, *47*, 3091–3094.
- [10] Alaimo, R.J.; Pelosi, S.S.; Freedman, R. Synthesis and Antibacterial Evaluation of 2-(Substituted Phenylureido)-4-thiocyanatobenzothiazoles. J. Pharm. Sci. **1978**, *67*, 281–282.

Synthesized PANI/Cu-NPs / Aloe-Vera thin films Biocomposites for ammine gas sensor stimulator.

Dr. D. B. Dupare@ *

1* @ Department of Chemistry, Shri R.G. Rathod Arts and Science College, Murtizapur, Di.Akola.

Abstract:

The synthesized polyaniline disperse Copper Nano particle (Cu-NPs) by the usage of ultrasonicator, microwave instrumentation approach to metal salt on Aloe Vera Leaf Extract thin film on glass substrate through chemically oxidative polymerization approach. The copper chloride metallic salt disperse Nano particle (Cu-NPs) Stabilized on Aloe Vera Leaf Extract. The secondary phytochemical of Aleovera leaf plant extract polyphenols stabilizing and capping system for the more balance the copper metallic chlorides. We synthesized PANI-Cu-NPs. Aloe Vera leaf extract studied their U.V., FTIR, XRD and Electronic Microscopy, Characterization for electrochemical behavior and current -voltage characteristics. The four -probe instrumentation system shows that the PANI-Cu-NPs modified electrode turned into accurate conductivity and stability on glass substrate. The thin film of PANI-Cu-NPs discovered gas sensing conduct for 10-50 ppm ammine gas sensor

Key word: Polyaniline, I-R Characterization, Thin film, PANI-Cu-NPs and Biocomposites

Introduction:

The biomaterial sciences include systematic study of engineering materials with various application purposes. A biomaterial is an engineering material which is specific range of properties like to evaluate the chemical, physical, mechanical and biological properties. Due to this synthetic polymer can be merged with biomaterial including metals, ceramics, composites and hybrid systems (1-2). The last three decay the numerous scientific efforts and publication reported related to biomaterial. The biomaterial science is a multidisciplinary area in science and technology included medicinal chemistry such as inert material gold, silver, and platinum, used in the early designed bone fracture plates like acrylic methyl methacrylate polymer or commercialized polymers such as Dacron used in the vascular implants and the heart valves (3-4).

Polyaniline exhibits excellent characteristic such as good electrical conductivity also environmental stability and an easy synthetic route. The synthetic biocompatible polymers show great physicochemical properties. The polymers PANI are the most commonly investigated IEPs because of several feature like good thermal stability, cost effectiveness of the used aniline less expensive monomer, simple synthetic procedure and good conductivity(5). PANI included metal salt materials have widespread application in the electronics, sensor, smart material batteries optical devices and biomaterial (6).

In this paper we reported the synthesis PANI-Cu-NPs -Aloe Vera hybrids thin film composites on glass substrate via simple chemical oxidative polymerization technique by using ultra sonicator. The Cu-NPs are first synthesized through the reduction of copper chlorides salts with Aloe -Vera leaf extracts of polyphenol. It is believed that these polyols can play a vital role as stabilizers/capping agents in the production of the Cu-NPs nanoparticles. The Novelty of this works is that plant extract polyols as well as flavonoids are used to stabilize the Copper particle in formation of thin films on glass substrate that is biomaterial or composites is synthesized and their utility for electrochemical characterizations in different application as sensor.

2. Materials and Methods

2.1 Materials and chemical

Aniline and Ammonium oxysulphides from Sd -Fine chemical are used. Aniline distilled prior to use. The copper (II) chloride hexahydrate ($\text{CuCl}_2 \cdot 5\text{H}_2\text{O}$, >98%) was from Sd-Fine chemicals. Aloe-Vera was bought from a local college medicinal garden. Double Distilled deionized water (DDW) was from the analytical laboratory, Chemistry Department, was used for all aqueous preparations.

2.2 Extraction of Aloe-Vera gel and Cu -NPs synthesis

We are collected the fresh leaves of Aloe-Vera was bought from our college medicinal garden and remove the hard green coat from leaf by using knife, the after near about 10 g semi liquid parts gel and 10 ml of double distilled water are mixed in 100ml beaker by using ultra sonicator for 20 minutes. The resultant supernatant was collected, filtered and stored at 10 °C before use. The CuNPs were prepared by adding 0.1 M to 0.01M Copper chloride solution to the Aloe-Vera extract (supernatant at ambient temperature) in a series of 1:1,1:2,1:3,1:4,1:5 and also 5:1,4:1,3:1, 2:1 volume ratio. The mixture was hand shaken for 1 min and allowed to stand at room temperature for 30 minutes in ultra sonicator at 40 to 70 °C to prepare the nanoparticles. The all beaker kept in refrigerator for 24 hour at 10°C.

2.1 Synthesis of PANI-Cu NPs of Aloe-Vera films.

The optimize stoichiometric concentration of 2ml aniline and 0.05, upto 0.1 M Concentration of Cu-NPs of Aloe-Vera extract solution added to in series of 100 ml beaker with glass substrate to oxidized with 0.5 M ammonium peroxodisulphate under continuous stirring at room temperature in hydrochloric acid solution and kept in ultrasonicator for 20 minutes then cool it below -10 °C freezers for 24 hours to obtained homogenous stable thin film formation. The thin films substrates wash with deionized water kept to dry at room temperature with drier. The Figure shown in Fig 1.1 is that Synthesis of PANI-CuNPs of Aloe-Vera films after oxidation the formation Biocomposites films of PANI-CuNPs and Fig 1.2 indicates the formation of thin films of PANI--CuNPs on Glass substrate.

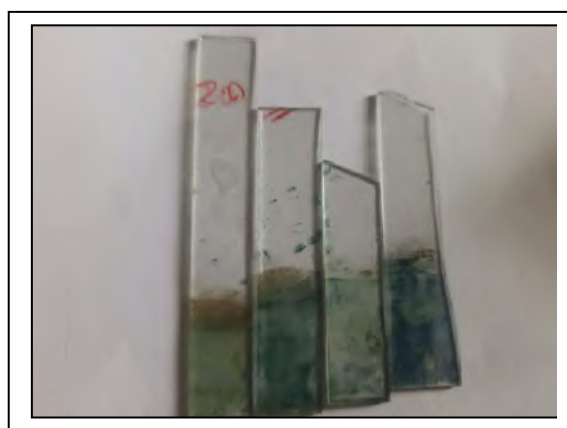


Fig 1.1 PANI-CuNPs of Aloe-Vera after oxidation Fig 1.2 thin films of PANI-CuNPs

2.2 Characterization Technique of the PANI-CuNPs

The Synthesized biocomposites of PANI-CuNPs dissolved in DMSO solvent to observe U.V.-Visible spectroscopy was recorded on UV- VIS Spectrophotometer Carry Agilent Tech at central instrumentation cell, Department of chemistry SGBAU, Amravati for formation of biocomposites and electronic transition is present to this biomaterial to show the electrochemical behaviors. The same composites solvent observed FTIR spectra were recorded on Bunker Alpha-T FT IR Spectrometer at central instrumentation cell, Department of chemistry SGBAU, Amravati for identification of functional group present and this functional group have vibration and rotation stretching of molecules. The XRD Spectra of dry powder observed by powder XRD spectroscopy for find the copper metal present in this biocomposites formation of biomaterials of Aleovera plants and metal dopant is this biocomposites. The application point if we need morphology of biocomposites is necessary this morphology observed by using High electron density microscopy by Department of Botany with in same institutes. The ectro-chemical behavior, Current –Voltage characteristics, and ammine gas sensing behavior were observed by four probe technique in Department of Physics BAMU university.

3. Results and Discussion.

3.1 Electron microscopy of PANI-CuNPs film.

To the view of application, we observed the morphology and structure of film for gas sensing application as well as I-V chaterization and other advance application like electronic device like ploy membrane, biomaterial, battery electrode or capacitor we need the uniform formation of films having their particular appearance of like tubular, granular or some Nano size metal slat occurrence of film observed.

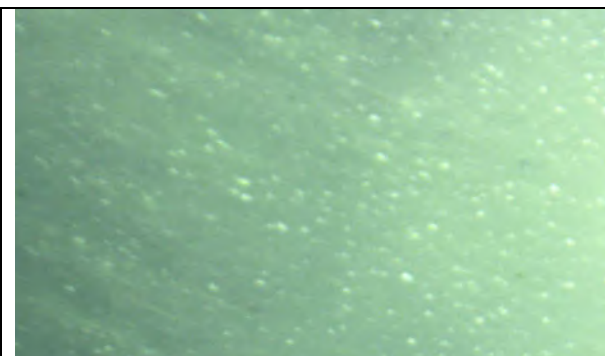


Fig 3.1 Electron microscopy of PANI

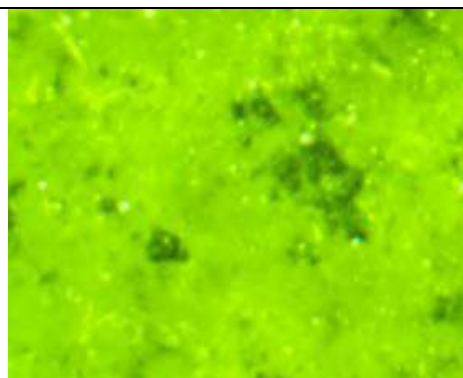


Fig 3.2 Electron microscopy of PANI-CuNPs

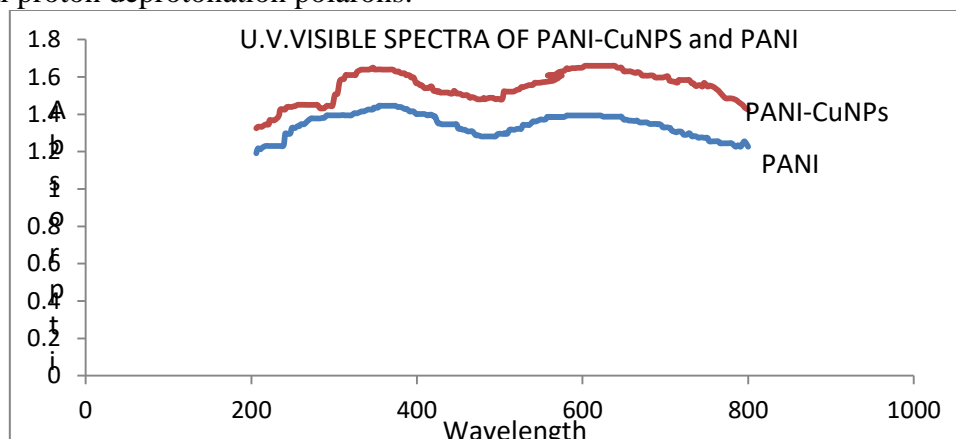
In Fig 3.1 observed that the Electron microscopy image of polyaniline films on glass substrate is uniform, having porous in morphology which applicable in chemical gas sensing as well as electrochemically behavior nature can be applicable for battery storage application as well as chemical and biological sensor. In Fig 3.2 observed that the Electron microscopy image of PANI-CuNPs Biocomposites of Aleovera plant which is uniform, porous dark green in colouration, the film having some dark globular spot confirm the presence of copper metal in granule morphology which have active role in gas sensor application. These two images confirm that there is formation PANI-CuNPs Biocomposites.

3.2 U.V Spectra of PANI-CuNPs film.

The U.V.-Visible spectroscopy was studied in range between 200nm to 700nm after dissolution of PANI and PANI/Cu-NPs / Aloe-Vera thin films in DMSO solvents. The spectrum shows a prominent peak at absorption maxima of 330 nm which has been assigned to the $\pi \rightarrow \pi^*$

transitions of the Aloe-Vera polyols. A broad peak extending from 310-390 nm with absorption maxima at 330 nm was seen.

The new peak formed was slightly shifted bathochromically compared to the 282 nm peak of the Aloe-Vera extracts. This peak at 282 nm and the smaller hub at around 330 nm have been shown to be due to the presence of the Cu-NPs nanoparticles in the Cu (II) state. It means the reductant polyols within the matrices successfully reduced the Cu (II) ions to indicating the formation of the Cu-NPs polyols hybrid. The PANI/ Cu-NPs / Aloe-Vera films composite films have conducting in nature it observed band at 560 nm to 690nm due to presence of conducting polaron of protonated ring of polyaniline. The PANI-Cu-NPs show in U.V. spectra it more intensive peak or activated to $n \rightarrow \pi^*$ at 684 nm to delocalization of lone pair of electron with Cu-metal proton deprotonation polarons.



In Fig 3.2 U.V Visible spectra of PANI-CuNPs

3.3 FTIR Spectra of PANI-CuNPs film.

FT-IR spectra of PANI-CuNPs exhibited the characteristic absorption bands of emeraldine salt at 1518 and 1616 cm^{-1} , which correspond to the C-C stretching vibration of benzenoid (N-B-N) and quinonoid (N=Q=N) ring, respectively [7]. The peaks in the range of $1300\text{--}1400\text{ cm}^{-1}$ as arise from C-N stretching vibrations of the secondary aromatic amines, while the intense absorption peak at 1193 cm^{-1} is associated to the B-NH-B and protonated $Q=NH^+-B$ stretching modes of PANI chains [8].

Figure 3.3 of the hybrid PANI/Cu-NPs/Aloe-Vera bio composite materials indicated a considerable red shift ($\sim 15\text{--}20\text{ cm}^{-1}$) of the N-B-N and N=Q=N vibrational bands at ~ 1501 and $\sim 1600\text{ cm}^{-1}$ respectively, suggesting interaction of PANI chains with anionic heteropolyacids. The IR spectra of the hybrid samples indicate the presence of Cu-Od (terminal bonds) and Cu-Ob-Cu (bridge bonds between the corner-sharing CuCl octahedra; M = Cu) stretching vibrations at $\sim 972\text{--}988$ and $\sim 879\text{--}890\text{ cm}^{-1}$ respectively [9]. The intense absorption bands at ~ 1140 and $\sim 1080\text{ cm}^{-1}$ observed in the samples of Cu-Nps-Aleovera and PANI-Cu-Nps-Aleovera are ascribed to the clusters, respectively. The aromatic C-N and O-H stretching occurs at 3550 cm^{-1} presence of aromatic Ar-OH and Ar-NH that alkolides and amino nature of fictional groups. The C-O, C-N Stretching at 1774 cm^{-1} and 1914 cm^{-1} . The various secondary metabolites all confirm by the presence of their functionality stretching and bending occurs in this FTIR spectra of PANI-Cu-Nps.

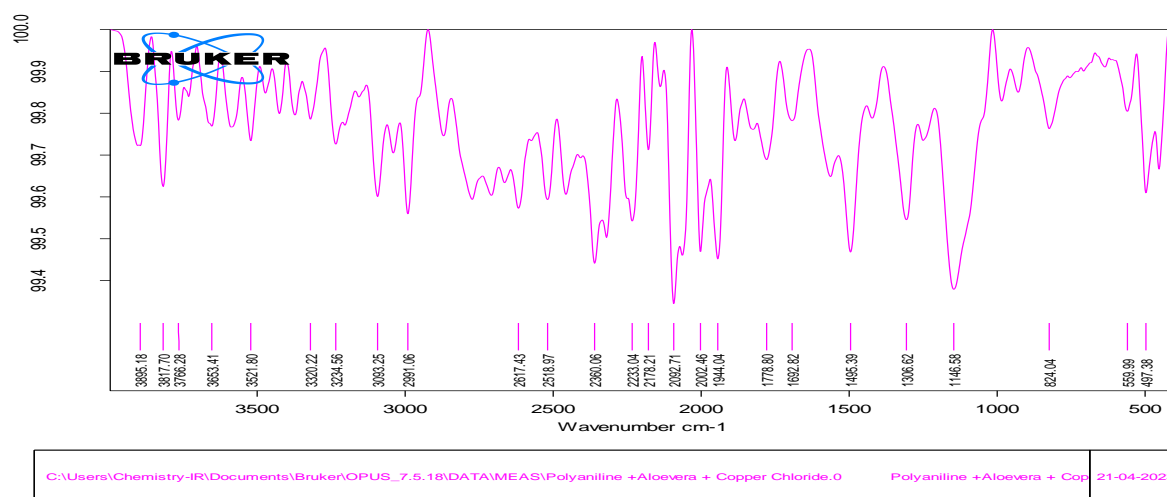
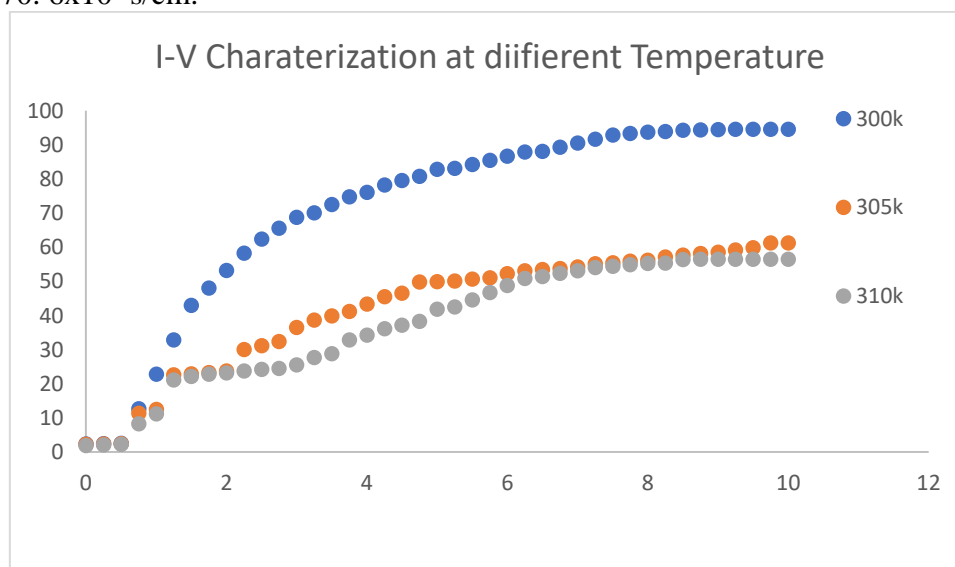


Figure 3.3 of the PANI/Cu-NPs / Aloe-Vera bio composite

3.4.I -V characterization of PANI-CuNPs film.

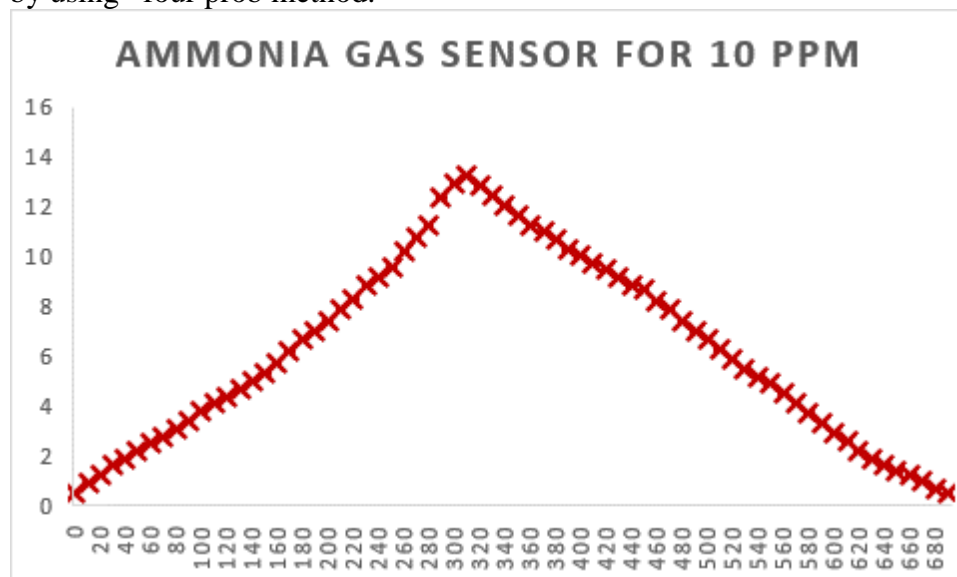
The I-V characterization measurement of the PANI /Cu-NPs /Aloe-Vera films was recorded by an indigenously developed computer controlled using four- probe method at room temperature. The current–voltage (I-V) characteristics of the synthesized PANI /Cu-NPs thin film was studied to ensure a ohmic or non ohmic behavior of the film. A linear and non linear relationship of the I-V characteristics shown in Fig.3.4. reveals that the PANI /Cu-NPs composites film has at 300k ,305 k and 310k of different temperature for applied the voltage at 0.5 to 10 voltages applied then for 300k it observed that initial from 0.5 ev potential to 3.5 it shown liner ohmic charter but to increase in voltage from 3.5 to 7ev voltage it shown bent or deflected in nature a then from 7 ev it stabilized and steady in nature appearance. The same film at 305k near about same behavior but 310k it disappears the linearity its non linear in nature. The average conductivity at 300k to applied the potential it shown in between $2.6 \times 10^{-5} \text{ s/cm}$ to $70.6 \times 10^{-5} \text{ s/cm}$.



3.5. Ammine gas for 10 -50ppm sensitivity PANI-CuNPs film.

The synthesized having good morphology film of PANI-CuNPs film observed ammine gas sensing conduction for low 10 ppm to change 50ppm hinger level. the films expose to 10 minutes for passing the ammine gas and observe the change in resistivity recorded by using computer control four probe system and to observer the recovery period the again expose to higher 50ppm ppm level. Due to present of Cu NPs biomaterial, it has recover and response are good because the film have conducive as well as uniform and porous in condition it

applicable to gas sensing behavior it can again expose to Carbon monoxide gas but it dangerous to handle at our laboratory to take care safety purpose. Fig 3.5 observed that the ammonia gas exposure for 10ppm level. 10 ppm ammonia gas exposed to gas sensor chamber for 5 minute (300 second) and observed the change in resistivity of film, which is continuously increasing but the for recovery of this gas the chamber is open and observed the change in resistivity it required 6.5 minutes (690 second) the recovery time is more as compared to response time by using four probe method.



Conclusion:

This paper deal with study of PANI /Cu-NPs / films biomaterial composite. The characterization techniques such as U.V, FTIR and EM analysis confirmed that Copper chloride metal salt with Aloe Vera were successfully dispersed into the PANI matrix. Effect of different concentration of copper with Aloe vera on structural, electrical and properties of PANI /Cu-NPs Biocomposites were studied. FTIR analysis showed good intermolecular interaction between PANI Cu-NPs / Aloe-Vera matrix. The surface morphology of PANI /Cu-NPs examined using EM analysis which is applicable for 10 ppm ammonia gas sensing behavior. The I-V Characterization at highest conductivity with a value of $2.6 \times 10^{-5} \text{Scm}^{-1}$, observed electrochemical behavior which is linear and nonlinear behavior.

References

1. George Soupions, Pantelitsa Georgiou and Loukas Zoumpoulakis "Polymer Composite Materials Fiber-Reinforced for the Reinforcement/Repair of Concrete Structures"Polymers 2020, 12(9), 2058 pp 1-14; <https://doi.org/10.3390/polym12092058>.
2. L S faeq "Thermal and Mechanical Properties of Polymer/Nickel Composites" 3rd International Conference on Sustainable Engineering Techniques (ICSET 2020) IOP Conf. Series: Materials Science and Engineering 881 (2020) 012092 IOP Publishing pp 1-8 [doi:10.1088/1757-899X/881/1/012092](https://doi.org/10.1088/1757-899X/881/1/012092).
3. Ewelina Mackiewicz, Tomasz Wejrzanowski , Bogusława Adamczyk-Cieślak and Graeme J. Oliver "Polymer–Nickel Composite Filaments for 3D Printing of Open Porous Materials"Materials 2022, 15(4), 1360 pp 1-15; <https://doi.org/10.3390/ma15041360>.
4. Hind Ahmed, Bahaa H. Rabee, Hussein Hakim, Ahmed Hashim and Saba R. Salman "Preparation and Study of Optical Properties of (Polymer-Nickel Nitrate) Composite"Advances in Physics Theories and Applications ,ISSN 2225-0638,Vol.20, 2013 pp 152-157.

5. R. K. Goyal, R. Sulakhe "Study on poly(vinylidene fluoride)/nickel composites with low percolation" *Adv. Mater. Lett.* 2015, 6(4), 309-317 DOI: 10.5185/amlett.2015.5627.
6. M. Lahelin a, I. Aaltio b, O. Heczko b, O. Söderberg b, Y. Ge b, B. Löfgren a, S.-P. Hannula b, J. Seppälä a "DMA testing of Ni–Mn–Ga/polymer composites" *Composites Part A: Applied Science and Manufacturing* publishes Volume 40, Issue 2, February 2009, Pages 125-129 <https://doi.org/10.1016/j.compositesa.2008.10.011>.
7. Hafiza Vaneeza Hussain, Mateeb Ahmad, Muhammad Tamoor Ansari, Ghulam M. Mustafa, Saira Ishaq, Shahzad Naseem, Ghulam Murtaza, Farah Kanwal and Shahid Atiq "Polymer based nickel ferrite as dielectric composite for energy storage applications" *Synthetic Metals*, Volume 268, October 2020, 116507 <https://doi.org/10.1016/j.synthmet.2020>.
8. Mohd Mohsin Nizam Ansari, Shakeel Khan and Naseem Ahmad "A comprehensive investigation of structural, thermal and electrical properties of $T_{0.35}Zn_{0.55}Cu_{0.1}Fe_2O_4$ (T = Mn, Ni) nano ferrites" *Physica B: Condensed Matter*, Volume 566, 1 August 2019, Pages 86-95. <https://doi.org/10.1016/j.physb.2019.05.003>.
9. A. Suhasinia and K. P. Vinod Kumar "Solubility and swelling studies of polymer hybrid-nickel oxide nanocomposite" *J. Indian Chem. Soc.*, Vol. 96, January 2019, pp. 7-8
10. Wangping Wu, Dingkai Xie, Jiaqi Huang, Qinqin Wang and Junjun Huang "Adhesion enhancement for nickel layer deposited on carbon fiber reinforced polymer (CFRP) composites by pretreatment processes for lightning strike" <https://doi.org/10.1080/00218464.2022.2082870>.

Structural and Ion-Exchange Properties of Copolymer Derived from 4, 4'-Biphenol - Benzidine - Formaldehyde

P. P. Kalbende^{1*}, M. S. Dhore², S. S. Butoliya³

^{1*}Department of Chemistry, Jagadamba Mahavidyalaya, Achalpur-444806, Dist.-Amravati, (MS) India.

E-mail:- pawankalbende@gmail.com

²Department of Chemistry, G. H. Rasoni University, Amravati-444701, (MS) India

³Department of Chemistry, Shri Ramdeobaba College of Engineering & Management, Nagpur-440 013, (MS) India

Abstract

A new copolymer resin has been synthesized by condensation polymerization reaction of 4,4'-Biphenol and Benzidine with Formaldehyde in presence of 2M hydrochloric acid as catalyst. Composition of resin was determined on the basis of their elemental analysis and further characterized by UV-Visible, Infra-red and Nuclear magnetic resonance spectroscopy to confine the most probable structure of synthesized copolymer.

Newly synthesized copolymer was proved to be a selective chelating ion-exchanger for certain metal ions and were studied for Fe^{3+} , Cu^{2+} , Ni^{2+} , Co^{2+} , Zn^{2+} , Cd^{2+} , Hg^{2+} and Pb^{2+} ions using their metal nitrate solutions. A batch equilibrium method was employed to study the selectivity of metal ions uptake involving the measurements of the distribution of a given metal ion between the copolymer sample and a solution containing the metal ion. The study was carried out over a wide pH range, shaking time and in media of different electrolytes at different ionic strengths. Distribution ratios of metal ions were found to be increased by rising pH of the solutions. Hence, it can be used to recover certain metal ions from waste water, for the purpose of purification of water and removal of iron from boiler water.

Key words Copolymers, Ion-exchangers, Distribution ratio, Metal ion uptake, Distribution ratio.

1. Introduction

Ion exchangers are often employed in chromatographic separation of cation mixture by using complexing agents to increase the efficiency of separation. Process of ion exchange between liquid and solid phase in which the complex equilibria are involved, includes conventional cation exchanger resin containing sulphonate or carboxylate group, is used which do not form the complexes with the cations present and the complexing agent is present as a solute in liquid phase. Chelating resins having a functional group as a complexing agent fixed to the matrix is used when either the liquid phase may or may not contain a complexing agent as a solute, permits the solution of some difficult analytical problems like separation of similar ions and the enrichment of trace elements in a simpler and far less tedious manner than the methods applied so far. This challenge has encouraged the numerous attempts by analytical chemists for synthesizing new chelating ion exchanger with definite selectivity towards certain ions or group of ions.

The introduction of ion exchange terpolymer resins offered new possibilities for the separation of species, and the application of various complexing agents has lead to much extremely effective separation procedure. In an analytical as well as synthetic inorganic chemistry, there exist a need for good chelating polymers that combines the ease of operation of conventional ion exchangers and selectivity of organic analytical reagents. The selectivity of most of the reagents for metals remains predominantly in their ability to form the complexes

with certain cations. Attempts have been made in the early fifties of the twentieth century to synthesize organic polymers which contain complex forming groups as exchanging functions. The selective behavior of these resins is based on the different stabilities of the metal complexes on the resin at appropriate pH values. The optimum conditions for maximum efficiency for given separation can be established by variation of the pH with time interval.

Selective removal, separation and recovery of metals from industrial effluents is a problem of environmental and economic concern, in consideration of the more stringent limits enforced for pollutants control and raising costs of raw materials. Ion exchange as a conservative technology allows for selective removal and recovery of heavy metals. Chelating ion exchangers are suitable for this purpose in presence of one or more donor atoms as Lewis bases which are able to coordinate most of the toxic polyvalent metal ions acting as Lewis acids. Accordingly, the selectivity scale of different chelating exchangers toward metals reflects the stability of the corresponding metal-ligand complexes in the liquid phase.

Toxic and heavy metal ions, traces of organic and inorganic contaminants, radioactive nuclides are widely occurred in aquatic systems as a result of rapid globalization and industrialization. Sorption processes such as electrodeposition, coprecipitation, solid liquid extraction, activated charcoal etc. have been used for the removal of these contaminants. In recent years, terpolymer ion-exchange resins have been developed due to their wide application in waste water treatment and pollution control, hydrometallurgy, antibiotic purification and separation of radioisotopes, identification of specific metal ion and metal recovery [1-4]. A batch equilibrium method has gained a rapid attention of researchers because of its acute degree of selectivity, variety of sorbent phases and enhanced hydrophilicity [5]. Some publications on the synthesis, characterization and applications of chelating ion exchange resins from other researchers [6-18] and from our research group on some terpolymer resins have been reported [19-23].

Lutfor et al [6] have prepared a chelating ion-exchange resin containing amidoxime functional group, was characterized by FT-IR spectra, TG and DSC analysis and the chelating behavior was studied with Cu^{2+} , Zn^{2+} , Ni^{2+} , Cd^{2+} and Pb^{2+} metal ions. Removal of transition metals from dilute aqueous solution by carboxylic acid group containing absorbent polymers has been studied by Liu Z S and Rempel G L [12].

Extensive literature is available to interpret the experimental results in the light of practical applicability of various terpolymer resins. Ion exchange properties of terpolymer resins derived from *o*-nitrophenol and thiourea with paraformaldehyde by A. Burkanudeen et al [7]; and salicylic acid, melamine and formaldehyde by Gurnule et al [8] have been studied. The terpolymer derived from 2,4-dichlorophenyl acrylate/8-quinolinyl methacrylate and acrylic terpolymer derived from 8-quinolinyl methacrylate were found to be a good cation exchanger as it has pendant ester-bound quinolinyl group [9, 10]. Terpolymers derived from salicylic acid and formaldehyde with resorcinol [11], 2,4-dihydroxybenzoic acid-urea-formaldehyde [13], salicylic acid-biuret-formaldehyde [14], 8-hydroxyquinoline, guanidine and formaldehyde [15], anthranilic acid-resorcinol-formaldehyde [16], 4-hydroxyacetophenone -biuret-formaldehyde [17] have been proved to be good ion exchangers. A detailed study on preparation and characterization of a new class of polymeric ligand exchangers for selective removal of trace contaminants from water has been reported by Henry and coworkers [18].

For chelating resin, however, reported in the publications with respect to the desired requirement is seldom presented. But only occasionally, it proved to be valuable for separation on laboratory scale. In this context, as reported earlier [19-23], the present study has been carried out on synthesis, characterization, selectivity and ion exchange capacity of copolymer resin (4,4'-BP-BD-F) derived from 4,4'-Biphenol (4,4'-BP) and Benzidine (BD) with Formaldehyde (F).

2. Experimental

2.1 Materials

The chemicals, 4,4'-biphenol and benzidine from Acros Chemicals, Belgium and formaldehyde (37%) from S. D. Fine Chemicals, India of analytical grade purity were purchased. All the solvents like N, N-dimethylformamide, dimethyl sulphoxide, tetrahydrofuran, acetone, diethyl ether were used after double distillation. All the metal nitrates, indicators, electrolytes and disodium salt of ethylenediaminetetraacetic acid of analytical grade purity were used, procured from Merck, India.

2.2 Synthesis of 4,4'-biphenol-benzidine-formaldehyde (4,4'-BP-BD-F) copolymer resin

A new copolymer was prepared by condensation polymerization reaction as shown in Figure 1, by using the molar proportion 3:2:8 of reacting monomers i.e. 4,4'-biphenol (5.58 gm, 0.3 mol) and Benzidine (4.00 gm, 0.2 mol) with formaldehyde (30 ml, 0.8 mol) in presence of 2M HCl as a catalyst at temperature 130 °C in an oil bath for about 3 h of continuous heating with occasional shaking. Dark reddish brown colored solid product was immediately removed, filtered and purified by dissolving in 1:1 (v/v) conc. NaOH/water with constant stirring and then filtered. The resulting polymer sample was washed several times with boiling water and dried in a desiccator at room temperature. Further dried polymeric sample extracted with diethyl ether to remove the excess 4,4'-biphenol-formaldehyde copolymer which might be present along with the 4,4'-BP-BD-F copolymer. Finally, the terpolymer was passed through 300-mesh size sieves and kept in a vacuum over silica gel.

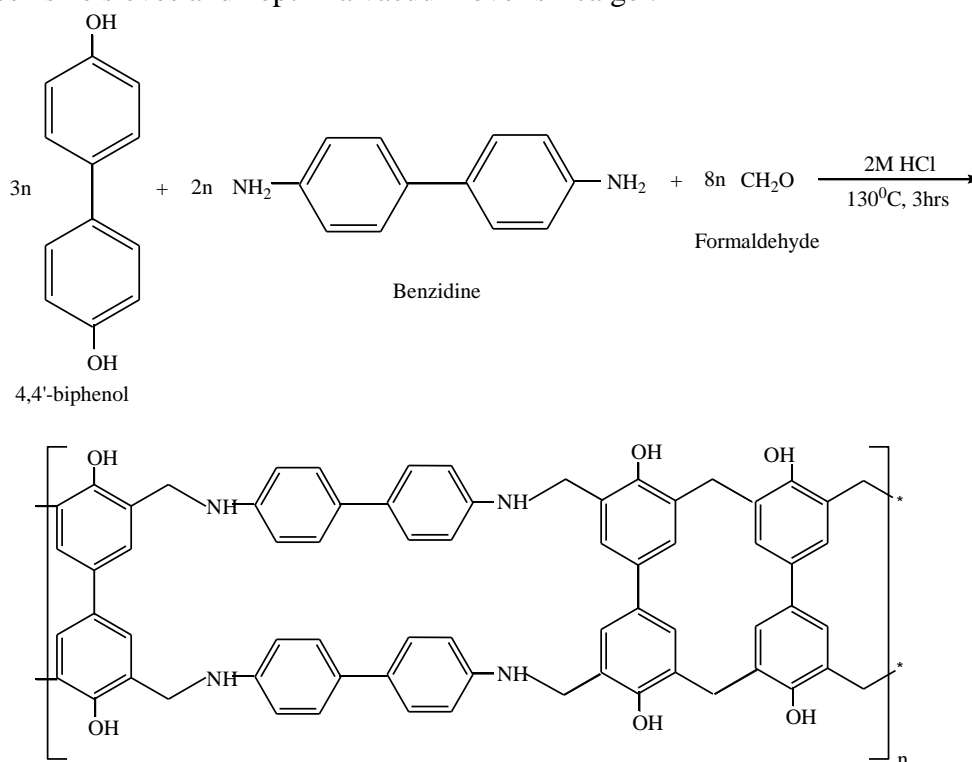


Fig. 1. Chemical reaction of 4,4'-BP-BD-F copolymer.

2.3 Characterization of copolymer by spectral studies

Terpolymer was subjected to elemental analysis for carbon, hydrogen and nitrogen on Perkin Elmer 2400 Elemental Analyser. UV-Visible spectra were recorded by preparing solution in dimethylsulphoxide on Shimadzu, UV-Visible double beam spectrophotometer in the range of 200-850 nm. Infrared spectra was recorded using KBr pellet in nujol mull on Perkin-Elmer-spectrum RX-I spectrophotometer in the range of 4000-500 cm^{-1} . $^1\text{H-NMR}$ studies were performed in solvent, dimethylsulphoxide, on Bruker Advance-II 400 MHz proton

NMR spectrophotometer. All the analytical and spectral studies were carried out at Sophisticated Analytical Instrumentation Facility (SAIF) Punjab University, Chandigarh.

2.4 Study of ion-exchange properties

As the batch equilibrium method has gained a rapid attention of researchers because of its acute degree of selectivity, variety of sorbent phases and enhanced hydrophilicity [5, 19-23] and hence has been applied to study the ion-exchange properties in the present investigation.

2.4.1. Determination of metal ions uptake in presence of electrolyte at different concentrations

The copolymer sample (25 mg) was suspended in an electrolyte solution (25 ml) of known concentration and the pH of the suspension was adjusted to required value by using either 0.1 M HNO₃ or/and 0.1 M NaOH, and was stirred for 24 h at 30 °C. To this suspension 2 ml of 0.1M solution of the metal ion was added and adjusted to required pH value, and then again stirred at temperature 30 °C for 24 h and filtered. The filtrate and washing of the solid product were combined together for the determination of metal ion content by titration against standardized ethylenediaminetetraacetic acid solution. The amount of metal ion taken up by copolymer was calculated from the difference between a blank reading and experimental reading. The experiment was repeated in the presence of several electrolytes at various ionic strength.

2.4.2 Evaluation of rate of metal ions uptake

Series of experiments, of the type described above, were carried out in order to estimate the time required to reach the state of equilibrium under the given experimental conditions, in which the metal ion taken up by the chelating resins was estimated from time to time, at temperature 30 °C, in presence of 25 ml of 1 M NaNO₃ solution. It was assumed that, under the given conditions, the state of equilibrium was established within 24 h. The rate of metal ions uptake is expressed as percentage of the amount of metal ions taken up after a certain time related to that at the state of equilibrium, using following relationship.

$$\text{Metal ion uptake} = \frac{\text{Amount of metal ion absorbed}}{\text{Amount of metal ion at equilibrium}} \times 100$$

2.4.3 Distribution of metal ions at different pH

The distribution of each one of the eight metal ions i.e. Fe³⁺, Cu²⁺, Hg²⁺, Ni²⁺, Co²⁺, Zn²⁺, Cd²⁺ and Pb²⁺ between the polymer phase and the aqueous phase was determined at temperature 30 °C in presence of 1 M NaNO₃ solution. The experiments were carried out as described above at different pH values and the distribution ratio (D), as defined, was calculated using following relationship.

$$D = \frac{\text{Weight (mg) of metal ion taken up by 1 gm of terpolymer}}{\text{Weight (mg) of metal ions present in 1ml of solution}}$$

3. Results and discussion

The resin sample was dark reddish brown in color and the solubility was tested in commonly used solvents and found to be soluble in DMF, DMSO, THF and pyridine without any precipitation and degradation. It was characterized by elemental and various spectral analyses and further studied their ion exchange behavior.

3.1. Characterization of terpolymer resin

3.1.1. Elemental analysis

Elemental analysis was carried out for Carbon, Hydrogen and Nitrogen contents which agrees well with theoretically calculated values, as compared in Table 1 and derived its empirical formula (C₆₈H₅₄N₄O) and empirical formula weight (1054).

Table 1. Elemental analysis data of terpolymer.

Terpolymer	Monomer empirical formula	Empirical formula weight	Elemental Analysis (%)					
			C		H		N	
			Cal.	Exp.	Cal.	Exp.	Cal.	Exp.
4,4'-BP-BD-F	$C_{68}H_{54}N_4O_6$	1022	77.41	76.62	5.12	5.02	5.31	5.24

3.1.2. UV-Visible spectra

Pure DMSO solvent was used to record the UV-visible spectrum of terpolymer sample in the wavelength region 200-850 nm and shown in Figure 2. The spectrum displayed two absorption maxima in the region 255 and 298 nm. The former and more intense band may be due to $n \rightarrow \pi^*$ transitions [24, 25] observed at 255 nm, indicates the presence of oxybiphenyl moiety. Hypsochromic shift observed in biphenyl may be due to introduction of -O- group between two phenyl groups which destroys the conjugation. Later and less intense band observed at 298 nm is accounted for $\pi \rightarrow \pi^*$ transition which may be due to biphenol group.

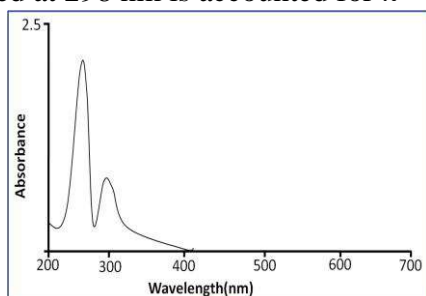


Fig. 2. UV-Visible spectrum of terpolymer.

3.1.3. FT-IR spectra

The FT-IR spectrum of terpolymer is represented in Figure 3 which shows a broad band, appeared at 3400.8 cm^{-1} , may be assigned to stretching vibration of the phenolic -OH groups, exhibiting intermolecular hydrogen bonding [26, 27]. Presence of weak peak at 2925.5 cm^{-1} describes the -NH- stretch in benzidine moiety which is present in terpolymeric chain [27]. Sharp and weak peak obtained at 2856.1 cm^{-1} indicates the presence of stretching vibrations of methylene -CH₂- group in the terpolymer chain [26]. Stretching vibration of $>C=C<$ in aromatics is represented by a medium band displayed at 1662.8 cm^{-1} . C-O stretching in phenol is represented at 1250.5 cm^{-1} . Bending, wagging and rocking vibrations can be accounted by the presence of bands appeared at 1460 cm^{-1} , $1345\text{--}1350\text{ cm}^{-1}$, $750\text{--}770\text{ cm}^{-1}$ respectively, may be due to presence of methylene bridges (-CH₂-) in the polymeric chain [28, 29]. The weak band appearing at 1010.5 and 837.7 cm^{-1} indicates the presence of tetrasubstitution in aromatic ring [27].

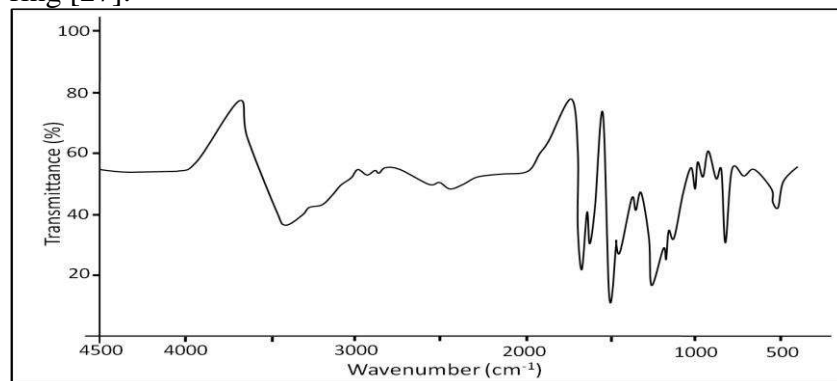


Fig. 3. FT-IR spectrum of terpolymer

3.1.4. ^1H - NMR spectra

Solvent DMSO- d_6 was used to record ^1H -NMR spectrum and is represented in Figure 4; which reveals different pattern of peaks, since each of it possesses set of proton having different proton environment.

A significant downfield in chemical shift of proton of phenolic -OH group, observed at δ 7.9 ppm is due to intermediate proton exchange reaction of phenolic -OH group [28]. Weak singlet is observed at δ 7.4 ppm is due to aromatic protons. Doublet signal observed at δ 6.8 ppm may be attributed to methylene protons of Ar- CH_2 -NH- moiety. In 4,4'-oxydianiline moiety, the doublet observed in the region δ 7.2 and δ 7.3 ppm is attributed to protons ortho to -NH and protons ortho to -O- respectively. A broad singlet observed at δ 6.7 ppm may be assigned to amino proton of -Ar-NH- CH_2 moiety and methylenic protons of Ar- CH_2 -Ar moiety may be recognized as signal appearing at δ 3.4 ppm [27, 28].

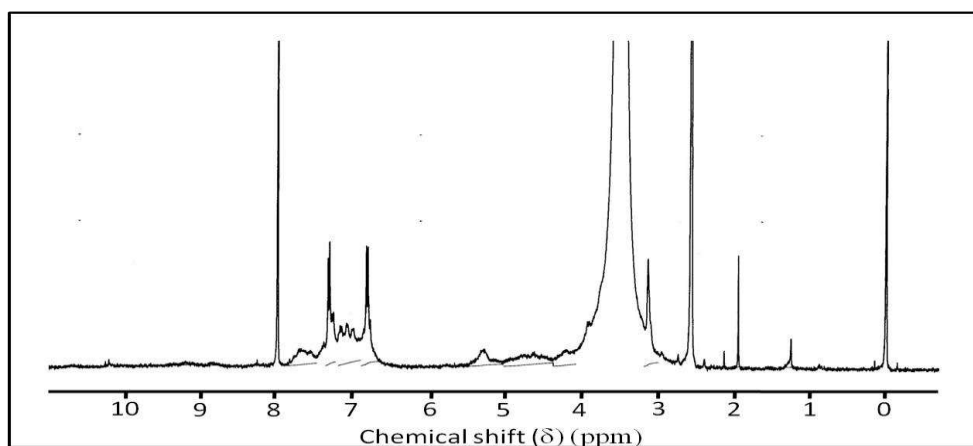


Figure 4. ^1H -NMR spectrum of terpolymer

On the basis of the nature and reactive position of the monomers, elemental analysis, UV-visible [24, 25], FT-IR [26, 27] and ^1H -NMR [27, 28] spectra, the most probable structure has been proposed as shown in Figure 1.

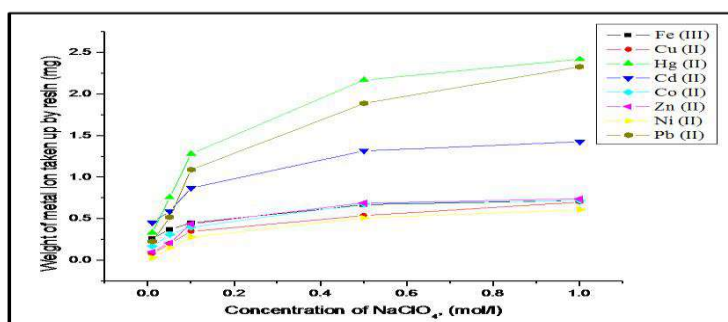
3.2 Study of ion exchange properties

To suggest the utility of newly synthesized terpolymer resins as ion exchanger for various applications, the study of influence of various electrolytes on the selectivity of metal ions, the rate of metal ion uptake and the distribution ratio of metal ions between the terpolymer and solution containing the metal ions, have been carried out. In a view to ascertain the selectivity of terpolymer resin, as ion exchanger, studies for the selected metal ions using batch equilibrium technique developed by Gregor et al and De Geiso [31] et al, have been carried out.

The results of batch equilibrium study are presented in Figures 5 to 10 in which aqueous solution of metal nitrate of Fe^{3+} , Cu^{2+} , Hg^{+2} , Ni^{2+} , Co^{2+} , Zn^{2+} , Cd^{2+} and Pb^{2+} ; and electrolytes NaNO_3 , NaCl , NaClO_4 and Na_2SO_4 were used. The ion exchange study was carried out using three experimental variables namely; a) Electrolytes at different ionic strength b) Shaking time and c) pH of the aqueous medium by keeping the two parameters constant. Only one parameter was varied at a time to evaluate its effect on metal ion uptake capacity of the copolymer [30, 31].

3.2.1 Effect of Electrolytes and their concentrations on metal ions uptake capacity.

The influence of ClO_4^- , NO_3^- , Cl^- and SO_4^{2-} at various concentrations on the equilibrium of metal-resin interaction has been studied and the results are expressed graphically shown in Figures 5 to 8. It shows that the amount of metal ions taken up by a given amount of copolymer depends on the nature and concentration of electrolyte present in solution. In presence of ClO_4^- , Cl^- and NO_3^- ions, the uptake of Fe^{+3} , Cu^{+2} , Hg^{+2} , Zn^{+2} , Cd^{+2} , Co^{+2} , Ni^{+2} and



Pb⁺² ions increases with rise in concentration of the electrolytes. Further, it was observed that in presence of SO₄⁻² ions, the amount of above metal ions taken up by the copolymers decreases with increasing concentration of electrolytes.

Moreover, higher increase in uptake of Fe⁺³, Hg⁺² and Pb⁺² ions with increasing concentration of ClO₄⁻, Cl⁻ and NO₃⁻ ions has been observed as compared to Cu⁺², Zn⁺², Cd⁺², Co⁺² and Ni⁺² ions, but it decreases in presence of SO₄⁻² ions. It was considered that the anions like ClO₄⁻, Cl⁻ and NO₃⁻ form weak association with the above metal ions while SO₄⁻² ions may form stronger complexes. Thus, this association may affect the equilibrium which may be explained on the basis of stability constants of complexes with these metal ions and the results agrees well as reported earlier [19, 20].

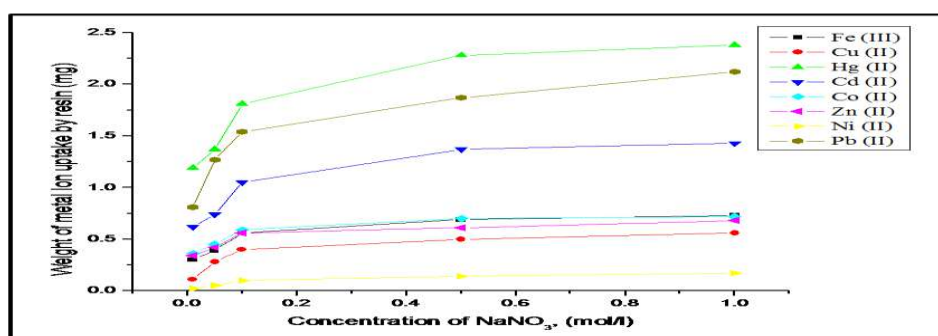


Fig. 5. Evaluation of the influence of different electrolytes on uptake of several metal ions^a by terpolymer resin at different concentrations of NaNO₃ electrolyte solution.
^a[M(NO₃)₂]=0.1 mol/l; volume of metal ion solution = 2 ml; volume of electrolyte solution = 25 ml; weight of resin = 25 mg; time = 24 h; at room temperature

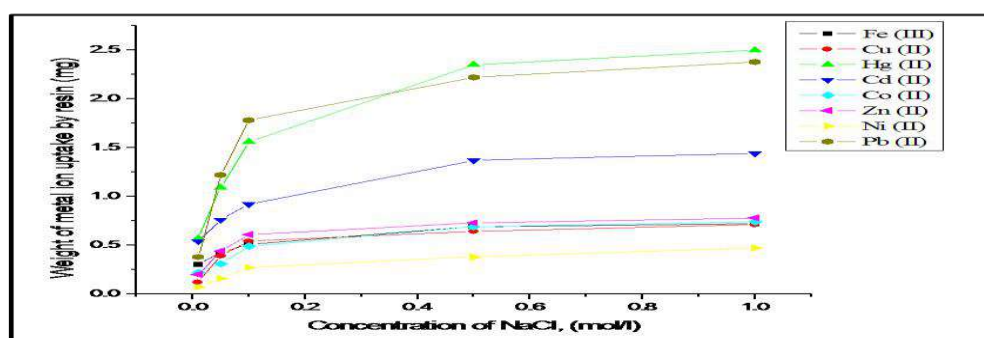


Fig. 6. Evaluation of the influence of different electrolytes on uptake of several metal ions^a by terpolymer resin at different concentrations of NaCl electrolyte solution.

Fig. 7. Evaluation of the influence of different electrolytes on uptake of several metal ions^a by terpolymer resin at different concentrations of NaClO₄ electrolyte solution.

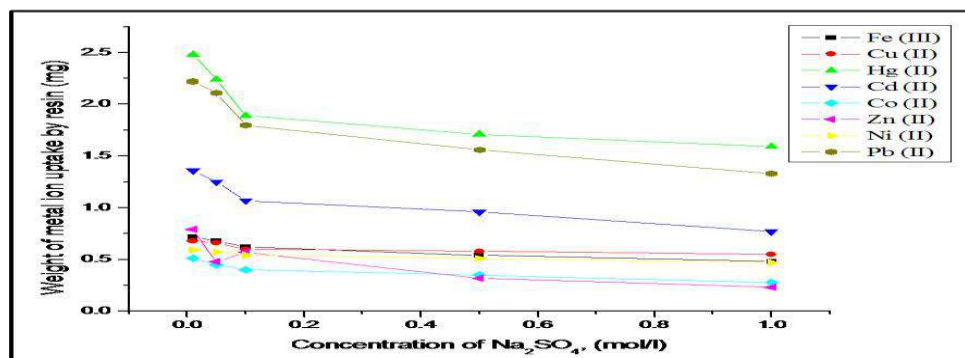


Fig. 8. Evaluation of the influence of different electrolytes on uptake of several metal ions^a by terpolymer resin at different concentrations of Na₂SO₄ electrolyte solution.

3.2.2 Rate of uptake for metal ions as a function of time

The rate of metal adsorption refers to the change in concentration of metal ions in aqueous solution which is in contact with given polymer and was determined to find out the shortest period of time for which equilibrium could be carried while operating as close to equilibrium conditions as possible. The results are expressed graphically shown in Figure 9, show that the time taken for the uptake of different metal ions at a given stage depends on the nature of metal ion under given conditions. It is found that Fe³⁺ ions required about 3 h for the establishment of the equilibrium, whereas Cu²⁺, Ni²⁺, Co²⁺ and Zn²⁺ required 5 h and Hg²⁺, Cd²⁺ and Pb²⁺ ions required about 7 h. Thus, the rate of metal ions uptake follows the order as Fe³⁺ > Ni²⁺ > Pb²⁺ > Cu²⁺ ≈ Co²⁺ > Cd²⁺ > Zn²⁺ > Hg²⁺ which agrees well with the results reported in literature [19, 20].

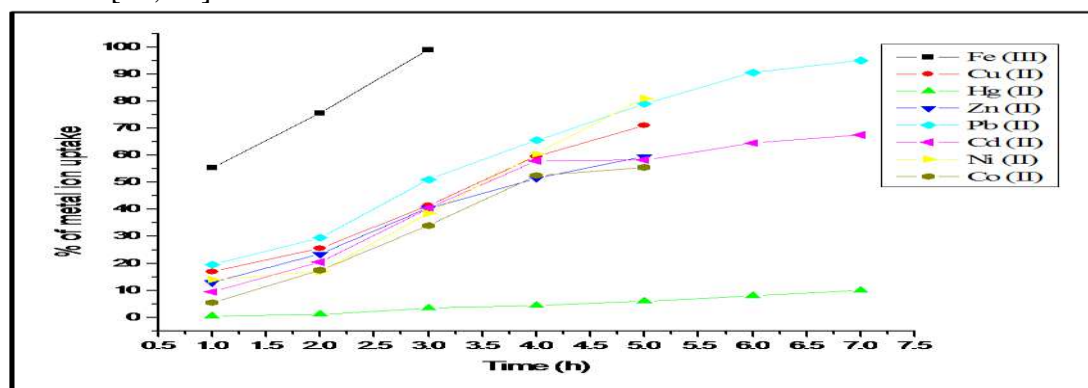


Fig. 9. Comparison of the rate of metal ions^a uptake^b by terpolymer, ^a [M(NO₃)₂] = 0.1 mol/l; volume : 2 ml; NaNO₃ = 1.0 mol/L; volume: 25 ml, room temperature.

^b Metal ion uptake = (Amount of metal ion absorbed x 100) / amount of metal ion absorbed at equilibrium.

3.2.3 Distribution ratio of metal ions at different pH

The effect of pH on the amount of metal ions distributed between two phases can be explained on the basis of results shown in Figure 10. The distribution ratio as a function of pH indicates that the relative amount of metal ion taken up by the terpolymer increases with rising pH of the medium, however, the magnitude of increase is different for each metal ion. The study was carried out only up to pH 6.5 in order to prevent hydrolysis of the metal ions at higher pH. In case of Fe³⁺ the highest working pH is 2.5. The terpolymer resin taken up Fe³⁺ ion more selectively than any other metal ions under study. The order of distribution ratio of

metal ions measured in pH range 2.5 - 6.5 is found to be as $\text{Fe}^{3+} > \text{Cd}^{2+} > \text{Co}^{2+} > \text{Zn}^{2+} > \text{Cu}^{2+} > \text{Hg}^{2+} > \text{Pb}^{2+} \approx \text{Ni}^{2+}$.

Thus, the results of this type of study are helpful in selecting the optimum pH for a selective uptake of a particular metal cation from a mixture of different metal ions [24]. For example, the result suggest the optimum pH 6.0, for the separation of Co^{2+} and Ni^{2+} with distribution ratio 'D' at 3000.0 and 568.90 respectively, using the present terpolymer resin as ion-exchanger. Similarly, for the separation of Cu^{2+} and Fe^{3+} the optimum pH is 3 at which the distribution ratio for Cu^{2+} is 1466.6 and that for Fe^{3+} is 3900.0. The lowering in the distribution of Fe^{3+} was found to be small and hence, efficient separation could be achieved.

In order to assess the utility of present terpolymer resin for the separation of Fe^{3+} ions from other metal ions, the following combinations of metal solutions were prepared: (1) Fe^{3+} and Cu^{2+} (2) Fe^{3+} and Ni^{2+} (3) Fe^{3+} and Co^{2+} (4) Fe^{3+} and Zn^{2+} (5) Fe^{3+} and Cd^{2+} (6) Fe^{3+} and Pb^{2+} etc. The solution for separation studies were prepared by mixing 1ml of 0.1M solutions of Fe^{3+} with 1ml of 0.1M solution of Cu^{2+} , Ni^{2+} , Co^{2+} , Zn^{2+} , Cd^{2+} , Hg^{2+} and Pb^{2+} . Selective uptake of the metal ions was studied by adjusting the optimum at pH 3. Distribution ratios of Fe^{3+} at pH 3 in the mixture with metal ions Cu^{2+} , Ni^{2+} , Co^{2+} , Zn^{2+} , Cd^{2+} and Pb^{2+} were found to be 1466.6, 568.90, 3000.0, 2537.0, 3700.0 and 870.70 respectively i.e. slightly lower than 3900.0 found when Fe^{3+} alone was studied. The lowering in the distribution ratios of Fe^{3+} was found to be small and hence efficient separation could be achieved which shows the importance of newly synthesized copolymer resins as an effective ion exchanger and can be explored for the separation of other metal ions.

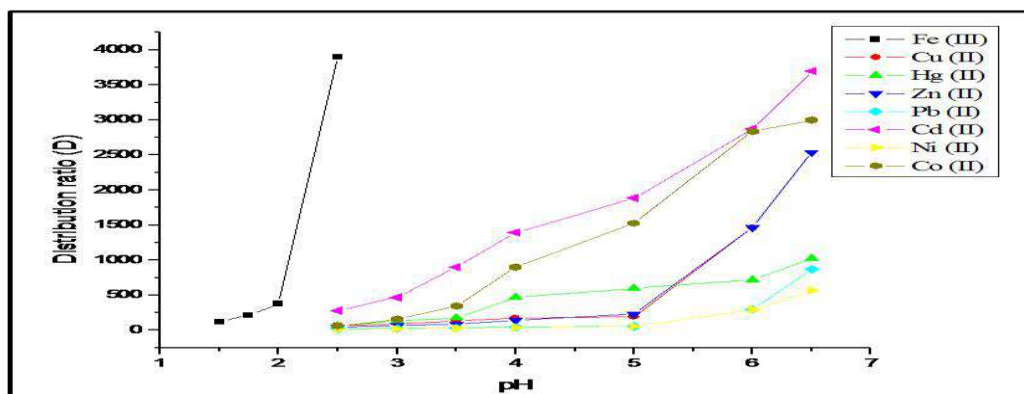


Fig. 10. Distribution ratio, D^a , of various metal ions^b as function of the pH by terpolymer
^a D = weight (in mg) of metal ions taken up by 1g of terpolymer/weight (in mg) of metal ions present in 1ml of solution.

^b $[\text{M}(\text{NO}_3)_2] = 0.1 \text{ mol/l}$; volume : 2 ml; $\text{NaNO}_3 = 1.0 \text{ mol/l}$; volume: 25 ml, time 24 h (equilibrium state) at room temperature.

4. Conclusion

A synthesis of new terpolymer 4,4'-BP-BD-F, based on the condensation reaction of 4,4'-biphenol and benzidine with formaldehyde in presence of acid catalyst was carried out and structure has been confirmed by elemental and spectral studies. It was proved to be selective chelating ion-exchanger for Fe^{3+} , Cu^{2+} , Ni^{2+} , Co^{2+} , Zn^{2+} , Cd^{2+} , Pb^{2+} and Hg^{2+} metal ions and has been successfully used for selective separation of ferric ions from other metal ions having combinations like a) ferric and cupric ion b) ferric and mercuric ion c) ferric and zinc ion and d) ferric and lead ion etc. This polymer showed higher selectivity for Fe^{3+} at pH 2.5 as compared to other metal ions.

To explore the use of this chelating resin for the separation of other metal ions in analytical chemistry appears to be advantageous when the separation problem can not be solved

by simpler means or when time can be saved. The area of application especially includes the concentration and the separation of chemically very similar ions. The use of this eco-friendly ion exchanger resin may effectively be explored in hydrometallurgy, antibiotics, purification and separation of radioisotope, in water treatment and pollution control, for the removal of hazardous and toxic metal ions like other ion exchangers.

Acknowledgement

The authors wish to express their sincere thanks to Principal, Jagadamba Mahavidyalaya, Achalpur for constant encouragement and support.

References

1. A. A. Atia, A. M. Donia, K. Z. Elwakeel, *React. Funct. Polym.* 65 (2005) 267-275.
2. L. K. Orazzhanova, M. G. Yashkarova, L. A. Bimendina, S. D. Kudaibergenov, *J. of Applied Polymer Science*, 87 (2003) 759-764.
3. D. Prabhakaran, M. S. Subramaniam, *Talanta* 59 (2003) 1227-1236.
4. F. Helfferich, *Ion-exchange*, McGraw Hill, New York, 1962.
5. M. M. Jadhav, L. J. Paliwal, N. S. Bhavne, *Desalination* 250 (2009) 120-129.
6. M. R. Lutfur, S. Silong, *European Polymer Journal* 36 (2000) 2105-2112.
7. A. Burkanudeen, M. Karunakaran, *Orient. J. Chem.* 18(1) (2002) 65-68.
8. W. B. Gurnule, H. D. Juneja and L. J. Paliwal, *Reactive and Functional Polymers* 50 (2002) 95-100.
9. J. M. Patel, M. G. Patel, H. J. Patel, K. H. Patel, R. M. Patel, *J. Mac. Mol. Sci.* 45 (2008) 281-288.
10. S. A. Patel, B. S. Shah, R. M. Patel, P. M. Patel, *Iran Polym. J.* 13(6) (2004) 445-453.
11. Bhavna Shah, Ajay Shah, Nayan Patel, *Iran Polym J.* 17(1) (2008) 3-17.
12. Z. S. Liu, G. L. Rempel, *Hydrology current research* 2(1) (2011) 107.
13. R. M. Joshi, M. M. Patel, *J. Makromol. Sci. Chem. A* 19(5) (1982) 351.
14. T. K. Pal, R. B. Kharat, *Die Angew Makromol Chem* 173 (1989) 55.
15. P. E. P. Michael, J. M. Barbe, H. D. Juneja, L. J. Paliwal, *European Polymer Journal*, 43 (2007) 4995-5000.
16. B. A. Shah, A. V. Shah, P. M. Shah, *Iran Polym. J.* 15(10) (2006) 809-819.
17. W. B. Gurnule, P. K. Rahangdale, L. J. Paliwal, *React Funct Polym.* 55 (2003) 255-265.
18. D. H. Wade, D. Zhao, A. K. Sengupta, C. Lange, *Reactive and Functional Polymers* 60 (2004) 109-120.
19. M. V. Tarase, A. B. Zade, W. B. Gurnule, *J. of Applied Polymer Science* 108(2) (2008) 738-746.
20. S. S. Rahangdale, A. B. Zade, W. B. Gurnule, *J. of Applied Polymer Science* 108(2) (2008) 747-756.
21. S. S. Butoliya, A. B. Zade, W. B. Gurnule, *J. of Applied Polymer Science* 113(1) (2009) 1-9.
22. M. V. Tarase, W. B. Gurnule, A. B. Zade, *e- Journal of Chemistry* 6(3) (2009) 639-650.
23. S. S. Rahangdale, W. B. Gurnule, A. B. Zade, *Indian Journal of Chemistry* 48(A) (2009) 531-535.
24. W. Kemp, *Organic Spectroscopy*, The Macmillan Press: Hong Kong, (1975).
25. R. M. Silverstein and G. C. Bassler, *Spectrometric Identification of Organic Compounds*, 2nd Ed; Wiley: New York, (1987).
26. K. Nakanishi, *Infra Red Absorption Spectroscopy Practical*; Nolden Day, INC and Nankodo Co. Ltd. Tokyo, (1967).
27. A. I. Vogel, *Text book of practical organic chemistry*; Longman Scientific and Technical: UK, (1989).
28. R. M. Silverstein, G. C. Bassler, T. C. Morrill, *Spectrometric Identification of Organic Compounds*, 5th Ed; Wiley: Singapore, (1991).
29. R. K. Samal, B. K. Senapati, T. B. Behuray, *J. Applied Poly Sci* 62 (1996) 655.
30. M. M. Jadhav, L. J. Paliwal, N. S. Bhavne, *J. Appl. Polym. Sci.* 109(1) (2008) 508-514.
31. J. R. Patel, D. H. Sutaria, M. N. Patel, *React. Polym.* 25 (1995) 17-23.
32. R. C. De Geiso, L. J. Donaruma, E. A. Tomic, *Jrg Chem* 27 (1962) 142.

Navigating the Therapeutic Landscape: Discovery and Pharmacophore Modeling of BRD4 Inhibitors for Prostate Cancer Precision Treatment

Mr. P S. Nawale¹, Ms. A D. Mehakare², Dr. J R. Bansod³, Prof. Capt. M M. Rathore⁴.

1. Department of chemistry, Vidya Bharati Mahavidyalay camp, Amravati

2. Department of chemistry, Vidya Bharati Mahavidyalay camp, Amravati

3. Department of chemistry, Vidya Bharati Mahavidyalay camp, Amravati

4. Department of chemistry, Vidya Bharati Mahavidyalay camp, Amravati

Abstract:-

This study represents a ground breaking exploration in the realm of prostate cancer therapeutics by focusing on the identification and optimization of inhibitors targeting Bromodomain-containing Protein 4 (BRD4). The research meticulously navigates the intricacies of BRD4 inhibition with a specific emphasis on tailoring these inhibitors for the treatment of prostate cancer. Employing a multifaceted approach, we delve into the process of identifying novel BRD4 inhibitors, breaking new ground in the field of cancer research. The study's core methodology involves not only the identification and optimization of BRD4 inhibitors but also their customization for precision treatment of prostate cancer. Pharmacophore modelling emerges as a pivotal tool in this endeavour, providing insights into the structural features crucial for effective inhibition. The interplay between innovative drug design and computational modelling techniques promises a refined understanding of the intricate molecular interactions between BRD4 inhibitors and their target. Through a comprehensive analysis, this research aims to contribute to the development of advanced therapeutic strategies for prostate cancer. The outcomes hold the potential to revolutionize precision medicine in the context of cancer treatment, offering new avenues for tailored therapeutic interventions. This study not only breaks new ground in the identification and optimization of BRD4 inhibitors but also paves the way for future advancements in prostate cancer therapeutics through the integration of pharmacophore modelling.

Keywords: Pharmacophore modelling, BRD4, Drug Discovery

1. Introduction:

Bromodomain-containing protein 4 (BRD4) is a crucial regulator involved in transcriptional and epigenetic processes, playing a pivotal role in various cellular functions and diseases. As a member of the BET (bromodomain and extra-terminal domain) family, BRD4 is known for its influence on gene expression and chromatin remodeling [1]. It has been extensively studied in the context of cancer, where it acts as a transcriptional and epigenetic regulator impacting cancer progression and inflammatory diseases [2][1]. Additionally, BRD4 has been associated with angiogenesis and is recognized as a potential therapeutic target for diseases involving abnormal cell growth [3] [4]. The interplay between BRD4 and the MYC proto-oncogene further highlights its significance in both normal development and disease pathogenesis [5].

BRD-4 inhibitors have emerged as promising therapeutic agents in various medical contexts. These inhibitors target the bromodomain-containing protein 4 (BRD-4) and are designed to modulate its activity. Treatment with BRD-4 inhibitors has been shown to reduce the expression of super-enhancer-associated oncogenes like MYC, E2F1, and BCL6, highlighting their potential in cancer therapy [6]. Moreover, BRD-4 inhibition has been associated with impaired DNA mismatch repair, induction of mismatch repair mutation signatures, and the creation of therapeutic vulnerabilities, particularly in immune-related responses [7]. Clinical studies have demonstrated the effectiveness of BRD-4 inhibitors in glioma, where BRD-4 expression is significantly higher than in adjacent normal brain tissue [9]. The development of

these inhibitors has traditionally focused on bromodomains, specifically bromodomain 1 and bromodomain 2, providing insights into potential therapeutic strategies [8].

The objective of the paper is to explore the molecular mechanisms underlying BRD-4 inhibition, focusing on how inhibitors interact with BRD-4 and modulate its activity. Utilize structural and biochemical studies to provide detailed insights into the binding interactions.

2. Methodology:

2.1 SMILES Collection: The SMILES notation provided a compact representation of the chemical structure, and the IC50 values has given an indication of each ligand's potency as an inhibitor, with lower values suggesting higher potency. Researchers have used this information to assess the effectiveness of compounds in inhibiting a specific target, in this case, BRD4.

Sr. No	LIGAND ID	Smiles	IC50nM [10]
1	SQ-9	<chem>CN1C2=CC=CC=C2C(OCCCC(NC3=CC=C(F)C=C3)=O)=CC1=O</chem>	80.54
2	SQ-17	<chem>CN1C2=CC=CC=C2C(OCCCC(NC3CCCCC3)=O)=CC1=O</chem>	95.88
3	SQ-12	<chem>CN1C2=CC=CC=C2C(OCCCC(NC3=CC=C(F)C=C3F)=O)=CC1=O</chem>	96.33
4	SQ-14	<chem>CN1C2=CC=CC=C2C(OCCCC(NC3=CC=CC=C3F)=O)=CC1=O</chem>	152.8
5	SQ-19	<chem>CN1C2=CC=CC=C2C(OCCCC(NC3=CC=C(C(C)C)C=C3)=O)=CC1=O</chem>	254.1
6	SQ-18	<chem>CN1C2=CC=CC=C2C(OCCCC(NC3=CC=C(CC)C=C3)=O)=CC1=O</chem>	392.6
7	SQ-21	<chem>CN1C2=CC=CC=C2C(OCCCC(NC3=CC=CC(C#N)=C3)=O)=CC1=O</chem>	585.5
8	SQ-13	<chem>CN1C2=CC=CC=C2C(OCCCC(NC3=CC(Cl)=CC=C3OC)=O)=CC1=O</chem>	623.8
9	SQ-15	<chem>CN1C2=CC=CC=C2C(OCCCC(NC3=CC=CC(OC)=C3)=O)=CC1=O</chem>	630
10	SQ-1	<chem>O=C3/C=C(/OCCCC(=O)NC=1/C=C(/[Cl])C=CC=1)C2=CC=CC=C2N3C</chem>	676.1
11	SQ-10	<chem>CN1C2=CC=CC=C2C(OCCCC(NC3=CC=CC(C(F)(F)F)=C3)=O)=CC1=O</chem>	1175
12	SQ-11	<chem>CN1C2=CC=CC=C2C(OCCCC(NC3=CC=C(C)C=C3Br)=O)=CC1=O</chem>	1177
13	SQ-20	<chem>CN1C2=CC=CC=C2C(OCCCC(NC3=C(OC)C=C(Cl)C(C)=C3)=O)=CC1=O</chem>	1256
14	SQ-8	<chem>CN1C2=CC=CC=C2C(OCCCC(NCC3=C(Cl)C=C(F)C=C3)=O)=CC1=O</chem>	1650
15	SQ-7	<chem>CN1C2=CC=CC=C2C(OCCCC(NCC3=CC=C(F)C=C3)=O)=CC1=O</chem>	1688
16	SQ-16	<chem>CN1C2=CC=CC=C2C(OCCCC(NC3=CC(Cl)=C(OC)C=C3OC)=O)=CC1=O</chem>	1781
17	SQ-5	<chem>CN1C2=CC=CC=C2C(OCC(NC3=CC=C(F)C=C3F)=O)=CC1=O</chem>	4747
18	SQ-3	<chem>CN1C2=CC=CC=C2C(OCC(NC3=CC=C(C)C=C3Br)=O)=CC1=O</chem>	5996
19	SQ-4	<chem>CN1C2=CC=CC=C2C(OCC(NC3=CC=C(C)C(F)=C3)=O)=CC1=O</chem>	9209
20	SQ-6	<chem>CN1C2=CC=CC=C2C(OCC(NC3=CC=C(Br)C=C3C)=O)=CC1=O</chem>	9307
21	SQ-2	<chem>CN1C2=CC=CC=C2C(OCC(NC3=CC=C(F)C=C3)=O)=CC1=O</chem>	25748

Note: - Not Determined [10]

Database Selection: Chose a reputable chemical data from literature [10] to collect SMILES notations of target molecules. Data Filtering: Filtered the dataset based on specific criteria, such as biological activity or structural features, to ensure relevance to our study.

2.2. SMILES to 3D Conversion:

Software Selection: Used molecular modeling software like RDKit, Open Babel, or Pybel to convert SMILES to 3D structures using MMFF94 force field. Conversion Process: Utilized the chosen software to convert SMILES notations into 3D molecular structures, ensuring proper handling of stereochemistry and atom coordinates.

2.3. Optimization: Geometry Optimization: Performed energy minimization and geometry optimization on the 3D structures to obtain stable conformations. Tools like RDKit and Open Babel provided optimization functionalities.

2.4. Saving as .SDF File:

File Format Conversion: Saved the optimized 3D structures in the Structure Data File (.sdf) format. Most molecular modeling software tools support this format for saving molecular

information. Consistency Check: Ensured that the saved .sdf file maintains the integrity and consistency of the molecular structures.

2.5. Pharmacophore Generation using PyMOL and Liquid Plugin: Software Installation: Executed PyMOL, a powerful molecular visualization tool, and the Liquid plugin for pharmacophore generation. Opened the saved .sdf file containing optimized structures in PyMOL.

Pharmacophore Generation: Used the Liquid plugin to generate pharmacophores based on specific features such as hydrogen bond donors/acceptors, hydrophobic regions, and aromatic centers. Visualization: Visualized the generated pharmacophores in PyMOL for further analysis.

3. Results and Discussion:

Our research represents a significant stride forward in the pursuit of enhanced therapeutics for prostate cancer. The systematic identification and optimization of BRD4 inhibitors, underscored by the innovative integration of pharmacophore modeling, have collectively marked a breakthrough in precision medicine for cancer treatment. The tailored design and optimization of these inhibitors exhibit a promising avenue for addressing the unique challenges posed by prostate cancer.

Through a meticulous exploration of molecular interactions and structural features, this study provides valuable insights that contribute to the refinement of BRD4 inhibitors. The potential impact of these findings extends beyond the laboratory, offering a blueprint for the development of targeted therapies in the clinical setting. The fusion of cutting-edge drug design strategies with computational modeling techniques not only breaks new ground but also lays a foundation for the evolution of personalized treatment approaches.

As we move forward, the outcomes of this research hold the potential to reshape the landscape of prostate cancer therapeutics. By breaking new ground in the identification and optimization of BRD4 inhibitors and harnessing the power of pharmacophore modeling, we chart a course towards more effective and tailored interventions. This study serves as a catalyst for future advancements, fostering a paradigm shift in the way we approach precision medicine for prostate cancer and potentially other malignancies.

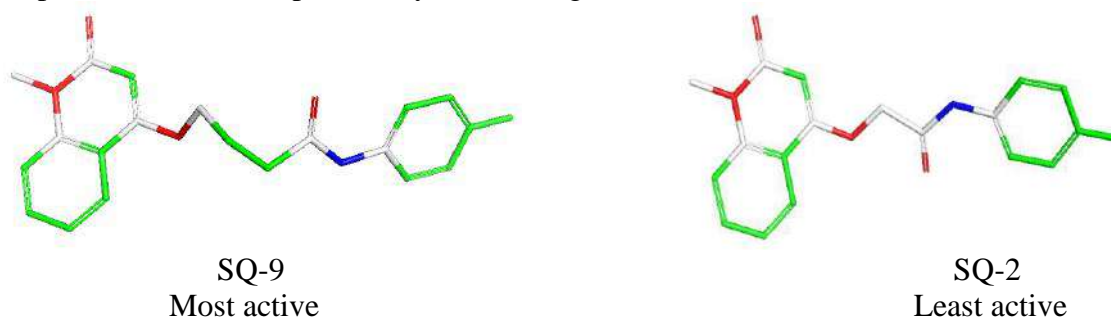


Figure3.1: - 3D Structure of most active and least active molecules, with distorted geometry of molecules.

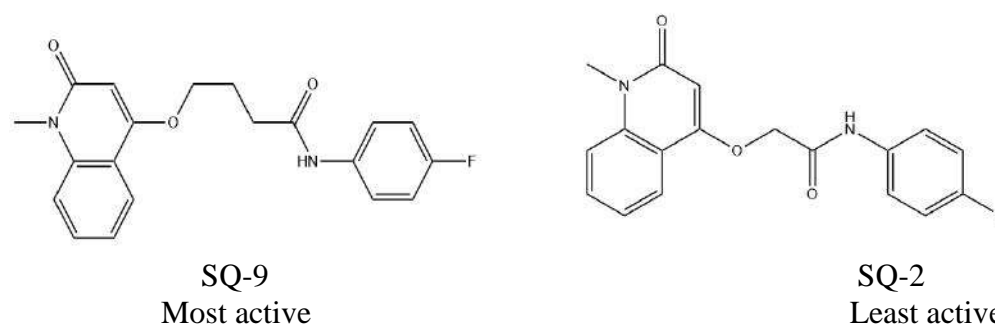
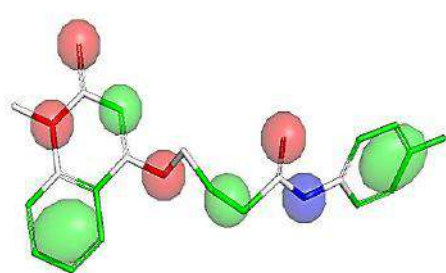
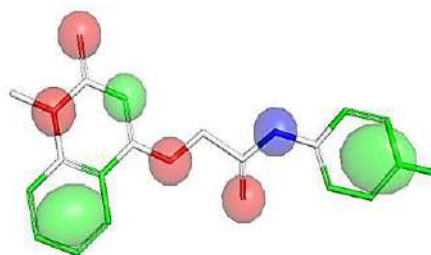


Figure3.2: - 2D Structure of most active and least active molecules.

SQ-9

Most active molecule

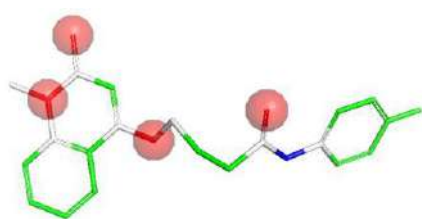


SQ-2

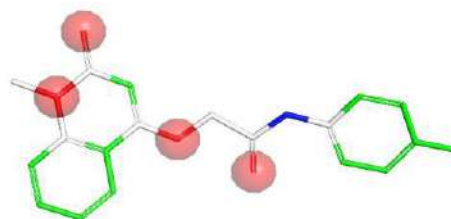
Least Active molecule

Figure3.3: - Above figure shows the pharmacophore model structure of most active and least active molecules.

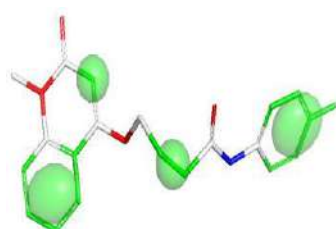
Pharmacophore modelling green colour for lipophilic, blue colour for H-donor and red colour for H-acceptor. In this figure SQ-2 structure shows three lipophilic, four H-acceptor and one H-donor molecules. In SQ-9 structure four lipophilic, four acceptor and one donor molecules.



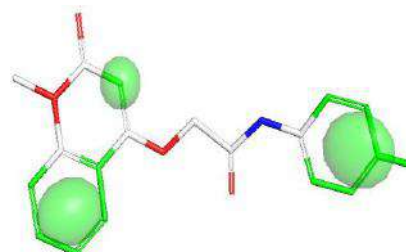
SQ-9



SQ-2

Figure 3.4: - In this above structure SQ-9 and SQ-2 both showing Same Number of H-acceptor

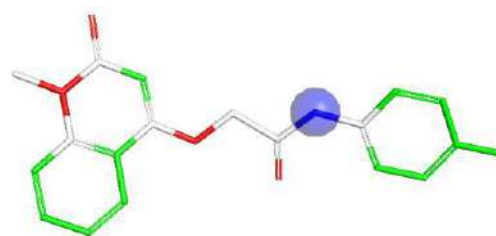
SQ-9



SQ-2

Figure 3.5: - SQ-9 having four lipophilic parts and SQ-2 having only three lipophilic part in this figure.

SQ-9



SQ-2

Figure 3.6: - In this above structure SQ-9 and SQ-2 both showing Same Number of H-donor (one H-Donor)

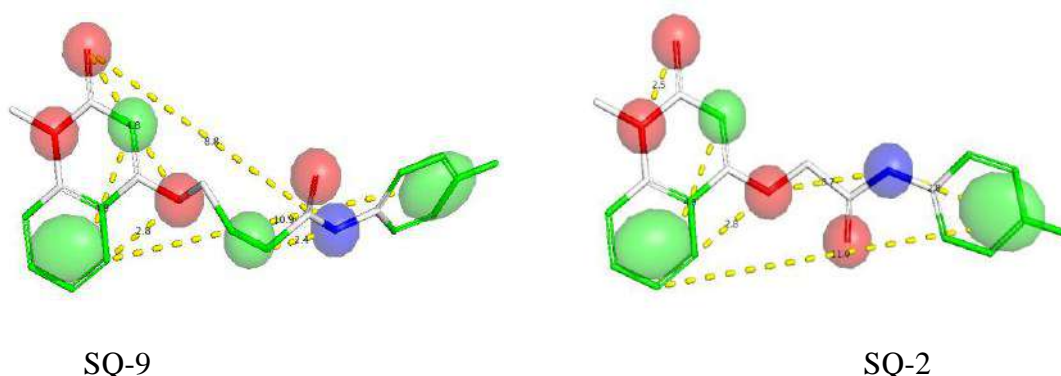


Figure3.7: - Measure distances between Lipophilic, H-acceptor and H-donor in most active and least active molecules.

In the SQ-9 shows distorted geometry with four lipophilic parts, the lipophilic to lipophilic higher distance is 10.9\AA and lowest distance is 4.9\AA , H-acceptor to H-acceptor distance is 4.2\AA , H-acceptor-Lipophilic distance is 2.8\AA and H-acceptor to H-donor distance is 8.8\AA . The SQ-2 having only three lipophilic parts in the molecule, in this structure lipophilic-lipophilic higher distance is 11.0\AA and lipophilic to lipophilic lowest distance is 4.9\AA , H-acceptor to H-acceptor distance is 2.5\AA , H-acceptor to Lipophilic distance is 2.8\AA , and H-acceptor to H-donor distance is 3.7\AA .

Conclusion:-

In conclusion, our research represents a significant stride forward in the pursuit of enhanced therapeutics for prostate cancer. The systematic identification and optimization of BRD4 inhibitors, underscored by the innovative integration of pharmacophore modeling, have collectively marked a breakthrough in precision medicine for cancer treatment. The tailored design and optimization of these inhibitors exhibit a promising avenue for addressing the unique challenges posed by prostate cancer. Through a meticulous exploration of molecular interactions and structural features, this study provides valuable insights that contribute to the refinement of BRD4 inhibitors. The potential impact of these findings extends beyond the laboratory, offering a blueprint for the development of targeted therapies in the clinical setting. The fusion of cutting-edge drug design strategies with computational modeling techniques not only breaks new ground but also lays a foundation for the evolution of personalized treatment approaches.

As we move forward, the outcomes of this research hold the potential to reshape the landscape of prostate cancer therapeutics. By breaking new ground in the identification and optimization of BRD4 inhibitors and harnessing the power of pharmacophore modeling, we chart a course towards more effective and tailored interventions. This study serves as a catalyst for future advancements, fostering a paradigm shift in the way we approach precision medicine for prostate cancer and, potentially, other malignancies.

"Sincere acknowledgement to Prof. Dr. Vijay H. Masand for his support throughout the research work."

References:

- 1] Ballachanda N. Devaiah, Anne Gegonne, and Dinah S. Singer¹ *J Leukoc Biol.* 2016 Oct; 100(4): 679–686. Published online 2016 Jul 22. doi: [10.1189/jlb.2RI0616-250R](https://doi.org/10.1189/jlb.2RI0616-250R)
- 2] Donati, B., Lorenzini, E. & Ciarrocchi, A. BRD4 and Cancer: going beyond transcriptional regulation. *Mol Cancer* 17, 164 (2018). <https://doi.org/10.1186/s12943-018-0915-9>
- 3] Zijun Zhou, Xiaoming Li, Zhiqing Liu, Lixun Huang, Yuying Yao, Liyou Li, Jian Chen, Rongxin Zhang, JiaZhou, Lijing Wang, Qian-Qian Zhang, Volume 11 - <https://doi.org/10.3389/fphar.2020.01043>.

- 4] Sheetal Uppal , Anne Gegonne , Qingrong Chen , PetriaS. Thompson , Dan Cheng , ie Mu, Daoud Meerzaman , Hari S. Misra , Dinah S. Singer Volume 29, Issue 8, 19 November 2019, Pages 2450-2460.e5 <https://doi.org/10.1016/j.celrep.2019.10.066>
- 5] Aparna Kotekar, Amit Kumar Singh, Ballachanda N. Devaiah The FEBS Journal Volume 290, Issue 20 p. 4820-4842, <https://doi.org/10.1111/febs.16580>
- 6] Qian, H., Zhu, M., Tan, X. *et al.* Super-enhancers and the super-enhancer reader BRD4: tumorigenic factors and therapeutic targets. *Cell Death Discov.* **9**, 470 (2023). <https://doi.org/10.1038/s41420-023-01775-6>.
- 7] BRD4 bromodomain containing 4 [*Homo sapiens* (human)] Gene ID: 23476, updated on 15-Jan-2024 <https://www.ncbi.nlm.nih.gov/gene/23476>
- 8] tudy Discovers Novel Region for BRD4 Transcription and Potential Therapeutic Target By Melissa RohmanJul 12, 2023 <https://news.feinberg.northwestern.edu/2023/07/12/study-discovers-novel-region-for-brd4-transcription-and-potential-therapeutic-target>
- 9] Hua Yang , Li Wei , Yang Xun , Anping Yang , Hua You, Volume 21, 25 June 2021, Pages 1-14, <https://doi.org/10.1016/j.omto.2021.03.005>
- 10] Haiyang Zhong, Xinyue Wang, Shicheng Chen, et al *J. Med. Chem.* 2024, 67, 1, 138–151 Publication Date:December 28, 2023. <https://doi.org/10.1021/acs.jmedchem.3c00996>
- 11] Siegel, R. and Ma, J. and Zou, Z. and Jemal, A. Cancer statistics, 2014, journal CA Cancer J. Clin, volume {64}, pages 9, 2014.
- 12] Torre, L. A. and Bray, F. and Siegel, R. L. and Ferlay, J. and Lortet-Tieulent, J. and Jemal, A. Global cancer statistics, 2012 journal of CA Cancer J. Clin volume {65}, pages 87, 2015
- 13] Chen, W. and Zheng, R and Baade, P. D. and Zhang, S. and Zeng, H. and Bray, F. and Jemal, A. and Yu, X. Q. and He, J. Cancer statistics in China, 2015, Journal of Ca-Cancer J. Clin., volume 66, pages 115, 2016.
- 14] Sung, H. and Ferlay, J. and Siegel, R. L. and Laversanne, M. and Soerjomataram, I. and Jemal, A. and Bray, F., Global Cancer Statistics 2020: GLOBOCAN Estimates of Incidence and Mortality Worldwide for 36 Cancers in 185 Countries, journal of CA Cancer J. Clin, volume 71, pages 209, 2021.
- 15] Katsogiannou, M. and Ziouziou, H. and Karaki, S. and Andrieu, C. and Henry de Villeneuve, M. and Rocchi, P., The hallmarks of castration-resistant prostate cancers, journal of Cancer Treat Rev., volume 41, pages 588, 2015.
- 16] Valenca, L. B. and Sweeney, C. J. and Pomerantz, M. M., Sequencing current therapies in the treatment of metastatic prostate cancer, journal of Cancer Treat Rev., volume 41, pages 332, 2015.
- 17] Wyatt, A. W. and Gleave, M. E., Targeting the adaptive molecular landscape of castration-resistant prostate cancer, journal of EMBO Mol. Med., volume 7, pages 878, 2015.
- 18] Antonarakis, E. S. and Lu, C. and Wang, H. and Lubber, B. and Nakazawa, M. and Roeser, J. C. and Chen, Y. and Mohammad, T. A. and Chen, Y. and Fedor, H. L., R-V7 and resistance to enzalutamide and abiraterone in prostate cancer, journal of N Engl J. Med., volume 371, pages 1028, 2014.

Vidya Bharati Mahavidyalaya, Amravati



Published by : SAI JYOTI PUBLICATION
Behind Chawla Sadi Center, Tin-nal Chowk,
Kasarpura, Itwari, Nagpur-440002
Phone : 9764673503, 9923593503
email : sajp10ng@gmail.com
Website : www.saijyoti.in

